NASA CR-132605-1

NASA CONTRACTOR
REPORT

(NASA-CR-132605-1) PREDICTION AND VERIFICATION OF CREEP BEHAVIOR IN METALLIC MATERIALS AND COMPONENTS, FOR THE SPACE SHUTTLE THERMAL PROTECTION SYSTEM. VOLUME 1, PHASE 1: CYCLIC (McDonnell-Douglas N75-21431 Unclas G3/26 18570

Prediction and Verification of Creep Behavior in Metallic Materials and Components for the Space Shuttle Thermal Protection System

VOLUME I

Phase I - Cyclic Materials Creep Predictions

November 1974

Prepared By **J. W. Davis** *and* **B. A. Cramer**

MCDONNELL DOUGLAS ASTRONAUTICS COMPANY • EAST

MCDONNELL DOUGLAS
CORPORATION

NATIONAL AERONAUTICS AND SPACE ADMINISTRATION • WASHINGTON, D.C. • NOVEMBER 1974

NASA CR-132605-1

Prediction and Verification of Creep Behavior in Metallic Materials and Components for the Space Shuttle Thermal Protection System

VOLUME I

Phase I - Cyclic Materials Creep Predictions

November 1974

J. W. Davis

B. A. Cramer

Prepared under contract NAS 1-11774

Prepared by McDonnell Douglas Astronautics Company-East

Saint Louis, Missouri

for National Aeronautics and Space Administration

Langley Research Center

Hampton, Virginia

MCDONNELL DOUGLAS ASTRONAUTICS COMPANY • EAST

Saint Louis, Missouri 63166 (314) 232-0232

MCDONNELL DOUGLAS

CORPORATION

FORWARD

This report was prepared by McDonnell Douglas Astronautics Company - East under contract NAS-1-11774 for the National Aeronautics and Space Administration, Langley Research Center, Hampton, Virginia. It was administered under the direction of the Materials Division, Materials Research Branch, with Mr. D. R. Rummler acting as the technical representative of the contracting officer. The McDonnell Douglas program manager was Mr. J. W. Davis. Others who participated in this program and in the preparation of this report are: Messrs. B. A. Cramer, W. J. Edens, and D. C. Ruhmann. The experimental portion were performed by Messrs. R. L. Hillman (steady state creep testing) and M. B. Munsell (cyclic creep testing). Statistical analysis was performed by Dr. J. F. Brady, Mr. W. J. Edens, Mr. R. K. Linback, and Mr. D. C. Ruhmann.

This report covers the period from July 1972 to June 1974.

SUMMARY

Phase I of this four-phase program was concerned with the steady-state and cyclic creep behavior of four materials in sheet form, L605, Ti-6Al-4V, Rene' 41, and TDNiCr, applicable to a metallic radiative thermal protection system (TPS).

A survey of the literature was conducted to gather available steady-state creep data for each of the materials. Empirical equations were developed for these data sets, using regression analysis techniques to express steady-state creep strains as functions of stress, temperature and time. In addition, the material gage and rolling direction were included as variables where applicable data were provided.

A series of supplemental steady-state creep tests were conducted on tensile specimens for each of the four materials. The majority of tests were conducted on thin gage sheet specimens ($\sim$.025 cm) in the longitudinal rolling direction although a limited number of tests were conducted to investigate effects of gage ($\sim$.060 cm) and transverse direction on creep response.

Cyclic tests were conducted to evaluate creep response characteristics under cyclic stress and temperature profiles typical of a Space Shuttle entry. These tests were as follows:

Basic Cycle - Stress and peak temperature were maintained constant for twenty minutes per cycle. Specimens of each material were cycled 100 times. Data from these tests were used to develop cyclic empirical creep equations for each material.

Stepped stress profiles - Stress and peak temperature were maintained constant for twenty minutes per cycle but stress level was varied as a function of cycle. This series of tests was designed to simulate stress redistribution, due to creep, occurring in a TPS panel.

<u>Complex trajectory</u> - Peak temperature was maintained constant for twenty minutes per cycle but stress was varied during the cycle. The stress was not varied between cycles. Data from the stepped stress profile and complex trajectory tests were used to investigate the applicability of the time and strain hardening theories of creep accumulation during cyclic creep exposures.

<u>Idealized trajectories</u> - Stress and temperature flight profiles were idealized into a series of constant steps. Specimens were repeatedly subjected to these profiles for up to 100 cycles.

<u>Simulated mission profiles</u> - Specimens were subjected to mission stress and temperature that changed with time as would occur in flight. These changes were conducted to 200 cycles.

Additional cyclic tests, conducted to assess the effect of time per cycle and effect of atmospheric pressure on creep strain, completed the cyclic creep testing.

Test results demonstrated that there is no significant difference between cyclic and steady-state creep strains (for the same total time at load) for the alloys L605, Ti-6Al-4V, Rene' 41, and TDNiCr. A single linear equation describing the combined steady-state and cyclic creep data, for each alloy, resulted in standard errors of estimate higher than desirable for the individual data sets. Well fitting creep strain equations were developed for either steady-state or cyclic creep data using linear least squares analysis techniques. A non-linear least squares analysis of the combined cyclic and steady-state data appeared to offer potential for lowering the standard error of estimate but time prevented further exploration in this area.

Predictions of strains that were produced by complex trajectory and simulated mission tests (using equations based on simple cycles) was successfully accomplished. A computer program was specifically written for this analysis. This computer program is based on time and strain hardening theories of creep accumulation. For Ti-6Al-4V,

and TDNiCr, the strain hardening theory of creep accumulation provided the best predictions, while for Rene' 41 time hardening, and for L605 a combination of strain and time hardening provided the best predictions.

A gage effect on creep response (thin gages crept faster) was noted in both the literature survey and the supplemental steady-state creep data bases for L605, Rene' 41, and TDNiCr. An effect of material rolling direction on creep strains was observed in TDNiCr.

No effects on creep strain due to variation of time per cycle (for the same total time) or atmospheric pressure were observed for any of the four materials. Comparison of data obtained from idealized and simulated mission tests indicates that adequate cyclic creep response analyses can be performed by expressing the trajectory conditions in a simplified step-wise form.

The International System of units (SI) are used in this report. U.S. Customary Units are also generally provided. Applicable conversion factors are presented in Appendix A.

TABLE OF CONTENTS

TABLE OF CONTENTS (Continued)

LIST OF FIGURES

LIST OF FIGURES (Continued)

LIST OF FIGURES (Continued)

LIST OF FIGURES (Continued)

LIST OF FIGURES (Continued)

LIST OF FIGURES (Continued)

LIST OF FIGURES (Continued)

LIST OF FIGURES (Continued)

LIST OF TABLES

LIST OF SYMBOLS

ε = strain, %

ε_{cy} = cyclic creep strain, %

ε_{ss} = supplemental steady-state creep strains, %

t = time, hrs.

LIST OF SYMBOLS (Continued)

Q	=	Apparent activation energy
R or R^2	=	correlation coefficient
R	=	universal gas constant
RT	=	Room temperature
T	=	Absolute Temperature, °K
σ	=	stress, MPa
σ_0	=	uniform tensile specimen stress
σ_1	=	principal stress
σ_2	=	principal stress
σ_T	=	tangential stress
S	=	structure factor
Ø	=	material thickness, cm.
θ	=	test direction
S_y	=	standard error of estimate
Z	=	dummy variable factor
<	=	less than
>	=	greater than

1.0 INTRODUCTION

One of the design requirements of reentry vehicle metallic thermal protection systems (TPS) is that deflections, occurring during ascent and entry mission phases, due to differential pressure and thermal loading, do not exceed design limits established to minimize localized aerodynamic heating and to minimize the need for panel refurbishment (Reference 1). Because these deflections include permanent deformation due to creep, the influence of cyclic entry conditions on material creep response and methods for predicting these deformations are needed.

Several experimental programs (References 2 to 6) have been conducted to determine if cyclic entry environments produce a different creep strain response than would be predicted based on data obtained from steady-state creep tests. These programs have produced varying, and at times, conflicting results as to whether a cyclic environment produces different results than those obtained in steady-state environments.

This four-phase program was initiated, in an effort to further investigate cyclic creep response and to develop design methods applicable to TPS structures subjected to environments causing creep to occur. Four alloys, in sheet form, Ti-6Al-4V, Rene' 41, L605 and TDNiCr, were studied. Although the work was initiated for application to Space Shuttle TPS, results are considered applicable to a wide variety of structures which are cyclicly exposed to creep producing thermal environments.

Phase I of this program was designed to investigate the steady-state (constant temperature and load) and cyclic creep response characteristics of the four alloys.

Steady-state creep data was gathered through a literature survey to establish a reference data base for each alloy. These data bases were used to develop empirical equations describing creep as a function of time, temperature, and stress.

These equations were the basis for establishing test parameters for supplemental steady-state creep tests conducted on tensile specimens. The purpose for these tests was to compare the creep response of sheet used in this program with that of the literature survey data base, and also to supplement the data base. Effects of variables such as material thickness and rolling direction were studied.

Tensile cyclic creep tests were conducted to characterize material cyclic creep response under varying loads and temperatures. These data were used to evaluate analytical methods to predict cyclic creep behavior. Basic cyclic tests, using simple constant stress and temperature cycles to represent flight conditions, provided data for comparison with steady-state response and development of empirical equations for cyclic creep. Other tests were conducted using these same cycles but with a varying stress as a function of cycle to simulate the changing stresses present in a creeping beam as a result of stress redistribution. Additional tests were conducted using complex stress and temperature profiles representative of Space Shuttle Orbiter trajectories. Tests were generally conducted for 100 simulated flight cycles.

A computer program was written, applying creep hardening theories in conjunction with empirical equations for creep, to aid in analysis of these test data.

In Phase II a computer program will be written to predict TPS panel creep deflections based on inputs of panel geometry, trajectory data, and empirical creep equation coefficients. Corrugation stiffened and rib stiffened sub-size panels will be tested to provide data for verification of prediction capability.

Phase III involves using methods of analysis developed in Phases I and II to analyze full size heat shield panel creep deformation data developed on other R/D programs (References 2 and 3).

In Phase IV recommended creep design procedures for the Space Shuttle TPS

will be established. These procedures provide methods for analyzing material creep data, procedures for design of TPS, and rules for inspection and measurement of panel deflections.

This report contains results of Phase I of the study. Included are data for steady-state and cyclic tests conducted and associated analysis for the four alloys studied.

2.0 TECHNICAL APPROACH

2.1 TPS DESIGN CRITERIA AND ENVIRONMENT

This program was associated with the use of metallic materials for the Space Shuttle TPS. Therefore, the test conditions were representative of the Reference (1) Shuttle design criteria and environments.

In the Reference (1) studies, entry trajectories were shaped to accommodate the type of TPS used. For example, trajectories for ablative and Reusable Surface Insulation (RSI) TPS were shaped so that high surface temperatures occur early in the entry trajectory. This resulted in low total heat to the TPS and a high surface temperature. Entry trajectories for metallic TPS were shaped to minimize peak surface temperatures so that the metals would not overheat. This resulted in high total heat input and a relatively long time at peak surface temperature. The Shuttle orbiter design ascent trajectory for a metallic TPS, based on Reference (1) studies is shown in Figure 2-1. Limit pressures resulting from this trajectory were multiplied by a 1.4 factor of safety to obtain design ultimate pressures shown in Figure 2-2. In addition to the aerodynamic pressure, a minimum vent pressure of +9.7 kPa ultimate was used over the entire vehicle for TPS design. These pressures occur while the panel temperature is less than 366°K.

The design entry trajectory is shown in Figure 2-3. Resulting ultimate differential pressures and bottom centerline temperatures are shown in Figures 2-4 and 2-5. Design limit temperatures for this trajectory over the Orbiter surface are shown in Figure 2-6.

Test temperatures and differential pressure profiles used in this study were based on the entry profiles shown. The cycle time of 20 minutes at peak temperature were used as a baseline throughout cycling testing. The entry temperature profile

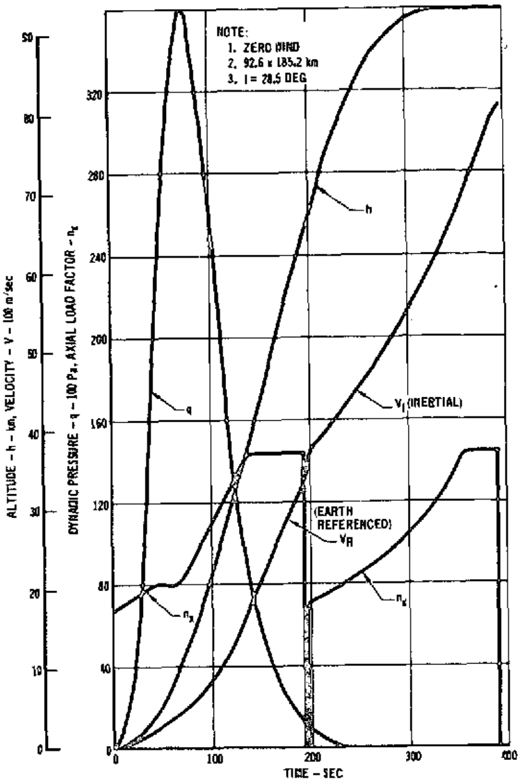

FIGURE 2-1 DESIGN ASCENT TRAJECTORY

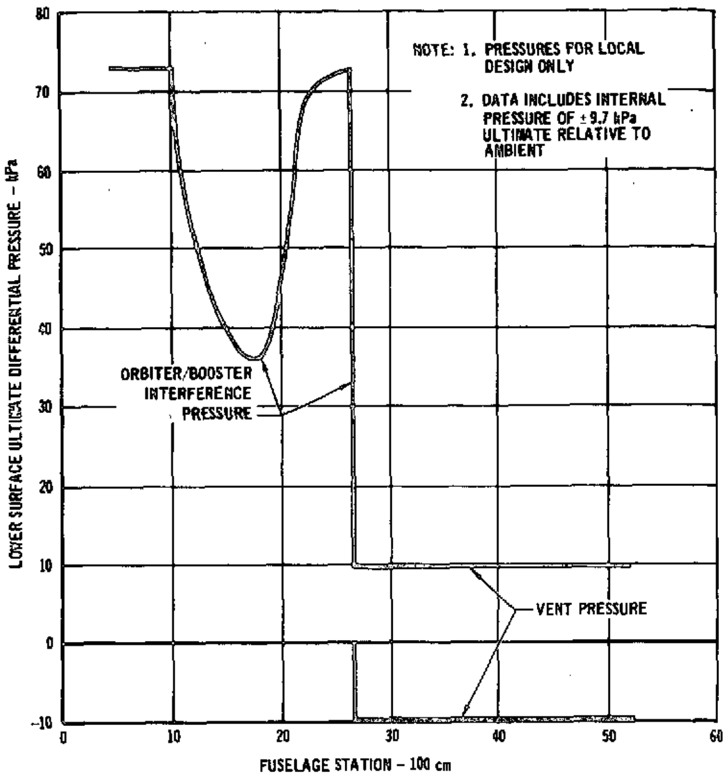

FIGURE 2-2 ENVELOPE OF ASCENT PRESSURES ON FUSELAGE LOWER SURFACE

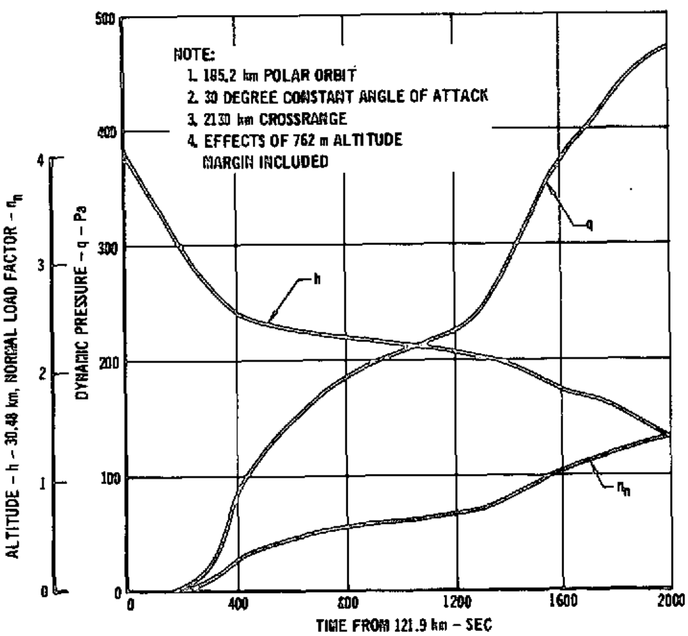

FIGURE 2-3 DESIGN ENTRY TRAJECTORY

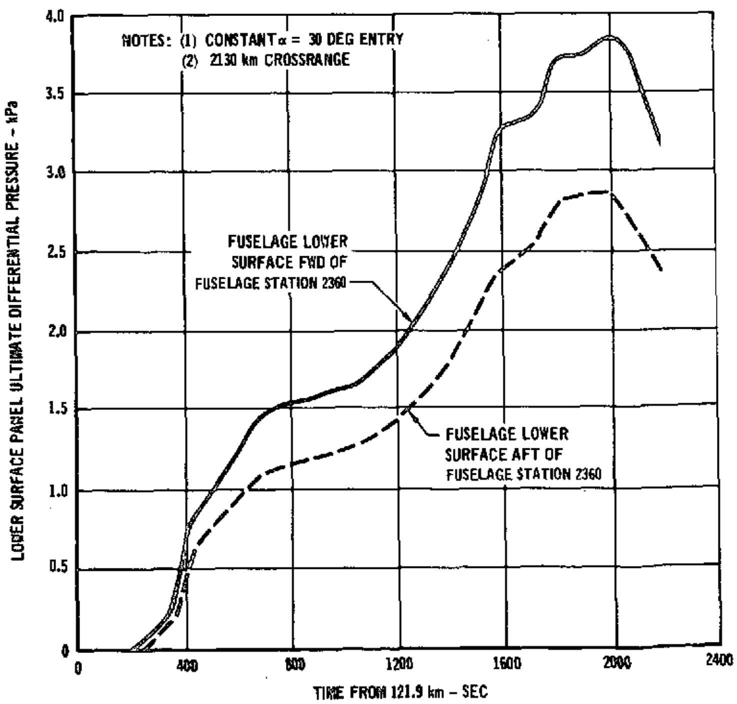

FIGURE 2-4 LOWER SURFACE ENTRY PRESSURE

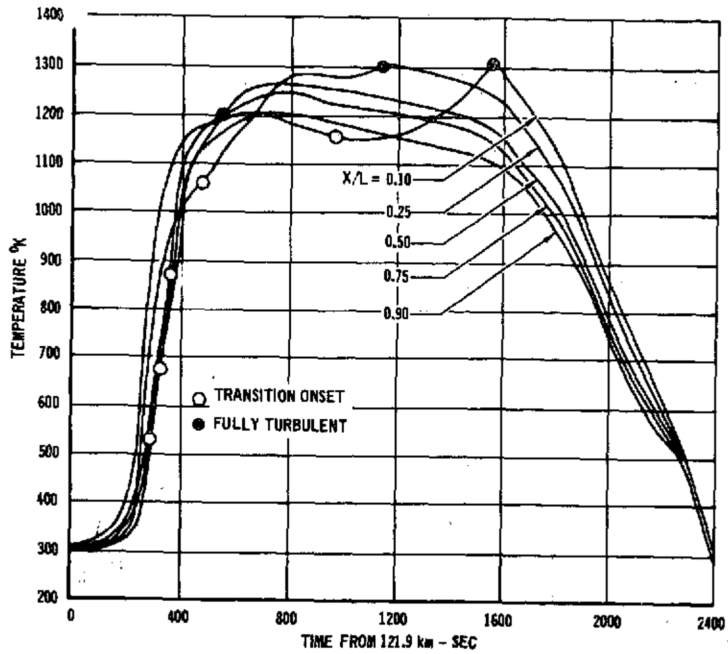

FIGURE 2-5 ORBITER BOTTOM CENTERLINE ENTRY TEMPERATURES

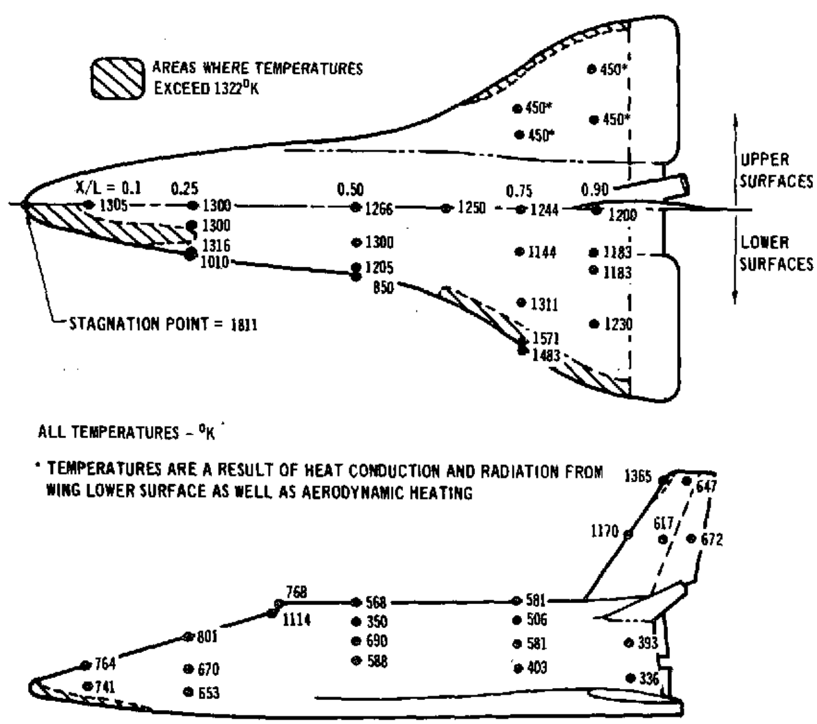

FIGURE 2-6 MAXIMUM ENTRY TEMPERATURE FOR A SPACE SHUTTLE WITH A METALLIC TPS

at X/L = .50 was used as typical for the basis of simulated mission and idealized cyclic trajectory tests for each of the materials.

Stress levels and temperature levels tested were designed to yield 100 cycle creep strains of up to approximately 0.5%. For typical 2.5 cm. deep corrugation and rib stiffened TPS panels, this creep strain level is consistent with the following allowable TPS deflection criterion:

$$\delta = .25 + .01L \text{ (cm)}$$

where δ = maximum elastic plus creep deflection at panel midspan

L = panel length (distance between supports)

This criterion was based on minimizing local panel heating as established through thermodynamic studies during the referenced Shuttle studies.

This criterion provides for a maximum deflection of .76 cm for the 50.8 cm panel length defined during the referenced studies.

Loads and temperatures resulting from design trajectories are normally used to size TPS panels for strength. However, in designing for creep deflections, nominal loads and temperatures are usually used. Reference (1) studies defined the differences in loads and temperatures for the design and nominal trajectories as (1) nominal pressures = design limit pressure/1.13 and (2) nominal temperatures = design temperatures -25°K (10°K per 304.8 m altitude dispersion from nominal trajectory).

2.2 SELECTION OF MATERIALS

Past Space Shuttle studies have shown that a combination of several metallic materials will provide the lightest weight metallic TPS. For example, up to 700°K, titanium alloys appear to provide the lightest panels. In the temperature range of 700-1144°K, the nickel base alloys offer weight advantage. For temperatures between 1144 and 1255°K, the cobalt base alloys are preferred, and, finally for temperatures between 1255 and 1500°K, the dispersion strengthened alloys appear to be the best choice.

Above this temperature coated refractory metals would have to be used. A typical distribution of metals on the Shuttle, based on temperature range of applicability, is presented in Figure 2-7.

During the Space Shuttle studies (Reference 1) a review was made of the most promising titanium, nickel, cobalt, and dispersion strengthened alloys to determine which alloy should be used on shuttle. The following topics were considered:

- Availability in thin sheet
- Thermal stability
- Fabrication
- Weldability
- Oxidation resistance
- Strength
- Creep resistance
- Cost to manufacture

Material properties for the nine alloys reviewed are presented in Table 2-1.

Based on the results of these studies (References 1 and 7) and the goals of this program, Ti-6Al-4V, in the annealed condition, was selected as the titanium alloy for evaluation. Another titanium alloy, Ti-6Al-2Sn-4Zr-2Mo, was also considered. The fabricability and thermal stability of Ti-6Al-4V and Ti-6Al-2Sn-4Zr-2Mo are the same. However, since Ti-6Al-4V has been in existence for over 10 years and was evaluated extensively for the Supersonic Transport (SST) program and for the Reference 1 studies, the data base for Ti-6Al-4V was greater than that for the newer alloy Ti-6Al-2Sn-4Zr-2Mo.

The nickel base alloy selected was Rene' 41. The basis for this selection was the fact that Rene' 41 was evaluated as full scale TPS panels in the Space Shuttle Supplementary Structural Test Program (SSTP), (Reference 2). In addition to panel evaluation, support components for the panels were designed, fabricated, and tested, to demonstrate their design feasibility and reuse capability.

MATERIAL	RANGE TEMPERATURE
RENE'41 (1172° AGED)	700°K–1144°K
L–605	1144°K–1255°K
TD–Ni–Cr	1255°K–1478°K
COLUMBIUM (FS–85)	1478°K–1644°K

RERADIATIVE TPS PANEL MATERIALS

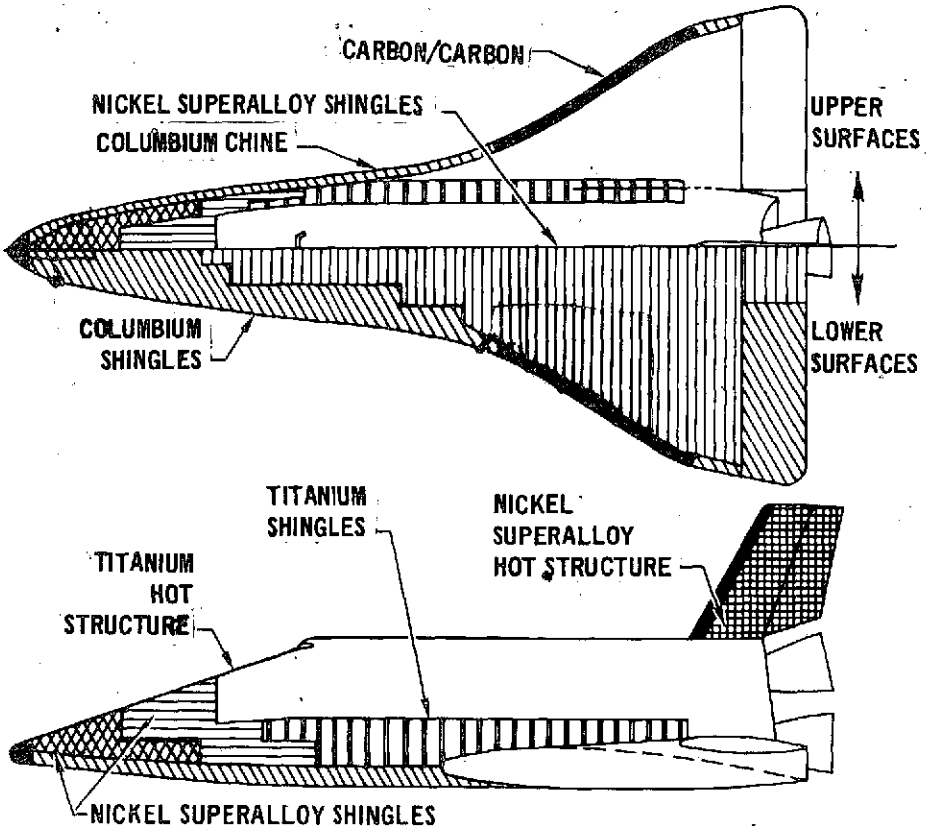

MATERIAL	AREA USED %	MATERIAL	AREA USED %
CARBON/CARBON	5.3	INCONEL 718–SHINGLES	2.42
COLUMBIUM (FS–85) SHINGLES	14.2	RENE'41–HOT STRUCTURE	4.65
HASTELLOY X SHINGLES	22.6	Ti SHINGLES	6.38
RENE'41–SHINGLES	2.15	Ti HOT STRUCTURE	42.3
		TOTAL	100.00

FIGURE 2–7 TYPICAL SHUTTLE METALLIC THERMAL PROTECTION SYSTEM

TABLE 2–1
MATERIAL PROPERTY COMPARISON

CLASS (TEMPERATURE USE RANGE °K)	MATERIAL	DENSITY $\rho \times 10^{-3}$ kg/m^3	ULTIMATE STRENGTH F_{TU} MPa (RT)	YIELD STRENGTH F_{TY} MPa (RT)	MODULUS E GPa (RT)
TITANIUM ALLOYS (590–811)	6Al–4V TITANIUM	4.43	1103	1000	110.3
	8Al–1 Mo–1V TITANIUM	4.37	1000	931	120.7
	6Al–2Sn–4Zr–2Mo (TRIPLEX ANNEALED) TITANIUM	4.54	1117	1027	110.3
NICKEL BASE SUPERALLOYS (811–1255)	RENE'41 (1394°K SOLN 1144°K AGE)	8.25	965	689	217.9
	HASTELLOY–X	8.22	758	345	197.2
	INCONEL 718	8.22	1241	1034	204.1
COBALT BASE SUPPERALLOYS (1144–1255)	L–605	9.13	896	365	235.8
	HAYNES 188	9.22	862	379	231.0
DISPERSION STRENGTHENED ALLOYS (1255–1500)	TD–Ni–Cr	8.44	689	448	140.7

There are a variety of heat treatments available for Rene' 41, each maximizing given property. For example, the 1339°K solution treatment, followed by an age at 1033°K, gives Rene' 41 the highest tensile strength compared to other Rene' 41 heat treatments but provides lower rupture strength than other heat treatments and limits reuse to below 1033°K (the aging temperature). For good stress-rupture strength, a solution treatment of 1450°K followed by an age at 1172°K is recommended. However, this heat treatment tends to increase the materials sensitivity to strain-age cracking during post weld heat treatments. A third heat treatment, which has reduced susceptibility to strain-age cracking, involves solution treating at 1394°K and aging at 1172°K. Creep properties achieved with the 1394°K solution closely approach the properties obtained with the 1450°K solution treatment and the material is not as crack sensitive (References 8 and 9). Because of the better crack resistance and dimensional stability, the 1394°K solution and the 1172°K age heat treatment was the heat treatment used on the Rene' 41 panels in the SSTP program and on in-house studies of cyclic creep, (References 2 and 4), and is the heat treatment selected for use on this program.

The cobalt base alloy selected was L605. This material was also used in fabrication and evaluation of full scale TPS panels in the Reference 2 program.

At the time of selection another cobalt base alloy, Haynes 188, was considered, which has properties similar to L605 but is more oxidation resistant above 1275°K than L605. It was not selected because there were no known large panel tests which could be analyzed in the third phase of this program.

A variety of dispersioned strengthened alloys exist ranging from the iron base alloys DH242 and GE1541, to the nickel base alloys Inconel 853, TDNiCr, and TDNiCrAl. However, above 1366°K only TDNiCr and TDNiCrAl possess the strength and oxidation resistance necessary for consideration in Space Shuttle TPS. TDNiCr was therefore selected because it has been developed to the point where it can be considered commercially available, and was also immediately available from an ongoing NASA

program (Reference 10).

In addition, a program to manufacture and test full scale TDNiCr panels (Reference 11) allowed data for prediction verification under Phase III of the program.

2.3 SURVEY OF LITERATURE

At the start of this program a search was performed to gather available creep data for thin gage sheet material, in order to establish a reference data base for the four alloys being studied. As part of this survey the following sources were consulted:

- NASA Scientific and Technical Information Facility.
- Defense Metals Information Center, Battelle Memorial Institute.
- McDonnell Douglas Research and Engineering Library.
- Material vendors, research laboratories, airframe and jet turbine manufacturers and others believed to be active in creep studies.

Fifty literature (Appendix B) sources out of approximately 600 dating from January 1962 to July 1972 were reviewed in detail.

This search revealed that most of the creep data was inadequate for establishing a data base. For example, much of the data was developed on rod and bar specimens rather than sheet or strip specimens. These data were rejected because the methods for manufacturing bar are different from those used to produce sheet.

There were, however, a few sources that presented enough detailed information, such as lot number, test direction, gauge, and plots or tabulation of strains vs time to establish a reasonable data base. These sources consisted of Reference (12) for Ti-6Al-4V, References (13) and (14) for Rene' 41, Reference (15) for L605, and References (16) to (21) for TDNiCr.

The Ti-6Al-4V reference contained data generated on sheet produced by two separate manufacturers and tested by two laboratories. One set of data was obtained from sheets 0.160 cm in thickness, manufactured by Mallory Sharon Titanium Company (now Reactive Metals Inc.) and tested by Joliet Metallurgical Laboratories. The second set of data was obtained from sheets 0.102 and 0.160 cm, manufactured by Titanium Metals Corporation of America (TIMET), and tested by Metcut Research Associates. These data were for approximately 120 creep tests at temperatures ranging from 589 to 811°K.

The heat treatment selected for Rene' 41 is relatively new (solution treat at 1394°K and age at 1172°K) and as a result the literature survey only produced two references. Reference (13) consisted of 10 creep tests performed on 0.127 cm thick material while Reference (14) contained 24 tests performed on 0.020 cm thick material. These two references had data for tests performed over the temperature range of 922 to 1255°K.

The reference for L605 (15) contained data from approximately 52 creep tests performed on sheet ranging in thickness from 0.013 to 0.203 cm in the temperature range of 922 to 1255°K.

TDNiCr had the largest number of sources available to establish a data base for a dispersion strengthened alloy (Reference 16 to 21). These references contained data performed on sheet ranging in thickness from .038 to .152 cm in the temperature range of 1033 to 1477°K.

2.4 PROCUREMENT OF MATERIALS

Past studies have shown that the weight of the TPS is dictated by minimum gage limits. Therefore, the baseline material gage selected for testing was thinnest sheet available of approximately .025 cm thickness (.025 for L605, .031 for titanium, .025 for TDNiCr, and .027 for Rene' 41). Thicker gage sheet (.064 for L605, .056 for titanium,

.051 for TDNiCr, and .054 for Rene' 41) was also obtained for each of the four alloys for use in comparison testing for gage effects and for application in TPS concept fabrication during Phase II.

To ensure that the material was representative of current technology, Rene' 41, L605, and Ti-6Al-4V sheet were procured to existing AMS or Military specifications. TDNiCr, not available commercially, was obtained from NASA. This material was produced for NASA's Lewis Research Center by Fansteel Inc., under NASA Contract NAS-3-13490. In addition, for each alloy, all material of the same gage was procured from one heat of material. This eliminated the possibility of chemistry and/or property variation in different heats of material from influencing the creep tests.

Summarized in Table 2-2 are the supplier certifications and purchase specifications of materials procured.

2.5 SELECTION OF CREEP SPECIMEN CONFIGURATION

Because both steady-state and cyclic testing were conducted on tensile specimens in this phase of the program, selection of specimen geometry required consideration of both types of test furnaces and measurement requirements. The same specimen geometry was used for both steady-state and cyclic tests to eliminate any possible variation in creep response due to specimen geometry.

The measurement of relative movement of scribe marks on a platinum slide rule attached to the creep test specimen is an accurate method applicable in steady-state testing where the furnace contains view-ports for continual readout of creep strains without distrubing the specimen. This approach does not require specimen tabs. However, in cyclic tests, where elastic loads are removed and reapplied, slide rule buckling or slippage can result in inaccurate creep measurements. For this type of testing the use of scribe marks on the specimen, read with a measuring microscope, are considered to provide a more reliable approach.

TABLE 2-2
SUPPLIER CERTIFICATION

ALLOY DESIGNATION	APPLICABLE SPECIFICATION	NOMINAL GAUGE (cm)	HEAT NO.	SUPPLIER	CHEMISTRY – % BY WEIGHT																			R. T. MECH. PROPERTIES				
					C	O	H	N	Al	Co	Cr	Fe	Mn	Mo	Ni	Ti	V	W	B	S	P	Si	ThO_2	F_{tu} MPa	F_{ty} MPa	E.LONG. %5.1cm	TEST DIR.	COND.
L605	AMS-5537	0.024	1860-2-1396	CABOT CORP	0.09	–	–	–	–	BAL	20.20	2.45	1.70	–	10.60	–	–	14.55	–	0.005	0.011	0.13	–	893.3	421.3	48%	T	A
L605	AMS-5537	0.064	1860-2-1399	CABOT CORP	0.09	–	–	–	–	BAL	19.95	2.30	1.25	–	10.55	–	–	14.50	– –	0.005	0.005	0.09	–	927.3	427.8	45%	T	A
RENE'41	AMS-5545	0.027	2490-0-8207	TELEDYNE-RODNEY	0.09	–	–	–	1.52	10.40	18.30	3.85	0.04	9.65	BAL	3.07	–	–	0.005	0.006	–	0.13	–	1144.5	710.2	32%	T	A
RENE'41	AMS-5545	0.051	2490-7-8279	TELEDYNE-RODNEY	0.08	–	–	–	1.50	11.48	19.05	0.24	0.01	9.87	BAL	3.15	–	–	0.005	0.003	–	0.07	–	–	–	–	–	A
Ti-6AL-4V	MIL-T-9046F TYPE 3 COMP C	0.031	N-0358	TIMET	0.026	0.100	0.009	0.011	6.0	–	–	0.06	–	–	–	BAL	4.0	–	–	–	–	–	–	1006.6 1013.5	910.1 923.9	10 10	T L	A
Ti-6AL-4V	MIL-T-9046F TYPE 3 COMP C	0.051	N-0263	TIMET	0.022	0.140	0.010	0.009	6.0	–	–	0.07	–	–	–	BAL	4.0	–	–	–	–	–	–	1006.6 1013.5	930.8 930.8	10 10	T L	A
TD-Ni-Cr	NONE	0.024	TC-3875	NASA	0.016	–	–	–	–	–	19.80	–	–	–	BAL	–	–	–	–	0.0057	–	–	1.94	766.2	547.1	16	T	A
TD-Ni-Cr	NONE	0.51	TC-3876	NASA	0.022	–	–	–	–	–	19.92	–	–	–	BAL	–	–	–	–	0.0051	–	–	1.96	887.4	592.5	20	T	A

A – ANNEALED
T – TRANSVERSE
L – LONGITUDINAL

To provide a location for the scribe marks, outside the specimen test zone, tabs were provided on the specimen as shown in Figure 2-8. Tabs were provided to eliminate possible adverse effects of locating the scribe marks in the test zone on the thin gage specimens. Holes were drilled in the tabs on Rene' 41, L605, and Ti-6Al-4V specimens in an initial effort to utilize holes as a reference point for creep strain measurements. Because scribe marks were subsequently used for this purpose, holes were not provided in TDNiCr specimens.

To investigate the effect that tabs and holes have on the stress distribution in the specimen test zone, both photoelastic and finite element analyses were performed. Results of the photoelastic analysis for a typical tab geometry are presented in Figure 2-9. Stress distributions, based on analyses of the fringe patterns,are shown along the free boundary where a uniaxial (tangent to the boundary) stress exists and across the specimen at the tab centerline where a biaxial stress state exists. Although the distribution across the specimen at the tab centerline is the difference in principal stresses, it approximates the longitudinal specimen stress distribution since stresses in the transverse direction are relatively small. A stress concentration factor of approximately 1.4 is shown to exist along the specimen boundary at the tab tangency point.

Finite element analysis was conducted using quadrilateral and triangular membrane plates to model the specimen for the NASTRAN Finite Element Computer Program. The resulting stress distribution based on this analysis is shown in Figure 2-10. Approximately seven percent of the specimen test zone area has greater than two percent variation from the uniform stress and approximately four percent of the specimen test zone area has greater than a five percent stress variation. The stress concentration factor of 1.4 at the tangent point of the specimen tab was substantiated in this analysis. Comparison of results for a specimen with a

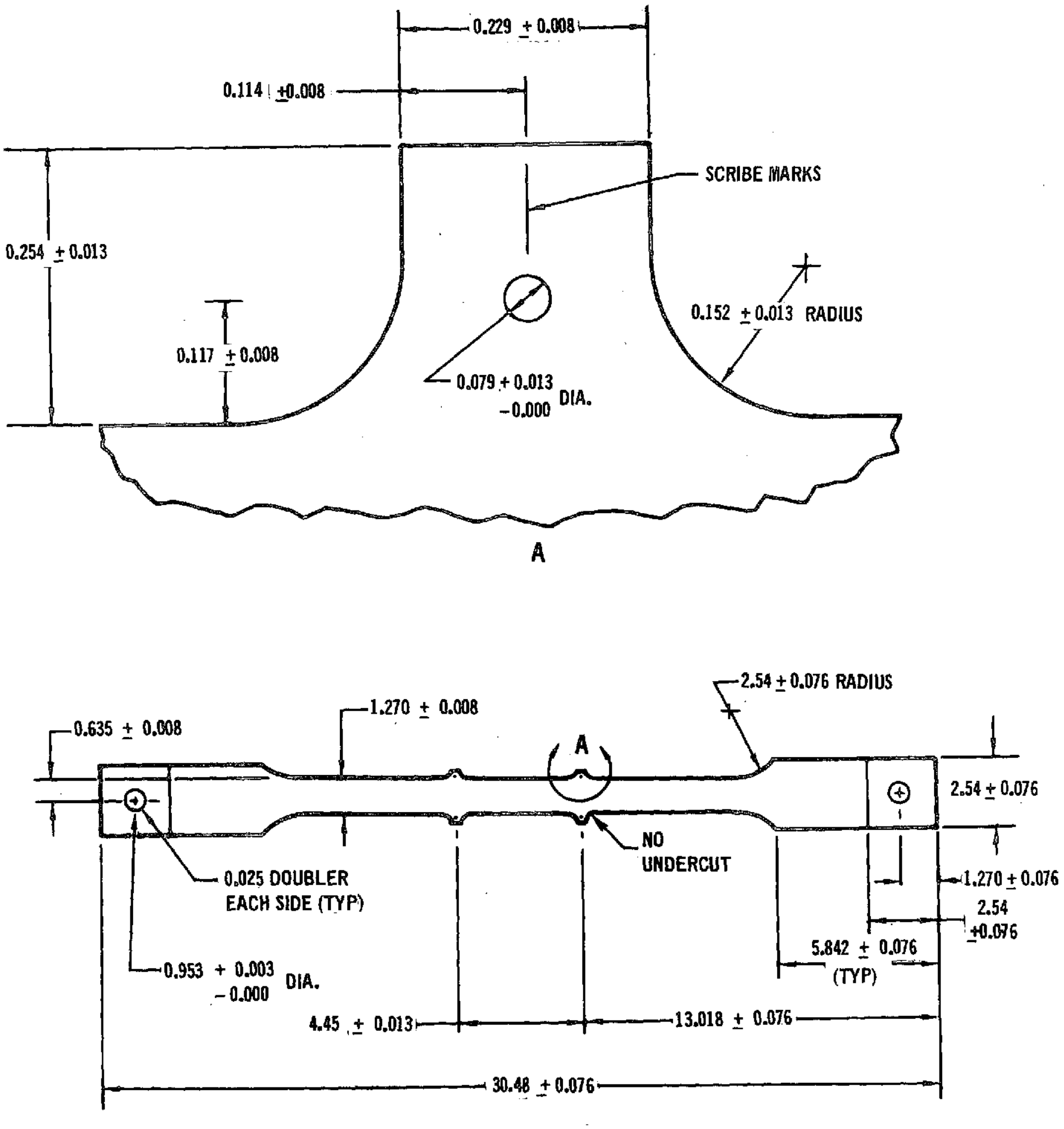

FIGURE 2-8 CREEP SPECIMEN GEOMETRY

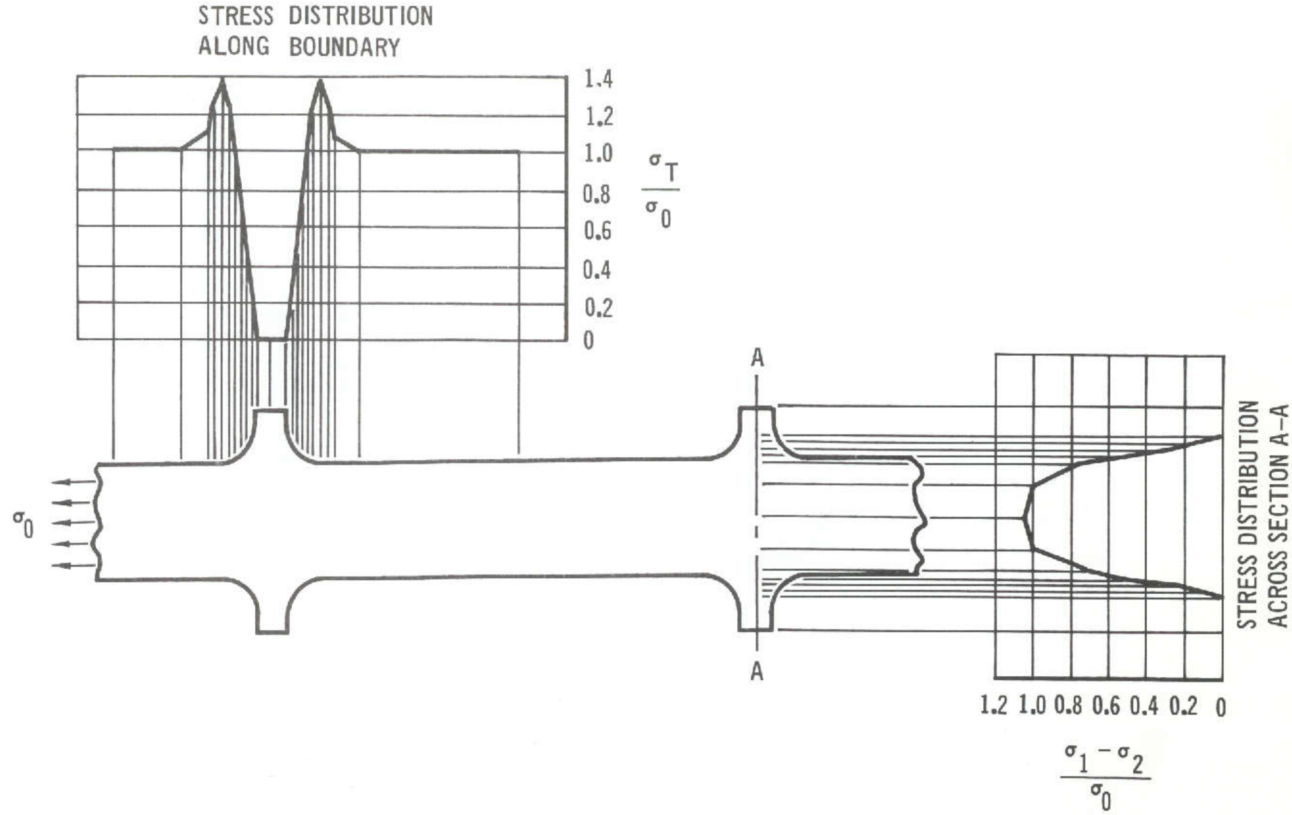

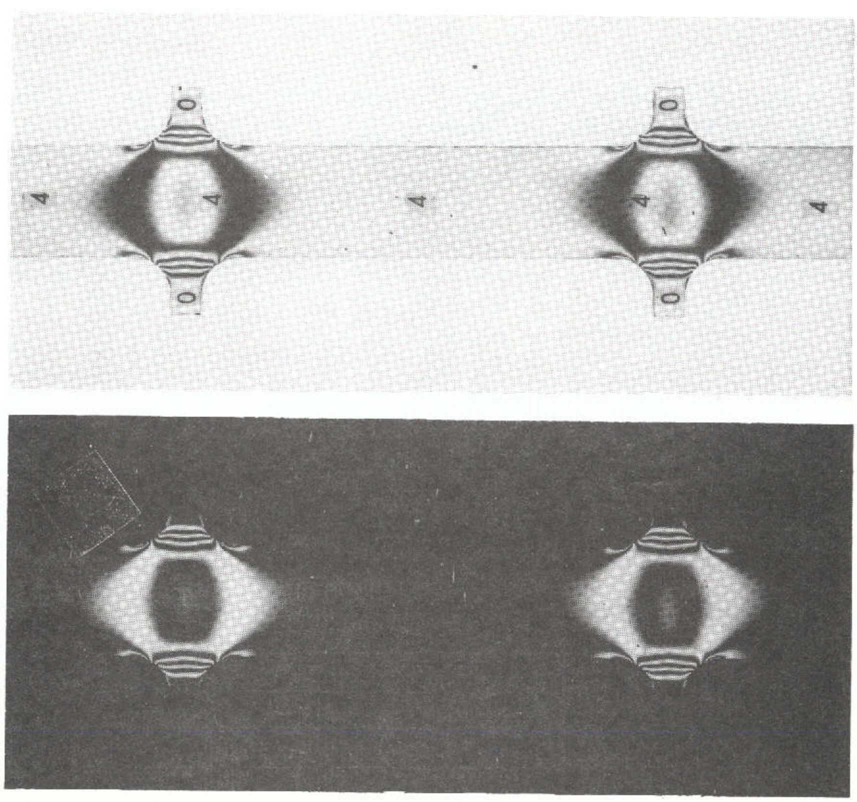

LIGHT FIELD
(LIGHT FRINGES ARE
INTEGRAL ORDER
n = 1, 2, 3 . . . .ETC.)

DARK FIELD
(LIGHT FRINGES ARE
1/2 ORDER n =
1/2, 1 1/2, 2 1/2. . .ETC)

FIGURE 2–9 TENSILE SPECIMEN PHOTOELASTIC ANALYSIS

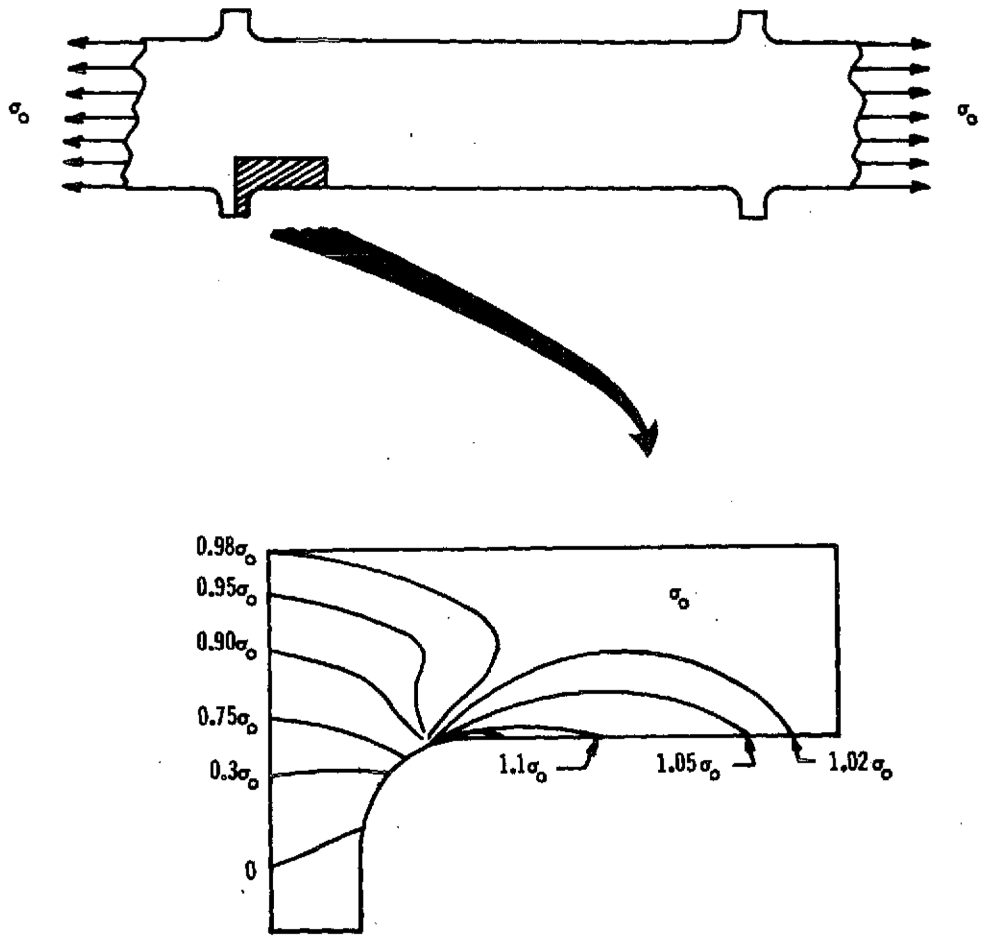

FIGURE 2-10 CREEP SPECIMEN STRESS DISTRIBUTION DETERMINED FROM FINITE ELEMENT ANALYSIS

hole in the tab with those for a specimen without the hole indicated that the hole (as defined in Figure 2-8) had a negligible effect on the resulting stress distribution.

The presence of the hole was shown to relieve the stress concentration factor due to the tab by impeding development of force gradients in the tab (Reference 22). However, for the geometry used, this effect was minimal (approximately 1%). Therefore, no further effort was made to optimize the hole location or size.

Minimizing tab width and tab fillet radius also reduces disturbances in the uniform stress distribution. The 0.229 cm tab width and 0.152 cm fillet radius used in the specimen design were considered minimums based on possibilities of bending the tab during handling.

The selected length of the specimens was 4.45 cm, which allowed creep measurements to be accomplished using a Unitron measuring microscope having a 5.08 cm field of travel. Doublers at the loading holes, shown in Figure 2-8, were provided to distribute bearing loads. Machining tolerances were based on McDonnell Douglas Standard tensile specimen design designated 6M118.

2.6 CREEP SPECIMEN MACHINING AND IDENTIFICATION

Prior to machining the tensile specimens, blanks were sheared from their respective sheets. These blanks which were 2.54 X 30.48 cm were then impression stamped at the ends with an identification code to insure proper specimen control. The code used is as follows. The first letter indicates the alloy, hence: L = L605, R = Rene' 41, T = Ti-6Al-4V, and TD = TDNiCr. The numbers start from 1 and identify an individual specimen. The last letter identifies the direction of rolling: L = longitudinal (parallel to the direction of rolling); T = transverse (normal to the direction of rolling). Therefore, specimen L50L is a L605 sheet specimen

number 50 that was taken from the longitudinal direction of the sheet. Specimens machined from the thicker gage sheet received the first ten numbers (01 thru 10) for each of the alloys.

After identification the strips were stacked and sandwiched between 2-2.54 cm thick aluminum plates (one pack per alloy). The packs were then drilled, bolted together, and machined to the dimensions shown in Figure 2-8. Specimen packs were separated after machining, individually deburred and the tab holes (reference Section 2.5) were drilled. An attempt was made to drill .040 cm tab holes. However, difficulty was encountered because the small drill could not be properly sharpened to cut through the superalloys without breakage. As a result, the hole diameter was increased to .079 cm. Doublers were spotwelded to specimens and specimens were cleaned and inspected to complete preparation for testing.

2.7 STEADY STATE TESTING PROCEDURES

2.7.1 TEST EQUIPMENT AND OPERATION

Steady-state tests were conducted using three Satec 7.62 cm (3 inch) diameter tube furnaces mounted on specially built creep frames. This test facility is shown in Figure 2-11.

2.7.1.1 Load Train. The creep frames were equipped with a self-aligning hemispherical seated bearing (Monoball) at the load support point, to minimize misalignment of the load train. The load train extended from the Monoball support through the furnace to a dead weight loading platform below the furnace. Test loads were provided by weight stacked on these platforms. The platform and weights were supported by a hydraulic jack which was slowly retracted to apply the load to the specimen.

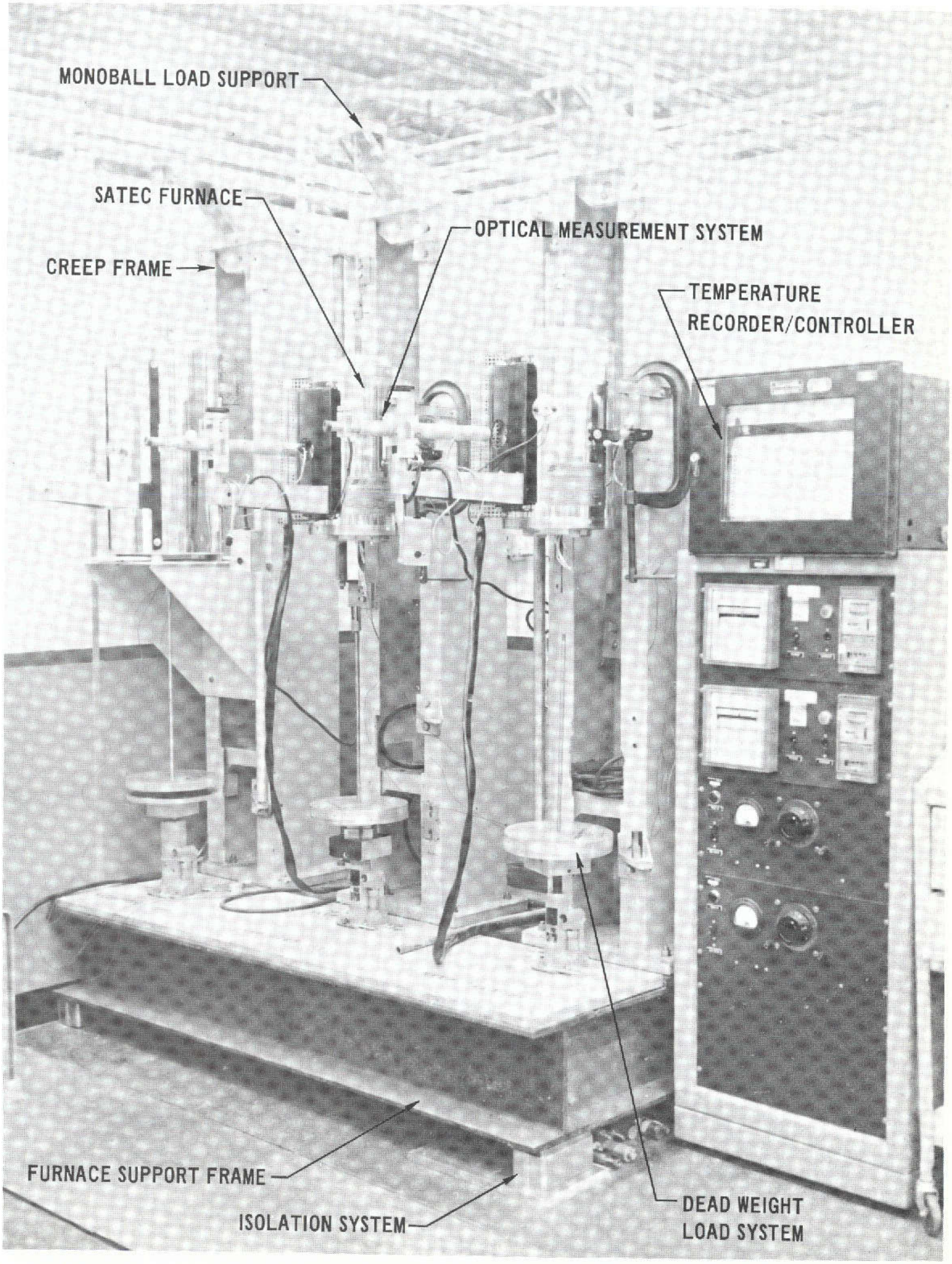

FIGURE 2–11 STEADY-STATE CREEP TEST FACILITY

2.7.1.2 Vibration Isolation. The creep frames were mounted on a support base as shown in Figure 2-11. In order to minimize possible vibration effects on the load train due to adjacent machinery, an isolation system was provided between this support base and the laboratory floor. This system consisted of MB Isomode vibration pads, piled to a compressed height of approximately 7 cm. Aluminum frames (boxes) were utilized to provide lateral support for the pads. Pad height was established to minimize response of the system. Seismometer readings taken showed that this system reduced response to approximately 34% of that without the system. Based on force transducer readings taken in the specimen load train, variations in applied load on the specimen caused by these vibrations was shown to be (<0.5%).

2.7.1.3 Optical Measuring System. Optical systems, for measuring strains, were mounted on brackets attached to the Satec Furnaces. Discussion of this system is presented in Section 2.7.2.

2.7.1.4 Temperature Measurement. Three Honeywell temperature recorders were used throughout steady state testing. A recorder having a range of 256°K (0°F) to 811°K (1000°F) was used in titanium testing and a recorder having a range of 922°K (1200°F) to 1255°K (1800°F) was used in L605 and Rene' 41 testing. Each of these two recorders was capable of recording temperatures to an accuracy of 0.5% of full scale deflection, (± 2.7°K and ± 1.7°K respectively). A third recorder having a range of 1089°K (1500°F) to 1642°K (2500°F) was used in testing TDNiCr specimens. This system (recorder, thermocouple and wire) was calibrated to within 2.8°K at the three nominal test temperatures utilized.

Chromel-alumel thermocouples were spot welded (at the center and at each end of the slide rule) on nichrome foil strips, which were in turn strapped to the

specimen (see Figure 2-12) to monitor temperature during testing. For each test the previous thermocouple bead was removed and a new bead and nichrome strip were made. In addition to the chromel-alumel thermocouples, Pt-Pt-10% Rh thermocouples were used for the TDNiCr tests.

2.7.2 STEADY STATE STRAIN MEASUREMENTS

Creep strains were observed through use of a 5.1 cm (2.0 inch gage length) precision formed polished, and scribed assembly spotwelded directly to the specimen as shown in Figure 2-12. Strains were obtained by measuring relative movements of scribe marks on the assembly. Initial attempts to use mechanical clamps for slide rule attachment resulted in some slipping under the clamps.

The optical system shown in Figure 2-13 was used to view the slide rule attached to the specimen suspended inside the furnace. This system was used to measure creep strains directly using an optical extensometer which incorporates a Gaertner filar micrometer microscope equipped with a 3.15 cm relay lens. Scribe marks on the platinum slide rule were located and the change in length recorded by moving cross-hairs controlled by micrometer slides on the microscope. The Gaertner filar micrometer microscope is capable of measuring length to 0.00005 cm. However, overall precision of the measurement system for creep strain was considered to be within ± .01% creep strain (e.g., 2% error on a creep strain of .5%, .490 to .510%) based on repeated measurements taken. This error includes variations in readings between different laboratory personnel.

Steady-state strain readings included elastic strains. These elastic strains were recorded at the beginning and completion of each test.

2.8 CYCLIC TESTING PROCEDURES

2.8.1 TEST EQUIPMENT AND OPERATION

2.8.1.1 Test Furnace. Cyclic tests were performed in the two 6.35 cm diameter

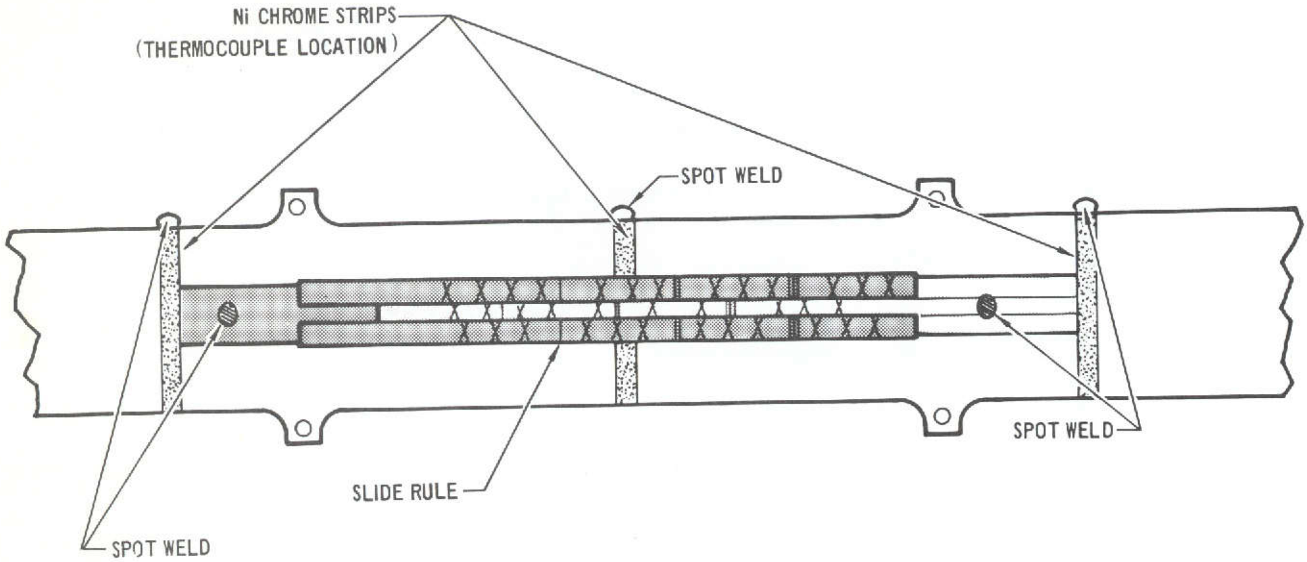

FIGURE 2-12 PLATINUM SLIDE RULE FOR STEADY-STATE CREEP MEASUREMENT

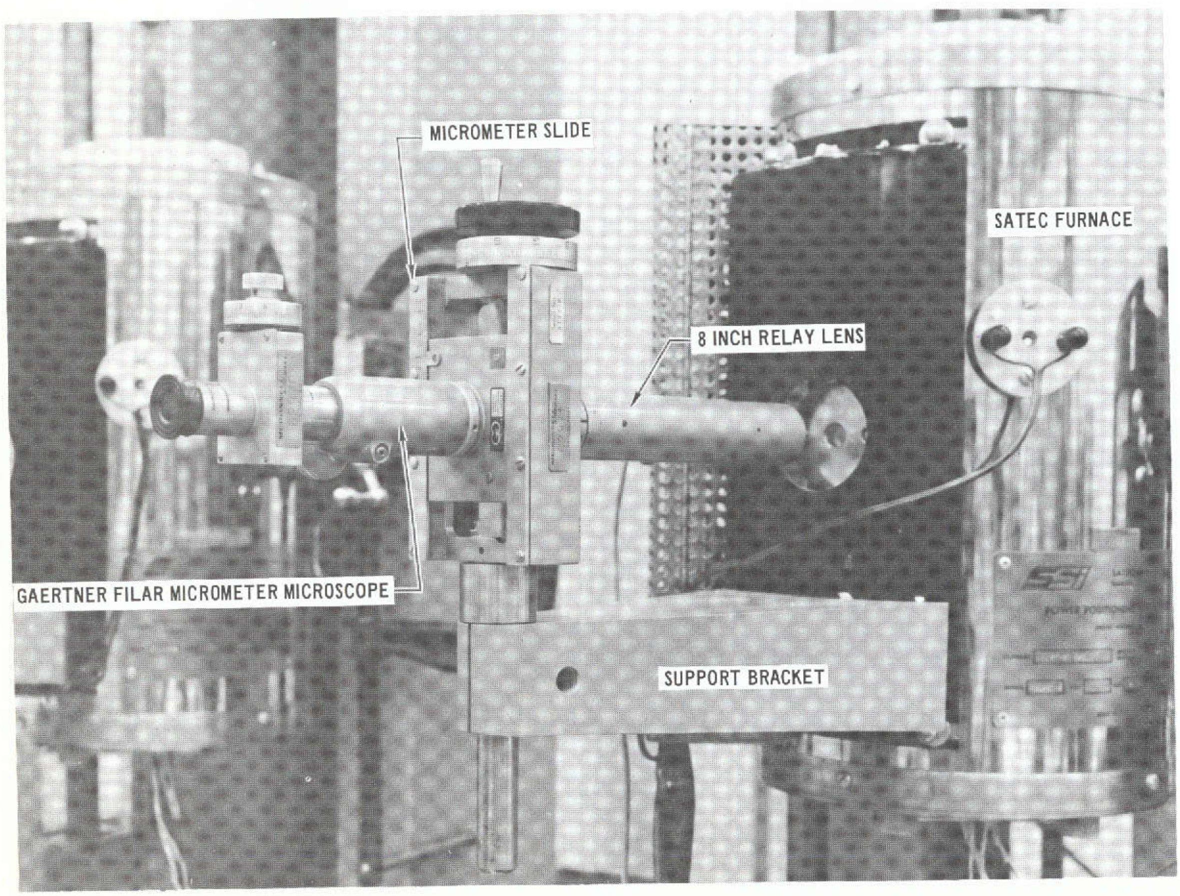

FIGURE 2-13 OPTICAL MEASURING SYSTEM FOR STEADY-STATE CREEP TESTING

furnaces shown in Figure 2-14. The upper part of each furnace contained a stainless steel extension assembly which houses the load dynamometers. A schematic diagram of the furnace test chamber is presented in Figure 2-15.

The furnace consists of a muffle tube which is heated by radiation from a resistance heated graphite element. A mullite tube was used in testing of Rene' 41, L605, and TDNiCr. Minimum test temperature for these materials was 977°K (1300°F). For testing titanium specimens at lower temperatures (660°K to 839°K) a stainless steel muffle tube was used. This was required to provide adequate temperature control in the furnace test zone at the low temperatures.

Water cooled jackets are provided at both ends of the furnace.

2.8.1.2 Furnace Extension Assembly. Each of the furnaces was modified by the addition of a stainless steel extension assembly to the furnace top. This assembly provided a housing for the load dynamometers. These dynamometers measure individual loads to each of three specimens in the furnace. Location of the dynamometers inside the furnace system reduced the possibility of load measurement errors which could have been caused by friction at the seal and load rod interface had the dynamometers been outside the furnace.

A series of radiation shields were positioned between the dynamometers and the furnace to minimize heat transfer from the furnace.

Thermocouples on the dynamometers were monitored during testing to verify that they remained within the calibration temperature range during test.

2.8.1.3 Whiffle-Tree Load Fixture. In order to test a large number of specimens at a reasonable cost, a whiffle tree load fixture was designed for use in the furnaces. This fixture is shown in the schematic diagram of Figure 2-15. The mechanism consists of two sets of loading pins and clevis fittings which serve as load dividers. In this manner the applied load is divided into three separate loads so that three specimens can be tested, at three different load levels, during

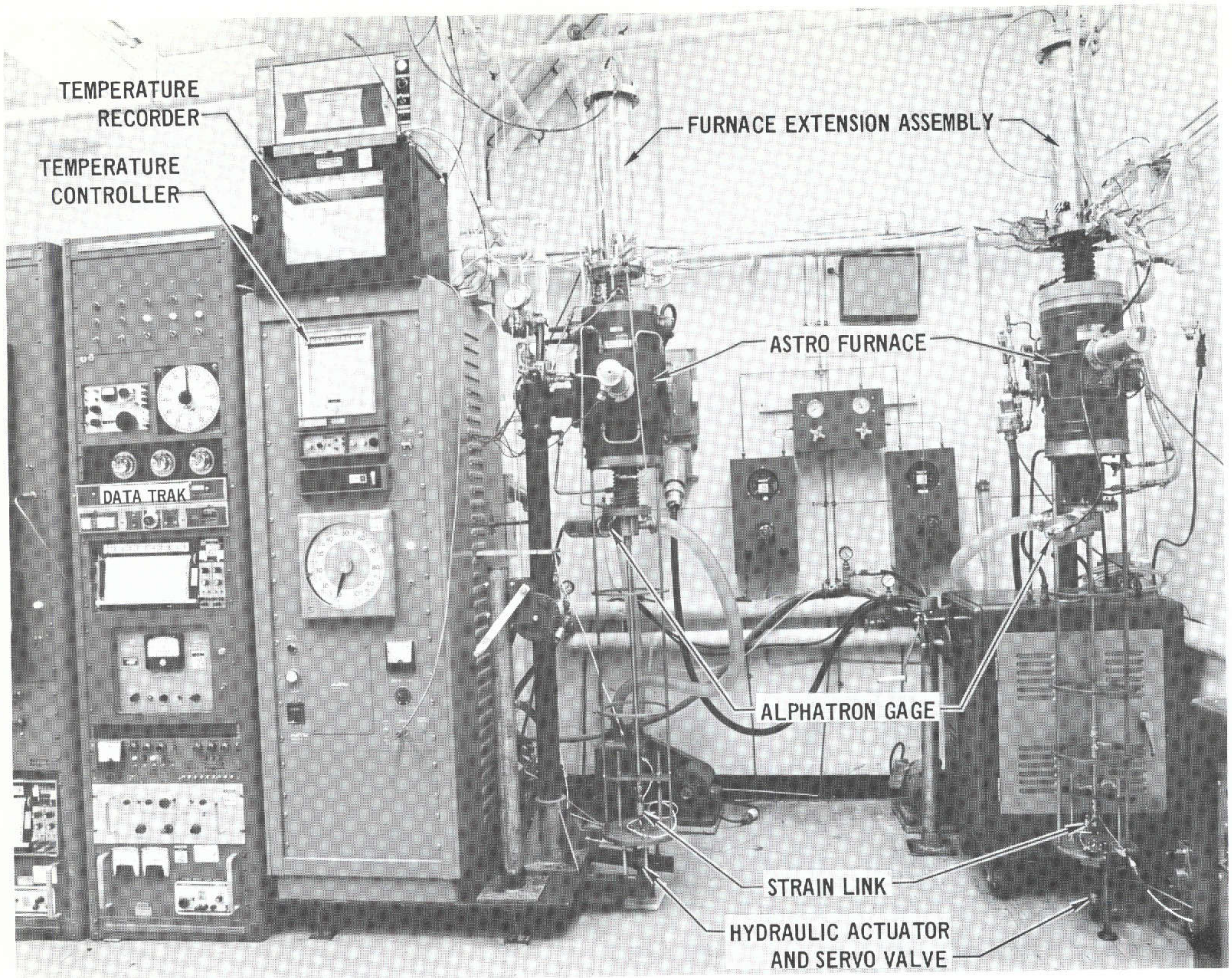

FIGURE 2–14 ASTROFURNACE CYCLIC TEST FACILITY

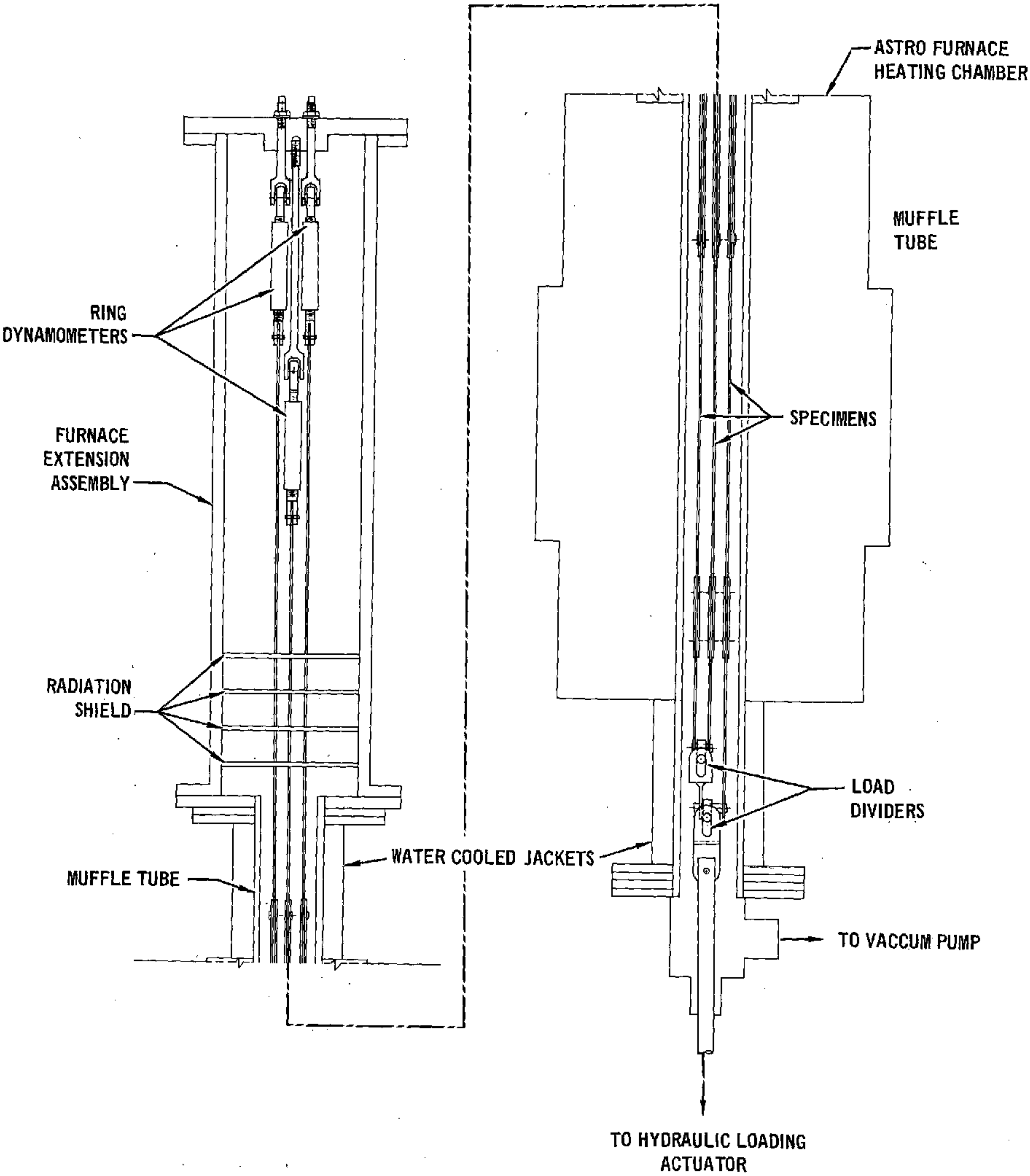

FIGURE 2-15 SCHEMATIC OF FURNACE TEST CHAMBER

a single furnace run. Two specimens can be tested during a single furnace run, if desired, by utilizing only one set of fittings.

Figure 2-16 shows a close-up of the pin and clevis fittings and their relationship to the specimens. By providing several pin fittings with different strap (specimen) attachment locations, several different load ratios were attained for use as required in the various tests. The following ratios were used:

1/1.66/2.58
1/1.23/1.44
1/1.37/1.75
1/1.47/1.94
1/1.78/2.00

Variation in specimen loads due to differential specimen strains was found to be negligible. Adjustment nuts were provided at the top of the furnace to allow initial alignment of the loading pins. Loads on each specimen were measured separately by the three load dynamometers provided at the top of the furnace extension assembly (reference Section 2.8.1.2).

The pin and clevis fittings were made from PH13-8Mo stainless steel alloy. Loading straps and specimen attachment pins were TDNiCr. A factor of safety of 2.10 with a limit load of 45.4 kg per specimen was used in designing the whiffle tree and related load train components.

2.8.1.4 Load Measurements. A 1.27 cm diameter stainless steel rod was connected to the load divider (whiffle tree) mechanism. This rod passed through an "O" ring vacuum seal and out through the bottom of the furnace where it was connected to a load cell through a clevis and Monoball. The load cell was connected to a hydraulic actuator through a second set of clevis and monoballs. Coupled to the actuator was a hydraulic servo valve. This provided a closed loop load control system with the electronic load controller. Load profiles were programmed into a time based analog programmer (Data Trak) which

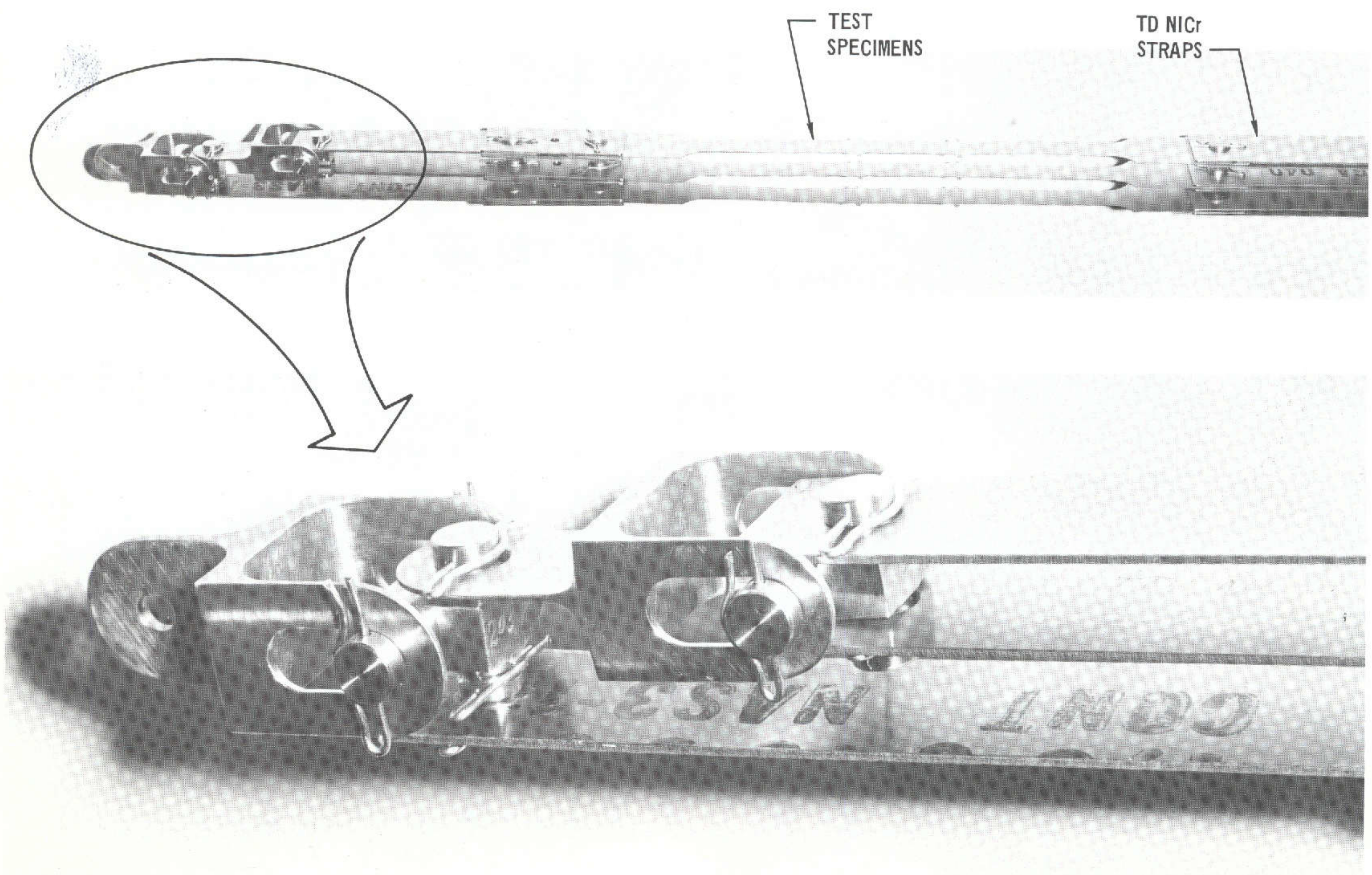

FIGURE 2–16 WHIFFLE TREE MECHANISM FOR CYCLIC TESTING

sent an electronic signal to the load controller which compared the signal to the output of the load cell. Variations between the two signals caused the servo valve to open or close, as required, to adjust the actual load to that of the programmed load.

Data acquisition during the cyclic creep testing was obtained from a specially designed digital data acquisition system. This system contained 50 channels which were scanned every 50 seconds. The accuracy of this system is ± 0.15%. The system recorded the data on tape, and also contained an 8-character digital printer which could be used to check the taped data. During testing the digital acquisition system recorded the outputs from the ring dynamometers and thermocouple positioned on the dynamometers. Control equipment is shown in Figure 2-17.

A Scientific Control Corporation Digital Computer (SCC-670-2) was programmed to calculate mean loads and standard deviations from the cassette tape data. A portion of a typical load profile, as recorded on a strip recorder, is shown in Figure 2-18. Load plots were offset on the time scale to facilitate reading of the data and eliminate any confusion between plots. Load data printout obtained from the digital acquisition system for other typical load cycles on 3 simultaneously tested specimens were as follows:

Cycle No.	Load Specimen 1		Load Specimen 2		Load Specimen 3		Total (Load)	
	MEAN	SIGMA	MEAN	SIGMA	MEAN	SIGMA	MEAN	SIGMA
72	44.660	0.108	53.733	0.269	34.948	0.081	134.762	0.179
73	44.681	0.134	53.523	0.278	34.878	0.109	134.546	0.358
74	44.866	0.094	53.528	0.245	34.974	0.091	134.843	0.255
75	44.867	0.074	53.616	0.302	35.089	0.086	134.616	0.378
76	44.784	0.125	53.485	0.226	35.040	0.091	134.654	0.315
77	45.013	0.102	53.530	0.256	35.167	0.084	134.789	0.243
78	44.894	0.068	53.547	0.295	35.162	0.066	134.924	0.235
79	44.942	0.055	53.564	0.273	35.182	0.048	134.951	0.124
80	45.032	0.074	53.706	0.255	35.301	0.034	135.085	0.160
81	45.073	0.090	53.723	0.226	35.342	0.072	135.003	0.274
82	44.795	0.079	53.273	0.267	35.113	0.057	134.735	0.277
83	44.768	0.090	53.453	0.288	35.208	0.049	134.750	0.258
OVERALL	45.650	0.083	54.310	0.286	35.696	0.075	134.847	0.267

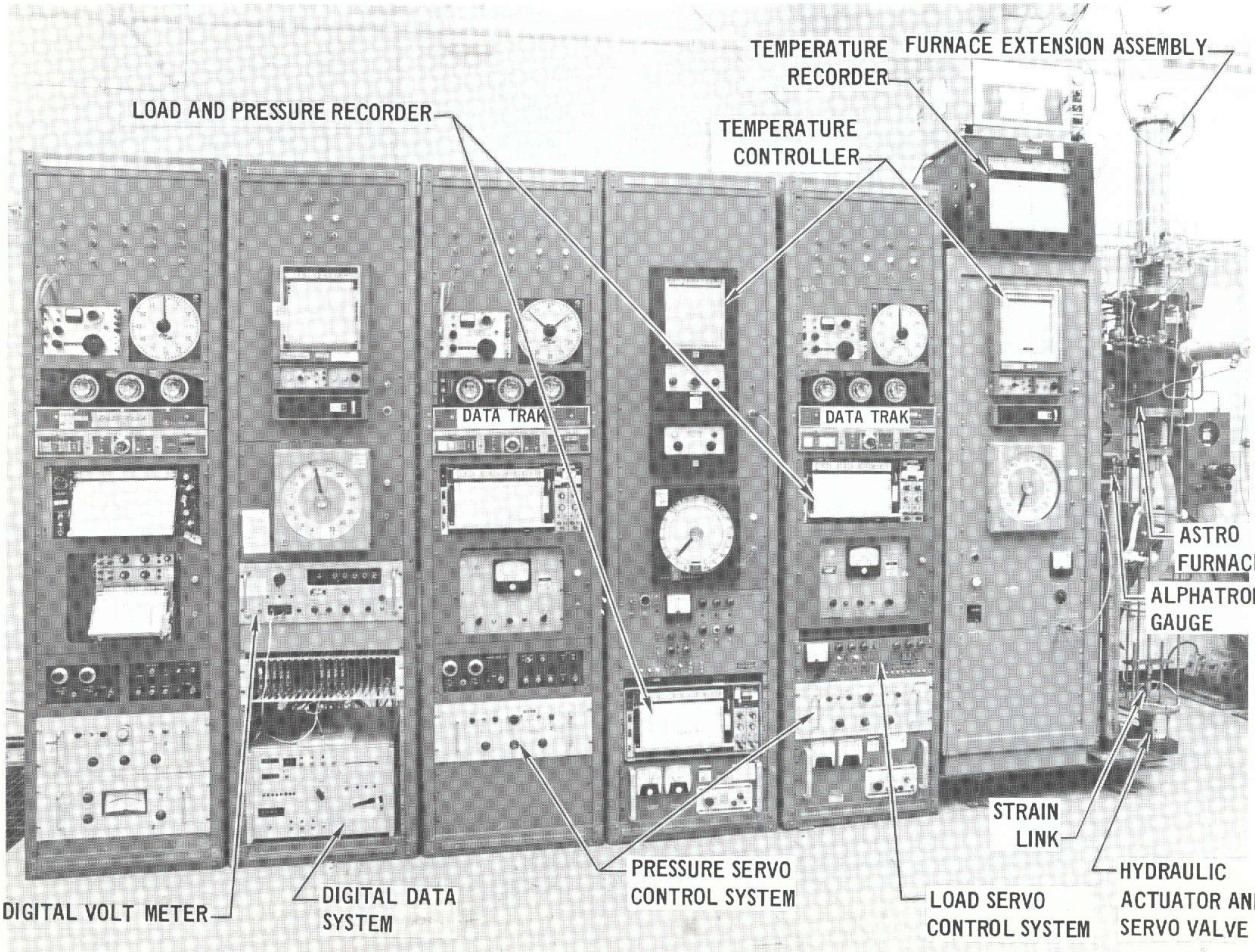

FIGURE 2-17 ASTROFURNACE CONTROL EQUIPMENT

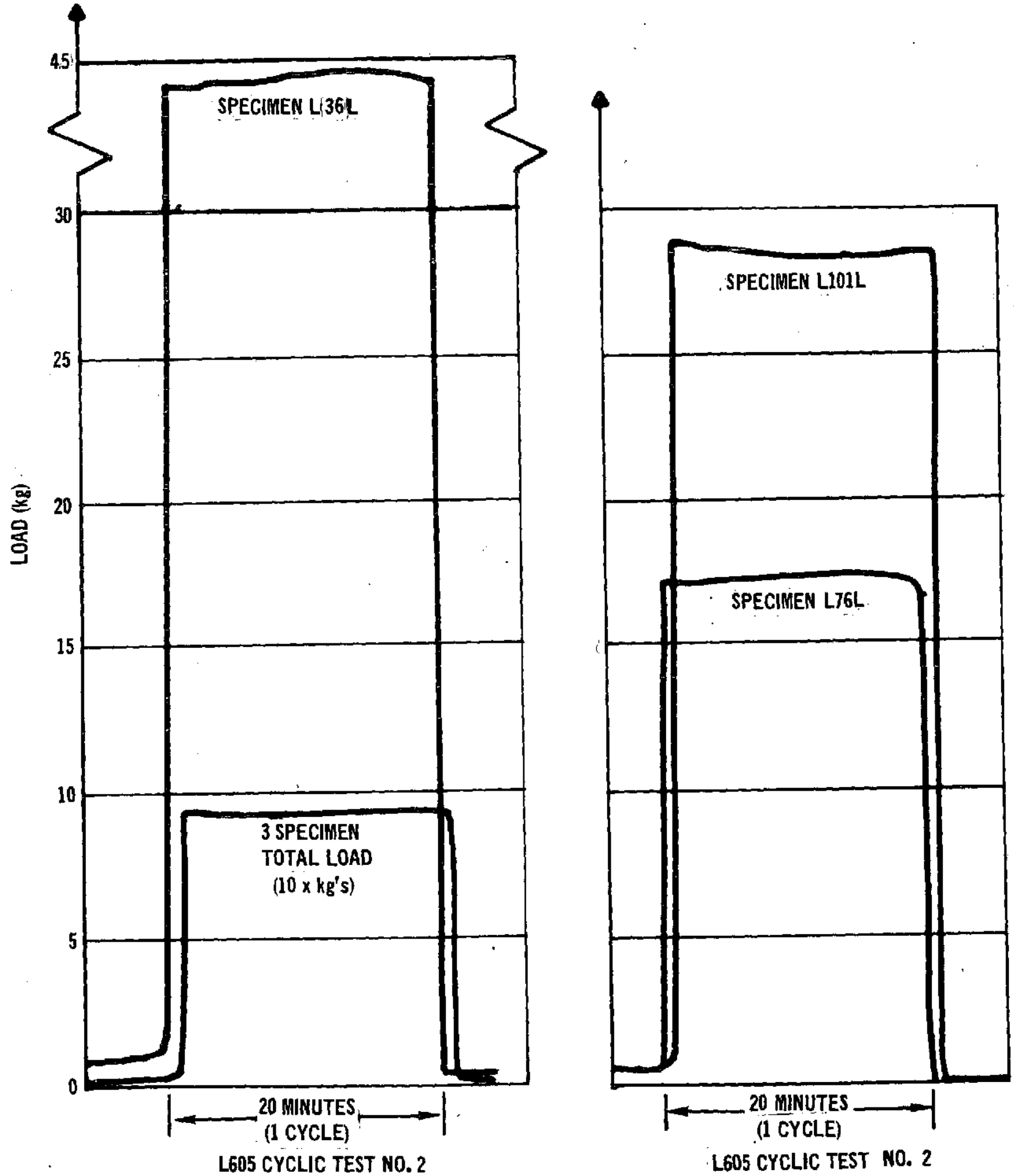

FIGURE 2-18 TYPICAL LOAD PROFILES OBTAINED IN CYCLIC TESTS

The mean value of load for each cycle was based on recorded loads at 50 second intervals across the test profile. An overall mean load and standard were calculated based on the mean values for each cycle. Average stress-time profiles for actual trajectory stress history tests were obtained by data averaging loads at common times in each cycle over the duration of the test. A load of approximately two percent of maximum load was maintained throughout each cycle to prevent slack in the whiffle tree mechanism.

2.8.1.5 Temperature Measurement. Within the hot zone of the furnace were two platinum-platinum-10% rhodium thermocouples. One of these thermocouples was used to measure the temperature within the hot zone, while the other controlled the furnace. Both of these thermocouples were connected to a thermocouple reference junction compensator, which maintained a constant reference to within 0.14°K. From this compensator the output of the measuring thermocouple was fed to a Honeywell strip chart recorder (Model #15, 30.48 cm. scale). Prior to testing the temperature recording system which included thermocouples, reference junction, and Honeywell strip recorder was calibrated and found to be accurate to within 1.7°K.

The output from the control thermocouple was fed from the reference junction to a Leeds and Northrup recorder/controller. This controller compared the electrical signal from the controlling thermocouple to one that was previously programmed into the Data Trak and adjusted the power input to the furnace to compensate for the differences in signal. The temperature control was found to be capable of controlling to within 1% of the desired temperature.

Prior to cyclic testing, calibrations were conducted to determine the magnitude of temperature variations on the specimens. Calibrations were accomplished using platinum/platinum-10% rhodium thermocouples spotwelded at the upper tab (location #1 Table 2-3) and at the lower tabs (location #3, Table 2-3). Testing was performed under a constant pressure of 1.33 Pa and temperature measurements were made immediately

TABLE 2-3

DETERMINATION OF TEMPERATURE GRADIENT IN CYCLIC TEST FURNACE

TEST	THERMOCOUPLE LOCATION	TARGET TEMP°K	CONTROL THERMO COUPLE-°K	SPECIMEN LOCATION AND TEMP.°K			MUFFLE TUBE MATERIAL
				SPECIMEN 1 (LEFT)	SPECIMEN 2 (CENTER)	SPECIMEN 3 (RIGHT)	
A	1 2 3	658	653	658 667 670	657 666 669	660 669 671	STAINLESS STEEL
B	1 2 3	714	718	710 718 721	708 716 719	711 720 723	STAINLESS STEEL
C	1 2 3	783	774	775 783 785	773 781 783	776 784 786	STAINLESS STEEL
D	1 2 3	839	832	831 839 841	829 836 839	832 840 842	STAINLESS STEEL
E	1 2 3	1033	1035	1033 1041 1040	1030 1039 1038	1033 1041 1039	MULLITE
F	1 2 3	1255	1257	1253 1262 1261	1249 1259 1258	1253 1262 1260	MULLITE

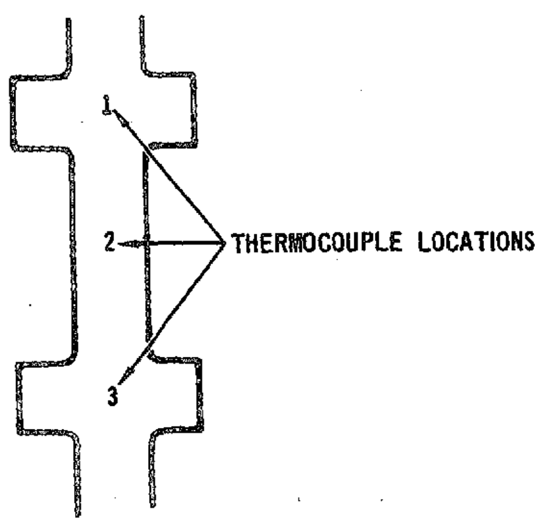

after the furnace stabilized at the set temperature. In the test the control thermocouple was located in the center part of the furnace in the same region as the #2 thermocouple. This allowed a direct comparison between the control thermocouple and the #2 thermocouple on the specimen.

Results of these calibrations are presented in Table 2-3. It can be seen that a 12°K maximum (∿2%) gradient existed within the specimen gage length (Test A and B). The maximum gradient from specimen to specimen was 4°K (Test B, D, and F). Variation between the control thermocouple reading and the center specimen temperature was less than 7°K for all tests except for test A where a 13°K variation was found. The general trend of these results is that temperature variations are reduced as test temperature is increased.

In addition to variations between the control thermocouple and the specimen temperature some variation from the planned temperature occurred as a function of time in each cycle. A typical result of calibrations made to measure this is shown in Figure 2-19. For a flat temperature profile at 1144°K (1600°F), variations of ± 6°K were observed.

2.8.1.6 <u>Pressure Measurement</u>. Pressure within the test chamber was controlled by a regulated leak rate operated by a servo-valve coupled to an Alphatron Vacuum gage (Model 530). The Alphatron gage sent an electrical signal to a Gran-Phillips automatic controller (series 213). The controller compared the signal from the Alphatron with that programmed on the Data Trak. The controller actuated the servo valve as required to control the air pressure. Control equipment is shown in Figure 2-17.

Some manual control of a bleed valve was necessary in the testing of specimens to an actual pressure profile (pressure variation from 1.33 Pa to one atmosphere). In these profiles the controller maintained a programmed change in pressure from 1.33 to 66.5 Pa.

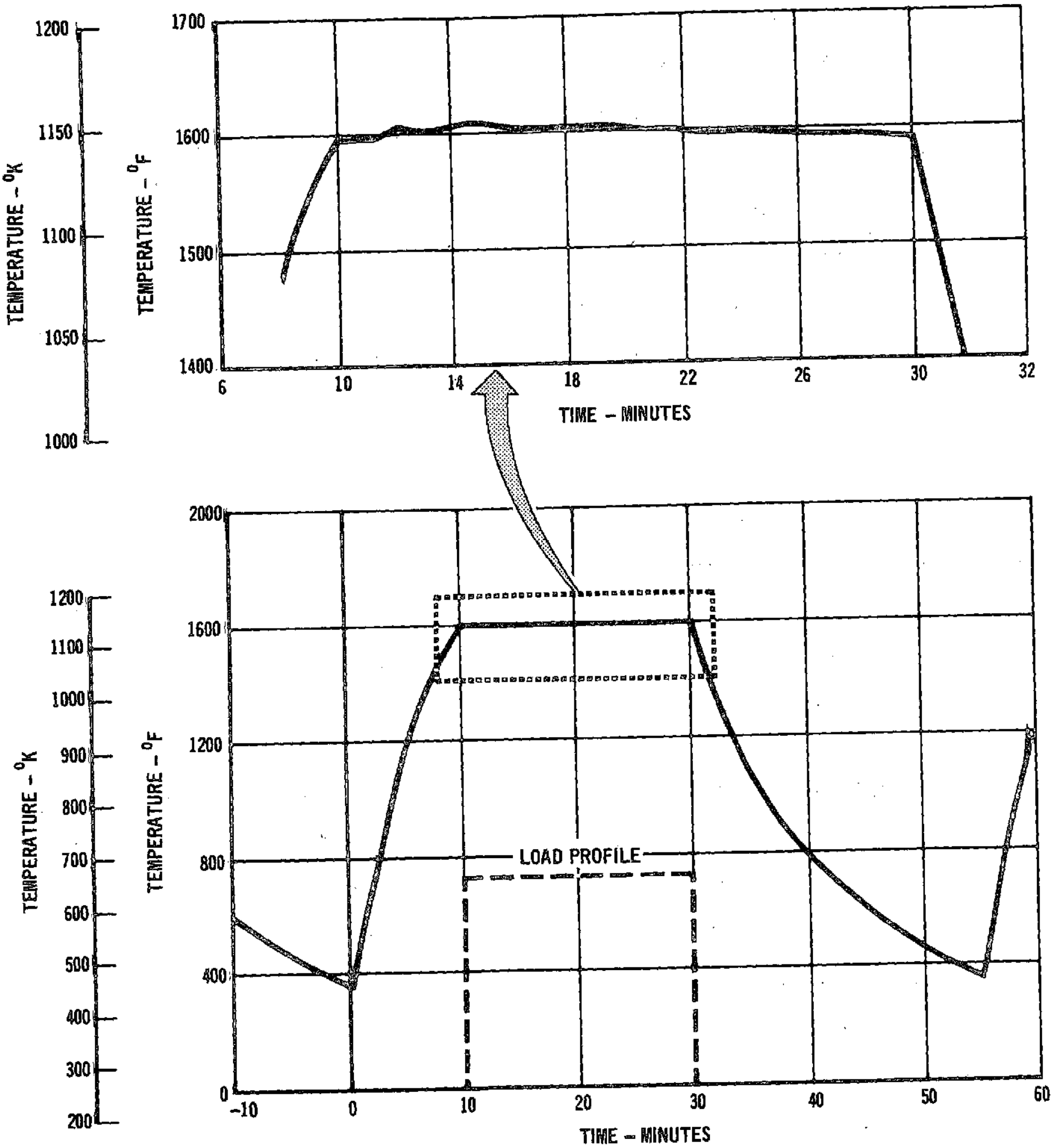

FIGURE 2-19 TYPICAL TEMPERATURE PROFILE OBTAINED IN CYCLIC TESTS

At that point the operatore changed scales and the controller continued the program from 66.5 to 2666 Pa. Beyond this point the vacuum pump was shut off and the pressure was allowed to stabilize at atmospheric pressure.

2.8.1.7 Cyclic Creep Strain Measurements. The cumulative creep strain of each specimen was measured after 1, 5, 15, 25, 50, 75, and 100 cycles (variations of this was made in some cases. See specific test data). To make the creep strain measurements, specimens were removed from the furnace. This was accomplished by separating the furnace extension assembly from the top of the furnace (see Section 2.8.1.2) and raising the assembly until the specimens were above the furnace.

The distances between the scribe marks on both sides of the specimen were determined by using a Unitron Measuring Microscope as shown in Figure 2-20. This scope is capable of measuring to within ± 0.00025 cm. However, actual precision in measurements based upon multiple measurements by several operators on the same creep specimens was found to be ± .00051 cm.

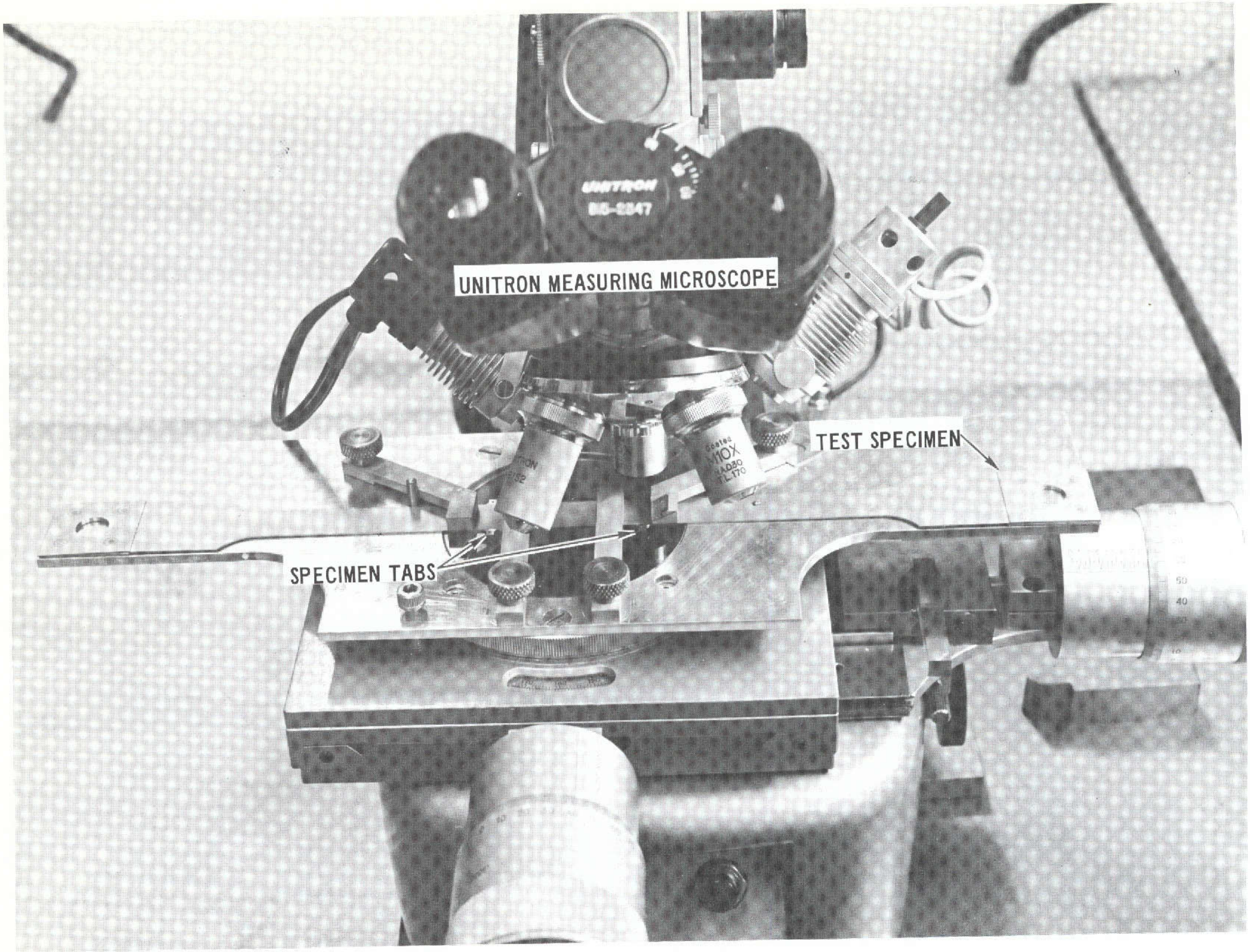

FIGURE 2-20 CYCLIC CREEP STRAIN MEASURING SYSTEM

2.9 DATA REQUIREMENTS AND TEST SELECTION

The approach toward selecting test conditions and types of tests for supplemental steady-state testing and cyclic testing, is presented in this section.

2.9.1 SUPPLEMENTAL STEADY-STATE TESTING

2.9.1.1 Data Requirements. The original intent of the supplemental steady-state creep tests was to use these tests to supplement the literature survey data base, and demonstrate that the material being studied was representative of that data base. The test matrix was established so that the resulting data could independently serve as the basis of an empirical equation for comparison with cyclic test results. In addition, a minimum number of tests for each alloy were planned for evaluation of the effects of material thickness and material rolling direction on creep response.

2.9.1.2 Selection of Conditions for Supplemental Steady-State Tests. Initially, several experimental designs were examined in an effort to identify combinations of test temperature and stress which would provide maximum useful data. The studies were based on the L605 equation developed from the literature survey (Reference Section 3.1.2).

$$\ln\varepsilon = 4.84599 + 2.12288 \ln \sigma + .48945 \ln t - .29601 \ln\phi - 19.50143(1/T) \quad (2\text{-}1)$$

where ε = creep strain, %

t = time, hours

σ = stress, MP_a

ϕ = material thickness, cm

T = temperature, °K

In this effort to obtain an experimental design, the following requirements as presented in Section 2.9.1.1 were considered.

(1) Test data should be amenable to development of an empirical creep strain equation. Applicability of each design for satisfying this requirement was checked by generating simulated creep strain data using equation 2-1, performing regression analyses, and evaluating the resulting prediction equation.

(2) Test temperatures should cover the ranges of interest for the material being tested.

(3) Test temperatures and stress levels should produce creep strains in the range of interest for metallic TPS. Maximum and minimum levels of creep strain considered reasonable for supplemental steady-state tests were .50% in 50 hours and .06% in 200 hours, respectively.

Some of the designs considered are presented in Figure 2-21. These designs include the simple 3 x 3 factorial design and an orthogonal composite design, described in References 23 and 24, and shown in Figures 2-21(a) and 2-21(b), respectively. While each of these designs satisfies the first requirement ((1) above), they do not satisfy the second or third requirement. This is evident from the figure since even for the narrow temperature range of 1089° to 1200°K and the stress range of 13.8 to 69 MPa, creep strains as low as .022% in 200 hours (13.8 MPa @ 1089°K) and as high as .6% in 6 hours (69 MPa @ 1200°K) result. These values are outside of the range of interest.

In addition to these two designs, the design shown in Figure 2-21(c) was considered because it provides a maximum coverage of the test temperature and stress range of interest for L605. Analysis of the simulated data using regression techniques, however, demonstrated that the resulting prediction equation based on this design was a function of time only.

A fourth design considered is a compromise between the other three. This design, shown in Figure 2-21(d) allowed testing over the temperature range of 978°K to 1255°K

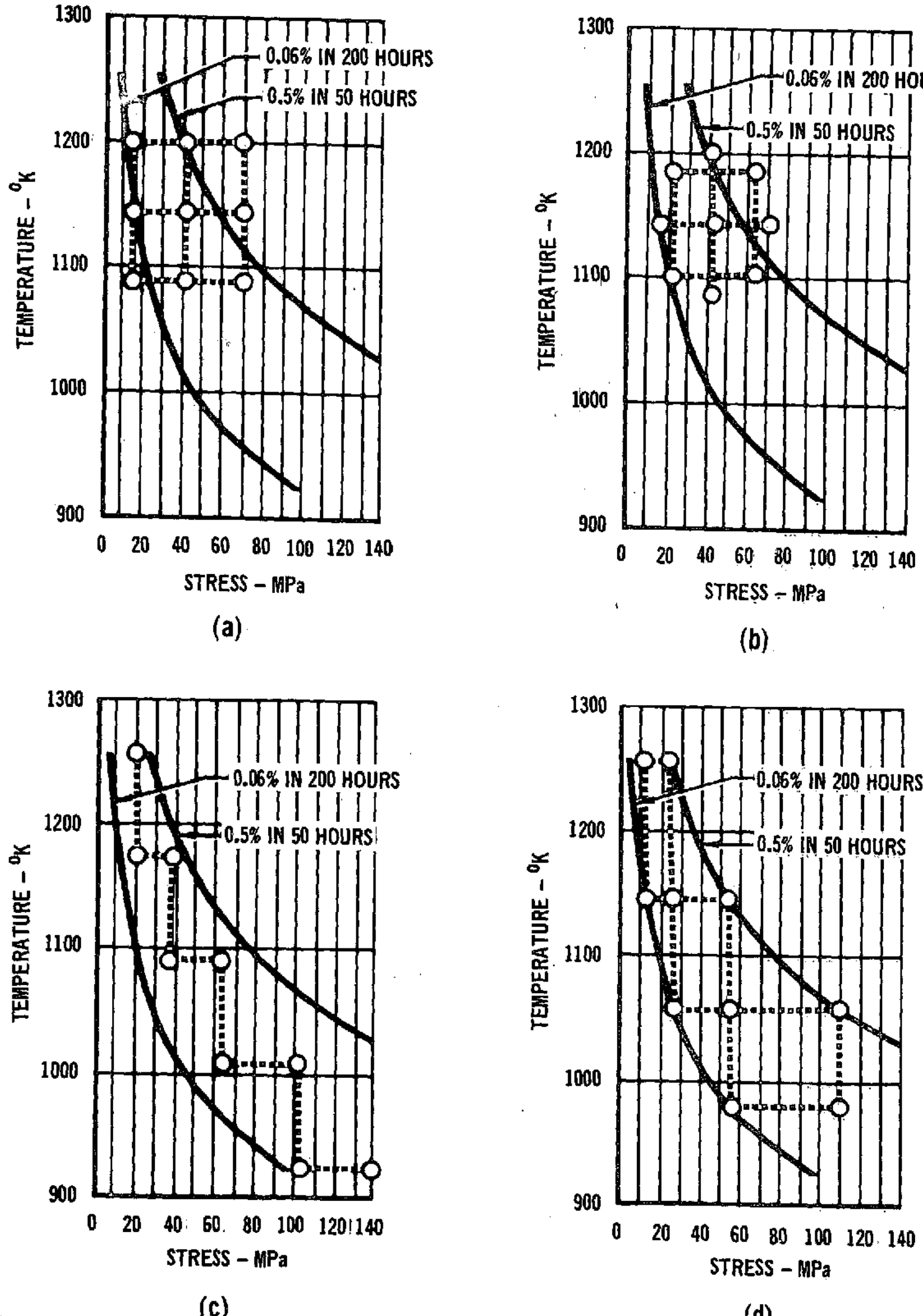

FIGURE 2–21 SUPPLEMENTAL STEADY-STATE EXPERIMENTAL DESIGNS

and stress range of 13.8 to 110.3 MPa. Values of temperature and stress were selected to be equally spaced in the variables log stress and 1/T (note form in Equation 2-1). This allowed for spacing of tests throughout the strain range of interest as well as the temperature and stress range. Study of this design using simulated data and regression techniques indicated that an empirical equation could be derived from the resulting test data. Therefore, due to the applicability of this design to regression analysis and its utilization of a relatively wide range of temperature and stress levels, this experimental design was used in the selection of supplemental steady state creep tests for L605, Titanium, and TDNiCr alloys. In the case of Rene' 41, the orthogonal composite design (Figure 2-21(b)) was used, based on a larger spread in the applicable creep range (see Section 3.3.2). Resulting test conditions for the basic matrix of supplemental steady-state tests are presented in Table 2-4. These tests were conducted using thin gage specimens tested in the longitudinal direction. To be consistent with the data base, L605, Titanium, and TDNiCr specimens were tested in the as-received condition and Rene' 41 specimens were tested with a heat oxidation coating obtained during the heat treat process (solution treating in air at 1394°K followed by aging in air for 4 hours at 1172°K). Some variations and additions were made to the test matrix in the case of Rene' 41 and TDNiCr. Additional discussion on test conditions for each of the alloys is presented in Section 3.

2.9.1.3 Selection of Tests for Evaluation of Other Variables. In addition to tests on thin gage material specimens in the longitudinal rolling directions as specified in Table 2-4, some tests were performed on each material to examine how material thickness and rolling direction effect creep.

In addition, for L605, the effect of an emittance coating on creep was briefly examined because panels will be coated to enhance emittance, which is essential for the efficient radiation of aerodynamic heat.

TABLE 2–4
SUPPLEMENTAL STEADY-STATE CREEP TESTS – BASIC MATRIX

TEST NO.	TEST[1] DIRECTION	L605 NOMINAL THICKNESS cm	L605 TEMP °K	L605 STRESS MPa	Ti-6Al-4V NOMINAL THICKNESS cm	Ti-6Al-4V TEMP °K	Ti-6Al-4V STRESS MPa	RENE '41[3] NOMINAL THICKNESS cm	RENE '41[3] TEMP °K	RENE '41[3] STRESS MPa	TDNiCr NOMINAL THICKNESS cm	TDNiCr TEMP °K	TDNiCr STRESS MPa
1	L	0.024	978	55.2	0.031	616	317.2	0.027	964	69.0	0.024	1089	62.1
2	L	0.024	978	110.3	0.031	616	475.7	0.027	983	121.4	0.024	1089	110.3
3	L	0.024	1053	27.6	0.031	658	165.5	0.027	1061	34.5	0.024	1200	34.5
4	L	0.024	1053	55.2	0.031	658	317.2	0.027	1061	69.0	0.024	1200	62.1
5	L	0.024	1053	110.3	0.031	658	475.7	0.027	1061	137.9	0.024	1200	110.3
6	L	0.024	1144	13.8	0.031	714	48.3	0.027	1111	69.0	0.024	1339	17.2
7	L	0.024	1144	27.6	0.031	714	165.5	0.027	1111	103.4	0.024	1339	34.5
8	L	0.024	1144	55.2	0.031	714	317.2	0.027	1155	39.3	0.024	1339	62.1
9	L	0.024	1255	13.8	0.031	783	48.3	0.027	1155	121.4	0.024	1478	17.2
10	L	0.024	1255	27.6	0.031	783	165.5	0.027	1180	69.0	0.024	1478	34.5
11	L	–	–	–	–	–	–	0.027	1155	55.2	0.024	1478	27.6

SUPPLEMENTAL STEADY-STATE CREEP TESTS – EVALUATION OF ADDITIONAL VARIABLES

TEST NO.	TEST[1] DIRECTION	L605 NOMINAL THICKNESS cm	L605 TEMP °K	L605 STRESS MPa	Ti-6Al-4V NOMINAL THICKNESS cm	Ti-6Al-4V TEMP °K	Ti-6Al-4V STRESS MPa	RENE '41[3] NOMINAL THICKNESS cm	RENE '41[3] TEMP °K	RENE '41[3] STRESS MPa	TDNiCr NOMINAL THICKNESS cm	TDNiCr TEMP °K	TDNiCr STRESS MPa
12	T	0.024	1053	55.2	0.031	658	317.2	0.027	1061	69.0	0.024	1200	62.1
13	T	0.024	1144	27.6	0.031	714	165.5	0.027	1111	69.0	0.024	1200	110.3
14	T	0.024	1144	55.2	0.031	714	317.2	0.027	1155	121.4	0.024	1339	62.1
15	L	0.064	1053	55.2	0.051	658	317.2	0.051	1061	69.0	0.051	1200	62.1
16	L	0.064	1144	27.6	0.051	714	165.5	0.051	1111	69.0	0.051	1200	110.3
17	L	0.064	1144	55.2	0.051	714	317.2	0.051	1155	121.4	0.051	1339	62.1
18	L	0.024	1053[2]	55.2	–	–	–	–	–	–	–	–	–
19	L	0.024	1144[2]	27.6	–	–	–	–	–	–	–	–	–
20	L	0.024	1144[2]	55.2	–	–	–	–	–	–	–	–	–

(1) TEST DIRECTION L = LONGITUDINAL; T = TRANSVERSE

(2) TESTED WITH HIGH EMITTANCE COATING. IN THIS CASE THE MATERIAL OXIDE WAS THE COATING MATERIAL.

(3) ALL RENE '41 SPECIMENS TESTED HAD OXIDE COATING.

For each material three specimens were tested in the transverse rolling direction using the thin gage material (same as the basic matrix). Three tests were also conducted on each alloy, in the longitudinal rolling direction, using the thicker gage material procured (see Section 2.4). In these six tests, stresses and temperatures were selected as replicates of conditions in the basic matrix.

Three tests were conducted on pre-oxidized L605 specimens. The surface coating used was the materials' own oxide obtained by heating the specimen in air to 1339°K, holding for 10 minutes and rapid cooling to room temperature. These were the thin gage, longitudinal rolling direction specimens as tested in the basic matrix. Test stresses and temperatures were replicates of conditions in the basic matrix.

2.9.2 CYCLIC TESTING

2.9.2.1 Data Requirements. This program is designed to provide a capability for the prediction of creep deflections for the Space Shuttle TPS panels. Toward developing the capability, the following requirements were established for cyclic testing:

(1) To provide data for determining material cyclic creep properties. To meet this requirement it is desirable to provide tests from which an empirical equation could be obtained, if required. Comparison of cyclic tests results with steady-state results is necessary in order to evaluate possible applicability of steady-state data bases to the prediction of cyclic creep.

(2) To provide data for investigation of creep accumulation (hardening) rules. These rules are required both in analyzing axially loaded components, where load or temperature changes with time, and in analyzing TPS panels subjected to bending loads. It is important to note that stresses in a

TPS panel, creeping under bending loads, will continuously change because of stress redistributions, even when applied bending loads are held constant.

(3) To provide data for investigating the applicability of resulting cyclic creep equations and hardening rules to trajectories having different time durations.

(4) To provide data for investigating possible effects of creep recovery.

(5) To provide data for establishing procedures applicable to analysis of TPS components subjected to general trajectories (varying temperatures and stresses within a cycle). In connection with this requirement the effect of atmospheric pressure on creep response was investigated.

(6) To provide cyclic creep response data for a typical Shuttle Mission trajectory. In connection with the requirement, stress and temperature profiles were applied with the goal of obtaining creep strains of approximately .5% after exposure to 200 simulated missions.

Cyclic tests to achieve these goals, were conducted under the following categories: (1) Basic Cyclic tests; (2) Variation of stress with cycle; (3) Variation of time per cycle; (4) Creep recovery tests; (5) Idealized trajectory tests and atmospheric pressure variation; (6) Simulated mission tests

For consistency of data, all cyclic tests were conducted using minimum gage specimens in the longitudinal rolling direction. Except for the variation of atmospheric pressure and aimulated mission tests, all cyclic tests were conducted at a constant atmospheric pressure of less than 1.3 Pa.

2.9.2.2 Basic Cyclic Tests. The Basic Cyclic tests form the cornerstone of all cyclic testing in this program because the data generated from these tests was used to develop the empirical equations relating stress, temperature, and time to creep strains. The profile used, shown in Figure 2-22, is a simplified trajectory consisting of a rapid heat-up, hold at temperature for twenty minutes, then rapidly cooling to approximately 422°K. The temperature profile was not taken to room temperature (299°K) because of cost and schedule consideration associated with an increased testing time. After cool-down the same profile was repeated for a 100 cycle test duration. Total time for each cycle was 55 minutes. The cycle time at maximum temperature and load of 20 minutes was based on the Shuttle design trajectory presented in Section 2.1 (See Figure 2-5).

Combinations of temperatures and stresses selected for each alloy were based on the experimental design used in steady-state testing. This design was particularly attractive for cyclic testing due to the whiffle tree test mechanism used (simultaneous testing of three specimens at one temperature and three different stress levels as discussed in Section 2.8).

Stress and temperature levels were also selected with the goal of obtaining 100 cycle creep strains up to 0.5%. A summary of these Basic Tests is presented in Table 2-5. More discussion of test selection for the Basic Cyclic Tests are presented for each material in Section 3.

2.9.2.3 Variation of Stress with Cycle. Stress redistribution occurs and residual stresses result within a beam due to creep. To include this effect in TPS creep analysis, theories describing hardening behavior are employed. To provide data

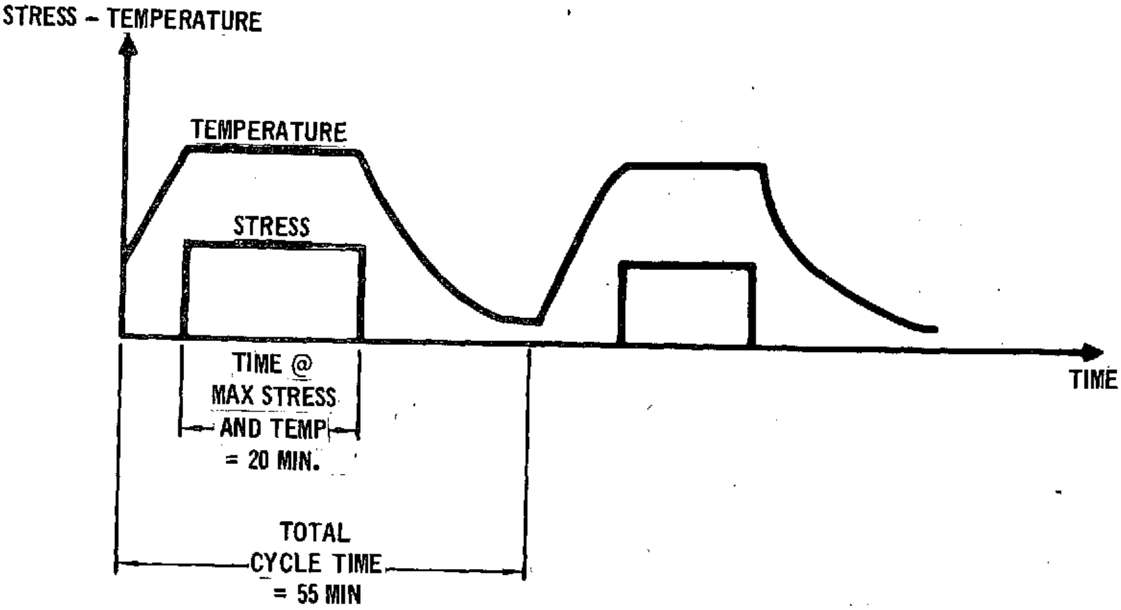

FIGURE 2–22 STRESS AND TEMPERATURE PROFILES FOR BASIC CYCLIC CREEP TESTS

TABLE 2–5
BASIC CYCLE TESTS

TEST NO.	ALLOY DESIGNATION							
	L605		RENE'41		Ti-6Al-4V		TDNiCr*	
	TEMP. °K	STRESS MPa	TEMP. °K	STRESS MPa	TEMP. °K	STRESS MPa	TEMP. °K	STRESS MPa
1	978	128.9 80.7 51.0	1111	104.1 68.7 39.0	658	399.0 299.2 207.0	1089	124.3– 85.7
2	1053	127.6 83.4 52.2	1155	66.5 57.0 46.8	714	295.9 192.0 114.7	1200	108.6– 57.2 9.0
3	1144	73.5 +47.2 29.6	1072	135.1 103.4 68.7	783	129.7 83.6 50.4	1339	60.3– 30.6
4	1255	33.8 20.6 13.2	1033	275.5 207.6 142.0	839	47.2 30.5 19.7	1478	44.3– 16.3

*A TOTAL OF 26 TDNiCr SPECIMENS WERE TESTED TO BASIC CYCLE PROFILES THROUGH THIS RANGE OF STRESS SHOWN. FOR FURTHER DISCUSSION OF THESE TESTS SEE SECTION 3.4.

for investigating this behavior, tests were conducted in which load (stress) level was varied as a function of cycle. Histories for these tests are shown in Figure 2-23. In these tests, the cycle profiles were the same as used in basic cyclic testing. Data obtained was used in conjunction with the Basic Cyclic Tests to evaluate the applicability of time or strain hardening theories to the individual alloys. Stress levels for the history shown in Figure 2-23(a) were selected to duplicate stresses in the Basic Cyclic Tests where possible, to allow direct comparison of data. The increasing and decreasing stress level tests, illustrated in Figures 2-23(b) and 2-23(c), respectively, were also used to assess and verify hardening behavior for Shuttle TPS conditions. These are representative of internal stresses at beam stresses which will gradually change due to creep during entry.

2.9.2.4 Variation of Time Per Cycle. In the previous discussions, analysis has been based on tests using trajectory profiles which have a time of 20 minutes at maximum temperature and load. Analysis, however, must be applicable to trajectories that have different times at maximum temperature and load.

To determine the effect of time at temperature for each material, a test (3 specimens) was conducted using a time of 10 minutes at maximum temperature and load. Total time per cycle was therefore 45 minutes, shortened by 10 minutes from the Basic Cyclic Test profile. Temperature and stresses for this test were the same as for one of the basic cyclic tests for each material to allow comparison with the basic cyclic results.

2.9.2.5 Creep Recovery Tests. These tests were designed to evaluate the effect of "recovery" time between loadings and the effect of overlapping stress and temperature profiles in time space. Two types of tests were conducted, as depicted in Figure 2-24.

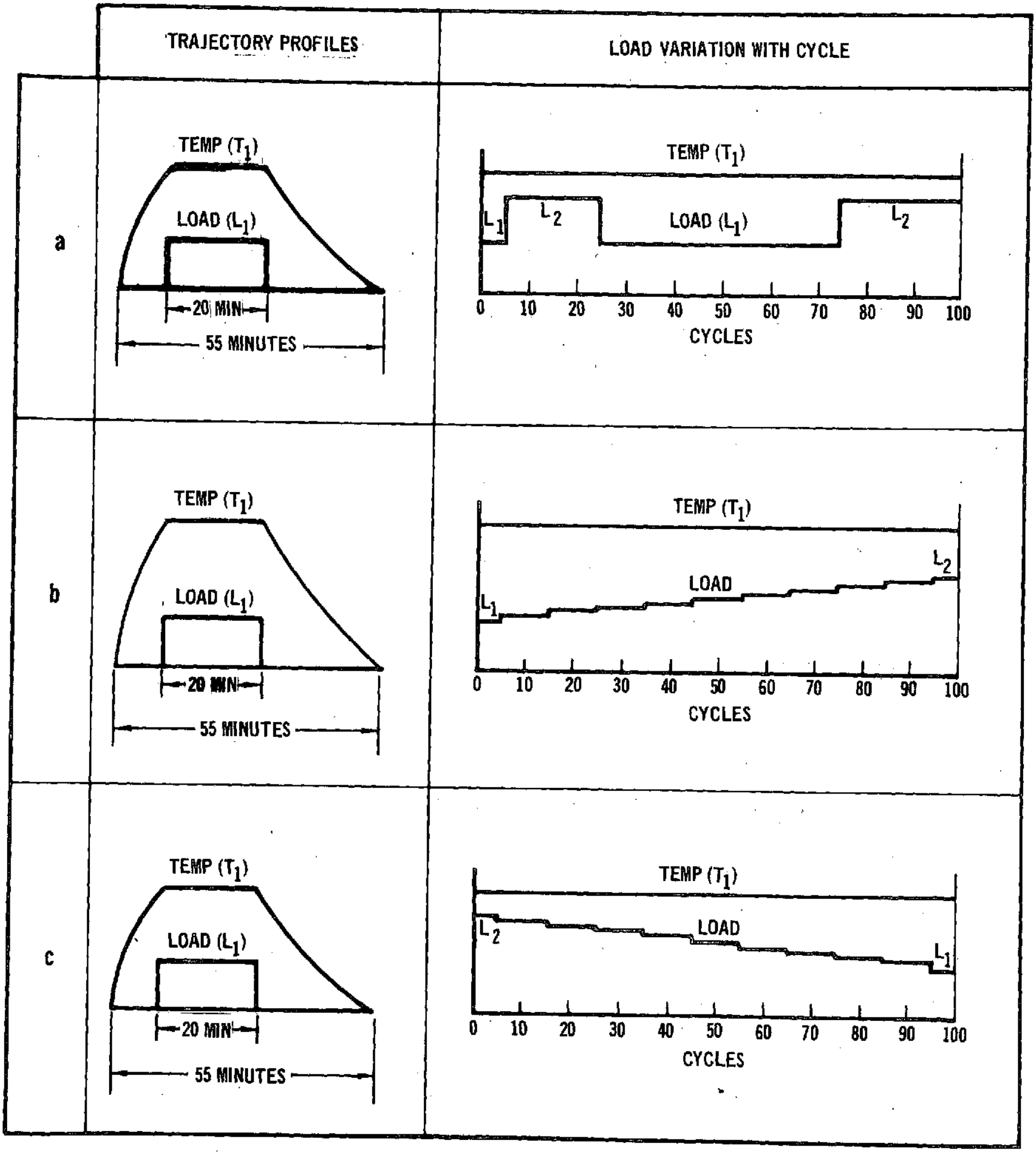

FIGURE 2-23 TESTS FOR EFFECTS OF VARIATION OF STRESS WITH CYCLE

The first test is a modified cyclic creep test in which the stress profile is extended until the temperature has been reduced to well below the maximum temperature (Figure 2-24(a)). In this manner, the possibility of "recovery" as a result of high temperature and no stress is greatly reduced. Time at maximum temperature in this test was 20 minutes. Temperature and load levels were selected to match those of one of the basic cyclic tests to allow direct data comparison. The purpose of the second test was to investigate the effect of a time delay typical of that which Shuttle vehicles will experience between missions. In this test, specimens tested in one of the Basic Cyclic Tests were recycled after a time delay (approximately 1 month). A schematic of this test is shown in Figure 2-24(b).

2.9.2.6 Idealized Trajectory Tests and Variation of Atmospheric Pressure. For purposes of analysis, an actual entry trajectory was idealized by dividing it into time increments for which stress and temperature are constant, as illustrated in Figure 2-25. To establish guidelines for idealizing continuous stress and temperature profiles, and to provide data for further evaluating the applicability of hardening theories when load (stress) and temperatures are changed within a cycle, idealized trajectory tests were performed.

The first type of test used a simplified two step stress profile as shown in Figure 2-26(a). For this test, two load levels of ten minutes each were applied sequentially to each specimen for the total trajectory time of twenty minutes. These data allow for initial comparisons with predictions using hardening rules in conjunction with the cyclic empirical creep equation (developed from Basic Cyclic data).

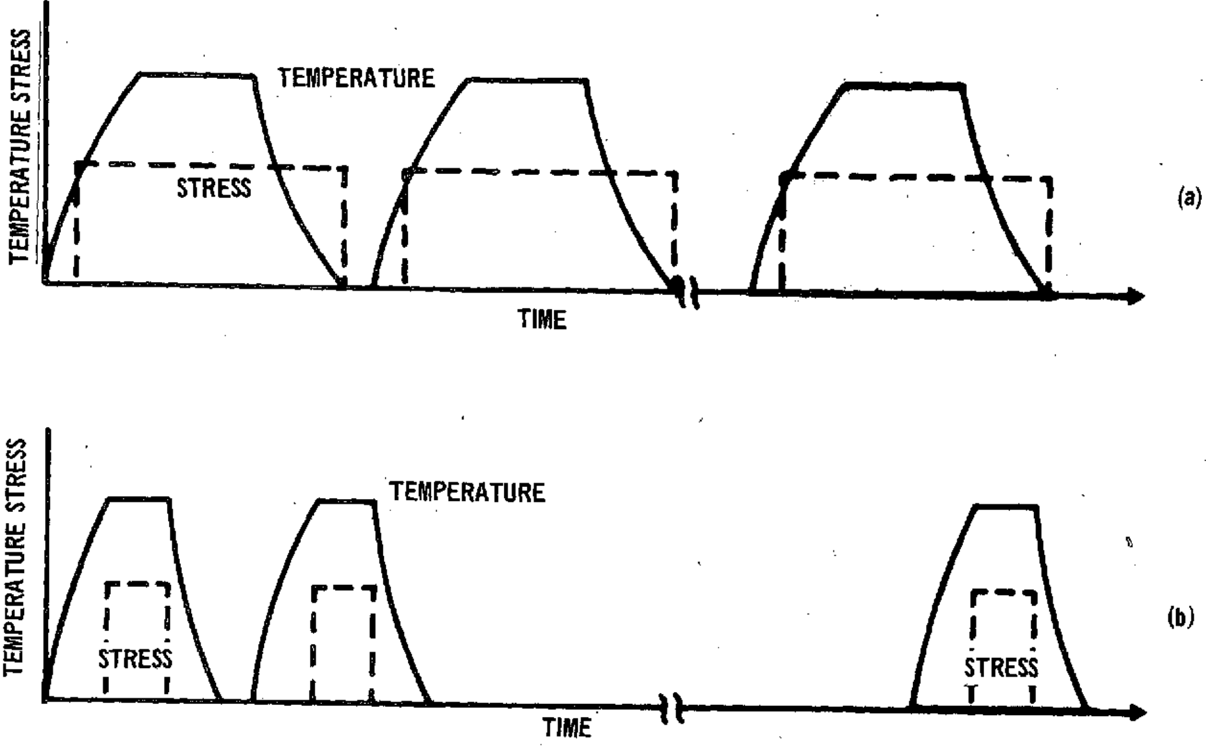

FIGURE 2-24 TESTS TO EVALUATE CREEP RECOVERY

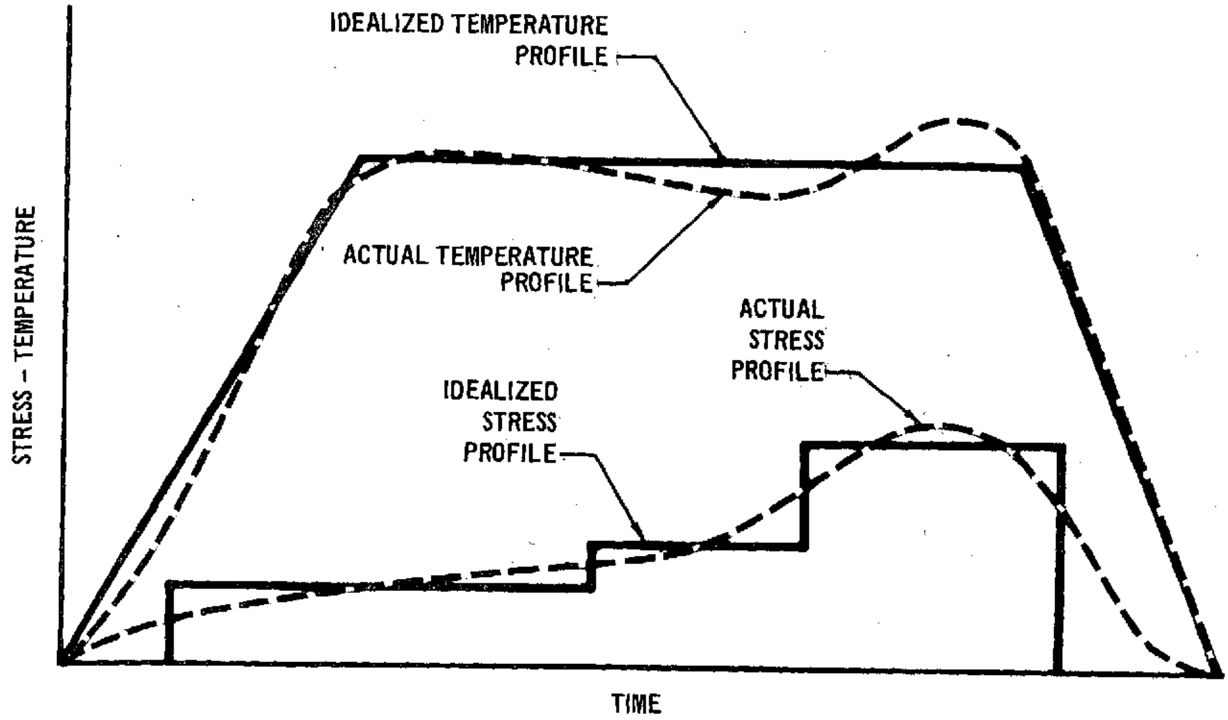

FIGURE 2-25 TYPICAL APPROACH FOR TRAJECTORY IDEALIZATION

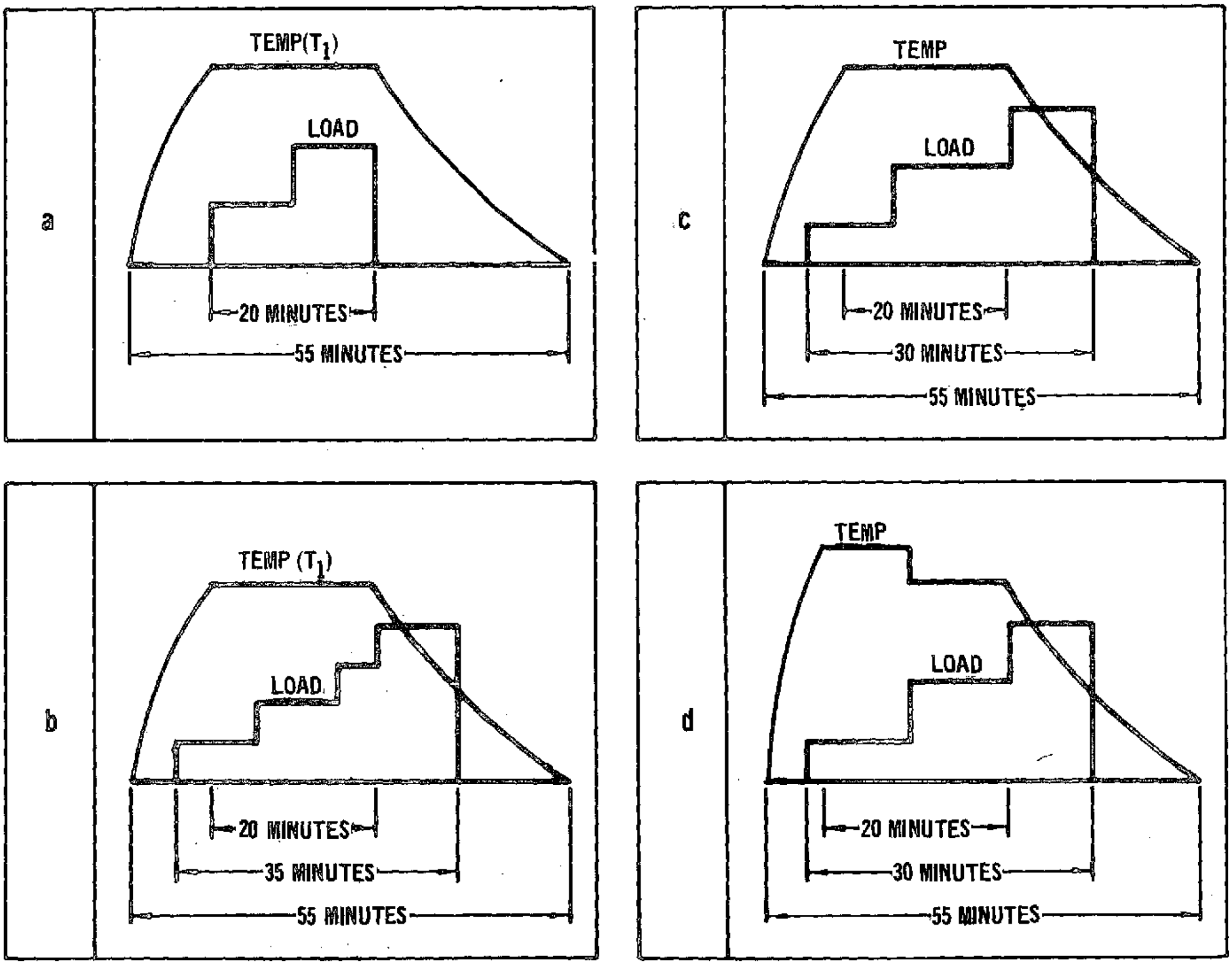

FIGURE 2–26 IDEALIZED TRAJECTORY PROFILES

The second type of test was conducted using idealizations of the projected Shuttle (load and temperature) missions. The number of steps in the idealized load trajectory was varied between materials in some cases. A four-step load profile was used in this test for L605 specimens, as depicted in Figure 2-26(b) and a three-step profile was used for testing Rene' 41, titanium, and TDNiCr specimens as shown in Figure 2-26(c) In addition, Rene' 41 specimens were tested using a two-level temperature distribution as shown in Figure 2-26(d). In general these tests were conducted for 100 cycles.

All cyclic tests discussed to the point were conducted with a constant atmospheric pressure of less than 1.3 Pa. To determine the effect of a changing pressure, one idealized trajectory test for each material was repeated using the simulated mission profile shown in Figure 2-27. This pressure profile is based on altitude versus time for the Phase B Space Shuttle Orbiter trajectory presented in Section 2.1.

2.9.2.7 Simulated Trajectory Tests. Testing of tensile specimens for each material to a simulated Shuttle mission, load, temperature, and pressure profiles, shown in Figure 2-27, completed the cyclic testing. Results of these tests provide data for final verification of predictive capability for cyclic creep in tension.

2.10 COMPUTER PROGRAMS

2.10.1 SELECTION OF REGRESSION ANALYSIS COMPUTER PROGRAM FOR DATA ANALYSIS (BMDO2R)

In the development of an empirical equation using a large volume of data, the use of regression analysis can be helpful. The computer program that was used in this study is referred to as BMDO2R and is part of the Biomedical Computer Programs developed by the Health Sciences Computing Facility, Department of Preventative Medicine, University of California (Reference 25). The regression analysis programs were designed to solve problems in medical research which involve data covering several variables for each case or several observations on a few variables. Of the

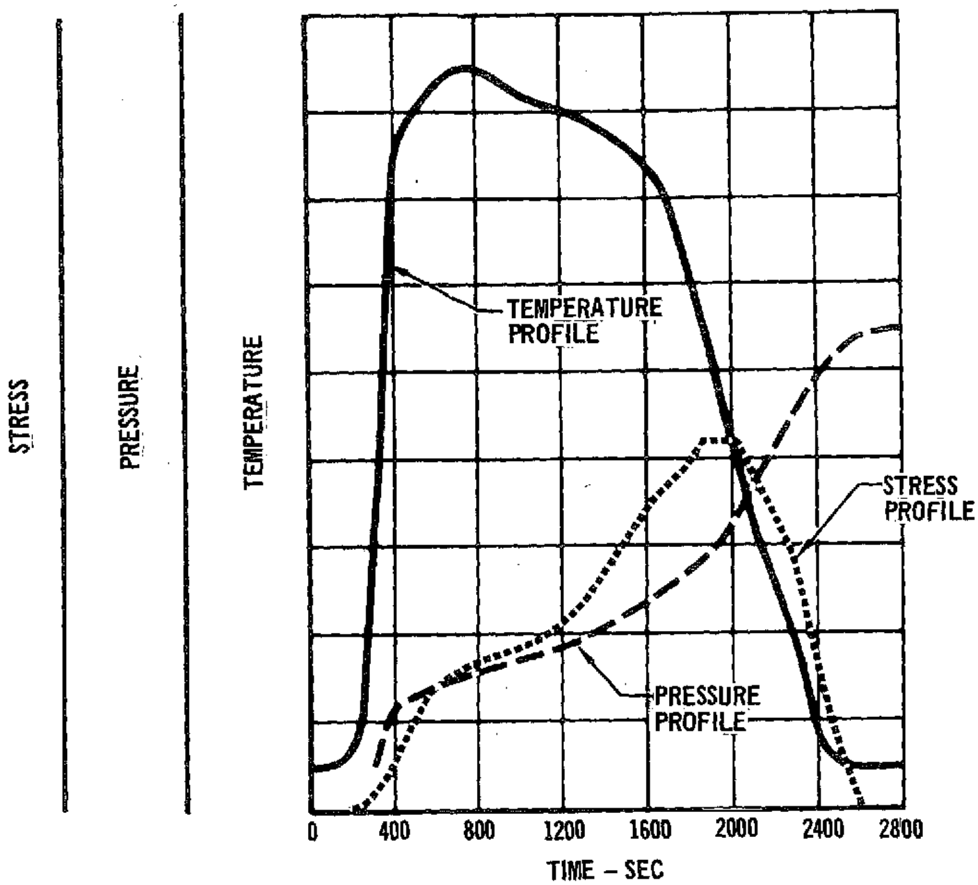

FIGURE 2–27 SIMULATED MISSION PROFILE

regression analysis category of six programs, the stepwise regression program (BMD02R) was selected.

The program is capable of computing a sequence of multiple linear equations in a stepwise manner. At each step, one variable is added to or deleted from the equation. The variable that is added is the one that makes the greatest reduction in the residual variance. In essence, the introduction of this variable produces the greatest overall "F" ratio (F = MSR/MSV, where MSR is the mean square due to regression and MSV is the mean square due to residual variation).

2.10.2 PROGRAM FOR TENSILE CREEP TRAJECTORY DATA ANALYSIS (CPCE)

The CPCE computer program was written in order to allow rapid analysis of cyclic tensile specimen trajectory test data. Creep strains are accumulated, based on hardening theories in conjunction with empirical equations for the creep.

Program input is based on the type of trajectory profiles conducted. For tests where stress is constant within each cycle but stepped as a function of cycle, input includes time per cycle and number of cycles at each stress and temperature. For tests where stress and temperature are varied within a cycle (idealized and simulated trajectory tests), input includes time, temperature and stress of each step in the trajectory and the number of cycles to be analyzed.

Analysis options are based on the time hardening and strain hardening theories of creep accumulation (Reference 26). Five analysis predictions are calculated and printed as functions of cycle and time within the cycle. The first two are time hardening and strain hardening, respectively. The other three accumulate creep strain increments for time or strain hardening, depending upon results of checks made on the trajectory. These three approaches are: 1) use of time hardening when stress increases and strain hardening when stress decreases; 2) use of time hardening when effective time (in strain hardening) is less than actual time and strain

hardening when effective time is greater than actual time; and 3) use of time hardening when strain rate increases and strain hardening when strain rate decreases. These three analysis approaches were formulated on the basis of initial analysis of L605 cyclic test data.

This program not only allows for analysis of the cyclic data but will supplement the TPS Beam prediction program for the analysis of TPS components subjected to axial load only.

2.11 STATISTICAL CONSIDERATIONS

During this program, major areas of work included (1) the development of predictive equations for the description of creep behavior based on previously conducted work as detailed in the literature, (2) the development of test matrices for the defintion of test parameters for required creep tests (both steady-state and cyclic), (3) the generation of new predictive equations for the description of steady-state and cyclic creep behavior as experimentally observed during this program, and (4) comparison of literature data with that obtained during this program. Each of these above areas of interest required the use of statistical considerations. For example, a very large number of equations are found in the literature which have been developed over the years to describe the complex physical process of creep. In addition, an infinite number of new relationships (or models) can be formulated for the description of the dependent variable creep as a function of the independent variables time, temperature, stress, structure, gage, etc. The use of regression analyses permits a determination of which "classical" equation or new equation best fits the previously existing and new creep data for each of the four alloys studied during this program. Also, time and funding limited the number of creep tests which could be performed during this program; therefore, statistical methods were used to choose test parameter combinations and to identify the

acceptable test data for establishing equations relating the test parameters and the creep for each alloy investigated. The various test parameter combinations are discussed separately under each of the four alloy discussions.

2.11.1 SELECTION OF EQUATIONS

The description of a creep equation involves the determination of the relationship between the dependent variable, strain, and the independent variable such as temperature, stress, time, thickness, and orientation. A convenient procedure for determining this relationship is the use of multiple regression techniques. Two parameters associated with this technique are (1) the multiple correlation coefficient, R, and (2) the standard error of estimate, S_y. The square of the multiple correlation coefficient is defined as the ratio of the sum of squares due to regression to the total sum of squares and is a measure of how well the fitted equation explains the variation in the data [27]. The closer the value of R^2 (or R) is to 1, the better the equation will fit the data.

The standard error of estimate is defined as the square root of the residual mean square and is an estimate of the variance about the regression. Therefore, the precision of the estimate would be considered better the lower the value of S_y. Accordingly, in the development of the various regression equations that were examined during the program, emphasis was placed in obtaining equations which resulted in large values of R and small values of S_y.

The development and selection of each predictive equation generally followed an iterative procedure as outlined below:

Step 1 - Select first order independent variables.

Step 2 - Using variables identified in Step 1, form new independent variables for the regression analysis consisting of higher order terms and interaction (first and higher order) terms. The computer program used to

perform the stepwise regression procedure (BMD-02R) is discussed in Section 2.10.2. A feature of the program is the capability of conveniently introducing new independent variables which may be interaction terms by simply including transgeneration cards.

Step 3 - Using the stepwise regression procedure, and the literature and/or program data, determine the significant variables from the total identified and constructed in Steps 1 and 2.

Step 4 - Review and record R and S_y for equation. If sufficient replication exists in data bank, compare the computed S_y with the internal estimate of error which is computed from the replicate observations.

Step 5 - Examine the residual of plots of the dependent variable vs. regressed variables. The residual is the difference between what is actually observed and what is predicted by the regression equation. If the proper variables were selected, the residual plots will have a uniform distribution with a zero mean. If the proper variables were not in the equation, then the residual plots tend to take a shape which indicates if the analysis should be weighted or a linear or quadratic term should have been used. An in-depth discussion of the examination of residuals and their significance is presented in Reference (27).

Step 6 - Repeat Step 3 using new variables and compare R and S_y with previously established values. Repeat Step 5 (i.e., review of plots of residuals) and form additional independent variables, if required.

Step 7 - Plot predicted creep responses and compare with experimentally observed creep curves with particular emphasis placed in identifying discrepancies in fit and general form of the predicted surfaces.

Step 8 - If major discrepancies are observed in Step 7, modify and/or add new independent variables and repeat from Step 3.

It should be noted that creep strains below 0.05 percent and above 0.5 percent were culled from the literature survey data base as were tests where the creep stress level was above the 0.2% offset yield stress at temperature. As a result, the predictive equations representing this data base are limited to this range. The justification for removing the creep data below 0.05 percent was that a significantly higher percent experimental error exists in the measurement of these very low creep strains, and that the standard error of estimate was being dominated by these large observation errors. It should be noted that a weighted least squares analysis could have been performed which would have accounted for the large variance in the low strain (0.05) regime [27]. However, the complexity of such an approach in view of the many data bases and variables was not considered practical.

Creep strains greater than 0.5 percent were removed to allow the model to more exactly describe the creep response up to strain limits normally imposed on TPS system. By excluding these higher strains, a small downward bias, as shown in Figure 2-28 is introduced in the predictive equations. Likewise, a small upward bias is introduced into the predictive equation at low strains as is also shown in Figure 2-28. A study was made with respect to the effect of this truncating, and the bias which is introduced was found to be negligible with respect to the goals of this program.

In general, the regression analyses were conducted using the natural logarithm of strain, $\ln\varepsilon$, as the dependent variable. There are two primary advantages in using logarithmic strain which are: (1) the model tends to come closer to minimizing the percentage deviations which is desirable in our application. This can be shown as follows:

The residual value, δ, in our case can be expressed as

$$\delta = \ln \left(\frac{\hat{Y}}{Y}\right) \tag{2-2}$$

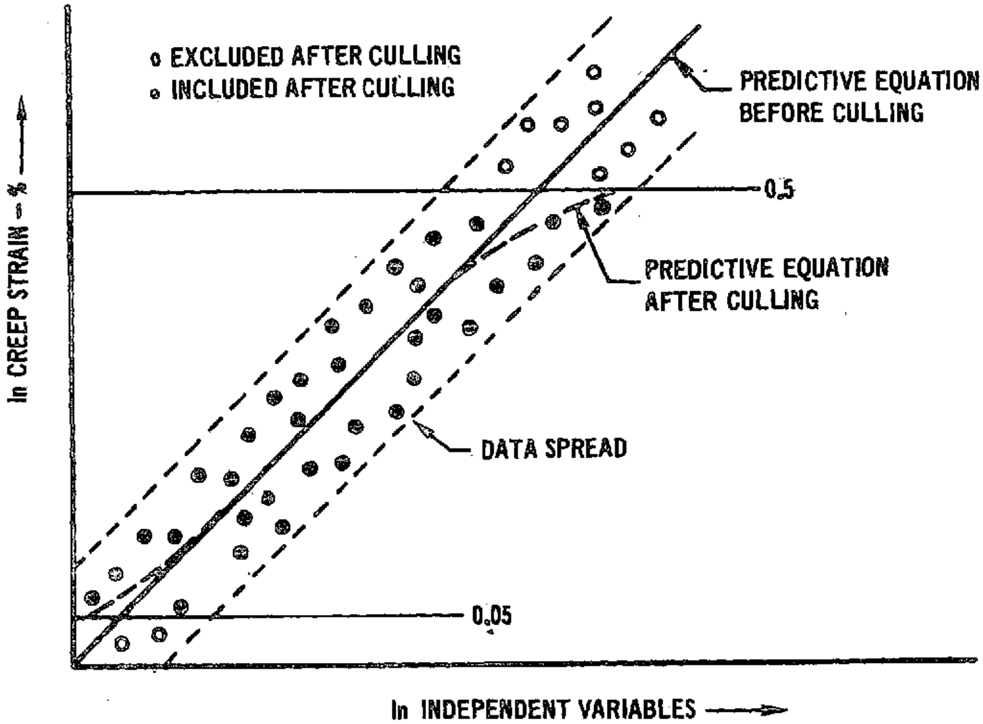

FIGURE 2-28 EFFECT OF CULLING LOW AND HIGH STRAIN DATA ON PREDICTIVE EQUATION DEVELOPMENT

where Y is the observed value and $\hat{Y}$ is the fitted value. Also

$$e^{\delta} = \frac{Y}{\hat{Y}} \tag{2-3}$$

and

$$e^{\delta} \cong 1 + \delta \quad \text{for small } \delta$$

and, therefore

$$1 + \delta \cong \frac{Y}{\hat{Y}} \tag{2-4}$$

As can be seen above, there is an inherent positive bias which results when regressing on logarithms and the magnitude of the bias is a function of the value of δ. With the standard error of estimates found during the program, this bias was very small. Regressing on the strain rather than the logarithm of strain results in the following expression for the residual value

$$\delta = y - \hat{y} \tag{2-5}$$

and with data such as observed for creep, the advantages of regressing on logarithm strain rather than strain are obvious.

(2) the model is forced to satisfy initial boundary value considerations. For example, the model

$$\ln \varepsilon = A_o + A_1 \ln\sigma + A_2 \ln t \tag{2-6}$$

when transformed back to strain space becomes

$$\varepsilon = e^{A_o} \sigma^{A_1} t^{A_2} \tag{2-7}$$

and if σ or t equal zero, the strain is forced to also equal zero. Note that the $\ln \varepsilon$ model can be used directly provided care is taken to account for the signs of the coefficients.

Finally, as is discussed in detail in Appendix G, an alternative approach to the generation of predictive equations was investigated during this program. This approach utilized finite difference techniques to minimize the effect of data dependency within individual tests since the regression equation is developed from

the difference in consecutive strain values rather than in their magnitude. Rather than being randomly distributed around the predicted curve, the data tend to run in strings of consecutive strains and this fact results in conventional regression techniques (e.g. least squares analysis) giving a consistent but not maximum liklihood estimate of the creep response. The two estimates converge if enough data sets are available.

2.11.2 DUMMY VARIABLE METHODS

Comparison in creep response surfaces computed from the literature search data bases were made with those computed from supplemental steady-state tests conducted during the program. In addition, comparisons were made between the steady-state and cyclic creep surfaces. One method used to make these comparisons was the dummy variable technique.

The regression model which incorporates the use of dummy variables is

$$y = \sum_{i=o}^{N} \alpha_i \, X_i + \beta_i \, (ZX_i) \tag{2-8}$$

where a_i and β_i are regression coefficients; X_i are the N independent variables (X_o has value of Unity) and Z is assigned values as follows:

Z = 0 if the observation is from data set A

Z = 1 if the observation is from data set B

If two data bases are statistically identical, the β_i's will be statistically insignificant and the response is described by $y = \sum_{i=o}^{N} \alpha_i X_i$ for all cases. In the event the data bases are different, some β_i's will have significant values, and, as a result of the presence of the β_i terms, the equation becomes

$$y = \sum_{i=o}^{N} K_i \, X_i \tag{2-9}$$

where

$K_i = \alpha_i$ for the case Z = 0

$K_i = \alpha_i + \beta_i$ for the case Z = 1 and the term β_i is significant

$K_i = \alpha_i$ for the case Z = 1 but the β_i term is not significant

In summary, the dummy variable method used in conjunction with the BMD-02R regression analysis program provides an efficient and convenient technique for the comparison of data and for the determination of significant differences, if any, between response surfaces from different data bases.

3.0 TEST AND DATA ANALYSIS

Presented in this section, by alloy, are the results of the literature survey and experimental portion of Phase I alloy with the analysis of the results.

3.1 L605 - RESULTS OF TESTS AND DATA ANALYSIS

3.1.1 STEADY STATE L605 DATA BASE

3.1.1.1 Literature Survey. A review of the literature revealed that Reference 15 contained enough data to develop a data base. This reference contained the results from 59 creep tests performed on various gages manufactured from the same heat of material. This data base is presented in Appendix C-1.

3.1.1.2 L605 Data Base Analysis. Figures 3-1 and 3-2 are graphical representations of stress, time, and temperature ranges for data base longitudinal and transverse tests respectively. Shaded areas indicate the ranges of stress, time, and temperature for which creep strain data less than 0.5% are available in the data set. At high temperatures (1144 and 1255°K) transverse specimens were generally tested for longer times than the longitudinal specimens. In working with this data base it is important to recognize that empirical equations based on this data base are applicable only for the range of data shown.

Data for five tests were removed from the data base. Two were tests at 922°K (206.8 MPa on 0.013 cm and 248.2 MPa on 0.102 cm). These tests had very high initial strain values (0.2% creep in 0.1 hour) which resulted in inconsistency between these tests and others of the same temperature and similar stress levels. Data for three additional tests were removed from the data base because the test points were erratic. Creep strains less than 0.05% were removed from the data base in an effort to weight the data in favor of the higher creep strains in the regression analysis (see Section 2.11.1).

Since the L605 data base tests were at temperatures greater than one half of the the melting point, the following high temperature creep model was used as the basis for obtaining an empirical equation.

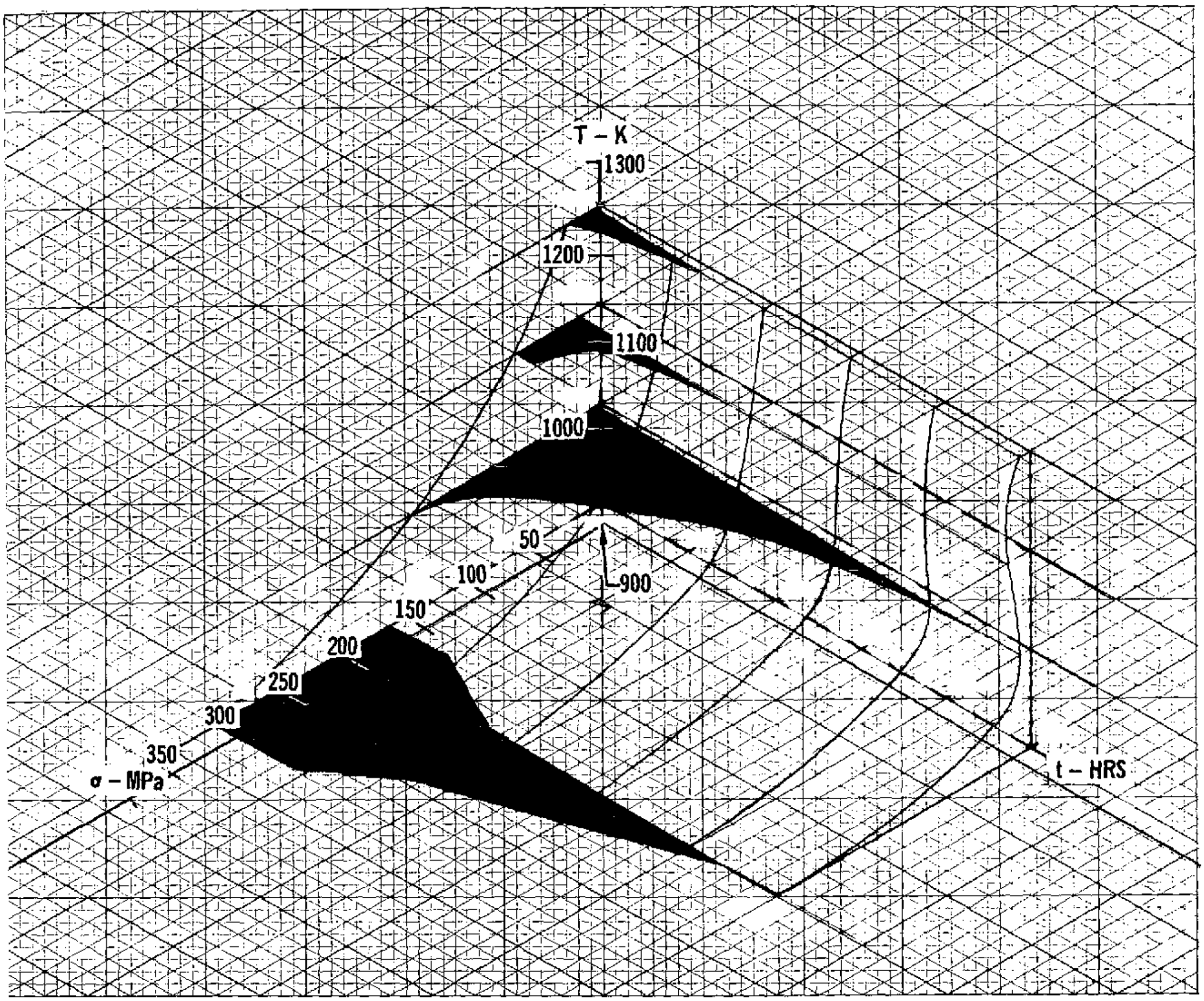

FIGURE 3-1 L-605 DATA RANGE – LONGITUDINAL ROLLING DIRECTION

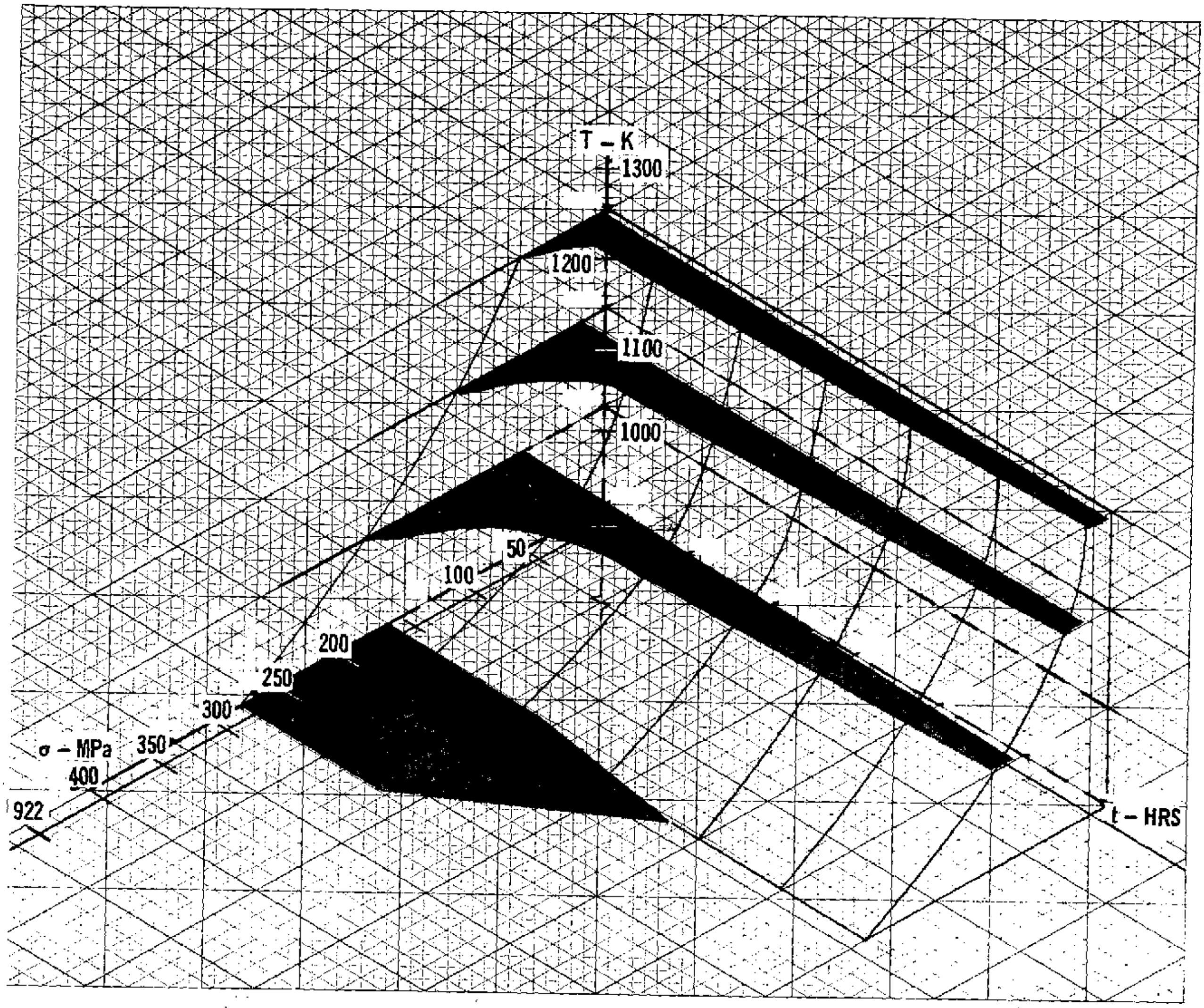

FIGURE 3–2 L–605 DATA RANGE – TRANSVERSE ROLLING DIRECTION

$$\varepsilon = f\,[\sigma,\ T,\ t,\ S,\ \exp\,(-Q/RT)] \tag{3-1}$$

Functional forms for stress (σ) and time (t) were based on References 24 and 25. Reference 24 showed that for low and moderate stresses, typical of the data base tests, the effect of stress on the rate of deformation in metals obeys the power stress law, $\dot{\varepsilon} = f\,(\sigma^n)$.

Based on Reference 26, the dependency of high temperature creep on time can be expressed by the Andrade power function, $\varepsilon = f'(t^k)$.

Because processing can effect crystal structure, dispersion of precipitates, and grain size (referred to as structure factors in References 26 and 28) in sheet products, one way to quantify this relationship is to include material thickness (ϕ) in the creep equation. The functional form selected was $\varepsilon = f\,(\phi)^m$.

Based on these functional relationships, the following equation format was obtained.

$$\ln \varepsilon = A_o + n \ln\sigma + k \ln t + m \ln\phi + {}^{A_1}/T \tag{3-2}$$

where A_o, n, k, m, A_1 are constants

Using this form, the following equation was obtained for the L605 data base

$$\ln \varepsilon = 4.84549 + 2.1288 \ln \sigma + .48945 \ln t - .29601 \ln\phi - 19.50143\ (1/T) \tag{3-3}$$

where ε = creep strain, %

σ = stress, MPa

t = time, hours

ϕ = material thickness, cm

T = Temperature, °K/1000°

The standard error of estimate (S_y), associated with this equation, based on the natural logarithm of strain is 0.2761 and the multiple correlation coefficient is 0.8913. The residual plots ($\ln \varepsilon_{actual} - \ln \varepsilon_{calculated}$ vs. variable) for this equation are shown in Figure 3-3. Data base creep strains are plotted against predicted values in Figure 3-4. The $\pm$ 1.96 S_y scatter band is also shown. This scatter band represents back transformed space (ε) rather than the transformed space that the

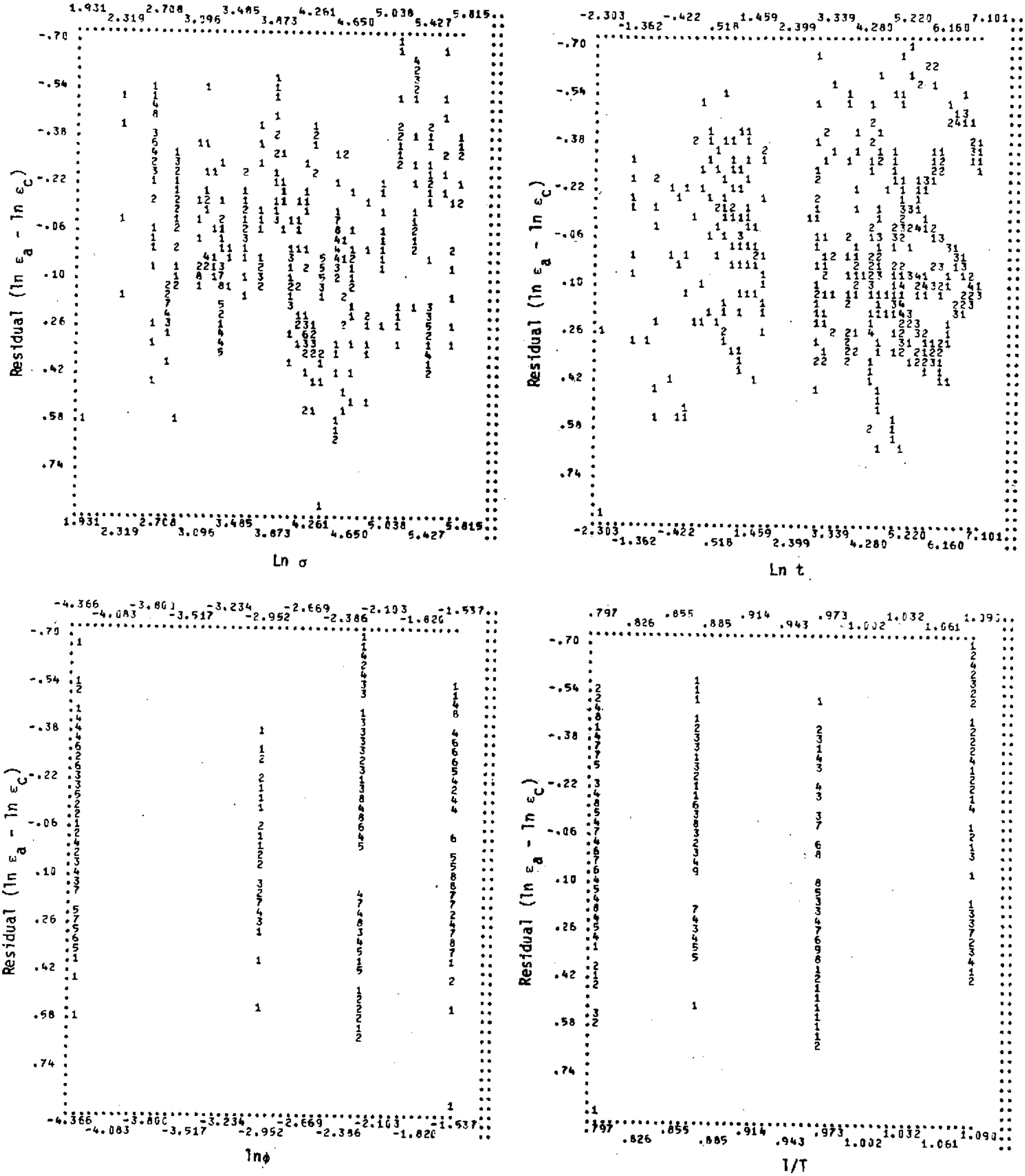

FIGURE 3-3 RESIDUAL PLOTS OF L605 LITERATURE SURVEY EQUATION (3-3)

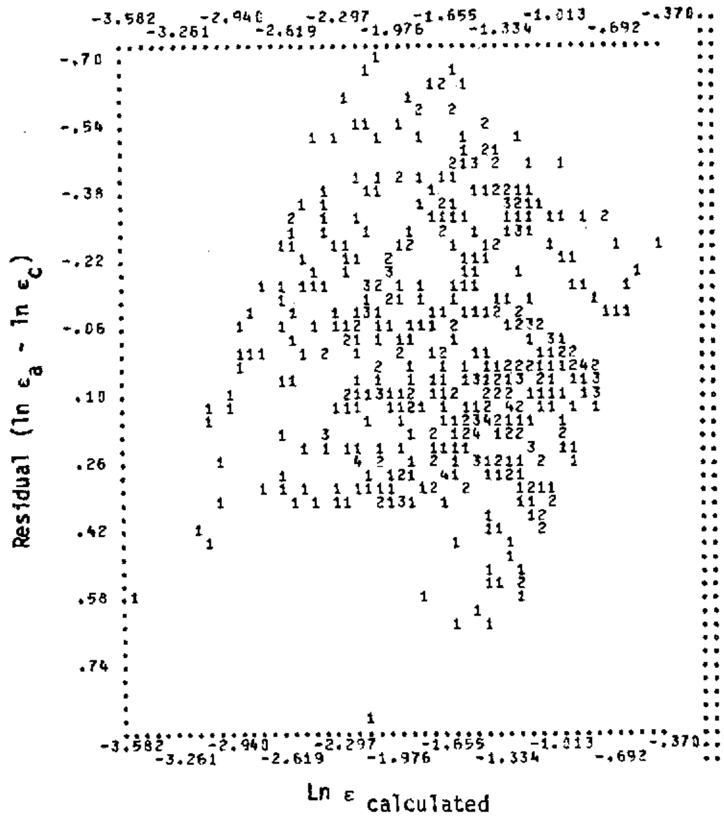

FIGURE3-3 RESIDUAL PLOTS OF L605 LITERATURE SURVEY EQUATION (3-3) (Continued)

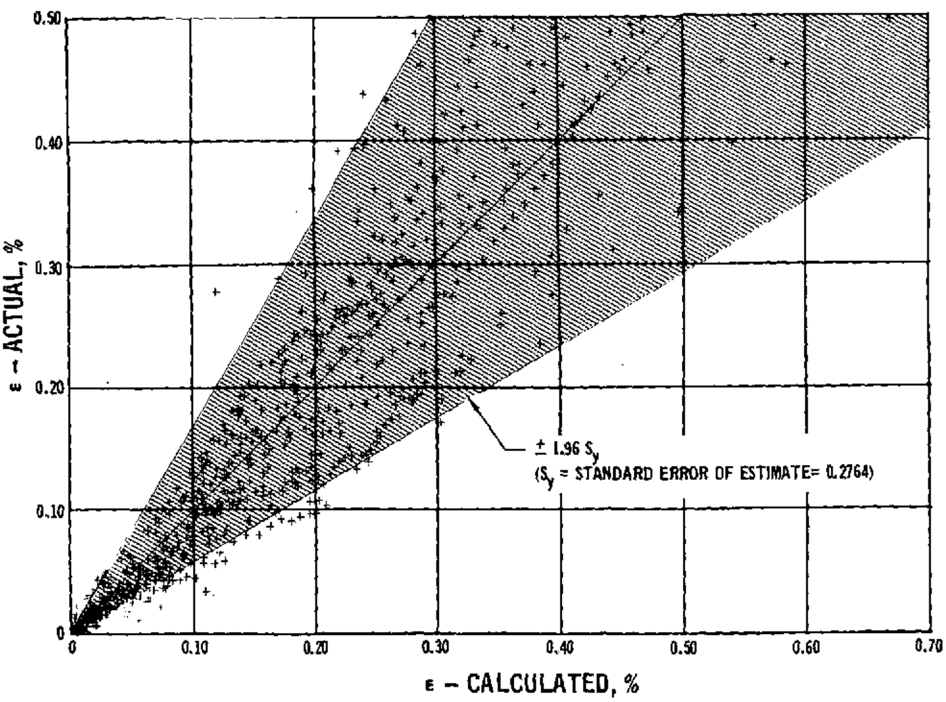

FIGURE 3-4 L605 EMPIRICAL EQUATION (3-3)

regression was performed on ($\ln\varepsilon$). Although creep strains less than 0.05% were not used in its derivation, the equation is capable of predicting these low strains because the required boundary conditions of zero creep strain at zero stress and time are satisfied.

Other equation forms which contained interaction terms of t, σ and T were examined through the use of the BMD-02R computer program, but were rejected in favor of Equation 3-3 because the improvement in curve fit was not sufficient to warrant using an equation with more complex terms.

3.1.2 L605 SUPPLEMENTAL STEADY-STATE TESTING

3.1.2.1 Supplemental Steady-State Test Matrix. A total of twenty-three steady-state creep tests were performed. The conditions for these tests are summarized in Table 3-1. From this table it can be seen that in addition to the ten tests selected in the basic experimental design, four tests were replicates; three were tested in the transverse direction to investigate the effect of specimen orientation on creep; three tests were run using specimens with a pre-oxidized surface layer (emittance coating) to determine the effect of this layer on creep; and three tests were performed on 0.064 cm thick material rather than .025 cm. material to evaluate the effect of thickness on creep.

The pre-oxidized surface layer was obtained by heating the specimens in air to 1339°K, holding for 10 minutes and rapid cooling to room temperature.

Raw data obtained for these twenty-three tests is presented in Appendix C-2. Included in this appendix are the elastic strains which were determined at the start and conclusion of the test.

The steady-state test matrix design, shown in Figure 2-21(d) allowed testing over the temperature range of 978 to 1255°K and a stress range of 13.8 to 110.3MPa. Values of temperature and stress are equally spaced in the variables log stress and $\frac{1}{T}$.

TABLE 3-1

L605 SUPPLEMENTAL STEADY-STATE TESTS
BASIC TEST MATRIX

TEST SPECIMEN	MATERIAL ROLLING DIRECTION	MATERIAL GAGE		TEMPERATURE		STRESS	
		CM	INCHES	°K	°F	MPa	KSI
L31L	LONGITUDINAL	0.025	0.010	978	1300	110.3	16.0
L42L	LONGITUDINAL	0.025	0.010	978	1300	110.3	16.0
L96L	LONGITUDINAL	0.025	0.010	978	1300	55.2	8.0
L50L	LONGITUDINAL	0.025	0.010	978	1300	55.2	8.0
L39L	LONGITUDINAL	0.025	0.010	1053	1435	110.3	16.0
L95L	LONGITUDINAL	0.025	0.010	1053	1435	55.2	8.0
L73L	LONGITUDINAL	0.025	0.010	1053	1435	27.6	4.0
L27L	LONGITUDINAL	0.025	0.010	1144	1600	55.2	8.0
L58L	LONGITUDINAL	0.025	0.010	1144	1600	55.2	8.0
L93L	LONGITUDINAL	0.025	0.010	1144	1600	27.6	4.0
L24L	LONGITUDINAL	0.025	0.010	1144	1600	13.8	2.0
L54L	LONGITUDINAL	0.025	0.010	1255	1800	27.6	4.0
L48L	LONGITUDINAL	0.025	0.010	1255	1800	13.8	2.0
L29L	LONGITUDINAL	0.025	0.010	1255	1800	13.8	2.0

L605 SUPPLEMENTAL STEADY-STATE TESTS
EVALUATION OF ADDITIONAL VARIABLES

TEST SPECIMEN	MATERIAL ROLLING DIRECTION	MATERIAL GATE		TEMPERATURE		STRESS	
		CM	INCHES	°K	°F	MPa	KSI
L17T	TRANSVERSE	0.025	0.010	1144	1600	55.2	8.0
L11T	TRANSVERSE	0.025	0.010	1144	1600	13.8	2.0
L18T	TRANSVERSE	0.025	0.010	1053	1435	55.2	8.0
L01L	LONGITUDINAL	0.064	0.025	1144	1600	55.2	8.0
L03L	LONGITUDINAL	0.064	0.025	1144	1600	27.6	4.0
L02L	LONGITUDINAL	0.064	0.025	1053	1435	55.2	8.0
L45L(PREOXIDIZED)	LONGITUDINAL	0.025	0.010	1144	1600	55.2	8.0
L78L(PREOXIDIZED)	LONGITUDINAL	0.025	0.010	1144	1600	27.6	4.0
L23L(PREOXIDIZED)	LONGITUDINAL	0.025	0.010	1053	1435	55.2	8.0

3.1.2.2 Test Data Evaluation - Basic Test Matrix. Data plots are presented in Figures 3-5 through 3-8 for the ten basic tests and four replicate tests conducted on .025 cm gage specimens in the longitudinal rolling direction. These data were for tests conducted at 978°K, 1053°K, and 1144°K, and 1255°K respectively. Data was obtained below 5 hours and is presented in Appendix C-2, however, for clarity these points are not shown in the Figures. Comparison of these plots indicates consistency in the data with respect to increasing strain with increasing stress and temperature. Comparison of replicate tests at 978°K, 1144°K, and 1255°K (Figures 3-5, 3-7, and 3-8 respectively) indicates close agreement. Replicate tests (specimens L58L and L27L at 1144°K (Figure 3-7) show the largest creep strain variation of .16% (.46% to .62% for the specimens respectively) at 60 hours. The largest variation in the other three replicates is .03% strain at 60 hours (specimens L50L and L96L).

The following equation was developed using data obtained from the hand faired curves of the basic supplemental tests 1 through 10. The data consisted of strain values taken at times of 1, 2, 5, 10 and 10 hour increments thereafter to the end of the individual test, from hand faired curves.

$$\ln\varepsilon = -3.92495 - .00237t + .45047 \ln t + 1.03087 \ln\sigma - 4.14348 \left(\frac{1}{T}\right) + .11052\ \sigma \ln T + .0000406\ (T\ \sigma\ t) \qquad (3\text{-}4)$$

The standard error of estimate (S_y) and multiple R, computed for this equation are .1499 and .9860, respectively. The residual plots ($\ln \varepsilon_{actual} - \ln \varepsilon_{calculated}$ vs. variable) for this equation are shown in Figure 3-9.

The interaction terms in this equation ($\sigma \ln T$ and $T\sigma t$) were found to significantly reduce S_y for the data since equations initially developed without these terms had S_y values in the range of .25 to .40.

Typical comparisons of creep strain predictions (based on Equation 3-4) with test results are shown in Figure 3-10 and 3-11.

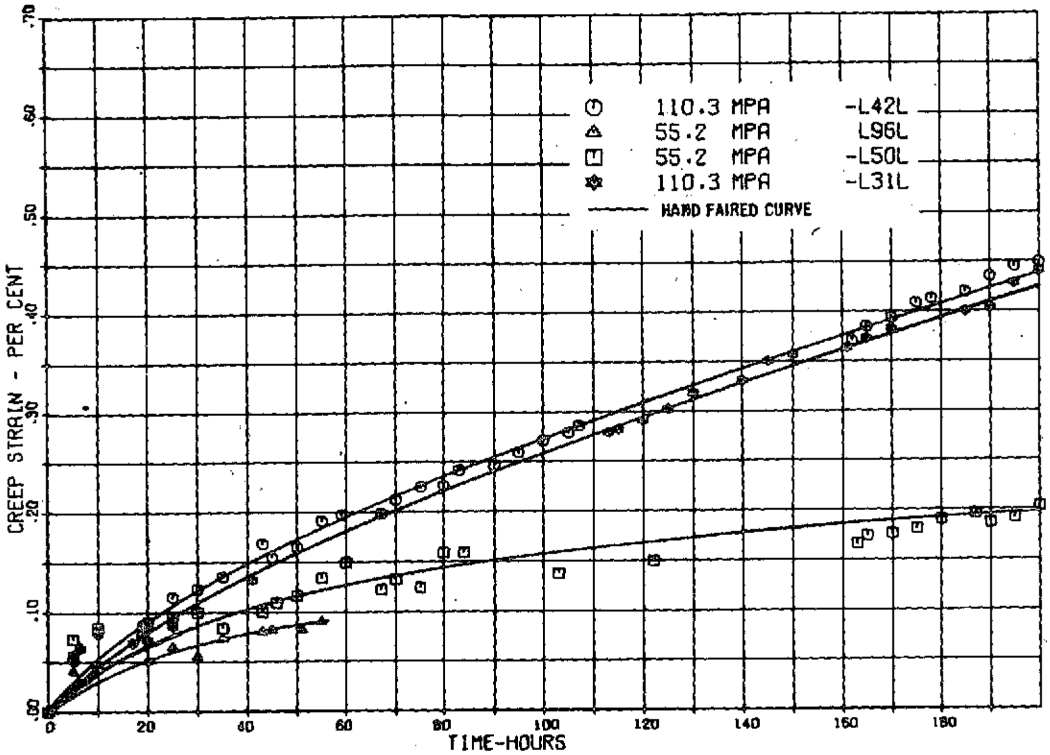

FIGURE 3-5 L605 SUPPLEMENTARY STEADY-STATE CREEP TESTS AT 978°K

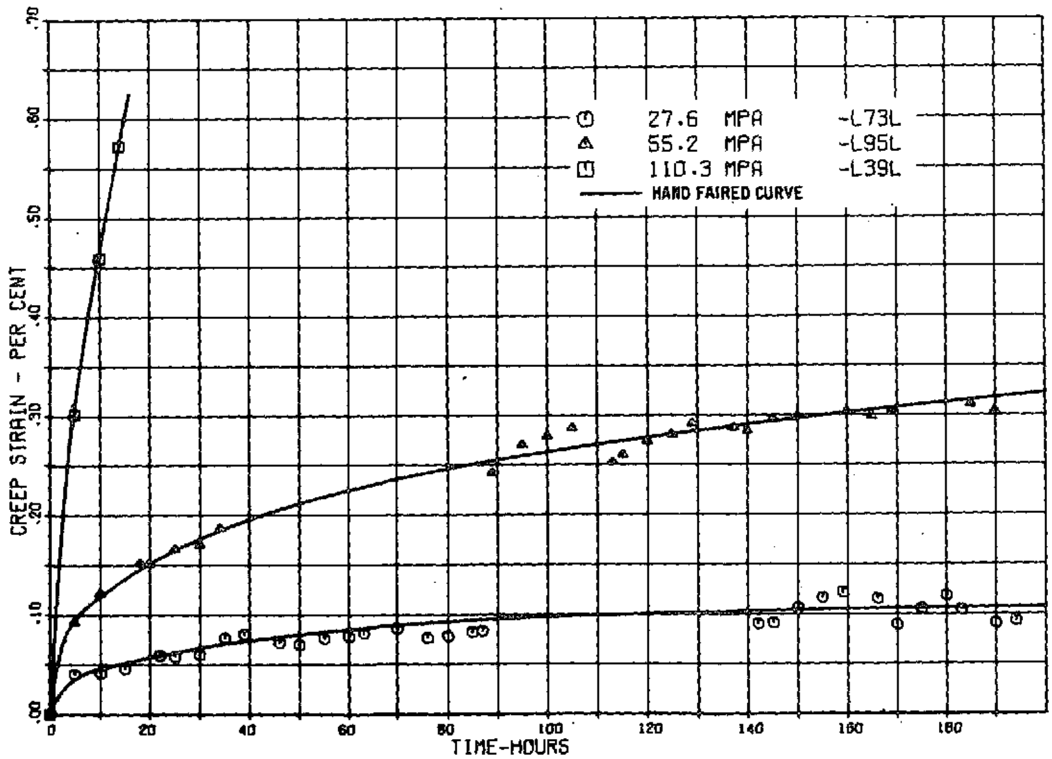

FIGURE 3-6 L605 SUPPLEMENTARY STEADY-STATE CREEP TESTS AT 1053°K

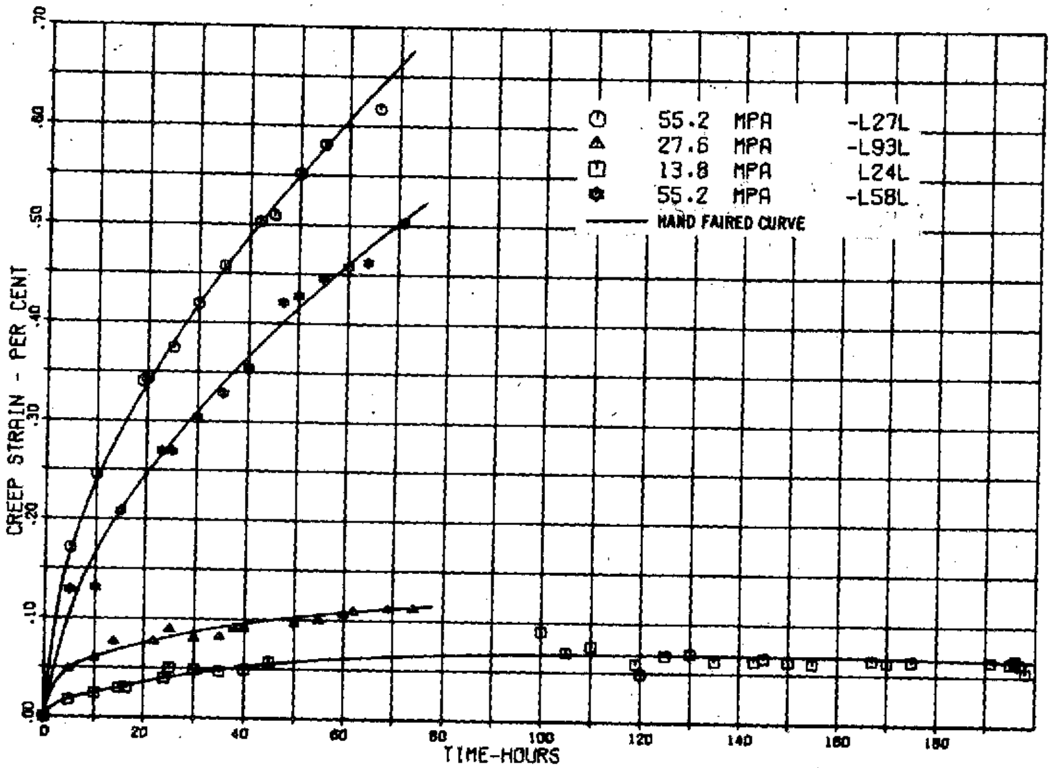

FIGURE 3-7 L605 SUPPLEMENTARY STEADY-STATE CREEP TESTS AT 1144°K

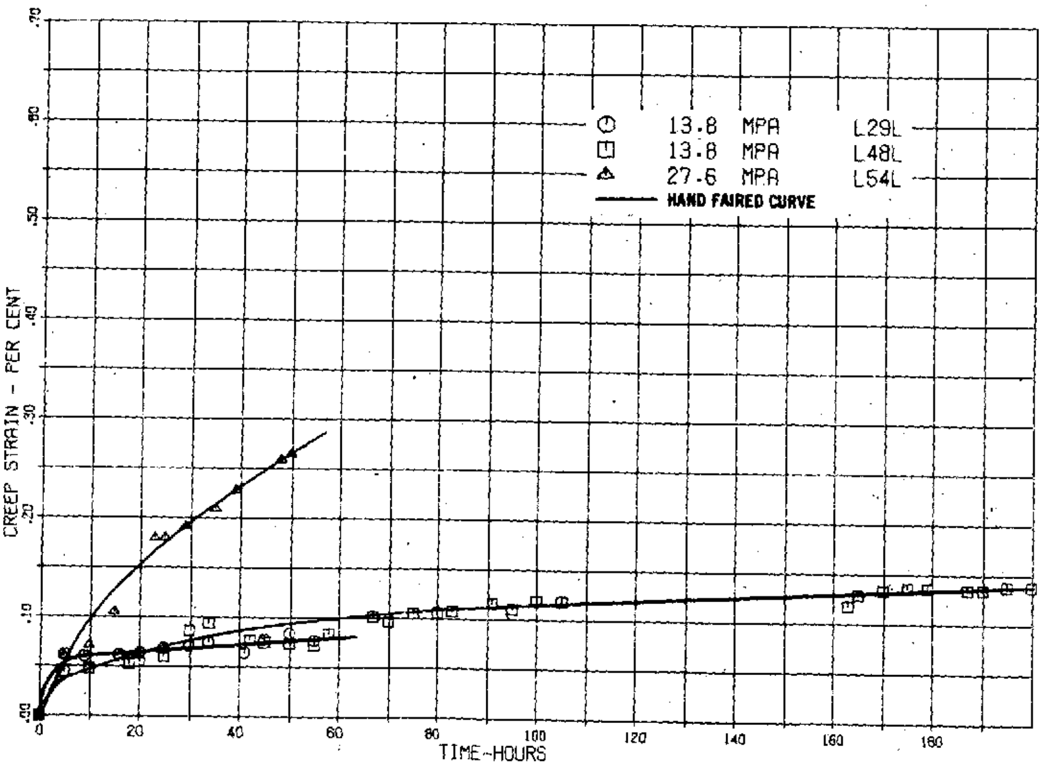

FIGURE 3-8 L605 SUPPLEMENTARY STEADY-STATE CREEP TESTS AT 1255°K

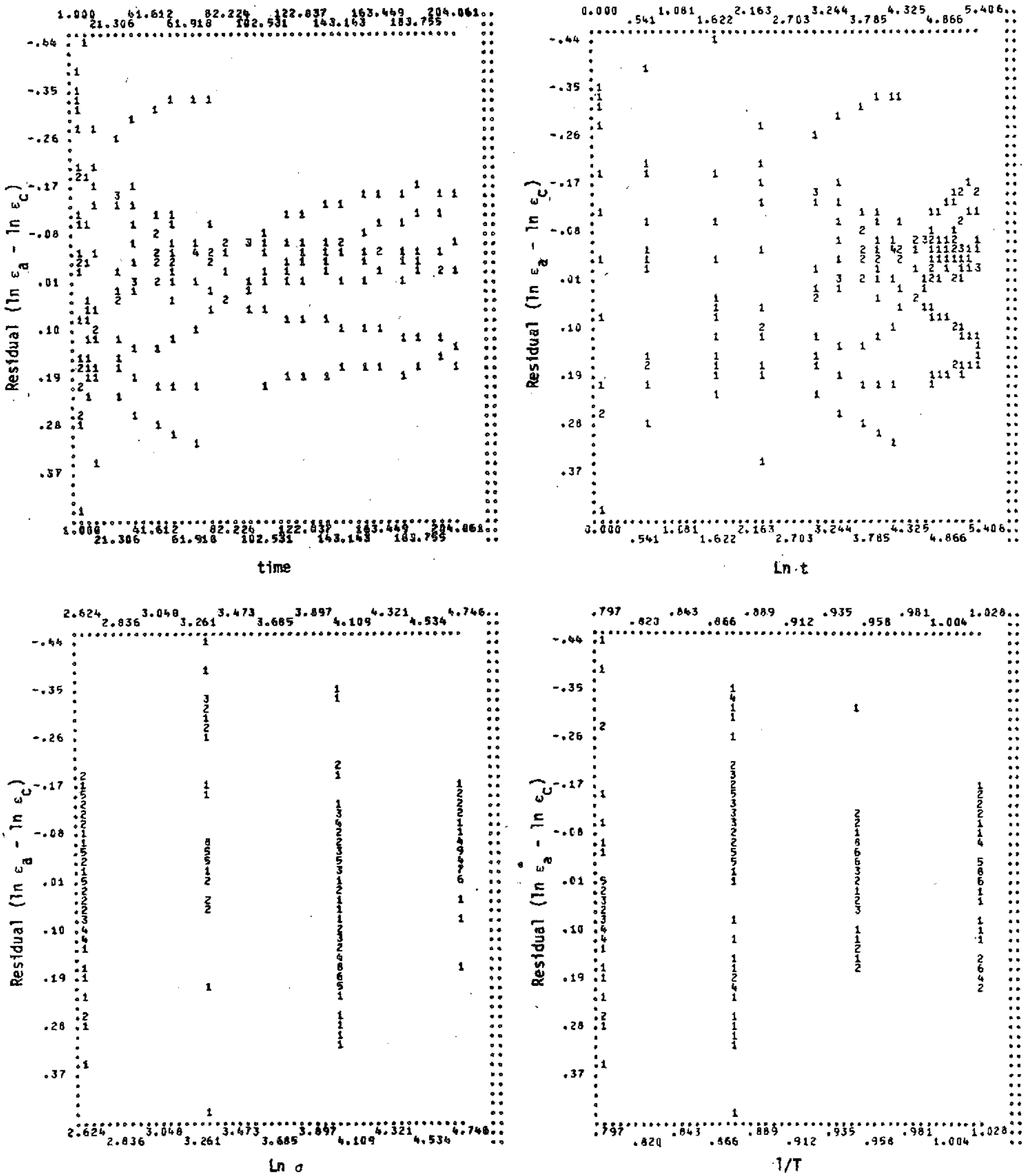

FIGURE 3-9 RESIDUAL PLOTS OF L605 SUPPLEMENTAL EQUATION (3-4)

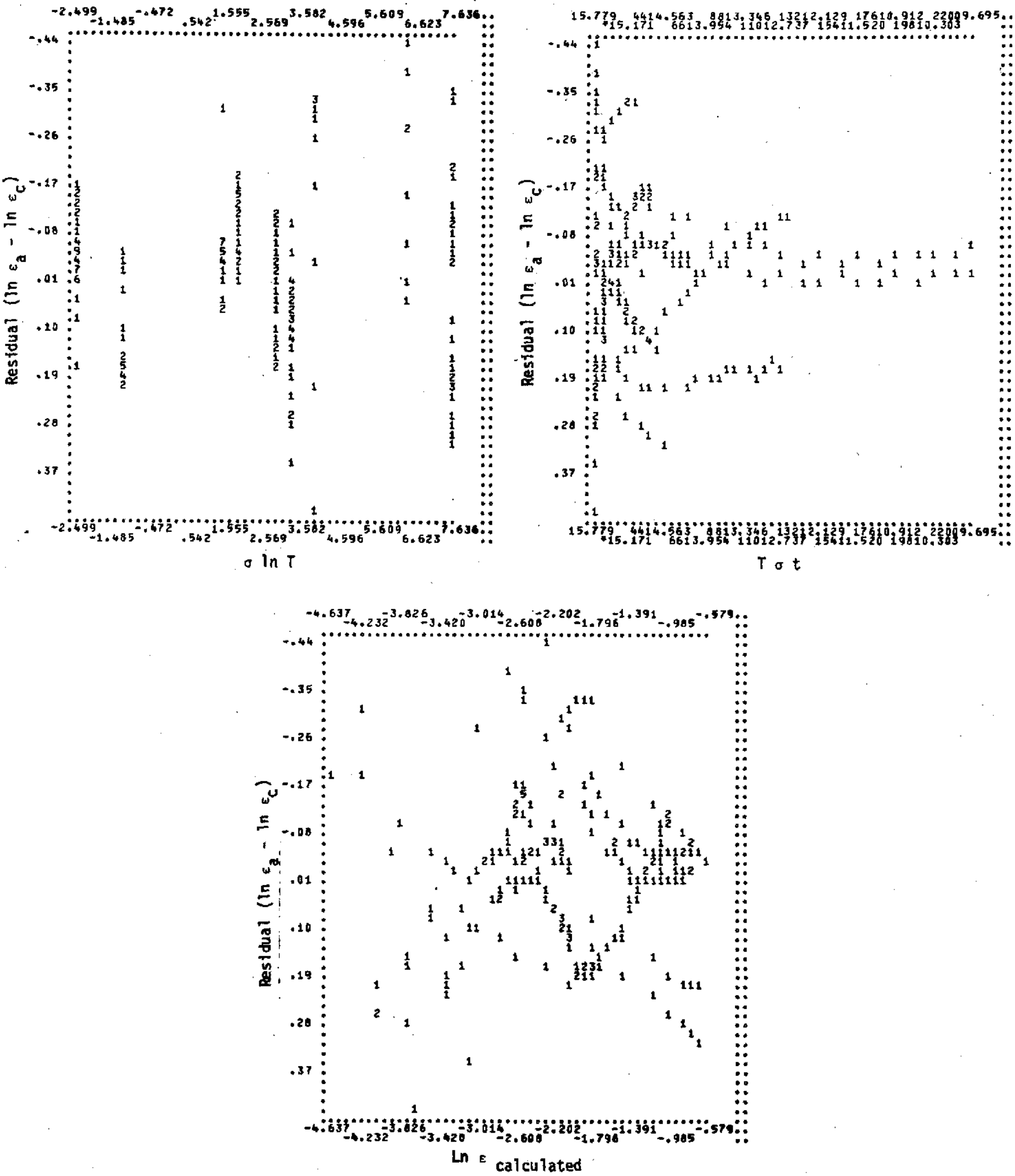

FIGURE 3–9 CONTINUATION OF RESIDUAL PLOTS OF L605 SUPPLEMENTAL EQUATION (3–4)

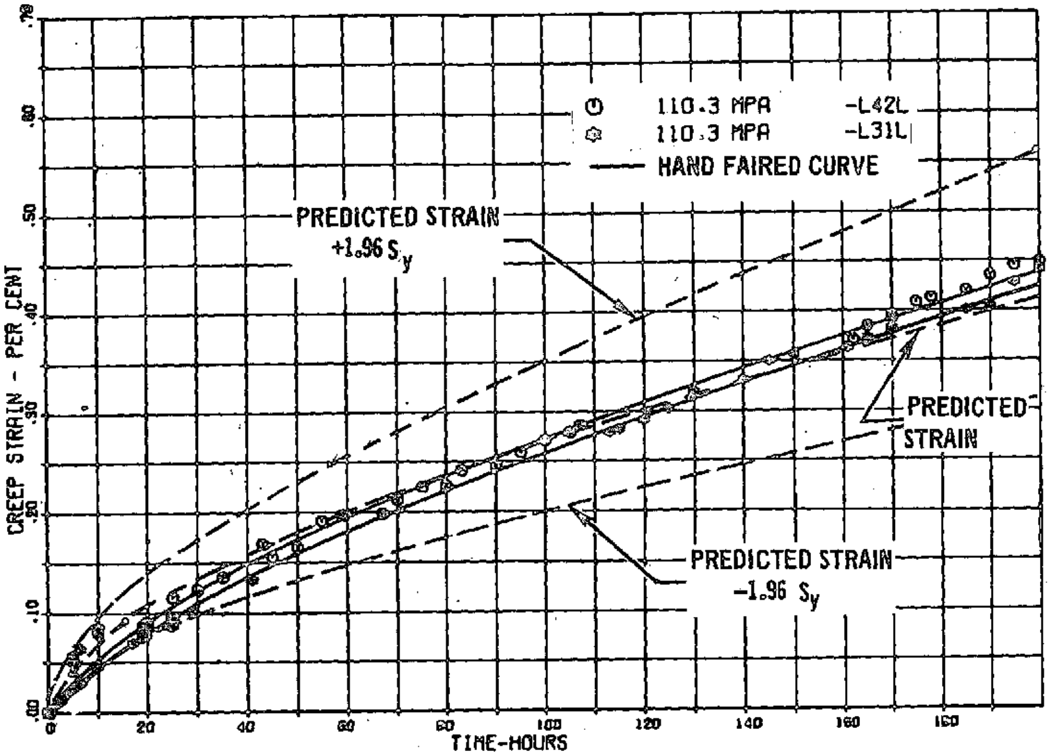

FIGURE 3-10 COMPARISON OF L605 CREEP STRAIN PREDICTIONS WITH TEST RESULTS AT 978 °K AND 110.3 MPa

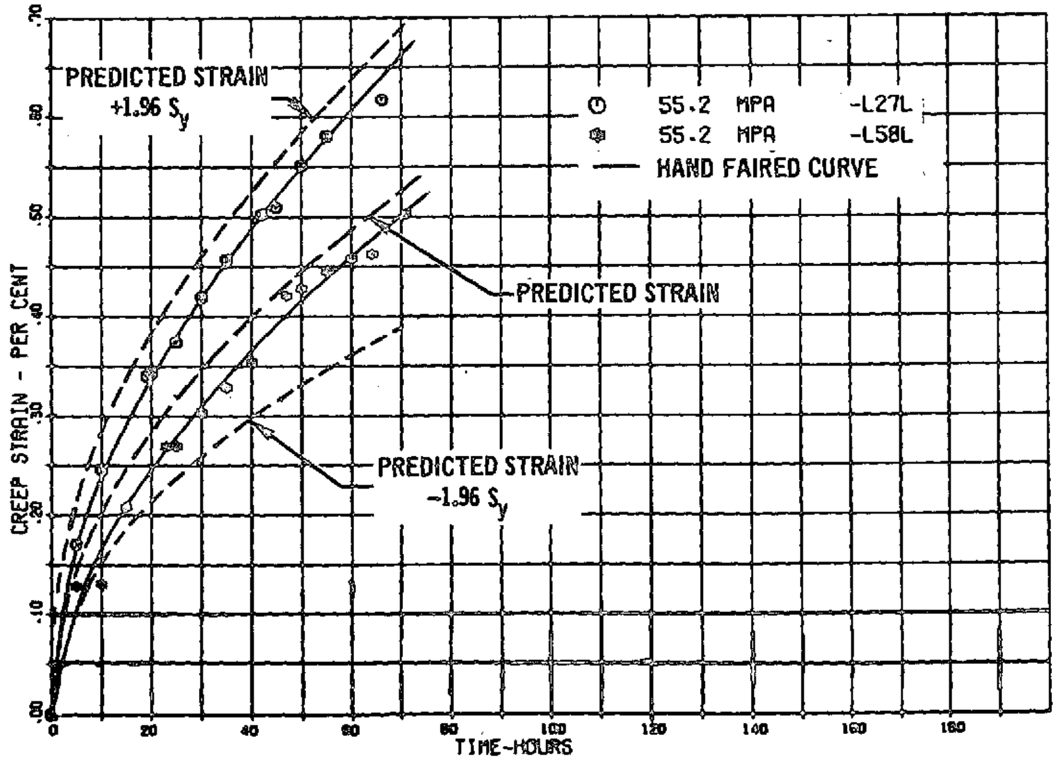

FIGURE 3-11 COMPARISON OF L605 CREEP STRAIN PREDICTIONS WITH TEST RESULTS AT 1144°K AND 55.2 MPa

3.1.2.3 Effects of Gage. Presented in Figures 3-12 through 3-14 are comparisons of creep strain data for supplemental tests conducted on .064 cm specimens with corresponding data for .025 cm specimens. Also included on the plots are the $\pm$ 1.96 S_y data bands based the standard error for Equation 3-4. In each of the three comparisons, the .064 cm specimens produced significantly lower creep strains than the .025 cm specimens.

3.1.2.4 Effect of Material Rolling Direction. Presented in Figures 3-15 through 3-17 are comparisons of creep strain data for supplemental tests conducted on transverse rolling direction specimens with corresponding data conducted on longitudinal rolling direction specimens. Also included on the plots are the $\pm$ 1.96 S_y data bands. Although the transverse test strain is less than the longitudinal test strain in two of the cases (Figures 3-15 and 3-16), it is greater than the third longitudinal test strain case (Figure 3-17). Therefore results as to the effect of this variable appear to be inconclusive.

3.1.2.5 Effect of Pre-Oxidation. Comparison of creep strain results for three specimens with a pre-oxidation coating with corresponding specimens having no coating are shown in Figures 3-18, 3-19, and 3-20. In the three cases the pre-oxidized specimen crept less than (Figure 3-18), equal to (Figure 3-19), and faster than (Figure 3-20), the corresponding non-pre-oxidized specimen respectively. Therefore, it is concluded that the pre-oxidation does not appear to significantly effect the specimen creep response.

3.1.3 COMPARISON OF L605 STEADY-STATE DATA BASE AND SUPPLEMENTAL TEST RESULTS

The following empirical equation was developed, using the dummy variable technique, for purposes of comparing the L605 data base and supplemental test data.

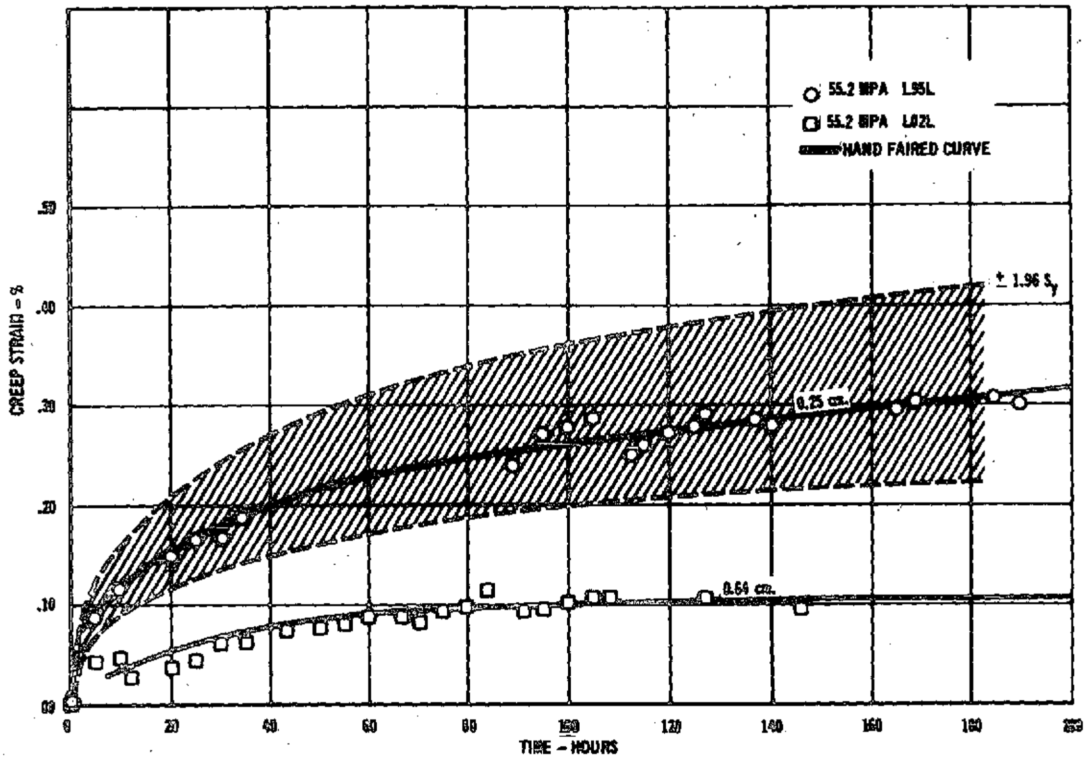

FIGURE 3-12 EFFECT OF GAGE ON L605 CREEP AT 1053 °K AND 55.2 MPa

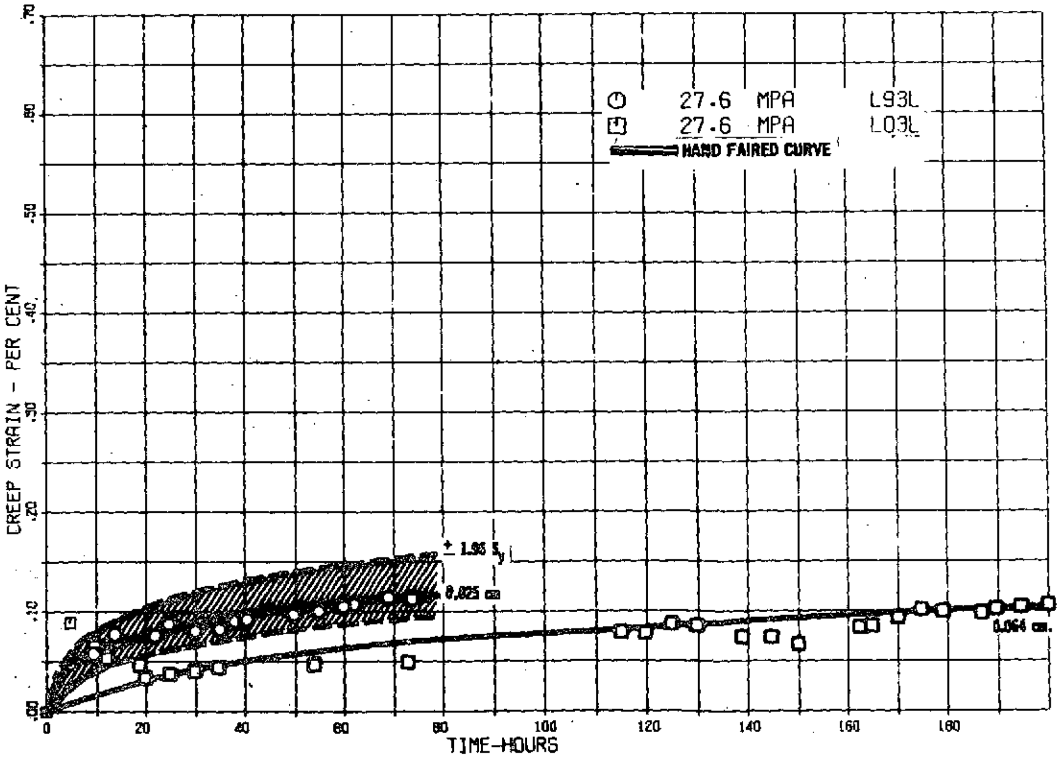

FIGURE 3-13 EFFECT OF GAGE IN L605 CREEP AT 1144 °K AND 27.6 MPa

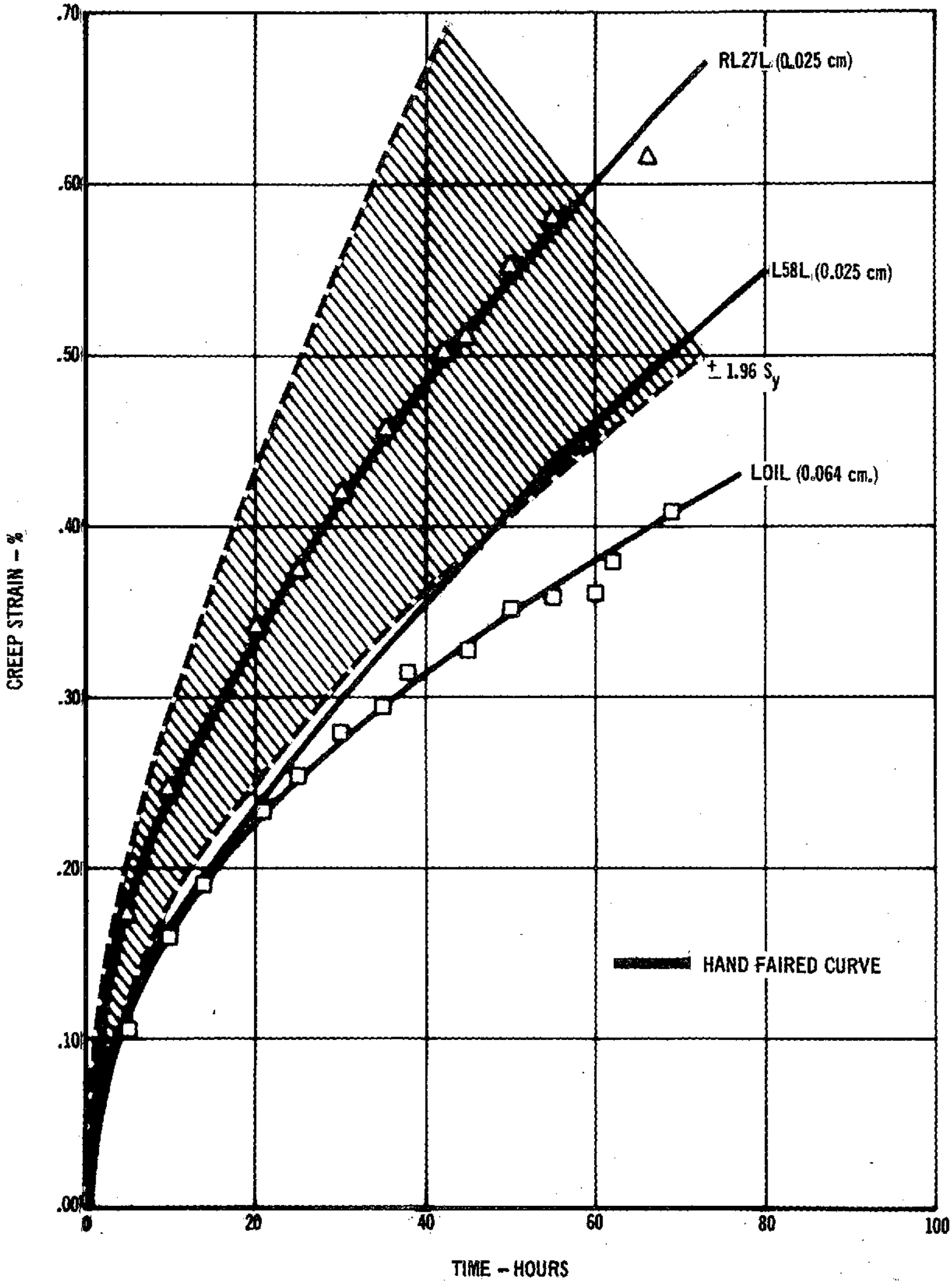

FIGURE 3-14 EFFECT OF GAGE ON L605 CREEP AT 1144°K AND 55.2 MPa

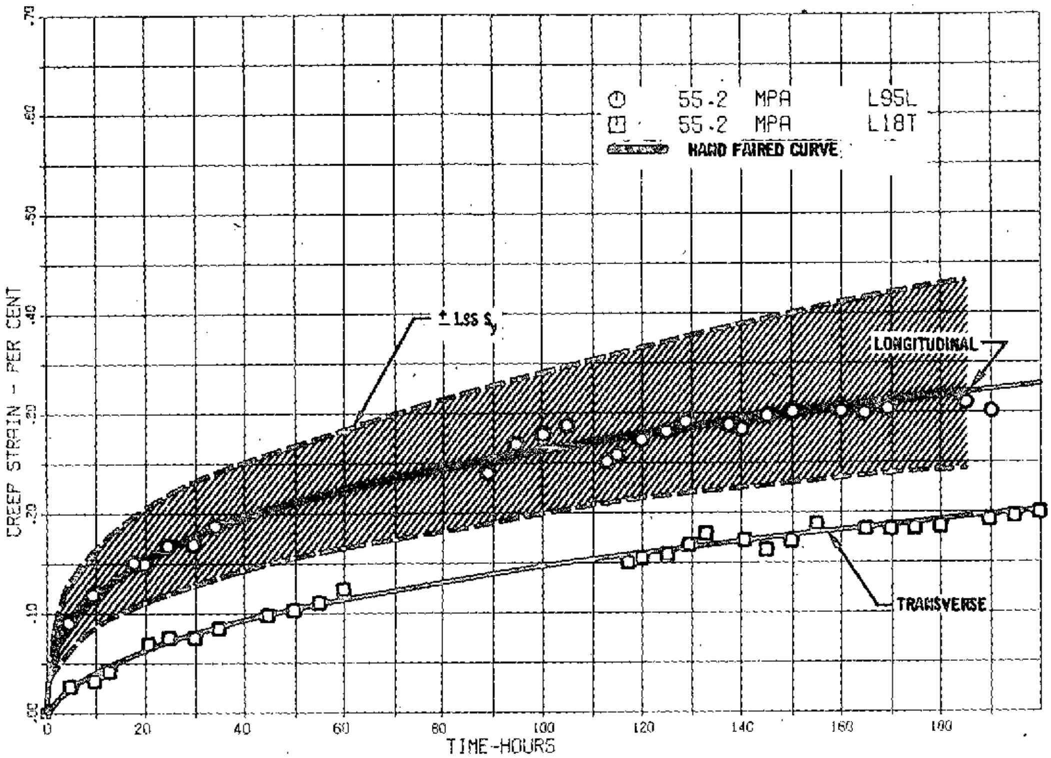

FIGURE 3-15 EFFECT OF ROLLING DIRECTION ON L605 CREEP AT 1053°K AND 55.2 MPa

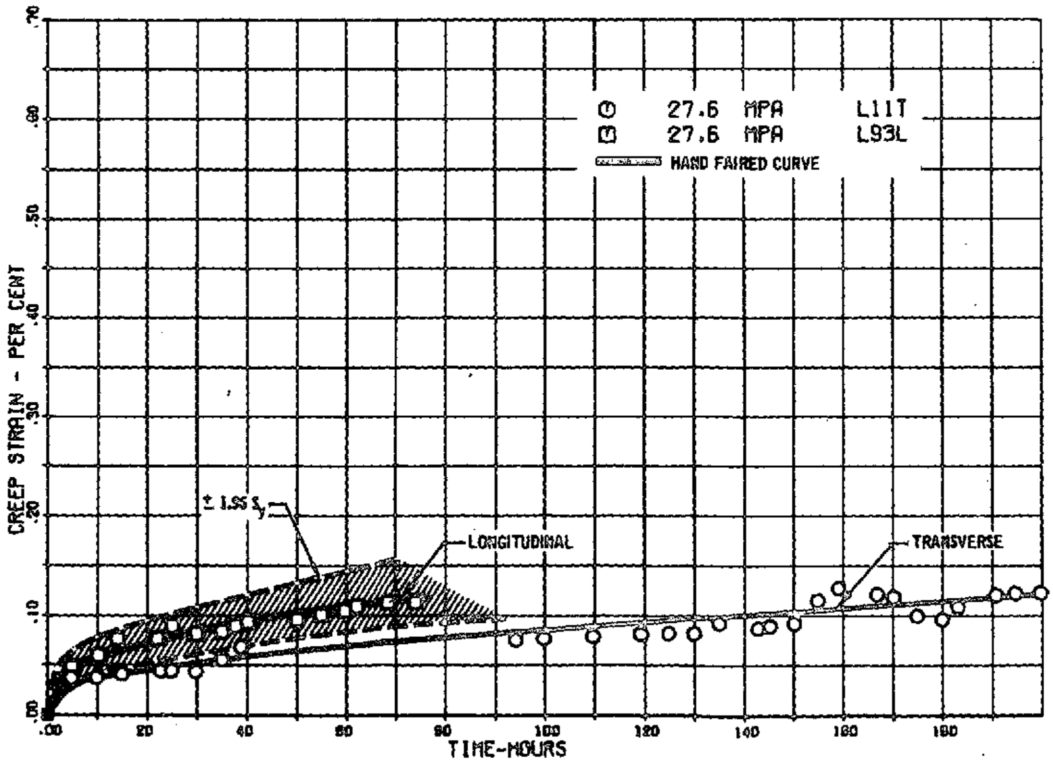

FIGURE 3-16 EFFECT OF ROLLING DIRECTION ON L605 CREEP AT 1144°K AND 27.6 MPa

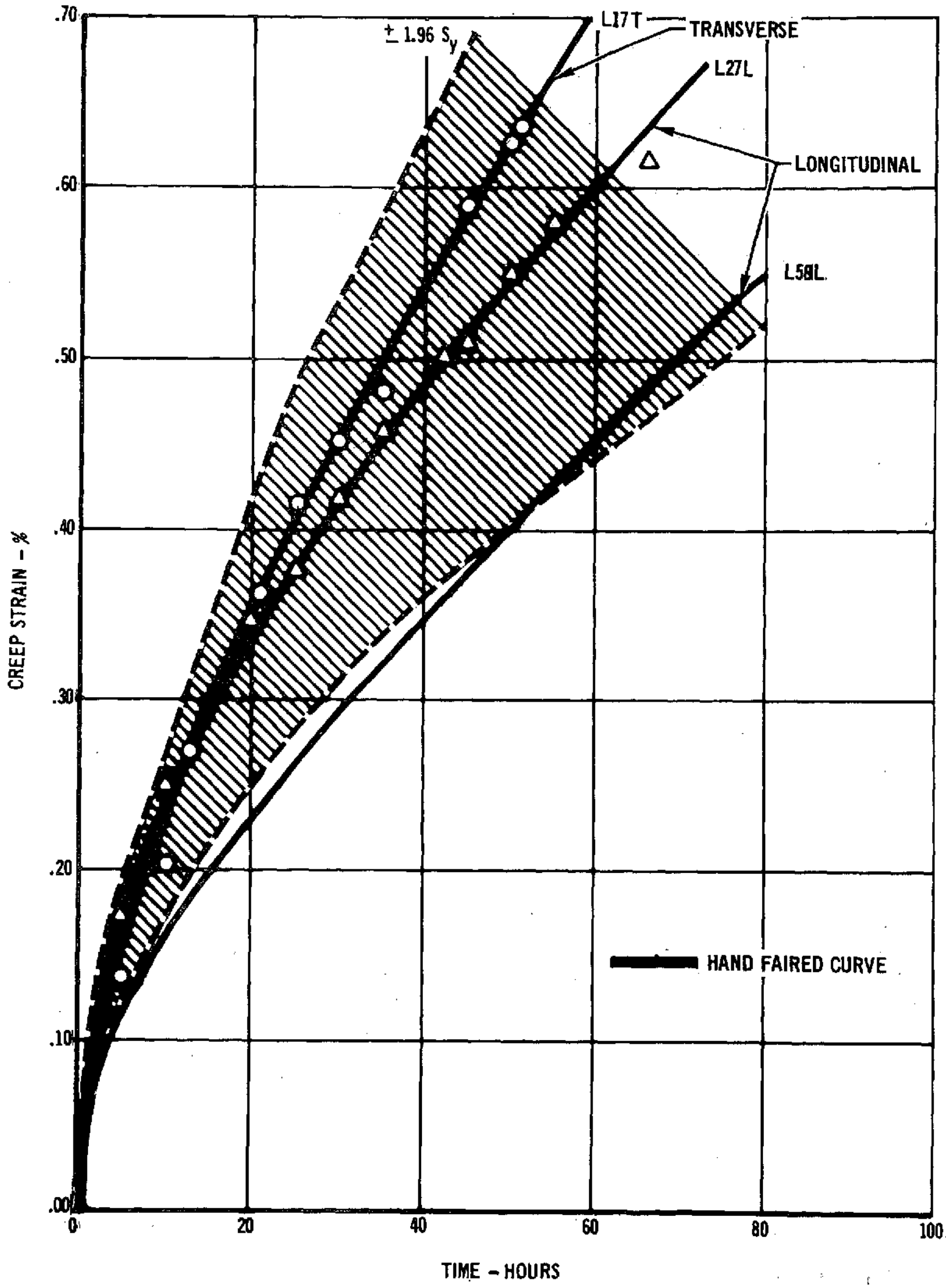

FIGURE 3–17 EFFECT OF ROLLING DIRECTION ON L605 CREEP AT 1144°K AND 55.2 MPa

C-2

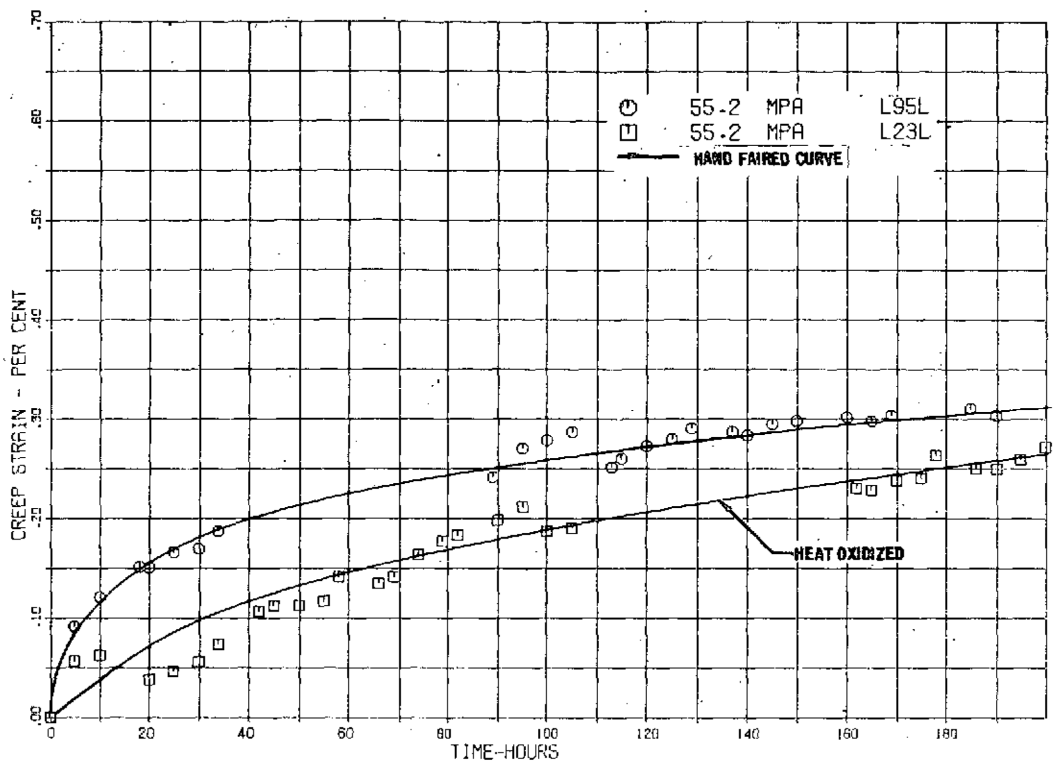

FIGURE 3–18 EFFECT OF PREOXIDATION ON CREEP OF L605 AT 1053°K AND 55.2 MPa

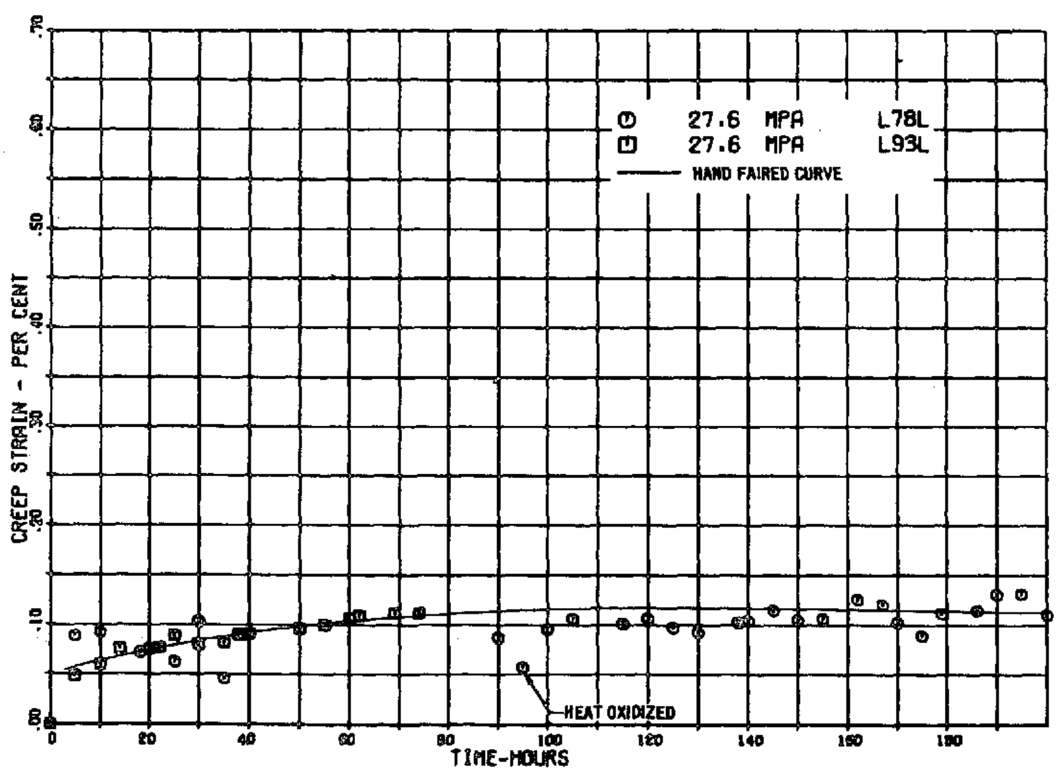

FIGURE 3–19 EFFECT OF PREOXIDATION ON CREEP OF L605 AT 1144° AND 27.6 MPa

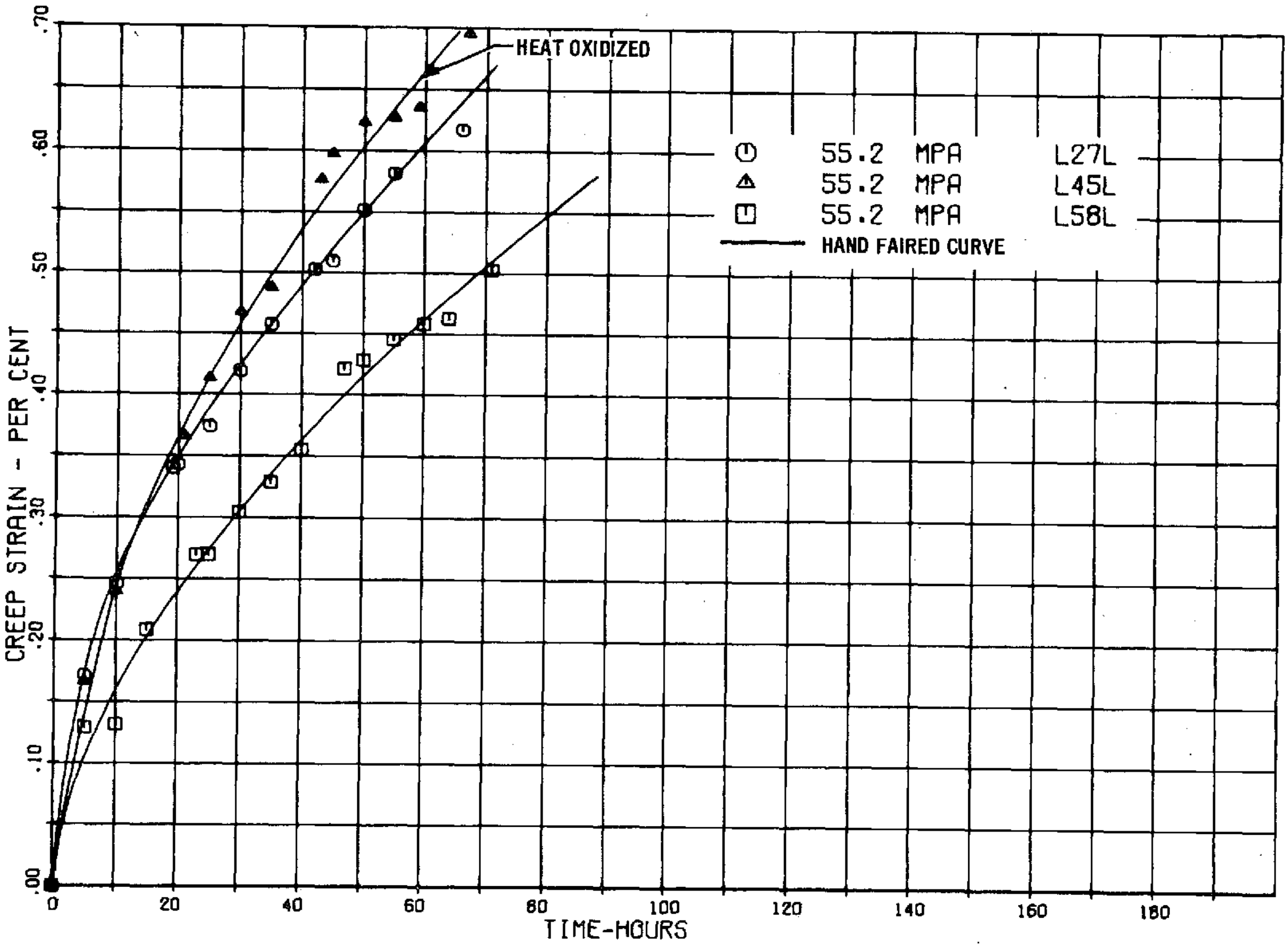

FIGURE 3–20 EFFECT OF PREOXIDATION ON CREEP OF L605 AT 1144°K AND 55.2 MPa

$$\ln\varepsilon = 2.553 + .336 \ln t + 1.145 (\ln\sigma - 1.931) - .243 (\ln\phi - .932) - 9{,}691 (1/T) + .081 Z(\ln t) + .327 Z (\ln\sigma - 1.931) + .246 Z (\ln\phi - .932) \quad (3\text{-}5)$$

where ε = creep strain, %

t = time, hours

σ = stress, MPa

T = Temperature, °K/1000

ϕ = material thickness, cm

$Z = \begin{matrix} 0 & \text{, Data Base} \\ 1 & \text{, Supplemental Data} \end{matrix}$

Because the Z terms are significant in fitting the data, it is concluded that there is a difference between the supplemental test data and the data base. It is of interest to note from the equation that for the supplemental data (Z = 1) the thickness terms cancel each other. This is because only the basic matrix of data (.025 cm) were used in the comparison.

There is a difference in the manufacturing process between thin gage (<.064 cm) and thicker gage material, based on contact with the material supplier. This processing difference, which occurs at approximately .063 cm, appears to be the cause of variations in creep response attributed to gage in both the data base (Section 3.1.1.2) and the supplemental tests (Section 3.1.2.3).

To investigate this, comparisons of data were made as shown in Figure 3-21 for 30 and 60 hours. The comparison in the figure is for tests at 1144°K where close agreement in the data base and supplemental data were found. These plots indicate that the data falls into two groups; (1) data for tests conducted are .013 cm and .025 cm specimens and, (2) data for tests conducted on

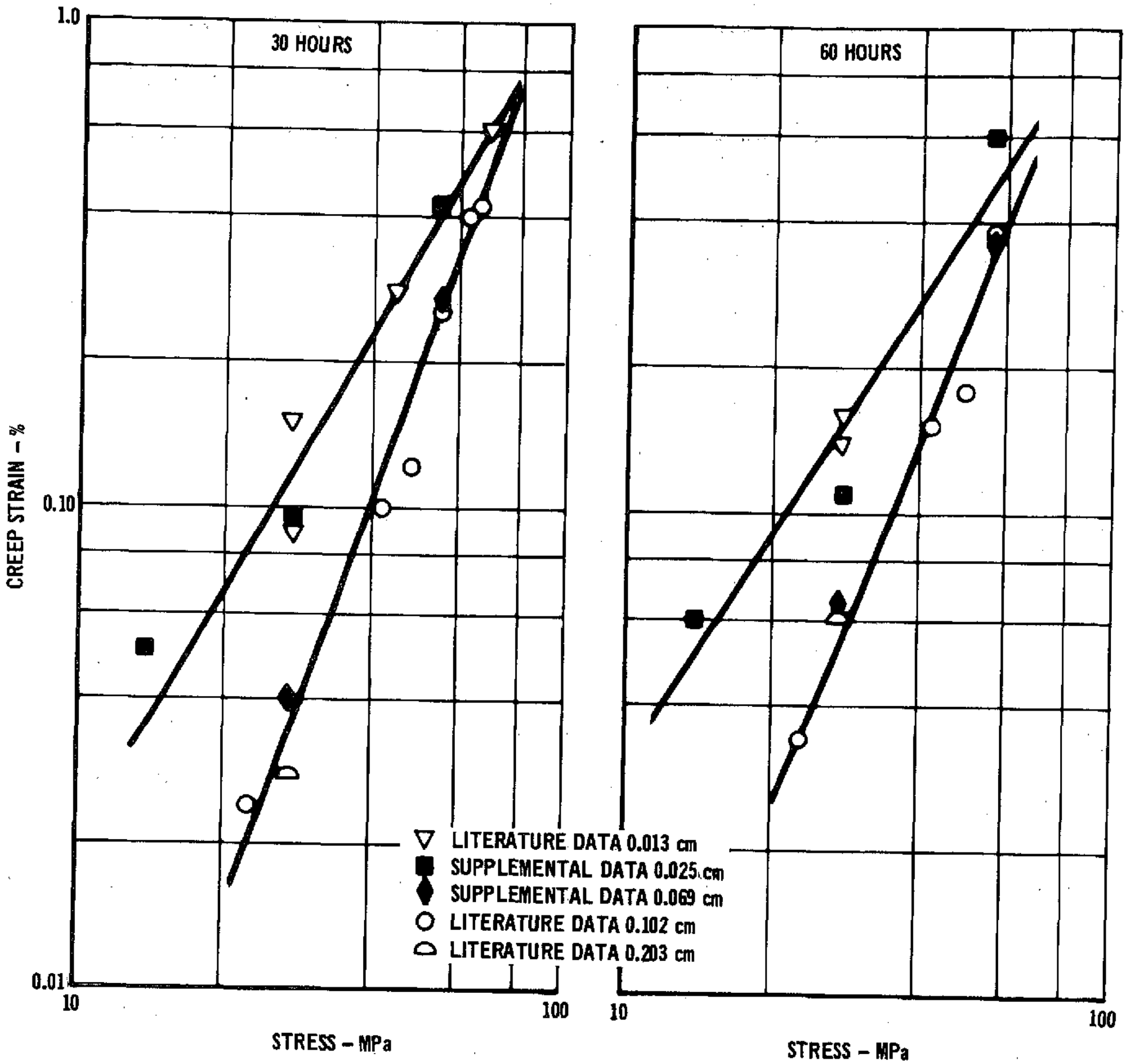

FIGURE 3–21 COMPARISON OF CREEP DATA FOR THICKNESS < 0.063 AND > 0.063 cm

.064 cm, .102 cm., and .203 cm specimens. Therefore, the "gage" effect appears to be a step difference attributable to manufacturing processing rather than a continuous gage effect as implied in the literature survey equation (Equation 3-3).

3.1.4 L605 BASIC CYCLIC TESTS

3.1.4.1 Basic Cyclic Test Matrix. Four 100 cycle tests (3 specimens per test) were conducted on .025 cm gage specimens to form the basic cyclic test matrix from which an empirical equation for cyclic creep can be derived. Each of the specimens was tested in the longitudinal rolling direction. Combinations of stress and temperature for these twelve specimens were based on the box type of experimental design (see Section 2.9.1.1) as shown in Figure 3-22. and listed in Table 3-2. The test temperatures of 978, 1053, 1144, and 1255°K are the same as those used for steady-state testing to allow direct comparison of results. The specific stress levels attained in testing, as listed in the table, are 100 cycle averages obtained using the whiffle tree test fixture (Section 2.8.1). The time at load for each cycle was 20 minutes, and total cycle time was 55 minutes including heat up and cool down portions of the profile.

This portion of the cyclic tests are designated as L605 cyclic tests 1 through 4. Data are presented in Appendix C-3.

3.1.4.2 Test Results and Analysis. Cyclic creep strain results for the twelve specimens in test 1 through 4 are presented in Figures 3-23 through 3-26.

The following equation was developed using data obtained from the hand faired curves of these twelve cyclic tests. This data consisted of strain values taken at 5 cycle intervals from the hand faired curves. Creep times were the accumulated cycle time at maximum load and temperature, therefore for the basic cycles the time was .33 hrs/cycle or 1.67 hrs/5 cycles.

$$\ln \varepsilon_{cy} = -2.89413 - .01743t + .54892 \ln t + 1.31015 \ln\sigma - 6.66548 (1/T) + .19131\, \sigma \ln T + .00021 (T\sigma t). \quad (3\text{-}6)$$

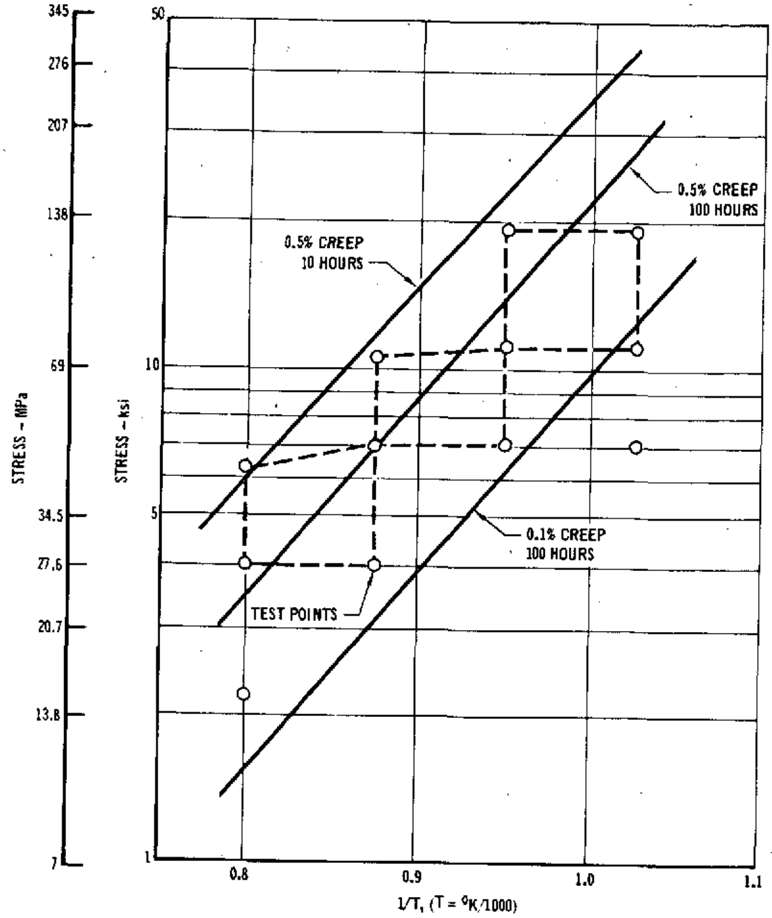

FIGURE 3–22 L605 BASIC CYCLIC EXPERIMENT DESIGN

TABLE 3–2
L605 BASIC CYCLIC TEST MATRIX

TEST NO.	SPECIMEN	TEST TEMPERATURE °K	TEST TEMPERATURE °F	STRESS MPa	STRESS ksi
1	L44L L52L L57L	978	1300	129.0 52.2 80.7	18.7 7.4 11.7
2	L36L L76L L101L	1053	1435	128.0 52.2 83.4	18.5 7.57 12.1
3	L53L L61L L37L	1144	1600	29.6 47.2 73.5	4.30 6.85 10.7
4	L65L L70L L91L	1255	1800	33.8 13.2 20.5	4.90 1.92 2.98

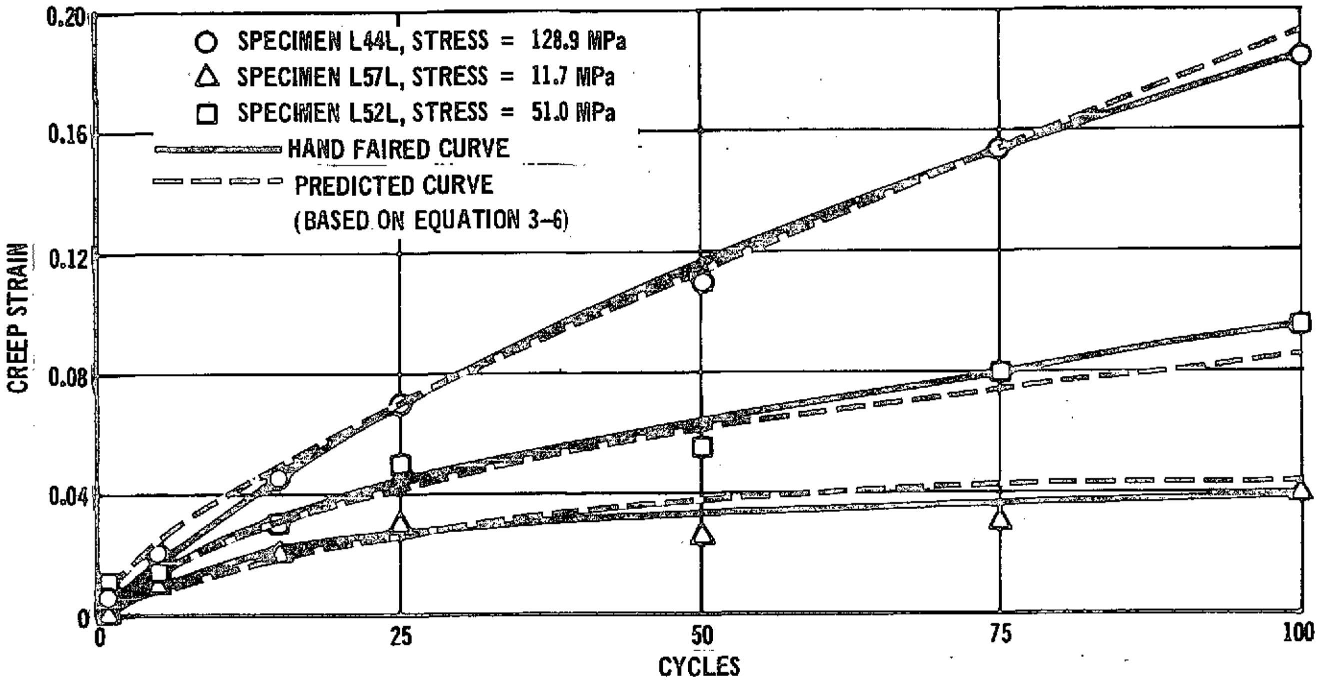

FIGURE 3-23 L-605 BASIC CYCLIC CREEP TEST AT 978°K

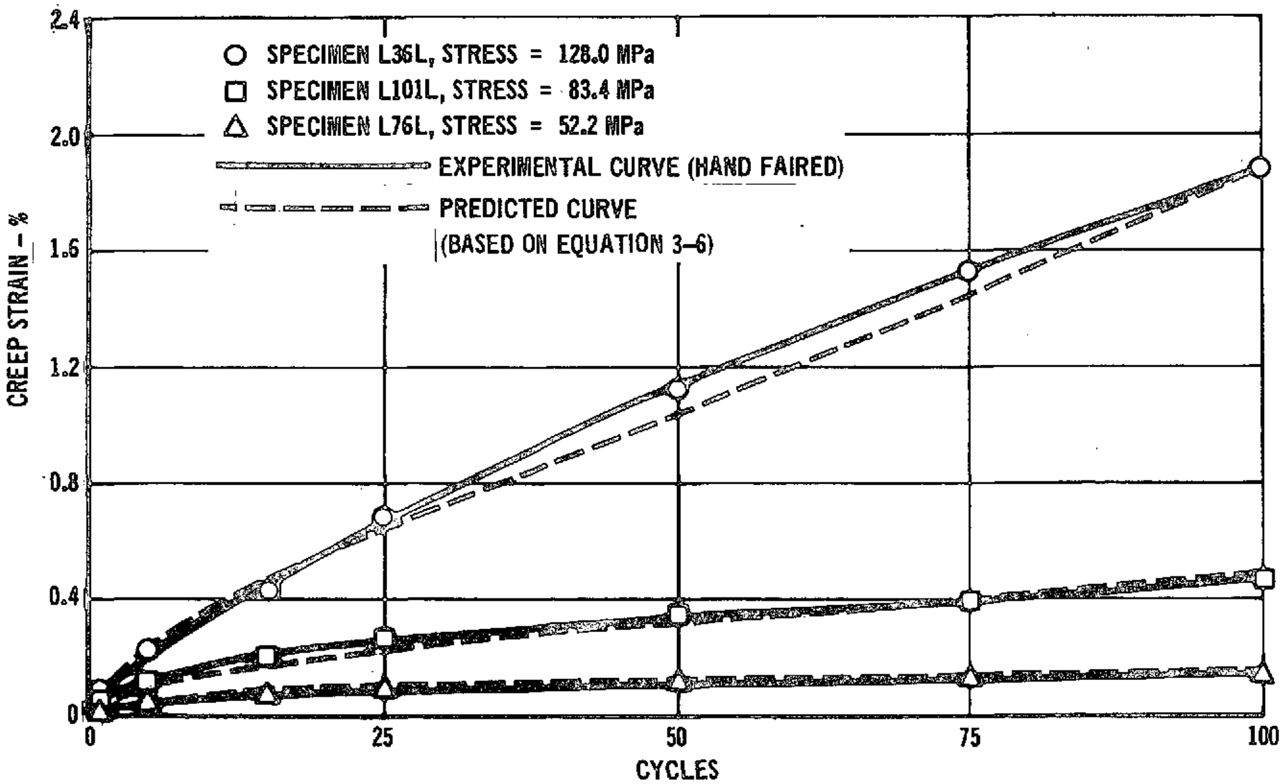

FIGURE 3-24 L-605 BASIC CYCLIC CREEP TEST AT 1053°K

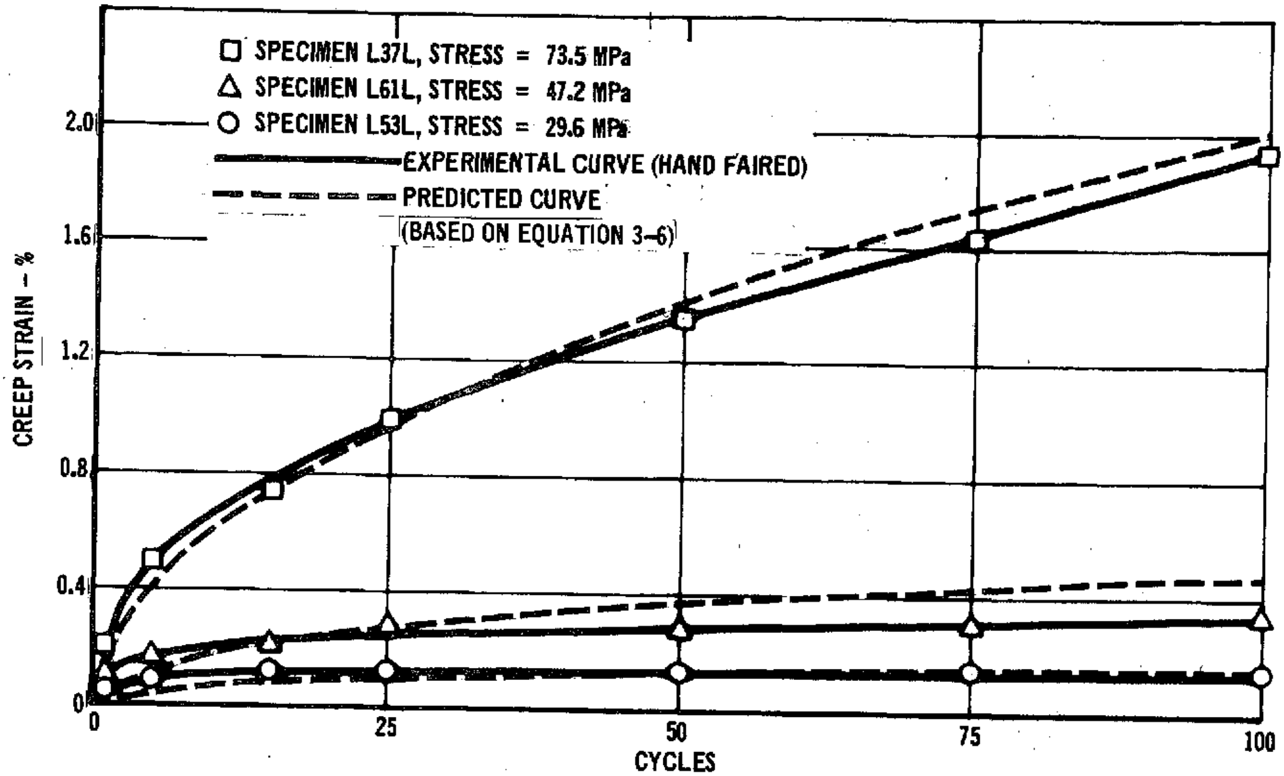

FIGURE 3-25 L-605 BASIC CYCLIC CREEP TEST AT 1144°K

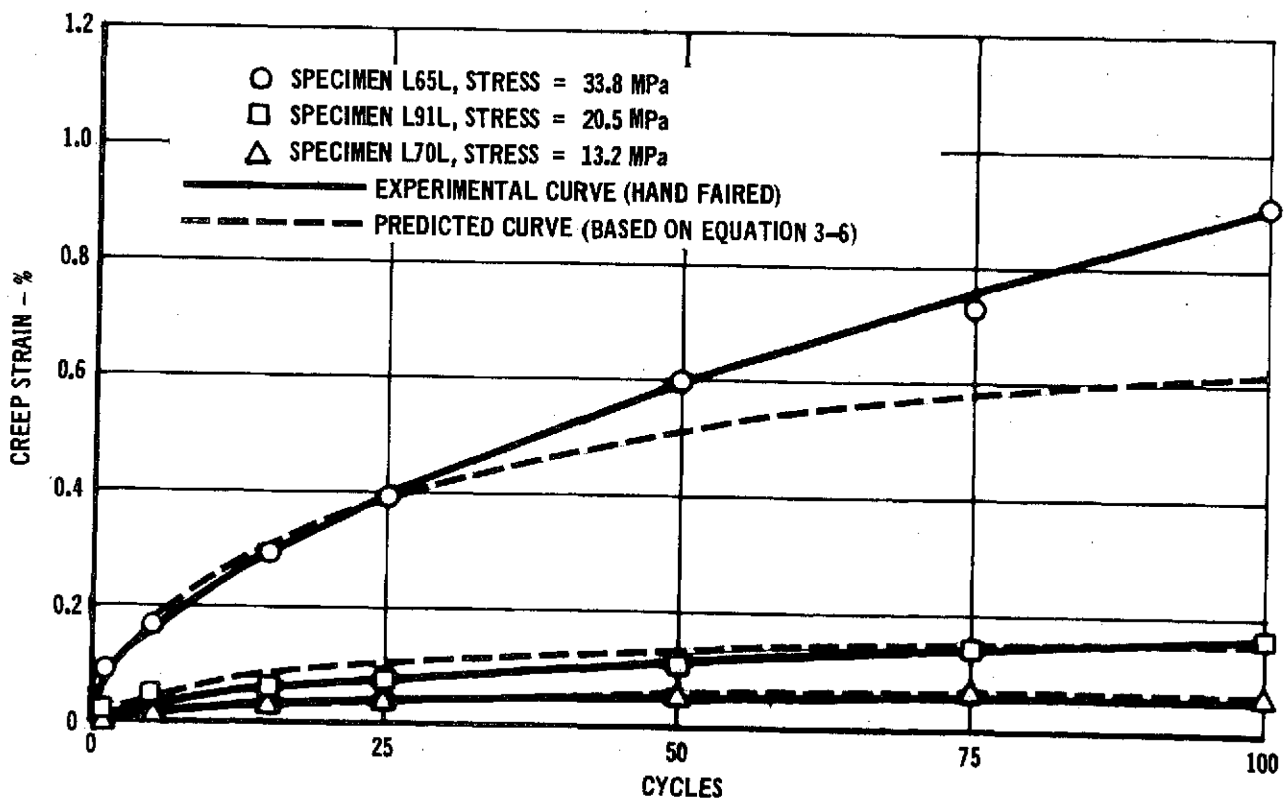

FIGURE 3-26 L-605 BASIC CYCLIC CREEP TEST AT 1255°K

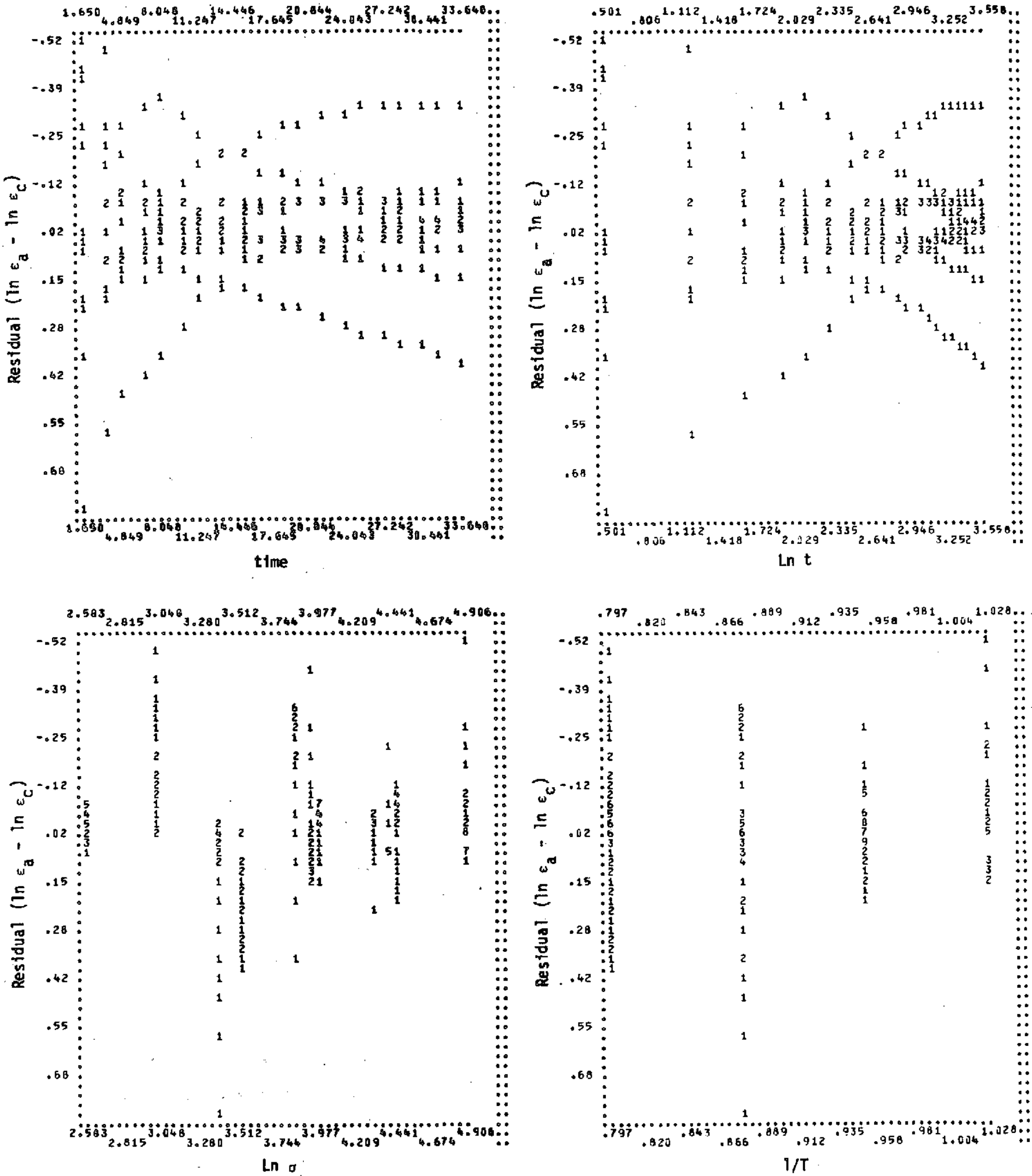

FIGURE 3-27 RESIDUAL PLOTS OF L605 CYCLIC EQUATION (3-6)

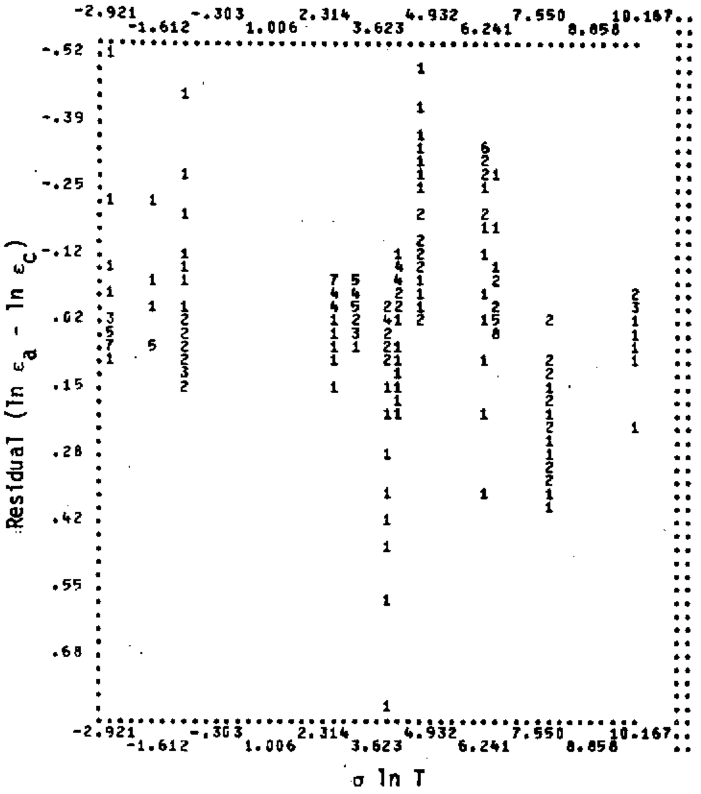

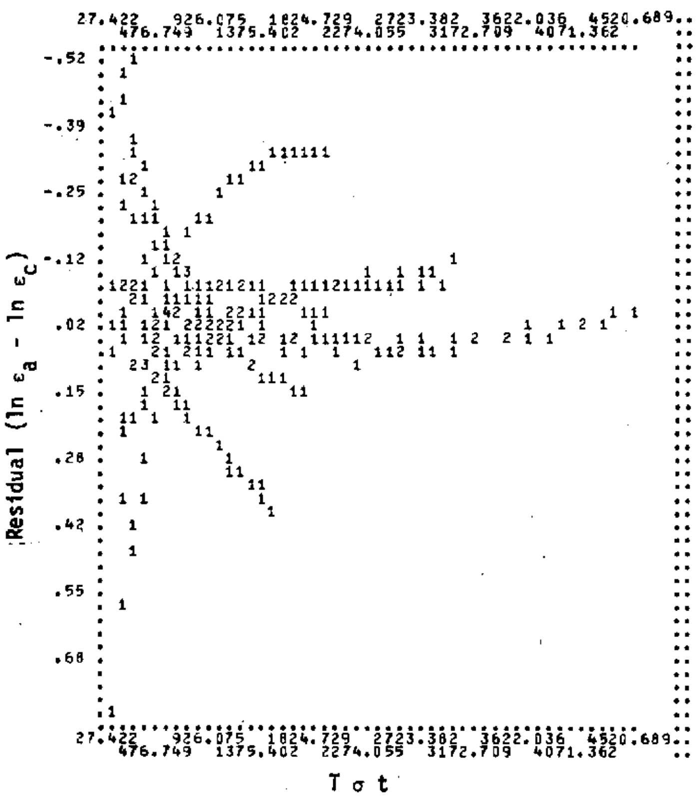

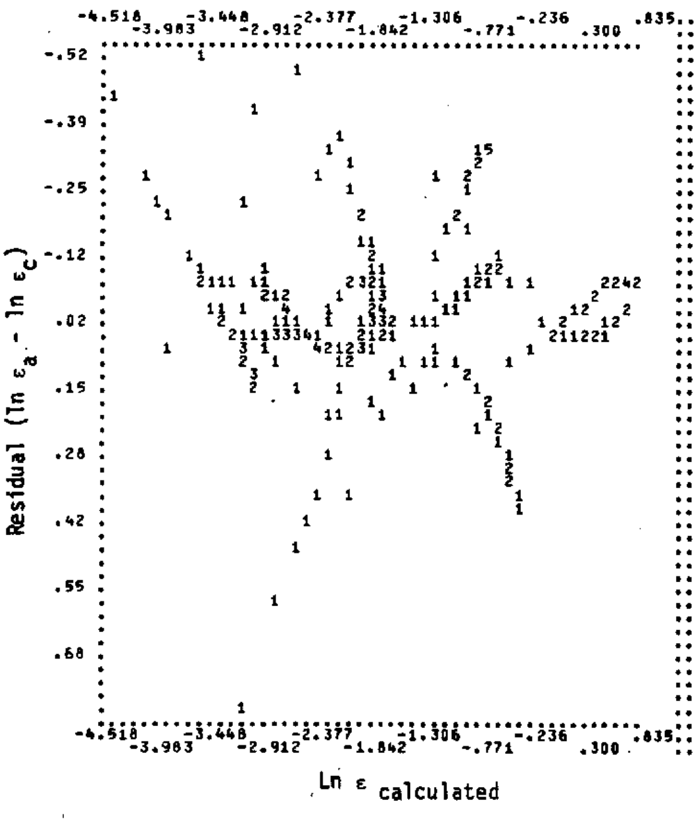

FIGURE 3–27 CONTINUATION OF RESIDUAL PLOTS OF L605 CYCLIC EQUATION (3–6)

The standard error of estimate (S_y) and multiple R computed for this equation are .1711 and .9904, respectively. The residual plots ($\ln \varepsilon_{actual} - \ln \varepsilon_{calculated}$ vs. variable) for the equation are shown in Figure 3-27.

Several equation forms which did not involve interaction terms were also explored. Equations containing interaction terms provided better fit of the data than those which did not contain interactions terms. Material gage is not a variable since all the data is for .025 cm specimens. The low value for the standard error of estimate and the high value for multiple R in the equation indicates that the empirical relationship, shown in this equation, describes the experimentally observed L605 cyclic creep response very well. This is illustrated in Figures 3-23 through 3-26 where the cyclic creep responses predicted by this Equation are shown together with the experimentally observed data for each of the Basic Cyclic Tests.

It should be noted that the cyclic creep equation (Equation 3-6) is only valid within the range of time, temperature, and stress values from which it was computed. The temperature range was 978°K to 1255°K. The stress range was 13.2 to 128.9 MPa. The time range was 0 to 33 hours. Outside of the data range invalid predictions may occur especially for times greater than 33 hours. Because of the functional form of the cyclic creep equation (Equation 3-6) calculated strains decrease with increasing times greater than 33 hours. This trend can be seen in Figure 3-28.

3.1.5 COMPARISON OF L605 CYCLIC AND SUPPLEMENTAL STEADY-STATE DATA

3.1.5.1 Test Data Comparison. Presented in Figures 3-29 and 3-30 are comparisons of L605 cyclic and steady-state data for times of 15 hours and 30 hours respectively. In this comparison the cyclic time was the accumulated time at maximum load and temperature (i.e., 100 cycles = 33.3 hours). Based on the close agreement in these data sets, it is concluded that no significant difference exists.

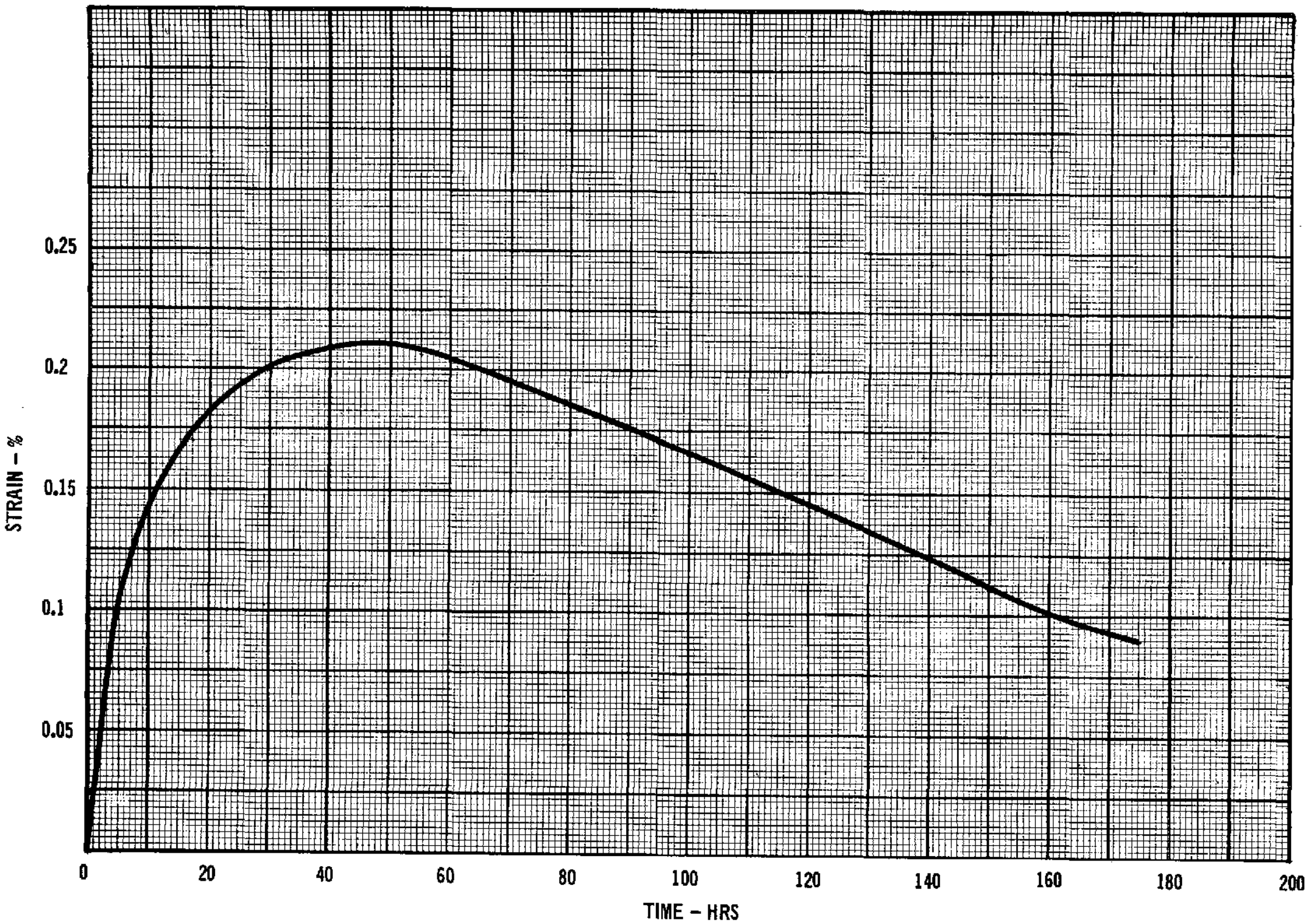

FIGURE 3-28 CHANGE IN STRAIN AS A FUNCTION OF TIME USING EQUATION (3-6)

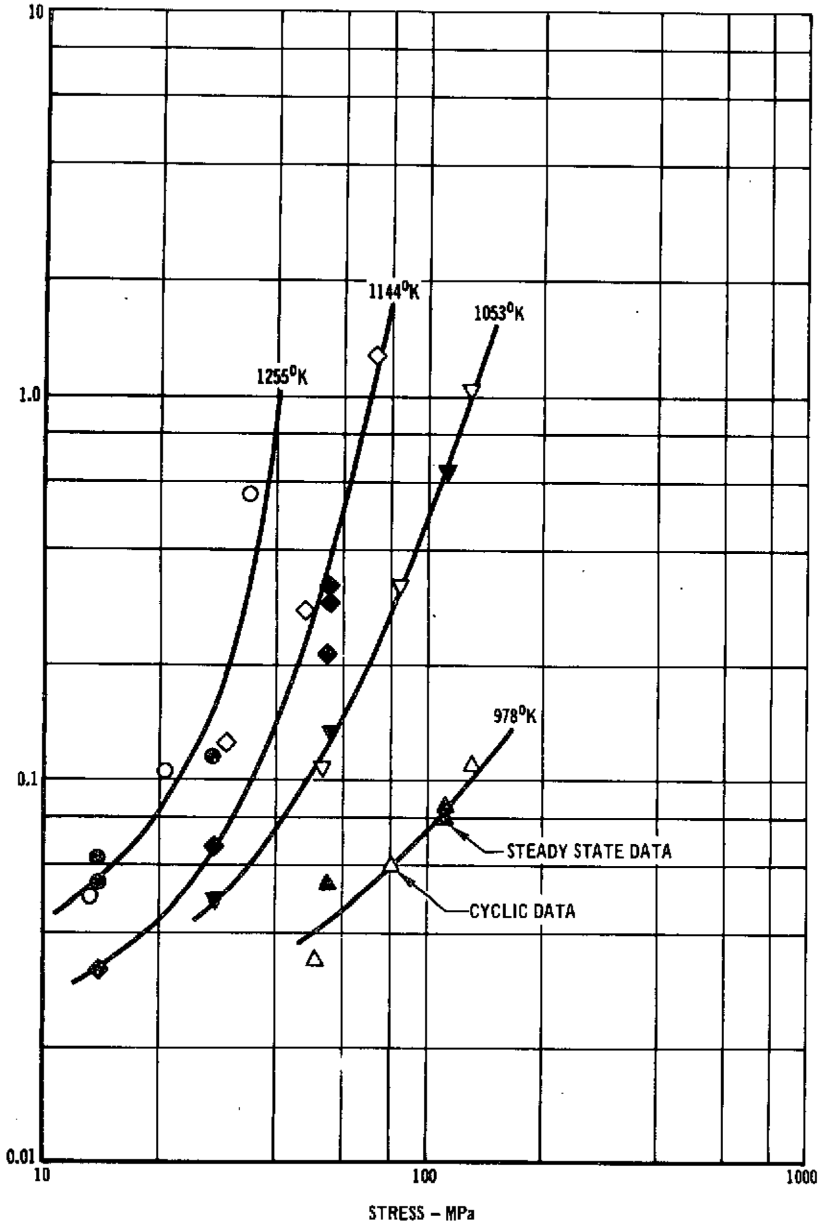

FIGURE 3–29 COMPARISON OF L605 CYCLIC AND STEADY-STATE DATA AT 15 HOURS

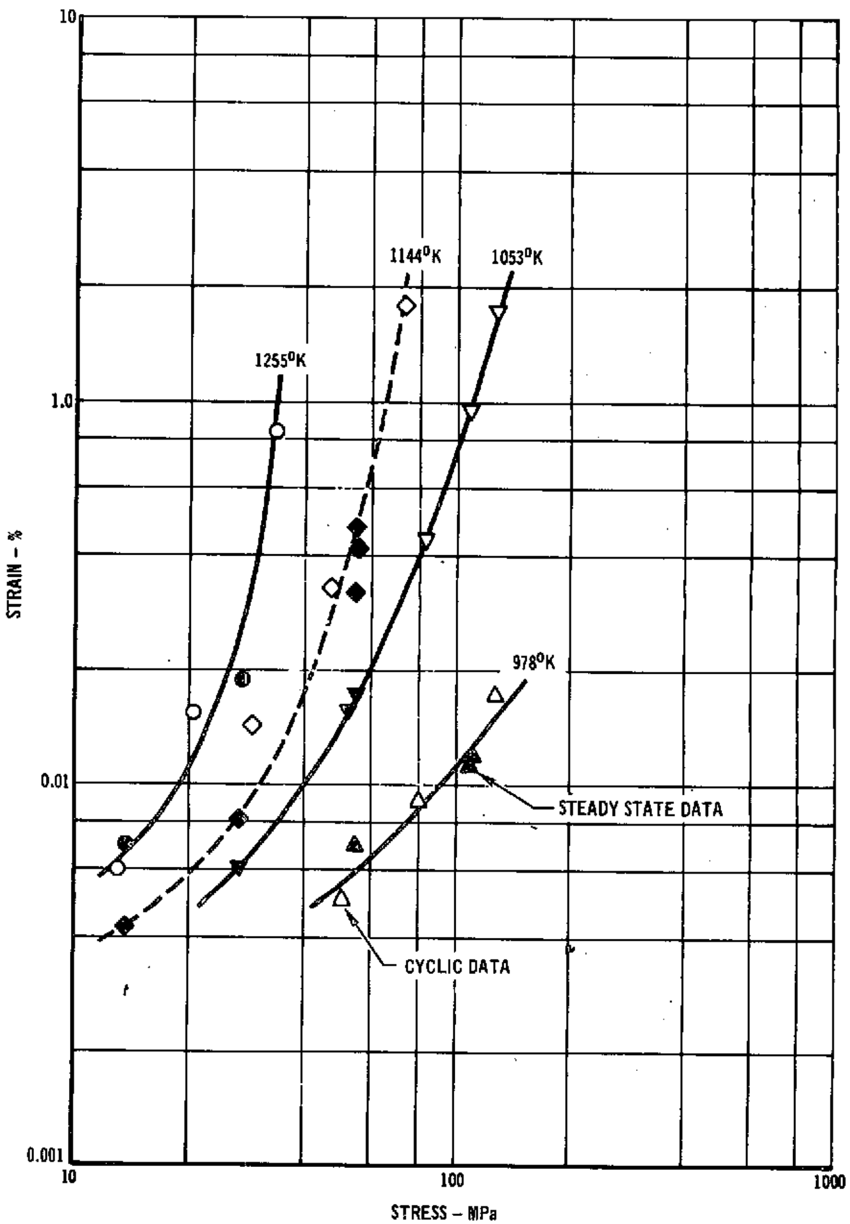

FIGURE 3–30 COMPARISON OF L605 CYCLIC AND STEADY-STATE DATA AT 30 HOURS

3.1.5.2 Microstructure Comparison. Samples representing steady-state and cyclic creep conditions were examined for microstructural features. The samples selected for examination were those that exhibited strains less than 0.5% at the end of the test. The results of this examination are presented in Figures 3-31, 3-32, and 3-33. From these figures it can be seen that there are no discernible differences, at 500X magnification, between the steady state and cyclic microstructures at any of the temperatures examined.

For comparison purposes the "as-received" microstructures are shown in Figure 3-31. Comparison of the as-received microstructure of L605 with that of the creep tested specimens shows that significant precipitation has occurred at 978°K, these precipitates are located only at the grain boundaries; according to Reference 29, these precipitates consist primarily of Laves phases and a Co-W intermetallic compound. At 1144°K and 1255°K, both grain boundary and matrix precipitation has occurred; these precipitates consist primarily of Laves phases and metal carbides. The carbides are primarily $M_{23}C_6$, at 1144°K, whereas at 1255°K, M_6C predominates. Examination of these photomicrographs also shows that testing at 1144°K and 1255°K has resulted in a depletion of carbides below the specimen surface. This subsurface layer is caused by preferential oxidation of less-noble alloying elements such as chromium.

3.1.6 L605 CYCLIC TESTS FOR EVALUATION OF ADDITIONAL VARIABLES

Described in Section 2.9.2 were a series of tests designed to study the effect of time per cycle, atmospheric pressure, and time between cycles on the cyclic creep of materials (creep recovery). This section discusses the results of those tests on L605. Raw creep data generated in these tests are presented in Appendix C-3.

3.1.6.1 Effect of Time Per Cycle. In the analysis of creep in a metallic TPS beam, the trajectory is idealized by dividing it into increments of time for which stress

ALLOY:	L–605
CONDITION:	AS-RECEIVED
ETCHANT:	HCl, H_2O_2 (ELECTROLYTIC)
MAG:	500X
ASTM GRAIN SIZE	3
THICKNESS	0.025 cm

ALLOY:	L–605
CONDITION:	TESTED (CYCLIC)
APPLIED STRESS:	80.7 MPa
TEST TEMPERATURE:	978°K
EXPOSURE TIME:	100 CYCLES
ETCHANT:	HCl, H_2O_2 (ELECTROLYTIC)
MAG:	500X
ASTM GRAIN SIZE	3
THICKNESS	0.025 cm

SPEC. NO. L57L

ALLOY:	L–605
CONDITION:	TESTED (STEADY STATE)
APPLIED STRESS:	55.2 MPa
TEST TEMPERATURE:	978°K
EXPOSURE TIME:	55 HOURS
ETCHANT:	HCl, H_2O_2 (ELECTROLYTIC)
MAG:	500X
ASTM GRAIN SIZE	3
THICKNESS	0.025 cm

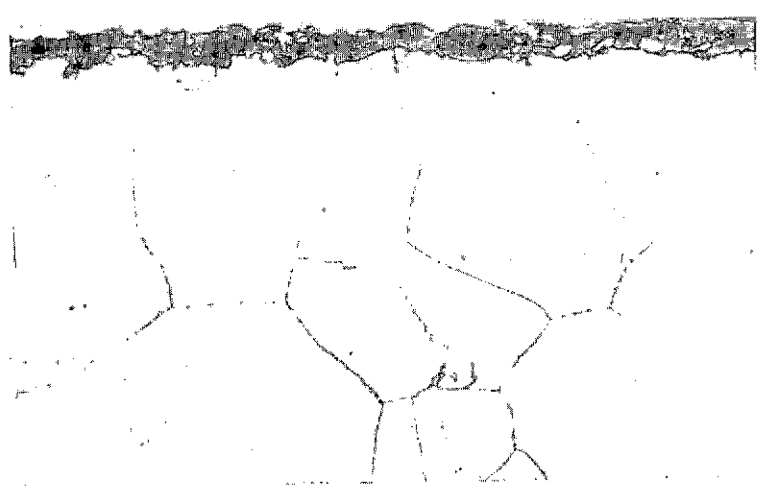

SPEC. NO. L96L

FIGURE 3–31 MICROSTRUCTURE OF L–605 BEFORE AND AFTER CREEP EXPOSURE AT 978°K

ALLOY:	L–605
CONDITION:	TESTED (STEADY STATE)
APPLIED STRESS:	55.2 MPa
TEST TEMPERATURE:	1144°K
EXPOSURE TIME:	66 HOURS
ETCHANT:	HCl, H_2O_2 (ELECTROLYTIC)
MAG:	500X
ASTM GRAIN SIZE	3
THICKNESS	0.025 cm

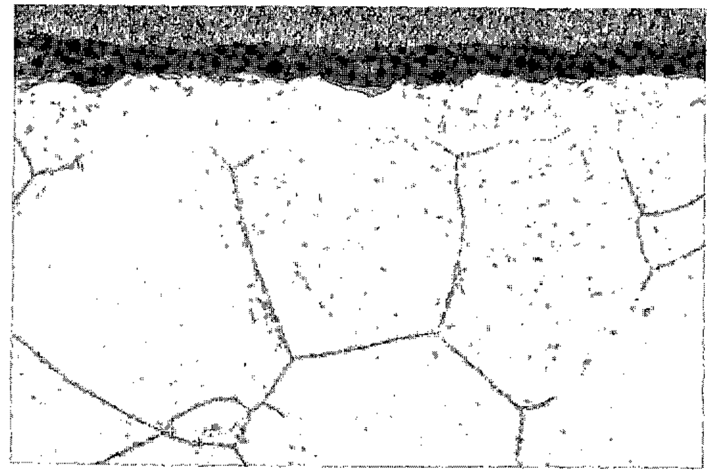

SPEC. NO. L27L

ALLOY:	L–605
CONDITION:	TESTED (CYCLIC)
APPLIED STRESS:	47.6 MPa
TEST TEMPERATURE:	1144°K
EXPOSURE TIME:	100 CYCLES
ETCHANT:	HCl, H_2O_2 (ELECTROLYTIC)
MAG:	500X
ASTM GRAIN SIZE	3
THICKNESS	0.025 cm

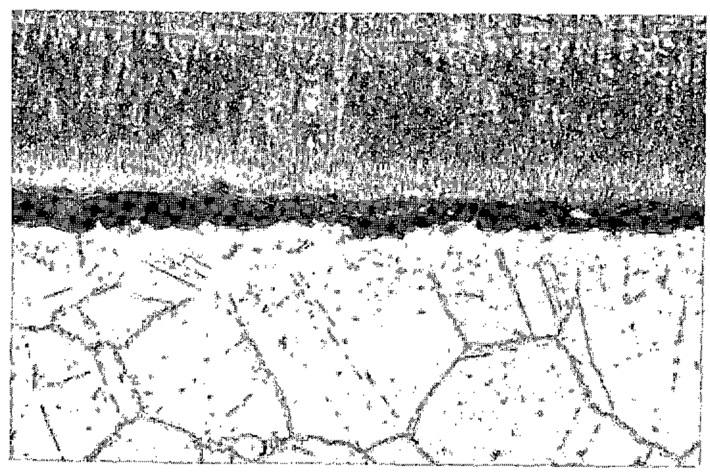

SPEC. NO. L61L

FIGURE 3–32 MICROSTRUCTURE OF L–605 AFTER CREEP EXPOSURE AT 1144°K

ALLOY:	L605
CONDITION:	TESTED (CYCLIC)
APPLIED STRESS:	20.7 MPa
TEST TEMPERATURE:	1255^oK
EXPOSURE TIME:	100 CYCLES
ETCHANT:	HCl, H_2O_2 (ELECTROLYTIC)
MAG:	500X
ASTM GRAIN SIZE	3
THICKNESS	0.025 cm

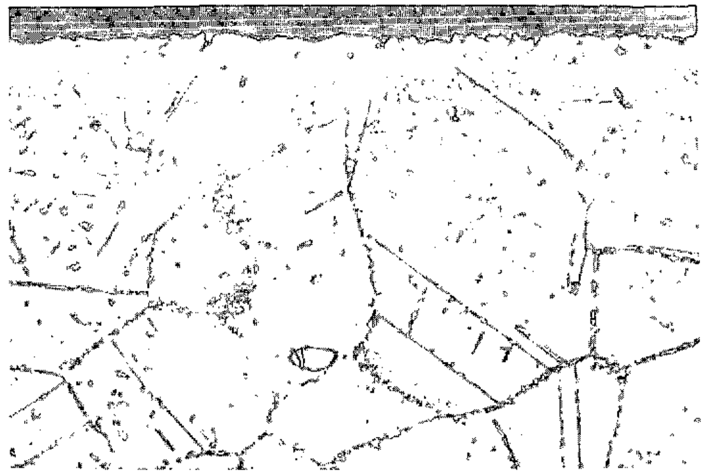

SPEC. NO. L91L

ALLOY:	L–605
CONDITION:	TESTED (STEADY STATE)
APPLIED STRESS:	27.6 MPa
TEST TEMPERATURE:	1255^oK
EXPOSURE TIME:	50 HOURS
ETCHANT:	HCl, H_2O_2 (ELECTROLYTIC)
MAG:	500X
ASTM GRAIN SIZE	3
THICKNESS	0.025 cm

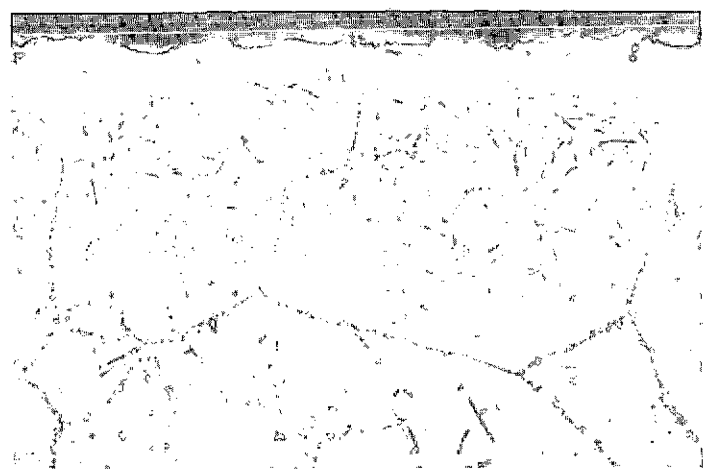

SPEC. NO. L54L

FIGURE 3–33 MICROSTRUCTURE OF L–605 AFTER CREEP EXPOSURE AT 1255^oK

and temperature are considered constant. Since the length of time of these increments will vary with the trajectory, the effect of time at temperature and load must be evaluated. To determine the magnitude of this effect, a test designated as L605 Cyclic Test #8 was performed using a cycle with a maximum time at temperature and stress of 10 minutes. A comparison of the data from this test with the data from the Basic Cyclic Test Number 3 (Figure 3-24) which had a maximum time at temperature and load of 20 minutes, is presented in Figure 3-34. Each of the data points in this figure represents a total cycle time at load and temperature (1146°K) of 16.67 hours (100 cycles at 10 minutes/cycle for Test #8 and 50 cycles at 20 minutes/cycle for Test #3). From this figure it appears that the cyclic creep strains are a function of total time at load and temperature only, for cycle times typical of Shuttle entry trajectories. Therefore, application of the L605 basic cyclic empirical creep strain equation to trajectories of varying time appears warranted.

3.1.6.2 Effect of Atmospheric Pressure. Cyclic tests 12 and 13 were replicate idealized trajectory tests, except that a simulated atmospheric pressure profile was applied in test 13 while in test 12 the pressure was maintained constant at <1.3Pa torr. Comparison of creep strain results for the corresponding specimens in these tests are shown in Figure 3-35. Based on the comparison, it cannot be concluded that atmospheric pressure has any effect on creep strain response.

Also shown in Figure 3-35 are creep strain results for actual stress and temperature profiles. These results will be discussed in Section 3.1.8.1.

3.1.6.3 Effects of Time Between Cycle. Tensile specimens L37L, L61L, and L53L were tested to 100 cycles at 1144°K (cycle test 3) as part of the basic cyclic tests for L605. Several weeks subsequent to the completion of this test, the specimens were tested for an additional 50 cycles (cyclic test 14). Creep strain results are shown in Figure 3-36. Comparison of creep rates at the end of test 3 with those obtained in test 14 shows no change. Therefore, room temperature recovery

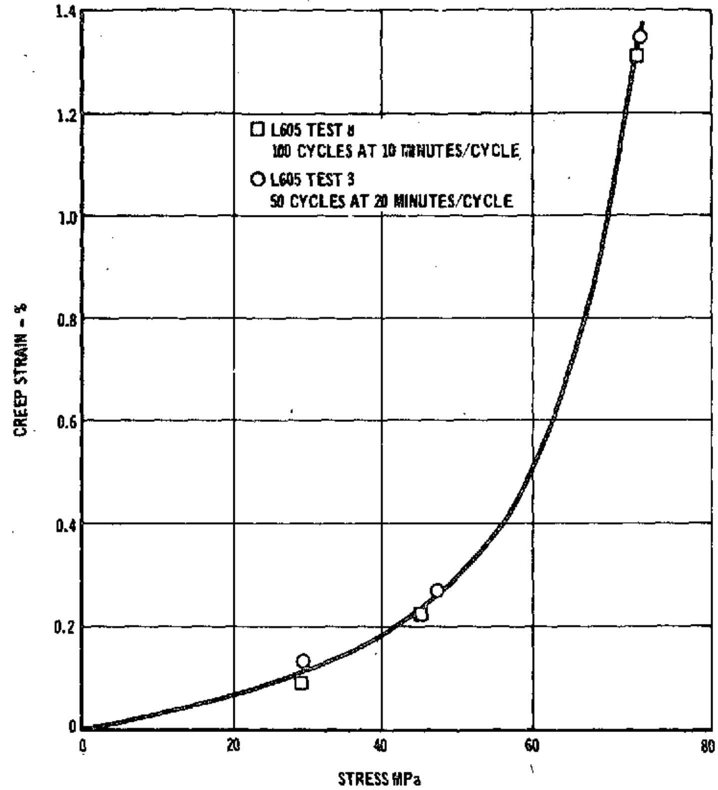

FIGURE 3–34 L605 CYCLIC CREEP STRAINS AS FUNCTION OF TOTAL TIME AT LOAD

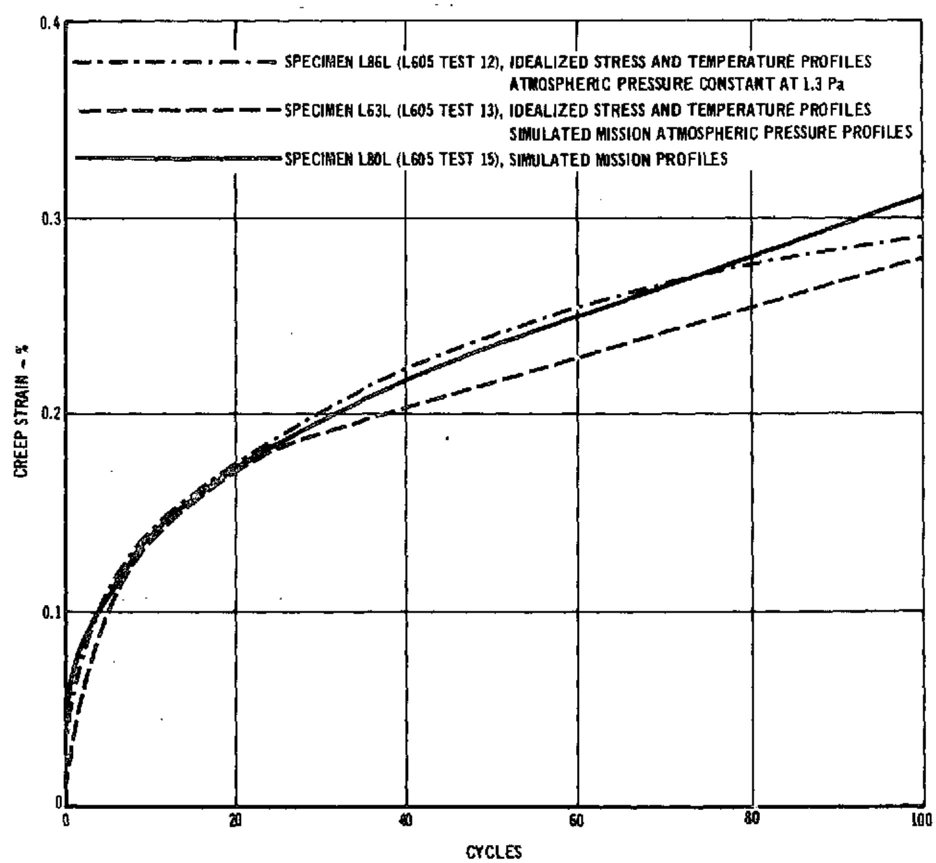

FIGURE 3–35 COMPARISON OF CYCLIC CREEP STRAINS FOR SIMULATED MISSION AND IDEALIZED TRAJECTORIES

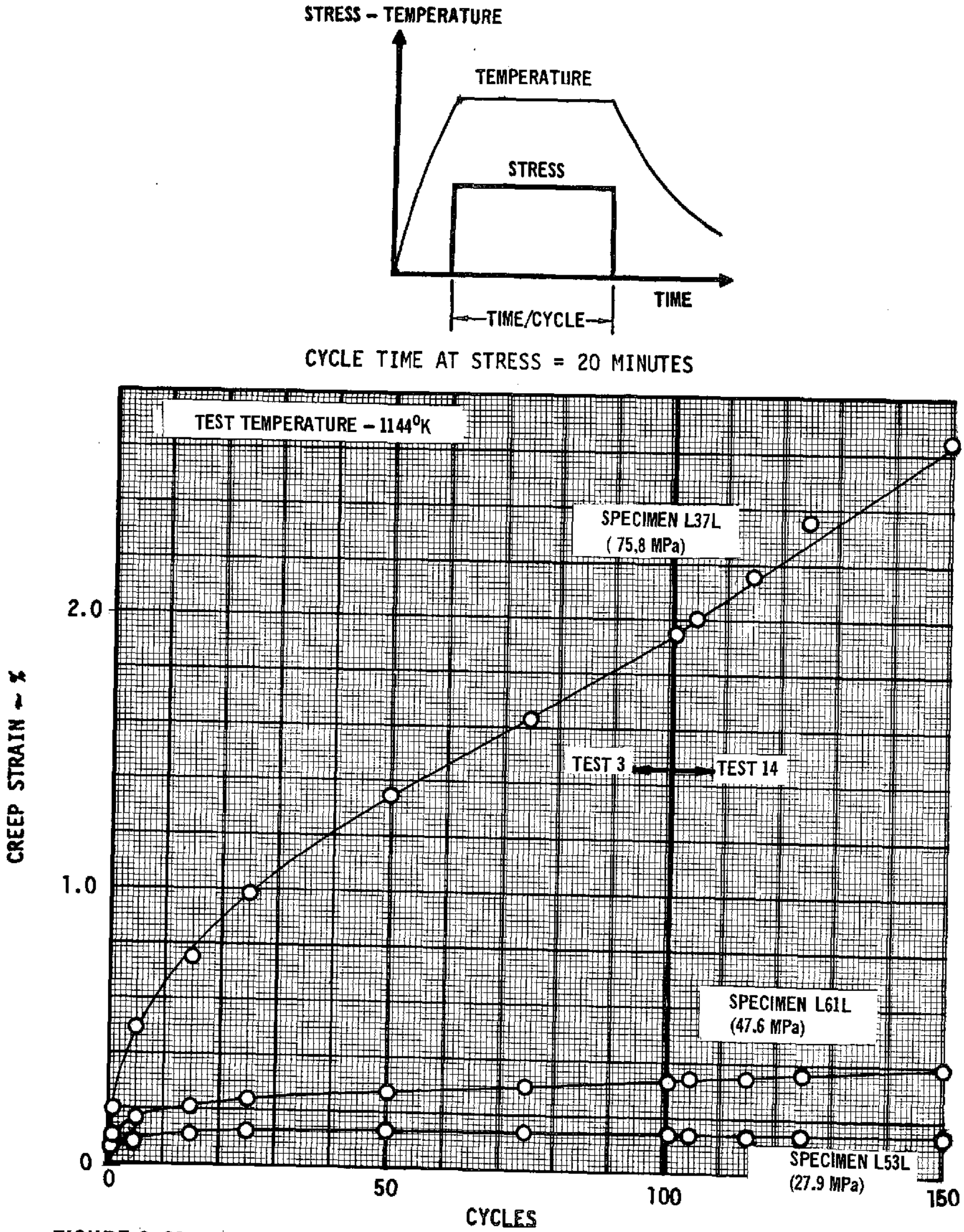

FIGURE 3-36 L605 CYCLIC TEST NO. 14 – CONTINUATION OF L605 BASIC CYCLIC TEST NO. 3

does not appear to be an important factor in the creep response behavior of L605.

Even though it did not appear that room temperature recovery was occurring, the possibility still existed that high temperature recovery was occurring in our basic cycle profile. High temperature recovery is a specimen relaxation during exposure to elevated temperature and no load conditions similar to what occurs in the basic cycle profile). To determine if high temperature recovery was occurring, an additional test was performed (test No. 11, specimens L43L and L38L) in which the load was mainained for 50 minutes (see Figure 2-24(a)) instead of the usual 20 minutes. By maintaining the load until the temperature is lowered, high temperature recovery should be prevented from occurring. Comparison of this test (No. 11), which did not have high temperature recovery, with one that could have high temperature recovery (test No. 3) revealed that there was no significant difference between the resultant creep strains for the two tests (See Figure 3-37). As a result neither room or high temperature recovery phenomena appear to be an important factor in L605 creep response.

3.1.7 STEPPED STRESS CYCLIC TESTS

Tests were designed to provide data for evaluation of various hardening rules applicable to TPS beam bending where stress varies as a function of time (see section 2.9.2.3). L605 tests 5, 6, and 7 were conducted at 1144°K and L605 test 10 was conducted at 1092°K. All tests were conducted using the typical cycle profile (20 minutes at load and peak temperature) shown in Figure 2-22. Load was varied, periodically, after a fixed number of cycles in each of the tests as indicated in Figures 3-38 to 3-41.

Stresses for Tests 5 and 10 were selected to duplicate portions of the creep strain curves from Test 3 and 2 respectively (Figure 3-25 and 3-24) to allow possible direct data comparisons.

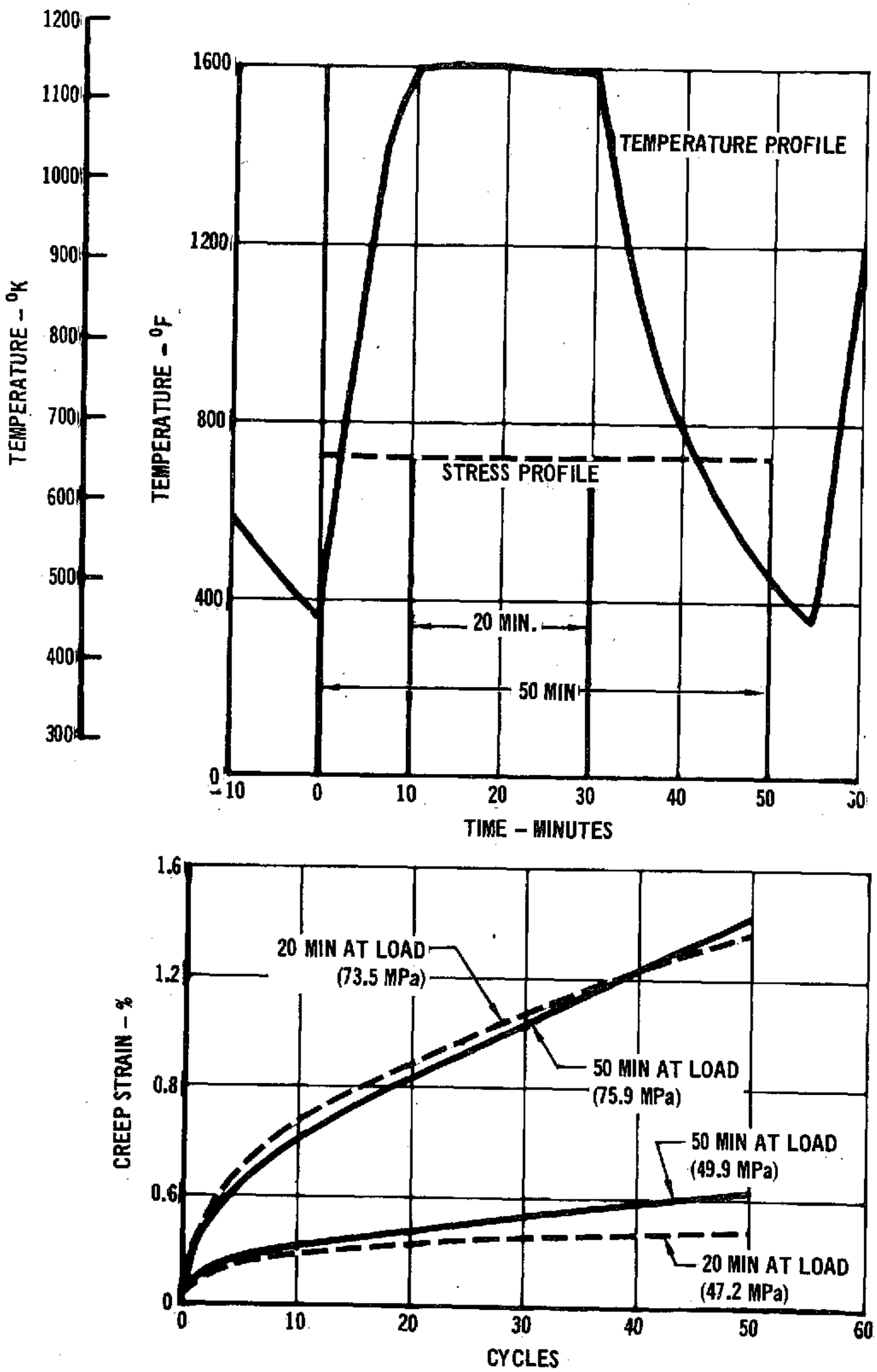

FIGURE 3-37 EFFECT OF TIME AT MAXIMUM LOAD FOR L605 CYCLIC TESTS AT 1144°K

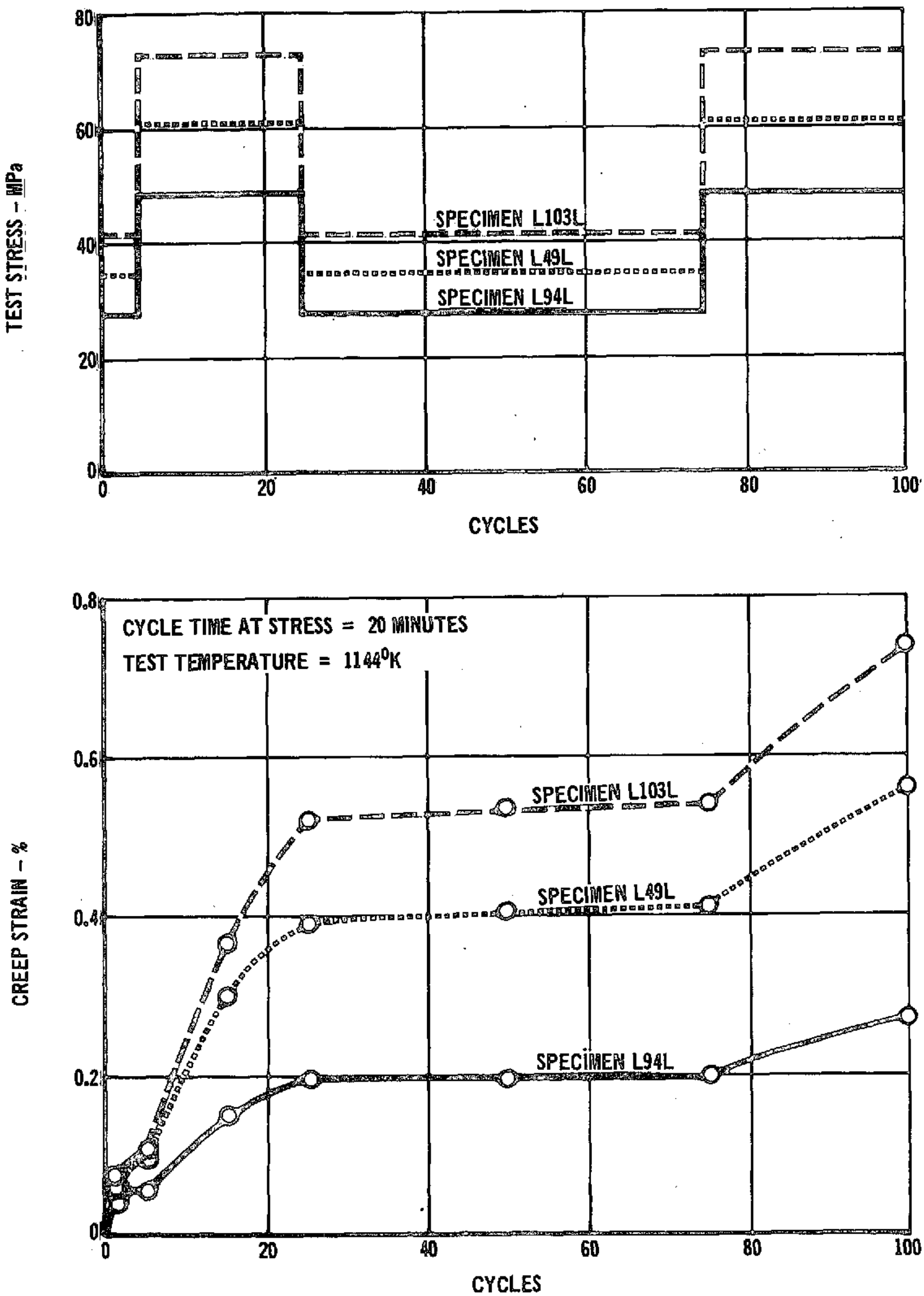

FIGURE 3-38 L605 CYCLIC TEST NO. 5 – STEPPED STRESS HISTORY AND RESULTANT CREEP

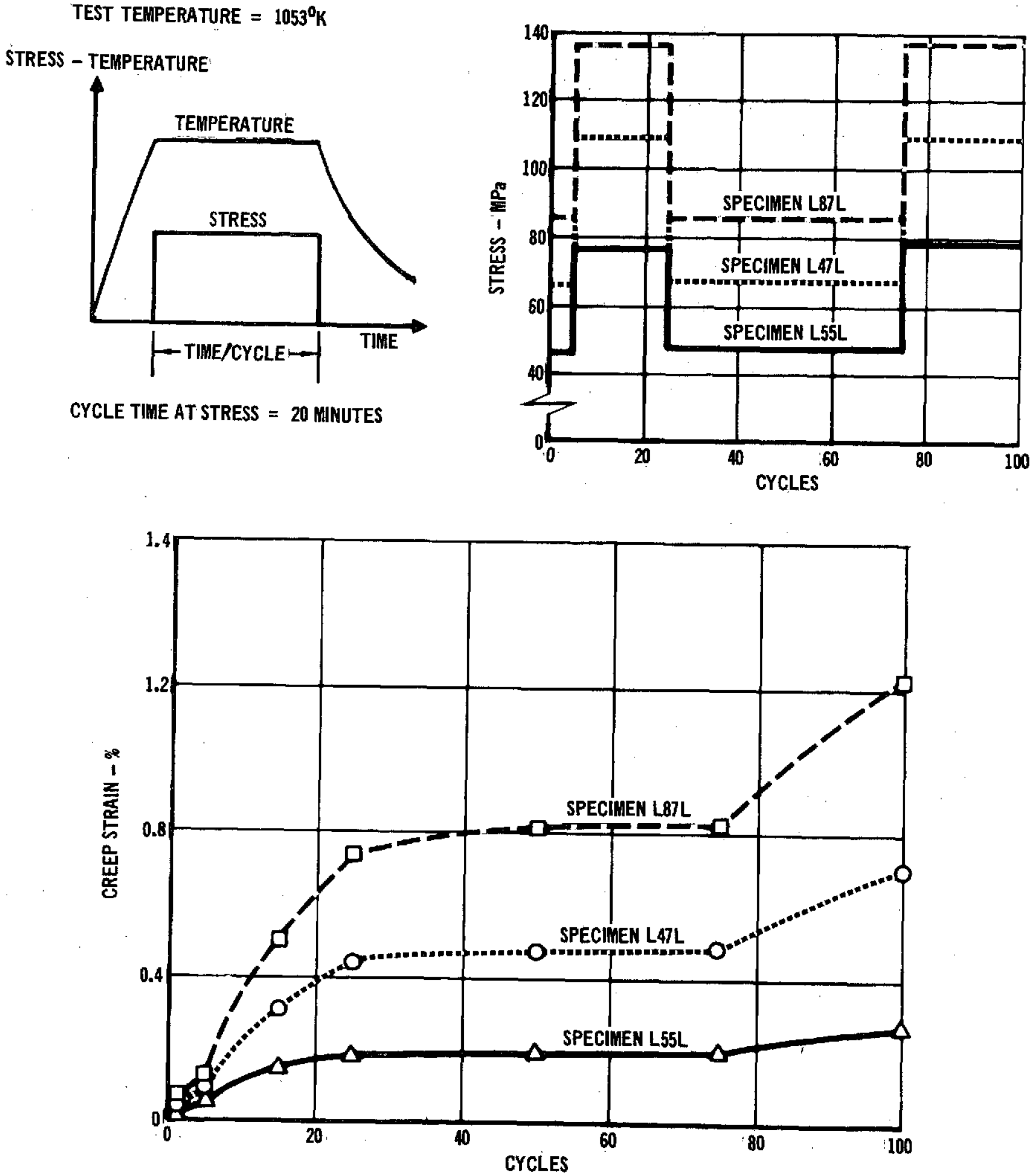

FIGURE 3–39 L605 CYCLIC TEST NO. 10 – STEPPED STRESS HISTORY AND RESULTANT CREEP

661 - 123

Test No. 6 and 7 (Figures 3-40 and 3-41) were conducted to simulate stress change as a function of cycle, which will occur in a TPS beam. A comparison of the results for these two tests indicates that the total creep strain is path dependent. For all three specimens, when stresses were high at the start of the test (Figure 3-41) and were lowered continuously during the test, the creep strains were greater than those obtained where the stresses were low at the start of the test, and increased continuously during the test (Figure 3-40).

Comparison of test results with predictions for specimens L26L test 6) and L75L (test 7) are presented in Figures 3-42(a) and 3-42(b). These predictions are based on application of the L605 cyclic creep equation (Equation 3-6), in conjunction with hardening theories of creep accumulation. In addition to predictions based on time hardening and strain hardening theories, a third approach is presented (rate dependent approach). This rate dependent approach is based on the results of L605 tests 6 and 7 because, as shown in the figure, time hardening provided the best predictions in the case of increasing stress (test 6) and strain hardening provided the best predictions in the case of decreasing stress (test 7). Therefore, the rate dependent approach was postulated as a combination of time hardening and strain hardening theories. For this approach the time hardening strain rate is calculated at each analysis time step and compared to the strain rate used in the previous time step. Then strain hardening or time hardening is applied depending on whether the strain rate has decreased or increased respectively.

Comparison of predictions with test results from tests 5 and 10 are shown in Figure 3-43(a) and 3-43(b). For these data the three hardening approaches provide comparable predictions with the strain hardening theory yielding highest strain predictions and the rate dependent approach yielding the lowest strain predictions. Further comparisons of predictions with test results are presented in the following section.

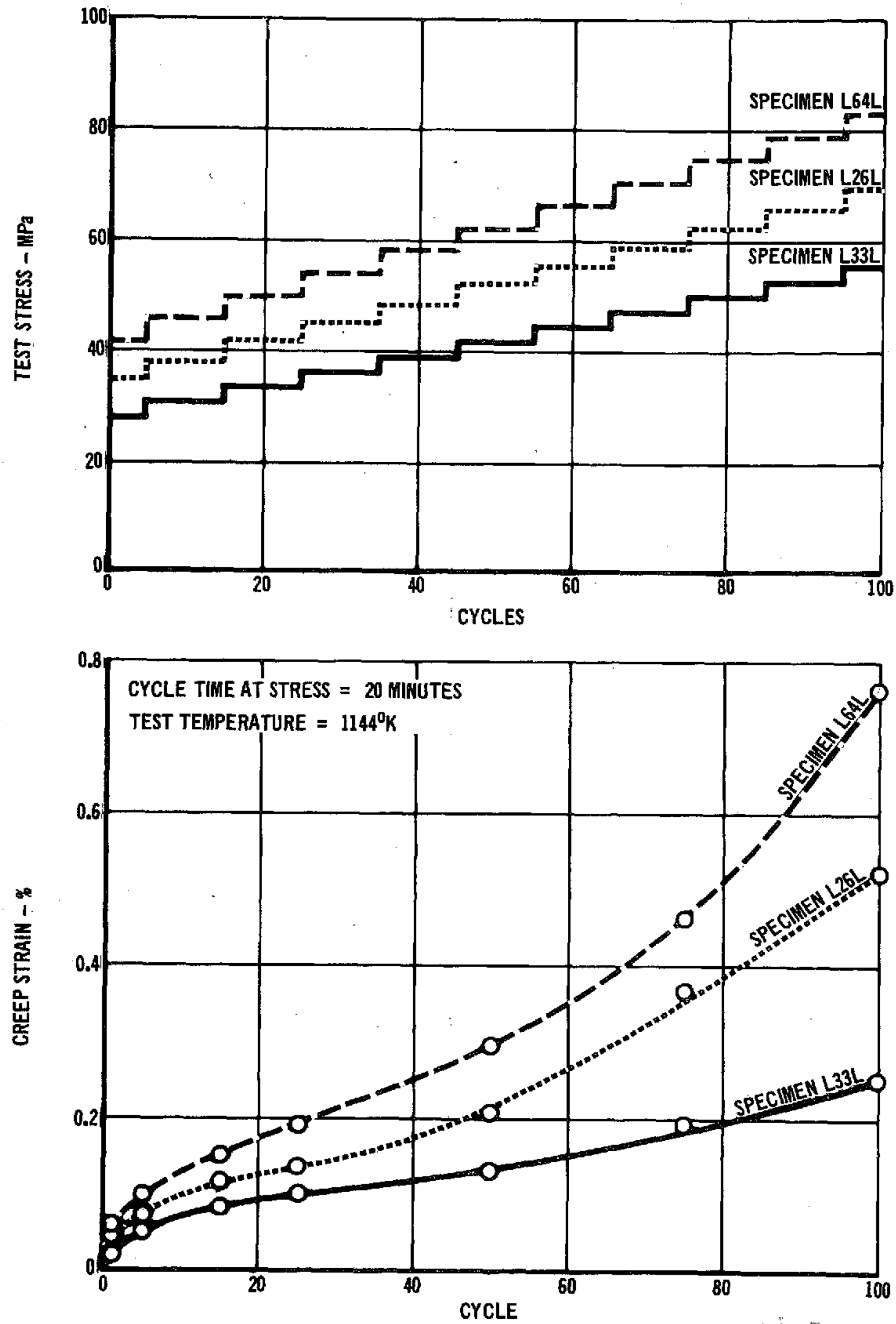

FIGURE 3–40 L605 CYCLIC TEST NO. 6 – INCREASING STRESS HISTORY AND RESULTANT CREEP

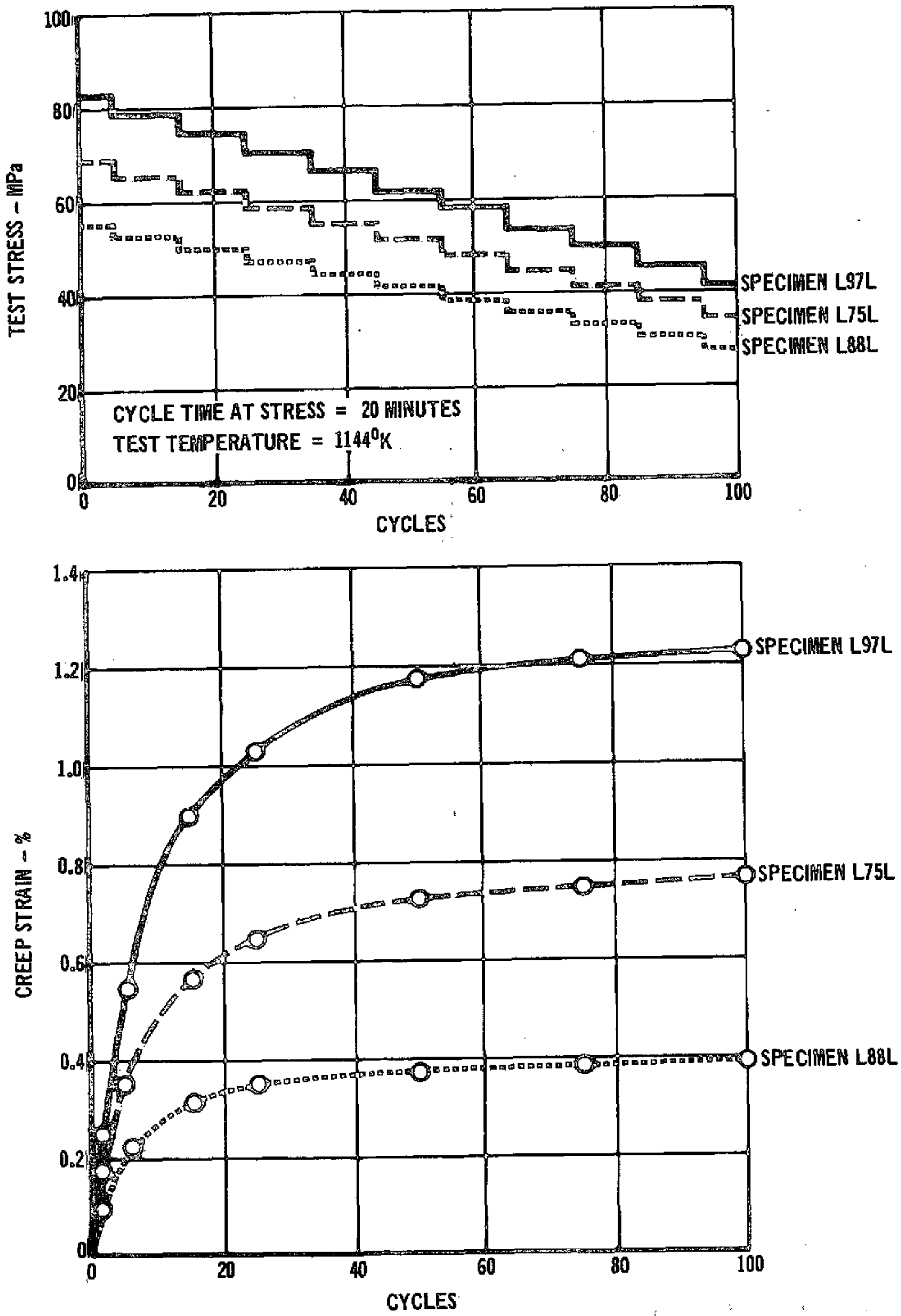

FIGURE 3-41 L605 CYCLIC TEST NO. 7 – DECREASING STRESS HISTORY AND RESULTANT CREEP

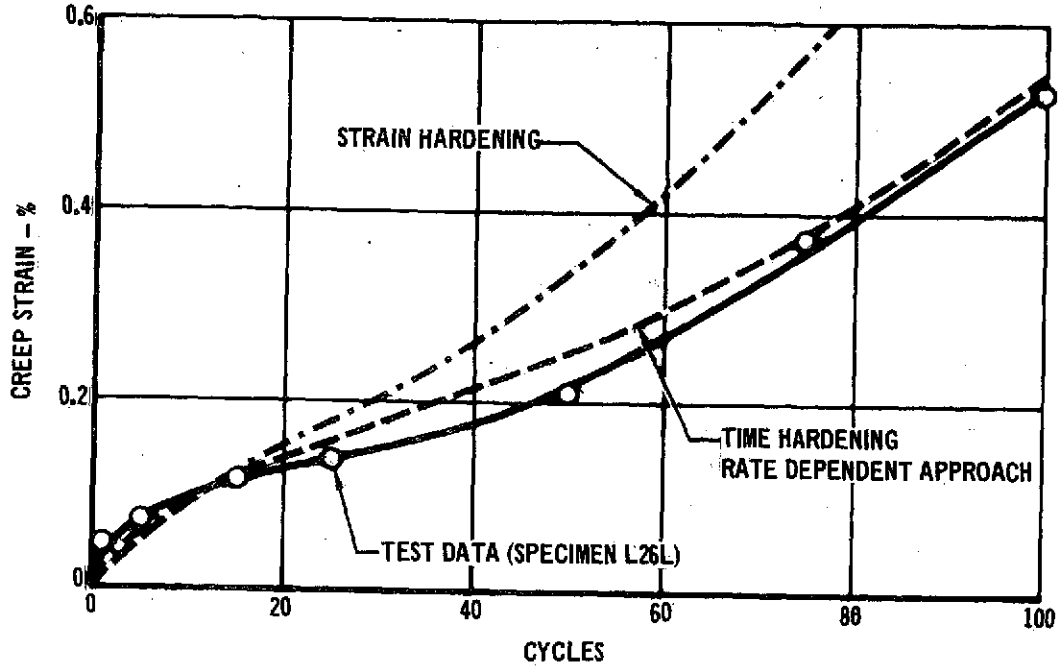

a) Increasing Stress History (L605 Test 6)

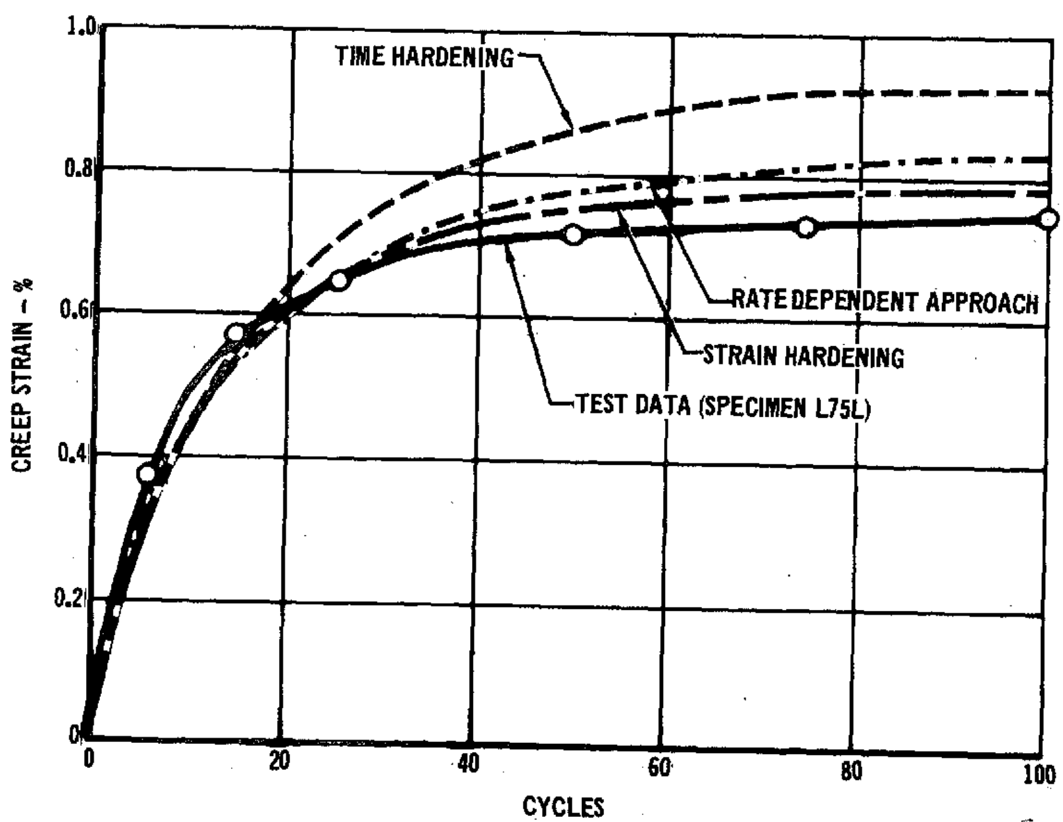

b) Decreasing Stress History (L605 Test 7)

FIGURE 3-42 COMPARISON OF HARDENING THEORIES

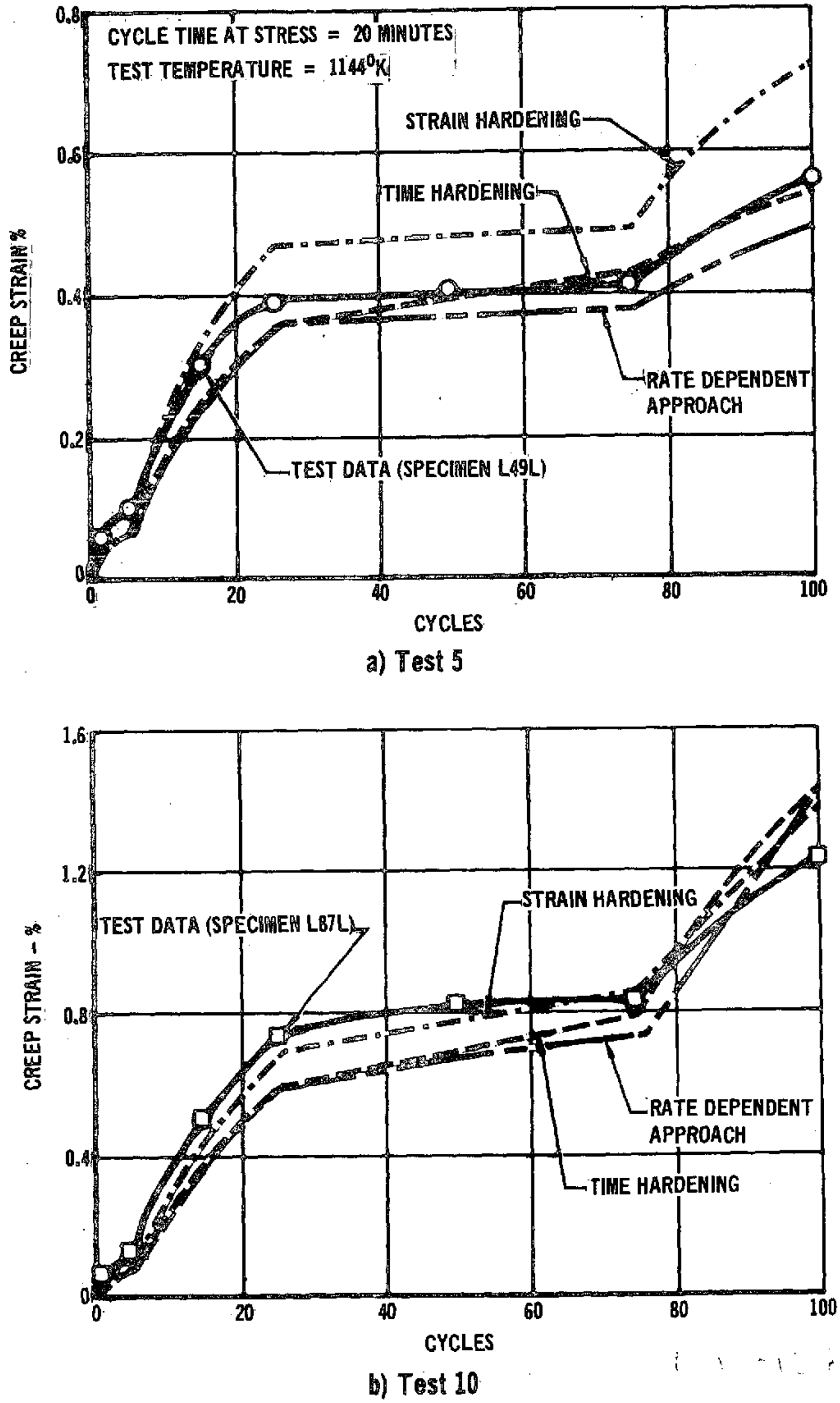

a) Test 5

b) Test 10

FIGURE 3-43 COMPARISON OF HARDENING THEORIES – STEPPED STRESS HISTORIES

3.1.8 TRAJECTORY TESTS

Four cyclic trajectory tests were conducted using L605 tensile specimens (.025 cm, longitudinal direction). These tests are a two-step stress trajectory profile with constant maximum temperature of 1144°K and constant pressure (test 9), two idealized trajectory tests (tests 12 and 13) with maximum temperatures of 1144°K (comparison of tests 12 and 13 on the basis of atmospheric pressure variation is presented in Section 3.1.6.2), and a simulated mission trajectory test (test 15) using representative Shuttle stress, temperature, and pressure profiles.

3.1.8.1 Idealized Trajectory Tests. One of the goals of cyclic testing in Phase I was to assess the suitability of approximating continuously varying stress and temperature profiles with a series of constant steps. It was considered necessary to minimize the number of analysis steps to reduce analysis and computer time to efficiently conduct TPS panel analysis.

The first test conducted on L605 specimens where stress was varied within a cycle was test No. 9. Comparison of results for these specimens with specimens tested at a constant stress (cyclic test No. 3) provide an initial estimate for idealizing the stress profiles. Shown in Figure 3-44 is the two-step stress profile for L605 test 9 and the resulting creep strains after 100 cycles for each of the three specimens (Specimens L30L, L07L, and L35L). Also shown are 100 cycle creep strain-stress data for the three specimens tested in L605 Test 3 (specimens L53L, L61L, and L37L). For purposes of the comparison, the two step stress profile (Test 9) could be idealized with a constant stress profile (Test 3). The objective of this idealization is to determine what stress applied for the entire 20 minute cycle, will produce the same 100 cycle creep strain as the two 10-minute stress levels. These stress levels are designated by the points of intersection (Δ) as shown in Figure 3-44. In this particular case, resulting "equivalent" or

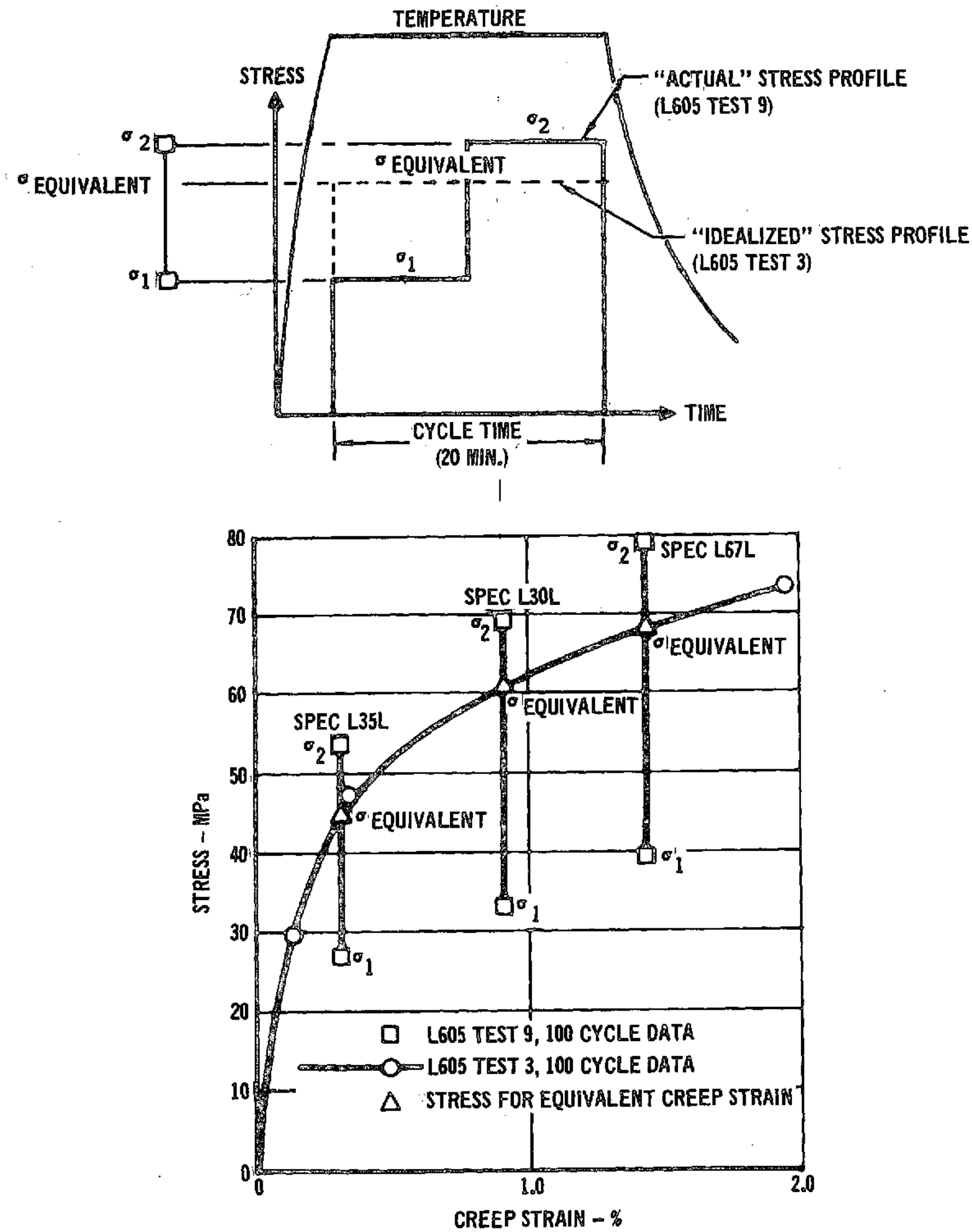

FIGURE 3–44 COMPARISON OF L605 CYCLIC TESTS 9 AND 3 – STRESS FOR EQUIVALENT CREEP STRAIN

"idealized" stress levels turned out to be the lower stress plus approximately 73% of the difference between the two stress levels (steps). This result indicates that the nonlinear nature of the creep-stress relationship should be considered in the process of idealizing a profile. The importance of making correct judgements in this idealization process becomes more critical as fewer steps are used in approximating the profiles.

For tests 12 and 13, the simulated mission stress profile was idealized into four steps as shown in Figure 3-45. The atmospheric pressure profile was varied between the tests in order to allow an assessment of the effects of this variable on creep strains (see Section 3.1.11.3).

For the idealized profiles it was considered desirable to maintain a constant peak temperature for twenty minutes to be consistent with basic cyclic and stepped stress tests. Therefore, the temperature profile, shown in the figure, represents an idealization for the entire twenty minute time period, based strictly on judgement. Stress levels shown were also based on judgement. Specifically, stresses in the first two time increments were established as somewhat lower than would be indicated by the previous discussion on L605 test 9 in an effort to offset higher temperatures and stress levels during the initial six minutes (200 seconds to 500 seconds).

A study using hardening theories in conjunction with cyclic equation 3-6 was conducted for the idealized trajectory tests. Typical comparisons of predictions with test data from tests 9 and 13 are presented in Figures 3-46 and 3-47. Results show that the rate dependent approach generally provides closer predictions than strain hardening or time hardening theories individually.

3.1.8.2 Simulated Mission Test. The final test of L605 tensile specimens (Test 15) was conducted using representative shuttle stress, temperature, and pressure profiles. The simulated mission profile and creep strain results are presented in Figure 3-48.

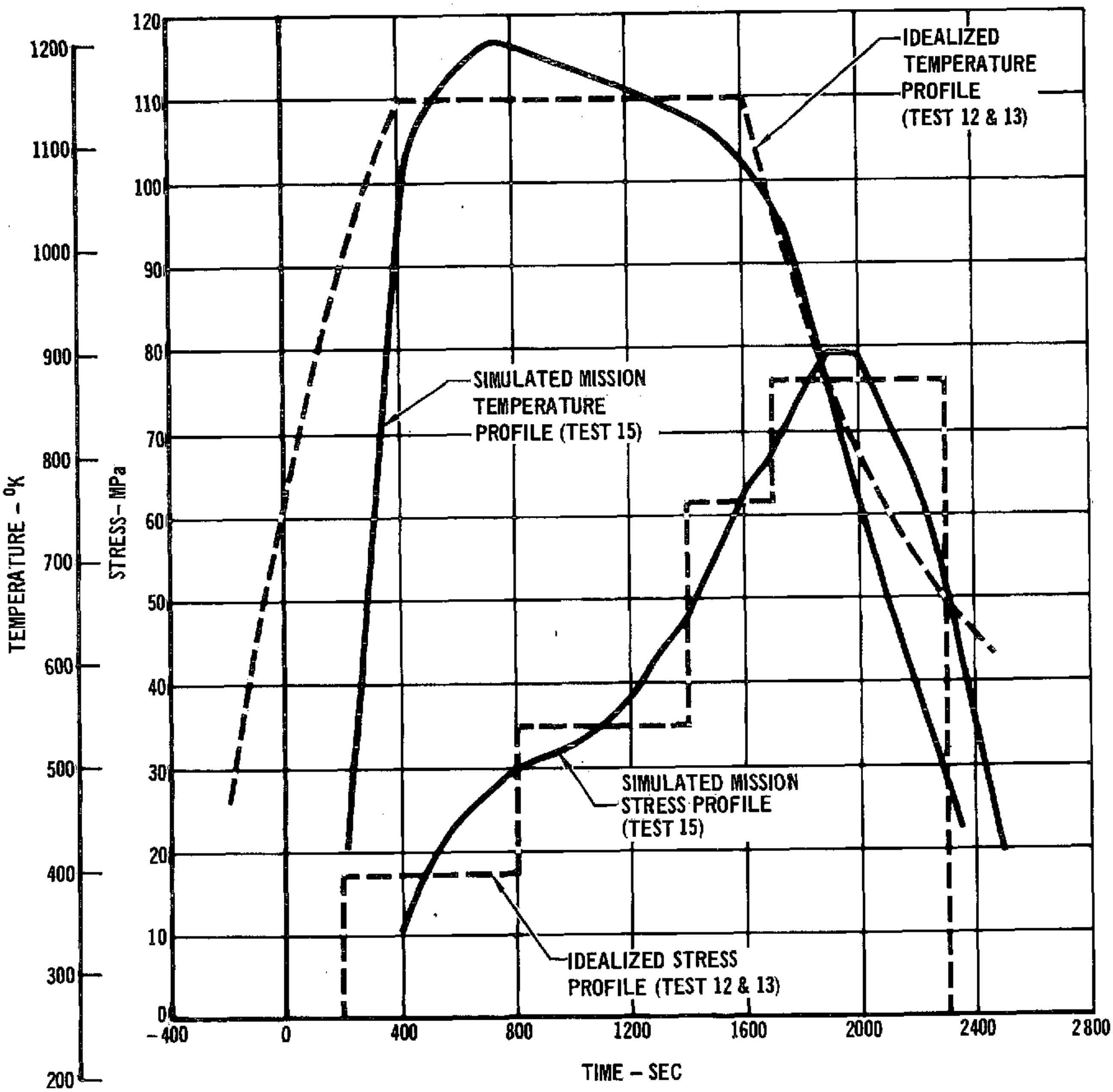

FIGURE 3–45 SIMULATED MISSION TRAJECTORY PROFILES FOR L605 CYCLIC TESTS 12, 13, AND 15

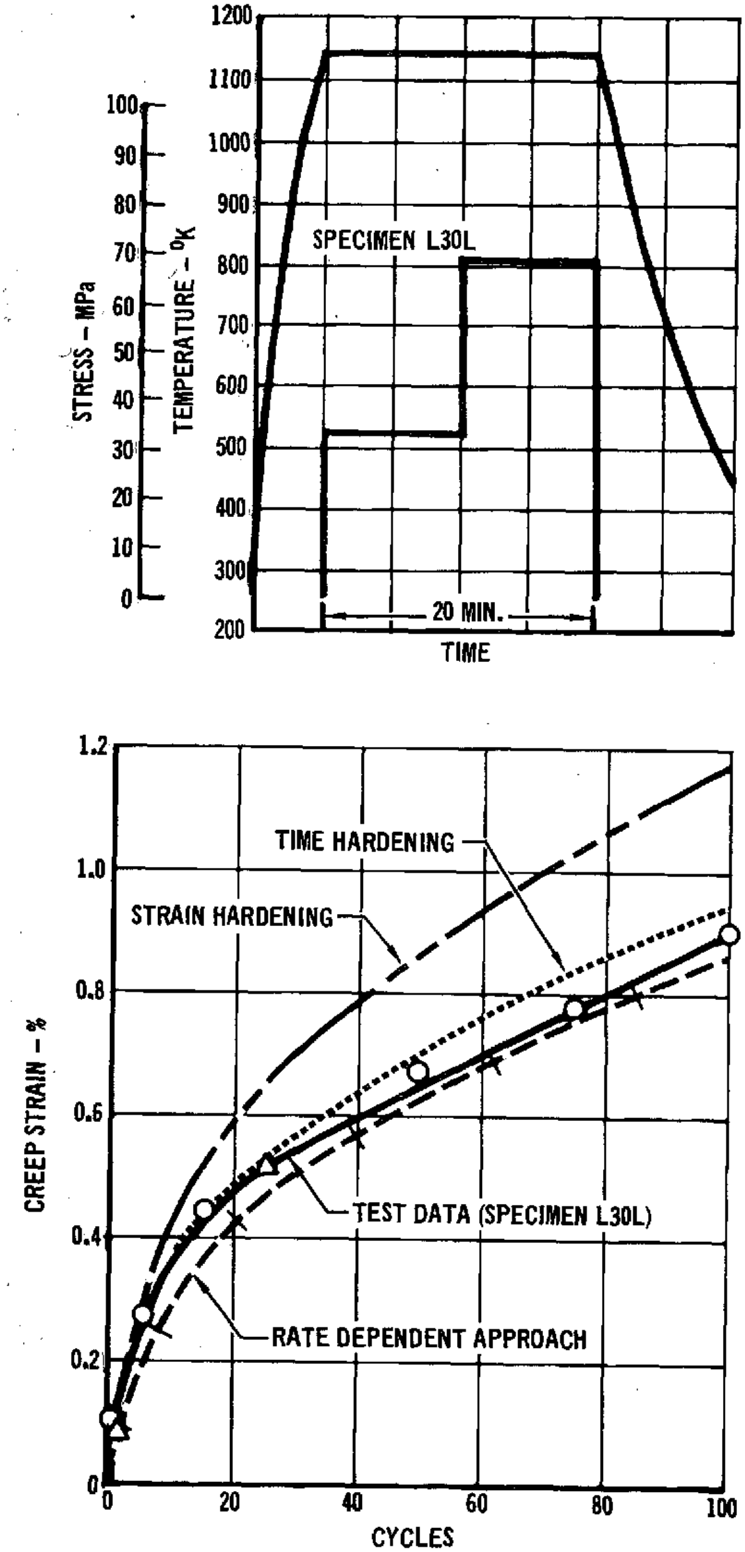

FIGURE 3-46 COMPARISON OF HARDENING THEORIES – L605 CYCLIC TEST NO. 9

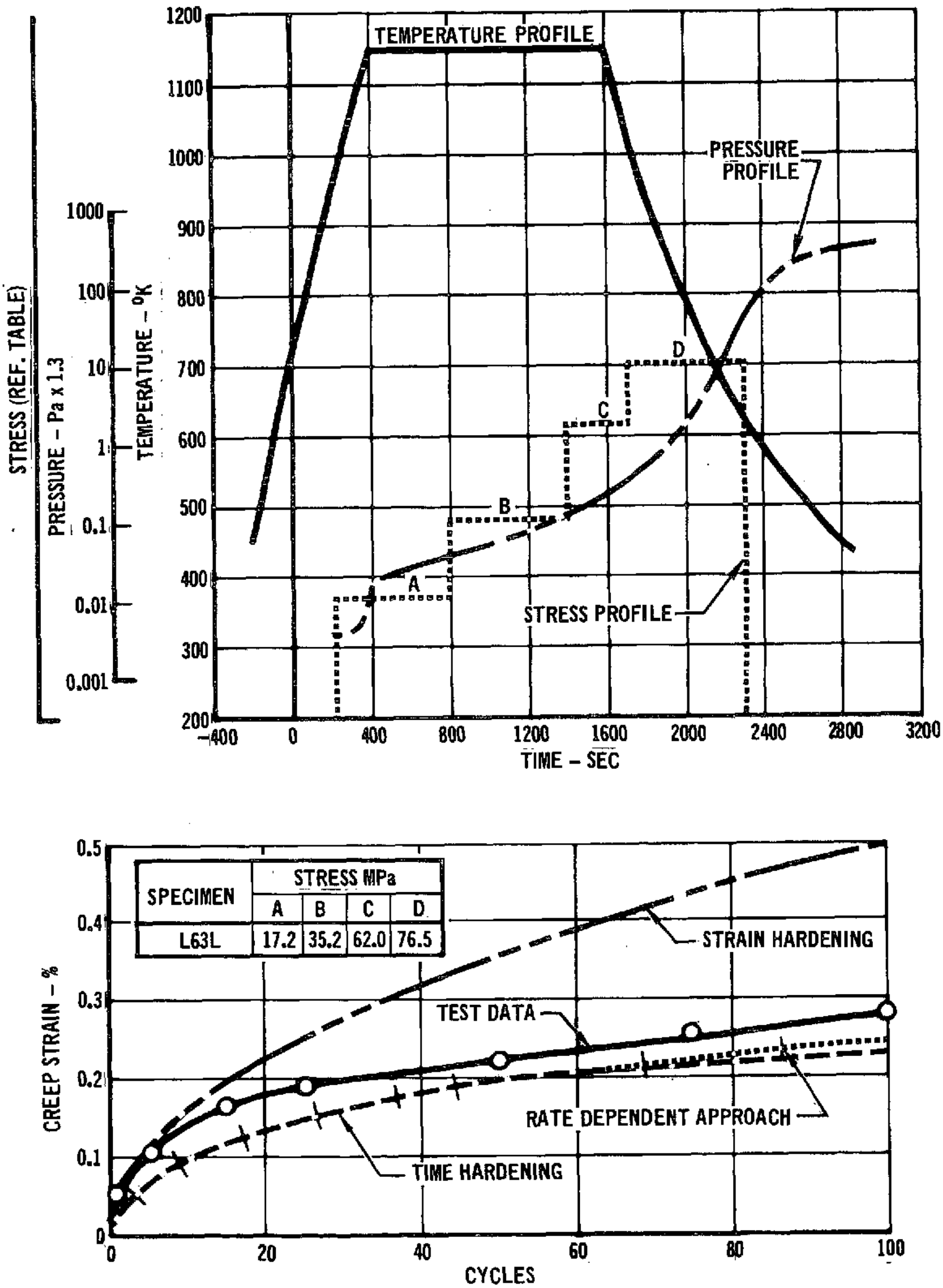

SPECIMEN	STRESS MPa			
	A	B	C	D
L63L	17.2	35.2	62.0	76.5

FIGURE 3-47 L605 CYCLIC TEST NO. 13 – IDEALIZED TRAJECTORY PROFILES AND RESULTANT CREEP

Comparison of idealized and simulated mission trajectory creep strain results are shown in Figure 3-35 where creep strain data are plotted for specimen L86L (L605 Test 12), specimen L63L (L605 Test 13), and specimen L80L (L605 Test 15). Specimen L80L (L605 Test 15) was tested to the simulated mission stress and temperature profile shown in Figure 3-45 while Specimens L86L and L63L (Test 12 and 13) were both tested to the idealized stress and temperature profiles shown in Figure 3-45. The difference between tests (Tests 12 and 13) was the atmospheric pressure profile (see Section 3.1.6.2). Because resulting creep strains for specimens L86L and L63L are not significantly different from those for specimen L80L, it can be suggested that the four step stress profile and corresponding flat temperature profile is a good idealization of the actual profiles.

In comparing predictions using the hardening theories for Test 15 data, it was shown that the strain hardening theory and the rate dependent approach closely approximate the test data. A typical comparison of test data and predictions is presented in Figure 3-49.

For analysis purposes the simulated mission stress and temperature profiles were idealized into 22 time steps or a total of 2200 steps for the 100 cycle creep accumulation analysis. The analysis steps used correspond to the 100 second increments in stress and temperature data for the profiles, as presented in appendix (C-3-23). Because the total time analyzed in each profile is 33 minutes (1.67 minutes per time step), the time of 33.3 hours maximum (100 cycles @ 20 minutes/cycle) for which the L605 cyclic creep empirical equation was derived, is exceeded at 55 cycles in Figure 3-48. Therefore, creep predictions beyond this time are outside equation limits and should not be used. This recommendation is based on the fact that the form of the cyclic equation (3-6) allows strains to decrease at accumulated times greater than 33 hours (see Figure 3-28). As a result, extrapolation beyond 33 hours results in incorrect strain predictions. This trend can be seen in Figure

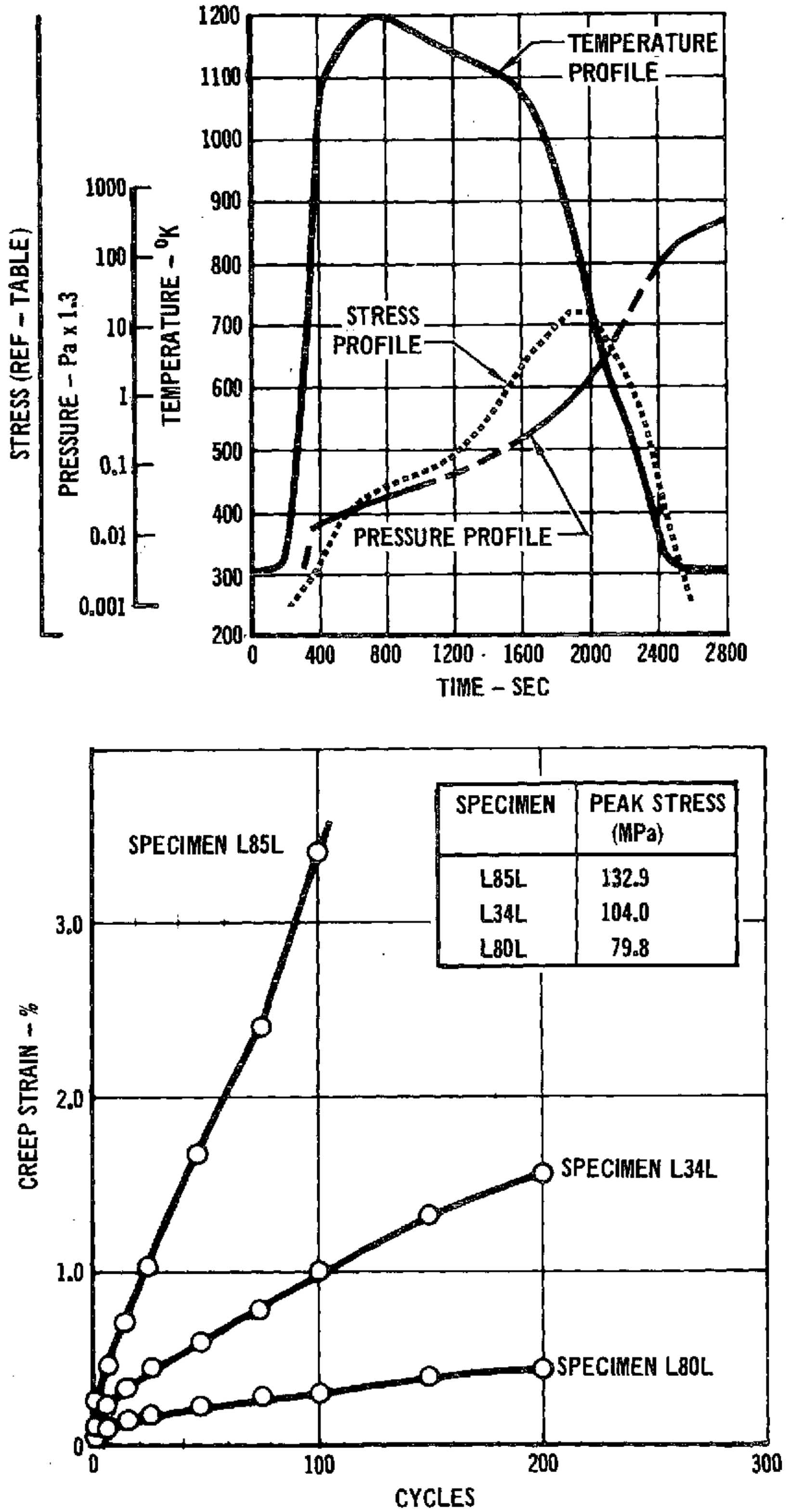

FIGURE 3-48 L605 CYCLIC TEST NO. 15 - SIMULATED MISSION TRAJECTORY PROFILES AND RESULTANT CREEP

6

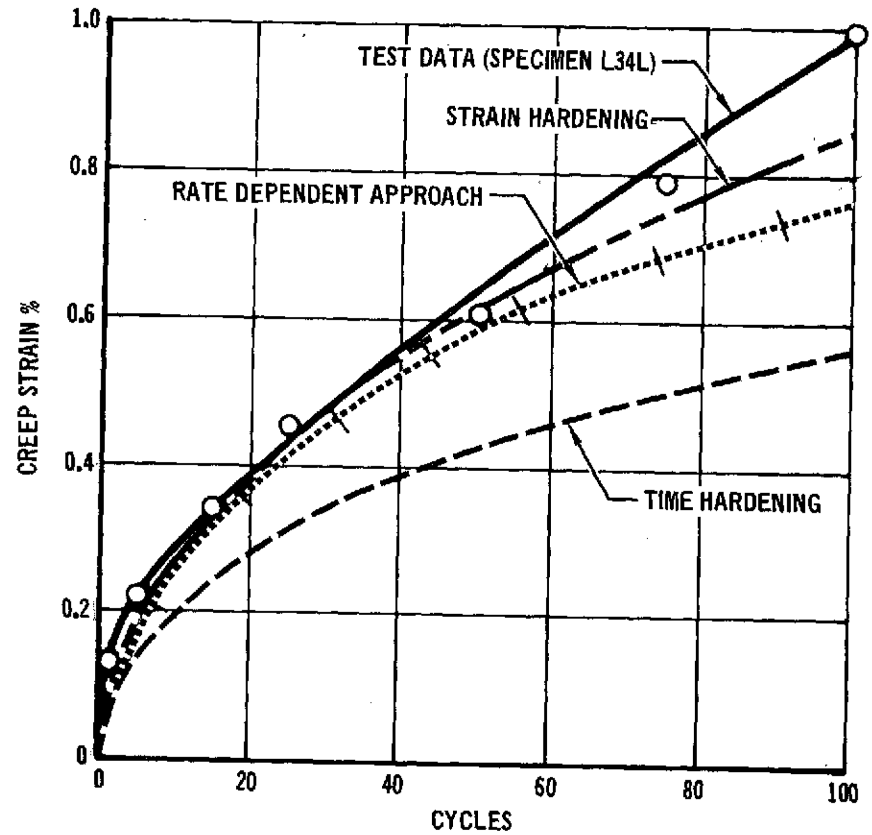

FIGURE 3-49 COMPARISON OF HARDENING THEORIES – L605 CYCLIC TEST NO. 15

3-49, where strain hardening closely approximates the test within the time range (55 cycles); however, outside this range the difference between the two becomes greater with increasing time.

3.1.9 L605 CONCLUSIONS

L605 tensile specimens were tested at steady-state conditions over the temperature range of 978°K (1300°F) to 1255°K (1800°F) for approximately 200 hours or creep strains of up to approximately .5% @ 50 hours. The following empirical regression equation was developed for data obtained in steady-state creep tests conducted under this phase of the program.

$$\ln \varepsilon = -3.92495 - .00237t + .45047 \ln t + 1.03087 \ln \sigma - 4.14348 \left(\frac{1}{T}\right) + .11052 \sigma \ln T + .0000406 (T\sigma t) \quad (3\text{-}4)$$

where ε = creep strain, %

t = time, hours

σ = stress, MPa

T = temperature, °K/1000.

An effect of gage on creep response (thin gages creep faster) was noted in both the steady-state literature data base and supplemental test data. This effect, however, is attributed to a change in material processing at about t = .064 cm. No differences in creep response due to rolling direction could be concluded.

The following empirical regression equation was developed for cyclic test data.

$$\ln \varepsilon = -2.89413 - .01743t + .54892 \ln t + 1.31015 \ln \sigma - 6.66548 \left(\frac{1}{T}\right) + .19131 \sigma \ln t + .00021 T\sigma t \quad (3\text{-}6)$$

This equation is applicable over the same temperature range as for the steady-state equation, for times of up to 33 hours (100 cycle test at 20 minutes per cycle).

It was demonstrated that no significant difference exists between steady-state and cyclic creep strain test results.

No effects on creep strain due to variation of time per cycle (for same total time) or atmospheric pressure could be determined. In addition, no evidence of a recovery phenomena was found.

A hardening approach for accumulating creep strains was developed which provided good predictions for trajectory test data. This approach utilized a combination of time hardening and strain hardening accumulation theories in conjunction with the cycle data empirical equation. Use of strain hardening in predicting results of trajectory tests yields greater strains than obtained in testing.

It was demonstrated that complex trajectory creep strains can be adequately predicted using only a few steps to represent the stress and temperature profiles.

3.2 Ti-6Al-4V - RESULTS OF TESTS AND DATA ANALYSIS

3.2.1 STEADY-STATE TITANIUM DATA BASE

3.2.1.1 Titanium Literature Survey. Ti-6Al-4V sheet is available in either annealed or solution treated and aged temper. The use of annealed temper is generally recommended for the thin gages required for reradiative TPS because warpage can occur using the solution treatment process. Therefore, only annealed sheet creep data was used for the data base.

One literature source, Reference 12, had the largest amount of data for annealed sheet. This source contained two separate sets of data: (1) results of creep testing performed by Joliet Metallurgical Laboratories on 0.160 cm sheet manufactured by Mallory Sharon (now Reactive Metals Div. of U.S. Steel); and (2) results of tests performed by Metcut Research Associates on 0.102-.160 cm sheet manufactured by Titanium Metals Corporation of America (TIMET). This data is presented in Appendix D-1.

3.2.1.2 Titanium Data Base Analysis. The Mallory Sharon data set consisted of 9 tests at 589°K, 12 tests at 700°K, and 11 tests at 811°K. Of these 32 tests, only 1

was a replicate. For the TIMET data set, 23 tests were at 589°K, 8 were replicates at 700°K, and 9 were replicates at 811°K. Examination of the two data sets revealed that the range of stresses were similar at 700 and 811°K; however, at 589°K, the Joliet Metallurgical tests were performed at lower stress levels than the Metcut tests. In the analysis of the titanium data, as with the L605 and Rene' 41 data, creep strains greater than 0.5% were eliminated along with the tests that were performed above the yield strength (F_{ty}) at temperature.

Initially the two data sets were analyzed separately to develop the following two equations:

For the Joliet Metallurgical tests

$$\varepsilon = 1.141\ \sigma^{.562}\ t^{.162}\ \exp\left(\frac{-3.453}{T}\right) \tag{3-7}$$

For the Metcut tests

$$\varepsilon = .6487\ \sigma^{.738}\ t^{.299}\ \exp\left(\frac{-4.208}{T}\right) \tag{3-8}$$

where ε = creep strain, %
σ = stress, MPa
t = time, hours
T = Temperature, °K/1000

The standard errors of estimate (S_y) for these two equations, based on the natural logarithm of strain, were .6009 and .6234 respectively. This standard error of estimate appears to be high, especially compared to the L605 and Rene' 41 equations. To determine how low the standard of estimate should be, a study was made of the scatter in data for individual tests and between tests at the same temperature and stress. This scatter is referred to as an internal estimate of error. It was possible to make this calculation for the Metcut data because of the large number of replicate tests. In the analysis of error, calculations were made using data from 20 sets of replicate tests performed by Metcut. These calculations revealed that the error due to testing (internal estimate of error) based on the natural logarithm of strain is 0.29. Therefore, the equation describing the Metcut data

still left a large portion of the data unexplained (S_y of .6234 compared to S_y of .29).

To improve the fit, interaction terms and power functions of σ and t were considered. Application of these types of terms resulted in the following empirical equations.

For Joliet Metallurgical test data

$$\ln \varepsilon = -24.19 + .0073\sigma + 22.79T + .95\ (\ln\sigma - 1.931) + .78\ \ln t - .01\ (\ln t)^2 - .06 \left(\frac{(\ln\sigma - 1.931)\ln t}{T}\right) \quad (3\text{-}9)$$

For Metcut tests

$$\ln \varepsilon = -23.44 + .0058\sigma + 22.73T + .89\ (\ln\sigma - 1.931) + .53\ \ln t - .03 \left(\frac{(\ln\sigma - 1.931)\ln t}{T}\right) \quad (3\text{-}10)$$

The standard error of estimate for these two equations, based on the natural logarithm of strain are .3202 and .4191, respectively. The standard error of estimate of 0.4191 represents the lowest value obtained for the Metcut data.

Because comparative plots of these two equations indicated no significant difference between their prediction capability, the two data bases were combined and used to develop the following equation for the Ti-6Al-4V data base:

$$\ln \varepsilon = -24.89504 + 21.40095(T) + 1.15998\ \ln\sigma + .63357\ \ln t + .00615\ (\ln t)^2 + 6.94 \times 10^{-6}\ (\sigma^2) - .03314\ \frac{(\ln\sigma)\ \ln t}{T} \quad (3\text{-}11)$$

The standard error of estimate (S_y) and multiple R computed for this equation are .4360 and .8783, respectively. This standard error of estimate appears to be limited by the Metcut test results. The residual plots ($\ln \varepsilon_{actual} - \ln \varepsilon_{calculated}$ vs. variable) for this equation are shown in Figure 3-50. Figure 3-51 shows the variation between the actual test points and their calculated values along with the $\pm$ 1.96 S_y error band lines.

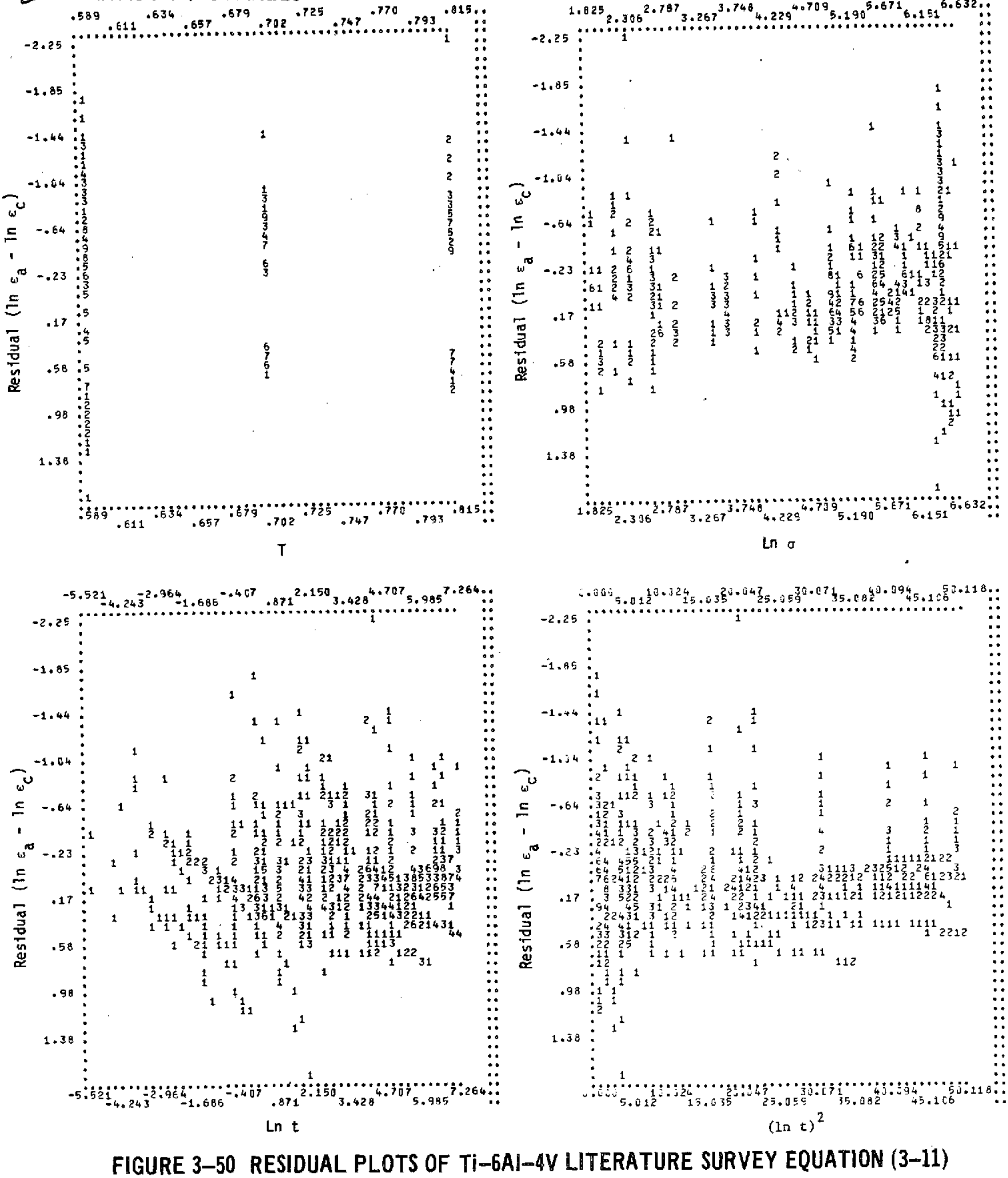

FIGURE 3–50 RESIDUAL PLOTS OF Ti–6Al–4V LITERATURE SURVEY EQUATION (3–11)

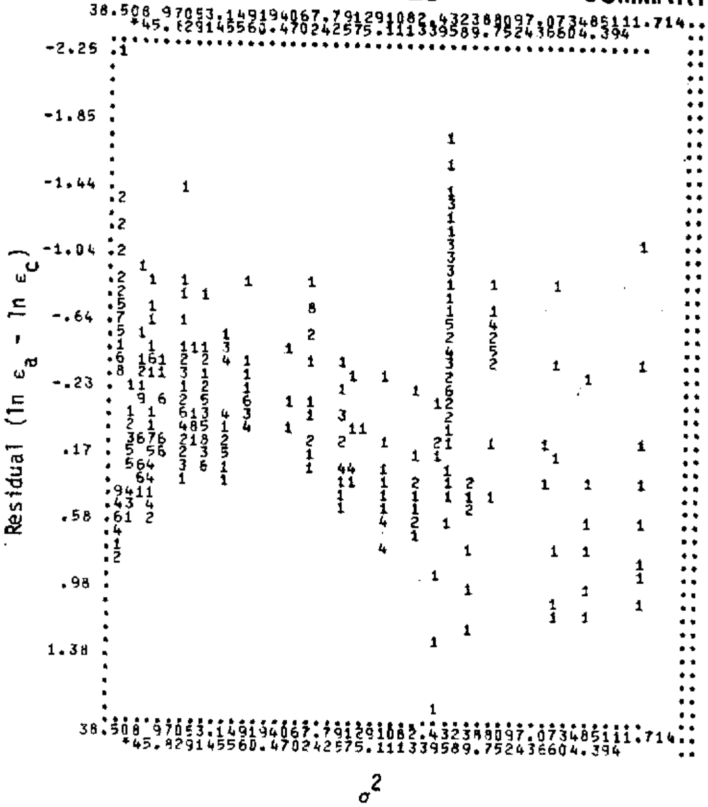

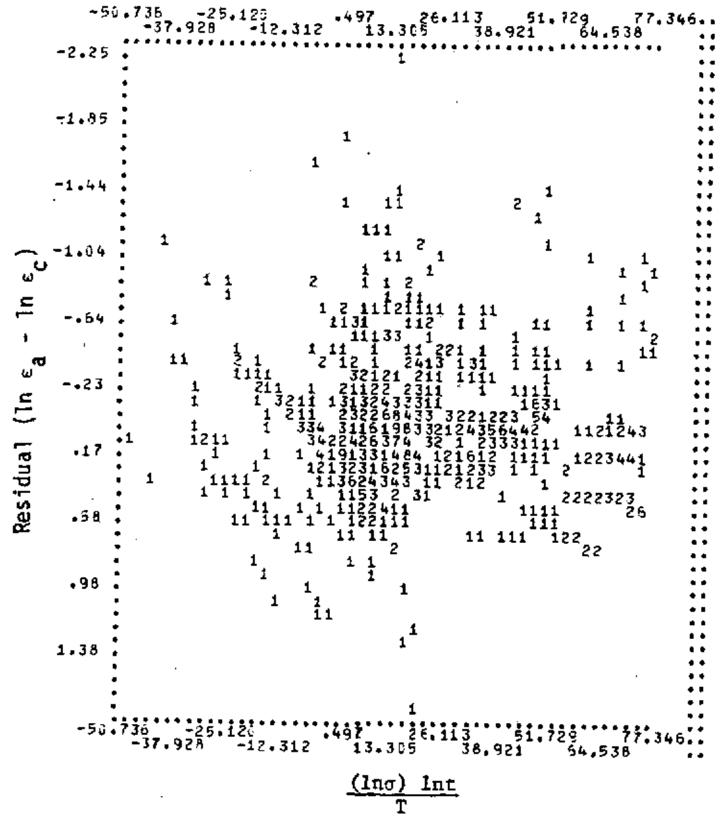

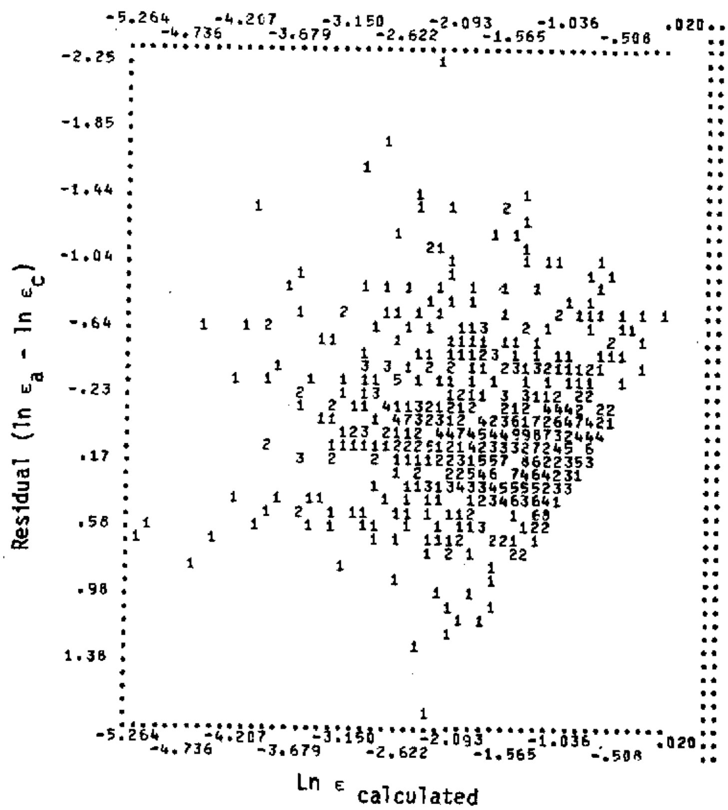

FIGURE 3-50 RESIDUAL PLOTS OF Ti-6Al-4V LITERATURE SURVEY EQUATION (3-11) (Continued)

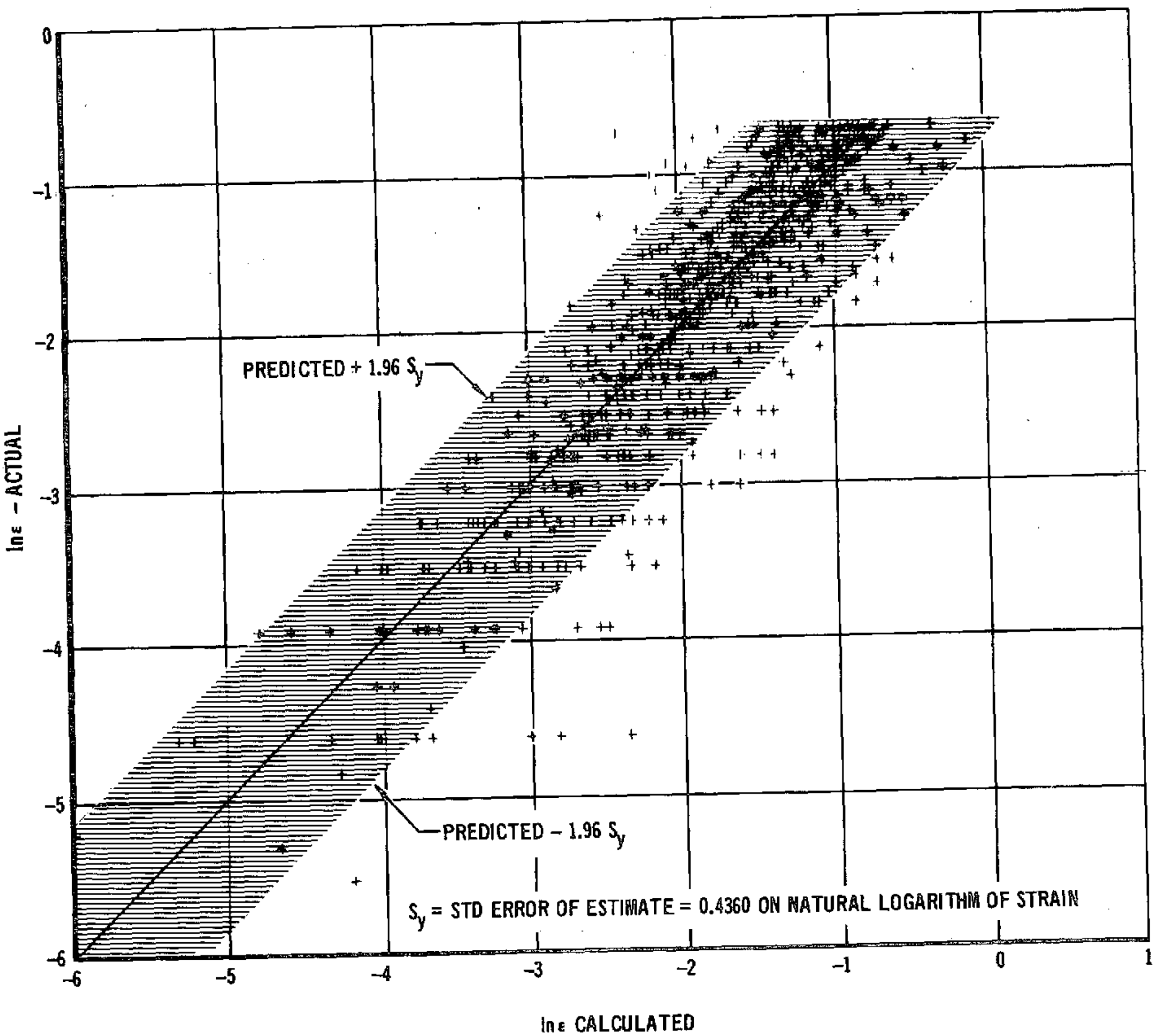

FIGURE 3-51 LOGARITHMIC RELATIONSHIP OF ACTUAL Ti-6Al-4V CREEP STRAIN vs PREDICTED VALUES USING EMPIRICAL REGRESSION EQUATION (3-11)

3.2.2 TITANIUM SUPPLEMENTAL STEADY-STATE TESTING

3.2.2.1 Titanium Supplemental Steady-State Test Matrix.

A total of 15 supplemental steady-state tests were conducted on 6Al-4V titanium tensile specimens. Combinations of temperature and stress selected were those which resulted in strains of approximately 0.50% in 50 hours, 0.33% in 200 hours, and 0.10% in 200 hours, as predicted by the literature survey creep equation (Equation 3-11). Lines of constant creep strain and the test points are indicated in Figure 3-52. Test points obtained from this figure are shown in Table 3-3.

Ten of these tests were for .036 cm (.014 inch) thick material tested in the longitudinal rolling direction. These ten tests make up the basic test matrix from which an empirical equation for supplemental steady-state data was determined. Of the five additional supplemental steady-state tests listed in Table 3-3, three were conducted on .036 cm thick specimens tested in the transverse rolling direction, and two were conducted on .058 cm thick specimens tested in the longitudinal rolling direction. Creep strain results for each of the supplemental steady-state tests are presented in Appendix D-2. Included in this appendix are the elastic strains which were determined at the start and conclusion of the test.

3.2.2.2 Test Data Evaluation - Basic Test Matrix. Agreement between data base predictions, based on the literature survey equation (Equation 3-11), and supplemental test results are noted throughout these tests. This was true even with the difference in gage between the data base supplemental tests.

The following equation was developed using data obtained from the hand faired curves of the basic supplemental tests 1 thru 10 (Figures 3-53 to 3-56). The data consisted of strain values taken at six points per test spaced in such a manner as to describe the curve. For example, a 40-hour test had strains selected at times of 1, 2, 5, 10, 20 and 40, while a 200-hour test had strains selected at

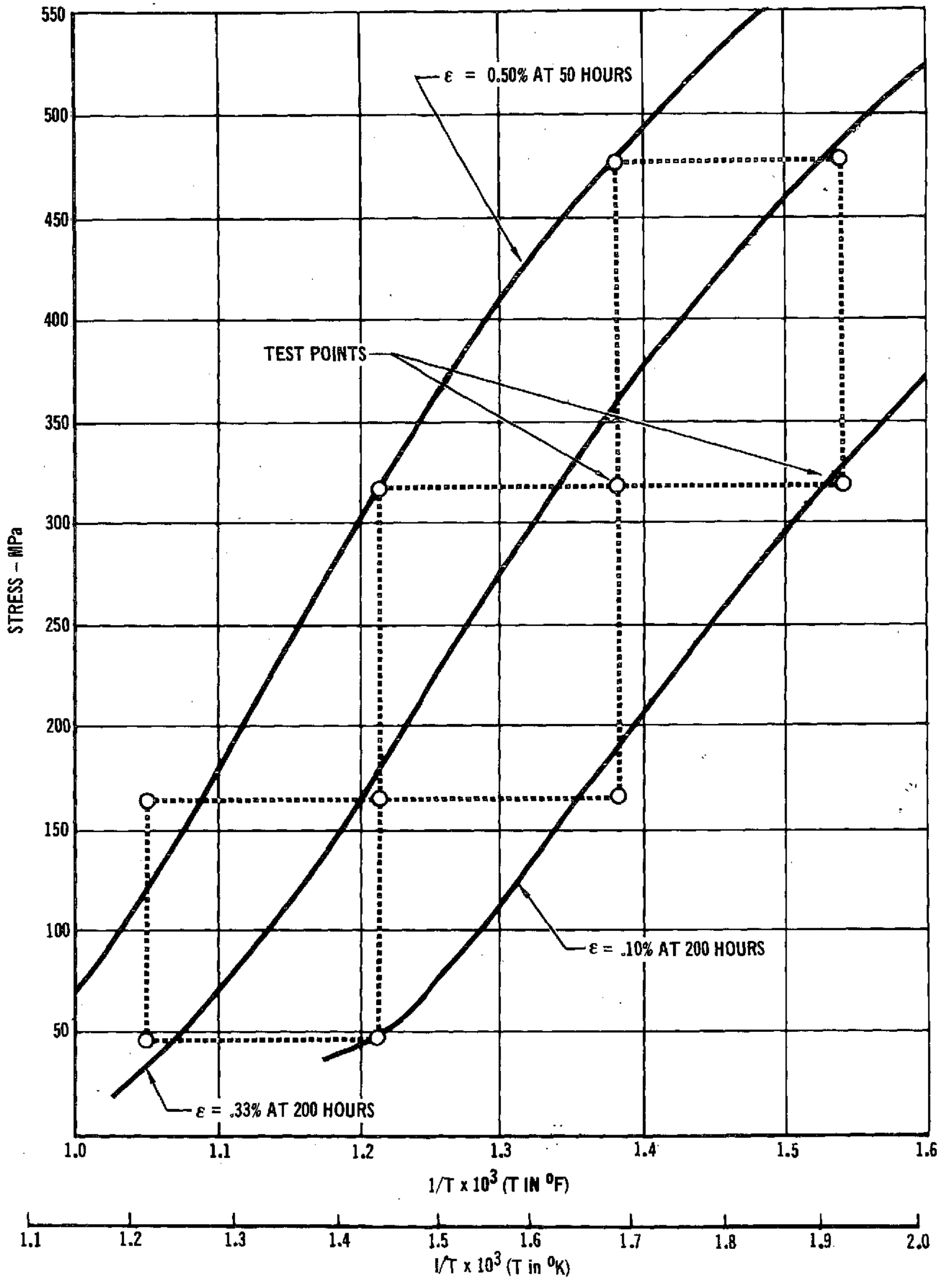

FIGURE 3–52 Ti–6Al–4V SUPPLEMENTAL STEADY-STATE EXPERIMENTAL DESIGN

TABLE 3–3
Ti–6Al–4V SUPPLEMENTAL STEADY-STATE TESTS

TEST NO.	TEST SPECIMEN	MATERIAL ROLLING DIRECTION	MATERIAL GAGE		TEMPERATURE		STRESS	
			CM	INCHES	°K	°F	MPa	KSI
1	T21L	LONGITUDINAL	0.036	0.014	783	950	165.5	24.0
2	T23L	LONGITUDINAL	0.036	0.014	783	950	48.3	7.0
3	T26L	LONGITUDINAL	0.036	0.014	714	825	317.2	46.0
4	T34L	LONGITUDINAL	0.036	0.014	714	825	165.5	24.0
5	T36L	LONGITUDINAL	0.036	0.014	714	825	48.3	7.0
6	T74L	LONGITUDINAL	0.036	0.014	658	725	475.8	69.0
7	T76L	LONGITUDINAL	0.036	0.014	658	725	317.2	46.0
8	T82L	LONGITUDINAL	0.036	0.014	658	725	165.5	24.0
9	T93L	LONGITUDINAL	0.036	0.014	617	650	475.8	69.0
10	T104L	LONGITUDINAL	0.036	0.014	617	650	317.2	46.0
11	T11T	TRANSVERSE	0.036	0.014	714	825	317.2	46.0
12	T12T	TRANSVERSE	0.036	0.014	658	725	317.2	46.0
13	T13T	TRANSVERSE	0.036	0.014	714	825	165.5	24.0
14	T1L	LONGITUDINAL	0.058	0.022	714	825	317.2	46.0
15	T3L	LONGITUDINAL	0.058	0.022	714	825	165.5	24.0

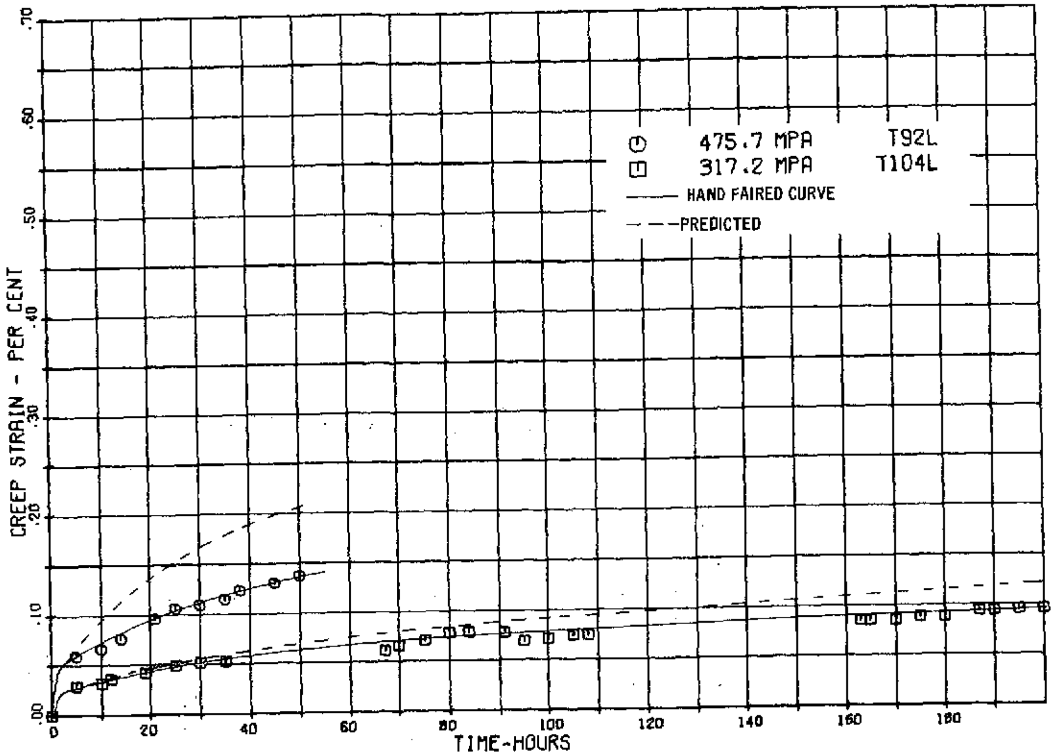

FIGURE 3-53 Ti-6Al-4V SUPPLEMENTAL STEADY-STATE CREEP DATA AT 616^{0}K

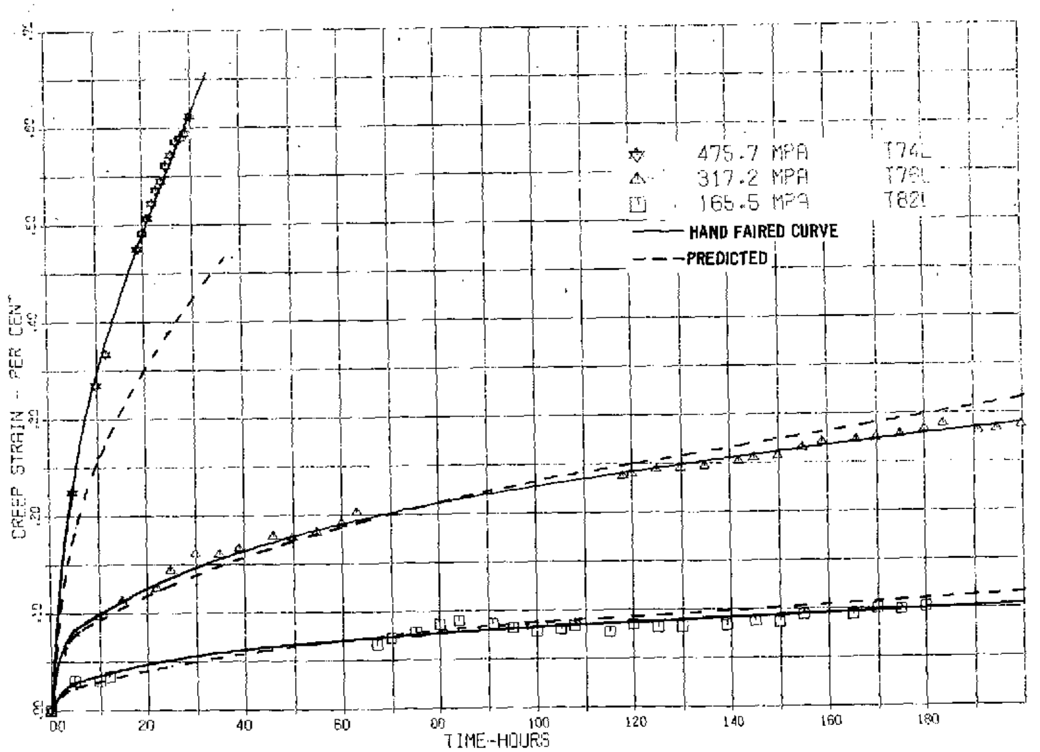

FIGURE 3-54 Ti-6Al-4V SUPPLEMENTAL STEADY-STATE CREEP DATA AT 658^{0}K

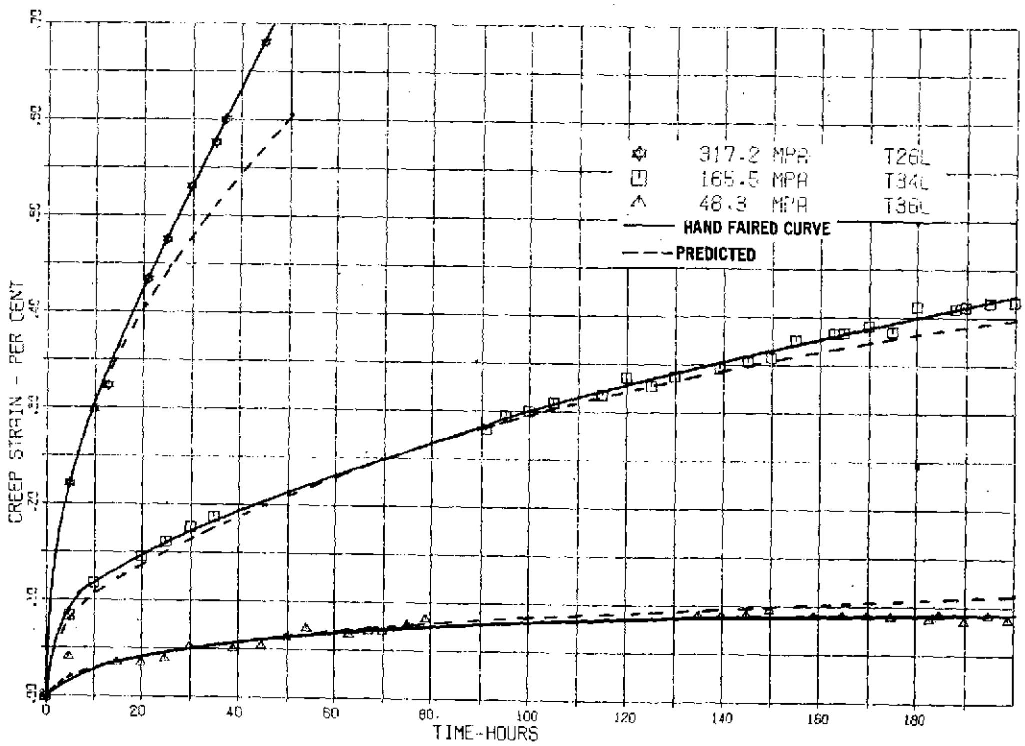

FIGURE 3-55 Ti-6Al-4V SUPPLEMENTARY STEADY-STATE CREEP DATA AT 714°K

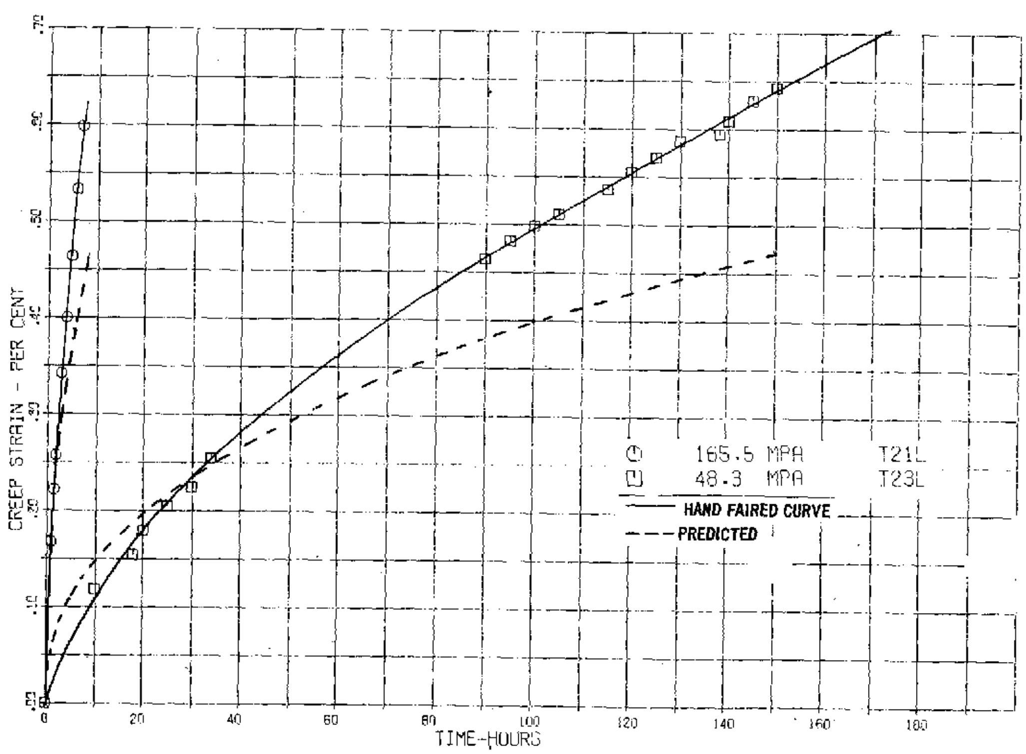

FIGURE 3-56 Ti-6Al-4V SUPPLEMENTARY STEADY-STATE CREEP DATA AT 783°K

1, 5, 20, 50, 100 and 200 hours from the hand faired curves.

$$\ln \varepsilon = -24.08576 + 22.53736\ T + 5.89 \times 10^{-6}\ \sigma^2 + .90505\ \ln\sigma + .43365\ \ln t \qquad (3\text{-}12)$$

The standard error of estimate (S_y) and multiple R computed for this equation are .2438 and .9729, respectively. The residual plots ($\ln \varepsilon_{actual} - \ln \varepsilon_{calculated}$ vs. variable) for this equation are shown in Figure 3-57.

Comparisons of creep strain predictions (based on Equation (3-13)) with test results are shown in Figures 3-53 thru 3-56.

3.2.2.3 Effects of Gage and Rolling Direction. The last five supplemental steady-state tests listed in Table 3-3 were conducted to investigate possible effects of material rolling direction and material gage on creep. Therefore, each of the three transverse specimens and two .058 cm (.022 inch) thick specimens were tested at stresses and temperatures at which testing had been conducted for the basic test matrix specimens. Comparative plots of creep strain results for these tests are shown in Figures 3-58 to 3-60. No significant difference in creep response due to thickness variation and rolling direction was observed.

3.2.3 COMPARISON OF TITANIUM STEADY-STATE DATA BASE AND SUPPLEMENTAL TEST RESULTS.

Comparison of the literature survey equation (Equation 3-11) with the supplemental creep equation (Equation 3-12) on a term-for-term basis indicated agreement between supplemental test results and the literature survey data base. The two terms $(\ln t)^2$ and $\ln\sigma \ln t/T$ in Equation 3-11, were not determined to be significant in fitting the supplemental test data.

Stress and temperature combinations required to produce three levels of creep strain (.50% @ 50 hours, .33% @ 200 hours, and .10% @ 200 hours) for the supplemental data equation are shown in Figure 3-52. Comparison of these constant strain lines with those for the data base equation indicates that creep occurred at a

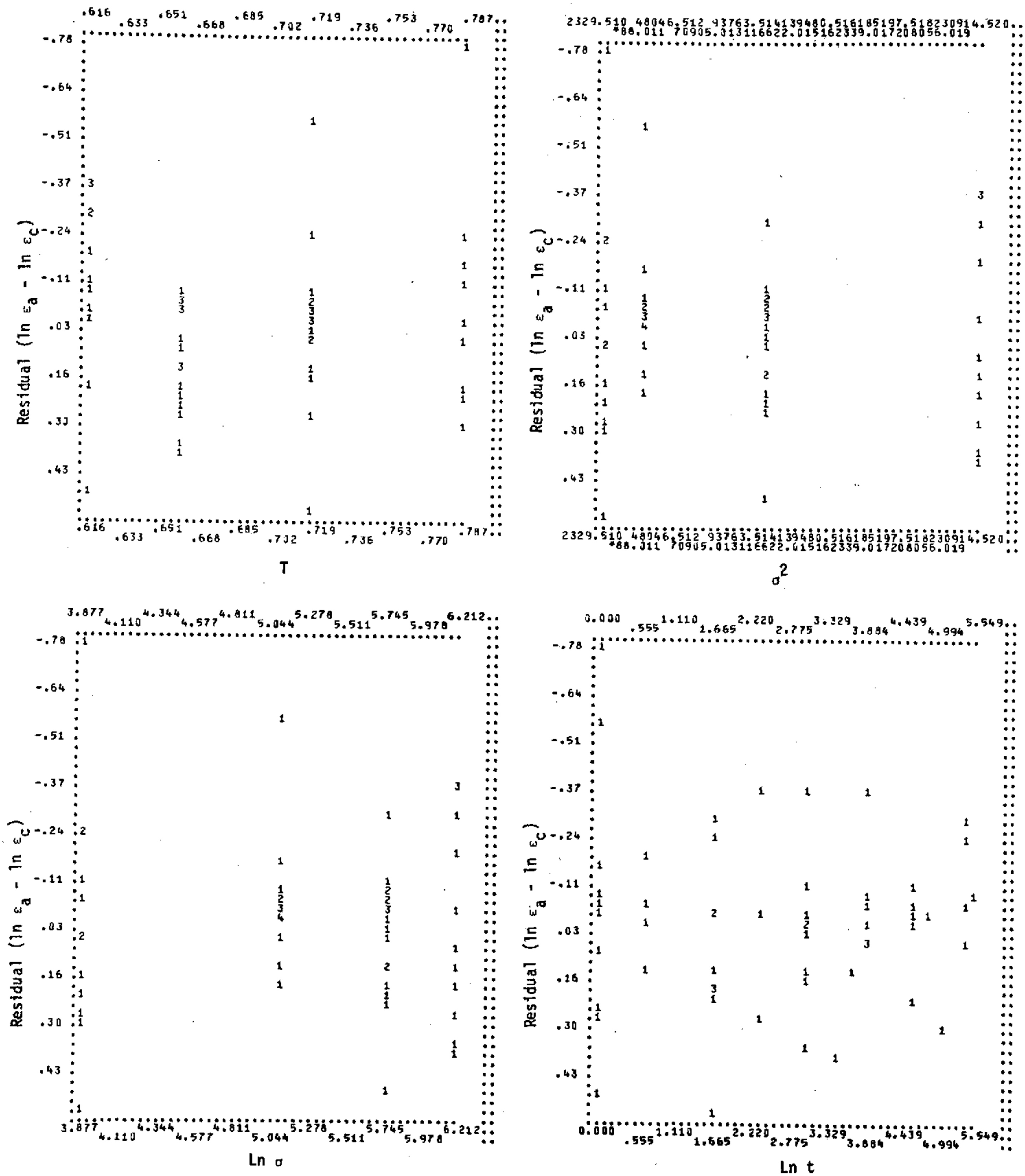

FIGURE 3-57 RESIDUAL PLOTS OF Ti-6Al-4V SUPPLEMENTAL STEADY-STATE EQUATION (3-12)

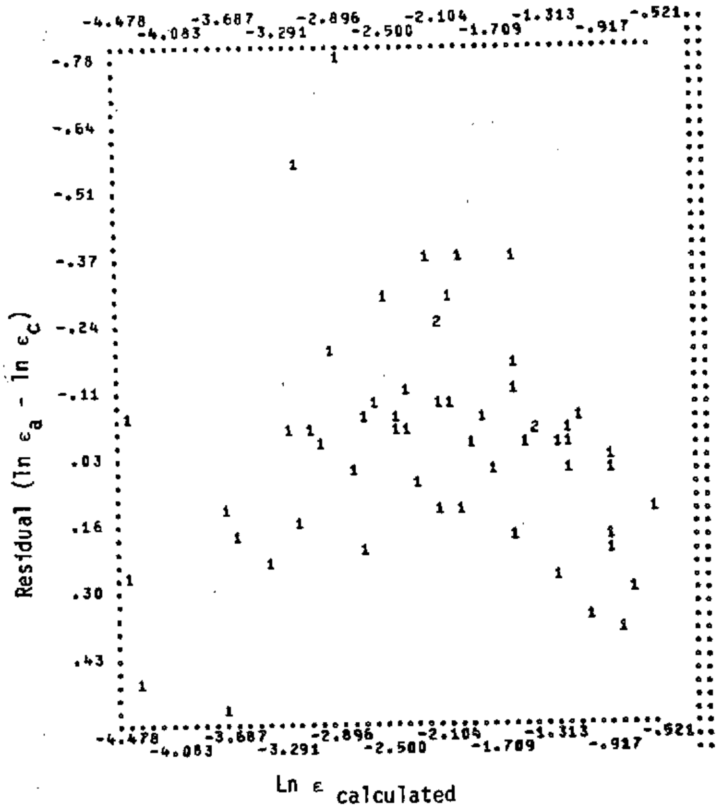

FIGURE 3–57 RESIDUAL PLOTS OF Ti–6Al–4V SUPPLEMENTAL STEADY-STATE EQUATION (3–12) (Continued)

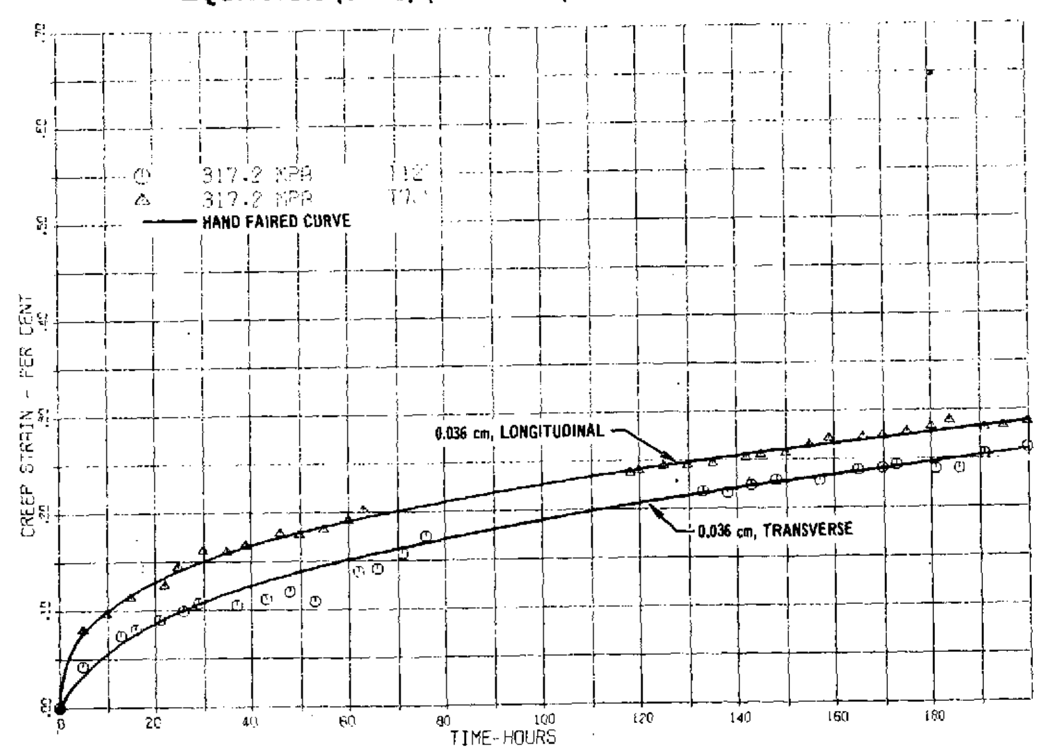

FIGURE 3–58 EFFECT OF ROLLING DIRECTION ON Ti–6Al–4V CREEP AT 658°K AND 317.2 MPa

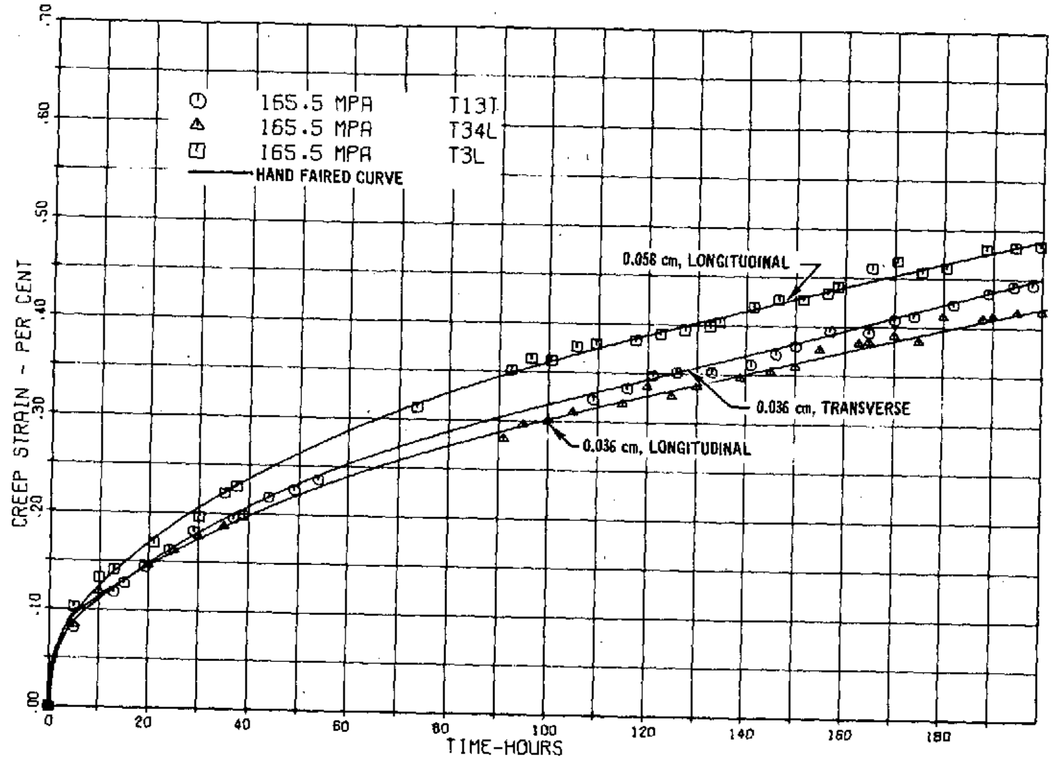

FIGURE 3-59 COMPARISON OF GAGE AND ROLLING DIRECTION ON Ti-6Al-4V CREEP AT 714°K AND 165.5 MPa

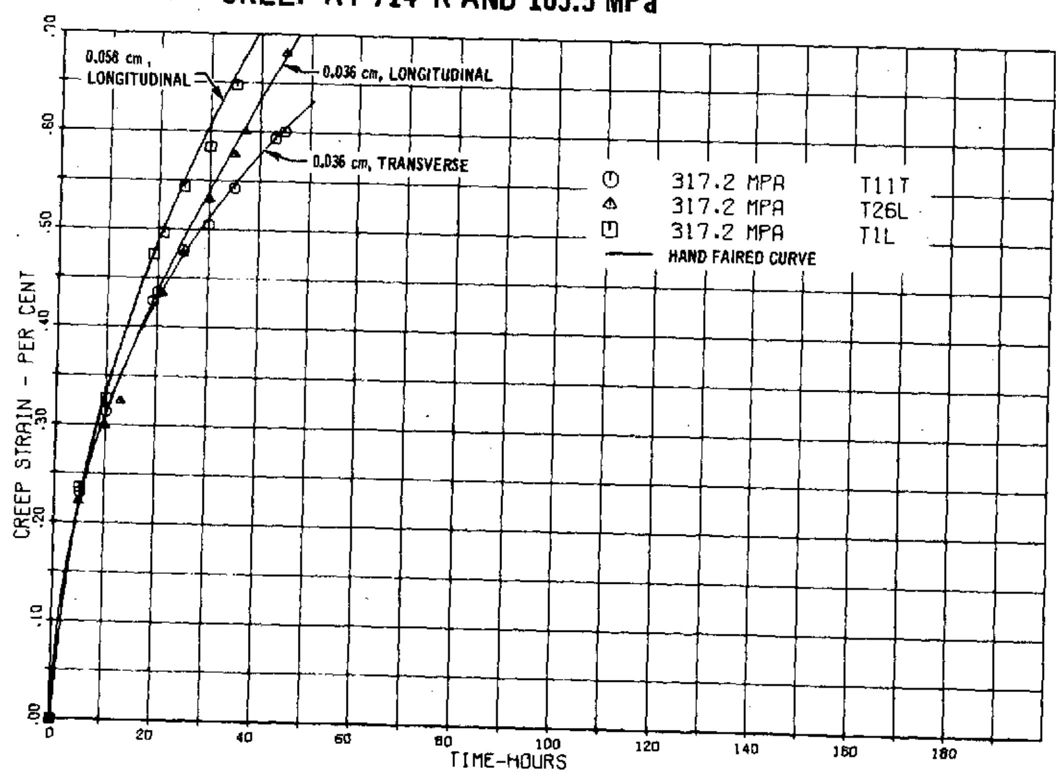

FIGURE 3-60 COMPARISON OF GAGE AND ROLLING DIRECTION ON Ti-6Al-4V CREEP AT 714°K AND 317.2 MPa

faster rate in the supplemental tests. Based on Figure 3-52, percentage variations is stress required to produce equal creep strains, at a typical temperature of 714°K, range from approximately 22% (@ 151.7 MPa) to 8% (@ 296.5 MPa).

Use of the supplemental creep equation (Equation 3-12) will yield conservative predictions relative to the literature survey equation (Equation 3-11). In addition, the use of Equation (3-12) would be recommended for use in predictions at low stresses and times since the boundary conditions of zero strain at zero stress and time are satisfied.

3.2.4 TITANIUM BASIC CYCLIC TESTS

3.2.4.1 Basic Cyclic Test Matrix. Basic cyclic tests were conducted on twelve .030 cm specimens at temperatures of 658°K (725°F), 714°K (825°F), 783°K (950°F, and 839°K (1050°F) as indicated in Table 3-4. Each of the specimens was tested in the longitudinal rolling direction. Each test was conducted for 100 cycles using the 55 minute cycle (20 minutes at load and peak temperatures) presented in Section 2.9.2.2. This portion of the cyclic tests are designated as titanium cyclic tests 1 thru 4 (3 specimens per test). Data are presented in Appendix D-3.

The 658°K, 714°K and 783°K test temperatures are the same as those tested in the supplemental steady-state tests. The 658°K temperature, however, was the minimum temperature at which loads could be applied within the whiffle tree mechanism design load capability and still obtain reasonable creep strains. Therefore, a test temperature of 839°K was used in test 4 instead of the 617°K temperature used in supplemental steady-state testing.

3.2.4.2 Test Results and Analysis. Cyclic creep strain results for the twelve specimens in test 1 through 4 are presented in Figures 3-61 through 3-64.

The following equation was developed using data obtained from the hand faired curves of these twelve tests. This data consisted of strain values taken at

TABLE 3-4 Ti-6AL-4V BASIC CYCLIC TESTS

CYCLIC TEST NO.	TEST SPECIMEN	TEMPERATURE		STRESS	
		°K	°F	MPa	KSI
1	T25L	658	725	207.0	30.02
1	T60L	658	725	299.2	43.40
	T51L	658	725	399.0	57.86
	T38L	714	825	114.7	16.63
2	T39L	714	825	192.0	27.85
	T31L	714	825	295.9	42.92
	T56L	783	950	49.9	7.23
3	T59L	783	950	82.9	12.03
	T41L	783	950	130.4	18.91
	T87L	839	1050	19.7	2.85
4	T89L	839	1050	30.5	4.43
	T64L	839	1050	47.2	6.85

NOTES
1. ALL SPECIMENS .030 CM
2. ALL SPECIMENS TESTED IN LONGITUDINAL ROLLING DIRECTION.
3. ALL TESTS – 20 MINUTES/CYCLE, 100 CYCLES.

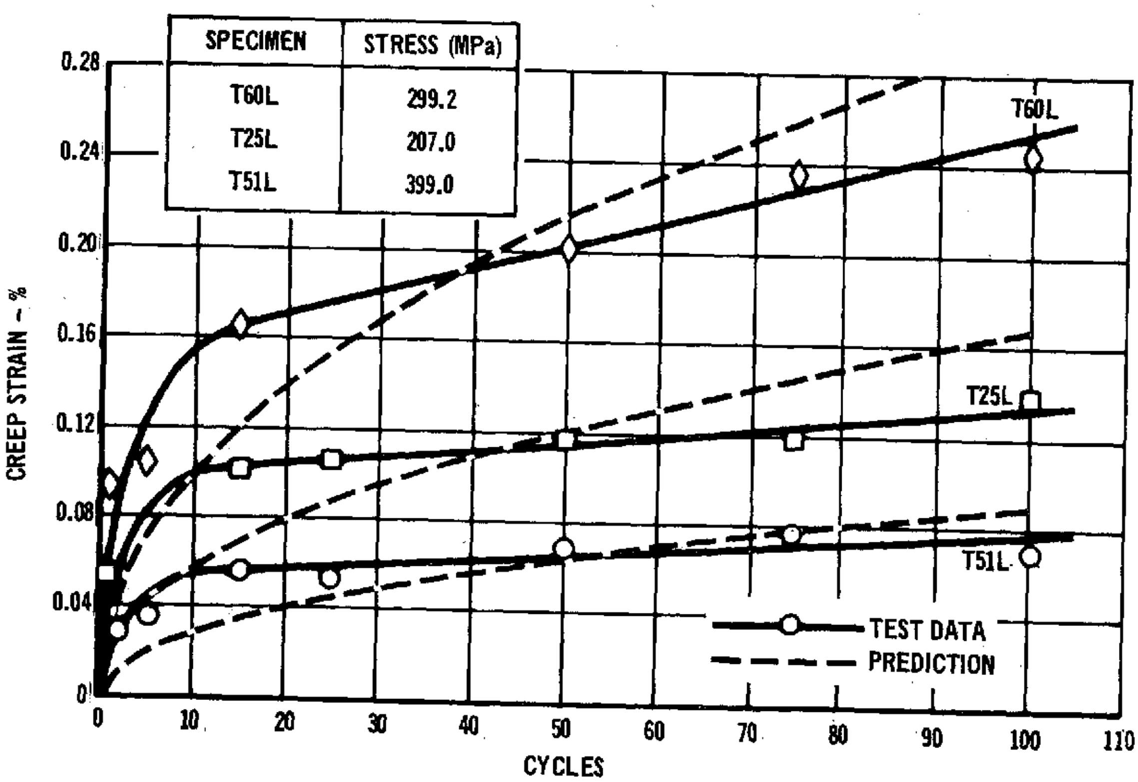

FIGURE 3-61 Ti-6Al-4V CYCLIC TEST NO. 1 – BASIC CYCLIC TEST AT 658°K

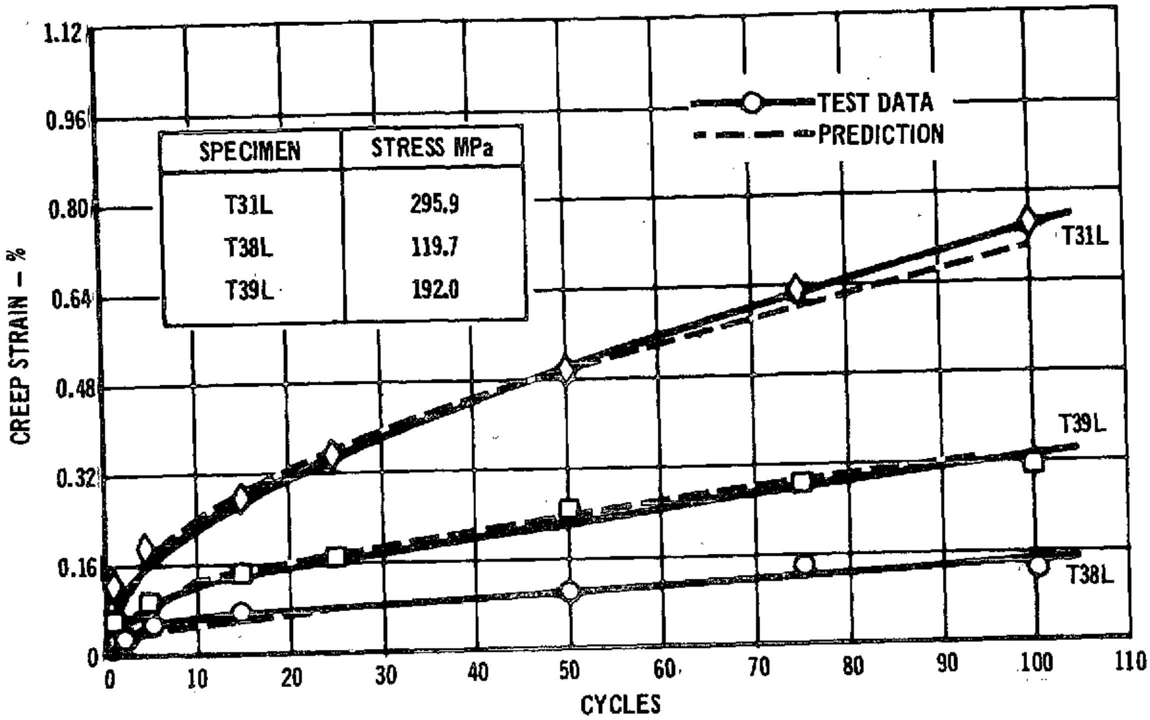

FIGURE 3-62 Ti-6Al-4V CYCLIC TEST NO. 2 – BASIC CYCLIC TEST AT 714°K

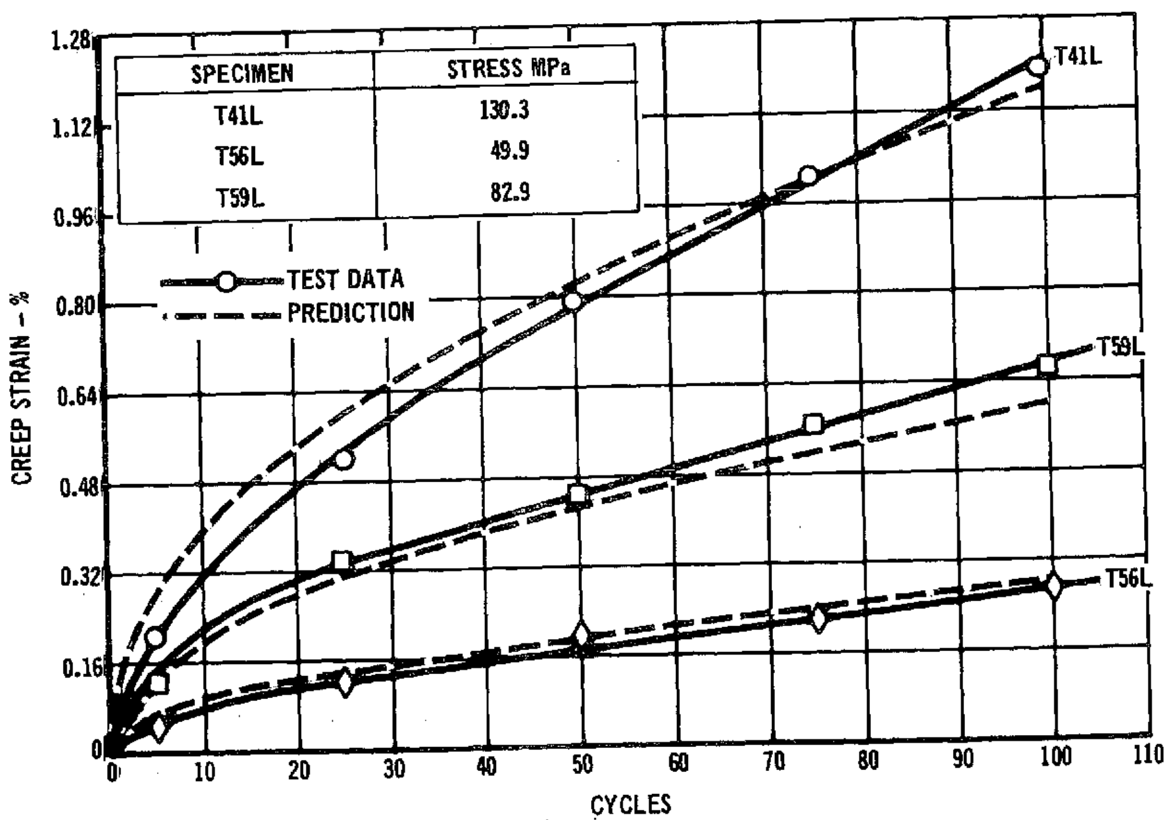

FIGURE 3-63 Ti-6Al-4V CYCLIC TEST NO. 3 – BASIC CYCLIC TEST AT 783°K

5 cycle intervals from the hand faired crrves. Creep times were the accumulated cycle time at maximum load and temperature, therefore, for the basic cycles the time was .33 hrs/cycle or 1.67 hrs/5 cycles.

$$\ln \varepsilon = -28.94077 + 26.24850\ T + 2.52 \times 10^{-6}\ \sigma^2 + 1.40406\ \ln\sigma + .46894\ \ln t \qquad (3\text{-}13)$$

The standard error of estimate (S_y) and multiple R computed for this equation are .1951 and .9755, respectively. The residual plots ($\ln \varepsilon_{actual} - \ln \varepsilon_{calculated}$ vs. variable) for the equation are shown in Figure 3-65. It is of the same form as that obtained for the supplemental steady state tests (Equation 3-12).

Comparison of predictions, using this equation, and the basic cyclic test data, are shown in Figures 3-61 through 3-64.

3.2.5 COMPARISON OF TITANIUM CYCLIC AND SUPPLEMENTAL STEADY-STATE DATA

3.2.5.1 Test Data Comparison. As was noted in Section 3.2.4 both supplemental steady-state and basic cyclic tests were conducted at three common temperatures (658°K, 714°K and 783°K). Direct comparisons of test data at these temperatures from these two series of tests are shown in Figures 3-66 and 3-67 for times of 5 hours (15 cycles) and 33.3 hours (100 cycles), respectively. In this comparison the cyclic time was the accumulated time at maximum load and temperature (i.e., 100 cycles = 33.3 hours). Based on this comparison, there does not appear to be any significant difference between cyclic and steady-state data for equal total times at load.

3.2.5.2 Microstructure Comparison. The microstructure of the as-received Ti-6Al-4V alloy (Figure 3-68) consists of slightly elongated grains of alpha phase in a beta phase matrix. Exposure to both cyclic and steady-state creep at temperatures as high as 783°K and stresses of 48.3 MPa has produced no observable change in the microstructure of this alloy relative to the as-received structure.

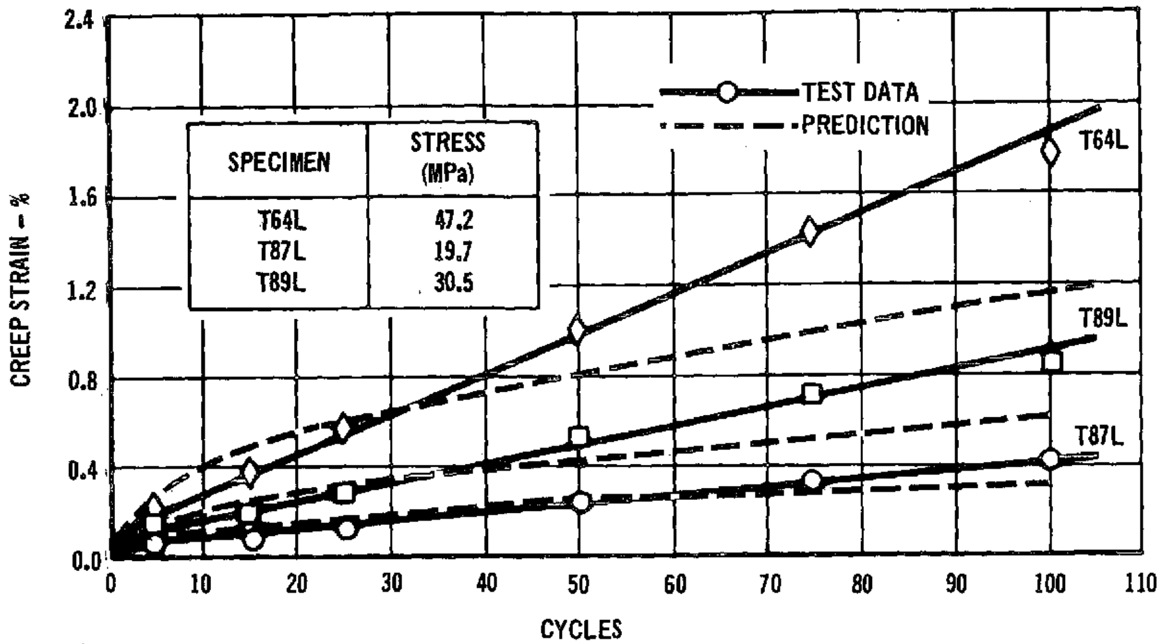

FIGURE 3-64 Ti-6Al-4V CYCLIC TEST NO. 4 – BASIC CYCLIC TEST AT 839° K

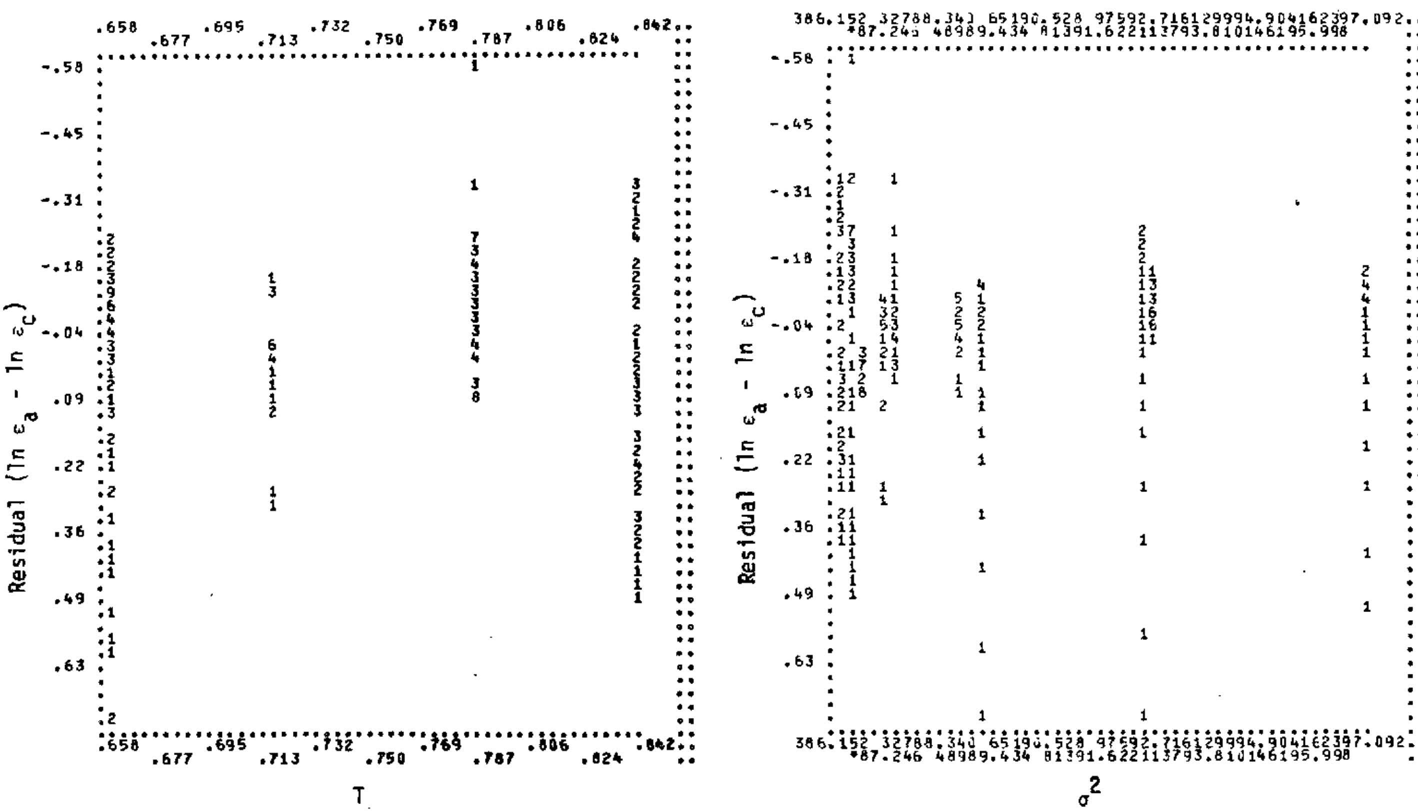

FIGURE 3-65 RESIDUAL PLOTS OF Ti-6Al-4V CYCLIC CREEP EQUATION (3-13)

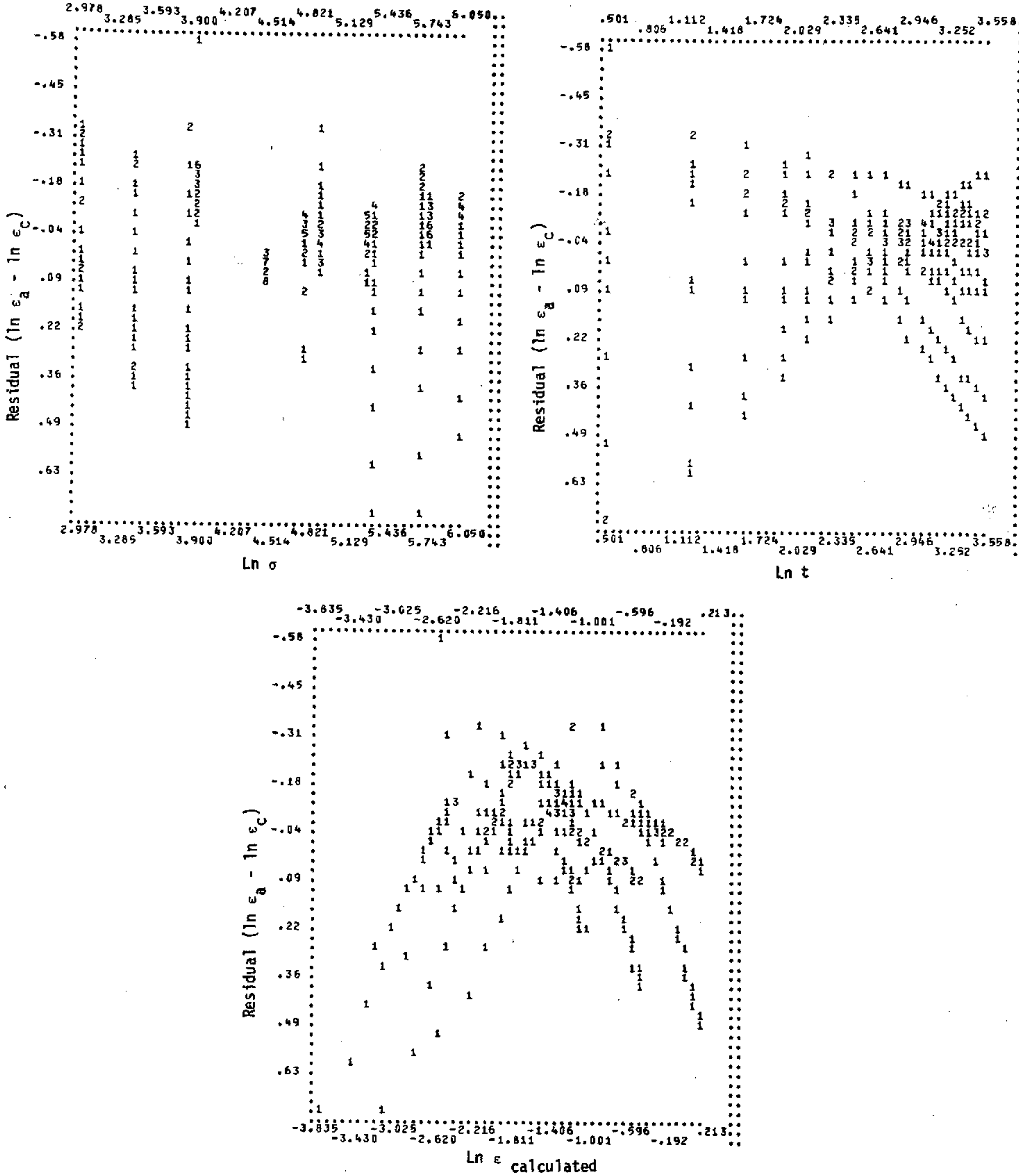

FIGURE 3-65 RESIDUAL PLOTS OF Ti-6Al-4V CYCLIC CREEP EQUATION (3-13)(Continued)

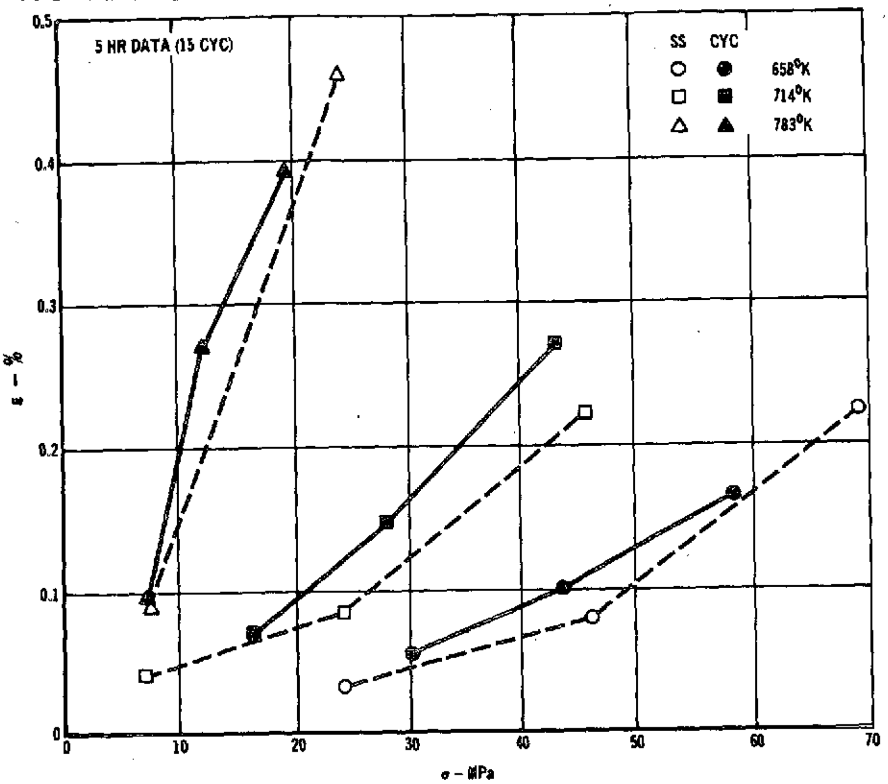

FIGURE 3-66 COMPARISON Ti-6Al-4V CYCLIC AND SUPPLEMENTAL STEADY-STATE DATA AT 5 HOURS

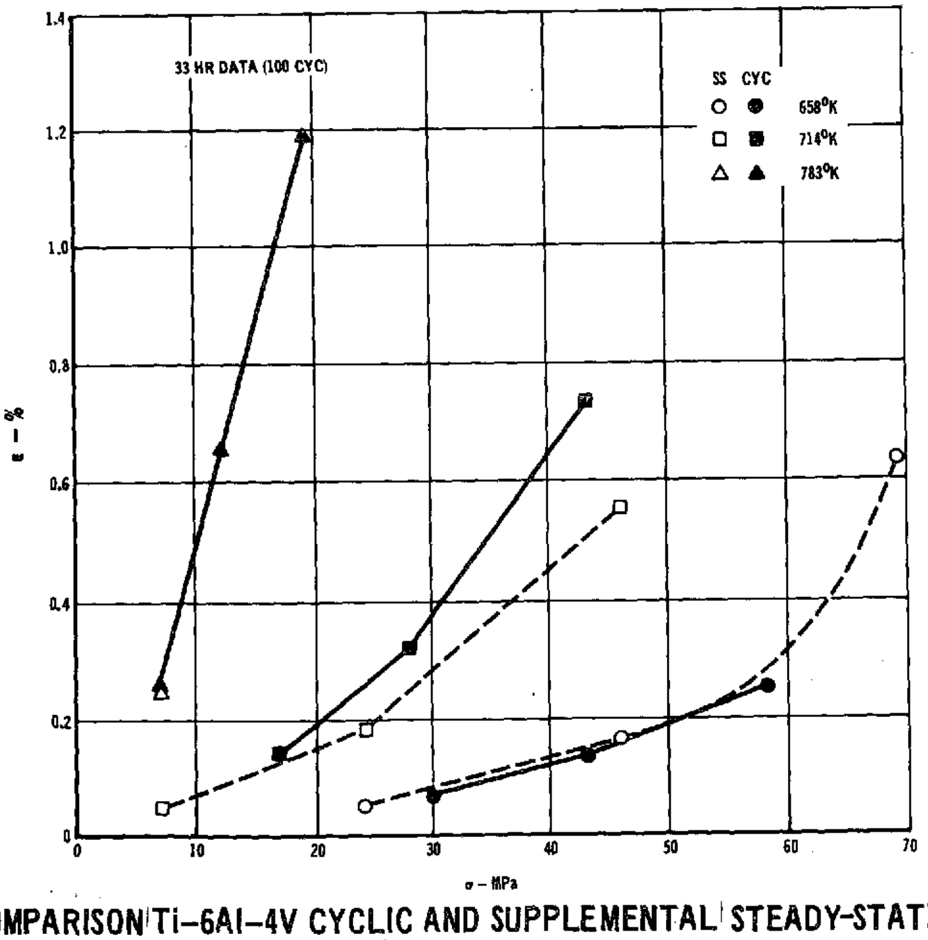

FIGURE 3-67 COMPARISON Ti-6Al-4V CYCLIC AND SUPPLEMENTAL STEADY-STATE DATA AT 33 HOURS

ALLOY: Ti-6Al-4V
CONDITION: AS RECEIVED
ETCHANT: KROLL'S REAGENT*
MAG: 500X
THICKNESS 0.031 cm

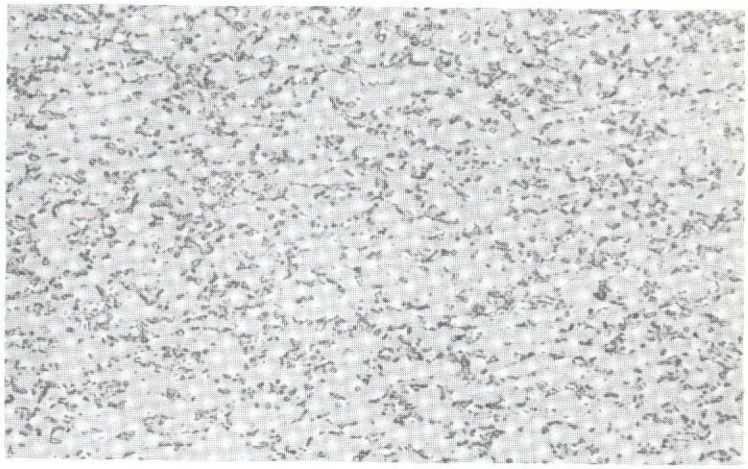

ALLOY: Ti-6Al-4V
CONDITION: TESTED (CYCLIC)
APPLIED STRESS: 48.3 MPa
TEST TEMPERATURE: 783°K
EXPOSURE TIME: 100 CYCLES (33.3 HRS)
ETCHANT: KROLL'S REAGENT
MAG: 500X
THICKNESS 0.034 cm

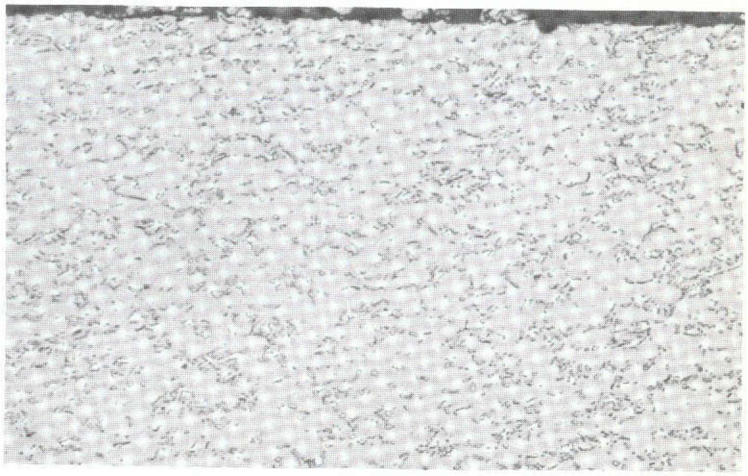

SPEC NO. T56L

ALLOY: Ti-6Al-4V
CONDITION: TESTED (STEADY STATE)
APPLIED STRESS: 48.3 MPa
TEST TEMPERATURE: 783°K
EXPOSURE TIME: 150 HOURS
ETCHANT: KROLL'S REAGENT
MAG: 500X
THICKNESS 0.035 cm

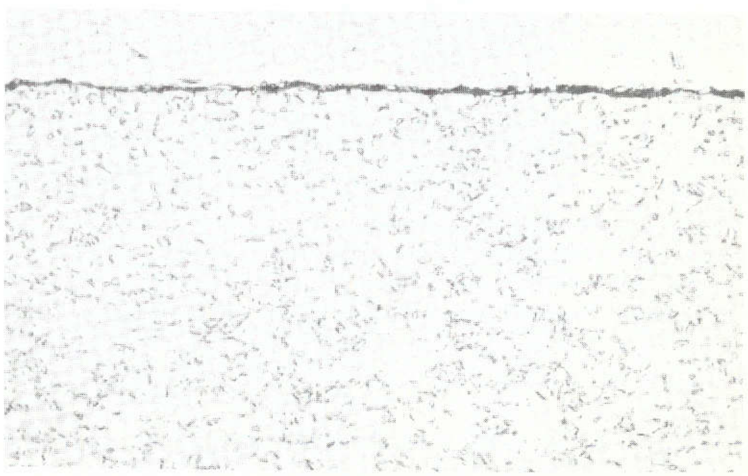

*2ml HF, 5ml HNO_3, 93ml H_2O

SPEC NO. T23L

FIGURE 3-68 MICROSTRUCTURE OF Ti-6Al-4V BEFORE AND AFTER CREEP EXPOSURE

3.2.6 TITANIUM CYCLIC TESTS FOR EVALUATION OF ADDITIONAL VARIABLES

3.2.6.1 Effect of Time Per Cycle. Results of titanium cyclic creep test No. 7 are presented in Figure 3-69. This test is a replicate of test 2, except that the time at load and maximum temperature is 10 minutes instead of the 20 minutes used in test 2. Comparison is made in Figure 3-69 between the two tests for equal total time at load. Also shown in the figure is the $\pm$ 1.96 S_y confidence band about the 20 minute per cycle data based on S_y = .1951 derived for the 20 minute-per-cycle basic cyclic equation (Equation 3-13). Although the 10 minute per cycle data are within this band, these data are consistently about 25% lower than the 20 minute per cycle data. Therefore it appears that there may be an effect due to time per cycle on titanium cyclic creep strains.

3.2.6.2 Effect of Atmospheric Pressure. Cyclic tests 10 and 11 were replicate idealized trajectory tests, except that a simulated atmospheric pressure profile was applied in test 11 while in test 10 the pressure was maintained constant at <1.3 pa. Comparison of creep strain results for the corresponding specimens in these tests are shown in Figure 3-70. Based on the comparison, it cannot be concluded that varying the atmospheric pressure has any effect on creep strain response.

3.2.6.3 Effects of Time Between Cycle. Specimens T41L, T56L, and T59L were tested to 100 cycles at 783°K (cyclic test No. 3) as part of the basic cyclic tests for titanium. Several weeks subsequent to completion of this test the specimens were tested for an additional 50 cycles. This additional cycling is designated as cyclic test No. 12. Creep strain results are shown in Figure 3-71. Comparison of the creep rates at the end of test 3 with those obtained in test 12 indicates a slight increase in slope. However, this increase is not

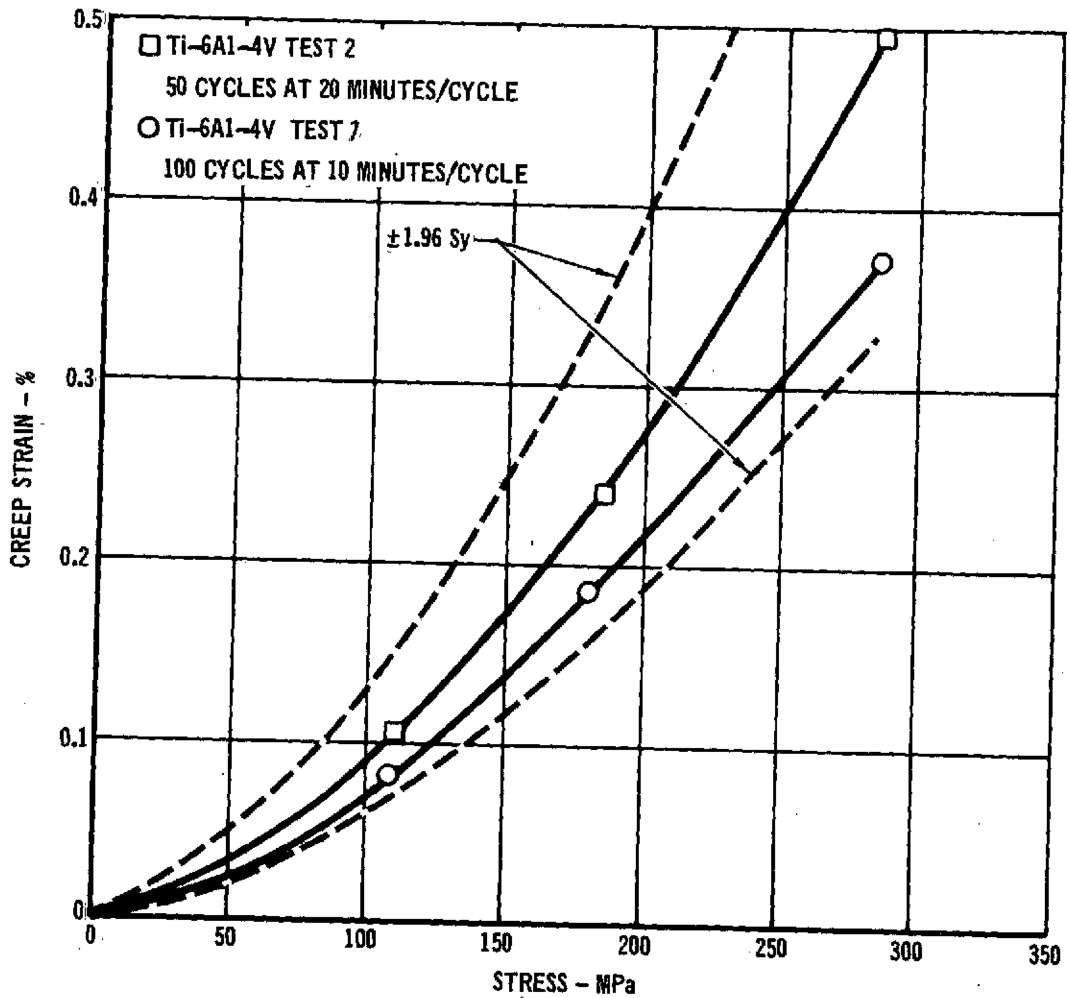

FIGURE 3-69 Ti-6AL-4V CYCLIC CREEP STRAINS AS A FUNCTION OF TIME PER CYCLE

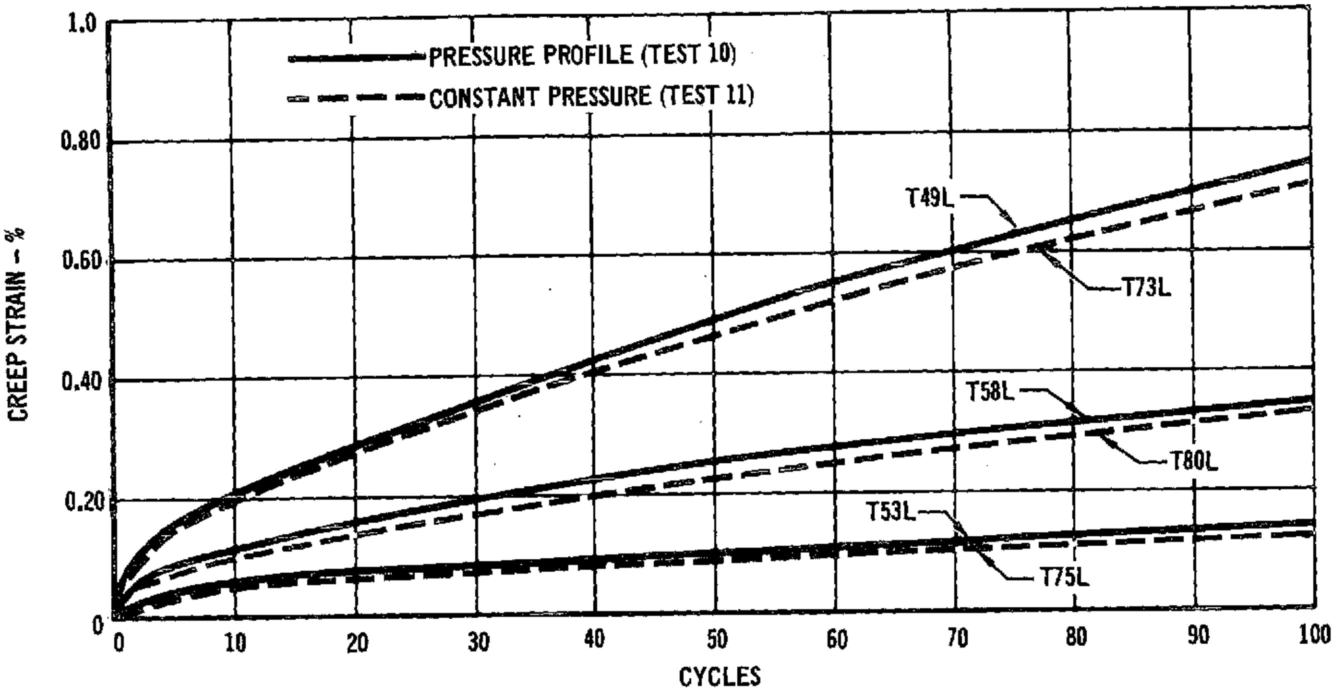

FIGURE 3-70 COMPARISON OF TITANIUM CYCLIC TEST DATA FOR EFFECTS OF ATMOSPHERIC PRESSURE

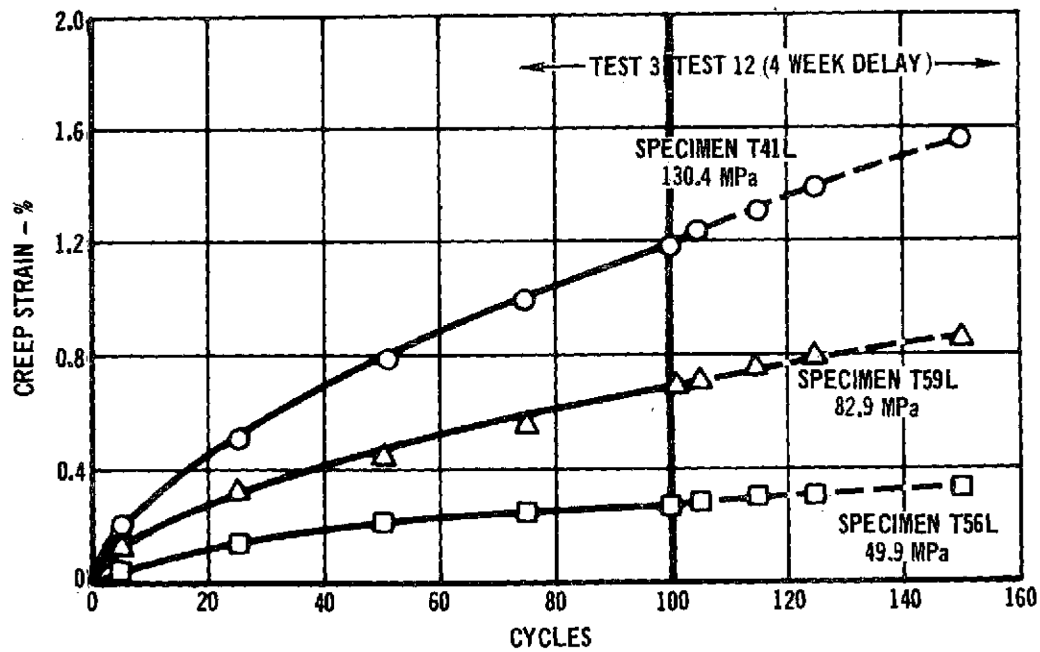

FIGURE 3-71 EFFECT OF TIME DELAY BETWEEN CYCLE TESTS ON THE CREEP BEHAVIOR OF Ti-6Al-4V

considered sufficient to conclude that the time delay has an effect on creep strains.

3.2.7 STEPPED STRESS CYCLIC TESTS

Increasing and decreasing stress history tests were conducted on titanium specimens. These were titanium cyclic test No. 5 (specimens T67L, T63L, T66L) and titanium cyclic test No. 6 (specimens T78L, T68L, T69L), respectively. Both tests were conducted at 783°K. Comparisons of creep strain tests results with predictions based on strain hardening and time hardening creep accumulation theories in conjunction with the cyclic creep equation (Equation 3-13) are shown in Figures 3-72 and 3-73. Predictions based on the time hardening theory are closest to test results in the case of the increasing stress history test (test 5) and predictions based on the strain hardening theory are closest to test results for the decreasing stress history test (test 6). Therefore, the analysis approach where strain is accumulated by using time hardening when strain rate increases and strain hardening when strain rate decreases (rate dependent approach) will be evaluated in the analysis of trajectory test data in the following section.

3.2.8 TRAJECTORY TESTS

Four cyclic trajectory tests (8, 9, 10 and 11) were conducted using titanium tensile specimens. These tests are a two-step stress trajectory profile with a constant maximum temperature of 783°K and constant pressure (test 8); an actual trajectory test (test 9) using actual Shuttle stress, temperature, and pressure profiles; and two idealized trajectory tests (tests 10 and 11) with maximum temperatures of 873°K. Comparison of test 10 and 11 results on the basic of atmospheric pressure variations, is presented in Section 3.2.6.2.

Comparison of creep strain results for tests 8, 9 and 10 with predictions based on the strain hardening theory of creem accumulation are shown in Figures 3-74 to

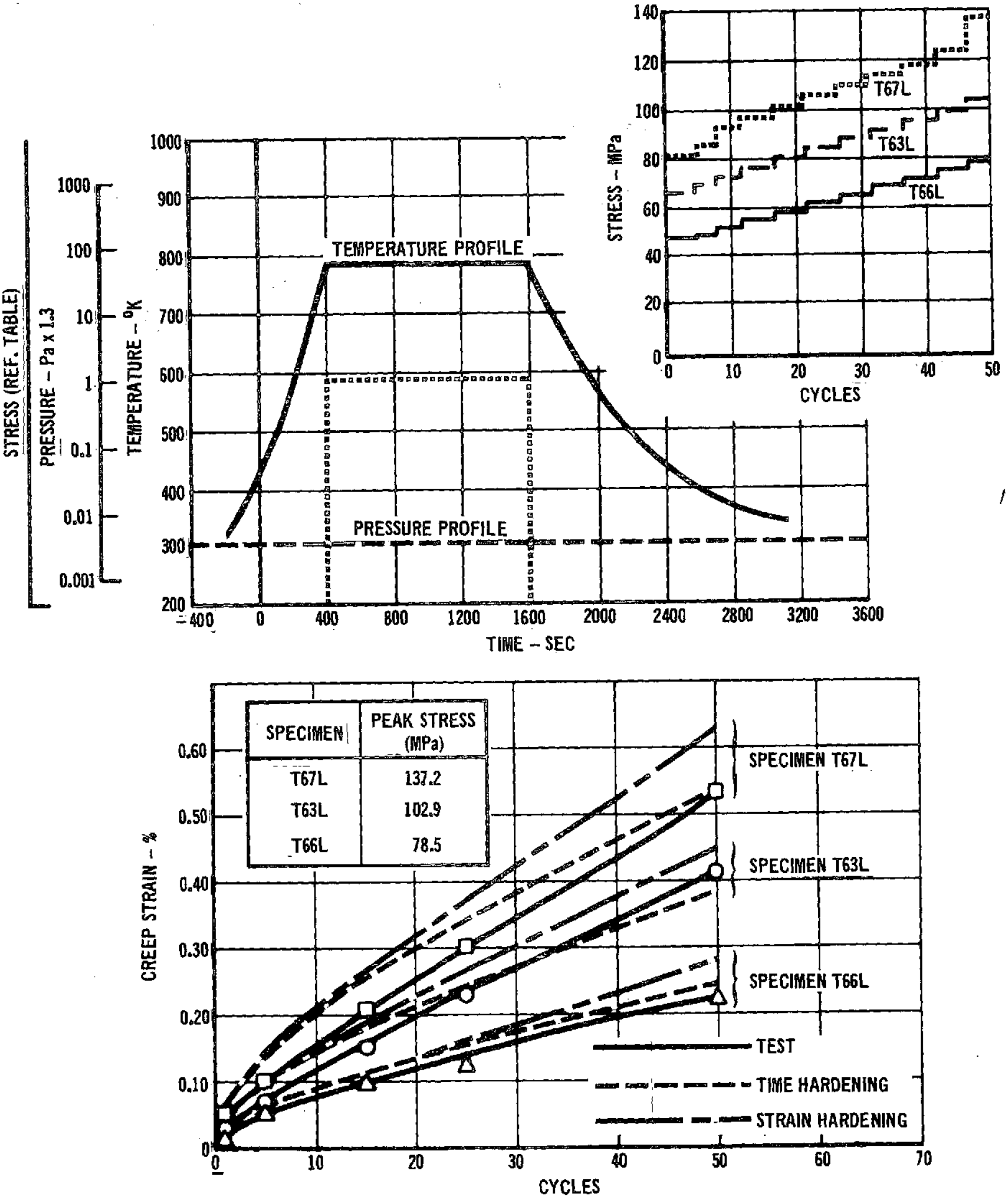

FIGURE 3-72 COMPARISON OF HARDENING THEORY PREDICTIONS WITH INCREASING STRESS TEST RESULTS (Ti-6Al-4V CYCLIC TEST 6)

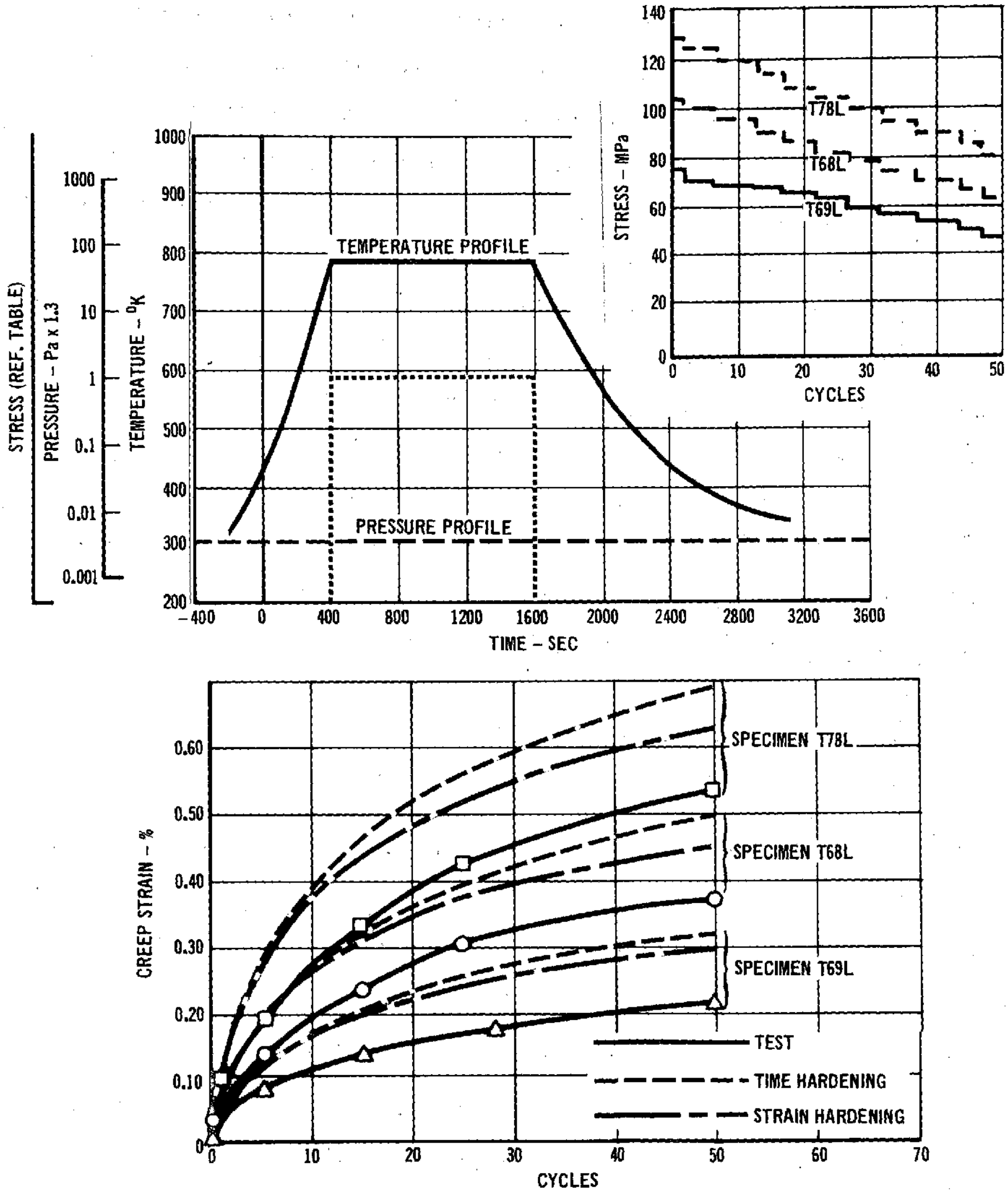

FIGURE 3-73 COMPARISON OF HARDENING THEORY PREDICTIONS WITH DECREASING STRESS TEST RESULTS (Ti-6Al-4V CYCLIC TEST 7)

3-76. The strain hardening theory was found to yield the best predictions for this series of tests, although all predictions resulted in lower creep strain than obtained in testing at the higher test times. The rate dependent approach, used successfully in predicting L605 data, yielded strains comparable to the time hardening predictions for these titanium data. These predictions were approximately 20% below the strain hardening predictions shown.

Steps used in idealizing the simulated mission stress and temperature profiles (test 9) for analysis purposes are indicated in Figure 3-75. Higher creep strains are predicted and obtained in the idealized trajectory tests (tests 10 and 11) than in the simulated mission test, (test 9) because the 783°K peak temperature is maintained over a longer period of time in tests 10 and 11.

The creep accumulation analysis for specimens in test 9 shows that approximately 95% of the creep strain occurs between 500 and 1500 seconds into the trajectory. Predictions for test 9 are shown to 200 cycles (total time of 73.3 hours) although the cyclic creep equation (Equation 3-13) are used in analysis was developed based on 100 cycle data (total time of 33.3 hours).

3.2.9 Ti-6Al-4V CONCLUSIONS

Ti-6Al-4V tensile specimens were tested at steady-state conditions over the temperature range of 616°K (650°F) to 783°K (950°F) for approximately 200 hours or creep strains of up to approximately .5% in 50 hours. The following empirical regression equation was developed for these data:

$$\ln \varepsilon = -24.08576 + 22.53736T + 5.89 \times 10^{-6}\,\sigma^2 + .90505 \ln \sigma + .43365 \ln t \qquad (3\text{-}11)$$

No effect could be seen in steady-state creep response due to material gage or rolling direction. Creep response obtained in supplemental testing was shown to be somewhat greater than that of the literature survey data base.

The following empirical regression equation was developed for cyclic test data.

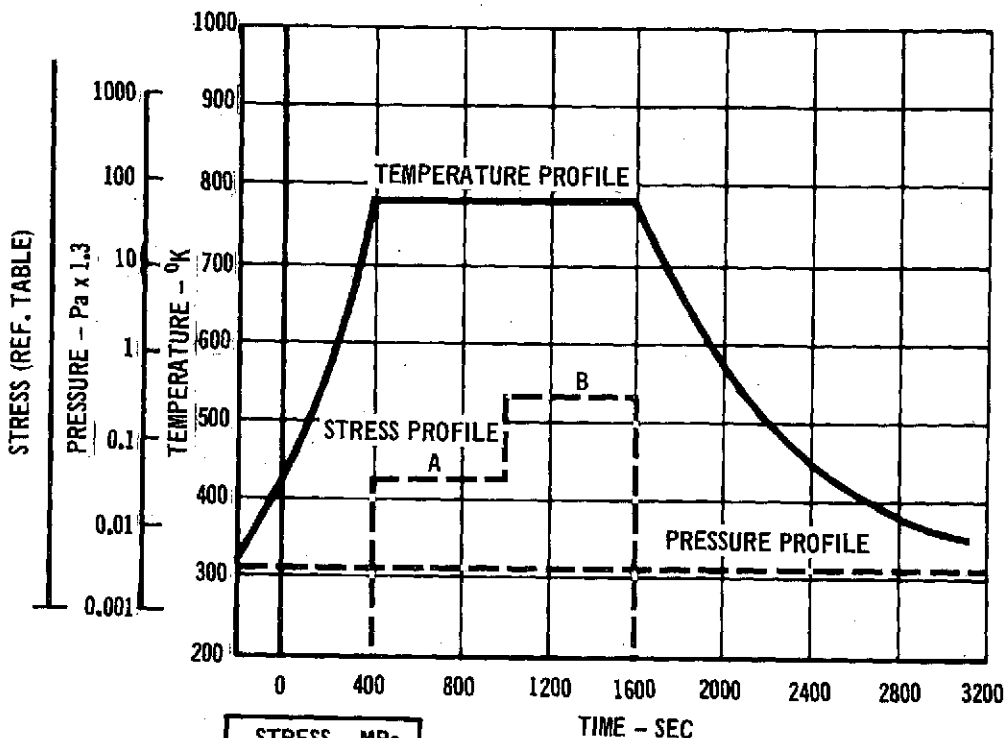

	STRESS – MPa	
SPECIMEN	A	B
T28L	65.4	102.6
T42L	48.8	77.2
T70L	86.4	132.0

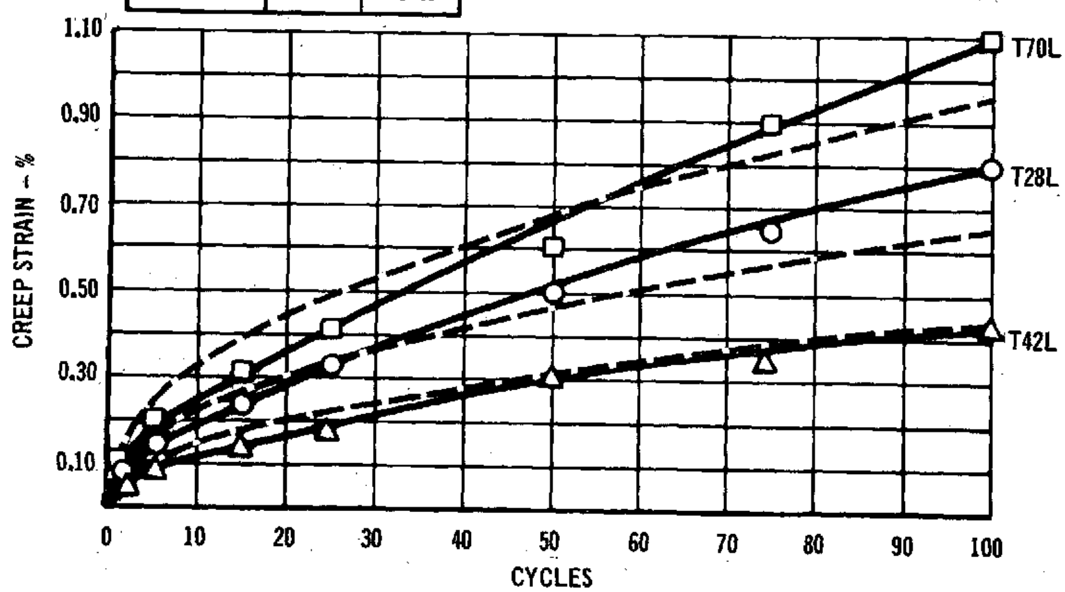

FIGURE 3–74 COMPARISON OF STRAIN HARDENING THEORY PREDICTIONS WITH TWO STEP TRAJECTORY TEST RESULTS (Ti–6Al–4V CYCLIC TEST 8)

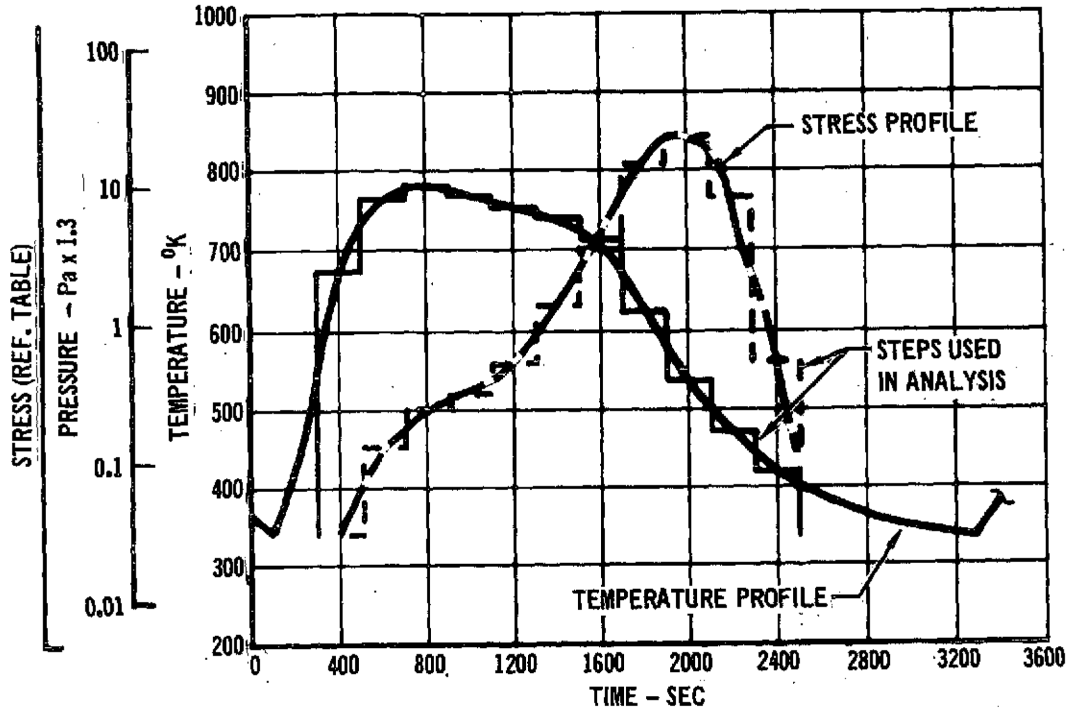

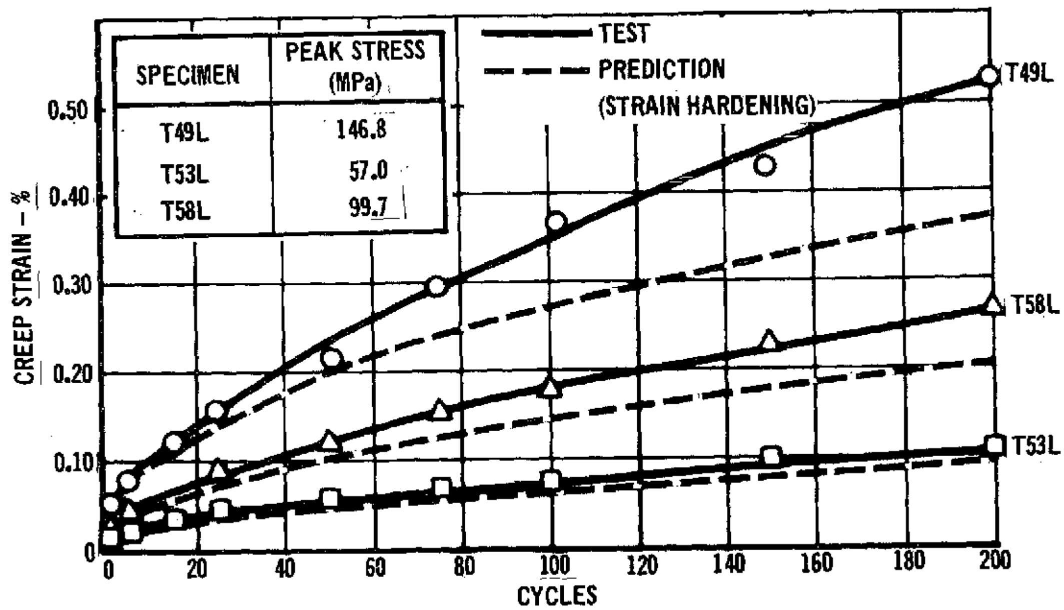

FIGURE 3-75 COMPARISON OF STRAIN HARDENING THEORY PREDICTIONS WITH SIMULATED MISSION TEST RESULTS (Ti-6Al-4V Cyclic Test 9)

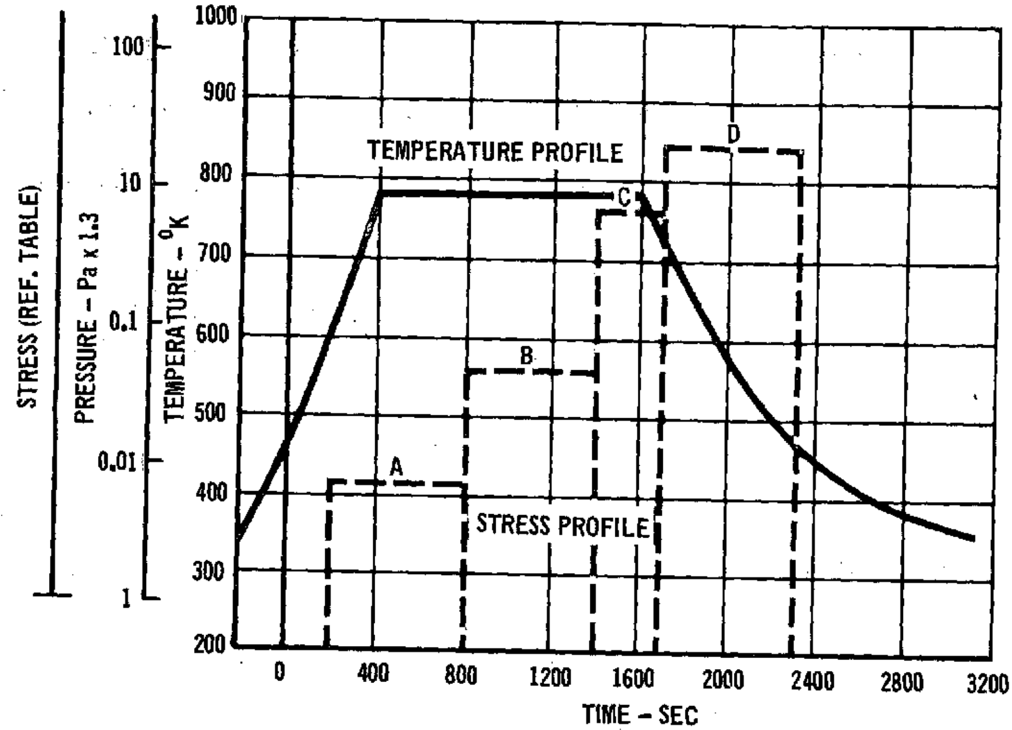

SPECIMEN	STRESS – MPa A	B	C	D
T73L	39.2	75.4	125.4	146.2
T80L	22.7	45.7	80.9	93.8
T75L	12.2	26.3	49.3	54.1

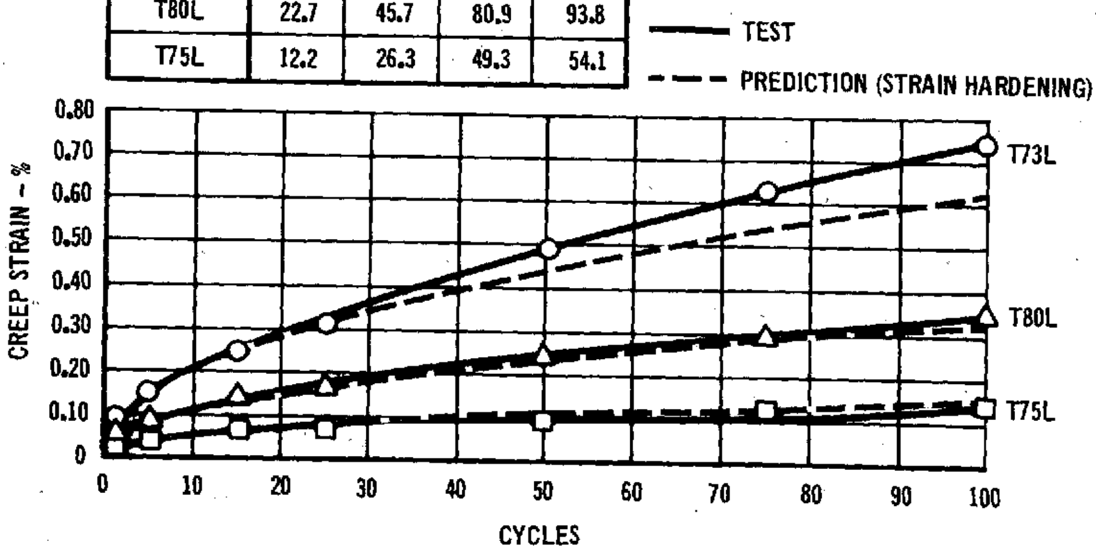

FIGURE 3-76 COMPARISON OF STRAIN HARDENING THEORY PREDICTIONS WITH IDEALIZED TRAJECTORY TEST RESULTS (Ti-6Al-4V CYCLIC TEST 10)

$$\ln \varepsilon = -28.94077 + 26.24850\ T + 2.52 \times 10^{-6}\ \sigma^2 + 1.40406\ \ln \sigma + .46894\ \ln t \quad (3\text{-}13)$$

This equation is applicable over the temperature range of 658°K (725°F) to 839°K (1050°F) for times up to 33 hours (100 cycles at 20 minutes per cycle).

No significant differences were observed between cyclic and steady state data for equal total times at load.

No effects on creep strain due to variation of time per cycle (for same total time) or atmospheric pressure could be determined.

The strain hardening theory of creep accumulation, used in conjunction with the empirical cyclic creep equation, provides good predictions of trajectory creep test data. Time hardening yielded lower (∿20%) predictions.

3.3 RENE' 41 RESULTS OF TESTS AND DATA ANALYSIS

3.3.1 RENE' 41 STEADY-STATE DATA BASE

3.3.1.1 Rene' 41 Literature Survey. Because Rene' 41 is a nickel base precipitation strengthened alloy, the type of heat treatment can effect its creep response. The steady-state literature survey data base was limited to the currently recommended solution treatment at 1394°K and aging at 1172°K (see Section 2.2). Only two sources, References 13 and 14, were found to contain creep data for this material heat treatment.

Reference 13 contains data from 13 creep tests performed on 0.127 cm thick material. Data from Reference 14 contains data from 24 creep tests performed on 0.020 cm thick material. Data from eleven of the tests in Reference 14, was noted to have erratic readings or low readings due to faulting or loosened extensometers, were eliminated from the data base. Remaining data are listed in Appendix E-1. Because the data of Reference 14, designated as MDAC-E-INTRNL was conducted on thin gage material (.020 cm) and also because these specimens were heat oxidized, they

are more representative of the material used on this program. Therefore, data from this source were used in development of the data base empirical equation.

3.3.1.2 Rene' 41 Data Base Analysis. The following empirical equation was developed for the Rene' 41 data base:

$$\ln \varepsilon = 3.81577 - 11.08783\ (1/T) + .57841\ \ln\sigma + .63366\ \ln t \tag{3-14}$$

where ε = creep strain, %

σ = stress, MPa

t = time, hours

T = temperature, °K/1000

This equation has a multiple R of .8889 and a standard error of estimate of .4278 on the natural logarithm of strain. The residual plots ($\ln \varepsilon_{actual} - \ln \varepsilon_{calculated}$ vs. variable) for this equation are shown in Figure 3-77.

Typical comparisons of test data with predictions based on equation (1) are shown in Figure 3-78.

3.3.2 SUPPLEMENTAL STEADY-STATE TESTING

3.3.2.1 Rene' 41 Supplemental Steady-State Test Matrix. A total of eighteen supplemental steady-state tests were conducted on Rene' 41 tensile specimens per conditions in Table 3-5. Twelve of these tests were for .028 cm (.011 inch) thick material tested in the longitudinal rolling direction. These twelve tests make up the basic test matrix from which an empirical equation for supplemental steady-state data is determined. Of the six additional tests listed in Table 3-5, three were conducted on .028 cm. (.011 inch) thick specimens tested in the transverse rolling direction, and three were conducted on .053 cm (.021 inch) thick specimens tested in the longitudinal rolling direction.

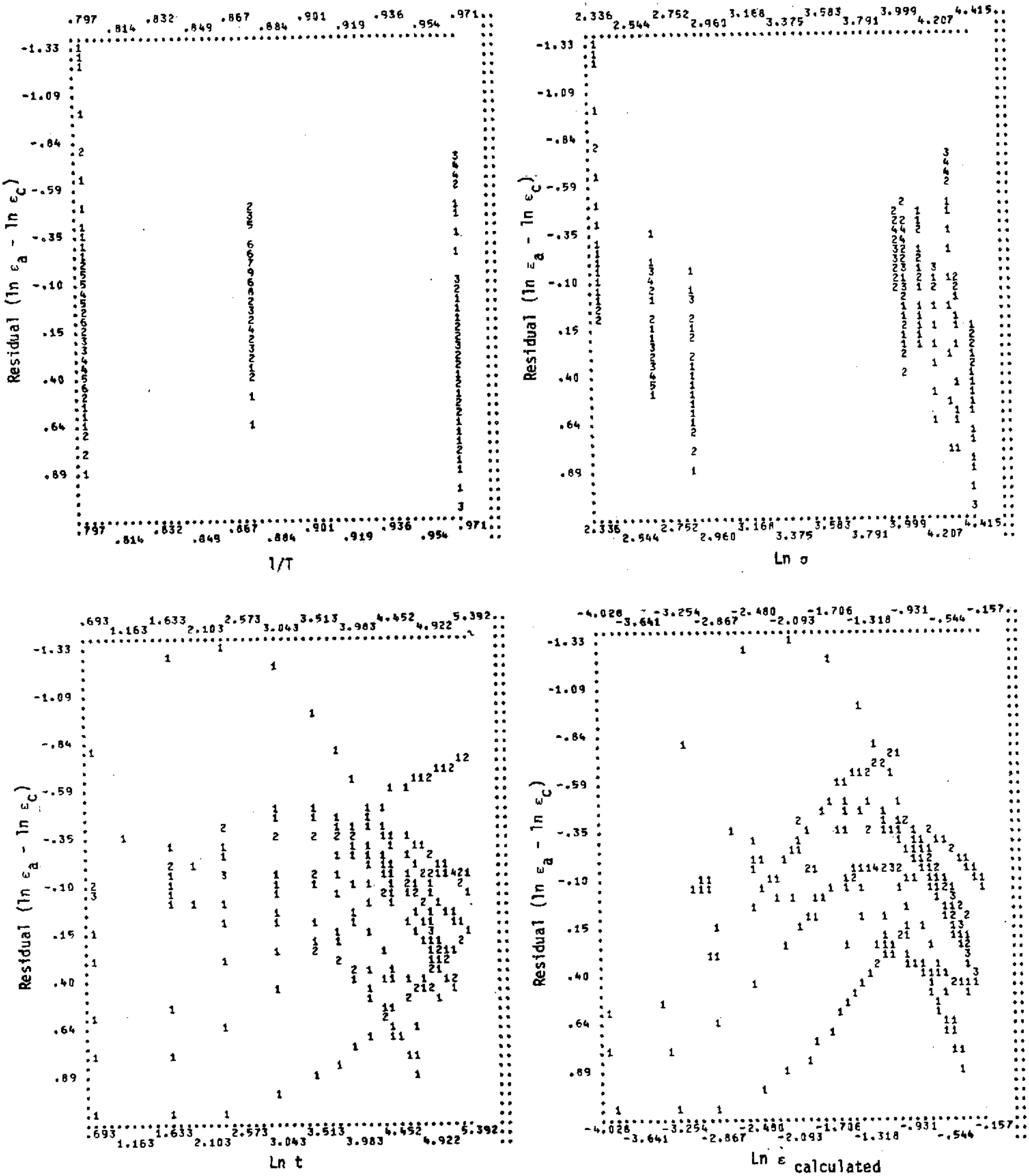

FIGURE 3-77 RESIDUAL PLOTS OF RENE'41 LITERATURE SURVEY EQUATION (3-14)

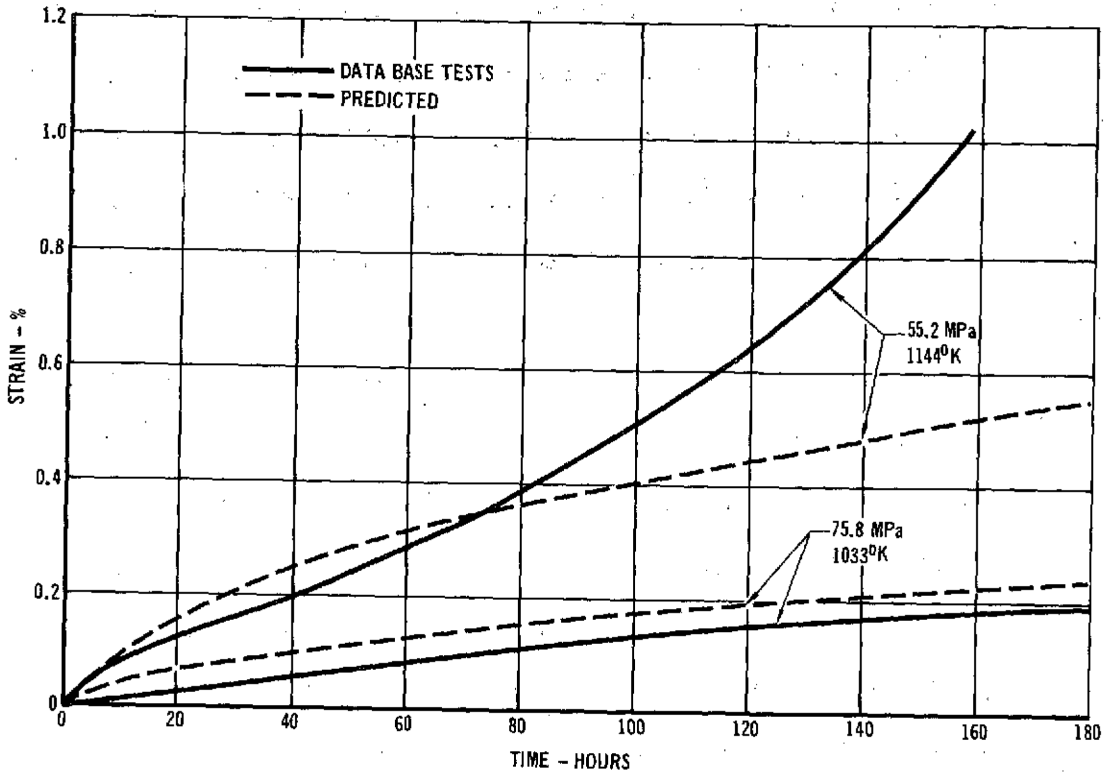

FIGURE 3-78 COMPARISON OF LITERATURE SURVEY CREEP EQUATION (3-14) WITH TEST RESULTS FOR RENE'41

TABLE 3-5 RENE' 41 SUPPLEMENTAL STEADY-STATE TESTS

TEST NO.	TEST SPECIMEN	MATERIAL ROLLING DIRECTION	MATERIAL GAGE		TEMPERATURE		STRESS	
			cm	in.	°K	°F	MPa	KSI
1	R21L	LONGITUDINAL	0.028	0.011	1180	1665	68.9	10.0
2	R22L	LONGITUDINAL	0.028	0.011	1155	1620	121.3	17.6
3	R31L	LONGITUDINAL	0.028	0.011	1155	1620	55.2	8.0
4	R23L	LONGITUDINAL	0.028	0.011	1155	1620	39.0	5.7
5	R29L	LONGITUDINAL	0.028	0.011	1111	1540	103.4	15.0
6	R30L	LONGITUDINAL	0.028	0.011	1111	1540	68.9	10.0
7	R28L	LONGITUDINAL	0.028	0.011	1061	1450	68.9	10.0
8	R104L	LONGITUDINAL	0.028	0.011	1061	1450	137.9	20.0
9	R24L	LONGITUDINAL	0.028	0.011	1061	1450	68.9	10.0
10	R26L	LONGITUDINAL	0.028	0.011	1061	1450	34.5	5.00
11	R27L	LONGITUDINAL	0.028	0.011	983	1310	121.3	17.6
12	R25L	LONGITUDINAL	0.028	0.011	964	1275	68.9	10.0
13	R11T	TRANSVERSE	0.028	0.011	1155	1620	121.3	17.6
14	R13T	TRANSVERSE	0.028	0.011	1111	1540	68.9	10.0
15	R12T	TRANSVERSE	0.028	0.011	1061	1450	68.9	10.0
16	R1L	LONGITUDINAL	0.053	0.021	1155	1620	121.3	17.6
17	R3L	LONGITUDINAL	0.053	0.021	1111	1540	68.9	10.0
18	R2L	LONGITUDINAL	0.053	0.021	1061	1450	68.9	10.0

The original test matrix, shown in Figure 3-79, is an orthogonal composite design (Reference 24). This design was selected because it provided a good distribution of test conditions within the strain range of .50% in 50 hours to .10% in 200 hours, based on Equation 3-14 predictions as indicated in the Figure 3-79. The box design utilized for L605, titanium, and TDNiCr did not fit the creep strain range well in this case.

Based on initial test results this matrix was modified resulting in completion of the tests shown in the table. The test at 983°K and 39.0 MPa was deleted, based on very low creep strains obtained in test 10 (1061°K and 34.5 MPa) and test 12 (964°K and 68.9 MPa). Tests 3 (1155°K and 55.2 MPa), 5 (1111°K and 103.4 MPa), and, 6 (1111°K and 68.9 MPa) were added. In addition test 9 was added as a replicate of test 7, based on erratic strain readings obtained in test 7. Creep strain results for each of the supplemental steady-state tests are presented in Appendix E-2. Included in this appendix are the elastic strains which were determined at the start and the conclusion of the test.

3.3.2.2 Test Data Evaluation - Basic Test Matrix. The following equation was developed using data obtained from the hand faired curves of the basic supplemental tests 1 thru 12 (Figures 3-80 thru 3-84). The data consisted of approximately 5 points per test spaced in such a manner as to describe the curve. For example, a 80-hour test had strains selected at times of 1, 5, 20, 50 and 80, while a 200 hour test had strains selected at 1, 5, 20, 50, 100 and 200 hours from the hand faired curves.

$$\ln \varepsilon = -35.21304 + 26.34069T + .55687 \ln t + .02807 (\ln \sigma)^3 \qquad (3\text{-}15)$$

This equation has a standard error of estimate of .3073 on the logarithm of strain and a multiple R of .9687. The residual plots ($\ln \varepsilon_{actual} - \ln \varepsilon_{calculated}$ vs. variable) for this equation are shown in Figure 3-85.

Comparisons of equation predictions with test results for several of the tests are presented in Figures 3-80 through 3-84. Review of these comparisons shows

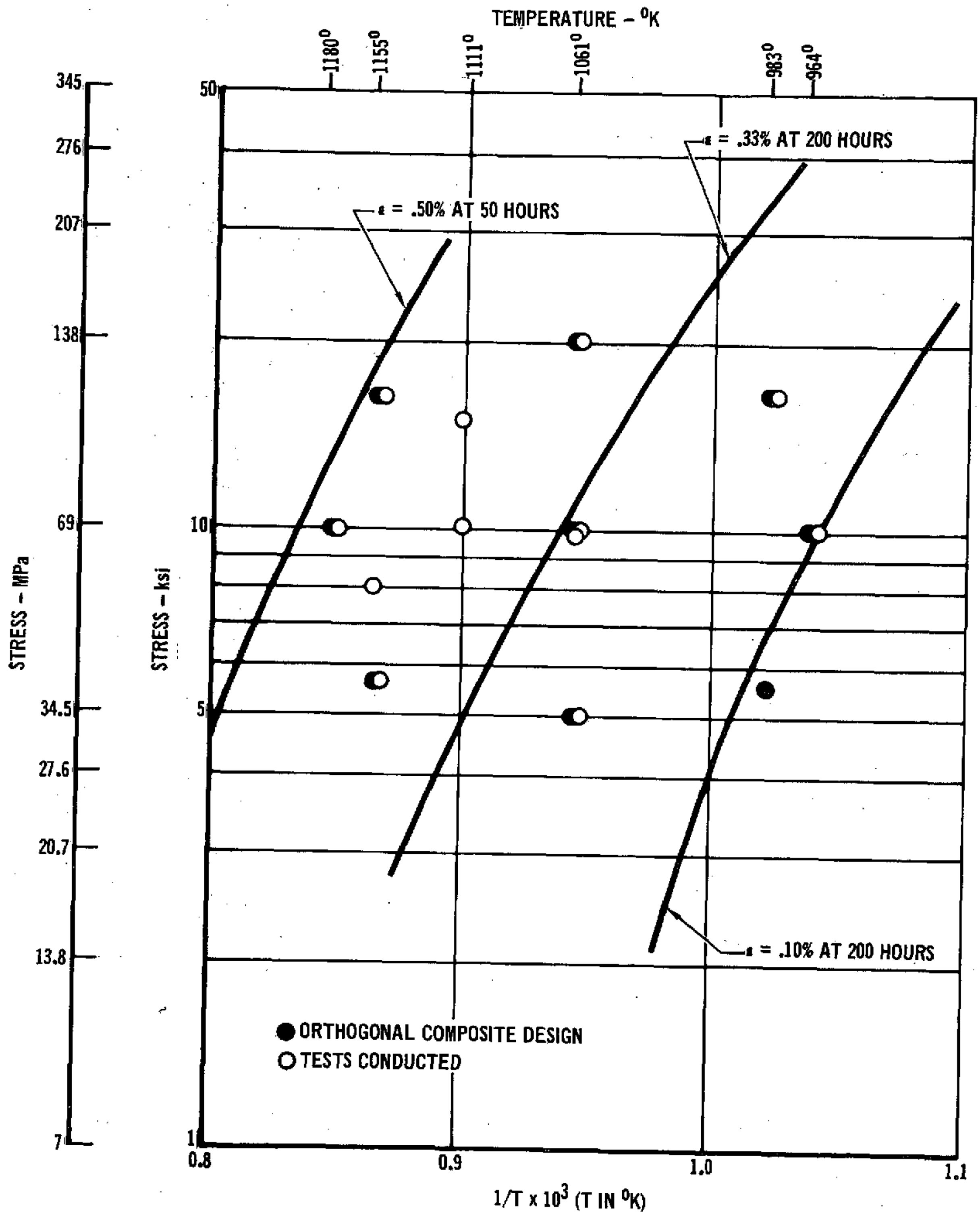

FIGURE 3–79 RENE'41 SUPPLEMENTAL STEADY-STATE TESTS

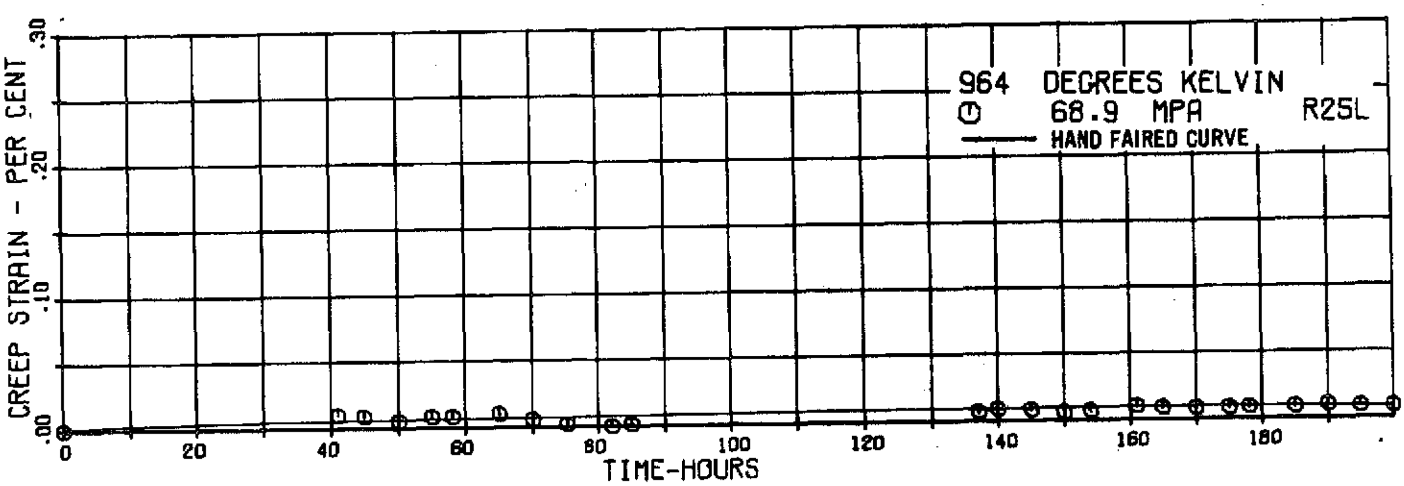

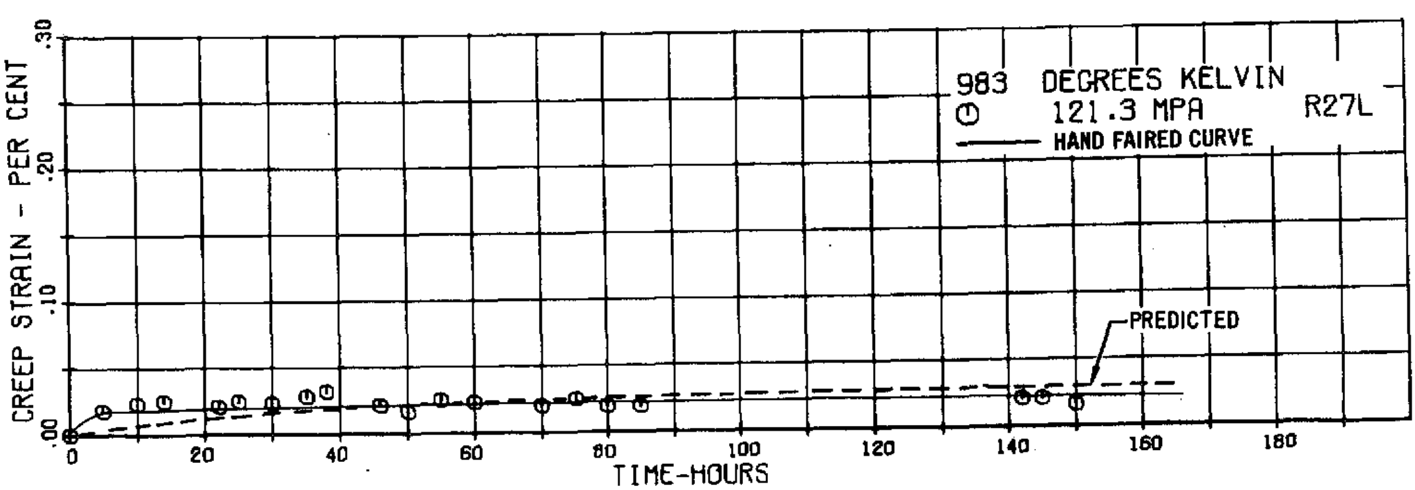

FIGURE 3-80 RENE '41 SUPPLEMENTARY STEADY-STATE CREEP DATA AT 964 AND 983°K

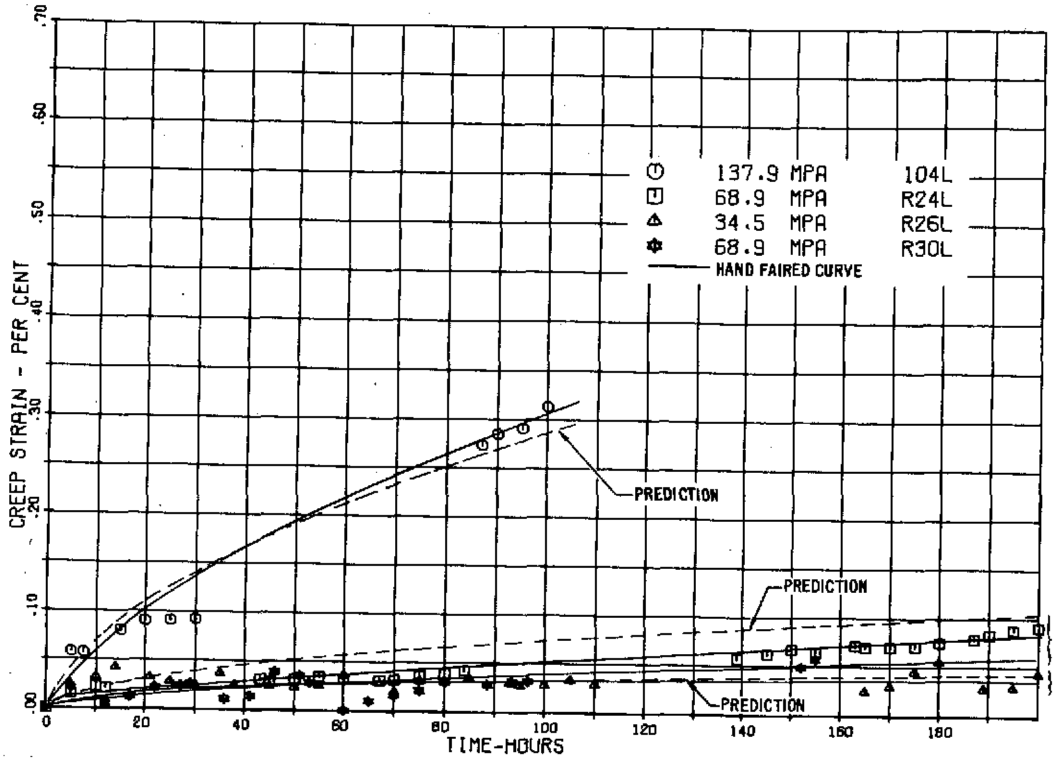

FIGURE 3–81 RENE'41 SUPPLEMENTARY STEADY-STATE CREEP DATA AT $1061^{0}K$

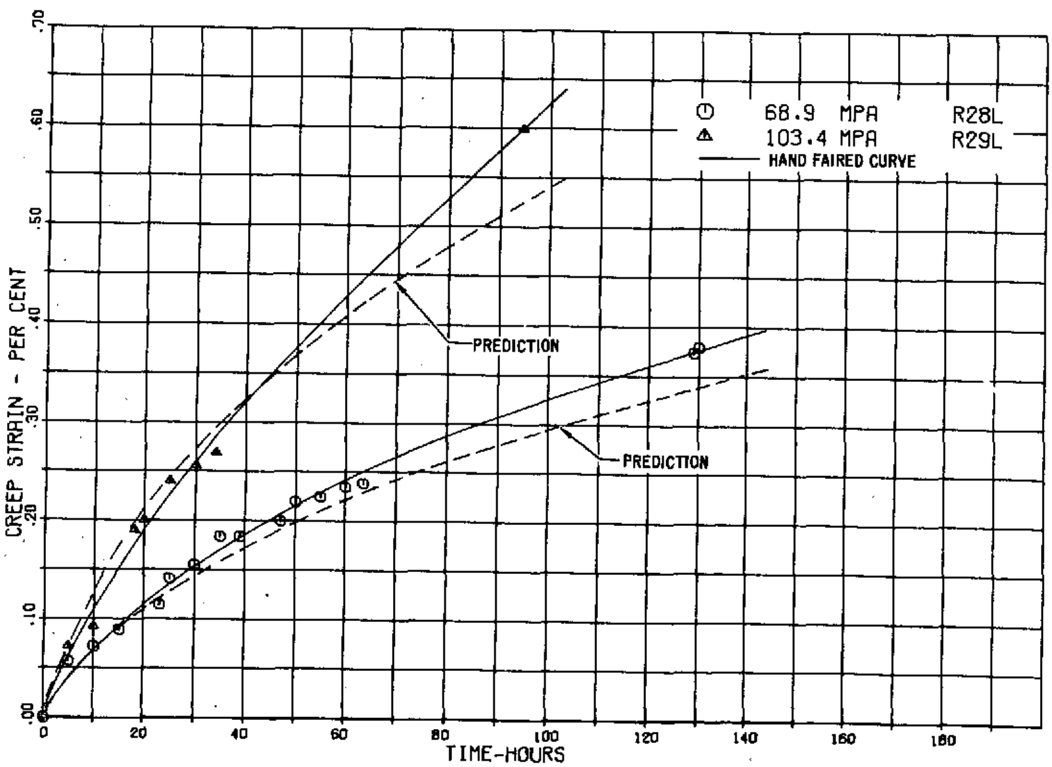

FIGURE 3–82 RENE'41 SUPPLEMENTARY STEADY-STATE CREEP DATA AT $1111^{0}K$

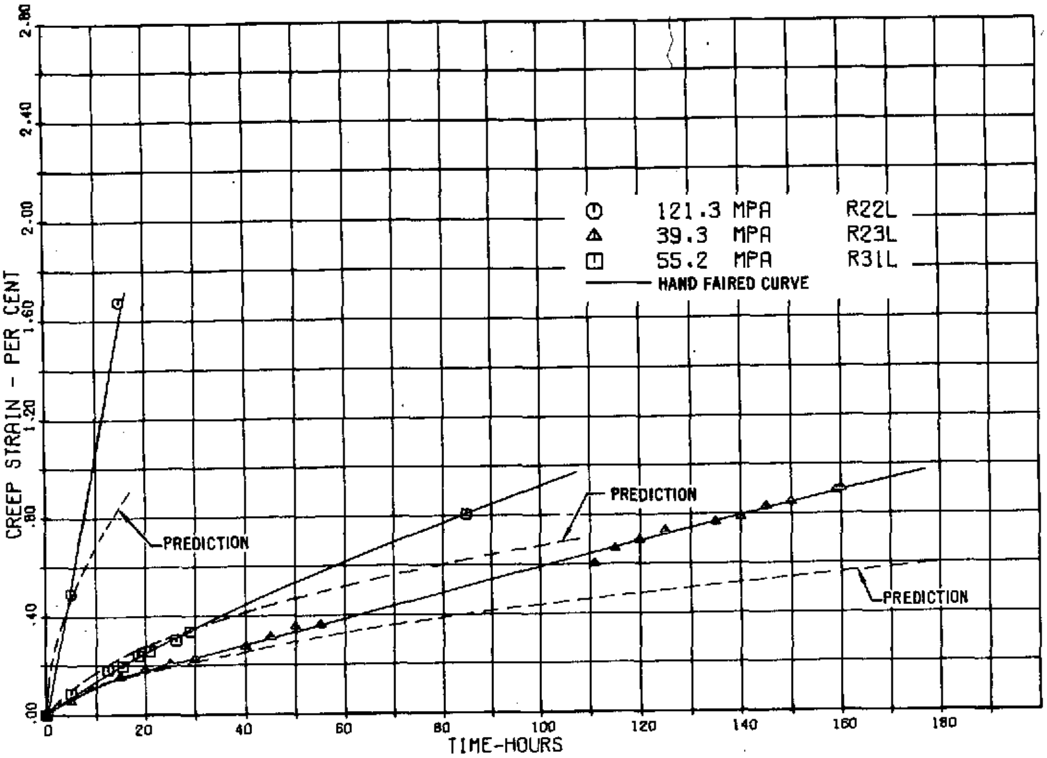

FIGURE 3-83 RENE'41 SUPPLEMENTARY STEADY-STATE CREEP DATA AT 1155°K

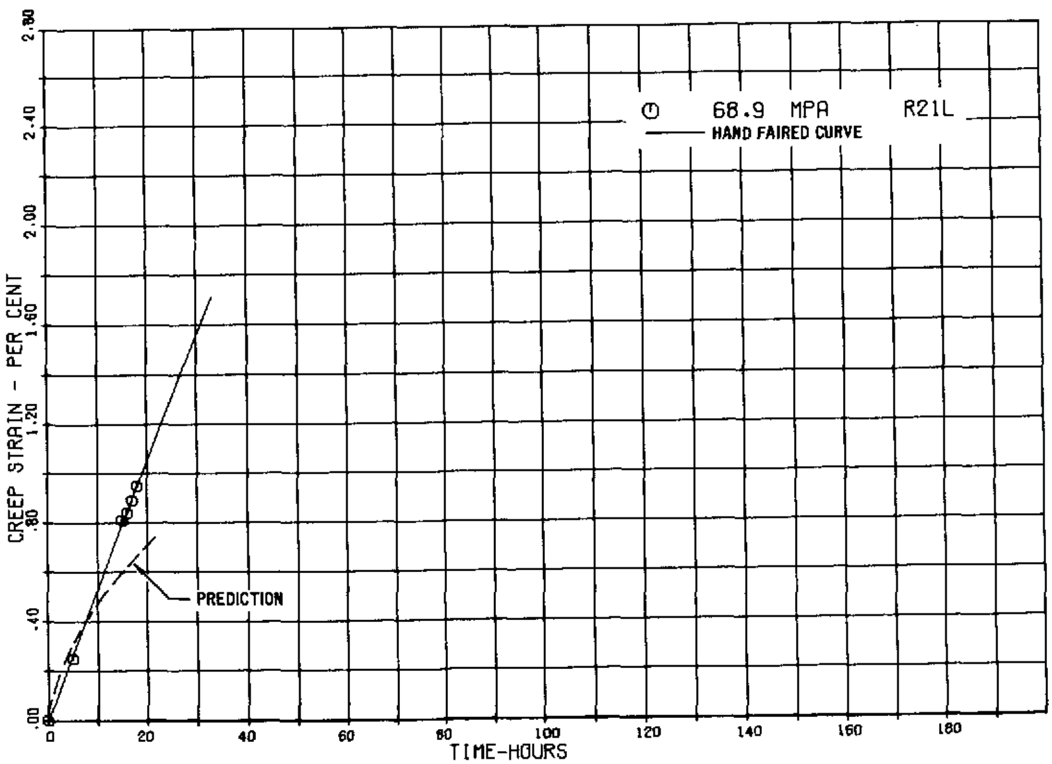

FIGURE 3-84 RENE'41 SUPPLEMENTARY STEADY-STATE CREEP DATA AT 1180°K

that the equation predicts lower strain rates than those accurring in the tests. Predicted strains are higher than test values during the initial test timer, cross the test values approximately midway through the test, and result in lower predictions at the test completion. This result indicates that additional time terms may be required to provide a better data fit. Terms such as $\ln \varepsilon = f(t^3)$, however, were found to be insignificant in fitting data from the supplemental steady-state basic test matrix (tests 1-12). The predictions for the 964 and 983°K tests are not presented in Figure 3-80 because the amount of strain is so small that the curve lies on the ordinate.

3.3.2.3 Effect of Gage and Rolling Direction on Rene' 41 Steady-State Creep. Rene' 41 supplemental steady-state tests 13 through 18 (Table 3-5) were conducted as replicates of basic matrix tests except for variations in rolling direction (tests 13, 14, 15 and in material thickness (tests 16, 17, 18). Comparison of creep strains for thest two variables are presented in Figures 3-86, 3-87, and 3-88.

In each of the three comparisons, the thicker gage specimen (0.53 cm) exhibits greater creep strain than either thin gage specimen. This difference is consistently a factor of approximately 2 times the creep strain values for .028 cm thick specimens tested in the longitudinal direction. One possibility for this effect is the fact that the 0.053 cm material had a finer grain size (ASTM 7-8) than the 0.028 cm material (ASTM 6). Since the amount of creep obtained for thicker material is greater than the factor of $\pm$ 1.81 based on $\pm$ 1.96 S_y scatter band for the supplemental steady-state creep equation (Equation 3-15), it can be concluded that the gage was significant variable for this series of tests.

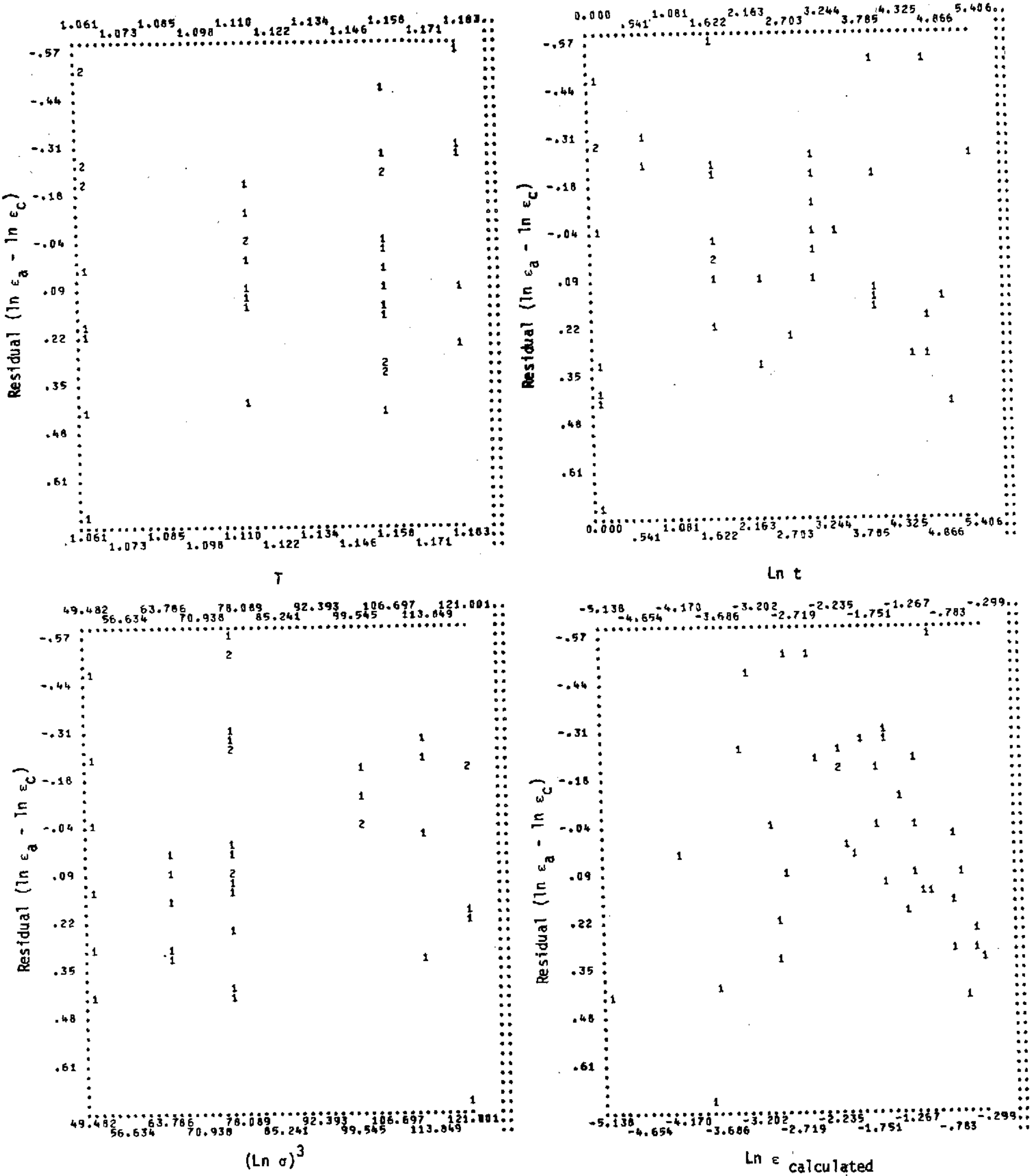

FIGURE 3-85 RESIDUAL PLOTS OF RENE'41 SUPPLEMENTAL EQUATION (3-15)

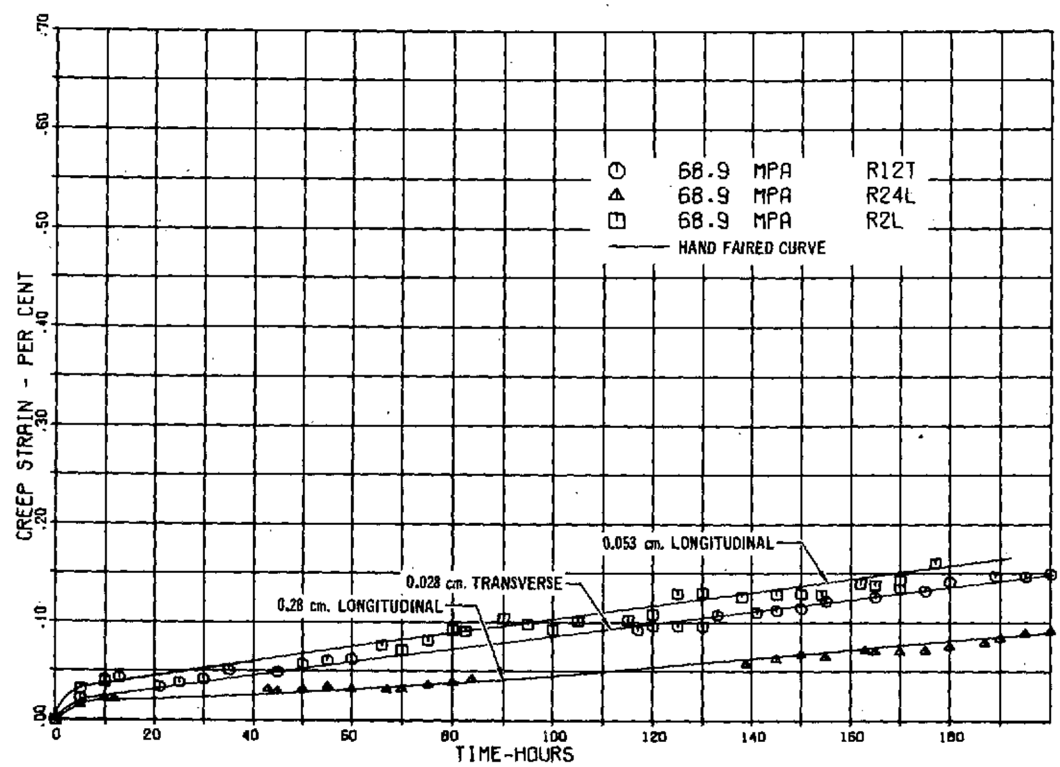

FIGURE 3–86 COMPARISON OF GAGE AND ROLLING DIRECTION ON CREEP OF RENE'41 AT 1061°K AND 68.9 MPa

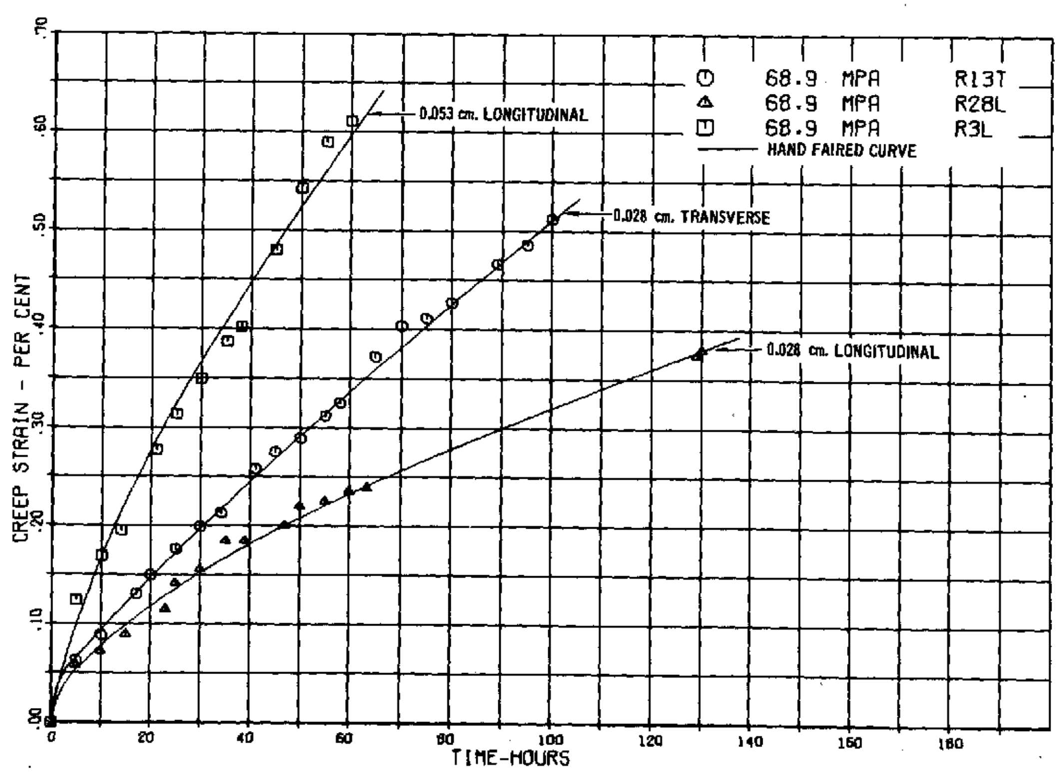

FIGURE 3–87 COMPARISON OF GAGE AND ROLLING DIRECTION ON CREEP OF RENE' 41 AT 1111°K AND 68.9 MPa

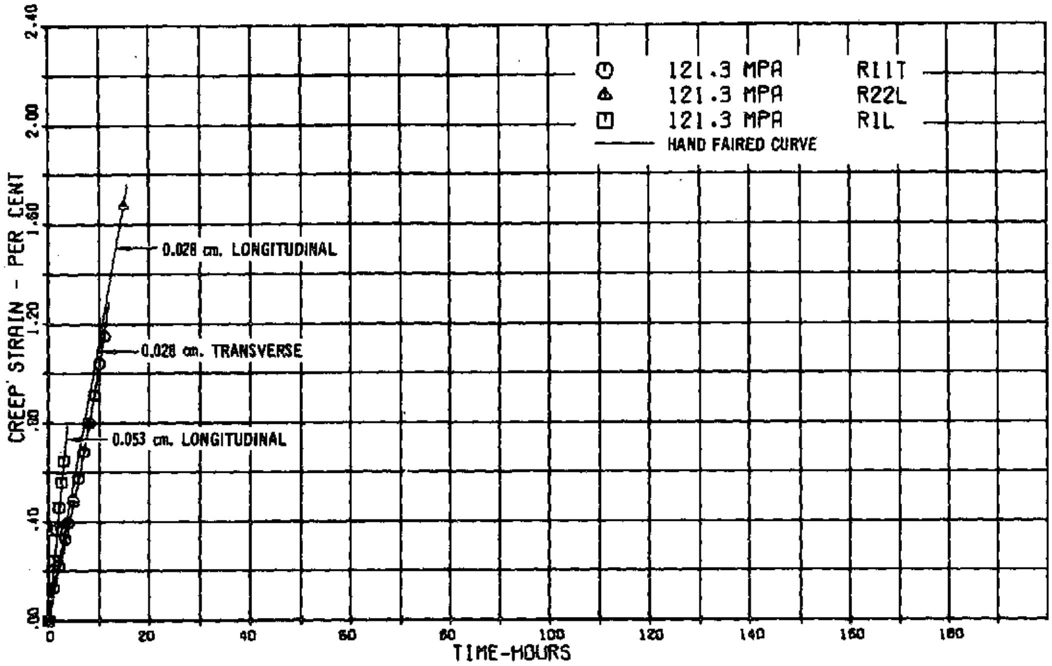

FIGURE 3–88 COMPARISON OF GAGE AND ROLLING DIRECTION ON CREEP OF RENE'41 AT 1155°K AND 121.3 MPa

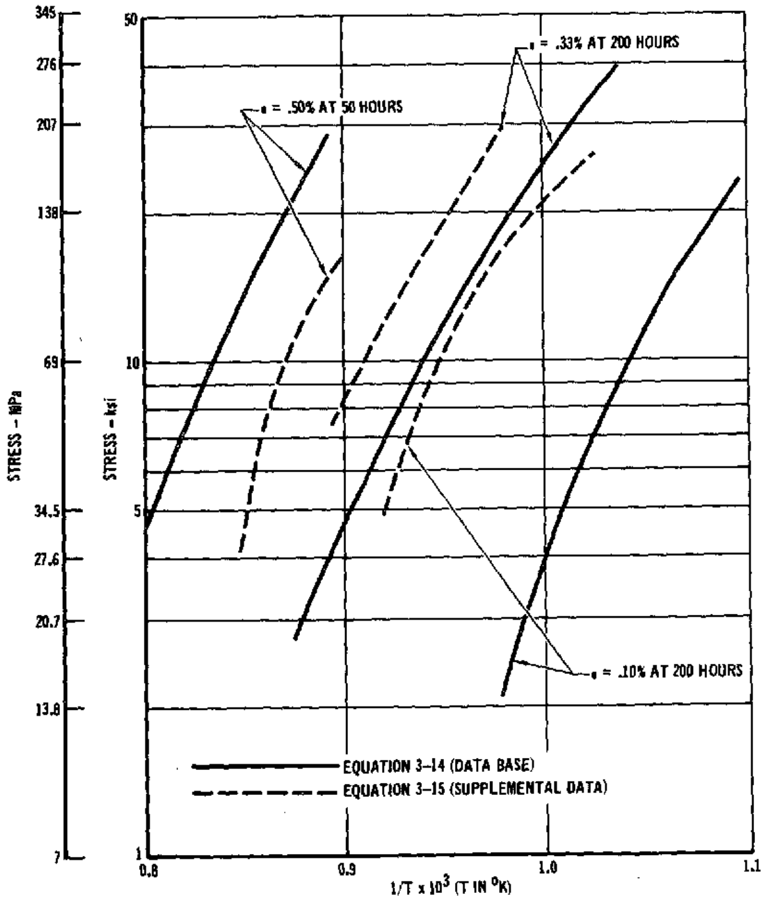

FIGURE 3–89 COMPARISON OF DATA BASE AND SUPPLEMENTAL TEST EQNS

Specimens tested in the transverse rolling direction also exhibit greater creep strain than those tested in the longitudinal direction in two of the three comparisons (Figures 3-86 to 3-88). However, the variation is not sufficient to firmly conclude that this variable has any effect on creep response.

3.3.3 COMPARISON OF RENE' 41 STEADY-STATE DATA BASE AND SUPPLEMENTAL TEST RESULTS

As indicated in Section 3.3.2.1, modification of the original test matrix was made in order to provide test data in the range of interest for metallic TPS. This implies a difference between the steady-state data base and the supplemental data. Comparisons of the lines of constant creep strain as predicted by the literature survey equation (Equation 3-14) and the supplemental creep equation (Equation 3-15) are shown in Figure 3-89. These results illustrate that the stress and temperature range over which creep strains of interest were attained in supplemental testing is less than that for the data base.

Further investigation into the comparison of these data sets using the dummy variable technique resulted in the following equation:

$$\begin{aligned} \ln\varepsilon = & -27.12779 + 18.63930T + .64311 \ln t \\ & + .25603 (\ln\sigma - 1.931)^3 \\ & - .14118 Z \ln t - .18620 Z (\ln\sigma - 1.931)^3 \end{aligned} \qquad (3\text{-}16)$$

where ε = creep strain, %

T = temperature, °K

t = time, hours

σ = stress, MPa

$Z = \begin{cases} 1, & \text{supplemental steady state data} \\ 0, & \text{steady state data base} \end{cases}$

Because the last three terms are significant in the equation, a difference between the two data sets is also indicated.

3.3.4 RENE' 41 BASIC CYCLIC TESTS

3.3.4.1 Basic Cyclic Test Matrix. Four 100 cycle tests (3 specimens per test) were conducted on .028 cm gage specimens to form the basic cyclic test matrix from which an empirical equation for cyclic creep can be derived. Each of the specimens was tested in the longitudinal rolling direction. Tests were conducted for 100 constant load and temperature cycles (20 minutes per cycle). The tests were conducted at temperatures of 1155, 1111, 1071, and 1031°K as listed in Table 3-6. Stress levels at each temperature were selected, based on results of supplemental steady-state results, to yield creep strains of up to .5%.

TABLE 3-6. RENE' 41 BASIC CYCLIC TEST MATRIX

Test No.	Specimen	Test Temperature °K	Test Temperature °F	Stress MPa	Stress Ksi
1	R39L	1111	1540	104.	15.1
	R41L			68.7	9.97
	R40L			39.0	5.66
2	R38L	1155	1620	66.5	9.65
	R36L			56.9	8.26
	R37L			46.7	6.78
3	R46L	1071	1470	135.	19.6
	R42L			103	15.0
	R43L			68.7	9.96
4	R54L	1031	1400	275.	39.9
	R52L			208.	30.1
	R53L			142.	20.6

This portion of the cyclic tests are designated as Rene' 41 cyclic tests 1 thru 4. Data are presented in Appendix E-3.

3.3.4.2 Test Results and Analysis. Cyclic creep strain results for the twelve specimens in test 1 through test 4 are presented in Figures 3-90 thru 3-93.

The following equation was developed using data obtained from the hand faired curves of these twelve tests. This data consisted of strain values taken at 5 cycle intervals from the hand faired curves. Creep times were the accumulated cycle time at maximum load and temperature, therefore for the basic cycles the time was 33 hours/cycle or 1.67 hours/5 cycles.

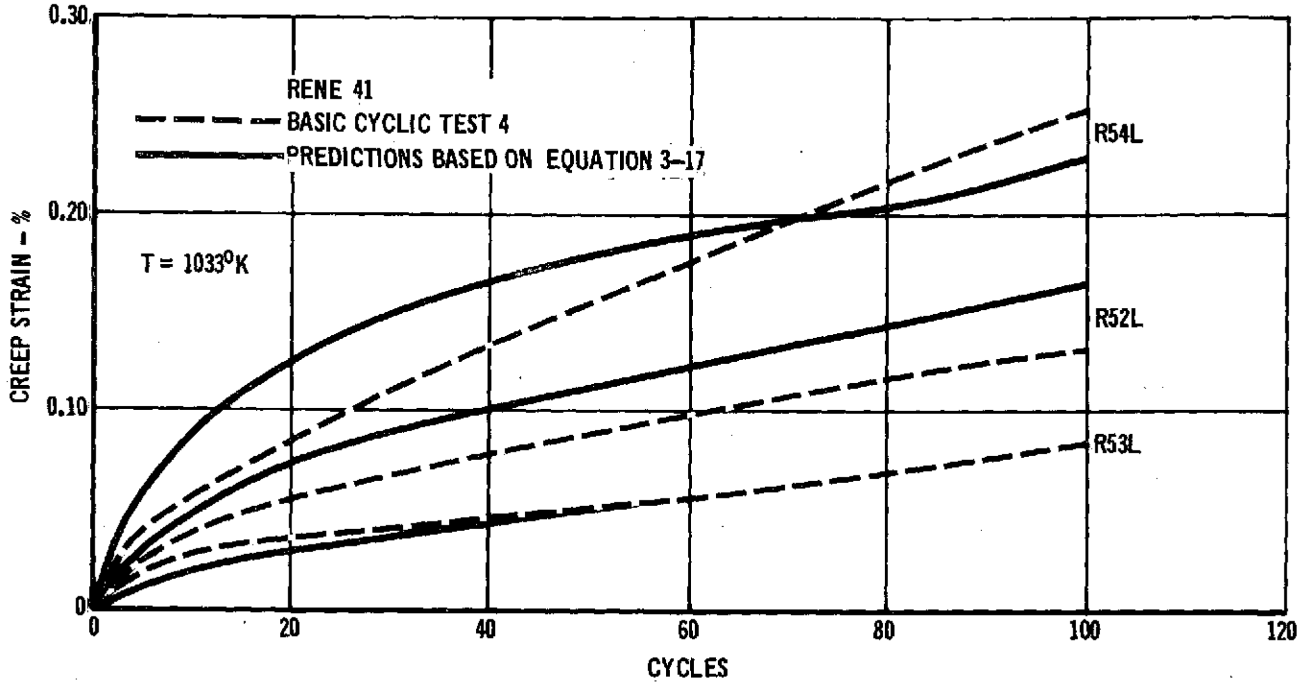

FIGURE 3–90 RENE'41 BASIC CYLIC CREEP TEST AT 1033°K

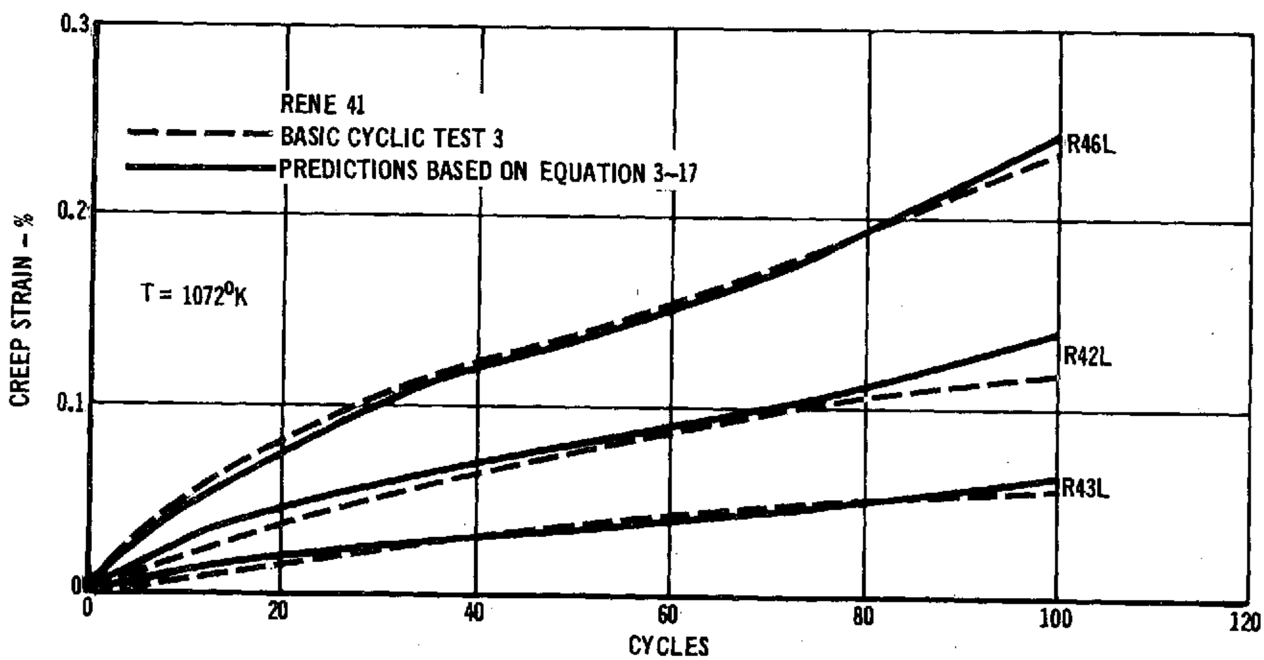

FIGURE 3–91 RENE '41 BASIC CYLIC CREEP TEST AT 1072°K

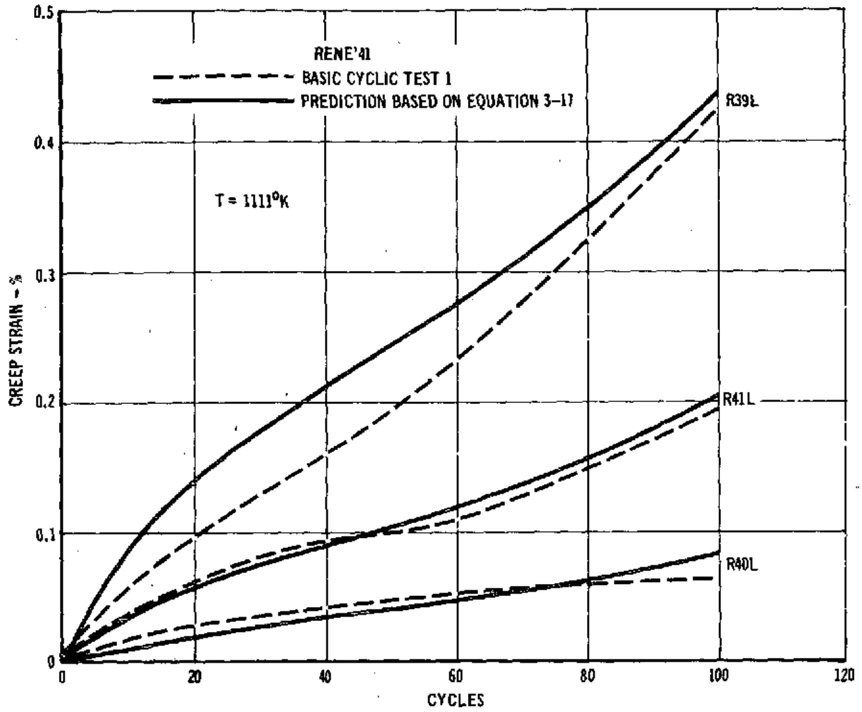

FIGURE 3-92 RENE'41 BASIC CYCLIC CREEP TEST AT 1111°K

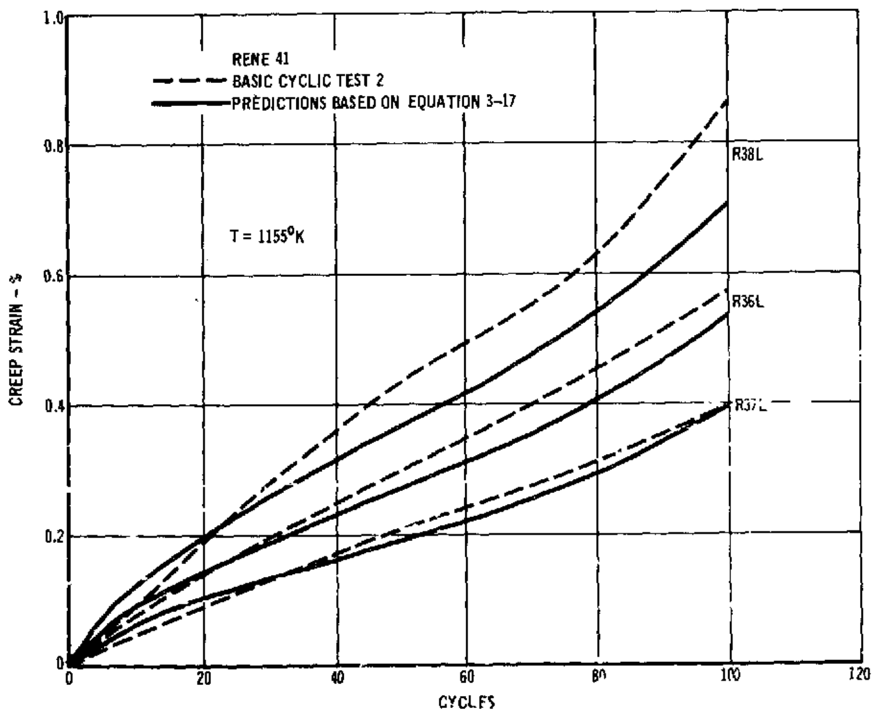

FIGURE 3-93 RENE'41 BASIC CYCLIC CREEP TEST AT 1155°K

$$\ln\varepsilon = -39.55860 + 29.13646T + .71922 \ln t + .92125 (\ln\sigma - 1.931) \quad (3\text{-}17)$$
$$-.000016\sigma^2 + .08183 (\ln\sigma - 1.931)^3 - .000125\ t\sigma T + .0000105t^3$$

This equation has a standard error of estimate of .1397 on the logarithm of strain and a multiple correlation coefficient of .9888. The residual plots ($\ln \varepsilon_{actual} - \ln \varepsilon_{calculated}$ vs. variable) for this equation are shown in Figure 3-94.

This equation is based on creep strain data read at 5 cycle intervals from the hand faired creep strain curves. In the basic cyclic tests 1, 3, and 4 (Appendix E-3) small negative creep strains were obtained up to 15 cycles. For analysis purposes the strains at 1 cycle, which were less than -.03%, were added to the creep curves so that all the creep data would be positive. Comparisons of creep strain predictions with test data are shown in Figures 3-90 through 3-93.

3.3.5 COMPARISON OF RENE' 41 CYCLIC AND SUPPLEMENTAL STEADY-STATE DATA

3.3.5.1 Test Data Comparison. Comparison of the supplemental steady-state equation (Equation 3-15) which the cyclic creep equation (Equation 3-17) reveals a difference in form. Specifically, the t^3 term in the cyclic creep equation which allows strain rate to increase with time (Reference Figures 3-90 to 3-93), and the $t\sigma T$ interaction term. However, in comparing the two data sets, using the dummy variable technique, no differences could be established. Analysis of the combined data sets resulted in an empirical equation of the same form as that for the supplemental steady state data (Equation 3-15). None of the terms indicating differences in the two data sets were determined to be significant.

Direct comparisons of supplemental steady-state and cyclic data are shown in Figure 3-95.

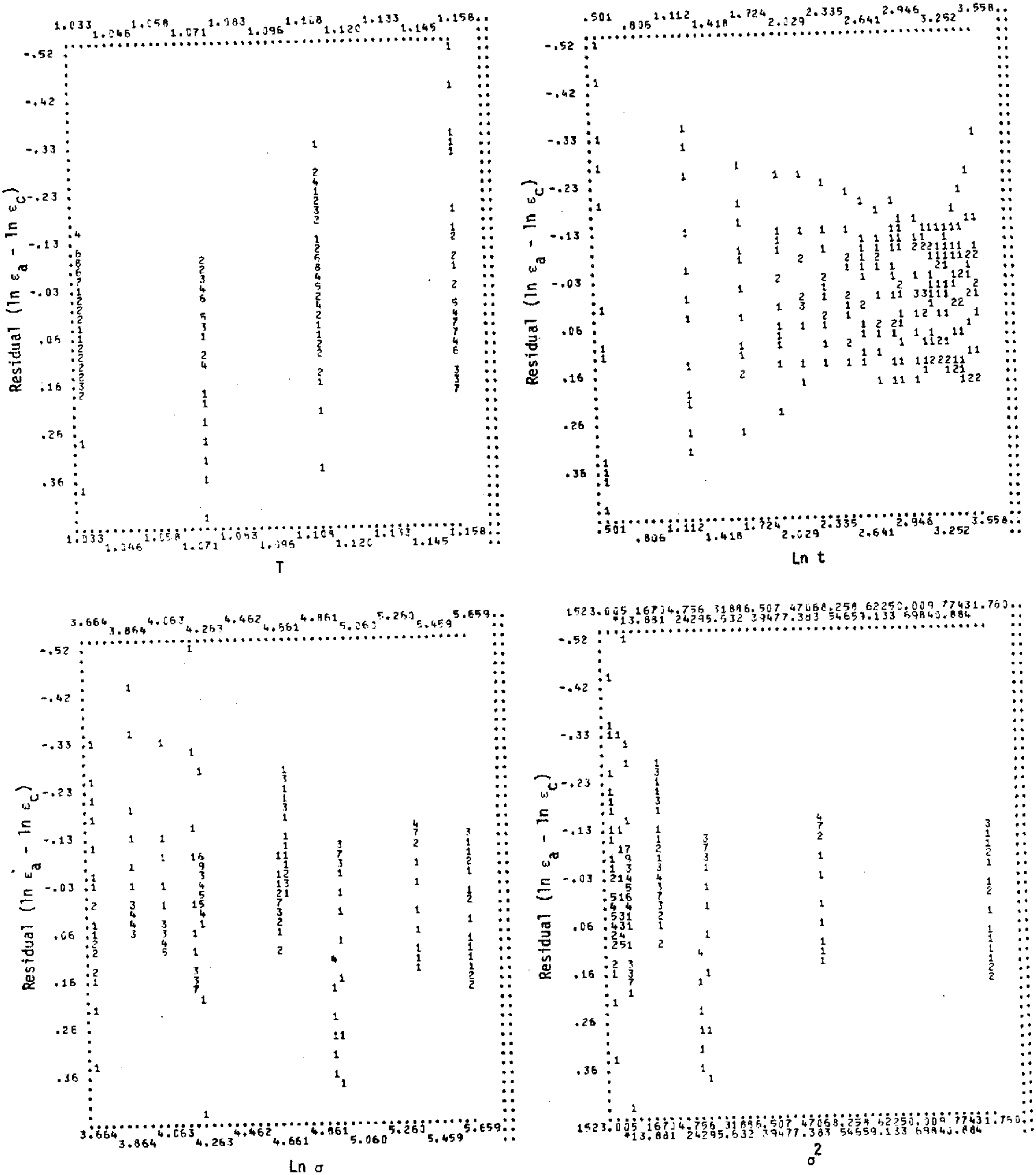

FIGURE 3-94 RESIDUAL PLOTS OF RENE'41 CYCLIC EQUATION (3-17)

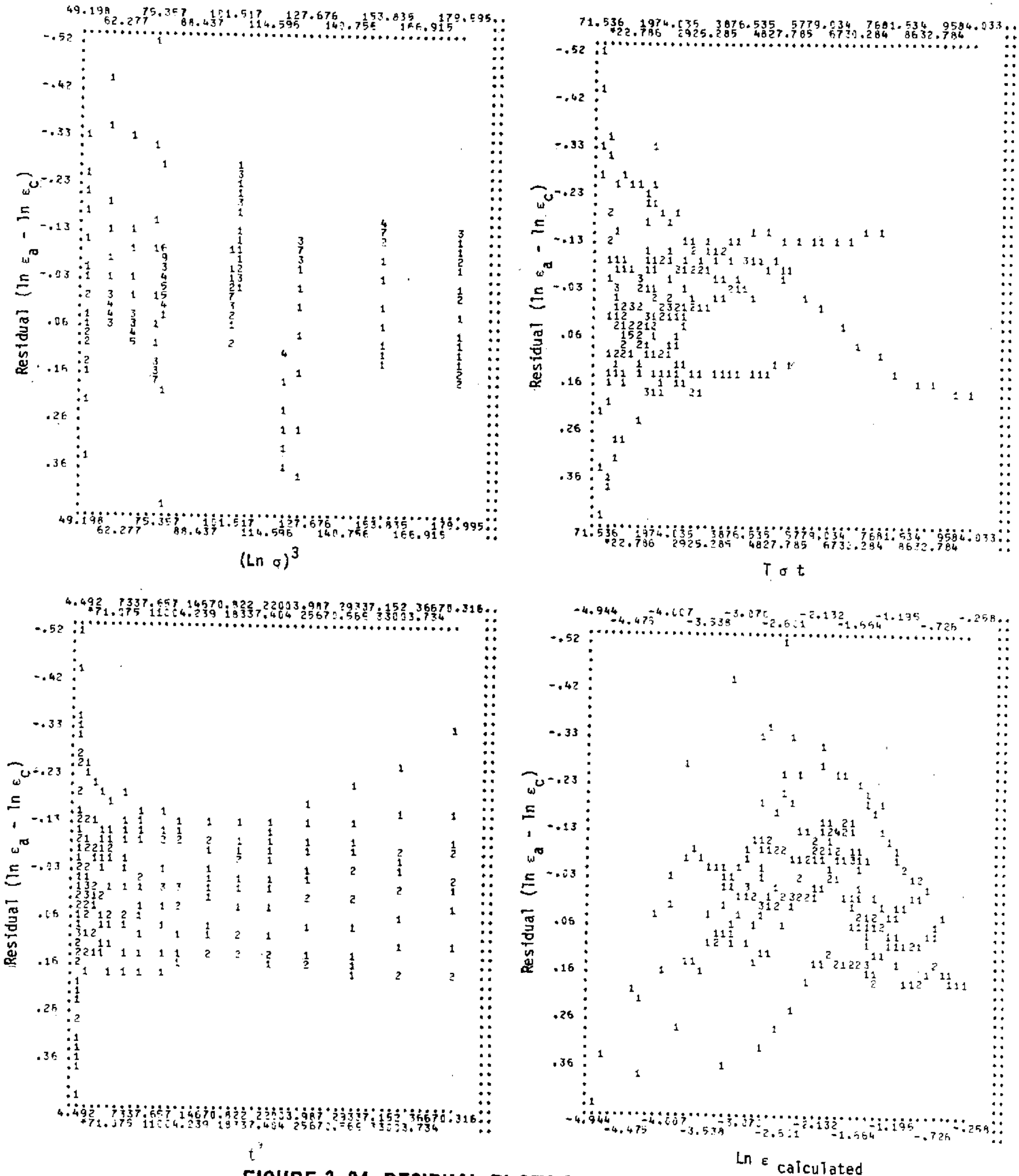

FIGURE 3-94 RESIDUAL PLOTS OF RENE'41 CYCLIC CREEP EQUATION (3-17)(Continued)

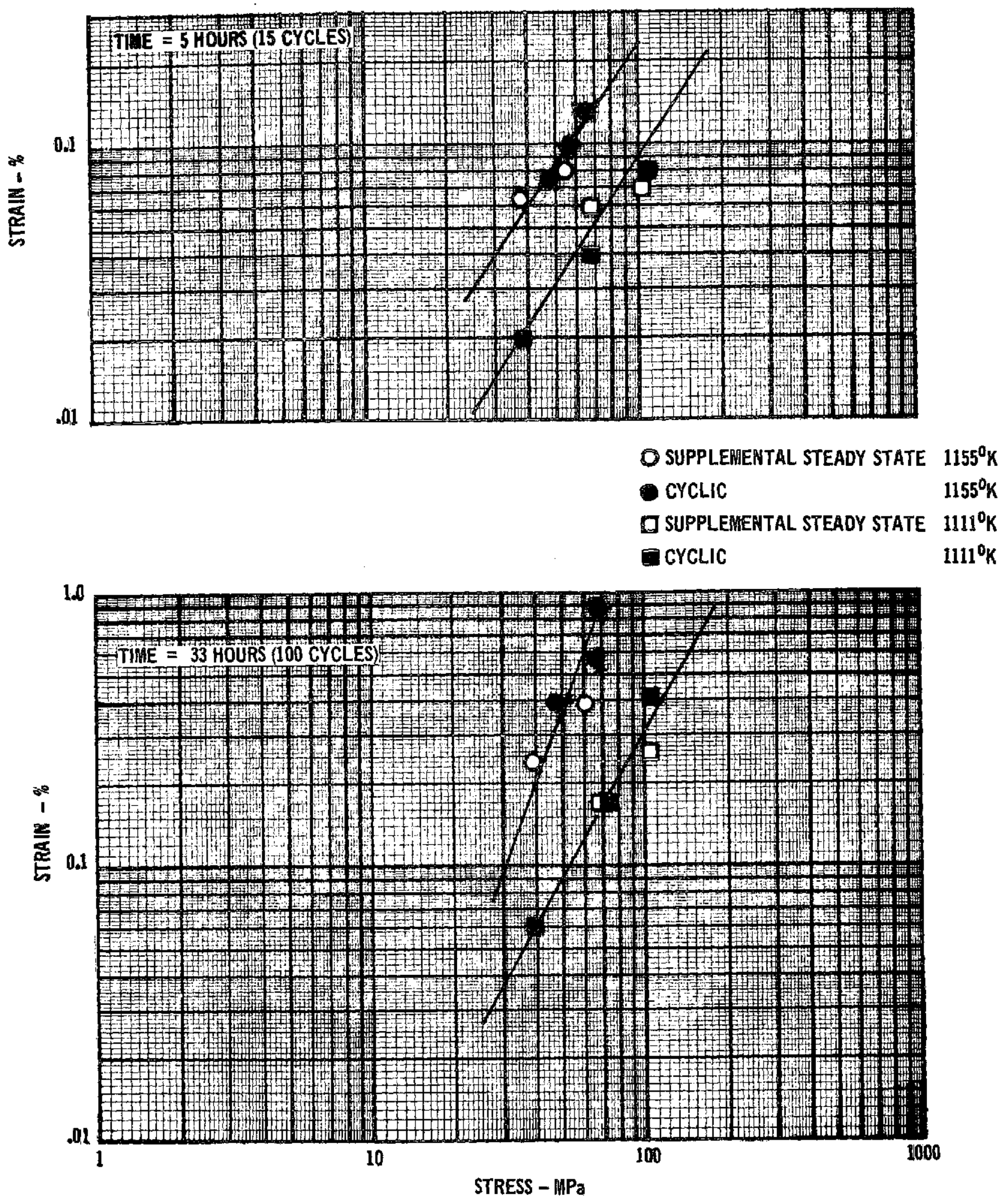

FIGURE 3-95 COMPARISON OF CYCLIC AND SUPPLEMENTAL STEADY-STATE CREEP DATA

3.3.5.2 Microstructure Comparison. The microstructure of the nickel-base Rene' 41 alloy before test is shown in Figure 3-96. Figures 3-97 and 3-98 show the structure after creep exposure. The as-received material has a typical solution annealed structure, consisting of stringers of carbides in a gamma solid solution matrix. After solution treatment and aging, carbide precipitation is evident at the grain boundaries and a subsurface zone depleted of precipitates has formed. Such zones are formed because diffusion and oxidation processes deplète the material adjacent to the surface of the less mobile alloying elements (such as chromium and aluminum).

Figures 3-97 and 3-98 show that pronounced changes have occurred in the microstructure of this alloy after creep exposure. Exposure at 1072°K and 137.9 MPa has caused coarsening of the grain boundary carbides and an increase in the extent of the subsurface depletion zone. Exposure at 1155°K and 41.4 MPa has a more pronounced effect, resulting in additional coarsening of precipitates both at the grain boundaries and within the grains, in addition to a more extensive subsurface depletion zone. However, no differences can be observed at this magnification between the cyclic and steady state microstructures of specimens creep tested at similar temperatures and stress levels.

3.3.6 RENE' 41 CYCLIC TESTS FOR EVALUATION OF ADDITIONAL VARIABLES

3.3.6.1 Effect of Time Per Cycle. Comparison of Rene' 41 cyclic test No. 8 (specimens R66L, R64L, and R65L) with Rene' 41 cyclic test No. 2 (specimens R37L, R36L, and R38L) are presented in Figure 3-99 for equal total times at load. Test 8 is a replicate of test 2 except that the time at load and maximum temperature is 10 minutes instead of the 20 minutes used in test 2. Based on the comparison, it cannot be concluded that time per cycle has any effect on Rene' 41 creep strains.

3.3.6.2 Effect of Atmospheric Pressure. Cyclic tests 13 and 14 were replicate idealized trajectory tests except that a simulated atmospheric pressure profile was

ALLOY:	RENE' 41
CONDITION:	AS-RECEIVED
ETCHANT:	KALLING'S REAGENT*
MAG:	500X
ASTM GRAIN SIZE	6
THICKNESS	0.027 cm

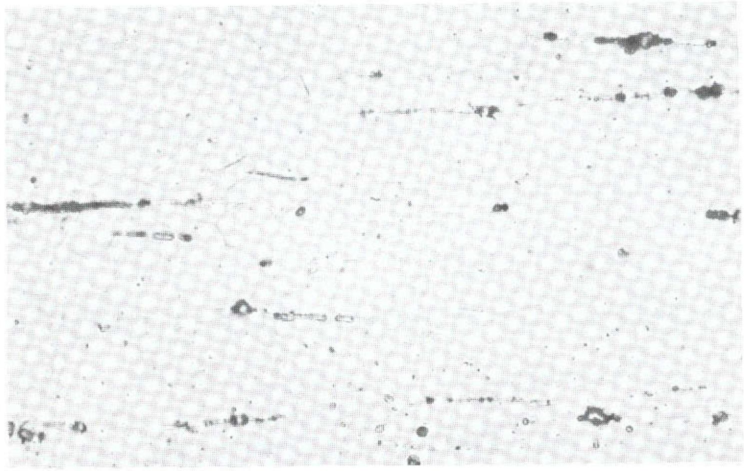

ALLOY:	RENE' 41
CONDITION:	SOLUTION TREATED AT 1394°K AGED AT 1172°K
ETCHANT:	KALLING'S REAGENT*
MAG:	500X
ASTM GRAIN SIZE	6
THICKNESS	0.027 cm

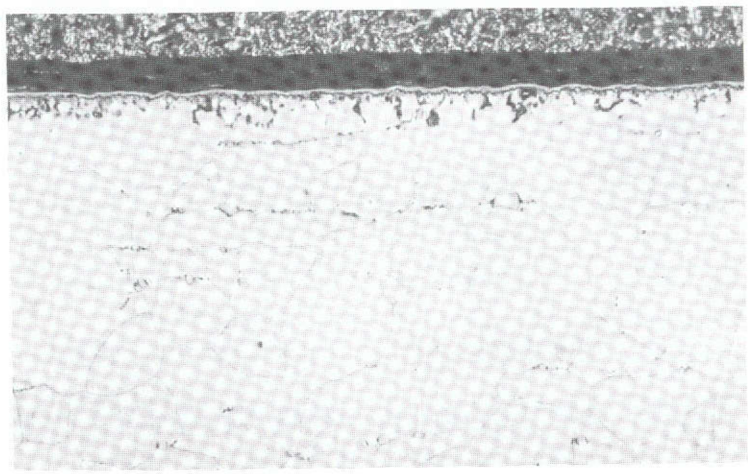

*2g$CuCl_2$, 40 ml HCl, 60 ml ETHONOL, 40 ml H_2O

FIGURE 3–96 MICROSTRUCTURE OF RENE' 41 PRIOR TO CREEP EXPOSURE

ALLOY:	RENE' 41
CONDITION:	TESTED (CYCLIC)
APPLIED STRESS:	55.2 MPa
TEST TEMPERATURE:	1155^{0}K
EXPOSURE TIME:	100 CYCLES
ETCHANT:	KALLING'S RAEGENT
MAG:	500X
ASTM GRAIN SIZE	6
THICKNESS	0.027 cm

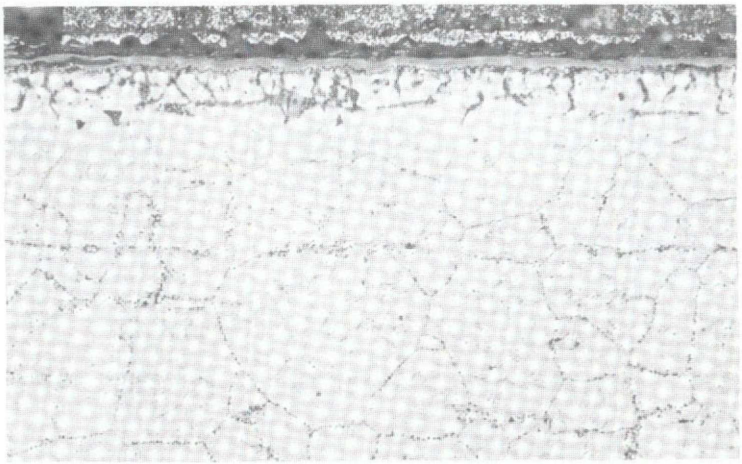

SPEC. NO. R36L

ALLOY:	RENE' 41
CONDITION:	TESTED (STEADY STATE)
APPLIED STRESS:	41.4 MPa
TEST TEMPERATURE:	1155^{0}K
EXPOSURE TIME:	160 HOURS
ETCHANT:	KALLING'S REAGENT
MAG:	500X
ASTM GRAIN SIZE	6
THICKNESS	0.028 cm

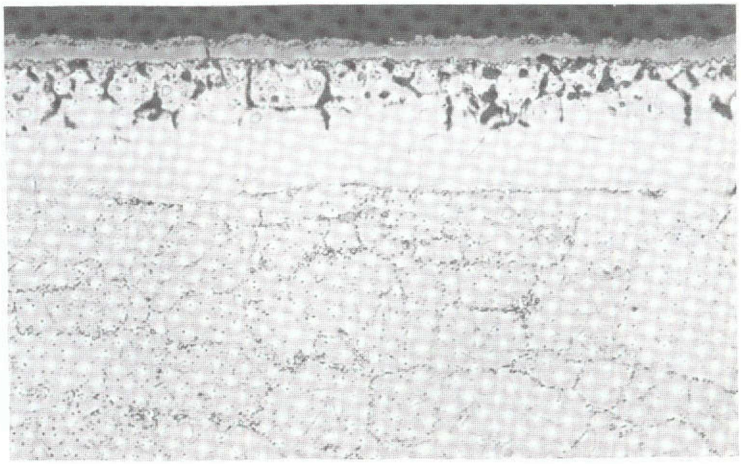

SPEC. NO. R23L

FIGURE 3–98 MICROSTRUCTURE OF RENE' 41 AFTER CREEP EXPOSURE AT 1155^{0}K

C-3

ALLOY:	RENE' 41
CONDITION:	TESTED (CYCLIC)
APPLIED STRESS:	137.9 MPa
TEST TEMPERATURE:	1072°K
EXPOSURE TIME:	100 CYCLES
ETCHANT:	KALLING'S REAGENT
MAG:	500X
ASTM GRAIN SIZE	6
THICKNESS	0.027 cm

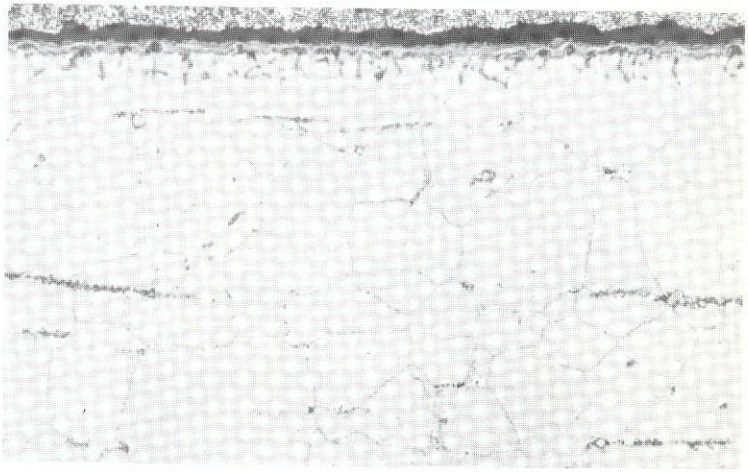

SPEC. NO. 46L

ALLOY:	RENE' 41
CONDITION:	TESTED (STEADY STATE)
APPLIED STRESS:	137.9 MPa
TEST TEMPERATURE:	1061°K
EXPOSURE TIME:	100 HOURS
ETCHANT:	KALLING'S RAEGENT
MAG:	500X
ASTM GRAIN SIZE	6
THICKNESS	0.027 cm

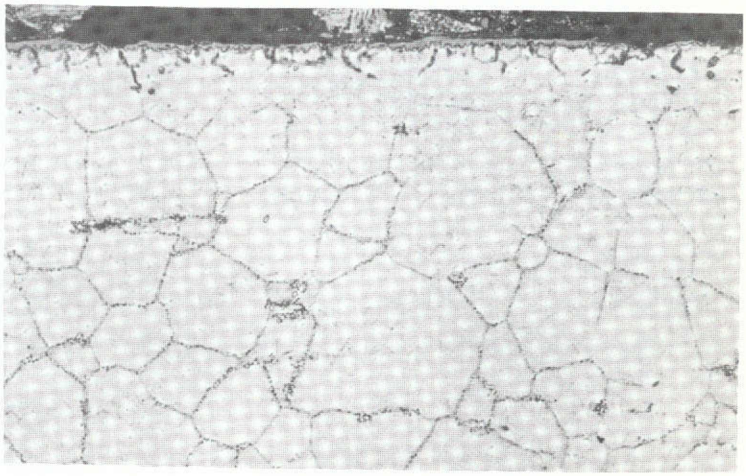

SPEC. NO. R104L

FIGURE 3–97 MICROSTRUCTURE OF RENE' 41 AFTER CREEP EXPOSURE AT 1061 AND 1072°K

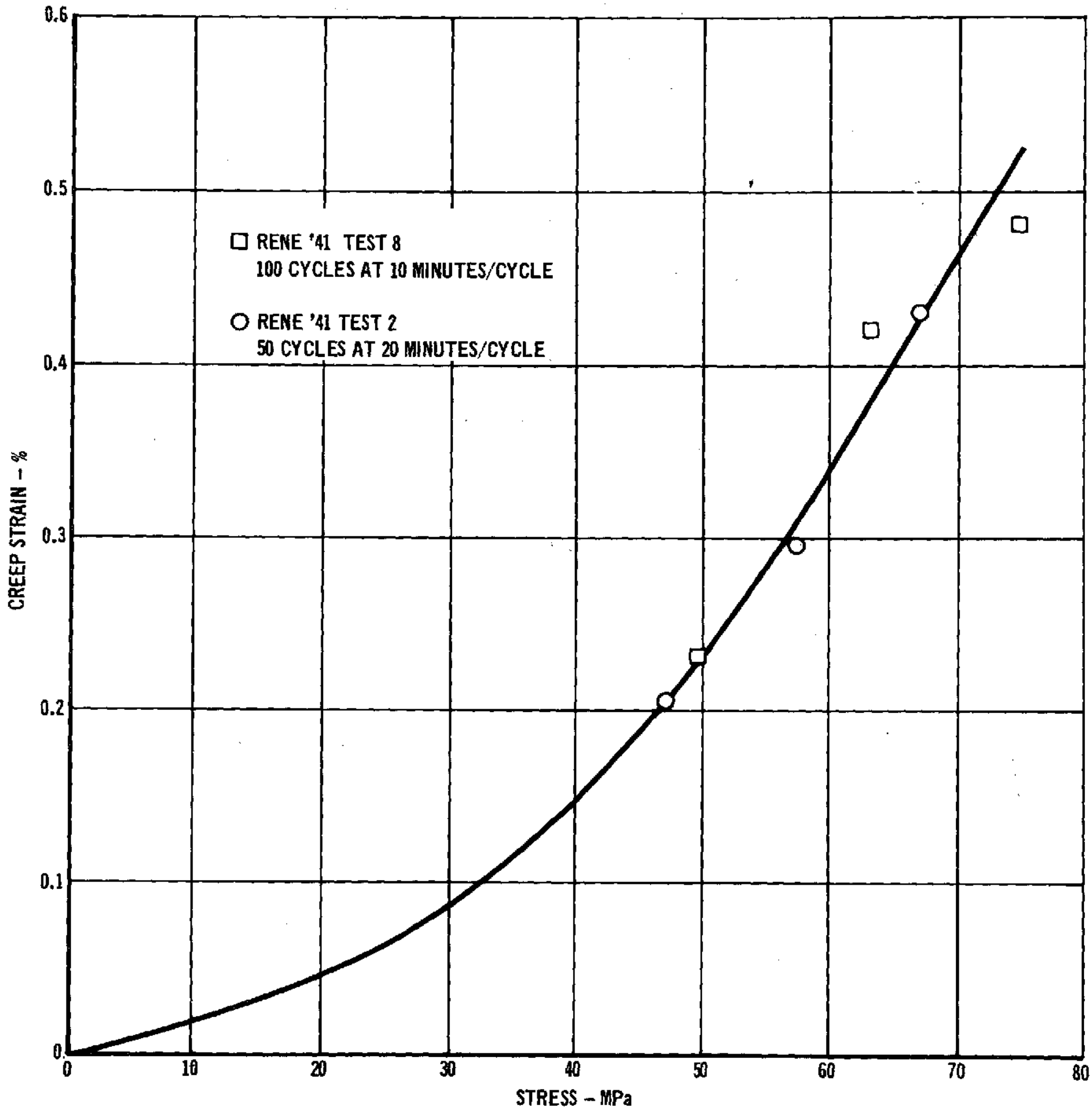

FIGURE 3–99 RENE '41 CYCLIC CREEP STRAINS AS A FUNCTION OF TOTAL TIME AT LOAD AT 1155°K

applied in test 14 while in test 13 the pressure was maintained constant at 1.3 Pa. Data for these two tests are presented in Appendix E-3. Comparison of creep strain results for the corresponding specimens in these tests are shown in Figure 3-100. Although the creep strains are higher for corresponding specimens using the constant pressure (test 13), the variation of approximately 10% is not sufficient to conclude that atmospheric pressure has any effect on a creep strain response.

3.3.6.3 Effects of Time Between Cycle. Tensile specimens R39L, R41L, and R40L were tested to 100 cycles at 1111°K (cyclic test No. 1) as part of the basic cyclic tests for Rene' 41. Several weeks subsequent to completion of this test, the specimens were tested for an additional 50 cycles. This additional cycling is designated as cyclic test No. 11. Data for the test are presented in Appendix E-3. Creep strain results are shown in Figure 3-101. Comparison of creep rates at the end of test 1 with those obtained in test 11 indicates a continuation of the slope. To determine if high temperature recovery was occurring, an additional test was performed (test No. 10, specimens R70L, R71L, and R72L) in which the load was maintained for 50 minutes (see Figure 2-24(a) instead of the usual 20 minutes. High temperature recovery usually occurs when a specimen is subjected to elevated temperature and no load conditions. By maintaining the load until the temperature is lowered, high temperature recovery should be prevented from occurring.

Data for the test are presented in Appendix E-3. Comparison of this test (No. 11), which did not have high temperature recovery, with one that could have high temperature recovery (test No. 1) revealed that there were differences between the two tests but not in the direction anticipated (See Figure 3-102). If high temperature recovery were occurring, the creep strains for test No. 1 should have been greater than test No. 10. Since the opposite is true, it does not appear that high temperature recovery is occurring. In addition, it appears that for test No. 10 a portion of the creep is occurring during the lower temperature portions of the profile.

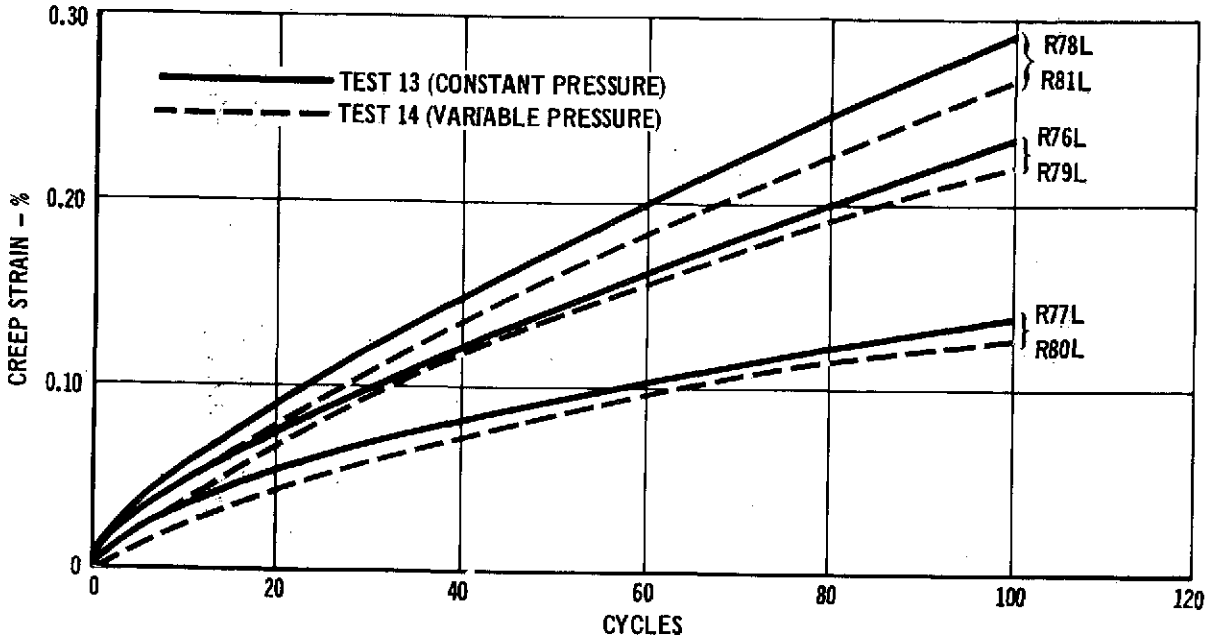

FIGURE 3–100 EFFECT OF PRESSURE ON THE CYCLIC CREEP OF RENE'41

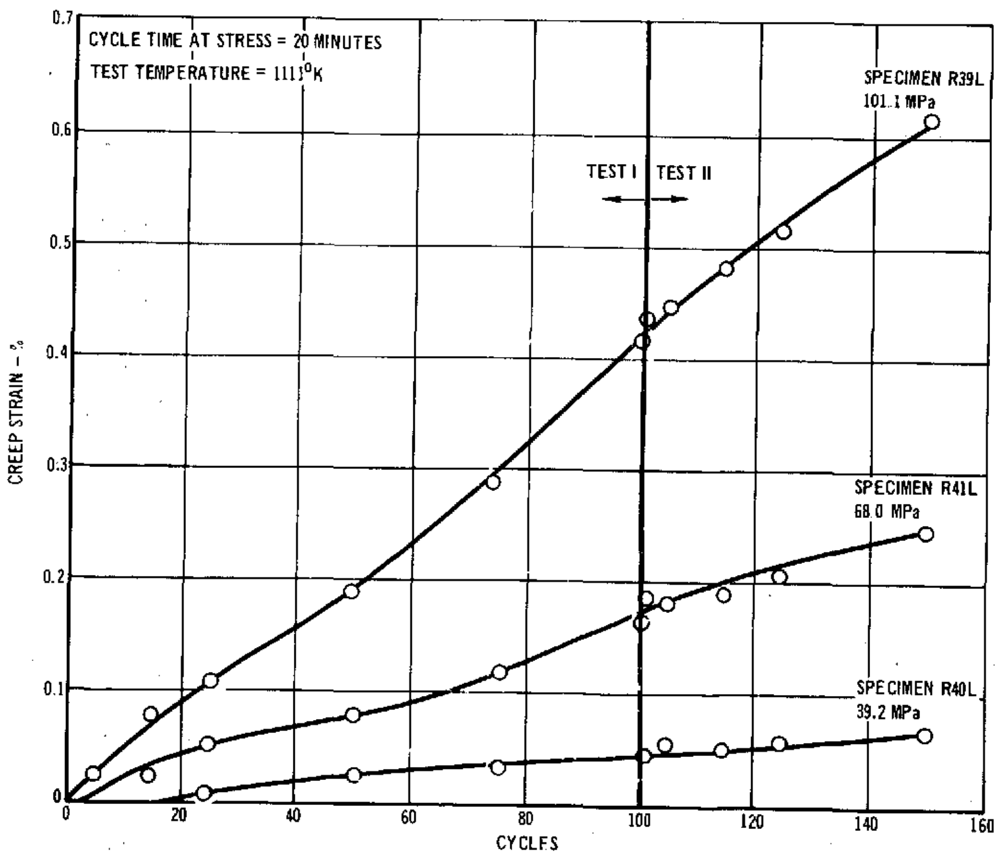

FIGURE 3–101 RENE '41 CYCLIC TEST NO. 11 – CONTINUATION OF RENE '41 BASIC CYCLIC TEST NO. 1

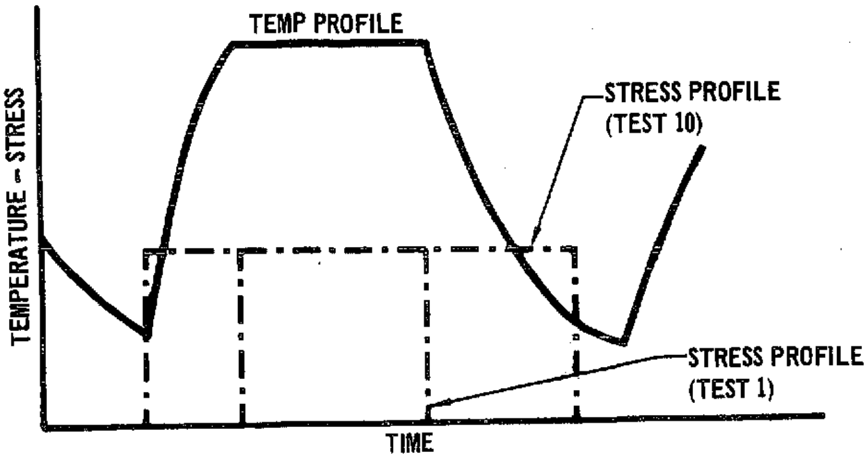

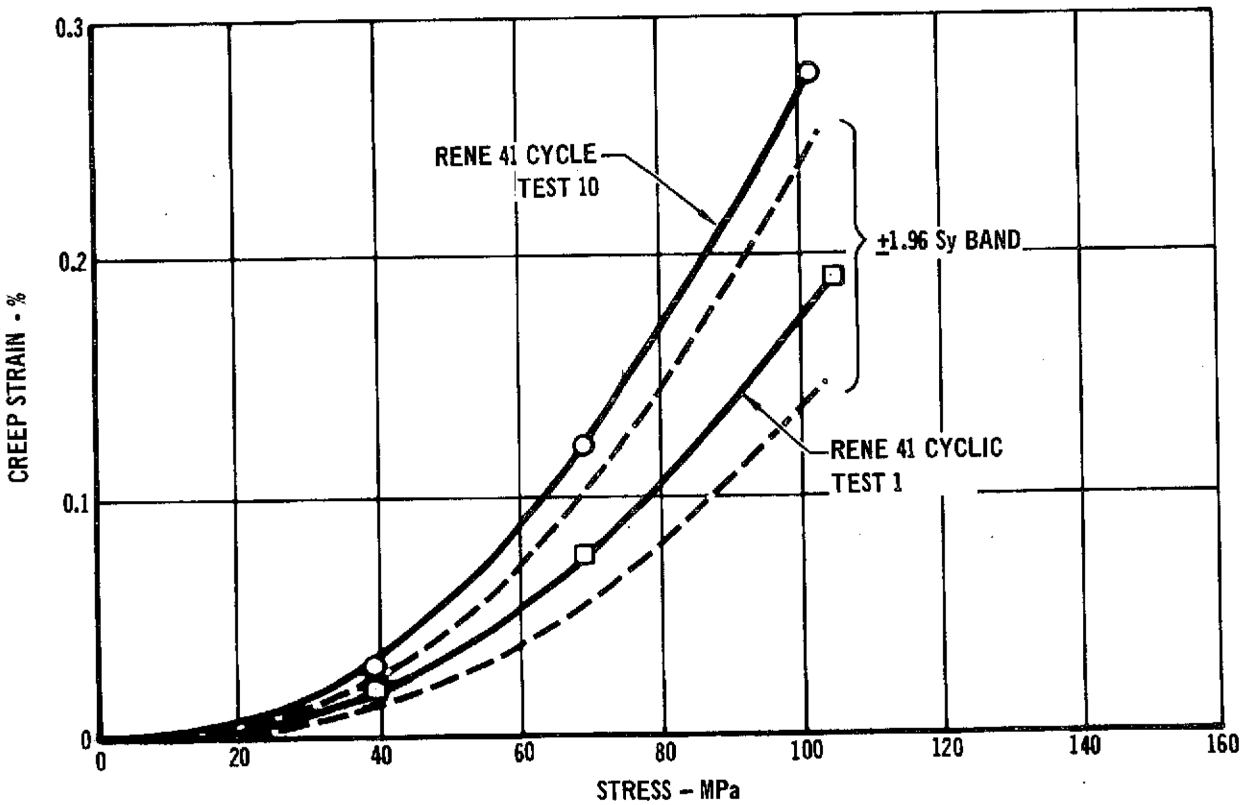

FIGURE 3-102 EFFECT OF INCREASED TIME AT LOAD ON RENE'41 AT 1111°K

3.3.7 STEPPED STRESS CYCLIC TESTS

Three cyclic tests were conducted where stress was maintained constant within each cycle but was varied as a function of cycle in order to allow an assessment of the materials hardening behavior. Data for these tests (Rene' 41 tests 5, 6, and 7 are presented in Appendix E-3.

In the first of these tests, Rene' 41 cyclic test 5 (specimens R51L, R47L, and R48L) stress was increased at cycle 16 through 50 and then decreased to the original level for the remaining 50 cycles as shown in Figure 3-103. Also shown in the figure are comparison of test results with predictions based on the time hardening theory of strain accumulation in conjunction with the cyclic creep equation (Equation 3-17). Predictions based on strain hardening (not shown) were up to 77% higher than those based on time hardening.

Increasing and decreasing stress history tests were also conducted on Rene' 41 tensile specimens. These were Rene' 41 cyclic test No. 6 (specimen R60L, R58L, and R59L) and Rene' 41 cyclic test No. 7 (specimens R63L, R61L, and R62L) respectively. Both tests were conducted at 1111°K (1540°F). Data for these tests are presented in Appendix E-3.

Comparisons of test creep strain results with predictions based on time hardening creep accumulation theories in conjunction with Equation (3-17) are shown in Figures 3-104 and 3-105. Predictions based on the strain hardening theory of creep accumulation were found to be approximately the same as for time hardening in predicting strains for test 6 (increasing stress). For test No. 7 however, strain hardening predictions were found to be up to 77% higher than the time hardening predictions which were already up to 30% higher than test values. Data comparisons show little creep strain difference between the increasing vs decreasing step stress tests at 100 missions.

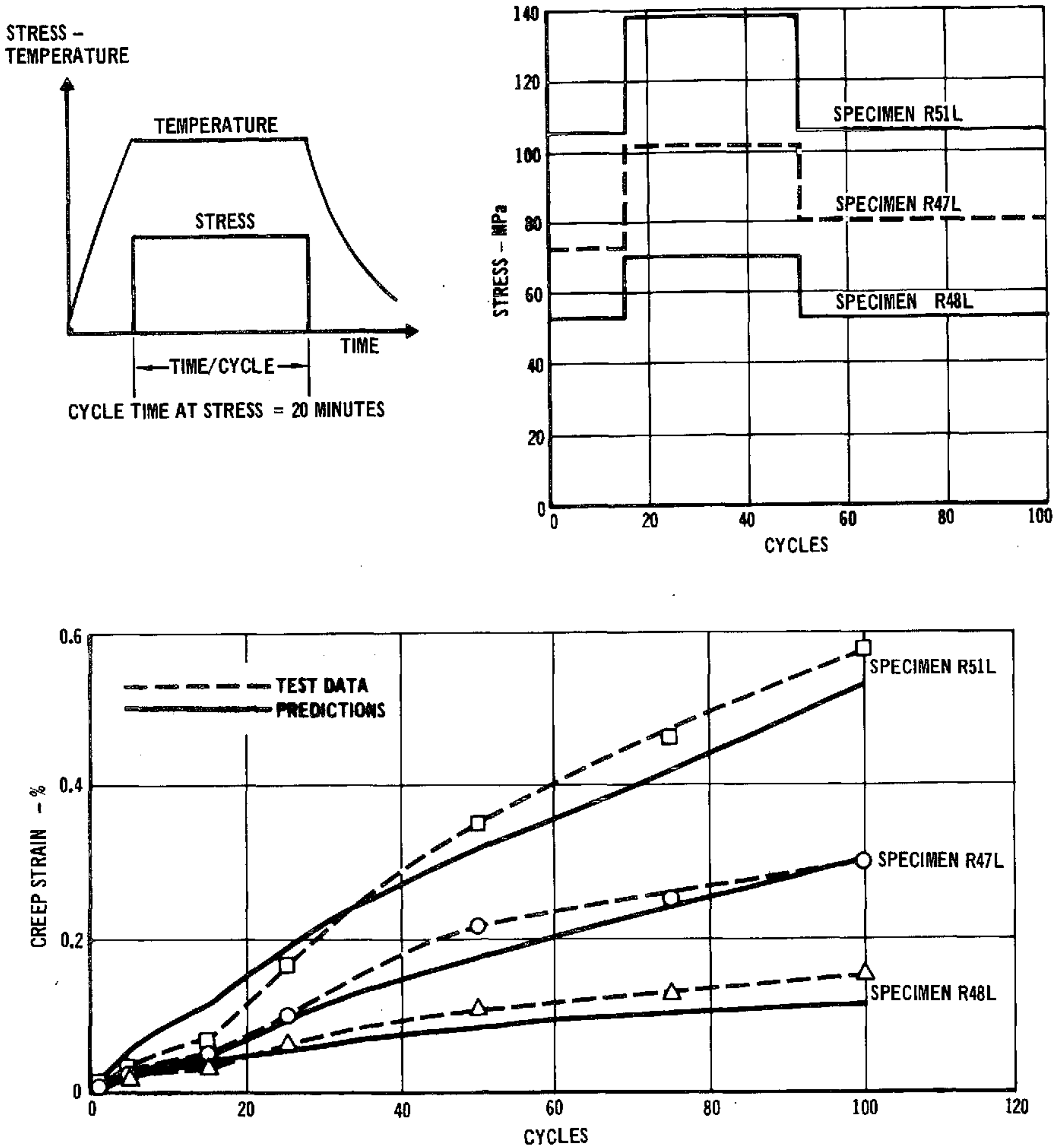

FIGURE 3–103 EFFECT OF VARIATION OF STRESS PROFILE BETWEEN CYCLES FOR RENE'41 AT 1111°K

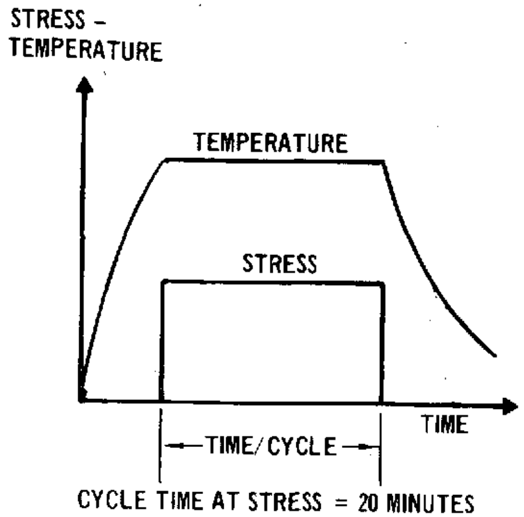

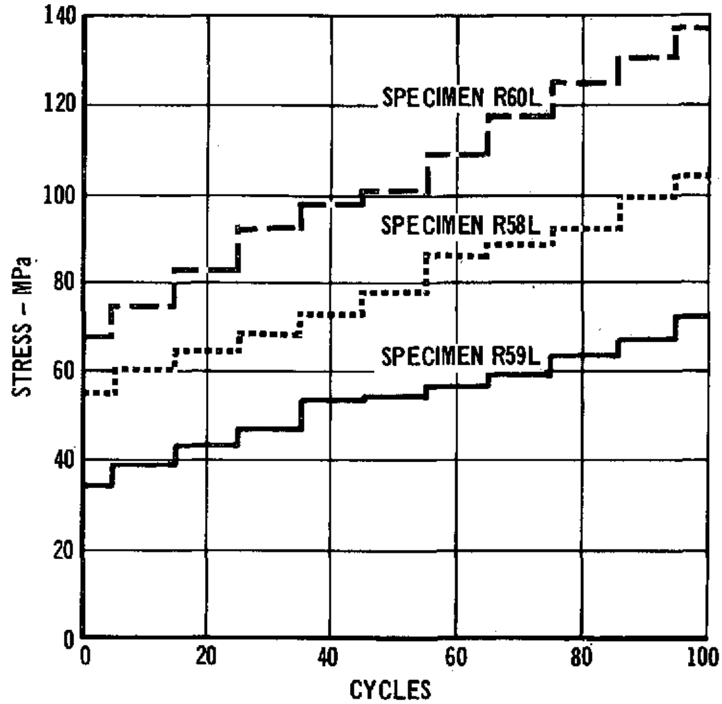

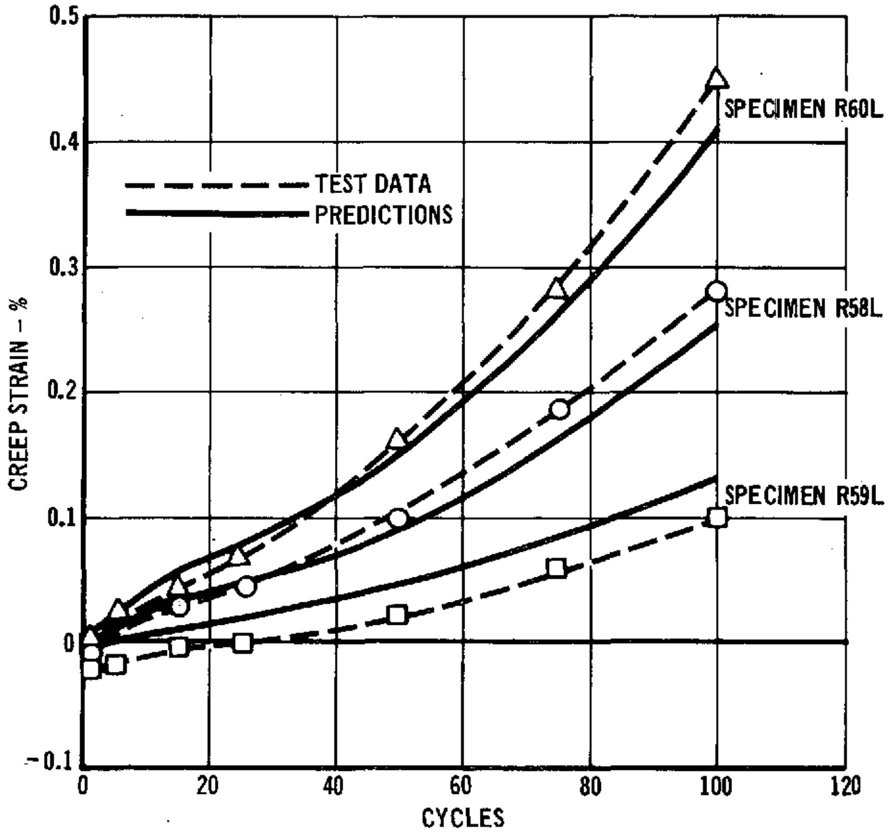

FIGURE 3-104 EFFECT OF INCREASING STRESS ON CREEP OF RENE'41 AT 1111°K

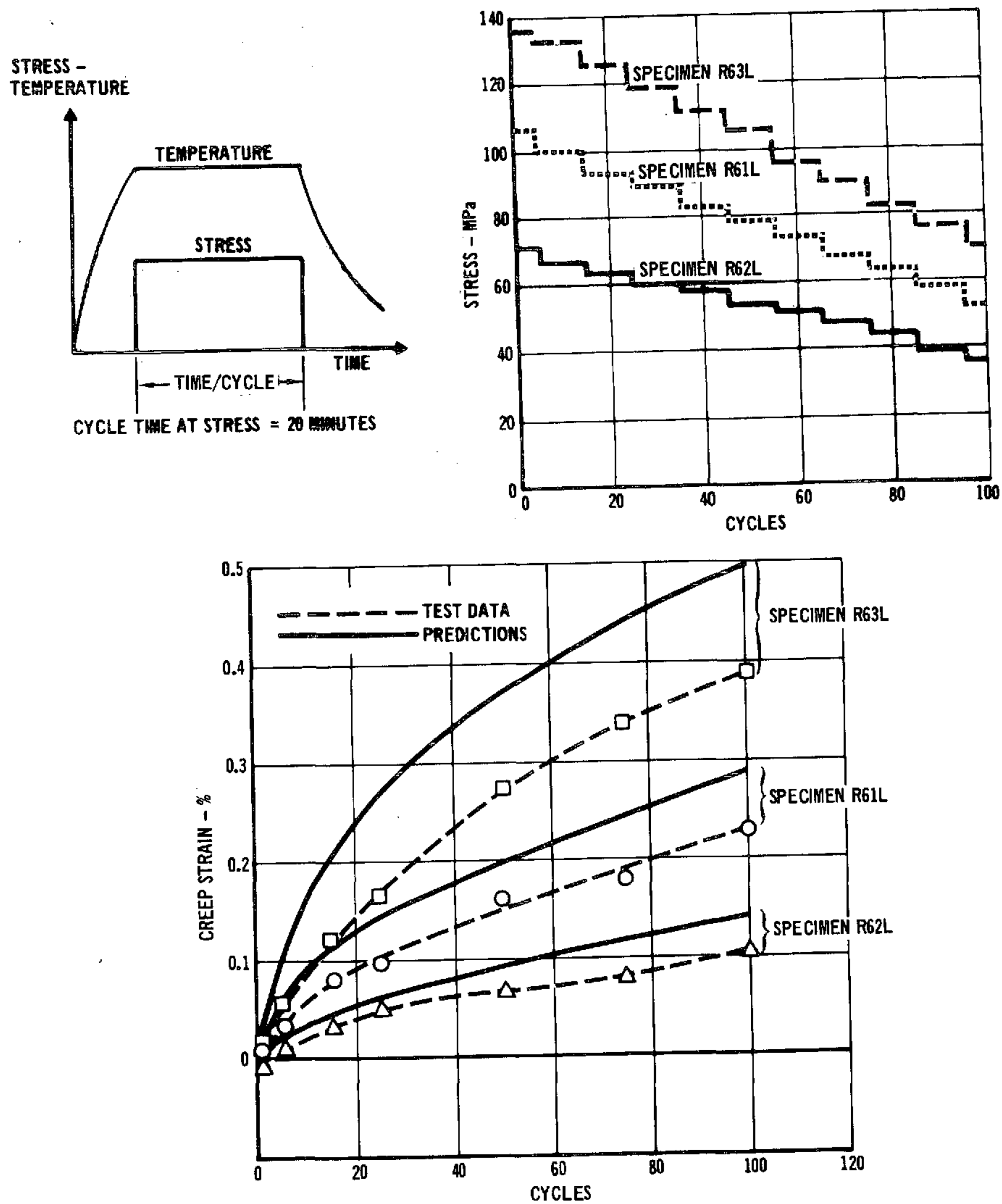

FIGURE 3-105 EFFECT OF DECREASING STRESS ON CREEP OF RENE'41 AT 1111°K

3.3.8 TRAJECTORY TESTS

Five cyclic trajectory tests were conducted using Rene'41 tensile specimens. Data for these tests, Rene' 41 cyclic tests 9, 12, 13, 14, and 15 are presented in Appendix E-3. These tests are a two-step stress trajectory profile with constant maximum temperature of 1111°K (1540°F) and constant pressure (test 9), an idealized trajectory test with a two-step temperature profile at 1155°K and 1111°K (test 12), two idealized trajectory tests (test 13 and 14) with a maximum temperature of 1111°K (comparison of test 13 and 14 on the basis of atmospheric pressure variation is presented in Section 3.3.6.2), and a simulated mission test (test 15) using representative Shuttle stress, temperature, and pressure profiles.

Comparison of creep strain results for tests 9, 12, 13, and 15, based on the time hardening theory of creep accumulation, are shown in Figures 3-106 through 3-109 respectively. Although the time hardening theory yielded the best predictions for this series of tests, all strain predictions are significantly lower than test results in the idealized and simulated mission tests where high stresses are maintained beyond the peak temperature portion of the profile. This behavior is the same as noted in comparing results of test 1 and 10 in Section 3.3.6.3.

The temperature and stress steps that were used to perform the trajectory analysis are presented in Appendix (E-3-25). In this analyses 10 steps of 200 seconds each were used starting with the data measured at 400 seconds into the trajectory.

3.3.9 Rene' 41 CONCLUSIONS

Rene' 41 tensile specimens were tested at stead-state conditions over the temperature range of 964°K (1275°F) to 1180°K (1665°F) over approximately 200 hours or creep strains of up to approximately .5% @ 50 hours. The following empirical regression equation was developed for these data:

$$\ln \varepsilon = -35.21304 + 26.34069\ T + .55687 \ln t + .02807 (\ln \sigma)^3 \qquad (3\text{-}15)$$

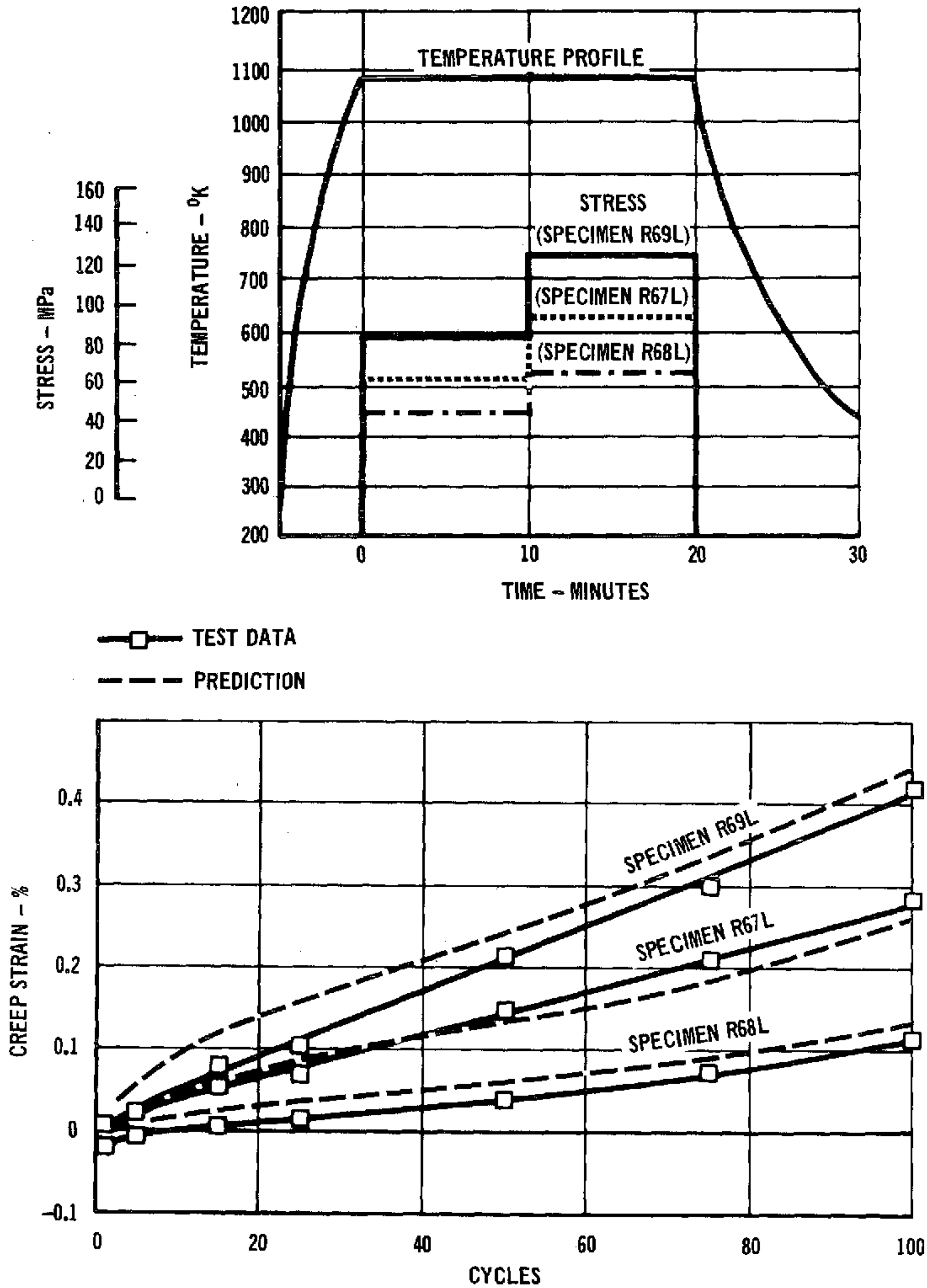

FIGURE 3–106 RENE'41 – TWO STEP STRESS TRAJECTORY DATA AND PREDICTIONS

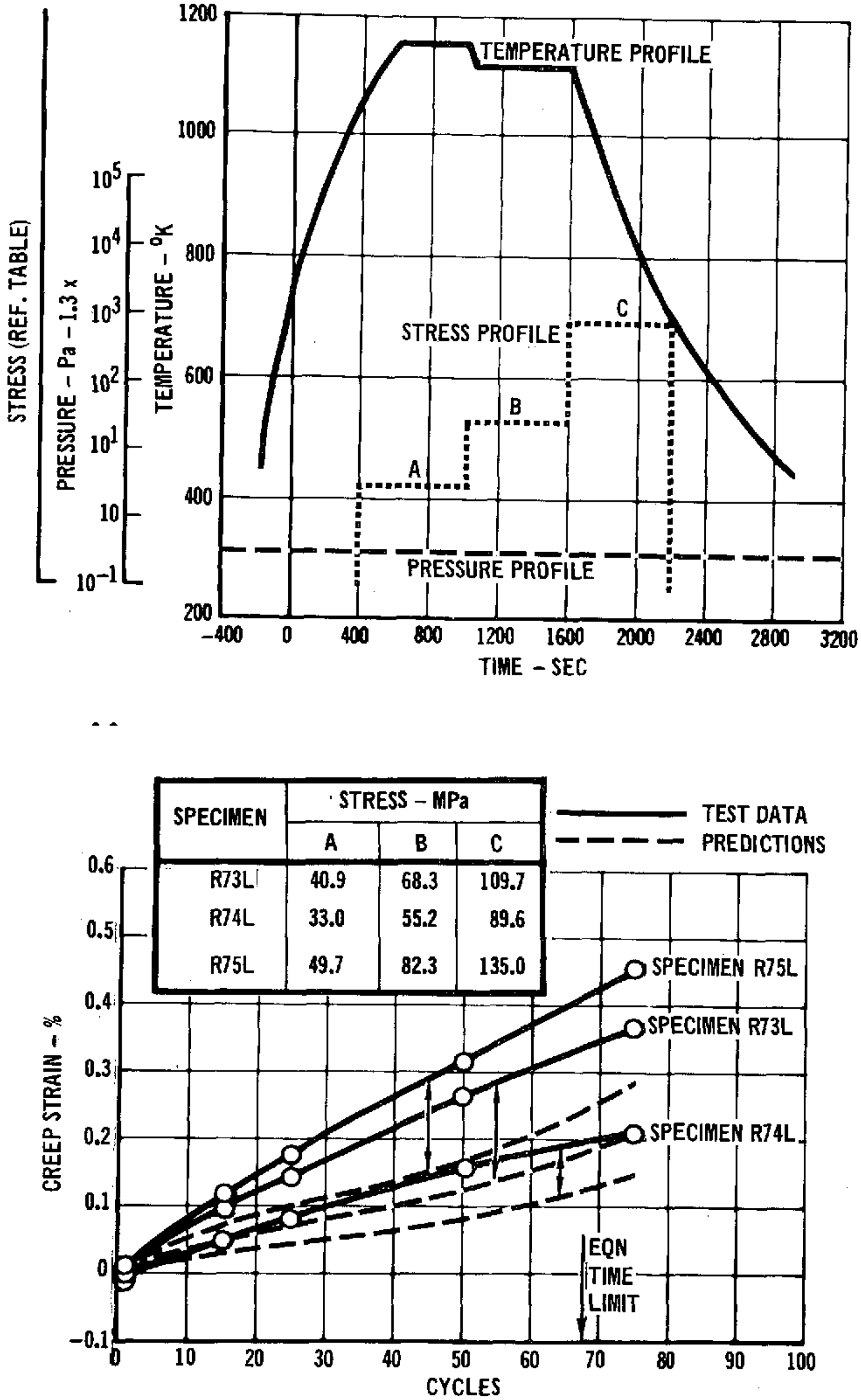

SPECIMEN	STRESS - MPa		
	A	B	C
R73L	40.9	68.3	109.7
R74L	33.0	55.2	89.6
R75L	49.7	82.3	135.0

FIGURE 3-107 RENE'41 – IDEALIZED TRAJECTORY PROFILES – CREEP DATA AND PREDICTIONS

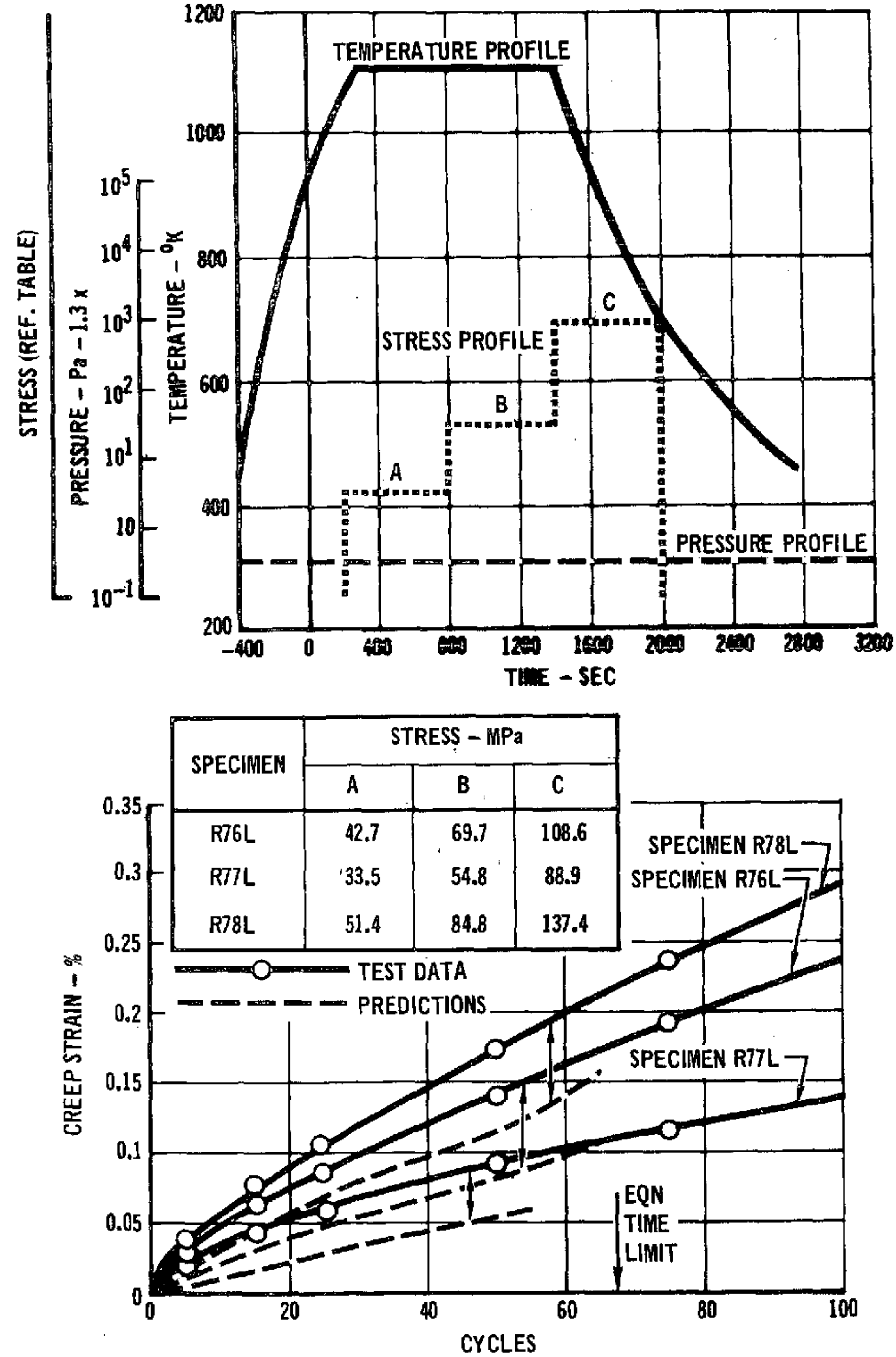

SPECIMEN	STRESS – MPa		
	A	B	C
R76L	42.7	69.7	108.6
R77L	33.5	54.8	88.9
R78L	51.4	84.8	137.4

FIGURE 3–108 RENE'41 CYCLIC TEST NO. 13 – IDEALIZED TRAJECTORY PROFILES – CREEP DATA AND PREDICTIONS

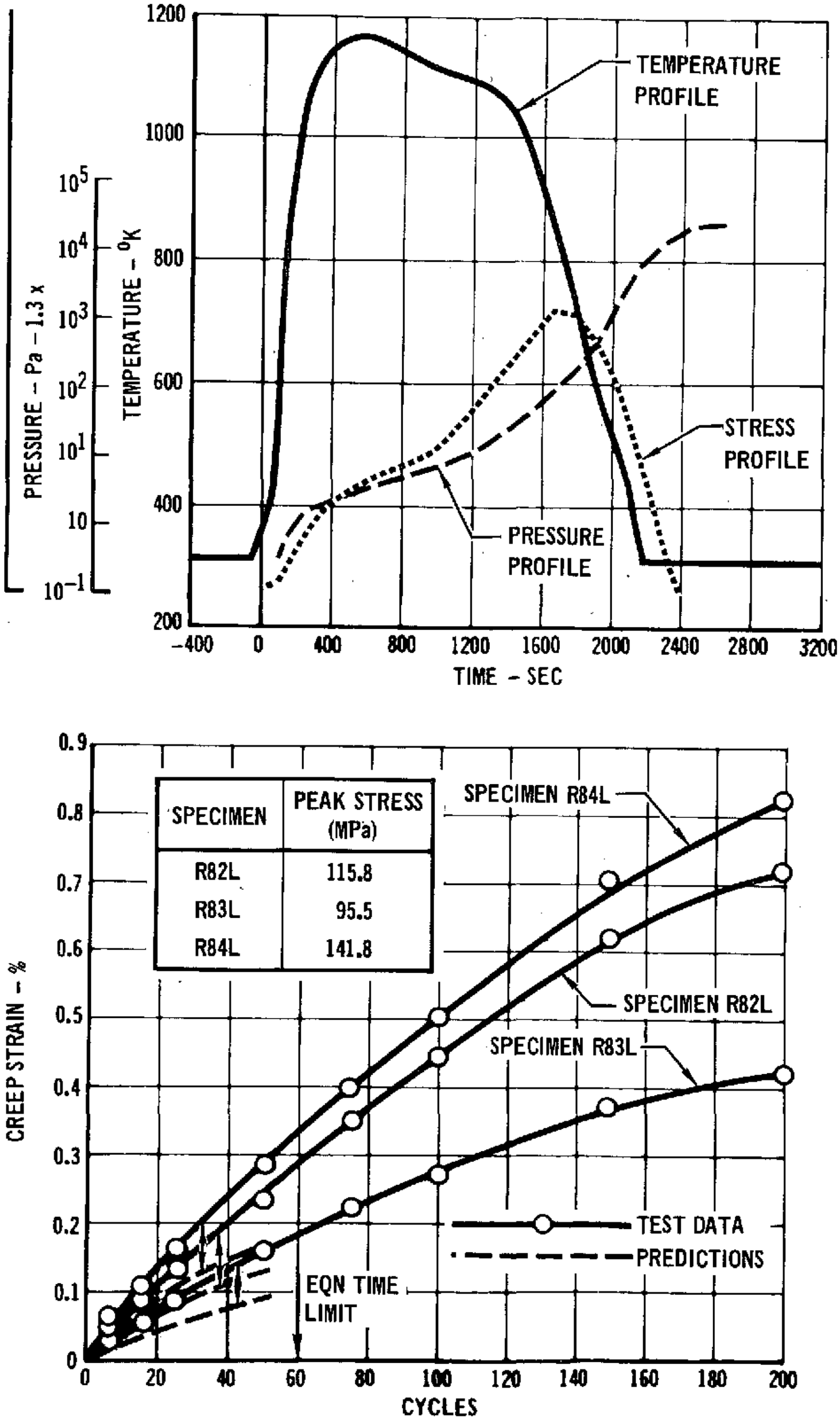

FIGURE 3-109 RENE'41 SIMULATED MISSION PROFILE - CREEP DATA AND PREDICTIONS

An effect of material gage on creep response was noted in both the literature survey data base and supplemental test results. Thicker gage specimens (.051 cm) were observed to creep faster than the thin gage (.027 cm) specimens in the supplemental tests. No differences in creep response due to material rolling direction were observed.

The following empirical regression equation was developed for cyclic test data:

$$\ln \varepsilon = -39.55860 + 29.13646\, T + .71922 \ln t - .92125 (\ln \sigma - 1.931) - .000016\, \sigma^2 + .08183 (\ln \sigma - 1.931)^3 - .000125\, t\sigma T + .0000105 t^3 \tag{3-17}$$

This equation is applicable over the temperature range of 1031°K (1400°F) to 1155°K (1620°F) for times up to 33 hours (100 cycles at 20 mintues per cycle).

Comparison of supplemental steady-state data and cyclic data showed that no difference existed in these data sets.

No effects on creep strain due to variation of time per cycle (for the same total time) or atmospheric pressure could be determined. Significant increases in creep strains were noted in tests where stress was maintained on the specimen while temperature was being decreased rapidly. This would indicate that creep can occur at a low temperature for Rene' 41.

Use of strain and time hardening creep accumulation theories in predicting the complex trajectory test data resulted in low predictions (approximately 40% below test value). The time hardening theory provided the best predictions. In predicting results for a simple two step trajectory however, the time hardening theory yielded good agreement with test data. The variation in prediction capability between simple and complex trajectories is attributed to the same phenomena demonstrated in the case where using a simple single stress profile, stress was maintained into the decreasing temperature portion of the cycle.

3.4 TDNiCr - RESULTS OF TESTS AND DATA ANALYSIS

3.4.1 TDNiCr DATA BASE

3.4.1.1 Literature Survey. The TDNiCr steady-state data base is comprised of 1897 data points obtained from the following sources: NASA Marshall (Reference 16), NASA Lewis (Reference 17), General Electric Company (References 18 and 19), and McDonnell Douglas Corporation (References 20 and 21). Data from the above sources were reviewed and tests with creep strains greater than approximately 0.5% at 100 hours were eliminated. Killpatrick (Reference 30) has found that TDNiCr creep tests which have creep strains greater than 0.5% at 100 hours are suspect of improper material condition. The literature data base is presented in Appendix F-1.

3.4.1.2 Data Base Analysis. Several equations of different forms were developed for the data base. The following equation was selected for use in development of a test matrix for TDNiCr.

$$\ln \varepsilon = -12.43906 + .01930\sigma + 2.80992T - .00022t - .38945\theta + 22.45187\phi + .35175 \ln t - 1.12398 \ln\phi \tag{3-18}$$

where ε = creep strain, %

T = temperature, °K/100

σ = stress, MPa

θ = 1, longitudinal material direction; 0, transverse material direction

ϕ = gage, cm

t = time, hours

This equation has a standard error of estimate of .6933, based on the logarithm of strain, and a multiple correlation coefficient of .7750, indicating a larger degree of scatter in this data than had been present for the other material data bases obtained for this program. Both material gage and rolling direction are indicated to be significant, independent variables. The residual plots ($\ln \varepsilon_{actual} - \ln \varepsilon_{calculated}$ vs. variable) for this equation are shown in Figure 3-110.

An empirical equation was also derived for a portion of the data base considered to be most representative of current TDNiCr manufacturing technology.

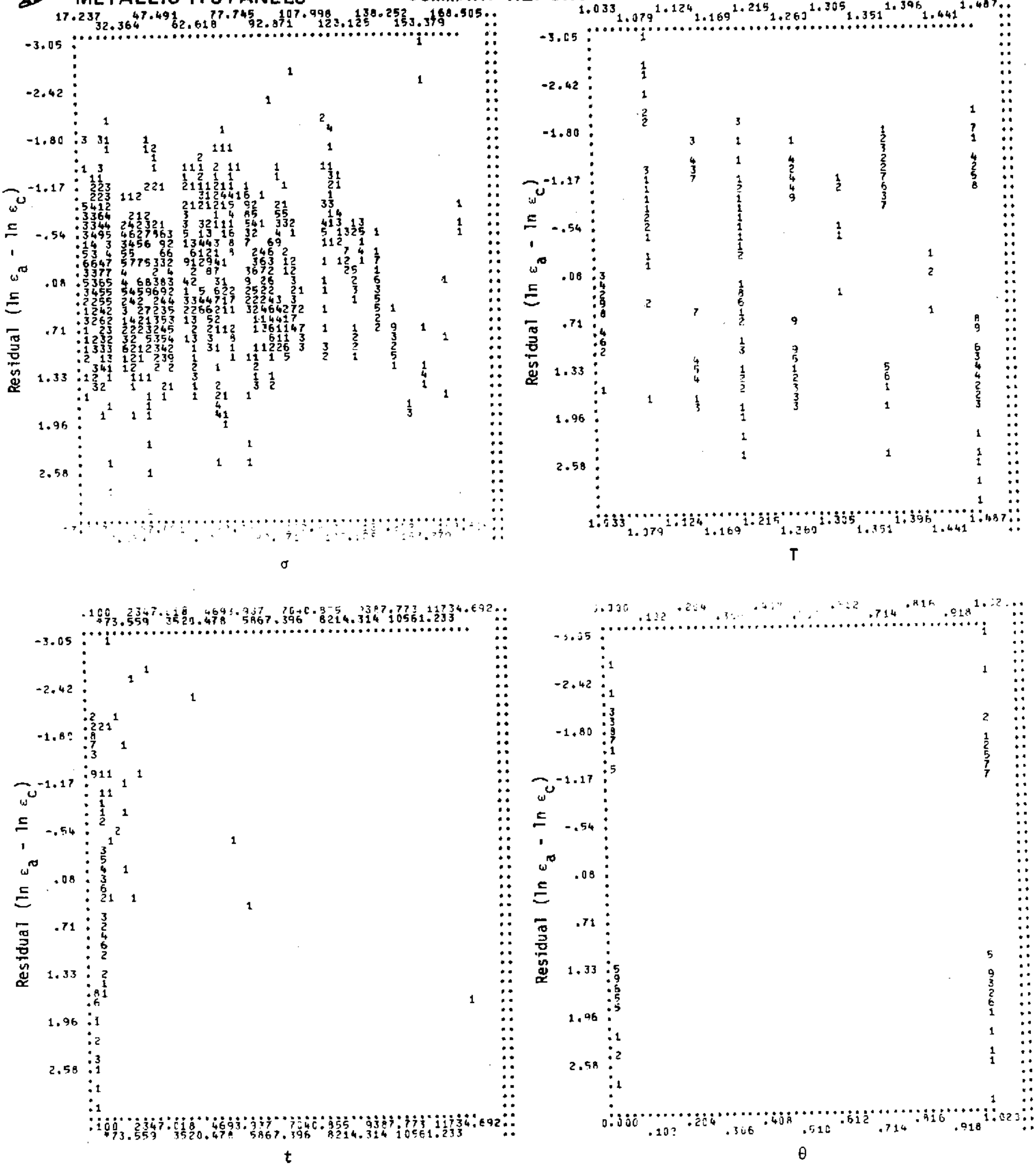

FIGURE 3-110 RESIDUAL PLOTS OF TDNiCr LITERATURE SURVEY EQUATION (3-18)

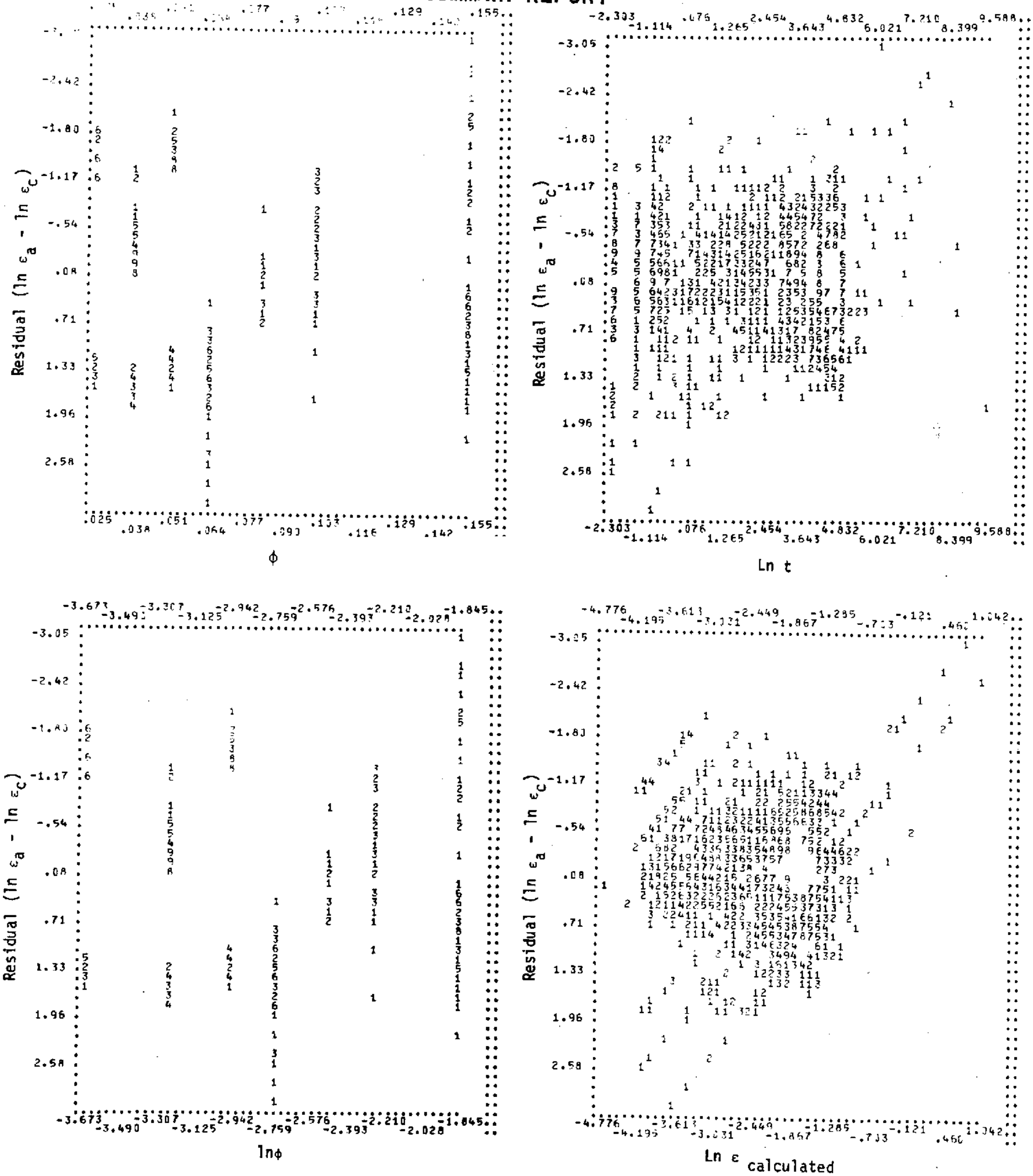

FIGURE 3-110 RESIDUAL PLOTS OF TDNiCr LITERATURE SURVEY EQUATION (3-18) (Continued)

These data, which were the portion of the data base obtained from NASA Lewis (Reference 17) resulted in the following empirical equation:

$$\ln \varepsilon = -3.16177 - 2.86860\ (1/T) + .36069 \ln t + .54690 \ln \sigma \qquad (3\text{-}19)$$

Material gage and rolling direction do not appear in this equation, since these data were all .025 gage tested in the longitudinal rolling direction.

The equation has a standard error of estimate of .5552 on the logarithm of strain and a multiple correlation coefficient of .8394. The residual plots (ln ($\ln \varepsilon_{actual} - \ln \varepsilon_{calculated}$ vs. variable) for this equation are shown in Figure 3-111. No attempts were made to incorporate interaction terms or to optimize for a better fit of the data. This equation will be used for purposes of comparing with cyclic data in Section 3.4.5.1.

3.4.2 TDNiCr SUPPLEMENTAL STEADY-STATE TESTING

3.4.2.1 TDNiCr Supplemental Steady-State Test Matrix - A total of sixteen supplemental steady-state tests were conducted per conditions in Table 3-7. Ten of the tests were for .0254 cm (.010 inch) thick material tested in the longitudinal rolling direction. Three of the remaining tests were conducted on .0533 cm (.021 inch) thick specimens tested in the longitudinal rolling direction, and three were conducted on .0254 cm. (.010 inch) specimens tested in the transverse rolling direction.

Test values of stress and temperature were designed to yield creep strains ranging from 0.33% in 200 hours to 0.10% in 200 hours based on Equation 3-18 predictions. These lines of constant creep strain and the test matrix are shown in Figure 3-112. The curve representing 0.33% strain in 200 hours is observed to be very close to the upper limit of the data base at temperatures greater than 1255°K.

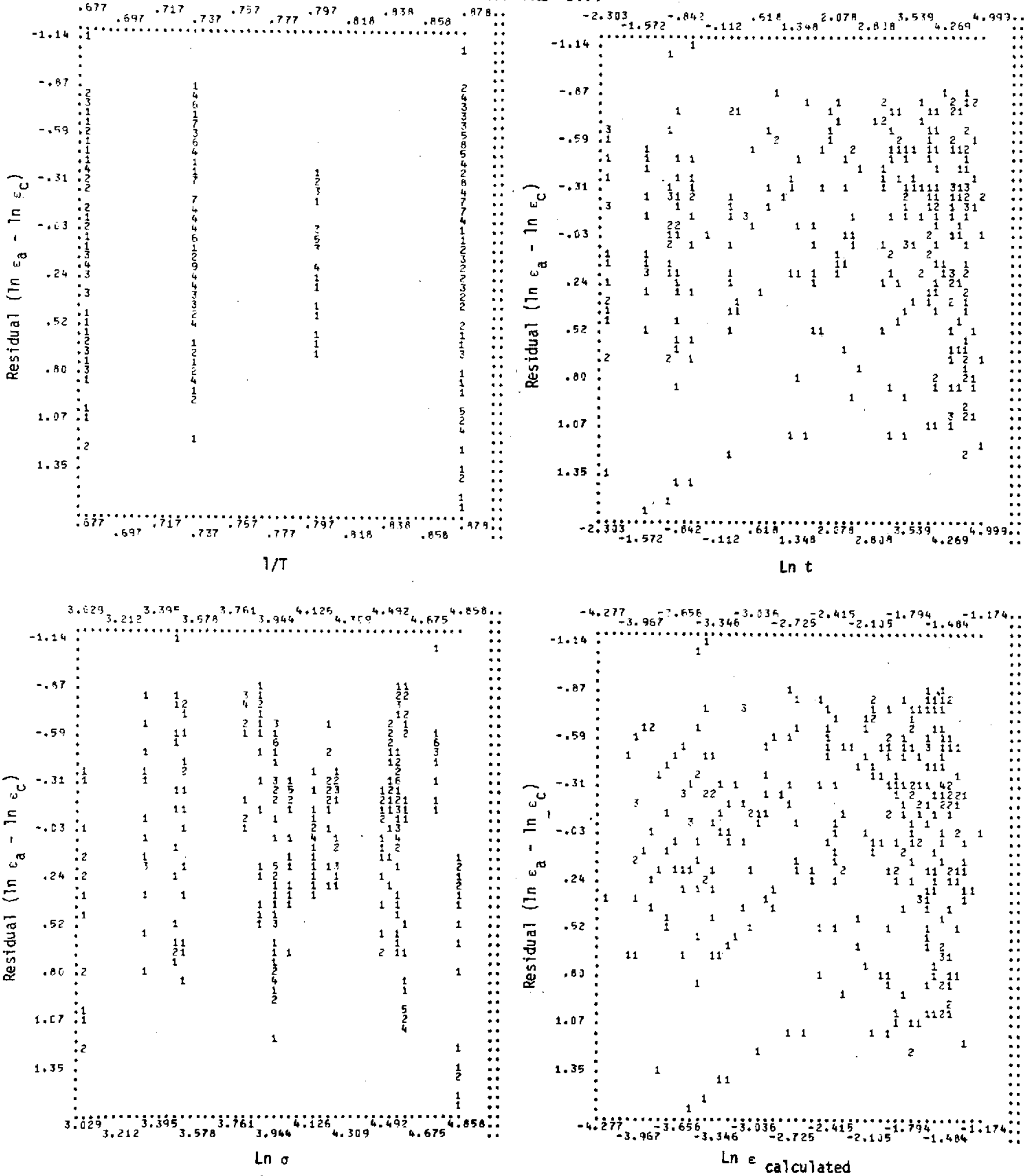

FIGURE 3-111 RESIDUAL PLOTS OF TDNiCr LITERATURE SURVEY EQUATION (3-19) (BASED ON NASA DATA ONLY)

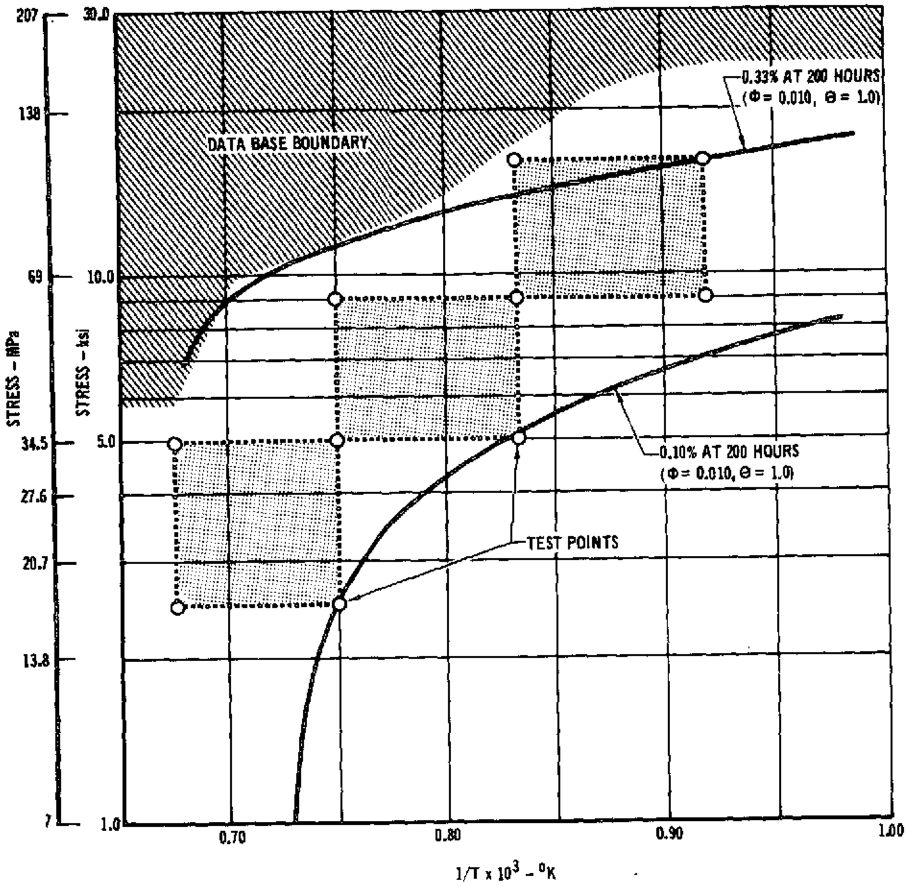

FIGURE 3–112 TD NiCr SUPPLEMENTAL STEADY-STATE EXPERIMENTAL DESIGN

TABLE 3–7 – TDNiCr SUPPLEMENTAL STEADY-STATE TESTS

TEST SPECIMEN	MATERIAL ROLLING DIRECTION	MATERIAL GAGE		TEMPERATURE		STRESS	
		CM	INCHES	°K	°F	MPa	ksi
TD21L	LONGITUDINAL	0.0254	0.010	1089	1500	110.3	16.0
TD25L				1200	1700	34.5	5.0
TD24L				1200	1700	62.1	9.0
TD23L				1200	1700	110.3	16.0
TD28L				1340	1950.	17.3	2.5
TD27L				1340	1950	34.5	5.0
TD26L				1340	1950	62.1	9.0
TD30L				1479	2200	17.2	2.5
TD32L				1479	2200	27.6	4.0
TD29L	LONGITUDINAL			1479	2200	34.5	5.0
TD12T	TRANSVERSE			1200	1700	62.1	9.0
TD11T				1200	1700	110.3	16.0
TD13T	TRANSVERSE	0.0254	0.010	1340	1950	62.1	9.0
TD2L	LONGITUDINAL	0.0533	0.021	1200	1700	62.1	9.0
TD1L				1200	1700	110.3	16.0
TD3L	LONGITUDINAL	0.0533	0.021	1340	1950	62.1	9.0

It should be noted that a curve for 0.50% strain at 50 hours is not shown, as has been done previously for the other materials under investigation, since this curve is outside the data base. This is indicative of the low creep strains obtained with TDNiCr material. The shaded area in Figure 3-112 represents the upper limits of the data for this material and is also where several specimen stress rupture failures occurred in the data base.

Creep strain results for each of the supplemental steady-state tests are presented in Appendix F-2. Included in this appendix are the elastic strains which were determined at the start and the conclusion of the test.

3.4.2.2 <u>Test Data Evaluation - Basic Test Matrix</u>. A review of the supplemental steady-state data indicates some inconsistency, in that some tests at 1340°K exhibit higher creep strains than those at 1479°K. This is demonstrated in the 50-hour creep strains shown in Figure 3-113. The usefulness of developing an equation for this data is, therefore, questionable.

Subsequent comparisons of cyclic and supplemental steady-state data are made (Section 3.4.5) which indicate no difference between these sets of data. Therefore, empirical equations developed for the basic cyclic tests (cyclic tests 1-6) will be considered applicable to the supplemental steady-state data also.

3.4.2.3 <u>Effects of Gage and Rolling Direction</u>. Comparisons of supplemental steady-state creep data for tests conducted on specimens of .0254 and .0533 cm and on specimens in longitudinal and transverse directions are shown in Table 3-8 for three different times. Review of the data indicates that the .0533 cm specimens experienced greater creep strains than the .0254 cm specimens, and that specimens tested in the transverse rolling direction experienced greater creep strain than those tested in the longitudinal rolling direction. The only exceptions to this trend were in the case of specimen TD12T (.0254 gage, transverse direction) where very low creep strains were attained, which may indicate an invalid test. These

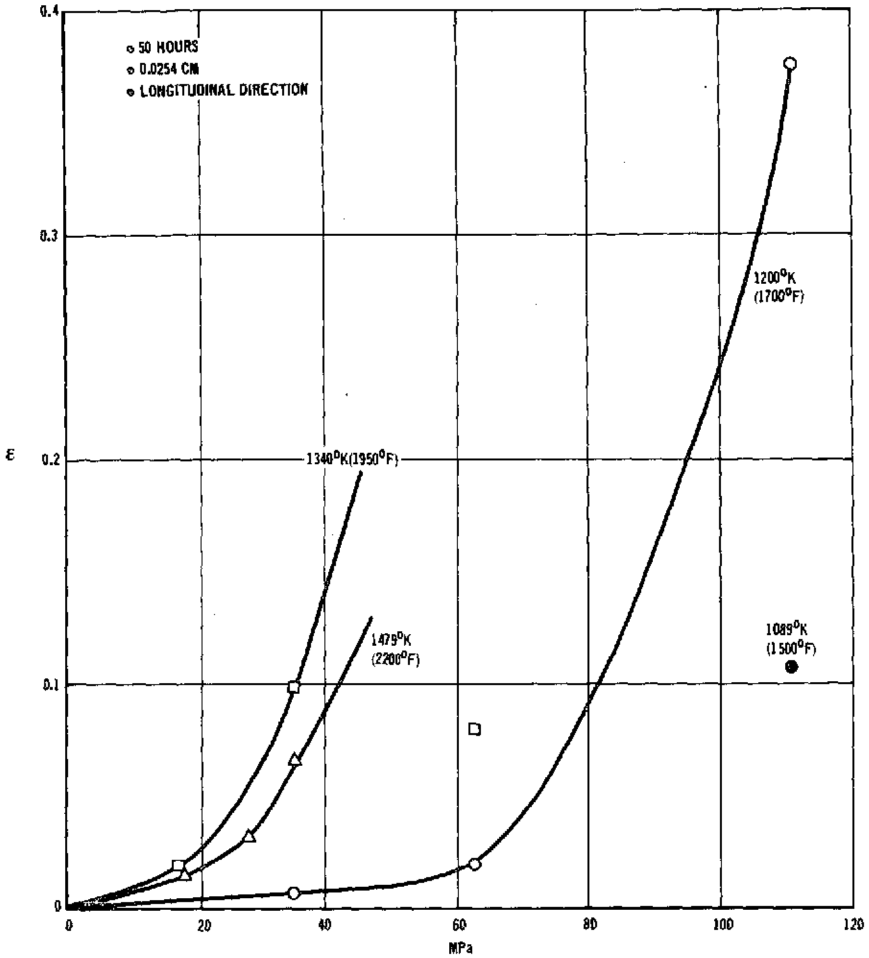

FIGURE 3–113 TDNiCr SUPPLEMENTAL STEADY-STATE DATA AT 50 HOURS

TABLE 3–8
COMPARISON OF GAGE AND ROLLING DIRECTION EFFECTS IN SUPPLEMENTAL STEADY-STATE TESTING

CONDITION	TIME = 0.25 HR			TIME = 20 HR			TIME = 100 HR		
	0.0254 LONGIT	0.0254 TRANS	0.0533 LONGIT	0.0254 LONGIT	0.0254 TRANS	0.0533 LONGIT	0.0254 LONGIT	0.0254 TRANS	0.0533 LONGIT
1200°K (1700°F) 110 mPa (16 ksi)	0.040 TD23L	0.094 TD11T	0.238 TD1L	0.290 TD23L	0.380 TD11L	–	0.473 TD23L	–	–
1200°K (1700°F) 62 mPa (9 ksi)	0.009 TD24L	0.002 TD12T	0.026 TD2L	0.026 TD24L	0.008 TD12T	0.037 TD2L	0.028 TD24L	0.032 TD12L	0.145 TD2L
1340°K (1950°F) 62 mPa (9 ksi)	0.004 TD26L	0.025 TD13T	0.039 TD3L	0.067 TD26L	0.300 TD13T	0.325 TD3L	0.131 TD26L	0.990 TD13T	–

results agree with the prediction for the steady-state data base in Equation 3-18 where creep strain increases with increasing gage, and is greater for the transverse direction (θ=0) than the longitudinal direction (θ=1).

3.4.3 COMPARISON OF STEADY-STATE DATA BASE AND SUPPLEMENTAL TEST RESULTS

Comparison of supplemental data at 5 hours and 50 hours, with predictions based on the data base equation (Equation 3-18) are shown in Figure 3-114. This comparison demonstrates that creep strains attained in supplemental testing are generally about one-half of strains predicted from the data base.

3.4.4 TDNiCr BASIC CYCLIC TESTS

3.4.4.1 Basic Cyclic Test Matrix. Evaluation of TDNiCr, from the standpoint of creep deflections in TPS panels, represents a completely different case than the other three materials studied under this program. This is primarily because relatively little creep is evident in this material before failures occur. Therefore, the requirement for definition of creep deflection is minimized in the design criteria for TDNiCr TPS. Because of this, less emphasis has been placed on evaluation of the steady-state data base and comparison of this data base with supplemental steady-state tests. More emphasis has been placed on definition of limits of temperature and stress at which failure occurs. In this effort, additional cyclic tests were conducted when necessary to obtain failures at each of four test temperatures. A summary of the basic cyclic tests performed is presented in Table 3-9.

Basic cyclic tests were conducted on .0254 cm specimens in the longitudinal direction at temperatures of 1089°K (1500°F), 1200°K (1700°F), 1340°K (1950°F), and 1479°K (2200°F). These tests consisted of cycling specimens at constant loads and temperatures for up to 100 cycles using a constant load and temperature over a 20-minute cycle time period. Test stress levels were based on the data base boundary as presented in Figure 3-112. Data for this portion of the cyclic

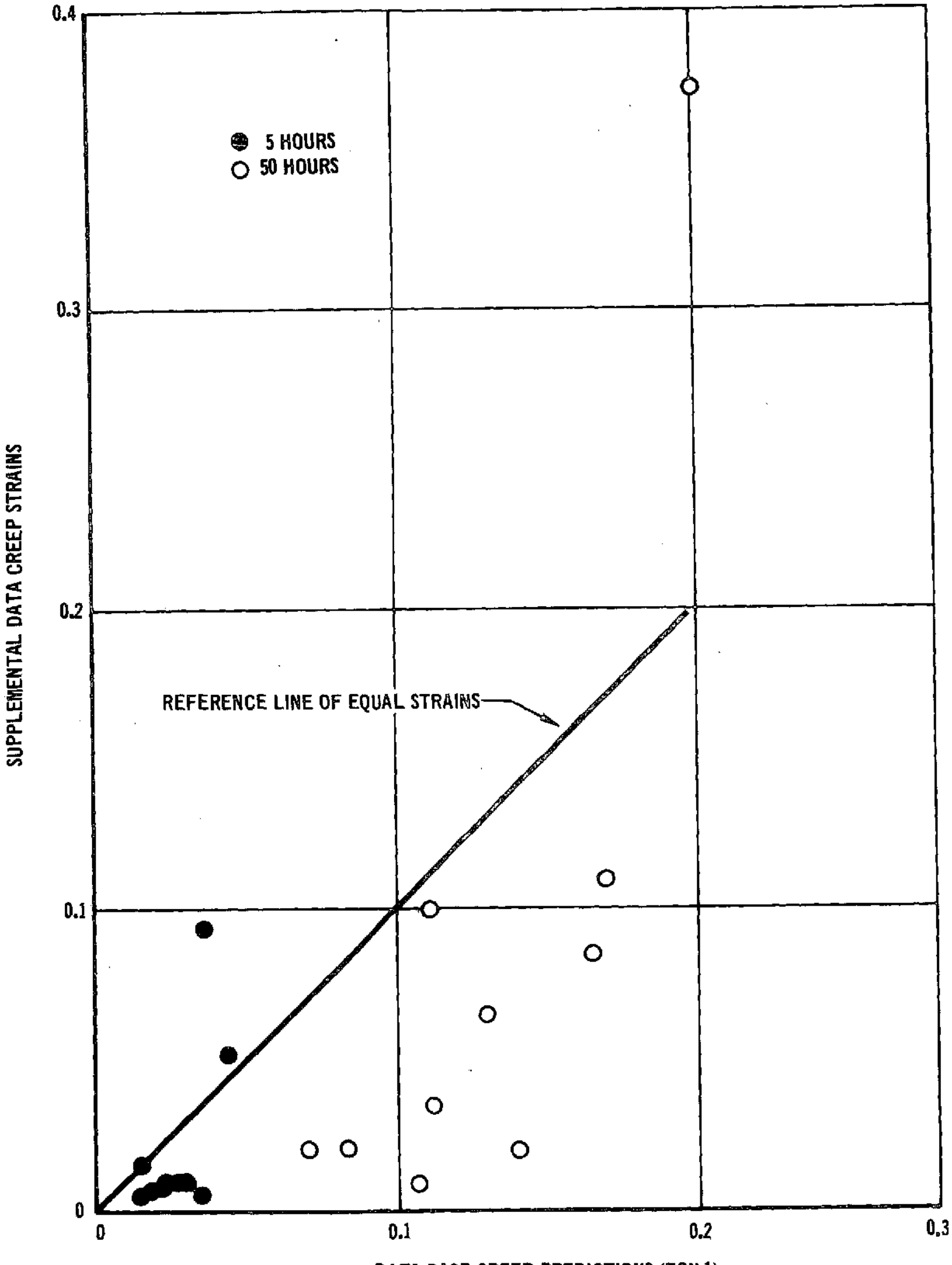

FIGURE 3-114 COMPARISON OF DATA BASE PREDICTIONS AND SUPPLEMENTAL TEST RESULTS

TABLE 3–9 TDNiCr BASIC CYCLIC TESTS

CYCLIC TEST NO.	TEST SPECIMEN	TEMPERATURE		STRESS	
		°K	°F	MPa	KSI
1	TD96L	1089	1500	85.7	12.43
	TD95L	1089	1500	103.3	14.98
	TD98L	1089	1500	124.2	18.02
2	TD80L	1200	1700	57.2	8.30
	TD44L	1200	1700	73.8	10.7
	TD81L	1200	1700	87.7	12.72
3	TD57L	1339	1950	30.6	4.44
	TD55L	1339	1950	47.6	6.90
	TD67L	1339	1950	59.2	8.59
	TD59L	1339	1950	60.3	8.74
4	TD62L	1478	2200	16.3	2.36
	TD63L	1478	2200	29.1	4.22
	TD35L	1478	2200	33.7	4.89
	TD102L	1478	2200	44.3	6.42

NOTES:
1. ALL SPECIMENS 0.024 CM
2. ALL SPECIMENS TESTED IN LONGITUDINAL ROLLING DIRECTION.
3. ALL TESTS – 20 MINUTES/CYCLE, 100 CYCLES.

tests, designated as Tests 1 through 6, are presented in Appendix F-3.

3.4.4.2 Test Results and Analysis. Cyclic test data was found to be generally more consistent (less scatter) than for the steady-state tests. The following equation was developed using data obtained from the hand faired basic cyclic creep curves (Figures 3-115 to 3-118). The data consisted of approximately 5 points per test spaced in such a manner as to describe the curve. For example, a test run for 60 cycles had strains selected at 6, 15, 30, and 60 cycles while the 100 cycle tests had strains selected at 6, 15, 30, 60 and 100 cycles from the hand faired curves. Creep times were the accumulated cycle time at maximum load and temperature, therefore, for the basic cycles the time was .33 hrs/cycle or 2 hrs/6 cycles.

$$\ln \varepsilon = -3.48443 - 10.37282 \left(\frac{1}{T}\right) +.28314 \ln t + 2.00118 \ln \sigma \qquad (3\text{-}20)$$

This equation has a standard error of estimate .2603 and a multiple R of .9128. The residual plots ($\ln \varepsilon_{actual} - \ln \varepsilon_{calculated}$) vs. variable for this equation are shown in Figure 3-119. Because of the low TDNiCr creep strains obtained, it was judged that further refinement of the equation would not have a significant effect on subsize panel predictions. Therefore, no attempts were made to add additional interaction terms to further optimize this equation for a better fit of the data.

Effort was placed on testing at stress levels such that some failures would be obtained at each of the test temperatures. Combination of stress and temperature at which failures occurred are indicated in Figure 3-120. Also shown are the last measured creep strain before failure and stresses at which tests were completed without failure. No creep strains are available for the 1200°K temperature tests, since all failures occurred during the first cycle before measurements could be obtained.

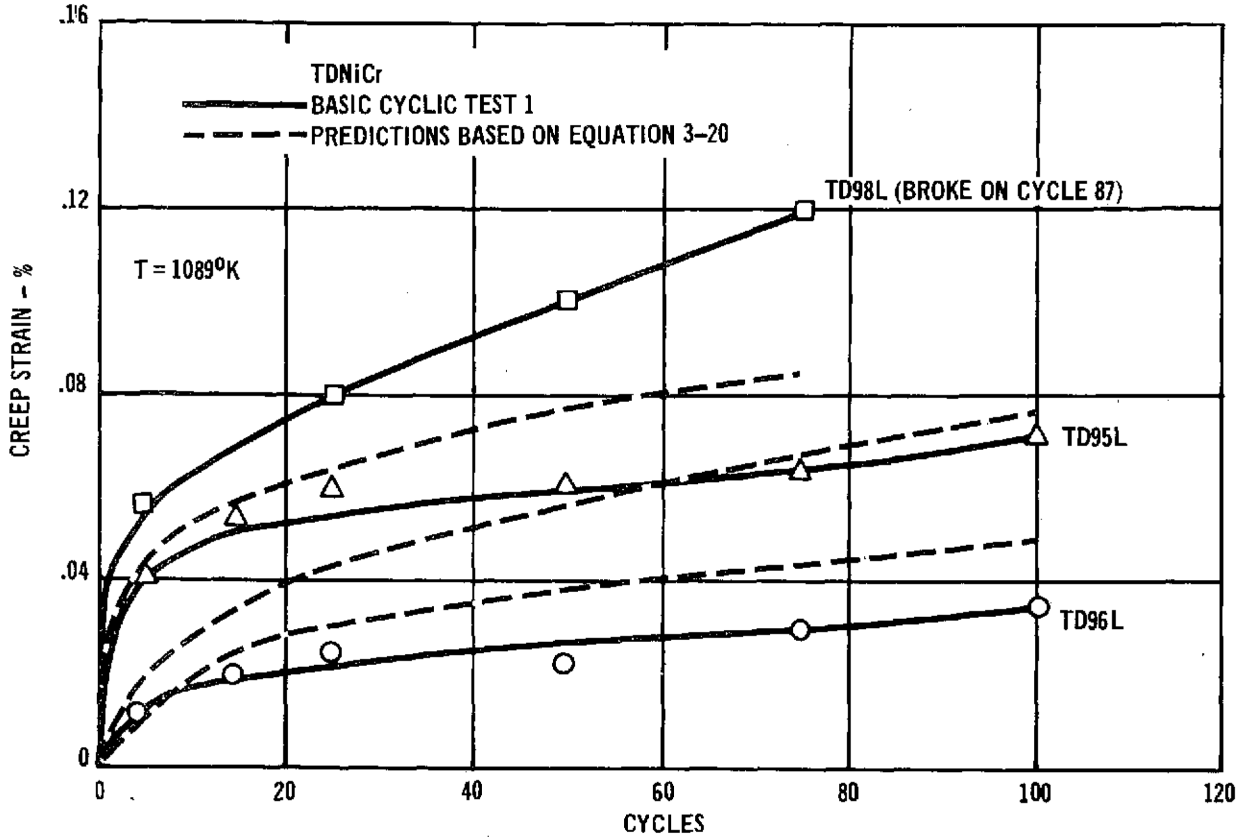

FIGURE 3-115 TDNiCr BASIC CYCLIC CREEP TEST AT 1089°K

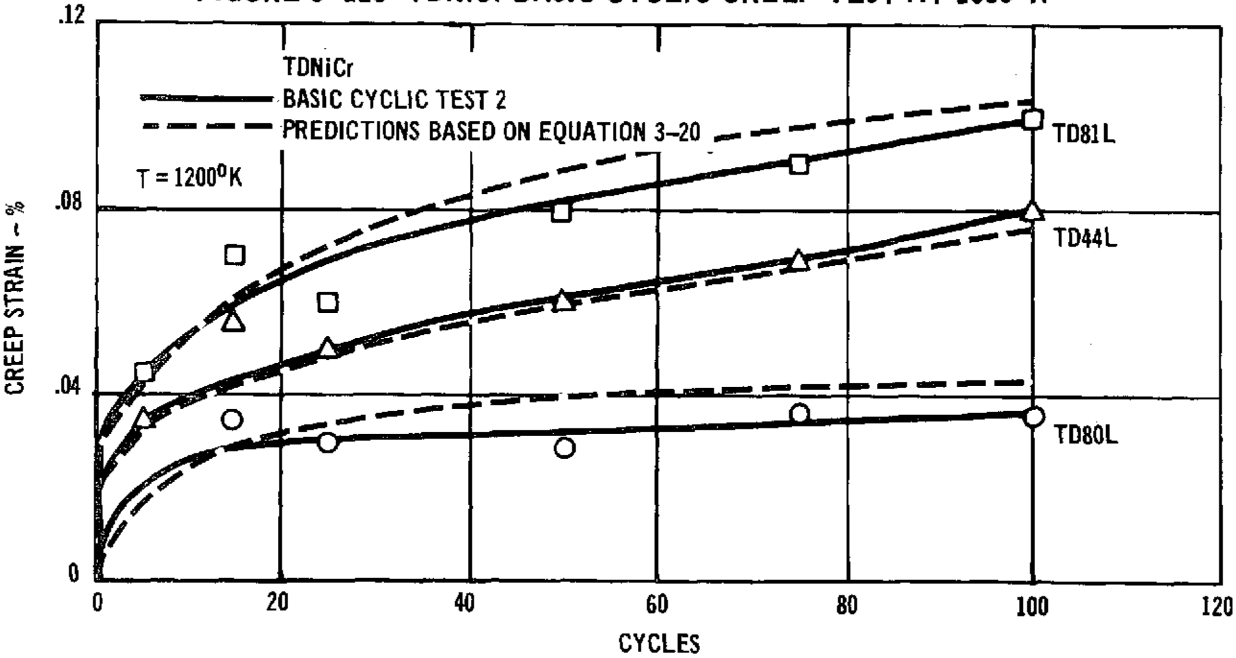

FIGURE 3-116 TNDiCr BASIC CYCLIC CREEP TEST AT 1200°K

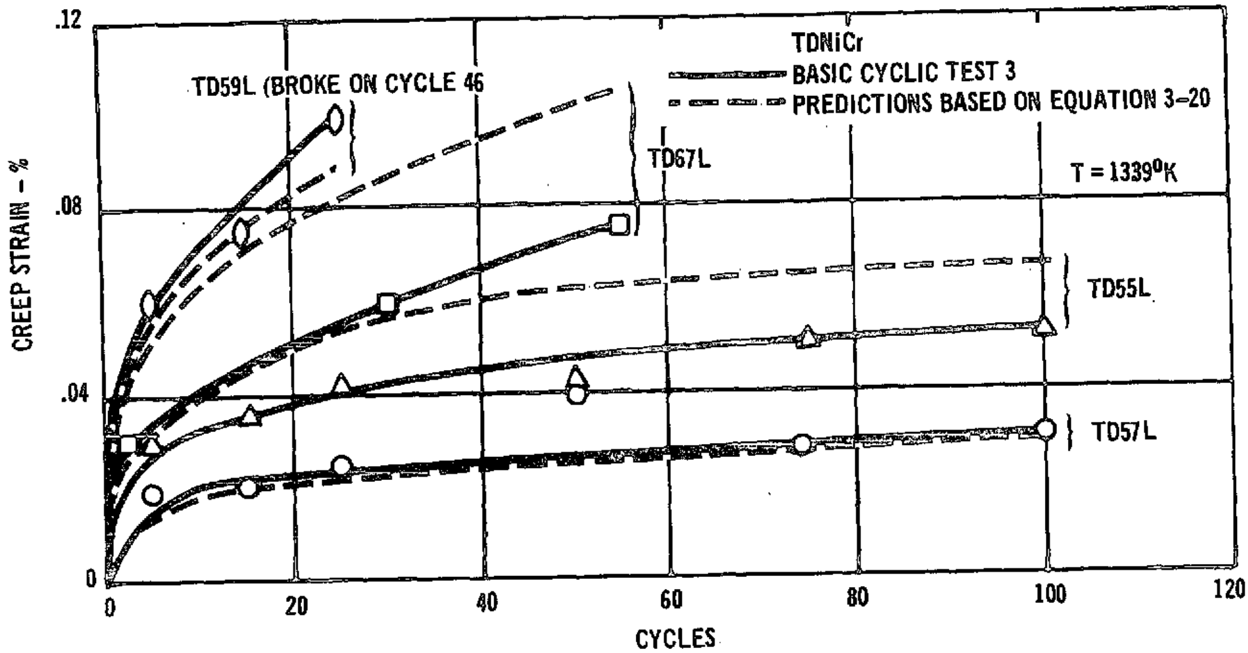

FIGURE 3-117 TDNiCr BASIC CYCLIC CREEP TEST AT 1339°K

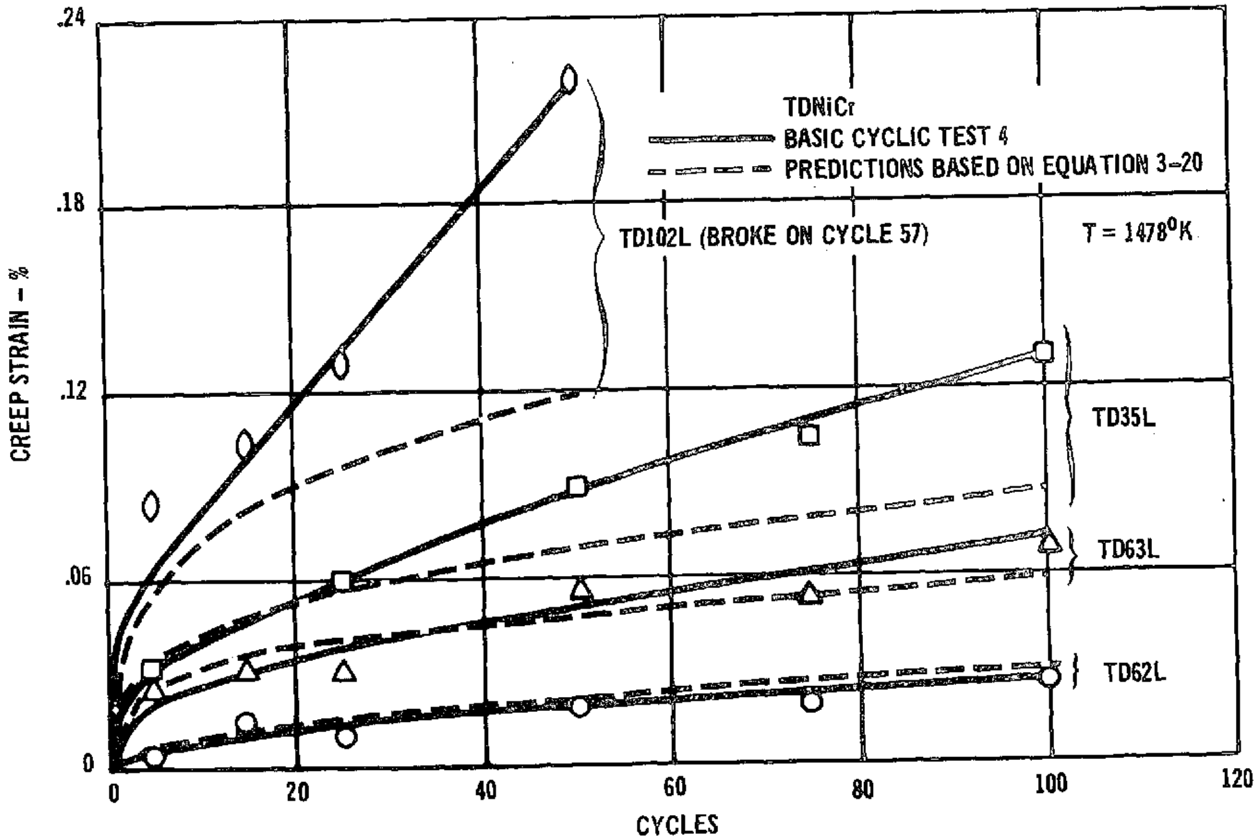

FIGURE 3-118 TDNiCr BASIC CYCLIC CREEP TEST AT 1478°K

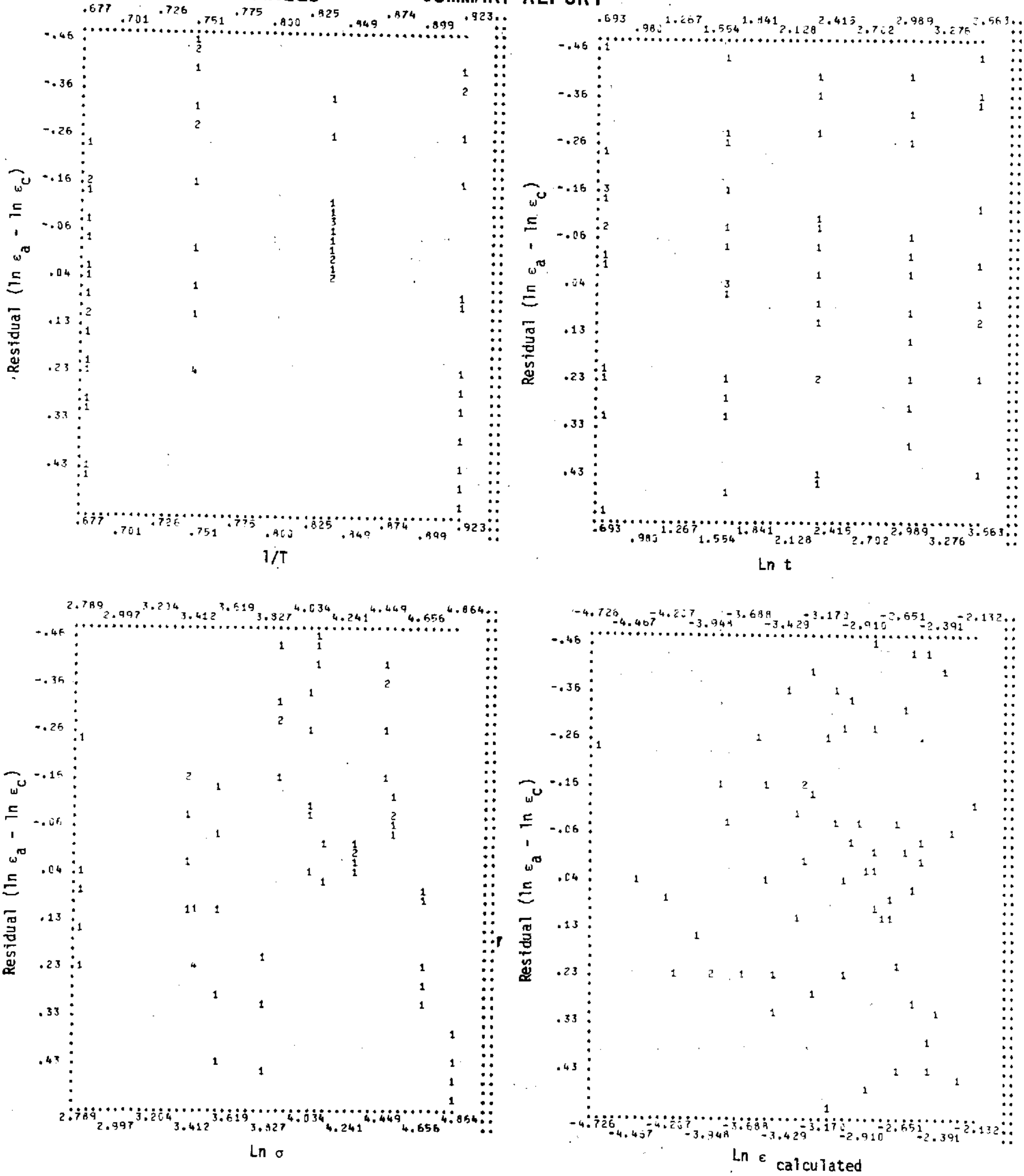

FIGURE 3-119 RESIDUAL PLOTS OF TDNiCr CYCLIC EQUATION (3-20)

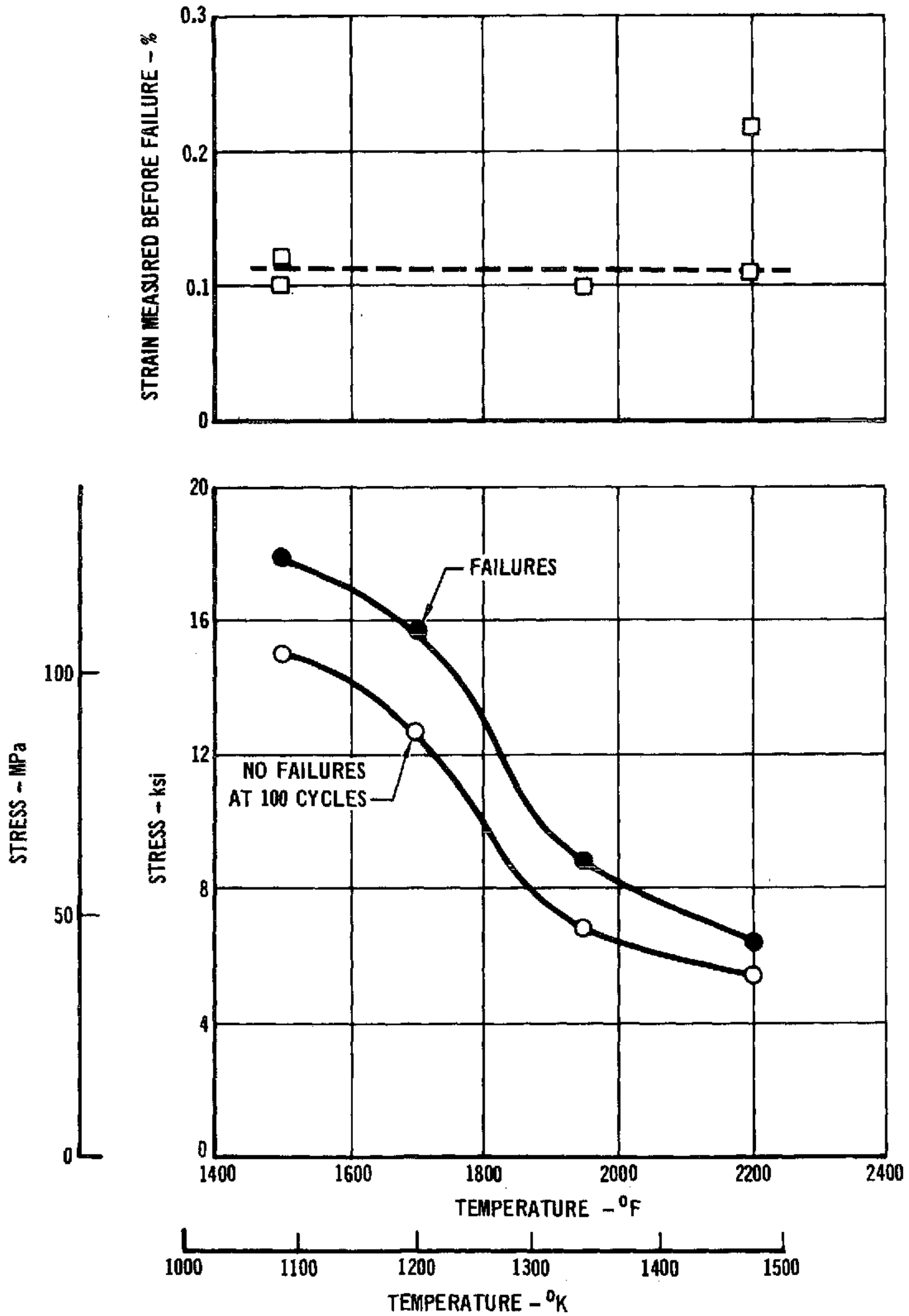

FIGURE 3–120 TDNiCr CYCLIC TEST DATA

3.4.5 COMPARISON OF CYCLIC AND STEADY-STATE DATA

3.4.5.1 Test Results. Comparison of the stress-temperature range of test data is shown in Figure 3-121 for the steady-state data base, supplemental steady-state tests, and the cyclic tests.

Comparison is made here between cyclic data and both the steady-state data base and supplemental steady-state results. Presented in Figures 3-122 and 3-123 are direct comparisons of cyclic and supplemental data, shown at 2 hours (6 cycles) and 20 hours (60 cycles) respectively. Because no clear difference between these data is indicated, the empirical equation developed for cyclic data (Equation 3-20) is considered applicable to the supplemental steady state data.

A comparison of cyclic and steady-state data base creep strains is shown in Figure 3-123. Plotted in the figure are ratios of creep strains as predicted by the literature survey steady-state creep equation (Equation 3-18) and the cyclic creep equation (Equation 3-20) for two different times. These ratios substantiate that the cyclic and supplemental steady-state test creep strains are less than those of the steady-state data base.

3.4.5.2 Microstructure Comparison. The microstructure of the TDNiCr alloy before and after creep exposure is shown in Figure 3-124. The as-received material is characterized by very large directional grains and a fine dispersion of thoria (not visible). Extensive grain boundary tearing was observed in both the cyclic and steady state creep specimens tested at 1339°K and 62.1 MPa. However, no differences between the cyclic and steady-state microstructures can be observed at 500X magnification.

3.4.6 CYCLIC TESTS FOR EVALUATION OF OTHER VARIABLES

3.4.6.1 Effect of Time Per Cycle. TDNiCr cyclic test 11 was conducted to provide data for evaluation of the effect of time per cycle on creep response. Data for

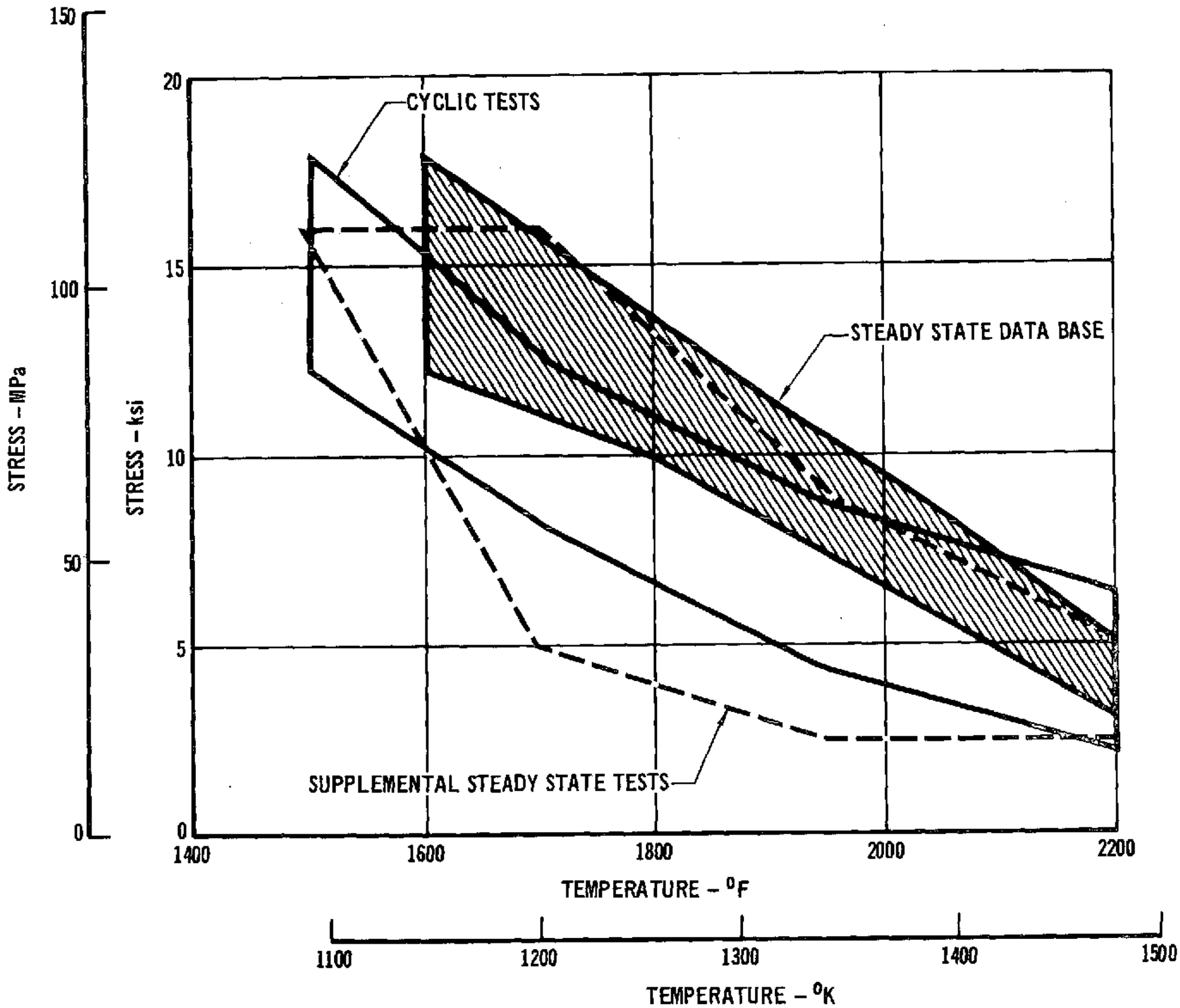

FIGURE 3–121 DATA RANGE COMPARISON – TDNiCr

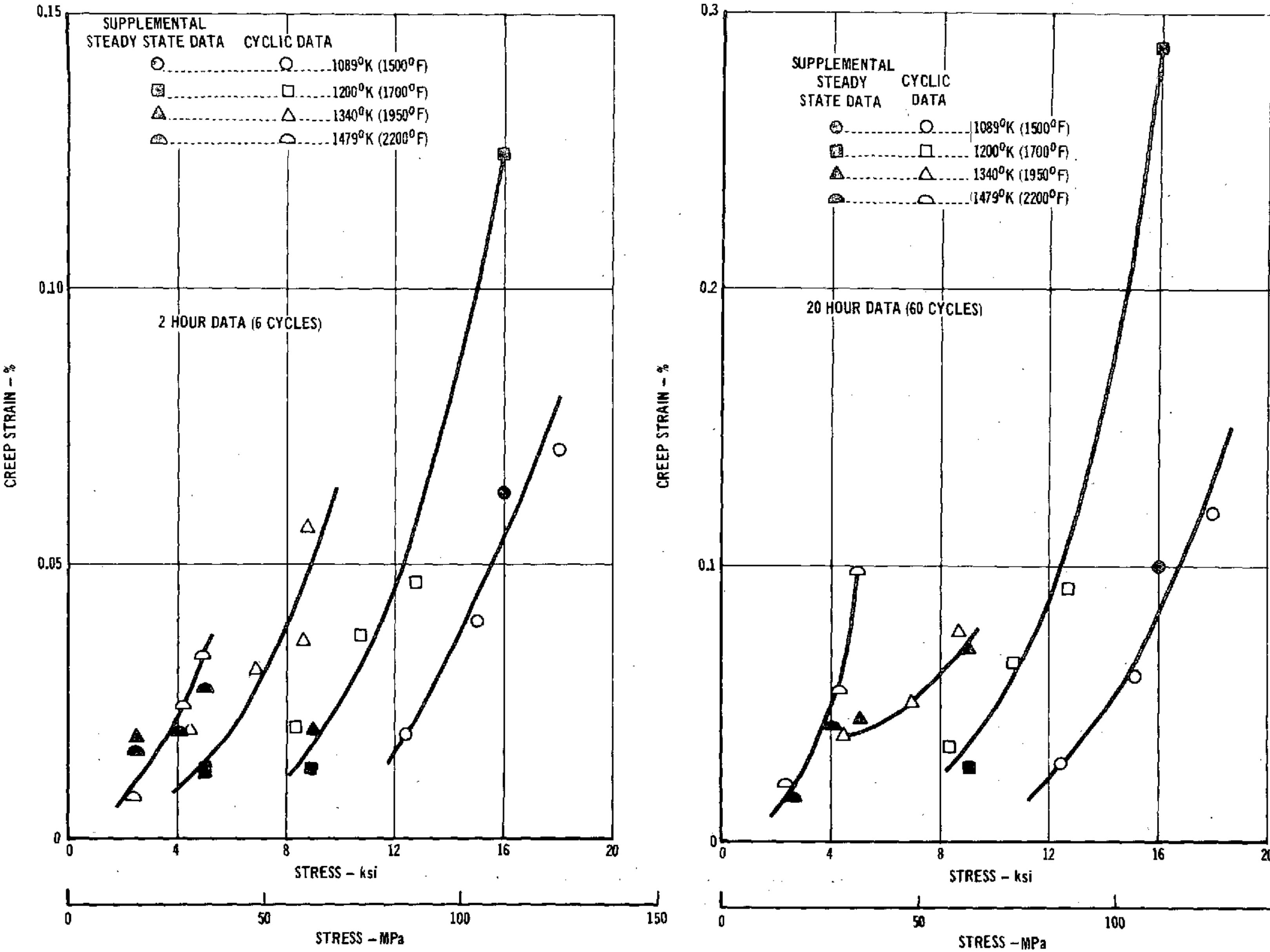

FIGURE 3–122 COMPARISON OF TD NiCR CYCLIC AND SUPPLEMENTAL STEADY-STATE DATA

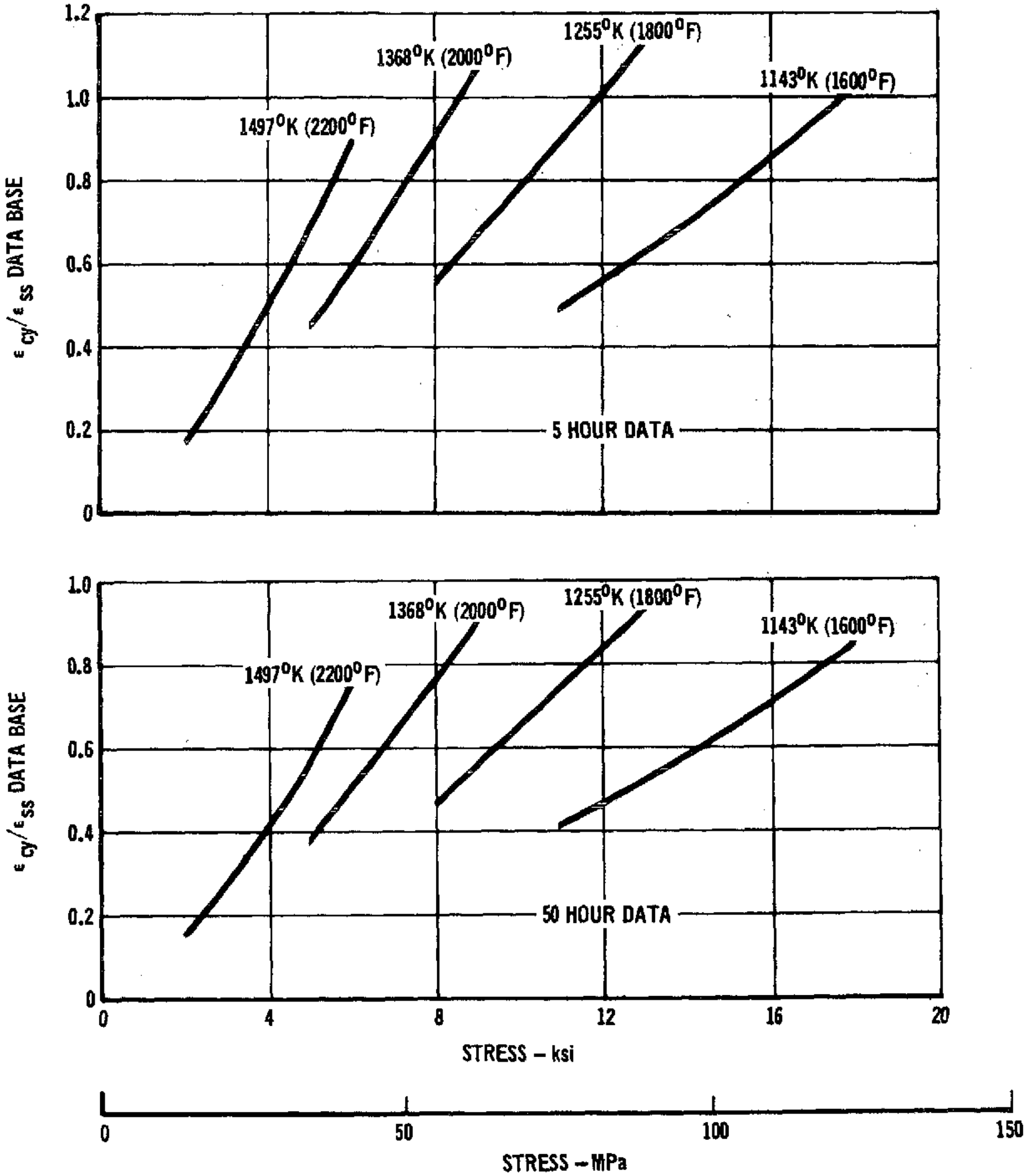

FIGURE 3-123 COMPARISON OF CALCULATED VALUES OF CYCLIC CREEP (ϵ_{CY}, EQN 3-20) AND STEADY-STATE DATA BASE CREEP (ϵ_{SS}, EQN 3-18)

ALLOY: TDNiCr
CONDITION: AS-RECEIVED
ETCHANT: 10% $(NH_4)_2S_2O_8$
MAG: 500X
THICKNESS 0.024 cm

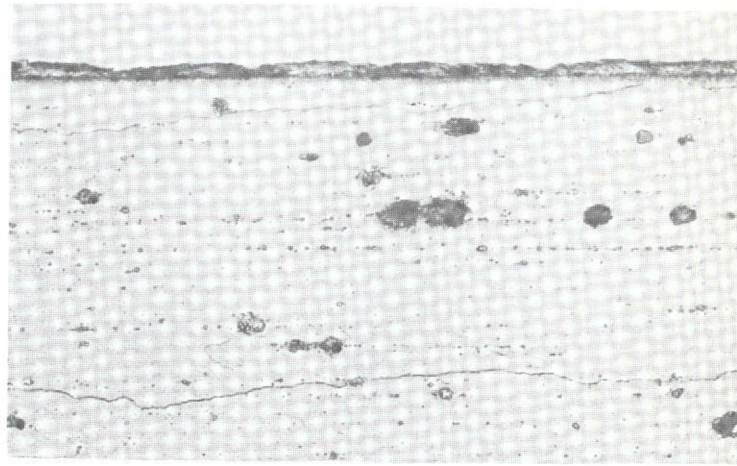

ALLOY: TDNiCr
CONDITION: TESTED (CYCLIC)
APPLIED STRESS: 60.3 MPa
TEST TEMPERATURE: 1338°K
EXPOSURE TIME: 100 CYCLES
ETCHANT: 10% $(NH_4)S_2O_8$
MAG: 500X
THICKNESS 0.026 cm

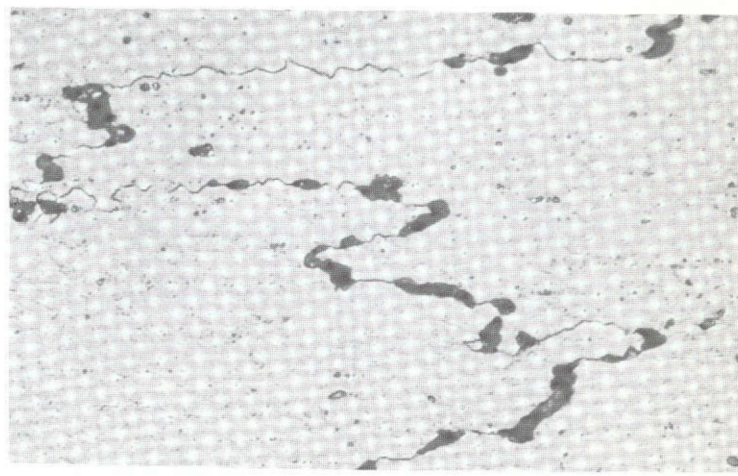

SPEC. NO. TD59L

ALLOY: TDNiCr
CONDITION: TESTED (STEADY STATE)
APPLIED STRESS: 62.1 MPa
TEST TEMPERATURE: 1338°K
EXPOSURE TIME: 100 HOURS
ETCHANT: 10% $(NH_4)S_2O_8$
MAG: 500X
THICKNESS 0.025 cm

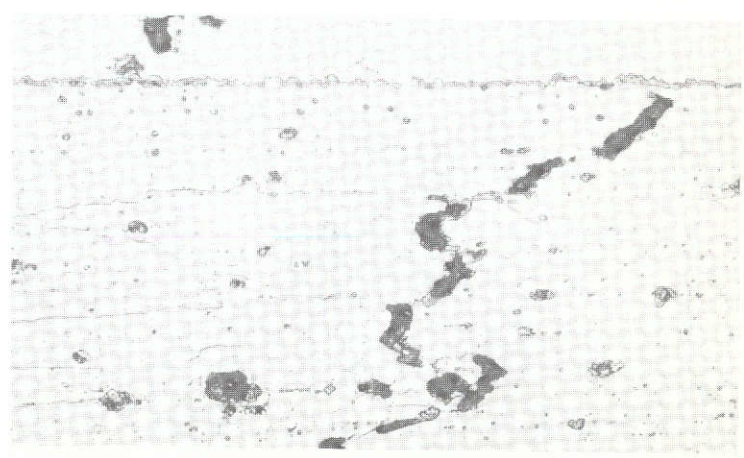

SPEC. NO. TD26L

FIGURE 3-124 MICROSTRUCTURE OF TDNiCr BEFORE AND AFTER CREEP EXPOSURE AT 1338°K

this test are presented in Appendix F-3. This test was conducted using 10 minutes per cycle at peak temperature (1532°K) and load. Comparison of results with data from basic test No. 5 (20 minutes per cycle) are shown in Figure 3-125. Because no effect of time per cycle on creep strain can be detected, it is assumed that the empirical equation developed for 20-mintes-per-cycle data (Equation 3-20) will be applicable to analysis of trajectory profiles where smaller analysis time increments are used.

3.4.6.2 <u>Effect of Atmoshperic Pressure</u>. TDNiCr cyclic test 8 and 10 are replicates, except that in test 8 the atmospheric pressure was held constant at approximately 1.33 Pa (1×10^{-2} torr), while in test 10 the atmospheric pressure was cycled to represent a simulated Shuttle profile. Data for these tests are presented in Appendix F-3. Comparison of creep strain results for corresponding specimens is shown in Figure 3-126. No significant variation can be attributed to the difference in pressure profiles.

3.4.6.3 <u>Effect of Time Between Cycles</u>. Specimens TD85L and TD77L, cycled at 1479°K in TDNiCr test 6, were retested for an additional 50 cycles in test 12. Data for this test are presented in Appendix F-3. This test was designed to determine if the creep rate is affected after specimens were allowed to relax for several weeks.

Results, shown in Figure 3-127, indicate that although some re-initiation of primary creep may have occurred, no significant strain rate changes can be detected between the completion of the 100 cycles in the basic test (test 6) and the initiation of the additional 50 cycles. Therefore, there is no clear sign that this time delay has an effect on subsequent creep strains.

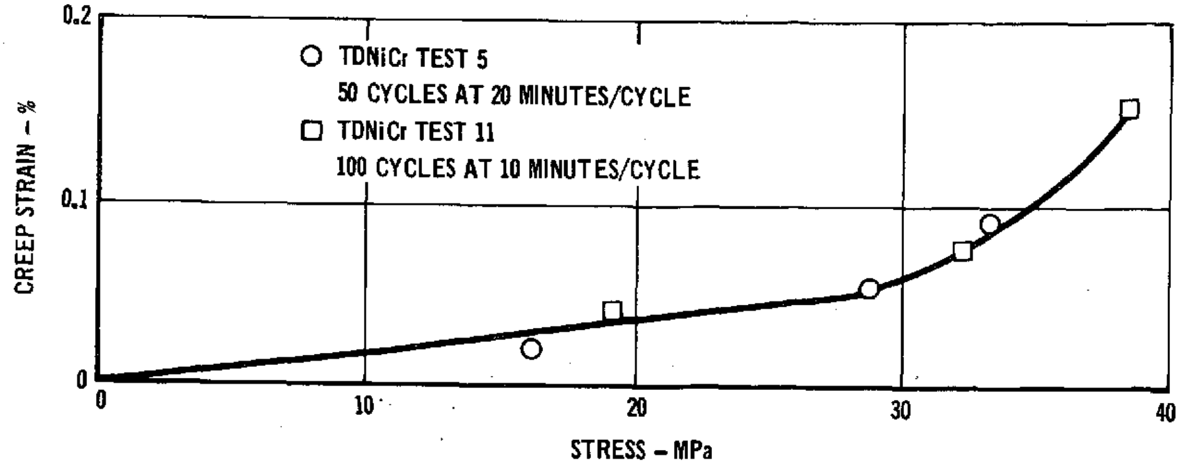

FIGURE 3–125 TDNiCr CYCLIC CREEP STRAINS AS A FUNCTION OF TOTAL TIME AT LOAD

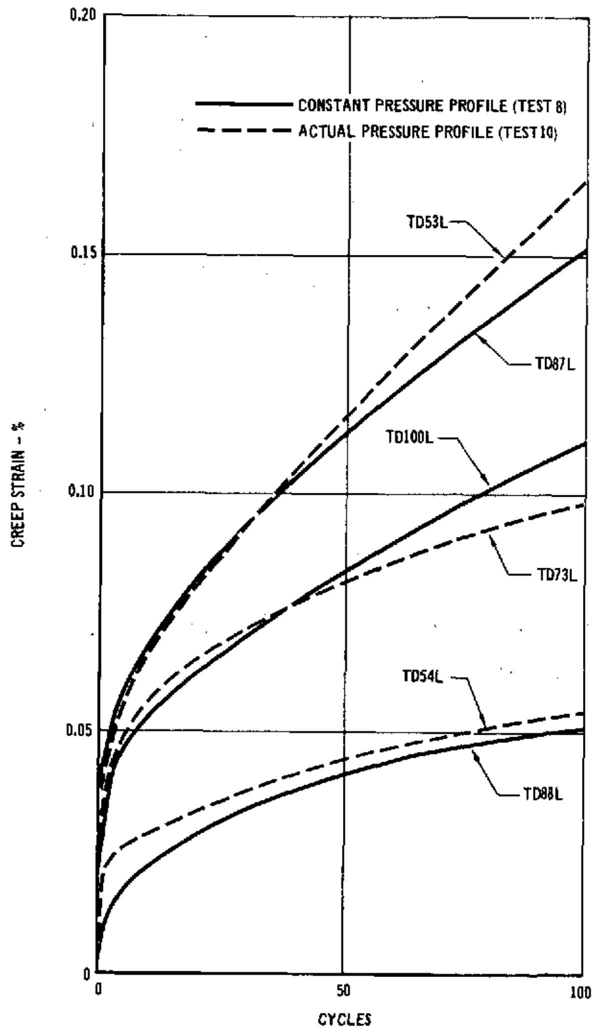

COMPARISON OF TDNiCr IDEALIZED TRAJECTORY TESTS FOR ATMOSPHERIC PRESSURE EFFECTS

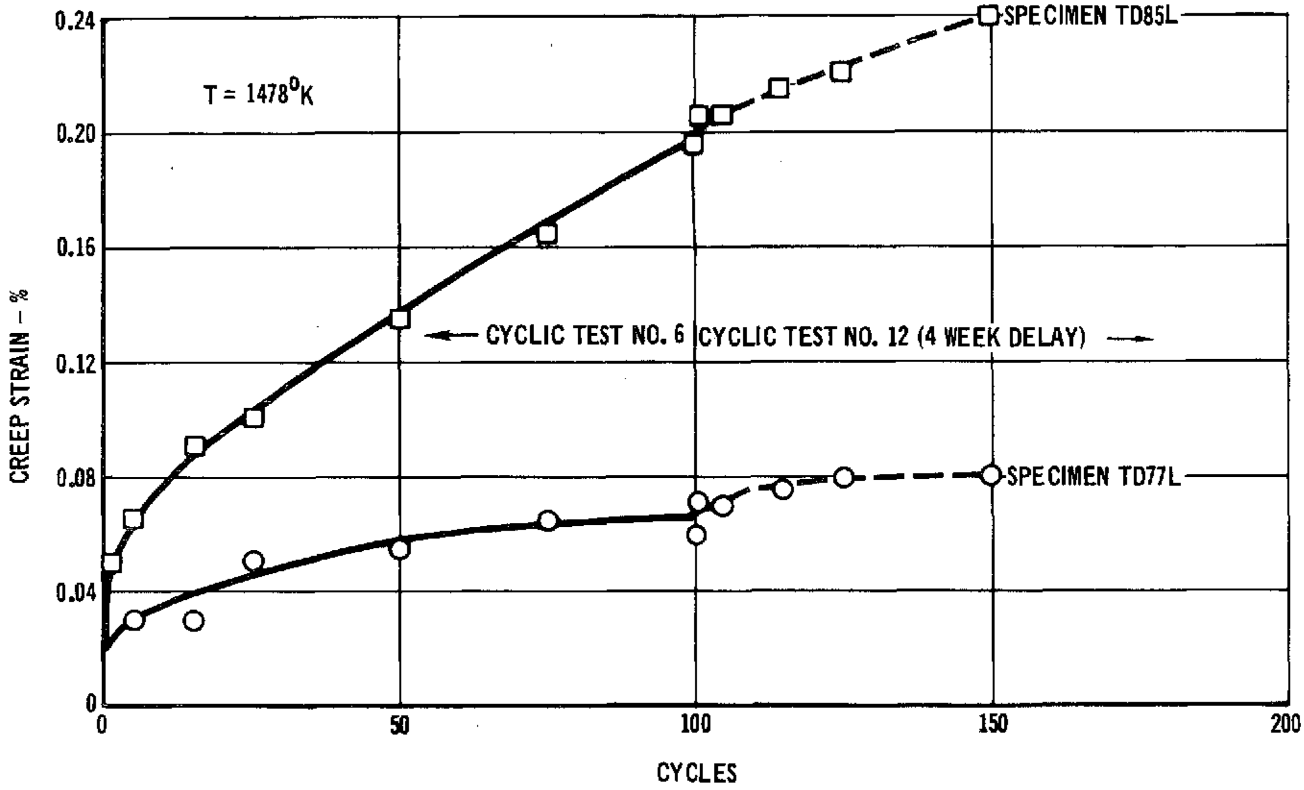

FIGURE 3–127 EFFECT OF TIME DELAY BETWEEN CYCLIC TESTS ON THE CREEP BEHAVIOR OF TD NiCr

3.4.7 COMPLEX TRAJECTORY CYCLIC TDNiCr TESTS

Four trajectory tests were conducted using TDNiCr tensile specimens. Data for these tests, designated as TDNiCr tests 7, 8, 9 and 10, are presented in Appendix F-3. These tests are: 1) a two-step stress trajectory profile with a maximum temperature of 1479°K and constant pressure (test 7); 2) two idealized trajectory tests (tests 8 and 100 with a maximum temperature of 1479°K; test 8 has a constant pressure profile and test 10 has a simulated pressure profile; 3) a simulated mission test (test 9) using representative Shuttle stress, temperature and pressure profiles. Comparison of tests 8 and 10 was made previously in Section 3.4.6.2. No stepped stress cyclic tests were conducted on TDNiCr specimens. Two comparisons of data from these tests will be investigated in this section.

The first comparison is between results of idealized trajectory tests (tests 8 and 10) and the simulated mission test (test 9). Creep strains resulting from the simulated mission test are approximately 50 to 70% of those attained in the idealized trajectory tests. This difference is attributable to the lower temperature in the simulated mission test. Although the peak temperature in test 9 was 1479°K at 800 seconds into the trajectory, temperature in the idealized trajectory tests was maintained at 1479°K over a longer period of time (Reference data in Appendix F-3).

A second comparison is between complex trajectory test results and predictions based on empirical equations (developed from tests 1-6) in conjunction with hardening theories. Predictions of creep strains for TDNiCr tests 7, 8, 9 and 10, using the cyclic creep equation (Equation 3-20), were found to be from 30% to 70% of test strains at 100 cycles. Investigation showed that this was at least partly due to prediction capability of (Equation 3-20) at 1479°K, where the complex trajectory tests had been conducted. Therefore, for purposes of evaluation of the complex trajectory tests, the following equation was developed for TDNiCr using 1479°K basic cyclic test

data (tests 5 and 6).

$$\ln \varepsilon = -11.4831 + 2.2404 \ln \sigma + .4127 \ln t \tag{3-21}$$

Comparisons of predictions using this equation in conjunction with the strain hardening theory of creep accumulation for the two-step stress profile (test 7) are shown in Figure 3-128. Predictions using the time hardening theory were approximately 90% of those using strain hardening.

Predictions using Equation 3-21 in conjunction with strain hardening are approximately 50% of values obtained in the idealized and simulated mission tests (tests 8, 9, and 10). This variation may be attributable to an effect of increasing creep response in the case where load is maintained into the portions of the trajectory profile where temperature is reduced. This effect was noted previously for Rene' 41.

3.4.8 TDNiCr CONCLUSIONS

Evaluation of TDNiCr, from the standpoint of creep deflections in TPS panels, represents a completely different case than the other three materials studied under this program. This is primarily because relatively little creep is evident in this material before failures occur. Therefore, the requirement for definition of creep deflection is minimized in the design criteria for TDNiCr TPS.

TDNiCr tensile specimens were tested at steady-state conditions over the temperature range of 1089°K (1500°F) to 1479°K (2200°F) to approximately 200 hours. Significant scatter was observed in both the literature survey data base and supplemental tests. The following empirical regression equation was developed for the data base, showing both material thickness and rolling direction to be significant variables.

$$\ln \varepsilon = -12.43906 + .01930\sigma + 2.80992T - .00022t - .38945\phi + 22.45187\phi \\ + .35175 \ln t - 1.12398 \ln\phi \tag{3-18}$$

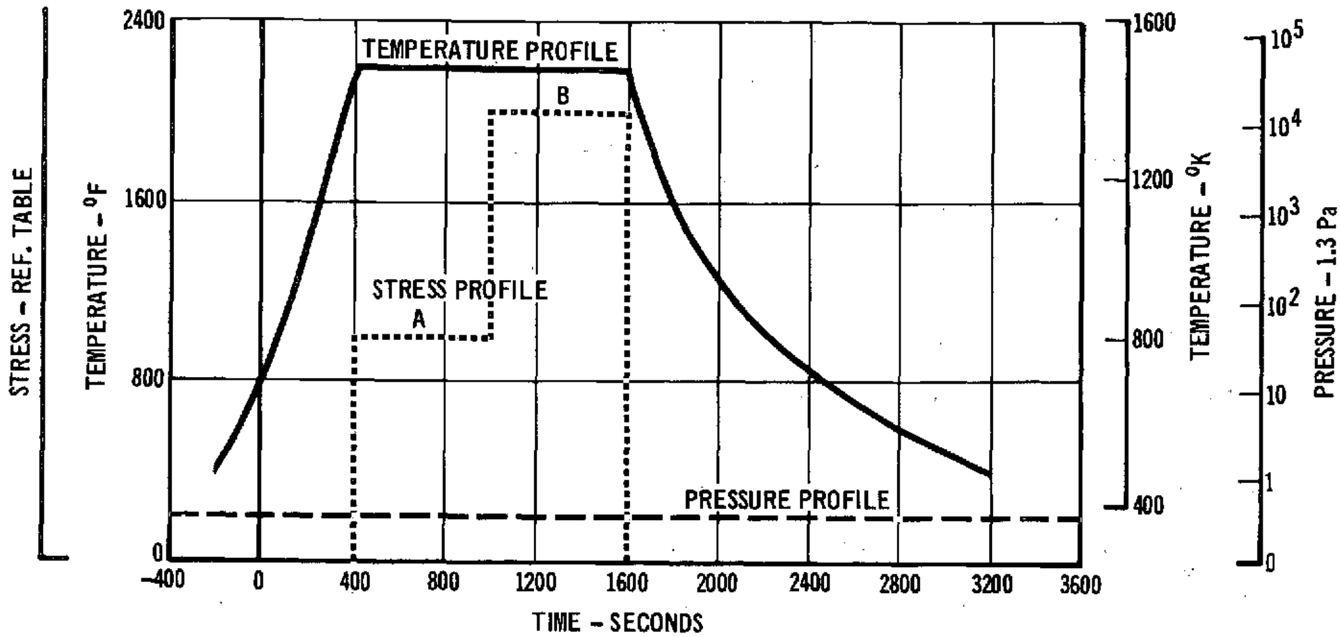

SPECIMEN	STRESS - MPa A	STRESS - MPa B
TD60L	30.0	38.3
TD61L	14.2	18.3
TD65L	25.8	33.4

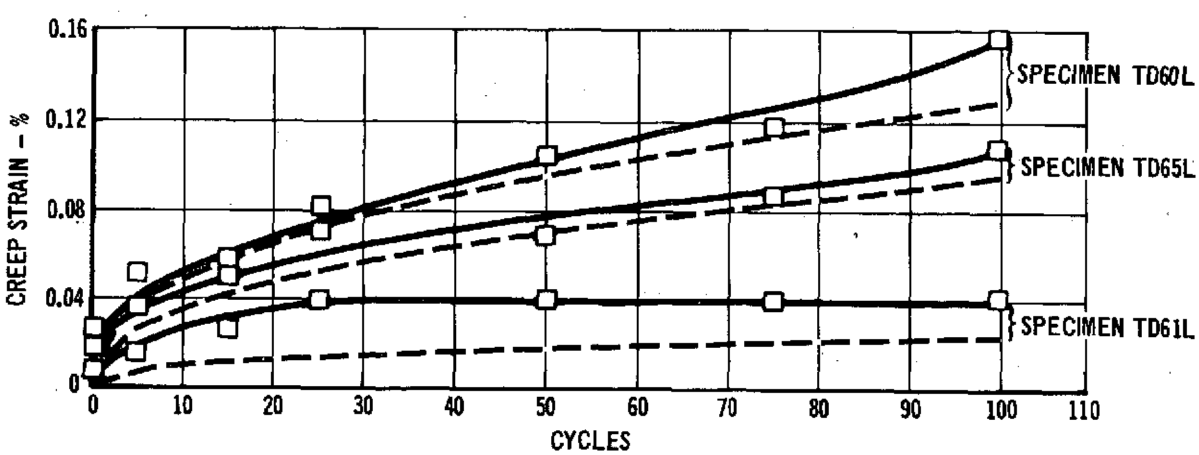

FIGURE 3-128 COMPARISON OF TEST DATA (TDNiCr TEST 7) AND PREDICTIONS (EQUATION 3-21)

Supplemental test results also showed that specimens tested in the transverse direction crept faster than those tested in the longitudinal direction and that, as is the case of Rene' 41, thinner gage crept less than the thicker material. This phenomenon for TD NiCr was observed in References 17 and 30. An extensive discussion of the possible causes of this are presented in Reference 30 but in general it appears to be a result of the variation in processing required to produce a "cubic texture" in the sheet.

The following empirical regression equation was developed for cyclic test data:

$$\ln \varepsilon = -3.48443 - 10.37282 \left(\frac{1}{T}\right) + .28314 \ln t + 2.00118 \ln\sigma \qquad (3\text{-}20)$$

This equation is applicable over the temperature range of 1089°K to 1479°K for times up to 33 hours (100 cycles at 20 minutes per cycle). No significant difference could be determined between supplemental steady-state test data and cyclic data sets.

Stress rupture failures were obtained at creep strains of approximately .11% throughout the cyclic test temperature range. No effect of time per cycle (for the same total time) or atmospheric pressure could be determined in cyclic testing.

Predictions were approximately 50% of trajectory cyclic creep test data. The strain hardening theory of creep accumulation provided the best predictions with time hardening theory yielding even lower values. This relationship between predictions and test strains is the same as obtained for Rene' 41.

Atmospheric pressure and time between cycling do not appear to have a significant effect on cyclic creep.

4.0 CONCLUSIONS

In this phase of the program test results have demonstrated that there is no significant difference between cyclic and steady-state creep strains (for the same total time at load) for the alloys L605, Ti-6Al-4V, Rene' 41, and TDNiCr. A single linear equation describing the combined steady-state and cyclic creep data, for each alloy, resulted in standard errors of estimate higher than obtained for the invividual data sets. Creep strain equations were developed for both steady-state and cyclic creep data using linear least squares analysis techniques. A non-linear least squares analysis appeared to offer potential for lowering the standard error of estimate but time prevented further exploration in this area. (See Appendix G-3.)

The prediction of strains that are produced by complex trajectory and simulated mission tests (using equations based on simple cycles) was successfully accomplished. A computer program was specifically written for this analysis. This computer program is based on time and strain hardening theories of creep accumulation. For Ti-6Al-4V, and TDNiCr, the strain hardening theory of creep accumulation provided the best predictions while for Rene' 41 time hardening and for L605 a combination of strain and time hardening provided the best predictions.

In general, for the four alloys studied, no effects on creep strain due to variation of time per cycle (for the same total time) or atmospheric pressure were observed. A gage effect on creep response was noted in both the literature survey and the supplemental steady-state creep data bases for L605, Rene' 41, and TDNiCr. For L605 the thin gage material crept faster than the thicker while in the case of Rene' 41 and TDNiCr the reverse was true. An effect of material rolling direction on creep strains was observed in TDNiCr.

Significant data scatter was found to exist for both the literature survey and supplemental steady-state creep data bases of TDNiCr. For TDNiCr stress-rupture failures were obtained at creep strains of approximately .11% throughout the cyclic test temperature range.

Comparison of data obtained from idealized and simulated mission tests indicates that cyclic creep response analyses can be performed through the use of the simpler idealized approach.

Specific conclusions as they relate to the individual alloys are presented in the specific alloy sections of this report.

5.0 REFERENCES

1. Space Shuttle Program Phase B Studies NAS-8-26016
2. Anon, "Supplementary Structural Test Plan (SSTP) Large Panel Tests", McDonnell Douglas Report MDC-E0562.
3. Harris, H. G., and Morman, K. N., "Creep of Metallic Thermal Protection Systems," NASA-TMX-2273, Presented at NASA Space Shuttle Technology Conference, NASA-Langley Research Center, March 2-4, 1971.
4. Davis, J. W., "Synergism of Stress and Temperature on the Cyclic Creep Behavior of Superalloys", Presented at NASA Mini Symposium on Creep of Materials for Space Shuttle TPS, Langley Research Center, December 1971.
5. Ecord, G. M., "Static and Cyclic Creep Exposure Test Results for 6Al-4V (STA) Titanium Alloy and 2219-T87 Aluminum", Presented at NASA Mini Symposium on Creep of Materials for Space Shuttle TPS, Langley Research Center, December 1971.
6. Black, W. E., "Coated Columbium Alloy Heat Shield Evaluation for Space Shuttle Application", Monthly Progress Report 14. NASA Contract NAS-1-9793, General Dynamics Convair Aerospace Division.
7. Anon, "Space Shuttle Data", Materials and Processes, McDonnell Douglas Report MDC-E0386, 30 June 1971.
8. Hughes, W. P., et. al., "A Study of the Strain-Age Crack Sensitivity of Rene' 41", AFML-TR-66-324, 1966.
9. Private Communications with General Electric Company.
10. Klingler, L. J., et. al., "Development of Dispersion Strengthened Nickel-Chromium Alloy (Ni-Cr-ThO_2) Sheet For Space Shuttle Vehicles", NASA-CR-120796, NASA Lewis Research Center.
11. Johnson, R. E., and Killpatrick, "Evaluation of Dispersion Strengthened Nickel-Base Alloy Heat Shields for Space Shuttle Application" NASA CR-132360, NASA Langley Research Center.

5.0 REFERENCES (Continued)

12. Anon, "Compilation of Tensile and Creep Rupture Data of Several Al, Mg, Ti, and Steel Alloys, AFML-TR-67-259, April 1968.

13. Data Obtained From General Electric.

14. Data from McDonnell Douglas Studies.

15. Green, A., et. al, Research Investigation to Determine Mechanical Properties of Nickel and Cobalt Base Alloys For Inclusion in Military Handbook-5, Volume II, AFML-TDR-116-Volume II, October 1964.

16. Data Generated for NASA Marshall Space Flight Center, by Vulcan Testing Laboratory under NASA Contract NAS 8-27189, 1971.

17. Data Generated for NASA Lewis Research Center by Metcut Research Associates under NASA Contract NAS 3-15558, Report CR- 121221.

18. Private Communications with General Electric Company, dated 15 September 1972. File Number 4662.

19. Private Communications with General Electric Company, dated 18 October 1972. File Number 5132.

20. Killpatrick, D. H., and Hocker, R. G.; Stress-Rupture and Creep in Dispersion Strengthened Nickel-Chromium Alloys. McDonnell Douglas Corporation Report Number DAC-62124, dated May 1968.

21. McDonnell Douglas Astronautics Corporation - West, in-house testing, 1971.

22. Durelli, A. J. and Sciammarella, C. A., "Elastoplastic Stress and Strain Distribution on a Finite Plate with a Circular Hole Subjected to a Uni-dimensional Load," Journal of Applied Mechanics, March 1963.

23. Lynch, J. H., "A Systematic Approach to Model Development by Comparison of Experimental and Analytical Regression Coefficients," NASA-TMX-1797, Lewis Research Center, 1969.

24. Davies, O. L., The Design and Analysis of Industrial Experiments, Second Edition, Hafner Publishing Company, 1956.

5.0 REFERENCES (Continued)

25. Dixon, W. J., "Biomedical Computer Programs (BMD)," Automatic Computation No. 2, University of California.

26. Dorn, J.E., Mechanical Behavior of Materials at Elevated Temperature, McGraw Hill Book Company, 1961, pages 79 - 93 and 455 - 457.

27. Draper, N. R., and Smith, H., Applied Regression Analysis, John Wiley pages 27, 77 - 105, and 134 - 142.

28. Garafalo, F., Fundamentals of Creep and Creep-Rupture in Metals, MacMillan Company, 1965, page 16.

29. Private Communications with R. B. Herchenroeder, Cabot Corporation.

30. Discussions with D. H. Killpatrick, MDAC-W, based on his work on "The Effect of Texture on the Elevated Temperature Mechanical Properties of Dispersion Strengthened Nickel-20 Chromium Alloys," McDonnell Douglas Corporation Report Number DAC-62153, dated February 1970.

APPENDIX A

CONVERSION OF U.S. CUSTOMARY UNITS TO SI UNITS

The International System of Units (designated SI) was adopted by the Eleventh General Conference on Weights and Measures in 1960. The units and conversion factors used in this report are taken from or based on NASA SP-7012, "The International System of Units, Physical Constants and Conversion Factors - Revised, 1969".

The following table expresses the definitions of miscellaneous units of measure as exact numerical multiples of coherent SI units, and provides multiplying factors for converting numbers and miscellaneous units to corresponding new numbers of SI units.

The first two digits of each numerical entry represent a power of 10. An asterisk follows each number that expresses an exact definition. For example, the entry "-02 2.54*" expresses the fact that 1 inch = 2.54 x 10^{-2} meter, exactly, by definition. Most of the definitions are extracted from National Bureau of Standards documents. Numbers not followed by an asterisk are only approximate representations of definitions, or are the results of physical measurements.

ALPHABETICAL LISTING

To convert from	to	multiply by
atmosphere (atm)	pascal (Pa)	+05 1.0133*
Fahrenheit (F)	kelvin (K)	$t_k = (5/9)(t_f + 459.67)$
foot (ft)	meter (m)	-01 3.048*
inch (in.)	meter (m)	-02 2.54*
mil	meter (m)	-05 2.54*
millimeter of mercury (mm Hg)	pascal (Pa)	+02 1.333
nautical mile, U.S. (n.mi.)	meter (m)	+03 1.852*
pound force (lb_f)	newton (N)	+00 4.448*
pound mass (lb_m)	kilogram (kg)	-01 4.536*
torr (0°C)	pascal (Pa)	+02 1.333

APPENDIX A - Continued

PHYSICAL QUANTITY LISTING

Area

To convert from	to	multiply by	
foot^2 (ft^2)	meter^2 (m^2)	-02	9.290*
inch^2 (in^2)	meter^2 (m^2)	-04	6.452*
inch^2 (in^2)	cemtimeter^2 (cm^2)	+00	6.452

Density

pound mass/foot^3 (pcf, lb_m/ft^3)	kilogram/meter^3 (kg/m^3)	+01	1.602
pound mass/inch^3 (lb_m/in^3)	kilogram/meter^3 (kg/m^3)	+04	2.768
pound mass/inch^3 (lb_m/in^3)	gram/centimeter^3 (g/cm^3)	+01	2.768

Force

kilogram force (kg_f)	newton (N)	+00	9.807*
pound force (lb_f)	newton (N)	+00	4.448*

Length

foot (ft)	meter (m)	-01	3.048*
inch (in.)	meter (m)	-02	2.54*
micron	meter (m)	-06	1.00*
mil	meter (m)	-05	2.54*
mile, U.S. nautical (n.mi.)	meter (m)	+03	1.852*

Mass

pound mass (lb_m)	kilogram (kg)	-01	4.536*

Pressure

atmosphere (atm)	pascal (Pa)	+05	1.013*
millimeter of mercury (mm Hg)	pascal (Pa)	+02	1.333
newton/meter	pascal (Pa)	00	1.00*
pound/foot^2 (psf, lb_f/ft^2)	pascal (Pa)	+01	4.788
pound/inch^2 (psi, lb_f/in^2)	pascal (Pa)	+03	6.895

Temperature

Fahrenheit (F)	Kelvin (K)	$t_k = (5/9)(t_f + 459.67)$

APPENDIX A - Continued

Volume

To convert from	to	multiply by	
foot^3 (ft^3)	meter^3 (m^3)	-02	2.832*
inch^3 (in^3)	meter^3 (m^3)	-05	1.639*
inch^3 (in^3)	centimeter^3 (cm^3, cc)	-01	1.639

PREFIXES

The names of multiples and submultiples of SI units may be formed by application of the prefixes:

Multiple	Prefix
10^{-6}	micro (μ)
10^{-3}	milli (m)
10^{-2}	centi (c)
10^{-1}	deci (d)
10^{3}	kilo (k)
10^{6}	mega (M)
10^{9}	giga (G)

APPENDIX B

BIBLIOGRAPHY ON CREEP IN METALS

1. Aaenes, M. N., and Tuttle, M. M.; "Presentation of Creep Data for Design Purposes," Aeronautical Systems Division Report ASD-TR-61-216, June 1961.

2. Alesch, C. W., "Onset of Creep Stress Measurement of Metallic Materials", NASA Report NASA-CR-91119, November 1967.

3. Anon, "Compilation of Tensile and Creep Rupture Data of Several Al, Mg, Ti, and Steel Alloys", AFML-TR-67-259, April 1968.

4. Anon, "Creep Behavior and Subsequent Room Temperauree Tensile Properties of Two Titanium Sheet Alloys (6Al-4V and 4Al-3Mo-1V) and One Titanium Bar Alloy (7Al-4Mo) in the Heat Treated Condition", Rockwell International, North American Aviation Division Report TFD-60-473, July 1960.

5. Anon, "Determination of Design Data for Heat Treated Titanium Alloy Sheet Vol. 3, Tables of Data Collected". Aeronautical Systems Division Report ASD-TDR-62-335, Vol. 3, December 1962.

6. Anon., "Investigation of Thermal Effects on Structural Fatigue," Aeronautical Systems Division, USAF, Report WADD-TR-60-410, Part II, August 1961.

7. Baucom, R. M., "Strain-Rate Sensitivity of Three Titanium Alloy Sheet Materials After Prolonged Exposure at 550°F (561°K)," Langley Research Center Report NASA-TN-D-4981, January 1969.

8. Blatherwick, A. A., and Cers, A. E., "Fatigue, Creep, and Stress-Rupture Properties of Several Superalloys, Air Force Materials Lab Report AFML-TR-69-12, January 1969.

9. Brackett, R. M., and Gottbrath, J. A.; "Development of Engineering Data on Titanium Extrusion for Use in Aerospace Design," Air Force Materials Lab. Report AFML-TR-67-189, July 1967.

10. Carew, W. F., "Engineering Effort to Obtain Long Time Creep Data on Structural Sheet Materials," Air Force Materials Lab Report AFML-TR-65-18,

11. Conrad, H., and White, J., "Correlation and Interpretation of High-Temperature Mechanical Properties of Certain Superalloys," Space Systems Division of U.S. Air Force Report SSD-TDR-63-26, March 1963.

12. Deel, O. L., and Mindlin, H.; "Engineering Data on New Aerospace Structural Materials; Air Force Materials Lab. Report AFML-TR-71-249, December 1971.

13. Deel, O. L., and Mindlin, H.; "Engineering Data on New and Emerging Structural Materials," Air Force Materials Lab. Report AFML-TR-70-252, October 1970.

14. Deel, O. L., and Hyler, W. S., "Engineering Data on Newly Developed Structural Materials," Air Force Materials Lab Report AFML-TR-67-418, April 1967.

15. Del Rio, J. A.,"Creep Testing of Ti-6Al-4V at 600°F", McDonnell Douglas Astronautics Company - Western Division Report MP51,364, January 1969.

16. Fritz, L. J., Laster, W. P., and Taylor, R. E.; Characterization of the Mechanical and Physical Properties of TD-NiCr (Ni-20Cr-2ThO_2) Alloy Sheet", Metcut Research Associates Report NASA-CR-121221, 1973.

17. Gerdeman, D. A., "The Evaluation of Materials for Aerospace Systems", Air Force Materials Lab. Report AFML-TR-69-178, June 1969.

18. Gluck, J. V., and Freeman, "Effect of Creep-Exposure on Mechanical Properties of Rene' 41", Aeronautical Systems Division of USAF Report ASD-TR-61-73.

19. Green, A., et.al, "Research Investigation to Determine Mechanical Properties of Nickel and Cobalt Base Alloys for Inclusion in Military Handbook-5", Volume II, AFML-TDR-116-Volume II, October 1964.

20. Grimm, E. E., "Long Time Elevated Temperature Exposure on Candidate Materials for the Supersonic Transport, Effects of", Douglas Aircraft Company Report DACO-LB-31587, November 1964.

21. Gearsman, R. D., "Nuclear Ramjet Propulsion System Applied Research and Advanced Technology (Project Pluto), Volume VI Structural Materials Investigation", Aeronautical Systems Division Report ASD-TDR-63-277, Volume VI, February 1963.

22. Halford, G. R., "Cyclic Creep Rupture Behavior of Three High Temperature Alloys", NASA-TN-D-6309, May 1971.

23. Herfert, R. E., "Metallurgical Study of Criteria Used To Achieve Compression Of Elevated Temperature Test Time", Air Force Materials Lab Report AFML-TR-70-57, June 1970.

24. Hirschberg, M. H., et. el., "Cyclic Creep and Fatigue of TD-Ni-Cr (Thoria-Dispersion-Strengthened Nickel-Chromium), TD-Ni, and NiCr Sheet at 1200°C", NASA, Lewis Research Center Report NASA TND-6649, February 1972.

25. Johnson, R., and Killpatrick, D. H.; "Dispersion-Strengthened Metal Structural Development", McDonnell Douglas Astronautics Company-West Report AFFDL-TR-68-130, July 1968.

26. Kattus, J. R., "Tensile and Creep Properties of Structural Alloys Under Conditions of Rapid Heating, Rapid Loading and Short Times At Temperature, Southern Research Institute Report 3962-867-2-1, April 1959.

27. Kay, R. C., "Tensile and Creep Properties of 0.010 And 0.050 Inch Rene' 41 Alloy Sheet From Room Temperature to 2000°F", Marquardt Report PR-281-1Q-1, September 1962.

28. Kiefer, T. F., and Schwartzberg, F. R., "Investigation of Low-Temperature Creep in Two Titanium Alloys", Martin-Marietta Corporation Report NASA-CR-92418, June 1967.

29. Killpatrick, D. H., and Hocker, R. G., "Stress Rupture and Creep in Dispersion Strengthened Nickel Chromium Alloys", McDonnell Douglas Corporation Report Number DAC-22124, dated May 1968.

30. King, E. J., "Short Time Tensile and Creep Properties of Commercially Pure Titanium Alloys", Bell Aerosystems Company Report BLR 62-24, December 1962.

31. Kramer, I. R., and Kumar, A., "Study of The Influence of Solid Films And Surface Layer On The Creep Behavior of Titanium", Naval Air Systems Command Report MCR-70-349, Sept. 1970.

32. Leggett, H., et. al., "Mechanical and Physical Properties of Super Alloy And Coated Refractory Alloy Foils", Air Force Materials Lab. Report AFML-TR-65-147.

33. Lloyd, R. D., and Dioguardo, P., "Investigation of the Effects of Rapid Loading and Elevated Temperature On The Mechanical Properties of Compressive And Column Members", Aeronautical Systems Division of USAF Report ASD-TR-61-499.

34. Malik, R. K., and Stetson, A. R., "Evaluation of Superalloys for Hypersonic Vehicle Heat Shields", Solar Division of International Harvester Company Report AFML-TR-68-292, Oct. 1968.

35. McBride, et. al., "Creep-Rupture Properties of Six Elevated Temperature Alloys" North East Materials Lab Report WADD-TR-61-199, August 1962.

36. Moon, D. P., Simon, R. C., and Faver, R. J., "The Elevated-Temperature Properties of Selected Superalloys", American Society for Testing and Materials Data Series DS-7-S1, 1968.

37. Popp, H. G., "Materials Property Data Compilation – L605 and Waspalloy", General Electric Company Report AD 288-267, November 1962.

38. Popp, H. G., "Titanium (Castings, Forgings and Sheet), (Ti-6Al-2.5Sn, Ti-6Al-4V, Ti-7Al-4Mo)" General Electric Report AD 296-143, February 1963.

39. Price, H. L., and Heimerl, G. J., "Tensile and Compressive Creep of 6Al-4V Titanium Alloy Sheet and Methods for Estimating The Minimum Creep Rate", Langley Research Center Report NASA-TN-D-805.

40. Reimann, W. H., "Room Temperature Creep in Ti-6Al-4V", Air Force Materials Lab. Report AFNL-TR-68-171, June 1968.

41. Sauvageat, A. B., "Development of A Titanium Alloy Foil and Sheet Rolling Process", Air Force Materials Lab. Report AFML-TR-67-386, December 1967.

42. Schwartz, D. B., "Hypersonic Aerospace-Vehicle Structures Program, Vol. I., General Structural Analyses Formulations", Martin-Marietta Report AFFDL-TR-68-129, Vol. I, August 1968.

43. Schwartzberg, F. R., et. al., "The Properties of Titanium Alloys at Elevated Temperature", Battelle Memorial Institute Report TML-82, Sept. 1957.

44. Swindeman, R. W., "Some Creep-Rupture Data for Newer Heats of Haynes Alloy No. 25 (L605)", Oak Ridge National Laboratory Report ORNL-TM-3028, Aug. 1970.

45. Thompson, O. N., and Jones, R. L., "Intermittent Creep and Stability of Materials for SST Applications", Air Force Materials Lab Report AFML-TR-66-407, January 1967.

46. White, D. L., and Watson, H. T., "Determination of Design Data for Heat Treated Titanium Alloy Sheet. Volume 2B, Test Techniques and Results for Creep and Fatigue". Aeronautical Systems Division Report ASD-TDR-62-335, Vol. 2B, December 1962.

47. Widmer, R., et el, "Mechanisms Associated with Long Time Creep Phenomena", New England Materials Laboratory Report AFML-TR-65-181, June 1965.

48. Wilcox, B. A., and Clauer, A. H., "High Temperature Deformation of Dispersion Strengthened Nickel Alloys", Part I - "The Influence of Initial Structure on Tensile and Creep Deformation of T.D. Nickel", Part II - "The Effect of Matrix Stacking Fault Energy on Creep of Ni-Cr-ThO_2 Alloys", Lewis Research Center Report NASA-CR-72367, February 1968.

49. Wood, R. A., "Aircraft Designers Handbook for Titanium and Titanium Alloys, Air Force Materials Lab. Report AFML-TR-67-142, March 1967.

50. Wurst, J. C., et. al., "The Evaluation of Materials for Aerospace Applications", Air Force Materials Lab. Report AFML-TR-67-165, June 1967.

APPENDIX C-1

L605 LITERATURE SURVEY CREEP DATA

This portion of Appendix C presents the literature survey data base. Portions of this data base were used to develop the literature survey equation (3-3). The source of this data is the Air Force Materials Laboratory report AFML-TDR64-116 (Reference 15).

All strains shown are total plastic strains. For informational purposes the elastic strains are presented below for the individual tests in order of their apperance in this section.

TEST #	TEMPERATURE °k	STRESS MPa	THICKNESS cm	ELASTIC STRAIN, %
1				
2	922	172.4	.013	.137
3		224.1		.177
4		275.8		.146
5		310.3		.813
6		172.4	.102	.087
7		189.6		.159
8		189.6		.111
9		224.1		.191
10		293.0		.212
11	1033	65.5	.013	.059
12		75.8		.131
13		96.5		.007
14		120.7		.074
15		224.1		.229
16		165.5	.051	.091
17		144.8		.066
18		75.8	.102	.048
19		86.2		.075
20		100.0		.074
21		103.4		.069
22		103.4		.071
23		165.5		.103
24		68.9	.203	.036
25		86.2		.053
26		137.9		.084
27		189.6		.163
28	1144	27.6	.013	.008
29		27.6		.020
30		62.1		.065
31		68.9		.132
32		22.8	.102	.019
33		41.4		.037
34		48.3		.019
35		55.2		.034
36		62.1		.056

TEST #	TEMPERATURE °k	STRESS MPa	THICKNESS cm	ELASTIC STRAIN, %
37		65.5		.057
38		120.7		.084
39		27.6	.203	.016
40	1255	10.3	.013	.011
41		17.2		.024
42		24.1		.030
43		34.5		.039
44		16.5	.051	.015
45		31.0		.182
46		51.7		.065
47		65.5		.076
48		6.9	.102	.003
49		24.1		.024
50		25.9		.020
51		34.5		.032
52		48.3		.065
53		65.5		.079
54		13.8	.203	.008
55		17.2		.013
56		34.5		.034
57		55.2		.069
58		68.9		.062
59		75.8		.094

ALLOY - L605
STRESS (MPA) - 172.4
TEMP. (KELVIN) - 922
THICKNESS (CM) - .013
SOURCE - AFMLTDR6-116

STRAIN (PCT.)	TIME (HOURS)
.007	.3
.017	.7
.023	1.1
.030	1.9
.042	2.5
.046	3.5
.107	22.0
.139	44.0
.172	70.2

ALLOY - L605
STRESS (MPA) - 275.8
TEMP. (KELVIN) - 922
THICKNESS (CM) - .013
SOURCE - AFMLTDR6-116

STRAIN (PCT.)	TIME (HOURS)
.011	1.3
.022	2.3
.098	18.2
.171	42.5
.235	69.0
.311	92.5
.341	116.0
.397	138.2
.460	162.3

ALLOY - L605
STRESS (MPA) - 224.1
TEMP. (KELVIN) - 922
THICKNESS (CM) - .013
SOURCE - AFMLTDR6-116

STRAIN (PCT.)	TIME (HOURS)
.011	.1
.025	.3
.029	.9
.033	2.0
.036	3.0
.040	4.0
.043	5.1
.048	5.7
.091	23.1
.128	45.7
.163	70.8
.194	94.0
.225	117.3
.259	142.1
.293	165.9
.327	190.0

ALLOY - L605
STRESS (MPA) - 310.3
TEMP. (KELVIN) - 922
THICKNESS (CM) - .013
SOURCE - AFMLTDR6-116

STRAIN (PCT.)	TIME (HOURS)
.030	.3
.048	.9
.067	1.8
.083	3.1
.176	19.9
.211	27.5
.274	43.6
.345	70.4
.464	93.4

ALLOY - L605
STRESS (MPA) - 172.4
TEMP. (KELVIN) - 922
THICKNESS (CM) - .102
SOURCE - AFMLTDR6-116

STRAIN (PCT.)	TIME (HOURS)
.006	.4
.010	1.1
.009	2.5
.010	3.4
.013	4.8
.024	22.0
.029	46.9
.035	70.1
.044	93.9
.045	122.5
.034	144.6
.057	165.7
.059	189.9

ALLOY - L605
STRESS (MPA) - 189.6
TEMP. (KELVIN) - 922
THICKNESS (CM) - .102
SOURCE - AFMLTDR6-116

STRAIN (PCT.)	TIME (HOURS)
.004	.2
.011	.5
.014	1.0
.019	2.0
.022	2.9
.026	4.1
.030	4.9
.050	24.4
.071	47.2
.089	70.9
.098	94.6
.104	117.8

ALLOY - L605
STRESS (MPA) - 189.6
TEMP. (KELVIN) - 922
THICKNESS (CM) - .102
SOURCE - AFMLTDR6-116

STRAIN (PCT.)	TIME (HOURS)
.002	.2
.003	.4
.004	.8
.009	1.2
.011	1.9
.009	2.7
.007	3.5
.032	20.8
.043	44.6
.046	69.5
.057	93.5
.066	116.9
.075	140.5
.080	163.7
.080	188.7
.087	212.1
.093	237.2
.091	261.1
.095	284.0
.097	306.6
.108	334.1
.104	356.0

ALLOY - L605
STRESS (MPA) - 224.1
TEMP. (KELVIN) - 922
THICKNESS (CM) - .102
SOURCE - AFMLTDR6-116

STRAIN (PCT.)	TIME (HOURS)
.003	.4
.014	1.4
.024	2.6
.027	3.1
.090	19.3
.101	21.3
.143	43.6
.161	67.2
.181	94.9
.203	119.1
.223	140.4
.237	163.5
.262	188.2
.284	211.5
.304	235.6
.319	260.0
.333	283.3
.353	307.1
.381	331.4
.399	355.5
.421	379.5
.443	404.4
.465	428.9
.488	453.2

ALLOY - L605
STRESS (MPA) - 293.0
TEMP. (KELVIN) - 922
THICKNESS (CM) - .102
SOURCE - AFMLTDR6-116

STRAIN (PCT.)	TIME (HOURS)
.002	.2
.010	.5
.023	1.1
.098	17.8
.176	42.9
.221	68.2
.270	92.6
.345	115.6
.412	140.2
.475	162.1

ORIGINAL PAGE IS OF POOR QUALITY

ALLOY - L605
STRESS (MPA) - 65.5
TEMP. (KELVIN) - 1033
THICKNESS (CM) - .013
SOURCE - AFMLTDR6-116

STRAIN (PCT.)	TIME (HOURS)
.018	.3
.019	.8
.038	1.5
.044	2.5
.111	18.5
.181	44.1
.218	67.6
.255	91.9
.285	120.1
.322	142.8
.337	162.8
.361	186.9
.398	212.9
.423	239.0
.443	259.2
.478	283.4
.490	307.0

ALLOY - L605
STRESS (MPA) - 75.8
TEMP. (KELVIN) - 1033
THICKNESS (CM) - .013
SOURCE - AFMLTDR6-116

STRAIN (PCT.)	TIME (HOURS)
.013	.3
.024	.7
.038	1.2
.050	2.2
.057	3.0
.181	20.1
.261	43.0
.334	67.5
.407	91.3

ALLOY - L605
STRESS (MPA) - 96.5
TEMP. (KELVIN) - 1033
THICKNESS (CM) - .013
SOURCE - AFMLTDR6-116

STRAIN (PCT.)	TIME (HOURS)
.021	.4
.031	.7
.039	1.2
.044	1.7
.053	2.3
.063	3.4
.214	19.4
.355	44.0
.491	67.7

ALLOY - L605
STRESS (MPA) - 12[illegible].7
TEMP. (KELVIN) - 1333
THICKNESS (CM) - .013
SOURCE - AFMLTDR6-116

STRAIN (PCT.)	TIME (HOURS)
.034	.2
.055	.5
.097	1.[illegible]
.137	1.9
.165	2.5
.193	3.2

ALLOY - L605
STRESS (MPA) - 224.1
TEMP. (KELVIN) - 1333
THICKNESS (CM) - .013
SOURCE - AFMLTDR6-116

STRAIN (PCT.)	TIME (HOURS)
.107	.2
.164	.5
.250	.7
.461	1.6

ALLOY - L605
STRESS (MPA) - 165.5
TEMP. (KELVIN) - 1333
THICKNESS (CM) - .051
SOURCE - AFMLTDR6-116

STRAIN (PCT.)	TIME (HOURS)
.018	.2
.035	.4
.084	1.5
.112	2.3
.134	3.2

ALLOY - L605
STRESS (MPA) - 144.8
TEMP. (KELVIN) - 1333
THICKNESS (CM) - .051
SOURCE - AFMLTDR6-116

STRAIN (PCT.)	TIME (HOURS)
.021	.3
.040	.6
.064	1.1
.097	2.2
.114	2.7
.137	3.5
.156	4.2
.176	4.9

ALLOY - L605
STRESS (MPA) - 75.8
TEMP. (KELVIN) - 1333
THICKNESS (CM) - .102
SOURCE - AFMLTDR6-116

STRAIN (PCT.)	TIME (HOURS)
.001	.2
.010	.6
.020	1.4
.026	2.3
.034	3.4
.074	21.3
.113	47.[illegible]
.138	69.3
.165	95.9
.183	120.4
.197	143.4
.213	166.3
.217	190.3
.230	215.3
.241	237.2
.259	263.2
.264	285.4
.271	311.3
.280	334.4
.286	357.2
.298	381.[illegible]
.307	405.6

ALLOY - L605
STRESS (MPA) - 86.2
TEMP. (KELVIN) - 1333
THICKNESS (CM) - .102
SOURCE - AFMLTDR6-116

STRAIN (PCT.)	TIME (HOURS)
.015	.4
.061	4.[illegible]
.131	22.2
.183	45.1
.288	69.4
.361	94.9
.391	117.9
.437	141.8

ALLOY - L605
STRESS (MPA) - 100.0
TEMP. (KELVIN) - 1033
THICKNESS (CM) - .102
SOURCE - AFMLTDR6-116

STRAIN (PCT.)	TIME (HOURS)
.008	.4
.015	1.0
.030	2.3
.035	3.2
.116	19.6
.208	43.5
.288	67.8
.412	93.3
.497	116.0

ALLOY - L605
STRESS (MPA) - 103.4
TEMP. (KELVIN) - 1033
THICKNESS (CM) - .102
SOURCE - AFMLTDR6-116

STRAIN (PCT.)	TIME (HOURS)
.008	.3
.019	.6
.021	1.1
.025	1.6
.033	2.3
.044	3.2
.107	19.3
.180	44.8
.242	67.9
.299	92.5
.345	120.8
.393	143.4
.439	163.5
.483	187.5

ALLOY - L605
STRESS (MPA) - 103.4
TEMP. (KELVIN) - 1033
THICKNESS (CM) - .102
SOURCE - AFMLTDR6-116

STRAIN (PCT.)	TIME (HOURS)
.016	.6
.030	1.1
.041	2.3
.054	3.1
.061	4.2
.154	21.1
.271	47.1
.360	69.7
.460	92.9

ALLOY - L605
STRESS (MPA) - 165.5
TEMP. (KELVIN) - 1033
THICKNESS (CM) - .102
SOURCE - AFMLTDR6-116

STRAIN (PCT.)	TIME (HOURS)
.038	.4
.052	1.1
.077	2.0
.092	3.0
.104	3.8
.122	4.8
.135	5.5
.461	22.4

ALLOY - L605
STRESS (MPA) - 68.9
TEMP. (KELVIN) - 1033
THICKNESS (CM) - .203
SOURCE - AFMLTDR6-116

STRAIN (PCT.)	TIME (HOURS)
.012	.4
.015	1.3
.021	2.1
.064	20.6
.094	45.7
.118	70.1
.130	91.9
.147	117.0
.157	140.0
.162	163.6

ALLOY - L605
STRESS (MPA) - 86.2
TEMP. (KELVIN) - 1033
THICKNESS (CM) - .203
SOURCE - AFMLTDR6-116

STRAIN (PCT.)	TIME (HOURS)
.001	.1
.005	.3
.006	1.2
.012	1.9
.015	2.[illegible]
.017	3.1
.054	21.4
.086	45.2
.123	68.7
.145	91.9
.163	116.7
.174	141.4
.183	164.8
.200	189.2
.207	213.3
.218	235.8
.229	26[illegible].9
.235	285.7
.251	310.1
.264	332.9
.275	351.9
.285	381.1
.295	404.9
.303	43[illegible].4
.318	452.7
.328	477.8
.337	500.6
.348	524.7
.360	548.9
.371	572.7
.380	595.9
.397	623.3
.402	645.2
.419	668.5
.425	692.7
.435	717.[illegible]
.451	74[illegible].7
.462	761.1
.465	789.1
.485	813.4
.498	838.1

ALLOY - L605
STRESS (MPA) - 137.9
TEMP. (KELVIN) - 1033
THICKNESS (CM) - .203
SOURCE - AFMLTDR6-116

STRAIN (PCT.)	TIME (HOURS)
.005	.4
.014	.9
.026	1.7
.037	2.6
.043	3.2
.162	2[illegible].5
.229	27.5
.370	43.7

ALLOY - L605
STRESS (MPA) - 189.6
TEMP. (KELVIN) - 1033
THICKNESS (CM) - .203
SOURCE - AFMLTDR6-116

STRAIN (PCT.)	TIME (HOURS)
.029	.3
.049	.6
.061	1.0
.085	1.6
.108	2.3
.135	3.1
.178	4.1
.249	5.6

ALLOY - L605
STRESS (MPA) - 27.6
TEMP. (KELVIN) - 1144
THICKNESS (CM) - .013
SOURCE - AFMLTDR6-116

STRAIN (PCT.)	TIME (HOURS)
.012	.2
.017	.7
.018	1.2
.025	1.5
.022	2.2
.028	3.2
.065	19.1
.118	45.6
.154	70.4
.190	93.1
.229	115.7
.257	140.[illegible]
.286	165.[illegible]
.296	187.8
.315	213.2

ALLOY - L605
STRESS (MPA) - 27.6
TEMP. (KELVIN) - 1144
THICKNESS (CM) - .013
SOURCE - AFMLTDR6-116

STRAIN (PCT.)	TIME (HOURS)
.017	.3
.021	.8
.041	2.1
.041	3.5
.049	4.5
.054	5.6
.108	21.9
.142	48.7
.186	71.7
.226	94.3
.257	117.9
.282	143.0
.303	166.[illegible]

ALLOY - L605
STRESS (MPA) - 62.1
TEMP. (KELVIN) - 1144
THICKNESS (CM) - .013
SOURCE - AFMLTDR6-116

STRAIN (PCT.)	TIME (HOURS)
.053	.2
.154	1.1
.221	2.1
.276	3.0
.351	5.5

ALLOY - L605
STRESS (MPA) - 63.3
TEMP. (KELVIN) - 1144
THICKNESS (CM) - .013
SOURCE - AFMLTDR6-116

STRAIN (PCT.)	TIME (HOURS)
.047	.2
.072	.4
.120	1.5
.151	2.3
.187	3.5
.222	4.8
.497	20.7

ALLOY - L605
STRESS (MPA) - 22.8
TEMP. (KELVIN) - 1144
THICKNESS (CM) - .102
SOURCE - AFMLTDR5-116

STRAIN (PCT.)	TIME (HOURS)
.020	22.4
.031	45.9
.037	74.5
.046	96.5
.054	117.6
.074	141.8
.085	166.4
.096	191.0
.110	213.8
.121	237.2
.127	261.5
.133	287.0
.139	309.9
.145	334.4
.147	358.9
.159	381.5
.156	408.7
.165	432.5
.160	453.6

ALLOY - L605
STRESS (MPA) - 41.4
TEMP. (KELVIN) - 1144
THICKNESS (CM) - .102
SOURCE - AFMLTDR6-116

STRAIN (PCT.)	TIME (HOURS)
.002	.1
.012	.3
.028	1.2
.036	2.0
.040	2.8
.046	4.0
.052	4.7
.080	21.6
.123	46.0
.162	69.4
.221	93.2
.259	117.9
.314	141.3
.349	164.9
.380	190.5
.412	213.5
.444	237.4
.459	261.3
.487	285.0
.493	308.7

ALLOY - L605
STRESS (MPA) - 48.3
TEMP. (KELVIN) - 1144
THICKNESS (CM) - .102
SOURCE - AFMLTDR6-116

STRAIN (PCT.)	TIME (HOURS)
.011	.2
.020	.7
.032	2.2
.035	3.2
.098	20.1
.107	27.6
.139	43.4
.190	68.0
.212	75.2
.250	91.7
.306	115.4
.355	139.8
.401	163.8
.435	188.0
.464	212.9
.492	236.1

ALLOY - L605
STRESS (MPA) - 55.2
TEMP. (KELVIN) - 1144
THICKNESS (CM) - .102
SOURCE - AFMLTDR6-116

STRAIN (PCT.)	TIME (HOURS)
.032	.4
.051	.8
.082	1.9
.107	3.2
.116	4.3
.134	5.6
.240	21.5
.331	46.0
.360	53.1
.412	69.7

ALLOY - L605
STRESS (MPA) - 62.1
TEMP. (KELVIN) - 1144
THICKNESS (CM) - .102
SOURCE - AFMLTDR6-116

STRAIN (PCT.)	TIME (HOURS)
.027	.4
.049	1.0
.078	2.1
.102	3.0
.107	3.5
.319	21.1
.370	27.2

ALLOY - L605
STRESS (MPA) - 120.7
TEMP. (KELVIN) - 1144
THICKNESS (CM) - .102
SOURCE - AFMLTDR6-116

STRAIN (PCT.)	TIME (HOURS)
.102	.2
.212	.4
.396	.8

ALLOY - L605
STRESS (MPA) - 17.2
TEMP. (KELVIN) - 1255
THICKNESS (CM) - .013
SOURCE - AFMLTDR6-116

STRAIN (PCT.)	TIME (HOURS)
.012	.3
.013	.7
.030	1.3
.124	17.5
.252	42.4
.486	67.8

ALLOY - L605
STRESS (MPA) - 55.5
TEMP. (KELVIN) - 1144
THICKNESS (CM) - .102
SOURCE - AFMLTDR6-116

STRAIN (PCT.)	TIME (HOURS)
.031	.4
.057	1.1
.080	1.9
.098	2.6
.117	3.6
.328	22.1
.487	44.0

ALLOY - L605
STRESS (MPA) - 10.3
TEMP. (KELVIN) - 1255
THICKNESS (CM) - .013
SOURCE - AFMLTDR6-116

STRAIN (PCT.)	TIME (HOURS)
.006	.2
.007	.8
.006	1.4
.015	2.3
.016	3.4
.016	4.5
.021	5.7
.028	22.5
.044	47.5
.057	70.7
.073	94.3
.114	121.2
.159	144.1

ALLOY - L605
STRESS (MPA) - 24.1
TEMP. (KELVIN) - 1255
THICKNESS (CM) - .013
SOURCE - AFMLTDR6-116

STRAIN (PCT.)	TIME (HOURS)
.040	.7
.047	1.2
.064	1.6
.062	2.2
.273	19.2

ALLOY - L605
STRESS (MPA) - 27.6
TEMP. (KELVIN) - 1144
THICKNESS (CM) - .203
SOURCE - AFMLTDR6-116

STRAIN (PCT.)	TIME (HOURS)
.006	.3
.008	.6
.011	1.2
.013	2.0
.013	2.9
.013	3.4
.036	20.9
.036	27.8
.047	44.1
.068	69.6
.080	91.4
.111	107.2
.131	140.0
.157	166.1
.170	189.6
.181	215.3
.193	237.8
.202	263.2
.201	287.6
.218	300.0
.220	333.6
.227	359.0
.231	380.0
.237	404.6
.241	427.1
.246	453.9
.243	478.7
.241	501.8
.243	526.4
.243	551.0
.248	573.7
.256	596.4
.263	621.2
.263	643.8
.261	671.1
.266	692.9
.267	718.8
.267	742.5
.279	767.9
.271	790.5
.275	812.7
.291	842.7
.298	861.6
.297	886.6
.298	910.2
.305	935.0
.303	956.0
.301	982.0
.314	1004.9

ALLOY - L605
STRESS (MPA) - 34.5
TEMP. (KELVIN) - 1255
THICKNESS (CM) - .013
SOURCE - AFMLTDR6-116

STRAIN (PCT.)	TIME (HOURS)
.054	.2
.076	.4
.105	.7
.162	1.6
.255	3.2
.297	4.2
.350	5.3

ALLOY - L605
STRESS (MPA) - 51.7
TEMP. (KELVIN) - 1255
THICKNESS (CM) - .051
SOURCE - AFMLTDR6-116

STRAIN (PCT.)	TIME (HOURS)
.079	.2
.130	.4
.170	.8
.233	1.4
.274	1.5

ALLOY - L605
STRESS (MPA) - 6.9
TEMP. (KELVIN) - 1255
THICKNESS (CM) - .102
SOURCE - AFMLTDR6-116

STRAIN (PCT.)	TIME (HOURS)
.006	.6
.013	1.9
.016	2.9
.021	3.9
.029	2[illegible].6
.031	28.1
.036	45.7
.044	69.8
.046	92.3
.050	117.0

ALLOY - L605
STRESS (MPA) - 16.5
TEMP. (KELVIN) - 1255
THICKNESS (CM) - .051
SOURCE - AFMLTDR6-115

STRAIN (PCT.)	TIME (HOURS)
.014	.5
.015	1.0
.025	2.0
.032	3.1
.036	3.5
.112	19.4
.126	23.8
.141	27.4
.179	43.5
.189	51.6
.206	67.5
.202	75.2
.230	95.5
.258	118.6
.282	139.8
.295	147.4
.317	165.3
.323	171.5
.335	187.5
.340	195.2
.367	211.8
.375	219.2
.392	235.7
.410	242.9
.484	258.7

ALLOY - L605
STRESS (MPA) - 25.9
TEMP. (KELVIN) - 1255
THICKNESS (CM) - .102
SOURCE - AFMLTDR6-116

STRAIN (PCT.)	TIME (HOURS)
.006	.2
.024	.7
.025	1.2
.027	2.0
.046	3.1
.145	19.4
.264	44.4
.380	69.9
.431	92.3
.457	117.2

ALLOY - L605
STRESS (MPA) - 31.0
TEMP. (KELVIN) - 1255
THICKNESS (CM) - .051
SOURCE - AFMLTDR6-116

STRAIN (PCT.)	TIME (HOURS)
.029	.3
.105	1.7
.127	2.3
.164	3.3

ALLOY - L605
STRESS (MPA) - 65.5
TEMP. (KELVIN) - 1255
THICKNESS (CM) - .051
SOURCE - AFMLTDR6-116

STRAIN (PCT.)	TIME (HOURS)
.194	.2
.432	.4

ALLOY - L605
STRESS (MPA) - 24.1
TEMP. (KELVIN) - 1255
THICKNESS (CM) - .102
SOURCE - AFMLTDR6-116

STRAIN (PCT.)	TIME (HOURS)
.020	.4
.035	1.2
.044	1.8
.051	2.5
.060	3.3
.059	3.9
.070	4.9
.188	23.4
.267	45.2
.332	71.2
.372	93.4
.413	119.5
.457	142.4

ALLOY - L605
STRESS (MPA) - 34.5
TEMP. (KELVIN) - 1255
THICKNESS (CM) - .102
SOURCE - AFMLTDR5-116

STRAIN (PCT.)	TIME (HOURS)
.040	.5
.096	1.7
.115	2.5
.139	3.1
.428	20.4

ALLOY - L605
STRESS (MPA) - 65.5
TEMP. (KELVIN) - 1255
THICKNESS (CM) - .102
SOURCE - AFMLTDR5-116

STRAIN (PCT.)	TIME (HOURS)
.136	.1
.243	.3
.344	.5
.500	.8

ALLOY - L605
STRESS (MPA) - 34.5
TEMP. (KELVIN) - 1255
THICKNESS (CM) - .203
SOURCE - AFMLTDR6-116

STRAIN (PCT.)	TIME (HOURS)
.022	.3
.059	1.0
.086	1.9
.105	2.6
.127	3.5
.332	20.8

ALLOY - L605
STRESS (MPA) - 48.3
TEMP. (KELVIN) - 1255
THICKNESS (CM) - .102
SOURCE - AFMLTDR6-116

STRAIN (PCT.)	TIME (HOURS)
.039	.2
.116	1.0
.146	1.4
.186	2.0

ALLOY - L605
STRESS (MPA) - 17.2
TEMP. (KELVIN) - 1255
THICKNESS (CM) - .203
SOURCE - AFMLTDR6-116

STRAIN (PCT.)	TIME (HOURS)
.003	.2
.005	.5
.016	1.5
.019	2.1
.022	3.2
.063	20.3
.077	25.8
.110	45.7
.122	51.0
.129	68.4
.142	91.3
.150	115.6
.159	141.1
.166	164.1
.172	188.4
.180	212.7
.185	236.8
.186	259.6
.192	285.5
.195	308.9
.198	333.5
.206	356.4
.211	379.7
.212	404.8

ALLOY - L605
STRESS (MPA) - 13.8
TEMP. (KELVIN) - 1255
THICKNESS (CM) - .203
SOURCE - AFMLTDR6-116

STRAIN (PCT.)	TIME (HOURS)
.010	.4
.034	1.3
.044	2.5
.067	20.7
.062	25.3
.084	43.6
.080	65.7
.089	91.5
.097	116.7
.100	140.4
.101	163.8
.107	189.8
.105	211.8
.109	237.7
.115	262.2
.119	284.7
.113	307.8
.123	357.1
.131	380.0
.131	401.5
.132	428.1
.124	453.0
.125	476.0
.121	500.7
.129	525.2
.135	547.9
.139	570.7
.142	596.7
.144	620.6
.133	645.5
.144	668.7
.145	692.9
.149	716.2
.155	742.4
.160	765.1
.169	789.2
.174	817.1
.185	835.7
.192	860.8
.190	883.9
.191	910.9
.189	931.4
.193	957.0
.211	980.2
.203	1003.9

ALLOY -	L605
STRESS (MPA) -	55.2
TEMP. (KELVIN) -	1255
THICKNESS (CM) -	.203
SOURCE -	AFMLTDR6-116

STRAIN (PCT.)	TIME (HOURS)
.106	.4
.164	.8
.211	1.1
.260	1.4
.347	2.0
.476	3.2

ALLOY -	L605
STRESS (MPA) -	68.9
TEMP. (KELVIN) -	1255
THICKNESS (CM) -	.203
SOURCE -	AFMLTDR6-116

STRAIN (PCT.)	TIME (HOURS)
.177	.2
.292	.4
.393	.6

ALLOY -	L605
STRESS (MPA) -	75.8
TEMP. (KELVIN) -	1255
THICKNESS (CM) -	.203
SOURCE -	AFMLTDR6-116

STRAIN (PCT.)	TIME (HOURS)
.277	.1

APPENDIX C-2

L605 SUPPLEMENTAL STEADY-STATE CREEP TESTS (RAW DATA)

This portion of Appendix C presents the results of the supplemental steady-state creep tests. All strains shown are total plastic strains. For informational purposes the elastic strains are presented below for the individual tests in order of their appearance in this section. Elastic strain "A" was measured at the start of the test while elastic strain "B" was measured at the conclusion of the test.

SPECIMEN #	ELASTIC STRAIN, %	
	A	B
L01L	.035	.028
L02L	.032	.023
L03L	.022	.014
L11T	.037	.024
L17T	.045	.024
L18T	.031	.032
L23L	.037	.062
L24L	.011	----
L27L	.036	.033
L29L	.015	----
L31L	.070	.070
L39L	----	.066
L42L	.070	.085
L45L	----	.028
L48L	.015	.013
L50L	.051	.070
L54L	.029	----
L58L	.042	.041
L73L	.016	.022
L78L	.022	.037
L93L	.021	----
L95L	.032	.031
L96L	.030	.048

ALLOY - L605
STRESS (MPA) - 55.2
TEMP. (KELVIN) - 978
THICKNESS (CM) - .025
SPECIMEN NO. - MDAC-E-L90L

STRAIN (PCT.)	TIME (HOURS)
.029	.1
.040	.2
.049	.3
.046	.5
.050	.8
.056	1.0
.058	1.5
.069	2.0
.059	3.0
.069	4.0
.073	5.0
.084	10.0
.078	19.0
.096	25.0
.100	30.0
.084	35.0
.100	43.0
.109	46.0
.116	50.0
.134	55.0
.149	60.0
.122	67.0
.132	70.0
.124	75.0
.159	80.0
.159	84.0
.137	103.0
.149	122.0
.165	163.0
.174	165.0
.176	170.0
.181	175.0
.193	180.0
.196	187.0
.187	190.0
.192	195.0
.203	200.0

ALLOY - L605
STRESS (MPA) - 55.2
TEMP. (KELVIN) - 978
THICKNESS (CM) - .025
SPECIMEN NO. - MDAC-E-L96L

STRAIN (PCT.)	TIME (HOURS)
.005	.1
.009	.2
.011	.3
.017	.5
.019	.8
.019	1.0
.022	1.5
.025	2.0
.030	3.0
.036	4.0
.040	5.0
.046	10.0
.051	20.0
.065	25.0
.055	30.0
.073	35.0
.080	43.0
.082	45.0
.087	51.0
.090	55.0

ALLOY - L605
STRESS (MPA) - 110.3
TEMP. (KELVIN) - 978
THICKNESS (CM) - .025
SPECIMEN NO. - MDAC-E-L31L

STRAIN (PCT.)	TIME (HOURS)
.011	.1
.017	.2
.018	.3
.029	.5
.035	.8
.039	1.0
.043	1.5
.048	2.0
.051	3.0
.053	4.0
.057	5.0
.064	6.5
.069	17.0
.072	20.0
.086	25.0
.132	41.0
.279	113.0
.282	115.0
.291	120.0
.302	125.0
.318	130.0
.331	140.0
.350	145.0
.356	150.0
.363	161.0
.373	165.0
.382	170.0
.400	185.0
.403	190.0
.428	195.0
.441	200.0
.450	209.0

ORIGINAL PAGE IS OF POOR QUALITY

ALLOY - L605
STRESS (MPA) - 110.3
TEMP. (KELVIN) - 978
THICKNESS (CM) - .025
SPECIMEN NO. - MDAC-E-L42L

STRAIN (PCT.)	TIME (HOURS)
.008	.1
.014	.2
.016	.3
.015	.5
.019	.8
.023	1.5
.024	2.0
.030	3.0
.050	4.0
.052	5.0
.080	10.0
.087	19.0
.090	20.0
.115	25.0
.123	30.0
.135	35.0
.168	43.0
.155	45.0
.165	50.0
.191	55.0
.197	59.0
.198	67.0
.212	70.0
.225	75.5
.226	80.0
.241	83.0
.246	90.0
.259	95.0
.271	100.0
.279	105.0
.286	107.0
.371	162.0
.385	165.0
.394	170.0
.408	175.0
.413	178.0
.420	185.0
.435	190.0
.445	195.0
.449	200.0
.453	202.0
.465	209.0

ALLOY - L605
STRESS (MPA) - 27.6
TEMP. (KELVIN) - 1053
THICKNESS (CM) - .025
SPECIMEN NO. - MDAC-E-L73L

STRAIN (PCT.)	TIME (HOURS)
.019	.1
.030	.2
.029	.3
.027	.5
.029	.8
.029	1.0
.028	1.5
.037	2.0
.040	3.0
.042	4.0
.040	5.0
.041	10.0
.046	15.0
.059	22.0
.058	25.0
.060	30.0
.076	35.0
.080	39.0
.072	46.0
.070	50.0
.076	55.0
.078	60.0
.081	63.0
.086	70.0
.076	76.0
.078	80.0
.082	85.0
.083	87.0
.090	142.0
.091	145.0
.106	150.0
.116	155.0
.121	159.0
.115	165.0
.089	170.0
.105	175.0
.118	18[illegible]
.104	183.0
.090	190.0
.093	194.0

ALLOY - L605
STRESS (MPA) - 55.2
TEMP. (KELVIN) - 1053
THICKNESS (CM) - .025
SPECIMEN NO. - MDAC-E-L23L

STRAIN (PCT.)	TIME (HOURS)
.018	.1
.020	.2
.014	.3
.026	.5
.031	.8
.041	1.0
.049	1.5
.034	2.0
.040	3.0
.046	4.0
.057	5.0
.063	10.0
.038	20.0
.047	25.0
.056	30.0
.074	34.0
.107	42.0
.113	45.0
.113	50.0
.117	55.0
.142	58.0
.139	66.0
.142	69.0
.164	74.0
.177	79.0
.183	82.0
.198	90.0
.212	95.0
.187	100.0
.191	105.0
.231	162.0
.229	165.0
.238	170.0
.241	175.0
.264	178.0
.250	186.0
.250	190.0
.259	195.0
.272	200.0

ORIGINAL PAGE IS
OF POOR QUALITY

ALLOY - L605
STRESS (MPA) - 55.2
TEMP. (KELVIN) - 1353
THICKNESS (CM) - .025
SPECIMEN NO. - MDAC-E-L05L

STRAIN (PCT.)	TIME (HOURS)
.002	.1
.009	.2
.012	.3
.020	.5
.027	.8
.032	1.0
.039	1.5
.049	2.0
.058	3.0
.080	4.0
.092	5.0
.121	10.0
.152	18.0
.151	20.0
.166	25.0
.170	30.0
.187	34.0
.242	89.0
.270	95.0
.279	100.0
.287	105.0
.252	113.0
.260	115.0
.273	120.0
.280	125.0
.291	129.0
.287	137.0
.284	140.0
.295	145.0
.298	150.0
.302	160.0
.298	165.0
.303	169.0
.310	185.0
.303	190.0

ALLOY - L605
STRESS (MPA) - 55.2
TEMP. (KELVIN) - 1353
THICKNESS (CM) - .025
SPECIMEN NO. - MDAC-E-L18T

STRAIN (PCT.)	TIME (HOURS)
.001	.1
.001	.2
.003	.3
.007	.5
.009	.8
.012	1.0
.013	1.5
.014	2.0
.017	3.0
.022	4.0
.027	5.0
.033	10.0
.042	13.0
.069	21.0
.076	25.0
.077	30.0
.085	35.0
.099	45.0
.102	50.0
.110	55.0
.125	60.0
.152	117.0
.156	120.0
.160	125.0
.170	130.0
.181	133.0
.174	141.0
.164	145.0
.172	150.0
.190	155.0
.184	165.0
.184	170.0
.186	175.0
.186	180.0
.193	190.0
.197	195.0
.202	200.0

ALLOY - L605
STRESS (MPA) - 55.2
TEMP. (KELVIN) - 1353
THICKNESS (CM) - .063
SPECIMEN NO. - MDAC-E-L02L

STRAIN (PCT.)	TIME (HOURS)
.014	.1
.019	.2
.025	.3
.031	.5
.039	.8
.041	1.0
.042	1.5
.049	2.0
.055	3.0
.057	4.0
.044	5.0
.046	10.0
.029	12.0
.039	20.0
.048	25.0
.064	30.0
.064	35.0
.076	43.0
.079	50.0
.081	55.0
.090	60.0
.089	67.0
.084	70.0
.094	75.0
.099	80.0
.116	84.0
.094	91.0
.096	95.0
.103	100.0
.110	105.0
.110	108.0
.107	127.0
.098	146.0
.105	187.0
.105	190.0
.106	195.0
.109	200.0

ORIGINAL PAGE IS
OF POOR QUALITY

ALLOY - L605
STRESS (MPA) - 11[illegible].3
TEMP. (KELVIN) - 1[illegible]53
THICKNESS (CM) - .025
SPECIMEN NO. - MDAC-E-L39L

STRAIN (PCT.)	TIME (HOURS)
.006	.1
.031	.2
.036	.3
.066	.5
.078	.8
.101	1.0
.125	1.5
.162	2.0
.21[illegible]	3.0
.246	4.0
.301	5.0
.459	10.0
.572	14.0
.748	21.0
.840	25.0
.854	26.0

ALLOY - L605
STRESS (MPA) - 13.8
TEMP. (KELVIN) - 1144
THICKNESS (CM) - .025
SPECIMEN NO. - MDAC-E- L24L

STRAIN (PCT.)	TIME (HOURS)
.006	.1
.006	.2
.006	.3
.009	.5
.011	.8
.011	1.0
.011	1.5
.011	2.0
.011	3.0
.014	4.0
.017	5.0
.024	10.0
.030	15.0
.030	16.5
.040	24.0
.050	25.0
.049	30.0
.047	35.0
.049	40.0
.057	45.0
.091	100.0
.078	105.0
.076	110.0
.059	119.0
.049	120.0
.068	125.0
.070	130.0
.062	135.0
.063	143.0
.066	145.0
.063	150.0
.061	155.0
.065	167.0
.063	170.0
.064	175.0
.065	191.0
.063	195.0
.066	196.0
.062	197.0
.054	198.0

ALLOY - L605
STRESS (MPA) - 27.6
TEMP. (KELVIN) - 1144
THICKNESS (CM) - .025
SPECIMEN NO. - MDAC-E-L78L

STRAIN (PCT.)	TIME (HOURS)
.024	.1
.029	.2
.028	.3
.028	.5
.026	.8
.028	1.0
.034	1.5
.041	2.0
.069	3.0
.083	4.0
.088	5.0
.092	10.0
.072	18.0
.075	20.0
.062	25.0
.103	30.0
.046	35.0
.087	90.0
.057	95.0
.095	100.0
.136	105.0
.101	115.0
.106	120.0
.097	125.0
.092	130.0
.102	138.0
.104	140.0
.114	145.0
.105	150.0
.106	155.0
.125	160.0
.120	167.0
.102	170.0
.089	175.0
.111	179.0
.114	186.0
.130	190.0
.131	195.0
.113	200.0

ALLOY - L605
STRESS (MPA) - 27.6
TEMP. (KELVIN) - 1144
THICKNESS (CM) - .025
SPECIMEN NO. - MDAC-E- L93L

STRAIN (PCT.)	TIME (HOURS)
.002	.1
.001	.2
.007	.3
.007	.5
.010	.8
.014	1.0
.014	1.5
.016	2.0
.016	3.0
.024	4.0
.048	5.0
.060	10.0
.076	14.0
.077	22.0
.089	25.0
.080	30.0
.082	35.0
.090	38.0
.091	40.0
.096	50.0
.100	55.0
.106	60.0
.109	62.0
.112	69.0
.112	74.0

ALLOY - L605
STRESS (MPA) - 27.6
TEMP. (KELVIN) - 1144
THICKNESS (CM) - .025
SPECIMEN NO. - MDAC-E-L11T

STRAIN (PCT.)	TIME (HOURS)
.009	.1
.011	.2
.014	.3
.019	.5
.021	.8
.019	1.0
.026	1.5
.030	2.0
.031	3.0
.028	4.0
.035	5.0
.039	10.0
.041	15.0
.043	23.0
.043	25.0
.044	30.0
.057	35.0
.068	39.0
.074	94.0
.077	100.0
.078	110.0
.081	119.0
.083	125.0
.082	130.0
.092	135.0
.087	143.0
.088	145.0
.091	150.0
.115	155.0
.128	159.0
.120	167.0
.117	170.0
.100	175.0
.096	180.0
.107	183.0
.120	191.0
.121	195.0
.122	200.0

ALLOY - L605
STRESS (MPA) - 27.6
TEMP. (KELVIN) - 1144
THICKNESS (CM) - .063
SPECIMEN NO. - MDAC-E-L[illegible]3L

STRAIN (PCT.)	TIME (HOURS)
.001	.1
.008	.2
.013	.3
.011	.5
.011	.8
.017	1.0
.015	1.5
.016	2.0
.021	3.0
.044	4.0
.089	5.0
.064	10.0
.054	12.0
.048	19.0
.036	20.0
.038	25.0
.041	30.0
.046	35.0
.049	54.0
.050	73.0
.079	115.0
.089	120.0
.089	125.0
.087	130.0
.075	139.0
.075	145.0
.069	150.0
.085	163.0
.087	165.0
.096	170.0
.102	175.0
.101	179.0
.098	187.0
.103	190.0
.104	195.0
.106	200.0

ALLOY - L605
STRESS (MPA) - 55.2
TEMP. (KELVIN) - 1144
THICKNESS (CM) - .025
SPECIMEN NO. - MDAC-E- L27L

STRAIN (PCT.)	TIME (HOURS)
.035	.2
.020	.3
.042	.5
.070	.8
.060	1.0
.078	1.5
.103	2.0
.114	3.0
.158	4.0
.171	5.0
.246	10.0
.340	19.0
.343	20.0
.374	25.0
.419	30.0
.457	35.0
.502	42.0
.509	45.0
.551	50.0
.581	55.0
.617	66.0

ALLOY - L605
STRESS (MPA) - 55.2
TEMP. (KELVIN) - 1144
THICKNESS (CM) - .025
SPECIMEN NO. - MDAC-E-L45L

STRAIN (PCT.)	TIME (HOURS)
.012	.1
.014	.2
.025	.3
.040	.5
.056	.8
.076	1.0
.090	1.5
.103	2.0
.146	3.0
.126	4.0
.166	5.0
.239	10.0
.366	21.0
.413	25.0
.467	30.0
.487	35.0
.576	43.0
.597	45.0
.623	50.0
.627	55.0
.635	59.0
.695	67.0

ALLOY - L605
STRESS (MPA) - 55.2
TEMP. (KELVIN) - 1144
THICKNESS (CM) - .025
SPECIMEN NO. - MDAC-E- L58L

STRAIN (PCT.)	TIME (HOURS)
.021	.1
.034	.2
.041	.3
.045	.5
.053	.8
.061	1.0
.072	1.5
.092	2.0
.103	3.0
.126	4.0
.128	5.0
.131	10.0
.208	15.0
.269	23.0
.269	25.0
.304	30.0
.328	35.0
.355	40.0
.421	47.0
.428	50.0
.445	55.0
.458	60.0
.462	64.0
.502	71.0

ORIGINAL PAGE IS OF POOR QUALITY

ALLOY - L605
STRESS (MPA) - 55.2
TEMP. (KELVIN) - 1144
THICKNESS (CM) - .025
SPECIMEN NO. - MOAC-E-L17T

STRAIN (PCT.)	TIME (HOURS)
.015	.1
.019	.2
.025	.3
.030	.5
.036	.8
.040	1.0
.047	1.5
.062	2.0
.077	3.0
.100	4.0
.133	5.0
.202	10.0
.270	13.0
.363	21.0
.415	25.0
.453	30.0
.482	35.0
.591	45.0
.629	50.0
.536	51.0

ALLOY - L605
STRESS (MPA) - 55.2
TEMP. (KELVIN) - 1144
THICKNESS (CM) - .063
SPECIMEN NO. - MOAC-E-L01L

STRAIN (PCT.)	TIME (HOURS)
.005	.1
.017	.2
.028	.3
.024	.5
.028	.8
.030	1.0
.042	1.5
.054	2.0
.070	3.0
.092	4.0
.105	5.0
.159	10.0
.189	14.0
.233	21.0
.253	25.0
.278	30.0
.294	35.0
.314	38.0
.327	45.0
.351	50.0
.358	55.0
.360	60.0
.379	62.0
.408	69.0

ALLOY - L605
STRESS (MPA) - 13.8
TEMP. (KELVIN) - 1255
THICKNESS (CM) - .025
SPECIMEN NO. - MOAC-E-L29L

STRAIN (PCT.)	TIME (HOURS)
.003	.1
.006	.2
.007	.3
.020	.5
.024	.8
.026	1.0
.033	1.5
.040	2.0
.046	3.0
.054	4.0
.062	5.0
.060	9.0
.062	16.0
.064	20.0
.069	25.0
.071	30.0
.075	34.0
.065	41.0
.078	45.0
.084	50.0
.077	55.0

ALLOY - L605
STRESS (MPA) - 13.8
TEMP. (KELVIN) - 1255
THICKNESS (CM) - .025
SPECIMEN NO. - MDAC-E-L48L

ALLOY - L605
STRESS (MPA) - 27.6
TEMP. (KELVIN) - 1255
THICKNESS (CM) - .025
SPECIMEN NO. - MDAC-E-L54L

STRAIN (PCT.)	TIME (HOURS)	STRAIN (PCT.)	TIME (HOURS)
.001	.1	.004	.1
.001	.2	.014	.2
.005	.3	.019	.3
.007	.5	.032	.5
.008	.8	.037	.8
.010	1.0	.042	1.0
.012	1.5	.045	1.5
.018	2.0	.043	2.0
.022	3.0	.050	3.0
.026	4.0	.054	4.0
.044	5.0	.060	5.0
.048	10.0	.071	10.0
.053	18.0	.105	15.0
.055	20.0	.180	23.0
.060	25.0	.180	25.0
.087	30.0	.192	29.0
.094	34.0	.209	35.0
.077	42.0	.228	39.0
.075	45.0	.259	48.0
.074	50.0	.265	50.0
.072	55.0		
.084	58.0		
.102	67.0		
.097	70.0		
.105	75.0		
.106	80.0		
.108	83.0		
.116	91.0		
.110	95.0		
.119	100.0		
.119	105.0		
.118	163.0		
.129	165.0		
.134	170.0		
.137	175.0		
.137	179.0		
.135	187.0		
.135	190.0		
.138	195.0		
.138	200.0		

APPENDIX C-3
L605 CYCLIC CREEP TESTS
(RAW DATA)

This section presents the results of the 15 cyclic creep tests that were performed on L605 tensile specimens.

Cobalt Cyclic Creep Data

Cyclic Test Number	1		
Alloy Designation	L605		
Heat Number	1860-2-1396		
Supplier	Cabot		
Test Temperature (°K)	978°K		
Test Direction	Longitudinal		
Sheet Thickness (cm.)	0.025 cm. + 0.003		
Specimen Number	L44L	L52L	L57L
Specimen Thickness (cm.)	.0251	.0254	.0254
Specimen Width (cm.)	1.2769	1.2776	1.2748
Applied Load (kg)	42.3	16.9	26.8
Test Stress (MPa)	128.9	51.0	80.7

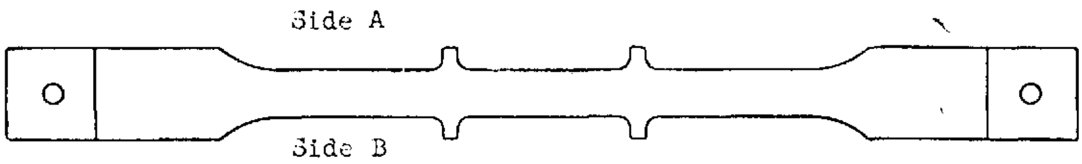

Cycle Number		% Creep L44L	% Creep L52L	% Creep L57L
1	Side A	.00	.00	.01
	Side B	.01	.00	.01
	Ave.	.005	.00	.01
5	Side A	.01	.006	.01
	Side B	.03	.006	.01
	Ave.	.02	.006	.01
15	Side A	.05	.017	.03
	Side B	.04	.017	.03
	Ave.	.045	.017	.03
25	Side A	.07	.017	.05
	Side B	.07	.029	.05
	Ave.	.07	.024	.05
50	Side A	.11	.034	.06
	Side B	.11	.029	.05
	Ave.	.11	.032	.055
75	Side A	.14	.011	.07
	Side B	.17	.046	.09
	Ave.	.155	.046	.08
100	Side A	.17	.029	.09
	Side B	.20	.051	.10
	Ave.	.185	.051	.095

Cobalt Cyclic Creep Data

Cyclic Test Number	2		
Alloy Designation	L605		
Heat Number	1860-2-1396		
Supplier	Cabot		
Test Temperature (°K)	1053°K		
Test Direction	Longitudinal		
Sheet Thickness (cm.)	0.025 cm. ± 0.003		
Specimen Number	L36L	L76L	L101L
Specimen Thickness (cm.)	.0267	.0269	.0267
Specimen Width (cm.)	1.2769	1.2786	1.2764
Applied Load (kg)	44.3	18.3	29.0
Test Stress (MPa)	127.6	52.2	83.4

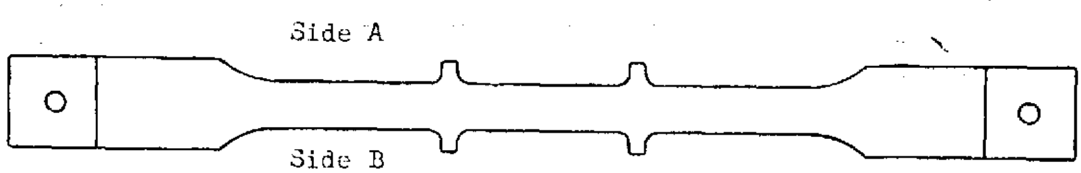

Cycle Number		% Creep L36L	% Creep L76L	% Creep L101L
1	Side A	.07	.02	.05
	Side B	.09	.01	.03
	Ave.	.08	.015	.04
5	Side A	.21	.05	.10
	Side B	.22	.04	.11
	Ave.	.215	.045	.105
15	Side A	.43	.08	.15
	Side B	.43	.07	.20
	Ave.	.43	.075	.175
25	Side A	.69	.09	.22
	Side B	.67	.09	.26
	Ave.	.68	.09	.24
50	Side A	1.13	.11	.32
	Side B	1.13	.11	.34
	Ave.	1.13	.11	.33
75	Side A	1.54	.13	.42
	Side B	1.53	.13	.39
	Ave.	1.535	.13	.405
100	Side A	1.91	.14	.47
	Side B	1.87	.15	.47
	Ave.	1.89	.145	.47

Cobalt Cyclic Creep Data

Cyclic Test Number	3		
Alloy Designation	L605		
Heat Number	1860-2-1396		
Supplier	Cabot		
Test Temperature (°K)	1144		
Test Direction	Longitudinal		
Sheet Thickness (cm)	0.025 ± 0.003		
Specimen Number	L53L	L61L	L37L
Specimen Thickness (cm)	0.025	0.025	0.025
Specimen Width (cm)	1.278	1.278	1.278
Applied Load (kg)	9.7	15.5	24.1
Test Stress (MPa)	29.6	47.2	73.5

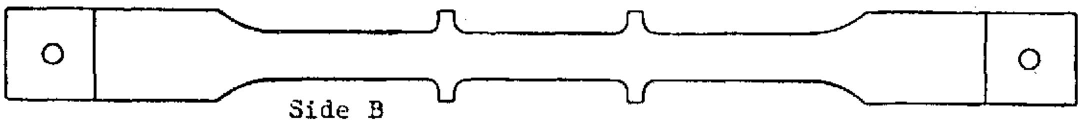

Cycle Number		% Creep L53L	L61L	L37L
1	Side A	.070	.090	.190
	Side B	.030	.100	.210
	Ave.	.050	.095	.200
5	Side A	.110	.170	.480
	Side B	.060	.160	.500
	Ave.	.085	.165	.490
15	Side A	.130	.190	.710
	Side B	.080	.220	.790
	Ave.	.105	.205	.750
25	Side A	.140	.220	.980
	Side B	.100	.250	1.000
	Ave.	.120	.235	.990
50	Side A	.150	.260	1.39
	Side B	.110	.280	1.31
	Ave.	.130	.270	1.35
75	Side A	.150	.300	1.640
	Side B	.120	.300	1.620
	Ave.	.135	.300	1.630
100	Side A	.160	.310	1.940
	Side B	.110	.350	1.930
	Ave.	.135	.330	1.935

Cobalt Cyclic Creep Data

Cyclic Test Number		4	
Alloy Designation		L605	
Heat Number		1860-2-1396	
Supplier		Cabot	
Test Temperature (°K)		1255	
Test Direction		Longitudinal	
Sheet Thickness (cm)		0.025 ± .003	
Specimen Number	L65L	L70L	L91L
Specimen Thickness (cm)	0.025	0.025	.025
Specimen Width (cm)	1.275	1.278	1.279
Applied Load (kg)	11.0	4.4	6.8
Test Stress (MPa)	33.8	13.2	20.5

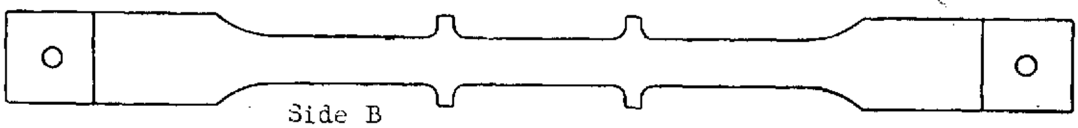

Cycle Number		% Creep L65L	L70L	L91L
1	Side A	.08	.00	.01
	Side B	.09	.00	.01
	Ave.	.085	.00	.01
5	Side A	.15	.03	.03
	Side B	.17	.01	.03
	Ave.	.16	.02	.03
15	Side A	.37	.03	.06
	Side B	.21	.03	.05
	Ave.	.29	.03	.055
25	Side A	.47	.05	.08
	Side B	.31	.03	.06
	Ave.	.39	.04	.07
50	Side A	.61	.05	.11
	Side B	.59	.05	.10
	Ave.	.60	.05	.105
75	Side A	.75	.06	.13
	Side B	.71	.06	.15
	Ave.	.73	.06	.14
100	Side A	.95	.06	.15
	Side B	.86	.06	.17
	Ave.	.905	.06	.16

Cobalt Cyclic Creep Data

Cyclic Test Number		5	
Alloy Designation		L605	
Heat Number		1860-2-1396	
Supplier		Cabot	
Test Temperature (°K)		1144	
Test Direction		Longitudinal	
Sheet Thickness (cm)		0.025 ± 0.003	
Specimen Number	L94L	L49L	L103L
Specimen Thickness (cm)	0.025	0.025	0.025
Specimen Width (cm)	1.276	1.277	1.275
Applied Load (Page C-3-7)			
Test Stress (Page C-3-7)			

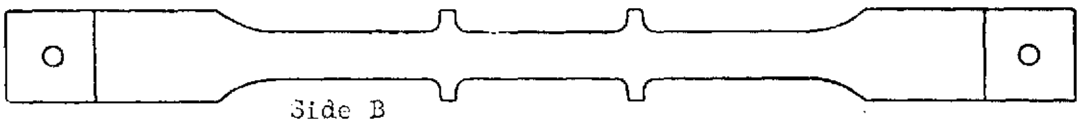

Cycle Number		% Creep L94L	L49L	L103L
1	Side A	.03	.06	.07
	Side B	.05	.06	.07
	Ave.	.04	.06	.07
5	Side A	.06	.11	.11
	Side B	.03	.09	.10
	Ave.	.055	.10	.105
15	Side A	.13	.31	.37
	Side B	.17	.29	.36
	Ave.	.15	.30	.365
25	Side A	.18	.39	.54
	Side B	.21	.39	.50
	Ave.	.195	.39	.52
50	Side A	.18	.39	.55
	Side B	.21	.42	.52
	Ave.	.195	.405	.535
75	Side A	.19	.40	.56
	Side B	.21	.42	.52
	Ave.	.20	.41	.54
100	Side A	.30	.55	.74
	Side B	.23	.56	.74
	Ave.	.27	.555	.74

L605 TEST 5

CYCLES	SPECIMEN L94L MEAN LOAD (LBS.) (kg)	STRESS (KSI) (MPa)	SPECIMEN L49L MEAN LOAD (LBS.) (kg)	STRESS (KSI) (MPa)	SPECIMEN L103L MEAN LOAD (LBS.) (kg)	STRESS (KSI) (MPa)
0-5	9.0	27.7	11.1	60.7	13.0	38.7
6-25	15.8	48.7	19.4	59.9	22.7	69.9
26-75	9.0	27.9	11.6	63.4	12.8	39.4
76-100	16.0	49.4	19.6	60.4	22.0	67.8

Cobalt Cyclic Creep Data

Cyclic Test Number		6	
Alloy Designation		L605	
Heat Number		1860-2-1396	
Supplier		Cabot	
Test Temperature (°K)		1144	
Test Direction		Longitudinal	
Sheet Thickness (cm)		0.025 + 0.003	
Specimen Number	L33L	L26L	L64L
Specimen Thickness (cm)	0.0255	0.0255	0.0259
Specimen Width (cm)	1.278	1.277	1.274
Applied Load (Page C-3-9)			
Test Stress (Page C-3-9)			

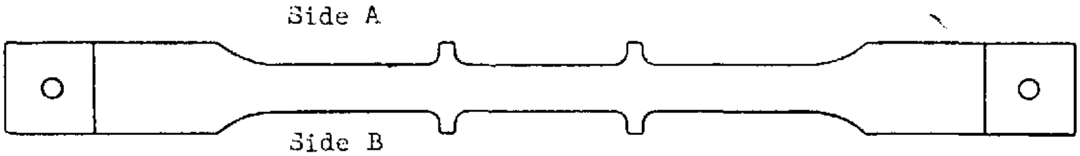

Cycle Number		% Creep L33L	% Creep L26L	% Creep L64L
1	Side A	.02	.05	.05
	Side B	.02	.04	.06
	Ave.	.02	.045	.055
5	Side A	.05	.08	.10
	Side B	.05	.06	.10
	Ave.	.05	.07	.10
15	Side A	.07	.13	.14
	Side B	.09	.10	.16
	Ave.	.08	.115	.15
25	Side A	.10	.14	.19
	Side B	.10	.13	.19
	Ave.	.10	.135	.19
50	Side A	.12	.22	.28
	Side B	.14	.19	.31
	Ave.	.13	.205	.295
75	Side A	.20	.36	.46
	Side B	.18	.37	.46
	Ave.	.19	.365	.46
100	Side A	.25	.54	.77
	Side B	.25	.50	.75
	Ave.	.25	.52	.76

L605 RUN 6

CYCLE	L33L LOAD (kg)	L33L STRESS (MPa)	L26L LOAD (kg)	L26L STRESS (MPa)	L64L LOAD (kg)	L64L STRESS (MPa)
0-5	9.1	27.6	11.1	33.7	13.8	41.0
6-15	10.2	30.8	12.4	37.6	14.8	44.1
16-25	10.9	33.3	13.7	41.6	16.2	48.3
26-35	12.0	36.5	14.7	44.7	17.0	51.7
36-45	12.9	39.2	15.7	47.6	18.2	54.2
46-55	14.0	42.5	17.1	52.1	19.8	58.9
56-66	15.1	45.9	18.4	55.8	2.10	62.5
67-75	16.1	49.0	19.5	59.3	22.2	66.1
76-86	16.7	50.8	20.7	62.8	23.7	70.5
86-95	18.2	55.4	26.4	66.3	24.7	73.5
96-100	19.2	58.3	23.1	70.1	25.9	77.2

Cobalt Cyclic Creep Data

Cyclic Test Number	7		
Alloy Designation	L605		
Heat Number	1820-2-1396		
Supplier	Cabot		
Test Temperature (°K)	1144		
Test Direction	Longitudinal		
Sheet Thickness (cm)	0.025 ± 0.003		
Specimen Number	L88L	L75L	L97L
Specimen Thickness (cm)	0.0254	0.0257	0.0259
Specimen Width (cm)	1.279	1.278	1.277
Applied Load (Page C-3-11)			
Test Stress (Page C-3-11)			

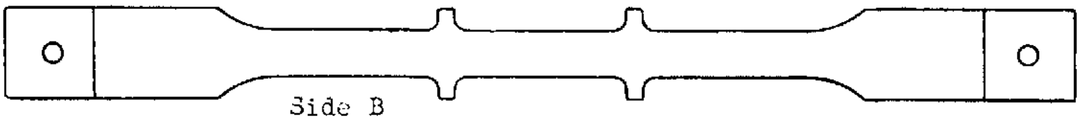

Cycle Number		% Creep L88L	% Creep L75L	% Creep L97L
1	Side A	.11	.18	.24
	Side B	.11	.19	.24
	Ave.	.11	.185	.24
5	Side A	.18	.36	.56
	Side B	.26	.39	.55
	Ave.	.22	.375	.555
15	Side A	.35	.55	.88
	Side B	.29	.60	.89
	Ave.	.32	.575	.885
25	Side A	.35	.64	.98
	Side B	.34	.66	1.09
	Ave.	.345	.65	1.035
50	Side A	.38	.72	1.09
	Side B	.37	.73	1.26
	Ave.	.375	.725	1.175
75	Side A	.38	.73	1.15
	Side B	.38	.76	1.27
	Ave.	.38	.745	1.21
100	Side A	.39	.74	1.19
	Side B	.38	.78	1.27
	Ave.	.389	.76	1.23

L605 RUN 7

CYCLE	SPECIMEN L88L MEAN LOAD (kg)	SPECIMEN L88L STRESS (MPa)	SPECIMEN L75L MEAN LOAD (kg)	SPECIMEN L75L STRESS (MPa)	SPECIMEN L97L MEAN LOAD (kg)	SPECIMEN L97L STRESS (MPa)
0-5	19.0	57.4	23.1	69.0	26.6	78.8
6-15	18.0	54.3	21.8	65.2	25.3	75.0
16-25	16.8	50.7	20.7	61.8	24.1	71.4
26-36	16.0	48.3	19.6	58.5	22.2	65.8
37-45	15.0	45.2	18.5	55.2	20.6	60.9
46-55	14.0	42.1	17.3	51.7	19.3	57.0
56-65	12.9	38.8	16.1	48.1	18.0	53.2
66-75	11.8	35.6	14.9	44.4	16.7	49.4
76-85	11.1	33.5	13.7	41.0	15.5	45.9
86-95	10.2	30.9	12.5	37.8	14.2	42.1
96-100	9.3	27.9	11.3	33.6	12.8	37.8

Cobalt Cyclic Creep Data

Cyclic Test Number		9	
Alloy Designation		L605	
Heat Number		1860-2-1396	
Supplier		Cabot	
Test Temperature (K°)		1144	
Test Direction		Longitudinal	
Sheet Thickness (cm)		0.025 ± 0.003	
Specimen Number	L35L	L30L	L67L
Specimen Thickness (cm)	.0246	.0249	.0249
Specimen Width (cm)	1.274	1.278	1.275
Applied Load (kg) (Per half cycle)	8.6/17.2	10.7/22.3	12.7/25.6
Test Stress (MPa) (Per half cycle)	26.9/53.7	33.0/68.6	39.2/78.9

Side A

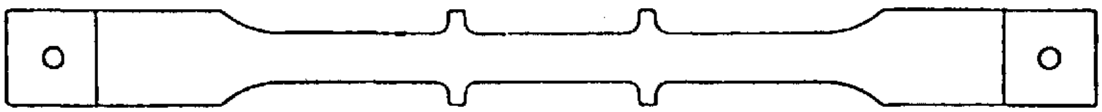

Side B

Cycle Number		% Creep L35L	% Creep L30L	% Creep L67L
1	Side A	.05	.10	.08
	Side B	.05	.10	.10
	Ave.	.05	.10	.09
5	Side A	.11	.25	.23
	Side B	.10	.28	.22
	Ave.	.105	.265	.225
15	Side A	.14	.42	.39
	Side B	.17	.45	.36
	Ave.	.155	.435	.375
25	Side A	.17	.49	.51
	Side B	.18	.53	.51
	Ave.	.175	.51	.51
50	Side A	.25	.65	.87
	Side B	.22	.69	.87
	Ave.	.235	.67	.87
75	Side A	.29	.79	1.17
	Side B	.25	.76	1.13
	Ave.	.27	.775	1.15
100	Side A	.30	.92	1.40
	Side B	.30	.89	1.42
	Ave.	.30	.905	1.41

Cobalt Cyclic Creep Data

Cyclic Test Number		10	
Alloy Designation		L605	
Heat Number		1860-2-1396	
Supplier		Cabot	
Test Temperature (°K)		1053	
Test Direction		Longitudinal	
Sheet Thickness (cm)		0.025 ± 0.003	
Specimen Number	L55L	L47L	L87L
Specimen Thickness (cm)	0.0246	0.0249	0.0246
Specimen Width (cm)	1.276	1.278	1.278
Applied Load (Page C-3-14)			
Test Stress (Page C-3-14)			

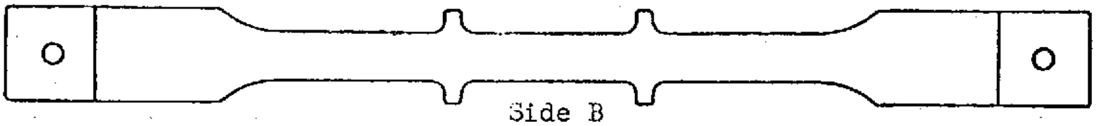

Cycle Number		% Creep L55L	% Creep L47L	% Creep L87L
1	Side A	.02	.04	.05
	Side B	.02	.03	.05
	Ave.	.02	.035	.05
5	Side A	.05	.09	.14
	Side B	.05	.09	.10
	Ave.	.05	.09	12
15	Side A	.13	.31	.51
	Side B	.16	.30	.48
	Ave.	.145	.305	.495
25	Side A	.19	.46	.74
	Side B	.18	.42	.72
	Ave.	.185	.44	.73
50	Side A	.21	.48	.78
	Side B	.18	.46	.84
	Ave.	.195	.47	.81
75	Side A	.21	.49	.82
	Side B	.19	.47	.82
	Ave.	.20	.48	.82
100	Side A	.28	.69	1.23
	Side B	.25	.71	1.21
	Ave.	.265	.70	1.22

L605 Test 10

	Specimen L55L		Specimen L47L		Specimen L87L	
Cycles	Mean Load (kg)	Stress (MPa)	Mean Load (kg)	Stress (MPa)	Mean Load (kg)	Stress (MPa)
1-5	14.7	45.6	21.2	65.6	27.6	85.6
6-25	27.1	76.9	35.3	109.4	44.1	136.7
26-75	15.3	47.5	21.7	67.2	27.6	85.4
76-100	25.4	78.6	35.4	109.6	44.3	137.3

Cobalt Cyclic Creep Data

Cyclic Test Number		8	
Alloy Designation		L605	
Heat Number		1860-2-1396	
Supplier		Cabot	
Test Temperature (°K)		1144	
Test Direction		Longitudinal	
Sheet Thickness (cm)		0.025 ± 0.003	
Specimen Number	L60L	L66L	L28L
Specimen Thickness (cm)	0.0264	0.0264	0.0264
Specimen Width (cm)	1.278	1.274	1.274
Applied Load (kg)	10.2	15.4	25.2
Test Stress (MPa)	29.4	45.3	73.1

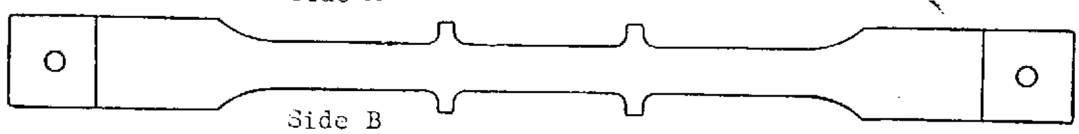

Cycle Number		% Creep L60L	L66L	L28L
2	Side A	.01	.05	.18
	Side B	.03	.06	.18
	Ave.	.02	.055	.18
10	Side A	.03	.10	.39
	Side B	.05	.11	.40
	Ave.	.04	.105	.395
30	Side A	.05	.14	.77
	Side B	.07	.16	.72
	Ave.	.06	.15	.745
50	Side A	.06	.17	.96
	Side B	.09	.20	.94
	Ave.	.075	.185	.95
100	Side A	.09	.21	1.34
	Side B	.09	.23	1.29
	Ave.	.09	.22	1.315

Cobalt Cyclic Creep Data

Cyclic Test Number	11	
Alloy Designation	L605	
Heat Number	1860-2-1396	
Supplier	Cabot	
Test Temperature (°K)	1144	
Test Direction	Longitudinal	
Sheet Thickness (cm)	0.025 ± 0.003	
Specimen Number	L38L	L43L
Specimen Thickness (cm)	0.0274	0.0257
Specimen Width (cm)	1.276	1.277
Applied Load (kg)	17.7	25.0
Test Stress (MPa)	49.9	75.9

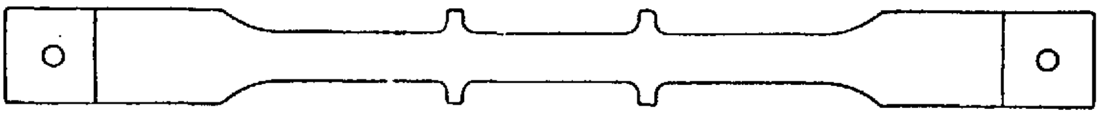

Cycle Number		% Creep L38L	% Creep L43L
1	Side A	.09	.22
	Side B	.09	.19
	Ave.	.09	.205
5	Side A	.17	.46
	Side B	.18	.46
	Ave.	.175	.46
15	Side A	.23	.78
	Side B	.25	.66
	Ave.	.24	.72
25	Side A	.33	.96
	Side B	.28	.87
	Ave.	.305	.915
50	Side A	.47	1.41
	Side B	.38	1.43
	Ave.	.425	1.42

Cobalt
Cyclic Creep Data

Cyclic Test Number	12		
Alloy Designation	L605		
Heat Number	1860-2-1396		
Supplier	Cabot		
Test Temperature (°K)	1144		
Test Direction	Longitudinal		
Sheet Thickness (cm)	0.025 ± 0.003		
Specimen Number	L77L	L71L	L86L
Specimen Thickness (cm)	0.0254	0.0249	0.0244
Specimen Width (cm)	1.2786	1.277	1.2788
Applied Load	See Table - Page C-3-18		
Test Stress	See Table - Page C-3-18		

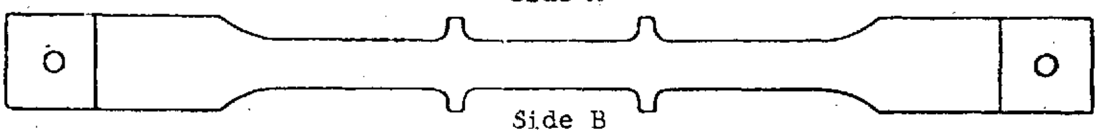

Cycle Number		% Creep L77L	% Creep L71L	% Creep L86L
1	Side A	.04	.06	.06
	Side B	.01	.07	.07
	Ave.	.025	.065	.065
5	Side A	.03	.08	.11
	Side B	.03	.10	.11
	Ave.	.03	.09	.11
15	Side A	.04	.11	.15
	Side B	.06	.13	.18
	Ave.	.05	.12	.165
25	Side A	.05	.15	.18
	Side B	.05	.13	.18
	Ave.	.05	.14	.18
50	Side A	.05	.15	.25
	Side B	.06	.17	.23
	Ave.	.055	.16	.24
75	Side A	.07	.19	.27
	Side B	.07	.18	.27
	Ave.	.07	.185	.27
100	Side A	.07	.19	.29
	Side B	.07	.19	.29
	Ave.	.07	.19	.29

L605 Test 12

SPECIMEN	LOAD ∿ Kg			
	1ST STEP (10 MINUTES)	2ND STEP (10 MINUTES)	3RD STEP (5 MINUTES)	4TH STEP (10 MINUTES)
L86L	5.5	11.2	19.7	24.4
L71L	4.5	9.3	16.4	19.6
L77L	3.4	6.4	11.3	13.7

SPECIMEN	STRESS ∿ MPa			
	1ST STEP (10 MINUTES)	2ND STEP (10 MINUTES)	3RD STEP (5 MINUTES)	4TH STEP (10 MINUTES)
L86L	17.2	35.2	62.0	76.6
L71L	13.8	28.6	50.7	60.3
L77L	9.2	19.4	34.1	41.3

Cobalt
Cyclic Creep Data

Cyclic Test Number	13		
Alloy Designation	L605		
Heat Number	1860-2-1396		
Supplier	Cabot		
Test Temperature (°K)	1144		
Test Direction	Longitudinal		
Sheet Thickness (cm.)	0.025 + 0.003		
Specimen Number	L41L	L32L	L63L
Specimen Thickness (cm.)	0.0251	0.0251	0.0254
Specimen Width (cm.)	1.2777	1.275	1.2778
Applied Load	See Table - Page C-3-20		
Test Stress	See Table - Page C-3-20		

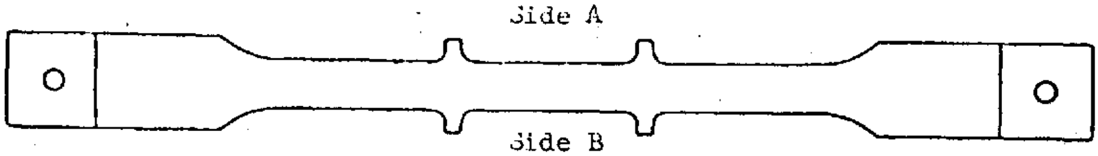

Cycle Number		% Creep L41L	L32L	L63L
1	Side A	.01	.04	.03
	Side B	.03	.05	.06
	Ave.	.02	.045	.045
5	Side A	.04	.07	.09
	Side B	.05	.09	.11
	Ave.	.045	.08	.10
15	Side A	.06	.10	.19
	Side B	.06	.13	.13
	Ave.	.06	.115	.16
25	Side A	.07	.11	.21
	Side B	.07	.15	.16
	Ave.	.07	.13	.185
50	Side A	.10	.14	.24
	Side B	.07	.17	.19
	Ave.	.085	.155	.215
75	Side A	.10	.19	.26
	Side B	.07	.18	.25
	Ave.	.085	.185	.255
100	Side A	.12	.18	.27
	Side B	.07	.20	.28
	Ave.	.095	.19	.275

L605 Test 13

	LOAD ∿ Kg			
SPECIMEN	1ST STEP (10 MINUTES)	2ND STEP (10 MINUTES)	3RD STEP (5 MINUTES)	4TH STEP (10 MINUTES)
L63L	5.7	11.7	20.6	25.4
L32L	4.6	9.3	16.2	19.1
L41L	3.5	7.1	12.4	14.9

	STRESS ∿ MPa			
SPECIMEN	1ST STEP (10 MINUTES)	2ND STEP (10 MINUTES)	3RD STEP (5 MINUTES)	4TH STEP (10 MINUTES)
L63L	17.2	35.2	62.1	76.7
L32L	14.1	28.4	49.6	58.4
L41L	10.8	21.8	37.8	45.5

Cobalt
Cyclic Creep Data

Cyclic Test Number	14 (Continuation of Test 3)		
Alloy Designation	L605		
Heat Number	1860-2-1396		
Supplier	Cabot		
Test Temperature (°K)	1144		
Test Direction	Longitudinal		
Sheet Thickness (cm)	0.025 ± 0.003		
Specimen Number	L53L	L61L	L37L
Specimen Thickness (cm)	0.025	0.025	0.025
Specimen Width (cm)	1.2778	1.2783	1.2776
Applied Load (kg)	9.1	15.6	24.8
Test Stress (MPa)	27.9	47.6	75.8

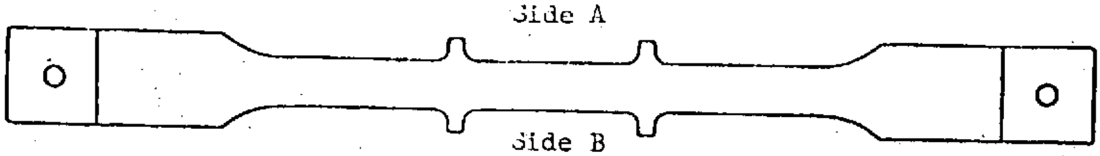

Cycle Number		% Creep * L53L	L61L	L37L
101	Side A	.00	-.01	.03
	Side B	-.01	.01	-.01
	Ave.	-.005	.00	.01
105	Side A	.00	.01	.08
	Side B	.00	.01	.10
	Ave.	.00	.01	.09
115	Side A	-.01	.01	.21
	Side B	.01	.01	.23
	Ave.	.00	.01	.22
125	Side A	.00	.04	.40
	Side B	.02	.02	.44
	Ave.	.01	.03	.42
150	Side A	.01	.08	.70
	Side B	.01	.05	.71
	Ave.	.01	.065	.705

* Creep strains are in addition to those obtained in Test 3.

C-4

Cobalt
Cyclic Creep Data

Cyclic Test Number	15		
Alloy Designation	L605		
Heat Number	1860-2-1396		
Supplier	Cabot		
Test Temperature	Trajectory (See Page C-3-23)		
Test Direction	Longitudinal		
Sheet Thickness (cm)	0.025 ± 0.003		
Specimen Number	L34L	L85L	L80L
Specimen Thickness (cm)	0.0251	0.0259	0.0256
Specimen Width (cm)	1.2743	1.2748	1.2781
Test Stress	(See Page C-3-23)		

Side A

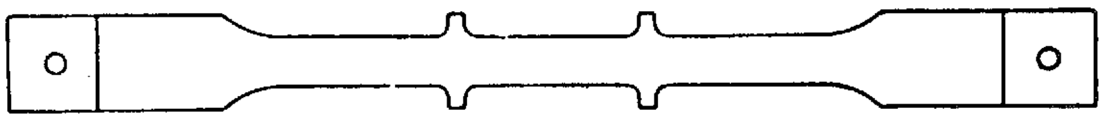

Side B

Cycle Number		% Creep L34L	% Creep L85L	% Creep L80L
1	Side A	.13	.27	.08
	Side B	.13	.25	.08
	Ave.	.13	.26	.08
5	Side A	.18	.52	.11
	Side B	.26	.40	.10
	Ave.	.22	.46	.105
15	Side A	.34	.75	.17
	Side B	.33	.66	.15
	Ave.	.335	.705	.16
25	Side A	.37	1.07	.19
	Side B	.35	1.03	.17
	Ave.	.36	1.05	.18
50	Side A	.55	1.68	.25
	Side B	.66	1.70	.22
	Ave.	.605	1.69	.235
75	Side A	.79	2.39	.29
	Side B	.79	2.41	.26
	Ave.	.79	2.40	.275
100	Side A	.97	3.40	.32
	Side B	1.02	3.43	.30
	Ave.	.995	3.415	.31
150	Side A	1.26	-	.37
	Side B	1.33		.38
	Ave.	1.295		.375
200	Side A	1.53	-	.44
	Side B	1.59		.38
	Ave.	1.55		.41

L605 TEST 15

CYCLE TIME (SEC)	TEMP. (°K)	PRESSURE- Pa.	STRESS ∿ MPa		
			SPEC L34L	SPEC L85L	SPEC L80L
300	561	.4	-	-	-
400	1005	2.0	14.9	19.4	10.8
500	1133	2.7	26.3	34.2	19.0
600	1178	3.3	33.2	43.1	24.1
700	1200	4.0	37.5	48.3	27.4
800	1200	4.7	41.1	52.2	30.2
900	1189	5.3	42.6	53.8	31.6
1000	1178	6.9	45.0	55.0	32.5
1100	1161	8.5	47.4	59.4	35.4
1200	1150	9.3	51.4	64.5	38.5
1300	1139	10.7	58.7	73.6	43.9
1400	1128	16.0	64.4	80.8	48.2
1500	1111	24.0	73.9	92.7	55.4
1600	1089	40.0	84.5	105.9	63.3
1700	1039	44.0	90.4	114.5	68.3
1800	955	80.0	99.0	125.8	75.7
1900	872	113.3	104.0	132.8	79.8
2000	744	200.0	103.4	132.9	79.5
2100	639	466.6	94.0	122.0	72.1
2200	550	1466.3	83.2	109.0	63.8
2300	478	4478.9	68.1	89.5	52.2
2400	311	11597.1	46.1	62.5	34.5
2500	311	18795.3	27.5	37.7	19.9

APPENDIX D-1

Ti-6Al-4V LITERATURE SURVEY RAW CREEP DATA

This section contains the raw creep data developed on sheet produced by two suppliers TIMET (data on pages D-1-2 to D-1-7) and Reactive Metals (data on pages D-1-8 to D-1-12).

ALLOY - T-6AL-4V
STRESS (MPA) - 551.6
TEMP. (KELVIN) - 589
THICKNESS (CM) - .160
SOURCE - AFMLTR6-259

STRAIN (PCT.)	TIME (HOURS)
.010	.5
.020	1.5
.030	5.0
.040	10.0
.050	50.0
.060	75.0
.080	100.0
.120	250.0
.160	500.0
.180	750.0
.210	1000.0

ALLOY - T-6AL-4V
STRESS (MPA) - 551.6
TEMP. (KELVIN) - 589
THICKNESS (CM) - .160
SOURCE - AFMLTR6-259

STRAIN (PCT.)	TIME (HOURS)
.030	.5
.040	1.0
.050	1.5
.060	5.0
.070	15.0
.080	25.0
.110	50.0
.120	75.0
.130	100.0
.160	250.0
.190	500.0
.210	750.0
.310	1000.0

ALLOY - T-6AL-4V
STRESS (MPA) - 551.6
TEMP. (KELVIN) - 589
THICKNESS (CM) - .160
SOURCE - AFMLTR6-259

STRAIN (PCT.)	TIME (HOURS)
.040	.5
.050	1.0
.060	1.5
.070	2.5
.080	5.0
.090	10.0
.100	15.0
.120	25.0
.160	50.0
.170	75.0
.190	100.0
.230	250.0
.280	500.0
.310	750.0
.340	1000.0

ALLOY - T-6AL-4V
STRESS (MPA) - 551.6
TEMP. (KELVIN) - 589
THICKNESS (CM) - .160
SOURCE - AFMLTR6-259

STRAIN (PCT.)	TIME (HOURS)
.010	1.0
.020	2.5
.030	5.0
.040	7.5
.050	50.0
.060	100.0

ALLOY - T-6AL-4V
STRESS (MPA) - 586.0
TEMP. (KELVIN) - 589
THICKNESS (CM) - .160
SOURCE - AFMLTR6-259

STRAIN (PCT.)	TIME (HOURS)
.030	.5
.040	1.0
.050	1.5
.060	2.5
.090	5.0
.100	10.0
.120	15.0
.140	25.0
.170	50.0
.190	75.0
.210	100.0
.250	250.0
.310	500.0
.370	750.0
.430	1000.0

ALLOY - T-6AL-4V
STRESS (MPA) - 275.8
TEMP. (KELVIN) - 700
THICKNESS (CM) - .102
SOURCE - AFMLTR6-259

STRAIN (PCT.)	TIME (HOURS)
.030	.5
.050	1.0
.060	1.55
.080	2.5
.120	5.0
.150	7.5
.180	10.0
.220	15.0
.270	25.0
.340	50.0
.400	75.0
.470	100.0

ALLOY - T-6AL-4V
STRESS (MPA) - 344.7
TEMP. (KELVIN) - 700
THICKNESS (CM) - .102
SOURCE - AFMLTR6-259

STRAIN (PCT.)	TIME (HOURS)
.080	.5
.100	1.0
.110	1.5
.120	2.5
.160	5.0
.190	7.5
.210	10.0
.240	15.0
.310	25.0
.460	50.0

ALLOY - T-6AL-4V
STRESS (MPA) - 137.9
TEMP. (KELVIN) - 700
THICKNESS (CM) - .160
SOURCE - AFMLTR6-259

STRAIN (PCT.)	TIME (HOURS)
.010	2.5
.020	5.0
.030	10.0
.040	15.0
.050	25.0
.090	50.0
.110	75.0
.130	100.0
.210	250.0
.270	500.0
.320	750.0
.360	1000.0

ALLOY - T-6AL-4V
STRESS (MPA) - 137.9
TEMP. (KELVIN) - 700
THICKNESS (CM) - .160
SOURCE - AFMLTR6-259

STRAIN (PCT.)	TIME (HOURS)
.040	10.0
.050	15.0
.070	25.0
.110	50.0
.130	75.0
.150	100.0
.180	250.0
.250	500.0
.300	750.0
.340	1000.0

ALLOY - T-6AL-4V
STRESS (MPA) - 172.4
TEMP. (KELVIN) - 700
THICKNESS (CM) - .160
SOURCE - AFMLTR6-259

STRAIN (PCT.)	TIME (HOURS)
.030	.5
.040	1.0
.050	1.5
.060	2.5
.080	5.0
.100	7.5
.110	15.0
.130	25.0
.160	50.0
.180	75.0
.210	100.0
.300	250.0
.380	500.0
.460	750.0

ALLOY - T-6AL-4V
STRESS (MPA) - 172.4
TEMP. (KELVIN) - 700
THICKNESS (CM) - .160
SOURCE - AFMLTR6-259

STRAIN (PCT.)	TIME (HOURS)
.020	5.0
.030	10.0
.040	15.0
.060	25.0
.080	50.0
.100	75.0
.120	100.0
.170	250.0
.230	500.0
.290	750.0
.330	1000.0

ALLOY - T-6AL-4V
STRESS (MPA) - 172.4
TEMP. (KELVIN) - 700
THICKNESS (CM) - .160
SOURCE - AFMLTR6-259

STRAIN (PCT.)	TIME (HOURS)
.020	.5
.030	1.0
.040	2.5
.050	5.0
.060	10.0
.080	15.0
.100	25.0
.170	50.0
.210	75.0
.240	100.0
.340	250.0
.430	500.0
.500	750.0

ALLOY - T-6AL-4V
STRESS (MPA) - 206.8
TEMP. (KELVIN) - 700
THICKNESS (CM) - .160
SOURCE - AFMLTR6-259

STRAIN (PCT.)	TIME (HOURS)
.030	.5
.040	1.0
.050	2.5
.060	5.0
.070	7.5
.080	10.0
.090	15.0
.120	25.0
.170	50.0
.210	75.0
.240	100.0
.370	250.0

ALLOY - T-6AL-4V
STRESS (MPA) - 241.3
TEMP. (KELVIN) - 700
THICKNESS (CM) - .160
SOURCE - AFMLTR6-259

STRAIN (PCT.)	TIME (HOURS)
.020	5.0
.040	7.5
.050	10.0
.070	15.0
.100	25.0
.140	50.0
.170	75.0
.200	100.0
.330	250.0
.430	500.0

ALLOY - T-6AL-4V
STRESS (MPA) - 241.3
TEMP. (KELVIN) - 700
THICKNESS (CM) - .160
SOURCE - AFMLTR6-259

STRAIN (PCT.)	TIME (HOURS)
.040	.5
.050	1.0
.070	1.5
.080	2.5
.090	5.0
.100	7.5
.110	10.0
.130	15.0
.150	25.0
.200	50.0
.240	75.0
.270	100.0
.390	250.0

ALLOY - T-6AL-4V
STRESS (MPA) - 241.3
TEMP. (KELVIN) - 700
THICKNESS (CM) - .160
SOURCE - AFMLTR6-259

STRAIN (PCT.)	TIME (HOURS)
.060	5.0
.080	7.5
.090	10.0
.120	15.0
.160	25.0
.260	50.0
.320	75.0
.370	100.0

ALLOY - T-6AL-4V
STRESS (MPA) - 310.3
TEMP. (KELVIN) - 700
THICKNESS (CM) - .160
SOURCE - AFMLTR6-259

STRAIN (PCT.)	TIME (HOURS)
.040	.5
.050	1.0
.060	1.5
.070	2.5
.080	5.0
.100	7.5
.120	10.0
.150	15.0
.250	25.0
.320	50.0
.400	75.0
.460	100.0

ALLOY - T-6AL-4V
STRESS (MPA) - 413.7
TEMP. (KELVIN) - 700
THICKNESS (CM) - .160
SOURCE - AFMLTR6-259

STRAIN (PCT.)	TIME (HOURS)
.060	.5
.090	1.0
.120	1.5
.140	2.5
.160	5.0
.180	7.5
.200	10.0
.230	15.0
.280	25.0
.380	50.0
.450	75.0

ALLOY - T-6AL-4V
STRESS (MPA) - 413.7
TEMP. (KELVIN) - 700
THICKNESS (CM) - .160
SOURCE - AFMLTR6-259

STRAIN (PCT.)	TIME (HOURS)
.200	1.5
.270	2.5
.390	5.0
.470	7.5

ALLOY - T-6AL-4V
STRESS (MPA) - 51.7
TEMP. (KELVIN) - 811
THICKNESS (CM) - .102
SOURCE - AFMLTR6-259

STRAIN (PCT.)	TIME (HOURS)
.020	.5
.030	1.0
.050	1.5
.070	2.5
.120	5.0
.180	7.5
.210	10.0
.290	15.0
.430	25.0

ALLOY - T-6AL-4V
STRESS (MPA) - 8.3
TEMP. (KELVIN) - 811
THICKNESS (CM) - .160
SOURCE - AFMLTR6-259

STRAIN (PCT.)	TIME (HOURS)
.020	2.5
.030	7.5
.040	25.0
.050	50.0
.070	75.0
.080	100.0
.160	250.0
.250	500.0
.320	750.0
.360	1000.0

ALLOY - T-6AL-4V
STRESS (MPA) - 27.6
TEMP. (KELVIN) - 811
THICKNESS (CM) - .102
SOURCE - AFMLTR6-259

STRAIN (PCT.)	TIME (HOURS)
.010	.5
.020	1.0
.030	1.5
.040	2.5
.060	5.0
.080	7.5
.090	10.0
.110	15.0
.150	25.0
.250	50.0
.340	75.0
.440	100.0

ALLOY - T-6AL-4V
STRESS (MPA) - 172.4
TEMP. (KELVIN) - 811
THICKNESS (CM) - .102
SOURCE - AFMLTR6-259

STRAIN (PCT.)	TIME (HOURS)
.200	.5
.330	1.0

ALLOY - T-6AL-4V
STRESS (MPA) - 8.3
TEMP. (KELVIN) - 811
THICKNESS (CM) - .160
SOURCE - AFMLTR6-259

STRAIN (PCT.)	TIME (HOURS)
.010	10.0
.020	25.0
.030	50.0
.040	100.0
.090	250.0
.170	500.0
.250	750.0
.310	1000.0

ALLOY - T-6AL-4V
STRESS (MPA) - 34.5
TEMP. (KELVIN) - 811
THICKNESS (CM) - .102
SOURCE - AFMLTR6-259

STRAIN (PCT.)	TIME (HOURS)
.020	.5
.030	1.0
.040	1.5
.060	2.5
.090	5.0
.100	7.5
.130	10.0
.170	15.0
.220	25.0
.360	50.0
.450	75.0

ALLOY - T-6AL-4V
STRESS (MPA) - 6.9
TEMP. (KELVIN) - 811
THICKNESS (CM) - .160
SOURCE - AFMLTR6-259

STRAIN (PCT.)	TIME (HOURS)
.010	1.0
.020	2.5
.030	7.5
.040	15.0
.050	25.0
.090	50.0
.120	75.0
.140	100.0
.200	250.0
.230	500.0
.240	750.0
.260	1000.0

ALLOY - T-6AL-4V
STRESS (MPA) - 10.3
TEMP. (KELVIN) - 811
THICKNESS (CM) - .160
SOURCE - AFMLTR6-259

STRAIN (PCT.)	TIME (HOURS)
.010	75.0
.030	100.0
.080	250.0
.160	500.0
.250	750.0
.330	1000.0

ALLOY - T-6AL-4V
STRESS (MPA) - 13.8
TEMP. (KELVIN) - 811
THICKNESS (CM) - .160
SOURCE - AFMLTR6-259

STRAIN (PCT.)	TIME (HOURS)
.010	2.5
.020	5.0
.030	10.0
.040	25.0
.050	50.0
.070	75.0
.080	100.0
.170	250.0
.320	500.0
.450	750.0

ALLOY - T-6AL-4V
STRESS (MPA) - 68.9
TEMP. (KELVIN) - 811
THICKNESS (CM) - .160
SOURCE - AFMLTR6-259

STRAIN (PCT.)	TIME (HOURS)
.050	5.0
.060	7.5
.080	10.0
.100	15.0
.170	25.0
.300	50.0
.400	75.0
.500	100.0

ALLOY - T-6AL-4V
STRESS (MPA) - 10.3
TEMP. (KELVIN) - 811
THICKNESS (CM) - .160
SOURCE - AFMLTR6-259

STRAIN (PCT.)	TIME (HOURS)
.010	2.5
.020	7.5
.030	15.0
.050	25.0
.120	50.0
.170	75.0
.230	100.0

ALLOY - T-6AL-4V
STRESS (MPA) - 13.8
TEMP. (KELVIN) - 811
THICKNESS (CM) - .160
SOURCE - AFMLTR6-259

STRAIN (PCT.)	TIME (HOURS)
.040	5.0
.060	7.5
.090	10.0
.100	15.0
.110	25.0
.150	50.0
.180	75.0
.210	100.0
.300	250.0
.410	500.0
.500	750.0

ALLOY - T-6AL-4V
STRESS (MPA) - 68.9
TEMP. (KELVIN) - 811
THICKNESS (CM) - .160
SOURCE - AFMLTR6-259

STRAIN (PCT.)	TIME (HOURS)
.100	1.0
.130	1.5
.150	2.5
.200	5.0
.250	7.5
.300	10.0
.400	15.0

ALLOY - T-6AL-4V
STRESS (MPA) - 10.3
TEMP. (KELVIN) - 811
THICKNESS (CM) - .160
SOURCE - AFMLTR6-259

STRAIN (PCT.)	TIME (HOURS)
.010	.5
.020	2.5
.030	7.5
.040	15.0
.050	25.0
.070	50.0
.090	75.0
.100	100.0
.160	250.0
.230	500.0
.290	750.0
.350	1000.0

ALLOY - T-6AL-4V
STRESS (MPA) - 13.8
TEMP. (KELVIN) - 811
THICKNESS (CM) - .160
SOURCE - AFMLTR6-259

STRAIN (PCT.)	TIME (HOURS)
.020	2.5
.030	7.5
.040	15.0
.050	25.0
.090	50.0
.110	75.0
.140	100.0
.260	250.0
.430	500.0

ALLOY - T-6AL-4V
STRESS (MPA) - 82.7
TEMP. (KELVIN) - 811
THICKNESS (CM) - .160
SOURCE - AFMLTR6-259

STRAIN (PCT.)	TIME (HOURS)
.310	5.0
.410	7.5
.480	10.0

ALLOY - T-6AL-4V
STRESS (MPA) - 82.7
TEMP. (KELVIN) - 811
THICKNESS (CM) - .160
SOURCE - AFMLTR6-259

STRAIN (PCT.)	TIME (HOURS)
.210	5.0
.270	7.5
.330	10.0
.440	15.0

ALLOY - T-6AL-4V
STRESS (MPA) - 86.2
TEMP. (KELVIN) - 811
THICKNESS (CM) - .160
SOURCE - AFMLTR6-259

STRAIN (PCT.)	TIME (HOURS)
.100	1.5
.150	2.5
.250	5.0
.330	7.5
.380	10.0

ALLOY - T-6AL-4V
STRESS (MPA) - 103.4
TEMP. (KELVIN) - 811
THICKNESS (CM) - .160
SOURCE - AFMLTR6-259

STRAIN (PCT.)	TIME (HOURS)
.200	1.5
.300	2.5
.450	5.0

ALLOY - T-6AL-4V
STRESS (MPA) - 103.4
TEMP. (KELVIN) - 811
THICKNESS (CM) - .160
SOURCE - AFMLTR6-259

STRAIN (PCT.)	TIME (HOURS)
.100	.5
.130	1.0
.170	1.5
.240	2.5
.400	5.0

ALLOY - T-6AL-4V
STRESS (MPA) - 110.3
TEMP. (KELVIN) - 811
THICKNESS (CM) - .160
SOURCE - AFMLTR6-259

STRAIN (PCT.)	TIME (HOURS)
.120	.5
.180	1.0
.240	1.5
.320	2.5
.500	5.0

ALLOY - T-6AL-4V
STRESS (MPA) - 137.9
TEMP. (KELVIN) - 811
THICKNESS (CM) - .160
SOURCE - AFMLTR6-259

STRAIN (PCT.)	TIME (HOURS)
.150	1.0
.250	1.5
.350	2.5

ALLOY - T-6AL-4V
STRESS (MPA) - 137.9
TEMP. (KELVIN) - 811
THICKNESS (CM) - .160
SOURCE - AFMLTR6-259

STRAIN (PCT.)	TIME (HOURS)
.200	.5
.270	1.0
.330	1.5
.440	2.5

ALLOY - TD NICR
STRESS (MPA) - 93.1
TEMP. (KELVIN) - 1033
THICKNESS (CM) - .038
TEST DIRECTION - TRANS.
SOURCE - NAS-8-27189

STRAIN (PCT.)	TIME (HOURS)
.095	2.0
.150	6.0
.195	18.0
.215	26.0
.234	40.0
.250	65.0
.270	120.0
.290	185.0
.310	240.0

ORIGINAL PAGE IS OF POOR QUALITY

ALLOY - T-6AL-4V
STRESS (MPA) - 448.2
TEMP. (KELVIN) - 589
THICKNESS (CM) - .160
SOURCE - AFMLTR6-259

STRAIN (PCT.)	TIME (HOURS)
.038	19.700
.069	45.200
.094	70.100
.099	93.000
.125	164.900
.135	213.800
.146	287.300
.152	359.900
.164	429.300
.168	477.300
.171	528.600
.182	597.400
.187	646.600
.190	721.500
.203	789.600
.206	820.400
.210	861.900
.216	933.400
.222	980.800
.229	1052.800
.235	1105.700

ALLOY - T-6AL-4V
STRESS (MPA) - 461.9
TEMP. (KELVIN) - 589
THICKNESS (CM) - .160
SOURCE - AFMLTR6-259

STRAIN (PCT.)	TIME (HOURS)
.048	19.800
.087	43.200
.117	65.500
.141	91.000
.156	115.300
.172	163.800
.177	186.800
.190	260.100
.198	306.200
.203	331.200
.211	378.900
.216	427.000
.229	470.700
.232	498.400
.236	546.400
.242	570.000
.246	594.300
.255	643.100
.263	691.000
.272	719.000
.275	769.200
.284	818.400
.289	865.500
.302	919.600
.307	943.000

ALLOY - T-6AL-4V
STRESS (MPA) - 475.7
TEMP. (KELVIN) - 589
THICKNESS (CM) - .160
SOURCE - AFMLTR6-259

STRAIN (PCT.)	TIME (HOURS)
.074	18.500
.139	44.100
.174	69.000
.192	92.000
.206	115.700
.220	140.100
.228	163.700
.242	191.100
.250	212.700
.255	236.100
.263	260.000
.269	285.200
.285	332.200
.291	358.800
.318	452.200
.323	476.200
.336	527.500
.348	571.800
.367	645.600
.370	693.500
.388	740.600
.409	788.500
.416	836.300
.424	860.800
.439	908.000
.451	956.200
.457	979.900
.474	1051.700
.481	1076.500
.488	1100.400

ALLOY - T-6AL-4V
STRESS (MPA) - 496.4
TEMP. (KELVIN) - 589
THICKNESS (CM) - .160
SOURCE - AFMLTR6-259

STRAIN (PCT.)	TIME (HOURS)
.033	2.500
.162	19.000
.184	26.700
.223	43.500
.228	50.400
.247	66.100
.266	91.500
.288	115.300
.292	122.600
.308	139.000
.327	162.700
.349	186.800
.365	211.100
.386	234.700
.434	283.000
.455	306.800
.473	331.300
.491	355.100

ALLOY - T-6AL-4V
STRESS (MPA) - 627.4
TEMP. (KELVIN) - 589
THICKNESS (CM) - .160
SOURCE - AFMLTR6-259

STRAIN (PCT.)	TIME (HOURS)
.026	.050
.049	.100
.100	.200
.221	.500
.335	.700
.398	.900

ALLOY - T-6AL-4V
STRESS (MPA) - 537.8
TEMP. (KELVIN) - 589
THICKNESS (CM) - .160
SOURCE - AFMLTR6-259

STRAIN (PCT.)	TIME (HOURS)
.037	.500
.060	.900
.063	1.600
.074	2.200
.160	2.300
.287	4.500
.489	6.300

ALLOY - T-6AL-4V
STRESS (MPA) - 565.4
TEMP. (KELVIN) - 589
THICKNESS (CM) - .160
SOURCE - AFMLTR6-259

STRAIN (PCT.)	TIME (HOURS)
.071	.200
.086	.500
.097	1.100
.112	1.600
.141	2.300
.189	3.100
.261	4.100
.373	5.500

ALLOY - T-6AL-4V
STRESS (MPA) - 655.0
TEMP. (KELVIN) - 589
THICKNESS (CM) - .160
SOURCE - AFMLTR6-259

STRAIN (PCT.)	TIME (HOURS)
.072	.100
.154	.200
.230	.300
.292	.400
.392	.500
.470	.600

ALLOY - T-6AL-4V
STRESS (MPA) - 689.5
TEMP. (KELVIN) - 589
THICKNESS (CM) - .160
SOURCE - AFMLTR6-259

STRAIN (PCT.)	TIME (HOURS)
.032	.020
.071	.030
.148	.070
.199	.100
.265	.130
.351	.170
.403	.200
.497	.250
.059	19.600
.068	25.300
.103	42.500
.137	66.100
.149	90.300
.171	114.800
.185	162.000
.192	186.200
.196	210.200
.202	233.600
.209	305.700
.212	330.300
.219	378.500
.219	426.200
.233	470.200
.235	497.700
.245	521.700
.252	593.600
.254	642.600
.273	717.700
.273	766.100
.282	815.000
.289	866.700
.295	916.200
.301	940.500
.305	949.700

ORIGINAL PAGE IS OF POOR QUALITY

ALLOY - T-6AL-4V
STRESS (MPA) - 205.9
TEMP. (KELVIN) - 700
THICKNESS (CM) - .160
SOURCE - AFMLTR6-259

STRAIN (PCT.)	TIME (HOURS)
.072	18.700
.159	43.900
.190	67.100
.221	91.500
.235	115.400
.259	139.300
.275	163.500
.282	187.200
.309	235.000
.322	259.300
.337	283.700
.343	307.800
.351	331.200
.356	354.400
.373	403.900
.394	451.100
.405	499.000
.429	571.700
.442	595.300
.445	619.600
.464	692.900
.485	738.500
.496	783.800

ALLOY - T-6AL-4V
STRESS (MPA) - 255.1
TEMP. (KELVIN) - 700
THICKNESS (CM) - .160
SOURCE - AFMLTR6-259

STRAIN (PCT.)	TIME (HOURS)
.099	18.200
.207	42.000
.269	66.000
.310	90.200
.347	113.800
.405	161.600
.419	185.900
.446	210.300
.452	234.900
.469	257.900
.490	281.000

ALLOY - T-6AL-4V
STRESS (MPA) - 279.2
TEMP. (KELVIN) - 700
THICKNESS (CM) - .160
SOURCE - AFMLTR6-259

STRAIN (PCT.)	TIME (HOURS)
.217	17.200
.239	24.200
.275	39.300
.332	65.000
.370	89.900
.409	112.800
.458	136.700
.492	161.100

ALLOY - T-6AL-4V
STRESS (MPA) - 310.3
TEMP. (KELVIN) - 700
THICKNESS (CM) - .160
SOURCE - AFMLTR6-259

STRAIN (PCT.)	TIME (HOURS)
.062	.300
.087	1.500
.195	4.600
.300	18.500
.317	26.200
.382	42.700
.409	50.300
.453	67.200
.465	74.100
.488	89.900

ALLOY - T-6AL-4V
STRESS (MPA) - 399.9
TEMP. (KELVIN) - 700
THICKNESS (CM) - .160
SOURCE - AFMLTR6-259

STRAIN (PCT.)	TIME (HOURS)
.090	.700
.188	2.500
.302	5.100

ALLOY - T-6AL-4V
STRESS (MPA) - 455.1
TEMP. (KELVIN) - 700
THICKNESS (CM) - .160
SOURCE - AFMLTR6-259

STRAIN (PCT.)	TIME (HOURS)
.096	.100
.179	.300
.261	.500
.287	.600
.299	.650
.304	.700
.362	.900
.408	1.100
.493	1.500

ALLOY - T-6AL-4V
STRESS (MPA) - 493.0
TEMP. (KELVIN) - 700
THICKNESS (CM) - .160
SOURCE - AFMLTR6-259

STRAIN (PCT.)	TIME (HOURS)
.153	.050
.225	.100
.278	.150
.332	.200
.420	.300
.497	.400

ALLOY - T-6AL-4V
STRESS (MPA) - 517.1
TEMP. (KELVIN) - 700
THICKNESS (CM) - .160
SOURCE - AFMLTR6-259

STRAIN (PCT.)	TIME (HOURS)
.107	.020
.187	.030
.243	.050
.275	.070
.317	.080
.363	.100
.421	.130
.470	.170
.499	.180

ORIGINAL PAGE IS OF POOR QUALITY

ALLOY - T-6AL-4V
STRESS (MPA) - 551.6
TEMP. (KELVIN) - 700
THICKNESS (CM) - .160
SOURCE - AFMLTR6-259

STRAIN (PCT.)	TIME (HOURS)
.084	.010
.192	.020
.229	.025
.283	.030
.334	.040
.387	.050
.472	.070

ALLOY - T-6AL-4V
STRESS (MPA) - 579.2
TEMP. (KELVIN) - 700
THICKNESS (CM) - .160
SOURCE - AFMLTR6-259

STRAIN (PCT.)	TIME (HOURS)
.287	.020
.445	.030

ALLOY - T-6AL-4V
STRESS (MPA) - 620.5
TEMP. (KELVIN) - 700
THICKNESS (CM) - .160
SOURCE - AFMLTR6-259

STRAIN (PCT.)	TIME (HOURS)
.275	.004
.413	.008
.005	3.800
.012	19.600
.043	68.300
.061	92.100
.105	165.600
.117	235.700
.125	260.500
.139	308.500
.142	351.900
.156	404.600
.171	455.000
.177	500.300
.182	549.200
.210	621.400
.232	670.500
.241	740.400
.257	790.100
.269	863.600
.290	932.700
.305	1004.100

ALLOY - T-6AL-4V
STRESS (MPA) - 10.3
TEMP. (KELVIN) - 811
THICKNESS (CM) - .160
SOURCE - AFMLTR6-259

STRAIN (PCT.)	TIME (HOURS)
.008	2.8
.014	4.3
.031	21.1
.043	28.6
.070	47.3
.101	69.8
.144	117.7
.164	142.4
.182	165.7
.216	217.0
.221	236.3
.248	286.0
.253	309.6
.266	335.0
.275	382.9
.302	430.0
.326	478.3
.345	549.6
.380	621.3
.393	645.7
.406	695.3
.429	740.7
.433	766.2
.442	789.9
.452	820.7
.470	845.1
.484	870.0
.491	895.3

ALLOY - T-6AL-4V
STRESS (MPA) - 15.2
TEMP. (KELVIN) - 811
THICKNESS (CM) - .160
SOURCE - AFMLTR6-259

STRAIN (PCT.)	TIME (HOURS)
.014	2.400
.018	5.600
.069	23.300
.105	46.800
.147	70.400
.202	94.700
.276	142.600
.325	194.000
.347	213.400
.411	263.000
.434	312.000
.493	359.900

ALLOY - T-6AL-4V
STRESS (MPA) - 34.5
TEMP. (KELVIN) - 811
THICKNESS (CM) - .160
SOURCE - AFMLTR6-259

STRAIN (PCT.)	TIME (HOURS)
.031	1.000
.052	3.100
.067	4.900
.142	17.000
.164	21.200
.181	23.400
.263	41.400
.291	48.100
.370	65.400
.466	89.000

ALLOY - T-6AL-4V
STRESS (MPA) - 17.2
TEMP. (KELVIN) - 811
THICKNESS (CM) - .160
SOURCE - AFMLTR6-259

STRAIN (PCT.)	TIME (HOURS)
.004	1.100
.060	17.600
.073	25.000
.121	40.500
.165	65.800
.218	90.400
.263	113.600
.300	137.600
.341	162.000
.384	186.100
.430	213.000
.465	234.400

ORIGINAL PAGE IS OF POOR QUALITY

ALLOY - T-6AL-4V
STRESS (MPA) - 75.8
TEMP. (KELVIN) - 811
THICKNESS (CM) - .160
SOURCE - AFMLTR6-259

STRAIN (PCT.)	TIME (HOURS)
.078	.500
.122	1.000
.152	1.600
.171	2.000
.199	3.000
.237	4.000
.260	4.900
.272	5.500
.285	6.200
.299	6.600
.305	7.100

ALLOY - T-6AL-4V
STRESS (MPA) - 151.7
TEMP. (KELVIN) - 811
THICKNESS (CM) - .160
SOURCE - AFMLTR6-259

STRAIN (PCT.)	TIME (HOURS)
.070	.100
.107	.200
.128	.300
.177	.500
.212	.700
.240	.900
.262	1.100
.290	1.300
.300	1.350
.382	2.000
.427	2.500
.473	3.000
.494	3.200

ALLOY - T-6AL-4V
STRESS (MPA) - 206.8
TEMP. (KELVIN) - 811
THICKNESS (CM) - .160
SOURCE - AFMLTR6-259

STRAIN (PCT.)	TIME (HOURS)
.079	.050
.118	.100
.167	.200
.211	.300
.250	.400
.278	.500
.300	.570
.320	.600
.346	.700
.392	.900
.426	1.000
.441	1.100
.468	1.200
.483	1.300

ALLOY - T-6AL-4V
STRESS (MPA) - 275.8
TEMP. (KELVIN) - 811
THICKNESS (CM) - .160
SOURCE - AFMLTR6-259

STRAIN (PCT.)	TIME (HOURS)
.065	.020
.103	.030
.138	.050
.168	.070
.186	.080
.205	.100
.244	.130
.259	.150
.282	.170
.298	.180
.315	.200
.356	.230
.382	.270
.410	.300
.441	.330
.469	.370
.499	.400

ALLOY - T-6AL-4V
STRESS (MPA) - 344.7
TEMP. (KELVIN) - 811
THICKNESS (CM) - .1[illegible]
SOURCE - AFMLTR6-259

STRAIN (PCT.)	TIME (HOURS)
.109	.020
.202	.030
.267	.050
.301	.060
.340	.070
.401	.080
.454	.100

ALLOY - T-6AL-4V
STRESS (MPA) - 413.7
TEMP. (KELVIN) - 811
THICKNESS (CM) - .160
SOURCE - AFMLTR6-259

STRAIN (PCT.)	TIME (HOURS)
.183	.004
.297	.008
.442	.012

APPENDIX D-2

Ti6Al-4V SUPPLEMENTAL STEADY-STATE CREEP TESTS (RAW DATA)

This portion of Appendix D presents the results of the supplemental steady-state creep tests. All strains shown are total plastic strains. For informational purposes the elastic strains are presented below for the individual tests in order of their appearance in this section. Elastic strain "A" was measured at the start of the test while elastic strain "B" was measured at the conclusion of the test.

SPECIMEN #	ELASTIC STRAIN, %	
	A	B
T01L	.419	.390
T03L	.198	.171
T11L	.417	.421
T12T	.381	.405
T13T	----	.208
T21L	.278	.186
T23L	.065	.055
T26L	.444	.449
T34L	.234	.202
T36L	.051	.055
T74L	.577	.563
T76L	.385	.378
T82L	.209	.221
T92L	.544	.548
T104L	.380	.372

ALLOY - TI-6AL-4V		ALLOY - TI-6AL-4V		ALLOY - TI-6AL-4V	
STRESS (MPA) - 475.7		STRESS (MPA) - 317.2		STRESS (MPA) - 165.5	
TEMP. (KELVIN) - 616		TEMP. (KELVIN) - 616		TEMP. (KELVIN) - 558	
THICKNESS (CM) - .033		THICKNESS (CM) - .033		THICKNESS (CM) - .033	
SPECIMEN NO. - MDAC-E- T92L		SPECIMEN NO. - MDAC-E- 104L		SPECIMEN NO. - MDAC-E- T82L	
STRAIN (PCT.)	TIME (HOURS)	STRAIN (PCT.)	TIME (HOURS)	STRAIN (PCT.)	TIME (HOURS)
.010	.1	.008	.1	.008	.1
.018	.2	.015	.2	.012	.2
.020	.3	.018	.3	.013	.3
.025	.5	.018	.5	.016	.5
.031	.8	.018	.8	.015	.8
.036	1.0	.019	1.0	.016	1.0
.039	1.5	.021	1.5	.018	1.5
.042	2.0	.021	2.0	.021	2.0
.051	3.0	.025	3.0	.023	3.0
.055	4.0	.028	4.0	.029	4.0
.059	5.0	.029	5.0	.031	5.0
.066	10.0	.032	10.0	.031	10.0
.076	14.0	.036	12.0	.035	12.0
.096	21.0	.042	19.0	.066	67.0
.106	25.0	.049	25.0	.073	70.0
.109	30.0	.052	30.0	.079	75.0
.115	35.0	.053	35.0	.087	80.0
.123	38.0	.061	67.0	.090	84.0
.130	45.0	.066	70.0	.087	91.0
.137	50.0	.071	75.0	.082	95.0
		.078	80.0	.078	100.0
		.079	84.0	.081	105.0
		.078	91.0	.084	108.0
		.069	95.0	.077	115.0
		.071	100.0	.085	120.0
		.074	105.0	.082	125.0
		.075	108.0	.082	130.0
		.085	163.0	.084	139.0
		.085	165.0	.088	145.0
		.085	170.0	.087	150.0
		.088	175.0	.094	155.0
		.088	180.0	.094	165.0
		.094	187.0	.100	170.0
		.094	190.0	.099	175.0
		.095	195.0	.102	180.0
		.095	200.0	.113	235.0

ORIGINAL PAGE IS
OF POOR QUALITY

ALLOY - TI-6AL-4V
STRESS (MPA) - 317.2
TEMP. (KELVIN) - 659
THICKNESS (CM) - .030
SPECIMEN NO. - MDAC-E- T76L

STRAIN (PCT.)	TIME (HOURS)
.014	.1
.018	.2
.024	.3
.032	.5
.034	.8
.040	1.0
.043	1.5
.049	2.0
.065	3.0
.074	4.0
.080	5.0
.097	10.0
.113	15.0
.126	22.0
.144	25.0
.161	30.0
.160	35.0
.166	39.0
.179	46.0
.177	50.0
.182	55.0
.192	60.0
.203	63.0
.237	118.0
.240	120.0
.244	125.0
.245	130.0
.247	135.0
.252	142.0
.255	145.0
.257	150.0
.265	155.0
.271	159.0
.273	166.0
.275	170.0
.278	175.0
.283	180.0
.289	184.0
.281	191.0
.283	195.0
.287	200.0

ALLOY - TI-6AL-4V
STRESS (MPA) - 317.2
TEMP. (KELVIN) - 658
THICKNESS (CM) - .030
SPECIMEN NO. - MDAC-E- T12T

STRAIN (PCT.)	TIME (HOURS)
.009	.1
.009	.2
.010	.3
.010	.5
.010	.8
.012	1.0
.029	1.5
.029	2.0
.026	3.0
.039	4.0
.043	5.0
.074	13.0
.081	16.0
.091	21.0
.099	26.0
.107	29.0
.105	37.0
.111	43.0
.119	48.0
.109	53.0
.139	62.0
.142	66.0
.157	71.0
.175	76.0
.218	133.0
.216	138.0
.224	143.0
.229	148.0
.228	157.0
.239	165.0
.241	170.0
.244	173.0
.240	181.0
.240	186.0
.255	191.0
.261	200.0
.253	209.0
.253	215.0
.266	217.5

ALLOY - TI-6AL-4V
STRESS (MPA) - 317.2
TEMP. (KELVIN) - 714
THICKNESS (CM) - .063
SPECIMEN NO. - MDAC-E-T1L

STRAIN (PCT.)	TIME (HOURS)
.020	.083
.034	.170
.045	.250
.065	.500
.090	.750
.104	1.000
.129	1.500
.153	2.000
.183	3.000
.204	4.000
.235	5.000
.326	10.000
.474	19.000
.496	21.000
.543	25.000
.584	30.000
.647	35.000
.718	43.000
.788	50.000
.799	52.000
.715	43.000
.788	50.000
.799	52.000

ORIGINAL PAGE IS OF POOR QUALITY

ALLOY - TI-6AL-4V
STRESS (MPA) - 165.5
TEMP. (KELVIN) - 714
THICKNESS (CM) - .030
SPECIMEN NO. - MDAC-E- T13T

STRAIN (PCT.)	TIME (HOURS)
.011	.1
.013	.2
.013	.3
.019	.5
.029	.8
.038	1.0
.044	1.5
.055	2.0
.059	3.0
.068	4.0
.081	5.0
.118	13.0
.127	15.0
.144	19.0
.162	24.0
.181	29.0
.195	37.0
.199	39.0
.217	44.0
.225	49.0
.236	54.0
.322	109.0
.334	116.0
.348	121.0
.351	126.0
.352	133.0
.360	141.0
.371	146.0
.379	150.0
.395	157.0
.394	165.0
.407	170.0
.411	174.0
.423	182.0
.435	189.0
.442	194.0
.443	198.0
.464	205.0
.458	208.0

ALLOY - TI-6AL-4V
STRESS (MPA) - 165.5
TEMP. (KELVIN) - 714
THICKNESS (CM) - .063
SPECIMEN NO. - MDAC-E-T3L

STRAIN (PCT.)	TIME (HOURS)
.016	.083
.028	.170
.035	.250
.043	.500
.046	.750
.055	1.000
.059	1.500
.068	2.000
.080	3.000
.090	4.000
.102	5.000
.133	10.000
.141	13.000
.169	21.000
.196	30.000
.221	35.000
.228	37.500
.312	73.500
.351	92.500
.363	96.500
.361	100.500
.376	105.500
.379	109.500
.383	117.500
.390	122.500
.394	127.500
.398	132.500
.403	134.500
.419	141.500
.427	146.500
.427	151.500
.434	156.500
.441	158.500
.460	165.500
.467	170.500
.455	175.500
.461	180.500
.480	188.500
.482	194.500
.484	199.500

ALLOY - TI-6AL-4V
STRESS (MPA) - 317.2
TEMP. (KELVIN) - 714
THICKNESS (CM) - .030
SPECIMEN NO. - MDAC-E- T26L

STRAIN (PCT.)	TIME (HOURS)
.014	.1
.035	.2
.045	.3
.065	.5
.077	.8
.102	1.0
.115	1.5
.139	2.0
.170	3.0
.191	4.0
.221	5.0
.298	10.0
.323	13.0
.434	21.0
.475	25.0
.530	30.0
.576	35.0
.600	37.0
.680	45.0

ALLOY - TI-6AL-4V
STRESS (MPA) - 475.7
TEMP. (KELVIN) - 658
THICKNESS (CM) - .030
SPECIMEN NO. - MDAC-E- T74L

STRAIN (PCT.)	TIME (HOURS)
.015	.1
.026	.2
.045	.3
.070	.5
.086	.8
.107	1.0
.125	1.5
.153	2.0
.183	3.0
.213	4.0
.225	5.0
.335	10.0
.367	12.0
.475	19.0
.491	20.0
.507	21.0
.522	22.0
.535	23.0
.545	24.0
.561	25.0
.572	26.0
.585	27.0
.589	28.0
.594	29.0
.612	30.0

ALLOY - TI-6AL-4V
STRESS (MPA) - 48.3
TEMP. (KELVIN) - 714
THICKNESS (CM) - .030
SPECIMEN NO. - MDAC-E- T36L

STRAIN (PCT.)	TIME (HOURS)
.002	.1
.017	.2
.019	.3
.020	.5
.024	.8
.031	1.0
.035	1.5
.039	2.0
.041	3.0
.041	4.0
.041	5.0
.035	15.0
.035	20.0
.039	25.0
.052	30.0
.050	39.0
.054	45.0
.063	50.0
.072	54.0
.066	63.0
.070	67.0
.070	70.0
.077	75.0
.083	79.0
.090	135.0
.090	140.0
.091	145.0
.096	150.0
.090	159.0
.090	165.0
.090	170.0
.089	175.0
.087	183.0
.092	185.0
.085	190.0
.091	195.0
.087	199.0
.090	207.0

ALLOY - TI-6AL-4V
STRESS (MPA) - 165.5
TEMP. (KELVIN) - 714
THICKNESS (CM) - .030
SPECIMEN NO. - MDAC-E- T34L

STRAIN (PCT.)	TIME (HOURS)
.006	.1
.011	.2
.021	.3
.024	.5
.026	.8
.039	1.0
.043	1.5
.056	2.0
.063	3.0
.074	4.0
.084	5.0
.118	10.0
.146	20.0
.161	25.0
.176	30.0
.187	35.0
.281	91.0
.296	95.0
.300	100.0
.309	105.0
.318	115.0
.336	120.0
.327	125.0
.337	130.0
.346	139.0
.353	145.0
.358	150.0
.376	155.0
.383	163.0
.384	165.0
.391	170.0
.385	175.0
.411	180.0
.409	188.0
.411	190.0
.415	195.0
.416	200.0

ORIGINAL PAGE IS OF POOR QUALITY

ALLOY - TI-6AL-4V
STRESS (MPA) - 317.2
TEMP. (KELVIN) - 714
THICKNESS (CM) - .330
SPECIMEN NO. - MDAC-E- T11T

STRAIN (PCT.)	TIME (HOURS)
.015	.1
.037	.2
.053	.3
.077	.5
.100	.8
.109	1.0
.139	1.5
.157	2.0
.179	3.0
.202	4.0
.230	5.0
.313	10.0
.426	19.0
.435	20.0
.479	25.0
.505	30.0
.542	35.0
.593	43.0
.601	45.0

ALLOY - TI-6AL-4V
STRESS (MPA) - 48.3
TEMP. (KELVIN) - 783
THICKNESS (CM) - .330
SPECIMEN NO. - MDAC-E- T23L

STRAIN (PCT.)	TIME (HOURS)
.018	.1
.022	.2
.028	.3
.034	.5
.036	.8
.040	1.0
.053	1.5
.065	2.0
.069	3.0
.078	4.0
.091	5.0
.119	10.0
.154	18.0
.180	20.0
.205	25.0
.225	30.0
.255	34.0
.463	90.0
.483	95.0
.498	100.0
.511	105.0
.537	115.0
.555	120.0
.570	125.0
.587	130.0
.595	138.0
.608	140.0
.629	145.0
.643	150.0

ALLOY - TI-6AL-4V
STRESS (MPA) - 165.5
TEMP. (KELVIN) - 783
THICKNESS (CM) - .330
SPECIMEN NO. - MDAC-E- T21L

STRAIN (PCT.)	TIME (HOURS)
.052	.1
.065	.2
.092	.3
.112	.5
.143	.8
.168	1.0
.222	1.5
.258	2.0
.342	3.0
.400	4.0
.463	5.0
.533	6.0
.598	7.0

ORIGINAL PAGE IS OF POOR QUALITY

APPENDIX D-3

Ti-6Al-4V CYCLIC CREEP TESTS

(RAW DATA)

Presented in this section are the results of the twelve cyclic tests performed on tensile specimens.

Titanium Cyclic Creep Data

Cyclic Test Number	1		
Alloy Designation	Ti-6Al-4V		
Heat Number	N-0358		
Supplier	Timet		
Test Temperature (°K)	658		
Test Direction	Longitudinal		
Sheet Thickness (cm)	0.031 ± 0.005		
Specimen Number	T25L	T51L	T60L
Specimen Thickness (cm)	.0363	.0361	.0356
Specimen Width (cm)	.8910	.8915	.8936
Applied Load (kg)	98.8	67.1	129.4
Test Stress (MPa)	299.2	207.0	399.0
Pressure (Pa)	Constant (<1.3)		

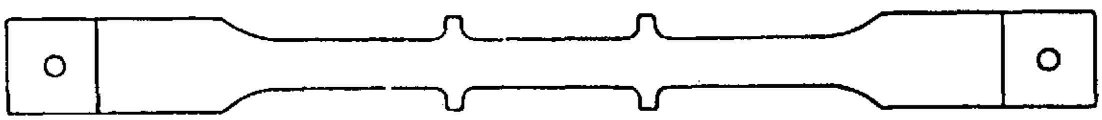

Side B

Cycle Number		% Creep T25L	% Creep T51L	% Creep T60L
1	Side A	.05	.03	.09
	Side B	.05	.02	.09
	Ave.	.05	.025	.09
5	Side A	.06	.04	.11
	Side B	.06	.03	.10
	Ave.	.06	.035	.105
15	Side A	.10	.05	.16
	Side B	.10	.06	.17
	Ave.	.10	.055	.165
25	Side A	.10	.05	.18
	Side B	.11	.06	.17
	Ave.	.105	.055	.175
50	Side A	.12	.06	.21
	Side B	.11	.07	.19
	Ave.	.115	.065	.20
75	Side A	.13	.08	.24
	Side B	.11	.07	.22
	Ave.	.12	.075	.23
100	Side A	.13	.07	.26
	Side B	.14	.07	.24
	Ave.	.135	.07	.25

Titanium Cyclic Creep Data

Cyclic Test Number	2		
Alloy Designation	Ti-6Al-4V		
Heat Number	N-0358		
Supplier	Timet		
Test Temperature (°K)	714		
Test Direction	Longitudinal		
Sheet Thickness (cm)	.031 ± .005		
Specimen Number	T31L	T38L	T39L
Specimen Thickness (cm)	.0343	.0343	.0345
Specimen Width (cm)	1.2743	1.2753	1.2748
Applied Load (kg)	132.0	51.2	86.3
Test Stress (MPa)	295.9	114.6	192.0
Pressure (Pa)	Constant (<1.3)		

Side A

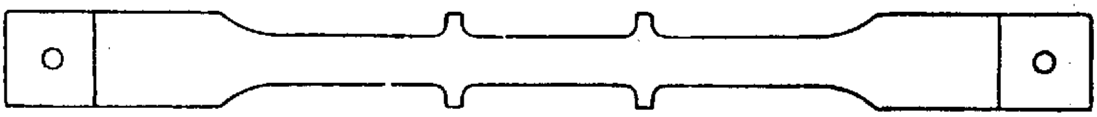

Side B

Cycle Number		% Creep T31L	T38L	T39L
1	Side A	.110	.03	.05
	Side B	.100	.03	.05
	Ave.	.105	.03	.05
5	Side A	.18	.05	.09
	Side B	.17	.05	.10
	Ave.	.175	.05	.095
15	Side A	.27	.07	.14
	Side B	.27	.07	.15
	Ave.	.27	.07	.145
25	Side A	.35	.08	.18
	Side B	.35	.09	.17
	Ave.	.35	.085	.175
50	Side A	.49	.10	.23
	Side B	.50	.11	.25
	Ave.	.495	.105	.24
75	Side A	.61	.13	.29
	Side B	.62	.14	.27
	Ave.	.615	.135	.28
100	Side A	.74	.14	.31
	Side B	.73	.14	.33
	Ave.	.735	.14	.32

Cyclic Test Number	3		
Alloy Designation	Ti-6Al-4V		
Heat Number	N-0358		
Supplier	Timet		
Test Temperature (°K)	783		
Test Direction	Longitudinal		
Sheet Thickness (cm)	0.031 ± 0.005		
Specimen Number	T41L	T56L	T59L
Specimen Thickness (cm)	.0343	.0343	.0345
Specimen Width (cm)	1.2753	1.2750	1.2750
Applied Load (kg)	57.9	22.5	37.6
Test Stress (MPa)	129.7	50.4	83.6
Pressure (Pa)	Constant (<1.3)		

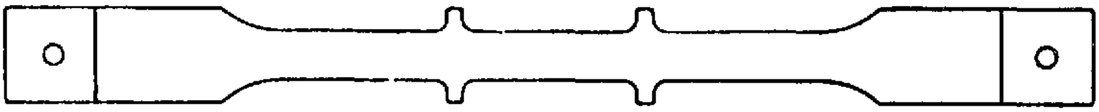

Cycle Number		% Creep T41L	% Creep T56L	% Creep T59L
1	Side A	.06	.02	.03
	Side B	.07	.02	.02
	Ave.	.065	.02	.025
5	Side A	.20	.04	.14
	Side B	.21	.05	.11
	Ave.	.205	.045	.125
15	Side A			
	Side B			
	Ave.			
25	Side A	.51	.13	.30
	Side B	.53	.12	.37
	Ave.	.52	.125	.335
50	Side A	.78	.21	.45
	Side B	.80	.21	.43
	Ave.	.79	.21	.44
75	Side A	.98	.23	.57
	Side B	1.02	.22	.55
	Ave.	1.00	.225	.56
100	Side A	1.17	.26	.65
	Side B	1.20	.26	.66
	Ave.	1.185	.26	.655

Titanium Cyclic Creep Data

Cyclic Test Number		4		
Alloy Designation		Ti-6Al-4V		
Heat Number		N-0358		
Supplier		Timet		
Test Temperature (°K)		839		
Test Direction		Longitudinal		
Sheet Thickness (cm)		0.031 ± 0.005		
Specimen Number		T64L	T87L	T89L
Specimen Thickness	(cm)	.0368	.0368	.0368
Specimen Width	(cm)	1.2741	1.2720	1.2723
Applied Load	(kg)	22.6	9.4	14.6
Test Stress	(MPa)	47.2	19.7	30.5
Pressure	(Pa)	Constant (<1.3)		

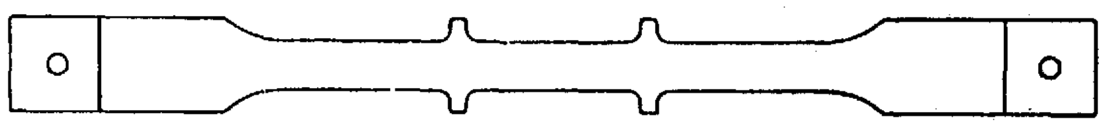

Cycle Number		% Creep T64L	T87L	T89L
1	Side A	.07	.02	.05
	Side B	.08	.02	.05
	Ave.	.075	.02	.05
5	Side A	.20	.06	.12
	Side B	.18	.06	.11
	Ave.	.19	.06	.115
15	Side A	.37	.10	.21
	Side B	.36	.08	.17
	Ave.	.365	.09	.19
25	Side A	.57	.15	.30
	Side B	.56	.14	.28
	Ave.	.565	.145	.29
50	Side A	1.03	.23	.51
	Side B	1.01	.24	.50
	Ave.	1.02	.235	.505
75	Side A	1.45	.32	.73
	Side B	1.38	.33	.67
	Ave.	1.415	.325	.70
100	Side A	1.80	.41	.86
	Side B	1.76	.39	.87
	Ave.	1.78	.40	.865

Titanium
Cyclic Creep Data

Cyclic Test Number	5
Alloy Designation	Ti-6Al-4V
Heat Number	N-0358
Supplier	Timet
Test Temperature (°K)	783
Test Direction	Longitudinal
Sheet Thickness (cm)	0.031 ± 0.0051
Specimen Number	T63L T66L T67L
Specimen Thickness (cm)	.0345 .0343 .0345
Specimen Width (cm)	1.2751 1.2743 1.2748
Applied Load	(See Table - Page D-3-6)
Test Stress	(See Table - Page D-3-6)
Pressure (Pa)	(Constant (<1.3)

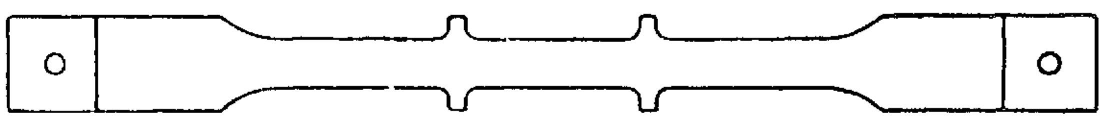

Cycle Number		% Creep T63L	T66L	T67L
1	Side A	.03	.03	.05
	Side B	.04	.02	.05
	Ave.	.035	.025	.05
5	Side A	.07	.05	.10
	Side B	.07	.05	.10
	Ave.	.07	.05	.10
15	Side A	.15	.09	.20
	Side B	.15	.10	.21
	Ave.	.15	.095	.205
25	Side A	.23	.12	.30
	Side B	.23	.13	.30
	Ave.	.23	.125	.30
50	Side A	.41	.23	.54
	Side B	.42	.22	.52
	Ave.	.415	.225	.53

TITANIUM TEST 5

	SPECIMEN T63L		SPECIMEN T67L		SPECIMEN T66L	
CYCLES	MEAN LOAD (kg)	STRESS (MPa)	MEAN LOAD (kg)	STRESS (MPa)	MEAN LOAD (kg)	STRESS (MPa)
1-5	29.8	66.2	36.4	80.9	21.4	48.1
7-8	31.2	69.4	39.3	87.4	21.8	48.9
9-12	32.8	72.9	41.1	92.3	23.2	51.9
13-17	34.4	76.6	43.3	96.3	24.8	55.7
18-22	36.3	80.7	45.5	101.2	26.1	58.6
23-27	37.8	84.1	47.5	105.7	27.7	62.2
28-32	39.3	87.3	49.6	110.4	29.0	64.9
33-37	41.0	91.3	51.5	114.5	30.5	68.5
38-42	42.8	95.1	53.9	119.8	31.6	70.8
43-47	44.5	98.9	55.9	124.2	33.3	74.6
48-50	46.3	102.9	57.7	137.3	35.0	78.5

Titanium
Cyclic Creep Data

Cyclic Test Number	6		
Alloy Designation	Ti-6A1-4V		
Heat Number	N-0358		
Supplier	Timet		
Test Temperature (°K)	783		
Test Direction	Longitudinal		
Sheet Thickness (cm)	0.031 ± 0.005		
Specimen Number	T68L	T69L	T78L
Specimen Thickness (cm)	.0343	.0343	.0345
Specimen Width (cm)	1.2748	1.2741	1.2741
Applied Load	(See Table - Page D-3-9)		
Test Stress	(See Table - Page D-3-9)		
Pressure (Pa)	(Constant <1.3)		

Side A

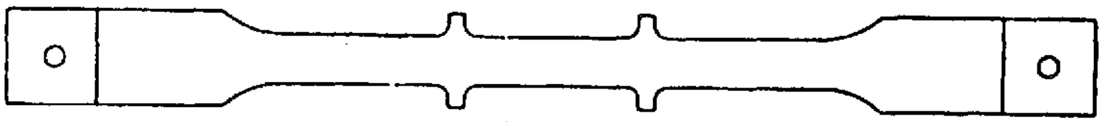

Side B

Cycle Number		% Creep T68L	% Creep T69L	% Creep T78L
1	Side A	.05	.05	.09
	Side B	.06	.05	.10
	Ave.	.055	.05	.095
5	Side A	.14	.09	.18
	Side B	.13	.07	.19
	Ave.	.135	.08	.185
15	Side A	.23	.14	.33
	Side B	.23	.12	.33
	Ave.	.23	.13	.33
25	Side A	.29	.18	.41
	Side B	.31	.17	.43
	Ave.	.30	.175	.42
50	Side A	.36	.22	.53
	Side B	.38	.21	.54
	Ave.	.37	.215	.535

TITANIUM TEST 6

	SPECIMEN T68L		SPECIMEN T78L		SPECIMEN T69L	
CYCLES	MEAN LOAD (kg)	STRESS (MPa)	MEAN LOAD (kg)	STRESS (MPa	MEAN LOAD (kg)	STRESS (MPa)
1-2	46.7	104.7	58.2	129.6	33.8	75.9
3-7	45.1	100.9	56.8	126.5	31.9	71.6
8-13	43.0	96.4	54.1	120.6	31.3	70.2
14-17	41.0	91.9	51.6	114.9	30.9	69.3
18-22	39.0	87.4	49.5	110.2	29.8	66.9
23-27	37.4	83.9	47.4	105.6	28.7	64.4
28-32	35.7	80.0	45.4	101.2	27.3	61.3
33-37	34.0	76.2	43.2	96.2	26.1	58.6
38-44	32.3	72.4	41.0	91.2	24.9	55.8
45-47	30.5	68.4	39.4	87.7	23.2	52.1
48-50	28.9	64.7	37.1	82.7	22.1	49.5

Titanium

Cyclic Creep Data

Cyclic Test Number	7		
Alloy Designation	Ti-6Al-4V		
Heat Number	N-0358		
Supplier	Timet		
Test Temperature (°K)	714		
Test Direction	Longitudinal		
Sheet Thickness (cm)	0.031 ± 0.005		
Specimen Number	T32L	T40L	T61L
Specimen Thickness (cm)	.0338	.0338	.0340
Specimen Width (cm)	1.2746	1.2748	1.2743
Applied Load (kg)	130.1	49.5	84.3
Test Stress (MPa)	296.0	112.6	190.4
Pressure (Pa)	(Constant (<1.3)		

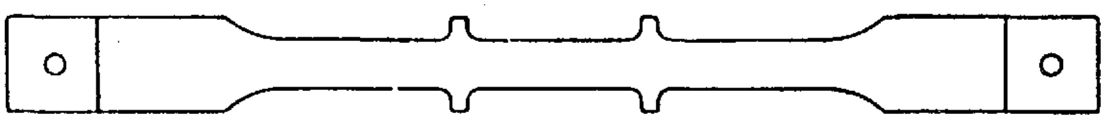

Cycle Number		% Creep T32L	T40L	T61L
1	Side A	.07	.02	.03
	Side B	.07	.02	.03
	Ave.	.07	.02	.03
5	Side A	.11	.03	.05
	Side B	.13	.03	.05
	Ave.	.12	.03	.05
10	Side A	.15	.03	.08
	Side B	.16	.03	.08
	Ave.	.155	.03	.08
30	Side A	.23	.04	.09
	Side B	.22	.03	.10
	Ave.	.225	.035	.095
50	Side A	.29	.06	.14
	Side B	.29	.07	.15
	Ave.	.29	.065	.145
100	Side A	.37	.07	.18
	Side B	.37	.09	.19
	Ave.	.37	.08	.185

Titanium
Cyclic Creep Data

Cyclic Test Number	8		
Alloy Designation	Ti-6A1-4V		
Heat Number	N-0358		
Supplier	Timet		
Test Temperature (°K)	783		
Test Direction	Longitudinal		
Sheet Thickness (cm)	0.031 ± 0.005		
Specimen Number	T28L	T42L	T70L
Specimen Thickness (cm)	.0353	.0353	.0353
Specimen Width (cm)	1.2741	1.2748	1.2743
Applied Load (kg)	(See Table - Page D-3-12)		
Test Stress (MPa)	(See Table - Page D-3-12)		
Pressure (Pa)	Constant (<1.3)		

Side A

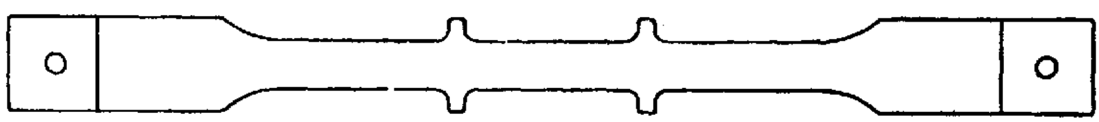

Side B

Cycle Number		% Creep T28L	T42L	T70L
1	Side A	.07	.04	.07
	Side B	.05	.04	.09
	Ave.	.06	.04	.08
5	Side A	.13	.08	.18
	Side B	.14	.10	.18
	Ave.	.135	.09	.18
15	Side A	.23	.13	.30
	Side B	.23	.14	.29
	Ave.	.23	.135	.295
25	Side A	.31	.19	.41
	Side B	.33	.18	.41
	Ave.	.32	.185	.41
50	Side A	.49	.28	.55
	Side B	.51	.29	.65
	Ave.	.50	.285	.60
75	Side A	.65	.37	.89
	Side B	.66	.34	.87
	Ave.	.655	.355	.88
100	Side A	.79	.42	1.09
	Side B	.81	.42	1.07
	Ave.	.80	.42	1.08

TITANIUM TEST NO. 8

	LOAD ∿ kg	
SPECIMEN	1ST STEP (10 MINUTES)	2ND STEP (10 MINUTES)
T28L	30.0	47.1
T42L	22.4	35.5
T70L	39.7	60.6

	STRESS ∿ MPa	
SPECIMEN	1ST STEP (10 MINUTES)	2ND STEP (10 MINUTES)
T28L	65.4	102.6
T42L	48.8	77.3
T70L	86.4	132.0

Titanium
Cyclic Creep Data

Cyclic Test Number	9		
Alloy Designation	Ti-6Al-4V		
Heat Number	N-0358		
Supplier	Timet		
Test Temperature (°K)	(See Table - Page D-3-15)		
Test Direction	Longitudinal		
Sheet Thickness (cm)	0.031 cm ±0.005		
Specimen Number	T49L	T53L	T58L
Specimen Thickness (cm)	.0351	.0351	.0348
Specimen Width (cm)	1.2751	1.2748	1.2748
Applied Load (Kg)	(See Table - Page D-3-15)		
Test Stress (MPa)	(See Table - Page D-3-15)		
Pressure (Pa)	(See Table - Page D-3-15)		

Side A

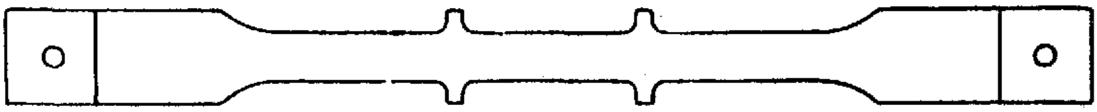

Side B

Cycle Number		% Creep T49L	T53L	T58L
1	Side A	.04	.02	.03
	Side B	.06	.02	.03
	Ave.	.05	.02	.03
5	Side A	.08	.02	.05
	Side B	.07	.02	.04
	Ave.	.075	.02	.045
15	Side A	.11	.03	.11
	Side B	.13	.03	.11
	Ave.	.12	.03	.11
25	Side A	.15	.03	.08
	Side B	.17	.06	.09
	Ave.	.16	.045	.085
50	Side A	.24	.05	.13
	Side B	.19	.06	.12
	Ave.	.215	.055	.125
75	Side A	.29	.07	.15
	Side B	.29	.06	.15
	Ave.	.29	.065	.15
100	Side A	.34	.07	.17
	Side B	.37	.07	.18
	Ave.	.355	.07	.175

		% Creep		
		T49L	T53L	T58L
150	Side A	.43	.08	.21
	Side B	.42	.11	.22
	Ave.	.425	.095	.225
200	Side A	.50	.10	.26
	Side B	.54	.11	.26
	Ave.	.52	.105	.26

TITANIUM TEST NO. 9

CYCLE TIME (SEC.)	TEMP. (°K)	PRESSURE Pa	STRESS ∿ MPa		
			T49L	T53L	T58L
300	555	1.5	-	-	-
400	674	2.4	21.1	6.1	13.1
500	741	4.0	31.6	12.4	24.1
600	766	5.2	49.7	16.6	31.3
700	781	6.4	53.5	19.4	35.7
800	782	7.2	61.3	21.6	39.1
900	778	8.3	63.5	22.6	40.5
1000	769	9.3	64.7	23.3	41.4
1100	764	10.4	69.2	25.2	44.4
1200	758	10.7	74.7	27.6	48.2
1300	750	12.5	85.0	31.9	55.2
1400	741	18.7	93.6	35.1	60.4
1500	733	33.3	104.6	40.3	68.8
1600	724	56.0	119.6	46.8	79.4
1700	669	77.3	128.0	50.1	86.0
1800	619	100.0	137.4	53.9	93.1
1900	578	126.6	146.0	57.0	99.4
2000	536	319.9	146.8	55.8	99.7
2100	500	693.2	137.5	49.7	92.1
2200	469	133.3	123.5	43.0	82.3
2300	440	41323	103.9	34.3	67.8
2400	422	101308	72.1	21.4	46.3
2500	400	101308	43.9	11.5	27.8

Titanium
Cyclic Creep Data

Cyclic Test Number	10		
Alloy Designation	Ti-6Al-4V		
Heat Number	N-0358		
Supplier	Timet		
Test Temperature (°K)	783		
Test Direction	Longitudinal		
Sheet Thickness (cm)	0.031 cm ±0.005		
Specimen Number	T73L	T75L	T80L
Specimen Thickness (cm)	.0353	.0356	.0356
Specimen Width (cm)	1.2743	1.3743	1.2748
Applied Load (Kg)	(See Table - Page D-3-17)		
Test Stress (MPa)	(See Table - Page D-3-17)		
Pressure (Pa)	Constant (< 1.333)		

Side A

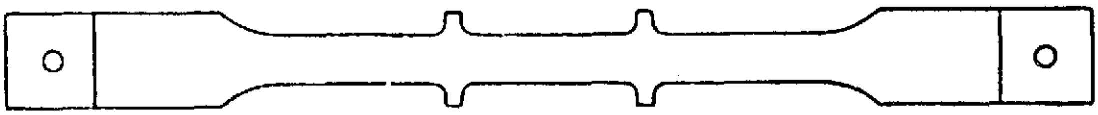

Side B

Cycle Number		% Creep T73L	T75L	T80L
1	Side A	.09	.03	.05
	Side B	.10	.02	.05
	Ave.	.095	.025	.05
5	Side A	.15	.03	.08
	Side B	.15	.03	.09
	Ave.	.15	.03	.085
15	Side A	.25	.06	.13
	Side B	.25	.06	.14
	Ave.	.25	.06	.135
25	Side A	.31	.07	.17
	Side B	.33	.06	.15
	Ave.	.32	.065	.16
50	Side A	.49	.10	.24
	Side B	.47	.09	.24
	Ave.	.48	.095	.24
75	Side A	.61	.11	.29
	Side B	.65	.13	.30
	Ave.	.63	.12	.295
100	Side A	.72	.13	.34
	Side B	.76	.14	.35
	Ave.	.74	.135	.345

TITANIUM TEST NO. 10

	LOAD ∿ Kg			
SPECIMEN	1ST STEP (10 MINUTES)	2ND STEP (10 MINUTES)	3RD STEP (5 MINUTES)	4TH STEP (10 MINUTES)
T73L	18.0	34.6	57.5	67.2
T80L	10.5	21.14	37.47	43.3
T75L	5.6	12.2	22.8	25.1

	STRESS ∿ MPa			
SPECIMEN	1ST STEP (10 MINUTES)	2ND STEP (10 MINUTES)	3RD STEP (5 MINUTES)	4TH STEP (10 MINUTES)
T73L	39.2	75.4	125.3	146.3
T80L	22.7	45.7	80.9	93.6
T75L	12.2	26.3	49.3	54.1

Titanium
Cyclic Creep Data

Cyclic Test Number	11		
Alloy Designation	Ti-6Al-4V		
Heat Number	N-0358		
Supplier	Timet		
Test Temperature (°K)	783		
Test Direction	Longitudinal		
Sheet Thickness (cm)	0.031 cm ±0.005		
Specimen Number	T29L	T45L	T46L
Specimen Thickness (cm)	.0348	.0348	.0348
Specimen Width (cm)	1.2751	1.2753	1.2751
Applied Load (Kg)	(See Table - Page D-3-19)		
Test Stress (MPa)	(See Table - Page D-3-19)		
Pressure (Pa)	(See Table - Page D-3-15)		

Side A

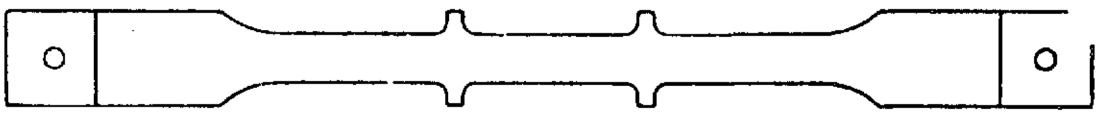

Side B

Cycle Number		% Creep T29L	T45L	T46L
1	Side A	.08	.01	.04
	Side B	.08	.02	.04
	Ave.	.08	.015	.04
5	Side A	.15	.02	.06
	Side B	.16	.04	.08
	Ave.	.155	.03	.07
15	Side A	.25	.04	.12
	Side B	.25	.05	.12
	Ave.	.25	.045	.12
25	Side A	.31	.05	.15
	Side B	.30	.07	.15
	Ave.	.305	.06	.15
50	Side A	.47	.09	.22
	Side B	.45	.10	.23
	Ave.	.46	.095	.225
75	Side A	.60	.11	.27
	Side B	.59	.12	.29
	Ave.	.595	.115	.28
100	Side A	.71	.11	.34
	Side B	.71	.13	.34
	Ave.	.71	.12	.34

TITANIUM TEST NO. 11

	LOAD ∿ Kg			
SPECIMEN	1ST STEP (10 MINUTES)	2ND STEP (10 MINUTES)	3RD STEP (5 MINUTES)	4TH STEP (10 MINUTES)
T29L	17.4	34.0	57.4	66.2
T46L	10.3	20.3	36.2	41.2
T45L	5.2	11.7	22.2	24.3

	STRESS ∿ MPa			
SPECIMEN	1ST STEP (10 MINUTES)	2ND STEP (10 MINTUES)	3RD STEP (5 MINUTES)	4TH STEP (10 MINUTES)
T29L	38.5	75.0	126.6	146.1
T46L	22.6	45.4	80.0	90.9
T45L	11.5	25.9	49.1	53.6

APPENDIX E-1

RENE' 41 LITERATURE SURVEY CREEP DATA

ALLOY - RENE 41
STRESS (MPA) - 68.9
TEMP. (KELVIN) - 1033
THICKNESS (CM) - .020
SOURCE - HF-MDAC-20

STRAIN (PCT.)	TIME (HOURS)
.040	2.000
.056	5.000
.065	10.000
.081	20.000
.091	30.000
.094	40.000
.097	50.000
.100	60.000
.104	70.000
.104	80.000
.108	91.000
.113	101.000
.116	110.000
.126	120.000
.133	130.000
.134	140.000
.137	150.000
.143	161.000
.146	171.000
.147	181.000
.150	191.000
.155	200.000

ALLOY - RENE 41
STRESS (MPA) - 72.4
TEMP. (KELVIN) - 1033
THICKNESS (CM) - .020
SOURCE - HF-MDAC-22

STRAIN (PCT.)	TIME (HOURS)
.034	2.000
.074	5.000
.095	10.000
.121	20.000
.131	30.000
.141	40.000
.154	50.000
.160	60.000
.168	70.000
.178	80.000
.188	90.000
.194	100.000
.202	110.000
.216	120.000
.224	130.000
.230	140.000
.243	150.000
.251	160.000
.259	170.000
.267	180.000
.281	190.000
.287	200.000

ALLOY - RENE 41
STRESS (MPA) - 79.3
TEMP. (KELVIN) - 1033
THICKNESS (CM) - .020
SOURCE - HF-MDAC-25

STRAIN (PCT.)	TIME (HOURS)
.056	2.000
.102	5.000
.159	10.000
.229	20.000
.268	30.000
.300	40.000
.319	50.000
.334	60.000
.340	70.000
.346	80.000
.356	90.000
.364	101.000
.365	110.000
.371	120.000
.377	130.000
.383	140.000
.391	150.000
.396	161.000
.404	180.000
.412	190.000
.422	205.000

ORIGINAL PAGE IS OF POOR QUALITY

ALLOY - RENE 41
STRESS (MPA) - 51.7
TEMP. (KELVIN) - 1144
THICKNESS (CM) - .020
SOURCE - HF-MDAC-8

STRAIN (PCT.)	TIME (HOURS)
.041	2.000
.063	5.000
.091	10.000
.128	20.000
.152	30.000
.182	40.000
.217	50.000
.247	60.000
.282	70.000
.314	80.000
.344	90.000
.381	100.000
.407	110.000
.444	120.000
.480	130.000
.518	140.000
.552	149.000
.589	160.000
.626	169.000
.665	180.000
.704	190.000
.752	200.000

ALLOY - RENE 41
STRESS (MPA) - 55.2
TEMP. (KELVIN) - 1144
THICKNESS (CM) - .020
SOURCE - HF-MDAC-10

STRAIN (PCT.)	TIME (HOURS)
.042	2.000
.068	5.000
.083	10.000
.115	20.000
.150	30.000
.196	40.000
.241	50.000
.282	60.000
.328	70.000
.380	80.000
.430	90.000
.491	99.000
.557	110.000
.635	120.000
.720	129.000
.819	140.000
.921	149.000
1.035	159.000

ALLOY - RENE 41
STRESS (MPA) - 55.2
TEMP. (KELVIN) - 1144
THICKNESS (CM) - .020
SOURCE - HF-MDAC-9

STRAIN (PCT.)	TIME (HOURS)
.059	5.000
.090	10.000
.136	20.000
.171	30.000
.214	40.000
.258	50.000
.299	60.000
.345	70.000
.396	80.000
.446	90.000
.507	100.000
.573	110.000
.643	120.000
.722	130.000
.818	140.000
.923	150.000
1.042	160.000

ALLOY - RENE 41
STRESS (MPA) - 1[illegible].3
TEMP. (KELVIN) - 1255
THICKNESS (CM) - .020
SOURCE - HF-MDAC-1

STRAIN (PCT.)	TIME (HOURS)
.018	2.000
.020	5.000
.029	10.000
.050	20.000
.083	30.000
.118	40.000
.159	50.000
.207	60.000
.253	70.000
.301	80.000
.347	90.000
.393	100.000
.439	110.000
.489	120.000
.535	130.000
.578	140.000
.626	149.000
.676	160.000
.718	170.000
.768	180.000

ALLOY - RENE 41
STRESS (MPA) - 58.6
TEMP. (KELVIN) - 1144
THICKNESS (CM) - .020
SOURCE - HF-MDAC-12

STRAIN (PCT.)	TIME (HOURS)
.041	2.000
.068	5.000
.085	10.000
.127	20.000
.177	30.000
.219	40.000
.275	50.000
.324	60.000
.383	70.000
.435	80.000
.497	90.000
.565	100.000
.633	110.000
.707	120.000
.797	130.000
.889	140.000

ALLOY - RENE 41
STRESS (MPA) - 65.5
TEMP. (KELVIN) - 1144
THICKNESS (CM) - .020
SOURCE - HF-MDAC-15

STRAIN (PCT.)	TIME (HOURS)
.046	2.000
.079	5.000
.116	10.000
.181	20.000
.238	30.000
.308	40.000
.389	50.000
.481	60.000
.588	70.000
.715	80.000
.877	90.000
1.088	100.000

ORIGINAL PAGE IS
OF POOR QUALITY

ALLOY - RENE 41
STRESS (MPA) - 13.8
TEMP. (KELVIN) - 1255
THICKNESS (CM) - .020
SOURCE - HF-MDAC-4

STRAIN (PCT.)	TIME (HOURS)
.042	2.000
.081	5.000
.141	10.000
.253	20.000
.341	30.000
.429	40.000
.504	50.000
.579	60.000
.649	70.000
.719	80.000
.790	90.000
.854	100.000
.922	110.000
.986	120.000
1.052	130.000
1.109	140.000

ALLOY - RENE 41
STRESS (MPA) - 13.8
TEMP. (KELVIN) - 1255
THICKNESS (CM) - .020
SOURCE - HF-MDAC-31

STRAIN (PCT.)	TIME (HOURS)
.042	3.000
.084	7.000
.112	10.000
.182	20.000
.228	30.000
.274	41.000
.322	50.000
.370	60.000
.429	70.000
.494	80.000
.569	90.000
.646	100.000
.731	110.000
.814	120.000
.906	130.000
.992	140.000
1.091	150.000
1.185	160.000

ALLOY - RENE 41
STRESS (MPA) - 17.2
TEMP. (KELVIN) - 1255
THICKNESS (CM) - .020
SOURCE - HF-MDAC-6

STRAIN (PCT.)	TIME (HOURS)
.061	2.000
.120	7.000
.150	10.000
.251	20.000
.356	30.000
.479	40.000
.615	50.000
.771	60.000
.927	70.000
1.111	80.000
1.309	90.000
1.513	99.000

ALLOY - RENE 41
STRESS (MPA) - 17.2
TEMP. (KELVIN) - 1255
THICKNESS (CM) - .020
SOURCE - HMDAC-5

STRAIN (PCT.)	TIME (HOURS)
.071	2.000
.095	5.000
.130	10.000
.221	20.000
.322	30.000
.439	40.000
.569	50.000
.713	60.000
.867	70.000
1.031	80.000
1.205	89.000
1.379	99.000

ORIGINAL PAGE IS OF POOR QUALITY

APPENDIX E-2

RENE' 41 SUPPLEMENTAL STEADY-STATE CREEP TESTS (RAW DATA)

This portion of Appendix E presents the results of the supplemental steady-state creep tests. All strains shown are total plastic strains. For informational purposes the elastic strains are presented below for the indivisual tests in order of their appearance in this section. Elastic strain "A" was measured at the start of the test while elastic strain "B" was measured at the conclusion of the test.

SPECIMEN #	ELASTIC STRAIN, %	
	A	B
R01L	.147	.128
R02L	.034	.053
R03L	.078	.055
R11T	.026	.098
R12T	.036	.020
R13T	.050	.043
R21L	.061	.054
R22L	.100	.106
R23L	.029	.031
R24L	.025	.039
R25L	.058	.037
R26L	.016	.018
R27L	.082	.081
R28L	.021	.037
R29L	.079	----
R30L	.044	.036
R31L	.088	.068
R104L	.104	.117

ALLOY - RENE 41
STRESS (MPA) - 68.9
TEMP. (KELVIN) - 964
THICKNESS (CM) - .025
SPECIMEN NO. - R25L

STRAIN (PCT.)	TIME (HOURS)
.015	.1
.016	.2
.018	.3
.019	.5
.022	.8
.021	1.0
.022	1.5
.021	2.0
.023	3.0
.023	4.0
.023	5.0
.021	10.0
.010	41.0
.009	45.0
.005	50.0
.008	55.0
.008	58.0
.010	65.0
.006	70.0
.002	75.0
.001	85.0
.000	82.0
.007	137.0
.009	140.0
.008	145.0
.006	150.0
.007	154.0
.010	161.0
.009	165.0
.008	170.0
.008	175.0
.009	178.0
.009	185.0
.010	190.0
.009	195.0
.009	200.0
.010	209.0

ALLOY - RENE 41
STRESS (MPA) - 121.3
TEMP. (KELVIN) - 983
THICKNESS (CM) - .025
SPECIMEN NO. - R27L

STRAIN (PCT.)	TIME (HOURS)
.008	.1
.009	.2
.008	.3
.009	.5
.011	.8
.011	1.0
.013	1.5
.015	2.0
.016	3.0
.015	4.0
.018	5.0
.023	10.0
.025	14.0
.021	22.0
.025	25.0
.023	30.0
.028	35.0
.032	38.0
.021	46.0
.016	50.0
.025	55.0
.023	60.0
.020	70.0
.025	75.0
.019	80.0
.019	85.0
.021	142.0
.021	145.0
.016	150.0

ALLOY - RENE 41
STRESS (MPA) - 34.5
TEMP. (KELVIN) - 1061
THICKNESS (CM) - .025
SPECIMEN NO. - R26L

STRAIN (PCT.)	TIME (HOURS)
.003	.1
.003	.2
.004	.3
.009	.5
.010	.8
.011	1.0
.012	1.5
.013	2.0
.016	3.0
.020	4.0
.024	5.0
.032	10.0
.042	14.0
.032	21.0
.028	25.0
.025	30.0
.037	35.0
.025	38.0
.024	45.0
.023	50.0
.025	55.0
.036	60.0
.020	70.0
.031	75.0
.031	80.0
.034	85.0
.029	93.0
.027	95.0
.028	100.0
.033	105.0
.029	110.0
.025	165.0
.030	170.0
.045	175.0
.055	180.0
.028	189.0
.029	195.0
.043	200.0

ORIGINAL PAGE IS
OF POOR QUALITY

ALLOY - RENE 41
STRESS (MPA) - 68.9
TEMP. (KELVIN) - 1061
THICKNESS (CM) - .025
SPECIMEN NO. - R30L

STRAIN (PCT.)	TIME (HOURS)
.003	.1
.003	.2
.003	.3
.012	.5
.017	.8
.024	1.0
.032	1.5
.034	2.0
.025	3.0
.020	4.0
.021	5.0
.005	12.0
.012	17.0
.022	22.0
.024	27.0
.026	29.0
.011	36.0
.014	41.0
.039	46.0
.035	51.0
.028	53.0
.000	60.0
.010	65.0
.016	70.0
.021	75.0
.030	80.0
.028	88.5
.031	93.5
.032	96.5
.049	152.0
.057	155.0

ALLOY - RENE 41
STRESS (MPA) - 68.9
TEMP. (KELVIN) - 1061
THICKNESS (CM) - .025
SPECIMEN NO. - R24L

STRAIN (PCT.)	TIME (HOURS)
.005	.1
.006	.2
.009	.3
.010	.5
.010	.8
.009	1.0
.011	1.5
.012	2.0
.013	3.0
.013	4.0
.015	5.0
.022	10.0
.021	12.0
.032	43.0
.029	45.0
.032	50.0
.034	55.0
.032	60.0
.031	67.0
.032	70.0
.036	75.0
.039	80.0
.042	84.0
.057	139.0
.062	145.0
.067	150.0
.064	155.0
.071	163.0
.070	165.0
.070	170.0
.071	175.0
.075	180.0
.079	187.0
.083	190.0
.088	195.0
.091	200.0

ALLOY - RENE 41
STRESS (MPA) - 68.9
TEMP. (KELVIN) - 1061
THICKNESS (CM) - .025
SPECIMEN NO. - R12T

STRAIN (PCT.)	TIME (HOURS)
.004	.1
.008	.2
.012	.3
.013	.5
.014	.8
.017	1.0
.017	1.5
.018	2.0
.020	3.0
.020	4.0
.022	5.0
.041	10.0
.043	13.0
.034	21.0
.039	25.0
.042	30.0
.051	35.0
.049	45.0
.057	50.0
.061	55.0
.062	60.0
.092	117.0
.096	120.0
.096	125.0
.095	130.0
.107	133.0
.110	141.0
.112	145.0
.114	150.0
.121	155.0
.126	165.0
.134	170.0
.132	175.0
.141	180.0
.147	189.0
.146	195.0
.149	200.0

ORIGINAL PAGE IS OF POOR QUALITY

ALLOY - RENE 41
STRESS (MPA) - 68.9
TEMP. (KELVIN) - 1061
THICKNESS (CM) - .063
SPECIMEN NO. - MDAC-E-R2L

STRAIN (PCT.)	TIME (HOURS)
.002	.083
.005	.170
.008	.250
.009	.500
.009	.750
.011	1.000
.016	1.500
.019	2.000
.019	3.000
.028	4.000
.032	5.000
.039	10.000
.076	66.000
.071	70.000
.081	75.000
.092	80.000
.091	82.500
.104	90.000
.098	95.000
.092	100.000
.101	105.000
.102	115.000
.108	120.000
.129	125.000
.130	130.000
.126	138.000
.128	145.000
.129	150.000
.128	154.000
.140	162.000
.138	165.000
.143	170.000
.160	177.000
.183	214.500
.186	234.000
.201	236.000

ALLOY - RENE 41
STRESS (MPA) - 137.9
TEMP. (KELVIN) - 1061
THICKNESS (CM) - .025
SPECIMEN NO. - 104L

STRAIN (PCT.)	TIME (HOURS)
.012	.1
.017	.2
.022	.3
.023	.5
.041	.8
.041	.1
.041	1.0
.043	1.5
.047	2.0
.042	3.0
.058	4.0
.058	5.0
.057	7.5
.080	15.0
.090	20.0
.091	25.0
.092	30.0
.274	87.0
.285	90.0
.291	95.0
.313	100.0

ALLOY - RENE 41
STRESS (MPA) - 68.9
TEMP. (KELVIN) - 1111
THICKNESS (CM) - .025
SPECIMEN NO. - R28L

STRAIN (PCT.)	TIME (HOURS)
.003	.1
.012	.2
.017	.3
.021	.5
.023	.8
.027	1.0
.035	1.5
.044	2.0
.054	3.0
.056	4.0
.057	5.0
.072	10.0
.089	15.0
.114	23.0
.141	25.0
.155	30.0
.184	35.0
.184	39.0
.200	47.0
.220	50.0
.225	55.0
.235	60.0
.239	63.5
.374	129.0
.380	130.0

ALLOY - RENE 41
STRESS (MPA) - 68.9
TEMP. (KELVIN) - 1111
THICKNESS (CM) - .025
SPECIMEN NO. - R13T

STRAIN (PCT.)	TIME (HOURS)
.010	.1
.015	.2
.017	.3
.018	.5
.022	.8
.026	1.0
.032	1.5
.039	2.0
.048	3.0
.055	4.0
.062	5.0
.088	10.0
.130	17.0
.149	20.0
.176	25.0
.199	30.0
.213	34.0
.258	41.0
.275	45.0
.289	50.0
.312	55.0
.325	58.0
.372	65.0
.403	70.0
.411	75.0
.427	80.0
.466	89.0
.486	95.0
.512	100.0

ALLOY - RENE 41
STRESS (MPA) - 68.9
TEMP. (KELVIN) - 1111
THICKNESS (CM) - .063
SPECIMEN NO. - MDAC-E-R3L

STRAIN (PCT.)	TIME (HOURS)
.015	.083
.025	.170
.027	.250
.037	.500
.053	.750
.058	1.000
.058	1.500
.069	2.000
.088	3.000
.112	4.000
.123	5.000
.168	10.000
.195	14.000
.277	21.000
.313	25.000
.349	30.000
.387	35.000
.402	38.000
.480	45.000
.542	50.000
.589	55.000
.611	60.000
.735	70.000

ALLOY - RENE 41
STRESS (MPA) - 103.4
TEMP. (KELVIN) - 1111
THICKNESS (CM) - .025
SPECIMEN NO. - R29L

STRAIN (PCT.)	TIME (HOURS)
.010	.1
.020	.2
.029	.3
.041	.5
.048	.8
.050	1.0
.053	1.5
.053	2.0
.064	3.0
.068	4.0
.072	5.0
.092	10.0
.190	18.0
.200	20.0
.240	25.0
.256	30.0
.269	34.0
.599	94.5

ORIGINAL PAGE IS OF POOR QUALITY

ALLOY - RENE 41
STRESS (MPA) - 39.3
TEMP. (KELVIN) - 1155
THICKNESS (CM) - .025
SPECIMEN NO. - R23L

STRAIN (PCT.)	TIME (HOURS)
.013	.1
.016	.2
.018	.3
.022	.5
.025	.8
.032	1.0
.038	1.5
.041	2.0
.050	3.0
.059	4.0
.056	5.0
.152	15.0
.182	20.0
.205	25.0
.227	30.0
.274	40.0
.312	45.0
.352	50.0
.361	55.0
.602	111.0
.664	115.0
.695	120.0
.733	125.0
.768	135.0
.788	140.0
.827	145.0
.847	150.0
.892	159.0
.902	160.0

ALLOY - RENE 41
STRESS (MPA) - 55.2
TEMP. (KELVIN) - 1155
THICKNESS (CM) - .025
SPECIMEN NO. - R31L

STRAIN (PCT.)	TIME (HOURS)
.009	.1
.014	.2
.018	.3
.028	.5
.030	.8
.033	1.0
.037	1.5
.048	2.0
.080	3.0
.076	4.0
.086	5.0
.180	12.5
.196	15.5
.240	18.5
.260	21.0
.299	26.0
.337	29.0
.805	85.0

ALLOY - RENE 41
STRESS (MPA) - 121.3
TEMP. (KELVIN) - 1155
THICKNESS (CM) - .025
SPECIMEN NO. - R22L

STRAIN (PCT.)	TIME (HOURS)
.055	.1
.071	.2
.086	.3
.114	.5
.165	.8
.173	1.0
.209	1.5
.252	2.0
.324	3.0
.406	4.0
.491	5.0
1.675	15.0

ALLOY - RENE 41
STRESS (MPA) - 121.3
TEMP. (KELVIN) - 1155
THICKNESS (CM) - .025
SPECIMEN NO. - R11T

STRAIN (PCT.)	TIME (HOURS)
.031	.1
.044	.2
.055	.3
.086	.5
.106	.8
.133	1.0
.220	2.0
.329	3.3
.394	4.0
.483	5.0
.573	6.0
.681	7.0
.799	8.0
.911	9.0
1.040	10.0
1.151	11.0

ALLOY - RENE 41
STRESS (MPA) - 68.9
TEMP. (KELVIN) - 1180
THICKNESS (CM) - .025
SPECIMEN NO. - R21L

STRAIN (PCT.)	TIME (HOURS)
.021	.1
.042	.2
.065	.3
.075	.5
.094	.8
.095	1.0
.125	1.5
.150	2.0
.194	3.0
.240	4.0
.246	5.0
.808	15.0
.837	16.0
.890	17.0
.948	18.0

ALLOY - RENE 41
STRESS (MPA) - 121.3
TEMP. (KELVIN) - 1155
THICKNESS (CM) - .063
SPECIMEN NO. - MDAC-E-R1L

STRAIN (PCT.)	TIME (HOURS)
.034	.083
.064	.170
.093	.500
.200	.750
.241	1.000
.366	1.500
.458	2.000
.558	2.500
.645	3.000

APPENDIX E-3

RENE' 41 CYCLIC CREEP TESTS

(RAW DATA)

This section presents the results of the 15 cyclic creep tests that were performed on Rene' 41 tensile specimens.

Nickel Cyclic Creep Data

Cyclic Test Number		1	
Alloy Designation		Rene' 41	
Heat Number		2490-0-8207	
Supplier		Teledyne Rodney	
Test Temperature (°K)		1111	
Test Direction		Longitudinal	
Sheet Thickness (cm)		0.025 ± 0.003	
Specimen Number	R40L	R41L	R39L
Specimen Thickness (cm)	0.02768	0.02768	0.02768
Specimen Width (cm)	1.2722	1.2725	1.2730
Applied Load (kg)	14.0	24.7	37.5
Test Stress (MPa)	39.0	68.7	104.1

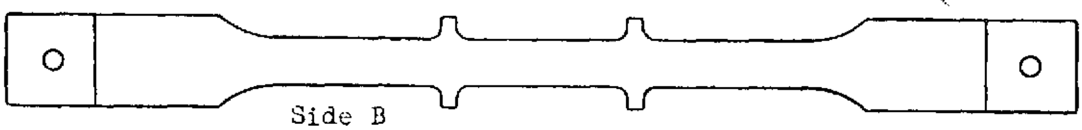

Cycle Number		% Creep R40L	% Creep R41L	% Creep R39L
1	Side A	-.02	-.01	.00
	Side B	-.02	-.02	.01
	Ave.	-.02	-.015	.005
5	Side A	-.01	.0	.01
	Side B	-.01	-.01	.04
	Ave.	-.01	-.005	.025
15	Side A	-.01	.02	.08
	Side B	.01	.03	.08
	Ave.	.0	.025	.08
25	Side A	-.01	.05	.10
	Side B	.02	.05	.11
	Ave.	.005	.05	.105
50	Side A	.02	.08	.17
	Side B	.02	.07	.21
	Ave.	.02	.075	.19
75	Side A	.03	.12	.28
	Side B	.04	.11	.29
	Ave.	.035	.115	.285
100	Side A	.03	.18	.41
	Side B	.05	.16	.43
	Ave.	.04	.17	.42

Nickel Cyclic Creep Data

Cyclic Test Number		2	
Alloy Designation		Rene' 41	
Heat Number		2490-0-8207	
Supplier		Teledyne Rodney	
Test Temperature (°K)		1155	
Test Direction		Longitudinal	
Sheet Thickness (cm)		0.025 ± 0.003	
Specimen Number	R37L	R36L	R38L
Specimen Thickness (cm)	0.0274	0.0274	0.0274
Specimen Width (cm)	1.2733	1.2740	1.2730
Applied Load (kg)	16.7	20.3	23.7
Test Stress (MPa)	46.7	57.0	66.5

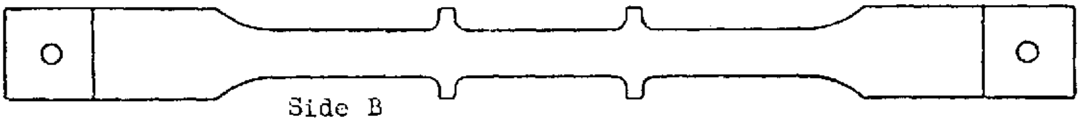

Cycle Number		% Creep R37L	R36L	R38L
1	Side A	.01	.01	.00
	Side B	.00	.00	.01
	Ave.	.005	.005	.005
5	Side A	.02	.05	.06
	Side B	.03	.04	.06
	Ave.	.025	.045	.06
15	Side A	.06	.11	.11
	Side B	.08	.09	.15
	Ave.	.07	.10	.13
25	Side A	.08	.17	.21
	Side B	.14	.17	.24
	Ave.	.11	.17	.225
50	Side A	.19	.29	.43
	Side B	.22	.30	.43
	Ave.	.205	.295	.43
75	Side A	.26	.43	.52
	Side B	.31	.43	.63
	Ave.	.285	.43	.575
100	Side A	.38	.55	.81
	Side B	.41	.58	.89
	Ave.	.395	.565	.85

Nickel Cyclic Creep Data

Cyclic Test Number	3		
Alloy Designation	Rene' 41		
Heat Number	2490-0-8207		
Supplier	Teledyne Rodney		
Test Temperature (°K)	1071		
Test Direction	Longitudinal		
Sheet Thickness (cm)	0.025 ± 0.003		
Specimen Number	R43L	R42L	R46L
Specimen Thickness (cm)	0.0274	0.0274	0.0274
Specimen Width (cm)	1.2750	1.2743	1.2758
Applied Load (kg)	24.5	36.9	48.3
Test Stress (MPa)	68.7	103.4	135.1

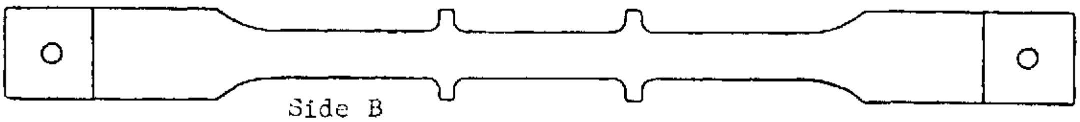

Cycle Number		% Creep R43L	R42L	R46L
1	Side A	-.02	-.02	.01
	Side B	-.03	-.01	.02
	Ave.	-.025	-.015	.015
5	Side A	-.02	-.02	.03
	Side B	-.01	.00	.03
	ve.	-.015	-.01	.03
15	Side A	-.02	-.01	.06
	Side B	-.01	.01	.07
	Ave.	-.015	.00	.065
25	Side A	.00	.02	.09
	Side B	-.01	.05	.09
	Ave.	-.005	.035	.09
50	Side A	.01	.05	.13
	Side B	.01	.05	.14
	Ave.	.01	.05	.135
75	Side A	.02	.08	.18
	Side B	.03	.09	.19
	Ave.	.025	.085	.185
100	Side A	.03	.10	.23
	Side B	.03	.10	.26
	Ave.	.03	.10	.245

Nickel Cyclic Creep Data

Cyclic Test Number		4	
Alloy Designation		Rene' 41	
Heat Number		2490-0-8207	
Supplier		Teledyne	
Test Temperature (°K)		1031	
Test Direction		Longitudinal	
Sheet Thickness (cm)		0.025 ± 0.003	
Specimen Number	R53L	R52L	R54L
Specimen Thickness(cm)	0.0272	0.0274	0.0272
Specimen Width (cm)	1.2769	1.2773	1.2766
Applied Load (kg)	50.3	74.2	97.6
Test Stress (MPa)	142.0	207.6	275.5

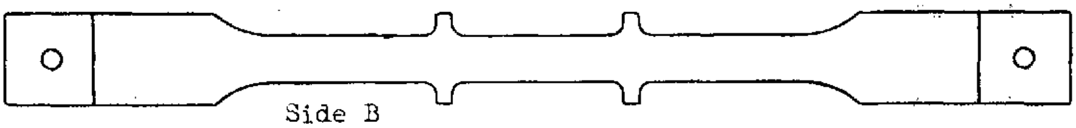

Cycle Number		% Creep R53L	R52L	R54L
1	Side A	-.02	-.02	.01
	Side B	-.03	.01	.02
	Ave.	-.025	-.005	.015
5	Side A	-.01	.01	.05
	Side B	-.01	.01	.03
	Ave.	-.01	.01	.04
15	Side A	.01	.03	.07
	Side B	.00	.03	.07
	Ave.	.005	.03	.07
25	Side A	.01	.05	.11
	Side B	.01	.05	.09
	Ave.	.01	.05	.10
50	Side A	.02	.05	.15
	Side B	.02	.10	.15
	Ave.	.02	.075	.15
75	Side A	.03	.08	.21
	Side B	.04	.12	.22
	Ave.	.035	.10	.215
100	Side A	.05	.10	.26
	Side B	.06	.14	.25
	Ave.	.055	.12	.255

Nickel Cyclic Creep Data

Cyclic Test Number			
Alloy Designation		Rene '41	
Heat Number		2490-0-8207	
Supplier		Teledyne Rodney	
Test Temperature (°K)		1111	
Test Direction		Longitudinal	
Sheet Thickness (cm)		0.025 + 0.003	
Specimen Number	R48L	R47L	R51L
Specimen Thickness (cm)	0.0274	0.0274	0.0272
Specimen Width (cm)	1.2764	1.2766	1.2769
Applied Load (Page E-3-7)			
Test Stress (Page E-3-7)			

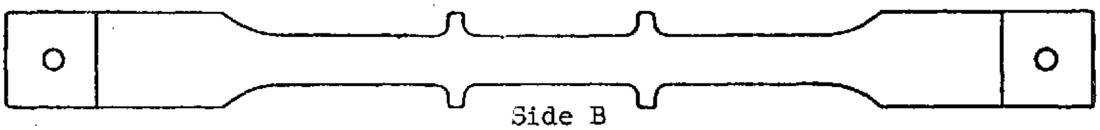

Cycle Number		% Creep R48L	% Creep R47L	% Creep R51L
1	Side A	.00	-.01	.00
	Side B	.02	.01	.01
	Ave.	.01	.00	.005
5	Side A	.01	.03	.02
	Side B	.03	.03	.04
	Ave.	.02	.03	.03
15	Side A	.01	.04	.06
	Side B	.05	.05	.07
	Ave.	.03	.045	.065
25	Side A	.05	.09	.16
	Side B	.07	.11	.17
	Ave.	.06	.10	.165
50	Side A	.10	.20	.35
	Side B	.11	.23	.35
	Ave.	.105	.215	.35
75	Side A	.10	.23	.47
	Side B	.15	.27	.45
	Ave.	.125	.25	.46
100	Side A	.13	.29	.58
	Side B	.17	.31	.57
	Ave.	.15	.30	.575

Rene '41 Test 5

	SPECIMEN R48L		SPECIMEN R47L		SPECIMEN R51L	
CYCLES	MEAN LOAD (kg)	STRESS (MPa)	MEAN LOAD (kg)	STRESS (MPa)	MEAN LOAD (kg)	STRESS (MPa)
1-15	18.5	52.1	25.1	70.6	36.1	101.4
16-50	24.7	69.4	36.3	102.2	48.5	136.4
51-100	18.7	52.7	28.2	79.4	36.9	103.8

Nickel Cyclic Creep Data

Cyclic Test Number		6	
Alloy Designation		Rene' 41	
Heat Number		2490-0-8207	
Supplier		Teledyne Rodney	
Test Temperature (°K)		1111	
Test Direction		Longitudinal	
Sheet Thickness (cm)		0.025 $\pm$ 0.003	
Specimen Number	R59L	R58L	R60L
Specimen Thickness (cm)	0.0271	0.0271	0.0271
Specimen Width (cm)	1.2768	1.2766	1.2768

Applied Load (See Table - Page E-3-9)
Test Stress (See Table - Page E-3-9)

Side A

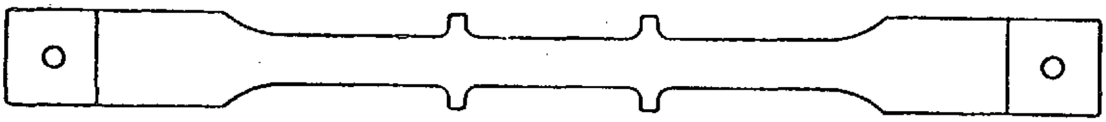

Side B

Cycle Number		% Creep R59L	R58L	R60L
1	Side A	-.03	-.01	-.01
	Side B	-.02	-.01	.01
	Ave.	-.025	-.01	.00
5	Side A	-.03	.01	.01
	Side B	-.01	.02	.02
	Ave.	-.02	.015	.015
15	Side A	-.02	.02	.03
	Side B	.01	.03	.05
	Ave.	-.005	.015	.04
25	Side A	-.02	.02	.06
	Side B	.01	.07	.07
	Ave.	-.005	.045	.065
50	Side A	.02	.05	.15
	Side B	.02	.14	.17
	Ave.	.02	.095	.16
75	Side A	.06	.14	.26
	Side B	.06	.23	.30
	Ave.	.06	.185	.28
100	Side A	.09	.26	.44
	Side B	.11	.30	.46
	Ave.	.10	.28	.45

Rene' 41 Test 6

	SPECIMEN R59L		SPECIMEN R58L		SPECIMEN R60L	
Cycles	Mean Load (kg)	Stress (MPa)	Mean Load (kg)	Stress (MPa)	Mean Load (kg)	Stress (MPa)
1-5	12.0	33.8	19.4	54.7	23.9	67.2
6-15	13.7	38.5	21.3	60.0	26.4	74.3
16-25	15.2	42.9	22.9	64.4	29.2	82.0
26-35	16.6	46.7	24.0	67.4	32.6	91.8
36-45	18.8	53.0	25.8	72.5	34.4	96.8
46-55	19.0	53.6	27.6	77.6	35.7	100.3
56-55	19.8	55.6	30.3	85.4	38.5	108.1
66-75	20.8	58.5	31.3	88.0	41.5	116.7
76-86	22.4	63.0	32.3	90.9	43.9	123.5
87-95	23.5	66.2	34.7	97.6	46.0	129.5
96-100	25.3	71.1	36.3	102.1	48.1	135.4

Nickel Cyclic Creep Data

Cyclic Test Number		7	
Alloy Designation		Rene '41	
Heat Number		2490-0-8207	
Supplier		Teledyne Rodney	
Test Temperature (°K)		1111	
Test Direction		Longitudinal	
Sheet Thickness (cm)		0.025 ± 0.003	
Specimen Number	R62L	R61L	R63L
Specimen Thickness (cm)	0.0272	0.0274	0.0274
Specimen Width (cm)	1.2756	1.2758	1.2756
Applied Load (See Table - Page E-3-11)			
Test Stress (See Table - Page E-3-11)			

Side A

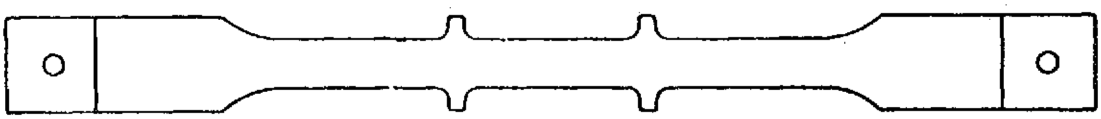

Side B

Cycle Number		% Creep R62L	R61L	R63L
1	Side A	-.01	.00	.00
	Side B	-.01	.01	.03
	Ave.	-.01	.005	.015
5	Side A	.00	.04	.04
	Side B	.02	.03	.07
	Ave.	.01	.035	.055
15	Side A	.01	.07	.10
	Side B	.05	.09	.14
	Ave.	.03	.08	.12
25	Side A	.05	.08	.15
	Side B	.05	.11	.18
	Ave.	.05	.095	.165
50	Side A	.06	.14	.25
	Side B	.07	.18	.29
	Ave.	.065	.16	.27
75	Side A	.09	.18	.31
	Side B	.07	.18	.37
	Ave.	.08	.18	.34
100	Side A	.10	.21	.37
	Side B	.11	.25	.41
	Ave.	.105	.23	.39

Rene' 41 Test 7

	SPECIMEN R62L		SPECIMEN R61L		SPECIMEN R63L	
Cycles	Mean Load (kg)	Stress (MPa)	Mean Load (kg)	Stress (MPa)	Mean Load (kg)	Stress (MPa)
0-5	25.1	70.6	37.3	104.7	47.6	134.0
6-15	23.4	65.9	35.0	98.4	46.3	130.2
16-25	22.3	62.7	32.6	91.6	43.8	123.1
26-35	21.0	59.2	31.1	87.4	41.4	116.5
36-45	20.3	57.1	29.0	81.6	38.7	108.9
46-55	18.8	52.7	27.2	76.4	36.7	103.3
56-65	17.9	50.3	25.5	72.2	33.4	94.0
66-75	16.8	47.2	23.4	65.9	31.3	88.0
76-85	15.1	42.4	22.0	61.8	28.7	80.7
86-95	13.6	38.2	20.0	56.2	26.6	74.7
96-100	12.5	35.2	18.2	51.2	24.3	68.4

Nickel Cyclic Creep Data

Cyclic Test Number		8	
Alloy Designation		Rene' 41	
Heat Number		2490-0-8207	
Supplier		Teledyne	
Test Temperature (°K)		1155	
Test Direction		Longitudinal	
Sheet Thickness (cm)		0.025 cm ±0.003	
Specimen Number	R65L	R64L	R66L
Specimen Thickness (cm)	0.0274	0.0274	0.0274
Specimen Width (cm)	1.2755	1.2760	1.2755
Applied Load (kg)	16.2	20.7	24.6
Test Stress (MPa)	49.1	62.6	74.9

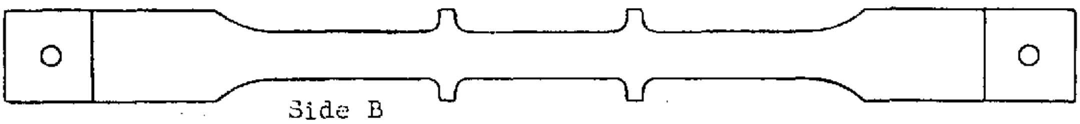

Cycle Number		% Creep R65L	R64L	R66L
2	Side A	-.01	.01	.00
	Side B	.01	.03	.06
	Ave.	.00	.02	.03
10	Side A	.02	.06	.06
	Side B	.05	.06	.06
	Ave.	.035	.06	.06
30	Side A	.06	.14	.19
	Side B	.09	.18	.14
	Ave.	.075	.16	.165
50	Side A	.09	.18	.27
	Side B	.16	.25	.21
	Ave.	.125	.215	.24
100	Side A	.19	.41	.48
	Side B	.27	.43	.48
	Ave.	.23	.42	.48

Nickel
Cyclic Creep Data

Cyclic Test Number		9	
Alloy Designation		Rene' 41	
Heat Number		2490-0-8207	
Supplier		Teledyne	
Test Temperature (°K)		1111	
Test Direction		Longitudinal	
Sheet Thickness (cm)		0.025 ± 0.003	
Specimen Number	R68L	R67L	R69L
Specimen Thickness (cm)	0.0274	0.0274	0.0274
Specimen Width (cm)	1.2758	1.2756	1.2753
Applied Load (kg)	14.6/22.0	21.7/32.5	29.3/43.7
Test Stress (MPa)	40.7/61.4	60.8/91.0	82.1/122.3

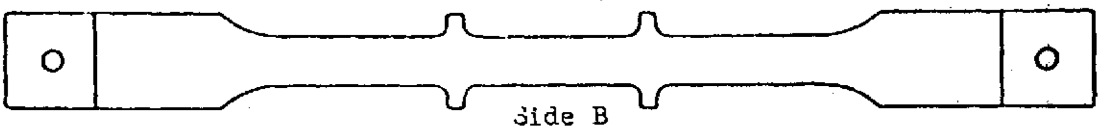

Cycle Number		% Creep R68L	% Creep R67L	% Creep R69L
1	Side A	-.03	.01	-.01
	Side B	-.01	.00	.01
	Ave.	-.02	.005	.00
5	Side A	-.01	.02	.02
	Side B	-.01	.02	.02
	Ave.	-.01	.02	.02
15	Side A	.00	.06	.07
	Side B	.01	.05	.09
	Ave.	.005	.055	.08
25	Side A	.00	.06	.10
	Side B	.03	.07	.11
	Ave.	.015	.065	.105
50	Side A	.03	.13	.19
	Side B	.05	.17	.24
	Ave.	.04	.15	.215
75	Side A	.05	.17	.27
	Side B	.09	.24	.33
	Ave.	.07	.205	.30
100	Side A	.09	.25	.39
	Side B	.13	.31	.44
	Ave.	.11	.28	.415

Nickel
Cyclic Creep Data

Cyclic Test Number	10		
Alloy Designation	Rene' 41		
Heat Number	2490-0-8207		
Supplier	Teledyne		
Test Temperature (°K)	1111		
Test Direction	Longitudinal		
Sheet Thickness (cm)	0.025 ± 0.003		
Specimen Number	R71L	R72L	R70L
Specimen Thickness (cm)	0.0274	0.0274	0.0274
Specimen Width (cm)	1.2758	1.2761	1.2756
Applied Load (kg)	13.9	24.7	36.6
Test Stress (MPa)	39.0	69.2	102.5

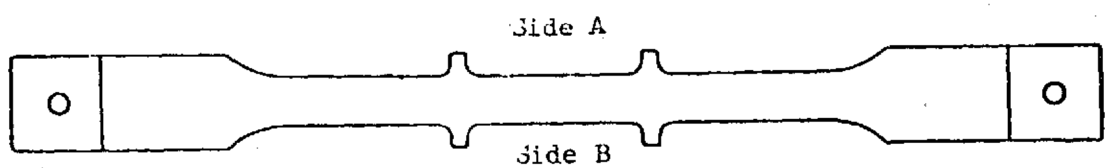

Cycle Number		% Creep R71L	% Creep R72L	% Creep R70L
1	Side A	.02	.01	.00
	Side B	.02	.00	.02
	Ave.	.02	.005	.01
5	Side A	.02	.01	.05
	Side B	.01	.03	.07
	Ave.	.015	.02	.06
15	Side A	-.01	.03	.09
	Side B	.01	.08	.13
	Ave.	.00	.055	.11
25	Side A	.01	.05	.15
	Side B	.00	.09	.15
	Ave.	.005	.07	.15
50	Side A	.02	.10	.25
	Side B	.04	.14	.30
	Ave.	.03	.12	.275

Nickel
Cyclic Creep Data

Cyclic Test Number		11 (Continuation of Rene' Test 1)		
Alloy Designation		Rene' 41		
Heat Number		2490-0-8207		
Supplier		Teledvne		
Test Temperature	(°K)	1111		
Test Direction		Longitudinal		
Sheet Thickness	(cm)	0.025 ± 0.003		
Specimen Number		R40L	R41L	R39L
Specimen Thickness	(cm)	0.0277	0.0277	0.0277
Specimen Width	(cm)	1.2723	1.2725	1.2730
Applied Load	(kg)	14.1	24.5	36.4
Test Stress	(MPa)	39.2	68.0	101.1

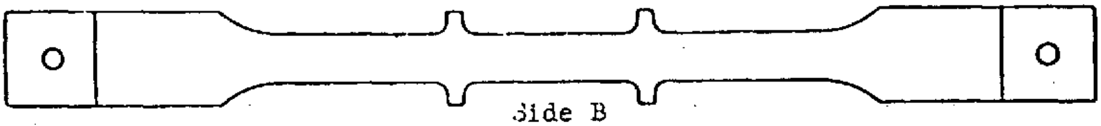

Cycle Number		% Creep * R40L	R41L	R39L
101	Side A	.01	.02	.02
	Side B	.00	.01	.01
	Ave.	.005	.015	.015
105	Side A	.01	.00	.02
	Side B	.02	.02	.03
	Ave.	.015	.01	.025
115	Side A	.01	.01	.04
	Side B	.01	.03	.08
	Ave.	.01	.02	.06
125	Side A	.01	.03	.06
	Side B	.02	.04	.13
	Ave.	.015	.035	.095
150	Side A	.02	.07	.15
	Side B	.03	.08	.24
	Ave.	.025	.075	.195

* Creep Strains are in addition to those obtained in Test 1.

Nickel
Cyclic Creep Data

Cyclic Test Number	12		
Alloy Designation	R41		
Heat Number	2490-0-8207		
Supplier	Teledyne Rodney		
Test Temperature (°K)	(See Figure 3-107)		
Test Direction	Longitudinal		
Sheet Thickness (cm)	0.025 ± 0.003		
Specimen Number	R73L	R74L	R75L
Specimen Thickness (cm)	0.0274	0.0274	0.0274
Specimen Width (cm)	1.2761	1.2758	1.2755
Applied Load (kg)	(See Table - Page E-3-17)		
Test Stress (MPa)	(See Table - Page E-3-17)		

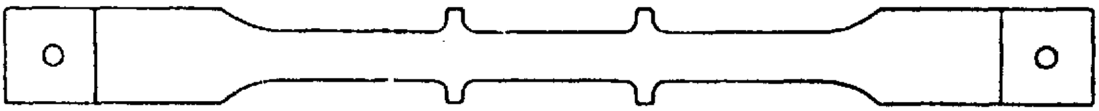

Cycle Number		% Creep R73L	R74L	R75L
1	Side A	.03	.00	.01
	Side B	-.01	-.02	.01
	Ave.	.01	-.01	.01
5	Side A	.03	.01	.06
	Side B	.05	.01	.03
	Ave.	.04	.01	.045
15	Side A	.09	.06	.09
	Side B	.10	.03	.13
	Ave.	.095	.045	.11
25	Side A	.13	.09	.17
	Side B	.15	.07	.17
	Ave.	.14	.08	.17
50	Side A	.23	.15	.31
	Side B	.30	.17	.33
	Ave.	.265	.16	.32
75	Side A	.31	.19	.41
	Side B	.43	.24	.50
	Ave.	.37	.215	.455

R41 TEST 12

SPECIMEN	LOAD ∿ (kg)		
	1ST STEP (10 MINUTES)	2ND STEP (10 MINUTES)	3RD STEP (10 MINUTES)
R73L	14.6	24.4	39.2
R74L	11.8	19.7	32.0
R75L	17.7	29.4	48.2

SPECIMEN	STRESS ∿ (MPa)		
	1ST STEP (10 MINUTES)	2ND STEP (10 MINUTES)	3RD STEP (10 MINUTES)
R73L	40.9	68.3	109.7
R74L	33.0	55.2	89.6
R75L	49.7	82.3	135.0

Nickel
Cyclic Creep Data

Cyclic Test Number	13		
Alloy Designation	R41		
Heat Number	2490-0-8207		
Supplier	Teledyne Rodney		
Test Temperature (°K)	1111		
Test Direction	Longitudinal		
Sheet Thickness (cm)	0.025 ± 0.003		
Specimen Number	R76L	R77L	R78L
Specimen Thickness (cm)	0.0272	0.0272	0.0272
Specimen Width (cm)	1.2756	1.2756	1.2753
Applied Load (kg)	(See Table - Page E-3-20)		
Test Stress (MPa)	(See Table - Page E-3-20)		

Side A

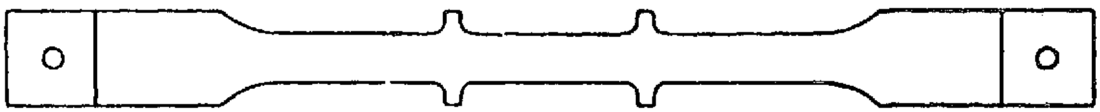

Side B

Cycle Number		% Creep R76L	% Creep R77L	% Creep R78L
1	Side A	.02	.01	.02
	Side B	.01	.01	.01
	Ave.	.015	.01	.015
5	Side A	.03	.02	.04
	Side B	.02	.02	.03
	Ave.	.025	.02	.035
15	Side A	.06	.04	.08
	Side B	.07	.05	.07
	Ave.	.065	.045	.075
25	Side A	.08	.04	.11
	Side B	.09	.07	.10
	Ave.	.085	.055	.105
50	Side A	.11	.07	.17
	Side B	.17	.11	.17
	Ave.	.14	.09	.17
75	Side A	.16	.11	.22
	Side B	.22	.12	.25
	Ave.	.19	.115	.235
100	Side A	.19	.13	.27
	Side B	.28	.15	.31
	Ave.	.235	.14	.29

R41 TEST 13

	LOAD ∿ (kg)		
SPECIMEN	1ST STEP (10 MINUTES)	2ND STEP (10 MINUTES)	3RD STEP (10 MINUTES)
R76L	15.1	24.6	38.4
R77L	11.8	19.4	31.4
R78L	18.2	30.0	48.6

	STRESS ∿ (MPa)		
SPECIMEN	1ST STEP (10 MINUTES)	2ND STEP (10 MINUTES)	3RD STEP (10 MINUTES)
R76L	42.7	69.7	108.6
R77L	33.5	54.8	88.9
R78L	51.4	84.8	137.4

Nickel
Cyclic Creep Data

Cyclic Test Number	14		
Alloy Designation	R41		
Heat Number	2490-0-8207		
Supplier	Teledyne Rodney		
Test Temperature (°K)	1111		
Test Direction	Longitudinal		
Sheet Thickness (cm)	0.025 ± 0.003		
Specimen Number	R79L	R80L	R81L
Specimen Thickness (cm)	0.0272	0.0272	0.0274
Specimen Width (cm)	1.2753	1.2748	1.2751
Applied Load (kg)	(See Table - Page E-3-22)		
Test Stress (MPa)	(See Table - Page E-3-22)		

Side A

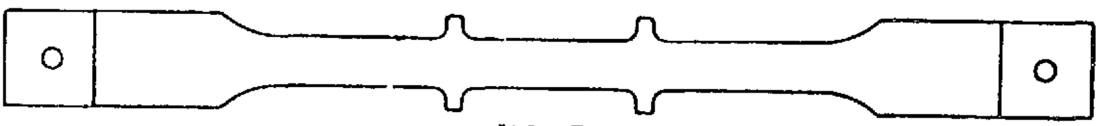

Side B

Cycle Number		% Creep R79L	R80L	R81L
1	Side A	-.01	-.01	.00
	Side B	.02	.01	.03
	Ave.	.005	.00	.015
5	Side A	.05	.02	.03
	Side B	.02	.01	.03
	Ave.	.035	.015	.03
15	Side A	.04	.02	.05
	Side B	.05	.05	.07
	Ave.	.045	.035	.06
25	Side A	.10	.03	.09
	Side B	.07	.05	.09
	Ave.	.085	.04	.09
50	Side A	.15	.07	.19
	Side B	.13	.07	.13
	Ave.	.14	.07	.16
75	Side A	.19	.11	.25
	Side B	.18	.11	.18
	Ave.	.185	.11	.215
100	Side A	.25	.16	.28
	Side B	.20	.10	.27
	Ave.	.225	.13	.275

R41 TEST 14

SPECIMEN	LOAD ∿ (kg) 1ST STEP (10 MINUTES)	2ND STEP (10 MINUTES)	3RD STEP (10 MINUTES)
R79L	14.5	24.2	38.8
R80L	11.9	19.9	32.1
R81L	18.0	29.8	48.6

SPECIMEN	STRESS ∿ (MPa) 1ST STEP (10 MINUTES)	2ND STEP (10 MINUTES)	3RD STEP (10 MINUTES)
R79L	41.0	68.6	109.8
R80L	33.7	56.2	90.9
R81L	50.5	83.4	136.3

Nickel
Cyclic Creep Data

Cyclic Test Number	15		
Alloy Designation	R41		
Heat Number	2490-0-8207		
Supplier	Teledyne Rodney		
Test Temperature (°K)	(See Table - Page E-2-24)		
Test Direction	Longitudinal		
Sheet Thickness (cm)	0.025 ± 0.003		
Specimen Number	R82L	R83L	R84L
Specimen Thickness (cm)	0.0272	0.0272	0.0272
Specimen Width (cm)	1.2748	1.2755	1.2751
Applied Load (kg)	(See Table - Page E-3-24)		
Test Stress (MPa)	(See Table - Page E-3-24)		

Side A

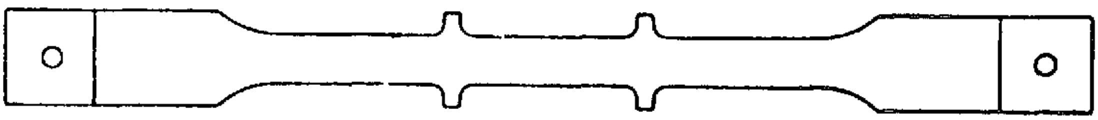

Side B

Cycle Number		% Creep R82L	R83L	R84L
1	Side A	.01	.00	.01
	Side B	.01	.01	.03
	Ave.	.01	.005	.02
5	Side A	.03	.02	.06
	Side B	.05	.03	.06
	Ave.	.04	.025	.06
15	Side A	.07	.06	.13
	Side B	.10	.04	.08
	Ave.	.085	.05	.105
25	Side A	.11	.10	.18
	Side B	.15	.07	.14
	Ave.	.13	.085	.16
50	Side A	.22	.21	.28
	Side B	.24	.10	.28
	Ave.	.23	.155	.28
75	Side A	.29	.25	.32
	Side B	.41	.20	.47
	Ave.	.35	.225	.395
100	Side A	.37	.31	.45
	Side B	.52	.23	.55
	Ave.	.445	.27	.50
150	Side A	.56	.38	.71
	Side B	.68	.37	.71
	Ave.	.62	.375	.71
200	Side A	.65	.42	.80
	Side B	.78	.42	.84
	Ave.	.715	.42	.82

RENE' 41 TEST 15

CYCLE TIME (SEC)	TEMP (°K)	PRESSURE-Pa.	STRESS ∿ (MPa)		
			R82L	R83L	R84L
300	551	.4	–	–	–
400	980	2.0	13.5	12.4	18.9
500	1104	2.7	28.4	22.9	34.9
600	1147	3 3	36.7	29.7	44.8
700	1169	4.0	41.9	33.9	50.7
800	1169	4.7	46.0	37.3	55.3
900	1158	5.3	47.7	38.8	56.9
1000	1147	6.9	48.7	39.7	57.8
1100	1131	8.5	52.5	42.7	62.1
1200	1120	9.3	57.1	46.5	67.4
1300	1109	10.7	65.4	53.1	77.1
1400	1099	16.0	72.3	58.0	84.5
1500	1083	24.0	81.5	66.0	96.4
1600	1061	40.0	93.7	75.9	111.0
1700	1013	44.0	100.3	81.6	120.3
1800	932	80.0	108.7	89.6	131.6
1900	851	113.3	115.8	95.5	141.1
2000	728	200.0	115.4	95.4	141.8
2100	626	466.4	106.3	88.0	131.9
2200	540	1466.3	94.4	78.6	118.5
2300	470	4478.9	78.8	65.7	99.8
2400	309	11597.1	54.5	45.0	69.6
2500	309	18795.3	33.7	30.4	44.3

Stress and Temperature Steps for Analysis of Rene '41 Mission Profile Tests (Test 15)

Step Number	Time Step Sec.	Temperature °K	Stress MPa		
			R82L	R83L	R84L
1	300 - 500	980	13.5	12.4	18.9
2	500 - 700	1147	36.7	29.7	44.8
3	700 - 900	1169	46.0	37.3	55.3
4	900 - 1100	1147	48.7	39.7	57.8
5	1100 - 1300	1120	57.1	46.5	67.4
6	1300 - 1500	1099	72.3	58.0	84.5
7	1500 - 1700	1061	93.7	75.9	111.0
8	1700 - 1900	932	108.7	89.6	131.6
9	1900 - 2100	728	115.4	95.4	141.8
10	2100 - 2300	540	94.4	78.6	118.5

APPENDIX F-1

TDNiCr LITERATURE SURVEY CREEP DATA

Sources of this data are:

DAC-62124	- Killpatrick, D. H., and Hocker, R. G., "Stress-Rupture and Creep in Dispersion Strengthened Nickel-Chromium Alloys," McDonnell Douglas Corporation Report DAC-62124, May 1968
G.E.-PVT-4662 and 5132	- Private Communications with General Electric Company File number 4662 and 5132, September and October 1972
MDAC-W-INTL	- McDonnell Douglas Astronautics Corporation - West, in-house testing, 1971
NAS-3-15558	- Data Generated for NASA Lewis Research Center by Metcut Research Associates under NASA contract NAS-3-15558 and reported in NASA CR-121221, 1973
NAS-8-27189	- Data Generated for Marshall Space Flight Center, by Vulcan Testing Laboratory under NASA contract NAS-8-27189, 1971

ALLOY - TD NICR
STRESS (MPA) - 100.0
TEMP. (KELVIN) - 1033
THICKNESS (CM) - .038
TEST DIRECTION - TRANS.
SOURCE - NAS-8-27189

STRAIN (PCT.)	TIME (HOURS)
.065	2.0
.105	4.0
.165	8.0
.250	18.0
.305	32.0
.335	44.0
.355	53.0
.375	68.0
.410	91.0
.414	116.0
.430	138.0
.440	163.0
.455	188.0
.465	212.0
.475	232.0
.484	258.0
.495	282.0

ALLOY - TD NICR
STRESS (MPA) - 103.4
TEMP. (KELVIN) - 1033
THICKNESS (CM) - .038
TEST DIRECTION - TRANS.
SOURCE - NAS-8-27189

STRAIN (PCT.)	TIME (HOURS)
.060	1.0
.105	2.0
.168	4.5
.212	7.0
.284	11.0
.375	23.0
.402	31.0
.430	46.0
.445	55.0
.462	71.8
.470	79.0
.485	96.0
.495	104.0
.500	121.0

ALLOY - TD NICR
STRESS (MPA) - 110.3
TEMP. (KELVIN) - 1033
THICKNESS (CM) - .038
TEST DIRECTION - TRANS.
SOURCE - NAS-8-27189

STRAIN (PCT.)	TIME (HOURS)
.050	.5
.085	1.0
.140	2.0
.230	4.0
.330	8.0
.390	13.2
.450	22.2
.480	33.0

ALLOY - TD NICR
STRESS (MPA) - 158.6
TEMP. (KELVIN) - 1033
THICKNESS (CM) - .038
TEST DIRECTION - TRANS.
SOURCE - NAS-8-27189

STRAIN (PCT.)	TIME (HOURS)
.070	.1
.180	.2
.450	.3
.010	1.0
.025	2.5
.040	5.0
.080	9.5
.155	23.0
.250	31.5
.349	46.0
.440	58.5

ALLOY - TD NICR
STRESS (MPA) - 75.8
TEMP. (KELVIN) - 1089
THICKNESS (CM) - .102
TEST DIRECTION - TRANS.
SOURCE - GE-PVT-4662

STRAIN (PCT.)	TIME (HOURS)
.100	500.0
.200	1320.0
.500	4720.0

ALLOY - TD NICR
STRESS (MPA) - 86.2
TEMP. (KELVIN) - 1089
THICKNESS (CM) - .102
TEST DIRECTION - TRANS.
SOURCE - GE-PVT-4662

STRAIN (PCT.)	TIME (HOURS)
.100	110.0
.200	336.0
.500	890.0

ALLOY - TD NICR
STRESS (MPA) - 100.0
TEMP. (KELVIN) - 1089
THICKNESS (CM) - .152
TEST DIRECTION - TRANS.
SOURCE - GE-PVT-4662

STRAIN (PCT.)	TIME (HOURS)
.100	1700.0

ALLOY - TD NICR
STRESS (MPA) - 110.3
TEMP. (KELVIN) - 1089
THICKNESS (CM) - .152
TEST DIRECTION - TRANS.
SOURCE - GE-PVT-4662

STRAIN (PCT.)	TIME (HOURS)
.100	70.0
.200	772.0

ALLOY - TD NICR
STRESS (MPA) - 115.1
TEMP. (KELVIN) - 1089
THICKNESS (CM) - .152
TEST DIRECTION - TRANS.
SOURCE - GE-PVT-4662

STRAIN (PCT.)	TIME (HOURS)
.100	30.0
.200	320.0
.100	450.0
.200	1250.0

ALLOY - TD NICR
STRESS (MPA) - 117.2
TEMP. (KELVIN) - 1089
THICKNESS (CM) - .102
TEST DIRECTION - LONG.
SOURCE - GE-PVT-4662

STRAIN (PCT.)	TIME (HOURS)
.100	120.0
.200	900.0

ALLOY - TD NICR
STRESS (MPA) - 131.[illegible]
TEMP. (KELVIN) - 1089
THICKNESS (CM) - .102
TEST DIRECTION - LONG.
SOURCE - GE-PVT-4662

STRAIN (PCT.)	TIME (HOURS)
.100	6.0
.200	13.0
.500	31.0
.100	370.0
.200	805.0
.500	1130.0

ALLOY - TD NICR
STRESS (MPA) - 165.5
TEMP. (KELVIN) - 1089
THICKNESS (CM) - .152
TEST DIRECTION - LONG.
SOURCE - GE-PVT-4662

STRAIN (PCT.)	TIME (HOURS)
.100	.2
.200	3.2
.500	15.0
.100	50.0

ALLOY - TD NICR
STRESS (MPA) - 65.5
TEMP. (KELVIN) - 1144
THICKNESS (CM) - .025
TEST DIRECTION - TRANS.
SOURCE - NAS-3-15558

STRAIN (PCT.)	TIME (HOURS)
.005	.1
.015	.3
.015	.4
.035	1.0
.085	6.1
.105	17.7
.145	25.1
.165	30.7
.180	49.1
.180	67.4
.200	73.1
.220	89.3
.230	96.5
.240	112.9

ALLOY - TD NICR
STRESS (MPA) - 68.9
TEMP. (KELVIN) - 1144
THICKNESS (CM) - .025
TEST DIRECTION - TRANS.
SOURCE - NAS-3-15558

STRAIN (PCT.)	TIME (HOURS)
.005	.3
.010	.5
.015	1.5
.015	3.3
.055	5.7
.060	12.6
.075	21.9
.080	29.7
.090	45.1
.100	53.6
.105	69.1
.115	77.9
.120	98.2
.120	117.4

ALLOY - TD NICR
STRESS (MPA) - 75.8
TEMP. (KELVIN) - 1144
THICKNESS (CM) - .025
TEST DIRECTION - TRANS.
SOURCE - NAS-3-15558

STRAIN (PCT.)	TIME (HOURS)
.010	.2
.015	.3
.020	.4
.030	3.2
.040	6.3
.050	10.9
.055	20.7
.060	[illegible]
.065	35.7
.070	45.1
.070	54.3
.075	78.3
.085	94.5
.085	101.9

ALLOY - TD NICR
STRESS (MPA) - 75.8
TEMP. (KELVIN) - 1144
THICKNESS (CM) - .025
TEST DIRECTION - TRANS.
SOURCE - NAS-3-15558

STRAIN (PCT.)	TIME (HOURS)
.015	.1
.035	.2
.045	.4
.055	.6
.065	1.0
.070	1.2
.200	7.6
.280	17.9
.330	25.3
.415	43.6
.440	48.7
.490	66.8
.505	73.1
.545	89.7
.565	96.9
.585	112.8

ALLOY - TD NICR
STRESS (MPA) - 75.8
TEMP. (KELVIN) - 1144
THICKNESS (CM) - .051
TEST DIRECTION - TRANS.
SOURCE - NAS-3-15558

STRAIN (PCT.)	TIME (HOURS)
.005	.1
.005	.2
.005	.4
.020	.5
.040	1.7
.035	3.6
.050	6.1
.050	10.7
.075	21.6
.070	29.3
.085	46.1
.100	53.6
.105	69.9
.095	77.5
.115	92.3
.130	100.1

ALLOY - TD NICR
STRESS (MPA) - 75.8
TEMP. (KELVIN) - 1144
THICKNESS (CM) - .051
TEST DIRECTION - TRANS.
SOURCE - NAS-3-15558

STRAIN (PCT.)	TIME (HOURS)
.020	.1
.035	.3
.025	.5
.030	1.0
.040	3.3
.055	6.1
.075	11.6
.090	23.4
.100	29.8
.120	46.0
.125	53.8
.140	69.3
.135	74.5
.150	93.0
.155	118.1

ALLOY - TD NICR
STRESS (MPA) - 75.8
TEMP. (KELVIN) - 1144
THICKNESS (CM) - .051
TEST DIRECTION - TRANS.
SOURCE - NAS-3-15558

STRAIN (PCT.)	TIME (HOURS)
.020	.1
.020	.2
.025	.3
.030	.5
.040	1.3
.065	5.5
.060	9.8
.105	23.3
.125	29.3
.130	46.1
.145	53.4
.150	69.1
.160	77.4
.155	98.5
.155	119.8

ALLOY - TD NICR
STRESS (MPA) - 79.3
TEMP. (KELVIN) - 1144
THICKNESS (CM) - .025
TEST DIRECTION - TRANS.
SOURCE - NAS-3-15558

STRAIN (PCT.)	TIME (HOURS)
.020	.2
.025	.3
.025	.4
.025	.5
.030	1.3
.035	3.7
.050	9.0
.055	19.9
.070	43.8
.085	51.6
.090	66.8
.095	75.6
.090	93.3
.095	100.0

ALLOY - TD NICR
STRESS (MPA) - 79.3
TEMP. (KELVIN) - 1144
THICKNESS (CM) - .051
TEST DIRECTION - TRANS.
SOURCE - NAS-3-15558

STRAIN (PCT.)	TIME (HOURS)
.020	.1
.020	.2
.030	.3
.030	.4
.040	1.9
.040	3.6
.075	9.7
.100	19.2
.100	27.7
.130	44.5
.120	51.7
.120	67.4
.130	75.3
.140	90.7
.140	95.8
.150	115.3

ALLOY - TD NICR
STRESS (MPA) - 80.7
TEMP. (KELVIN) - 1144
THICKNESS (CM) - .025
TEST DIRECTION - TRANS.
SOURCE - NAS-3-15558

STRAIN (PCT.)	TIME (HOURS)
.020	.1
.020	.2
.030	.3
.030	.4
.035	.6
.050	1.4
.050	3.8
.060	5.6
.050	11.1
.060	21.9
.065	30.0
.070	34.5
.065	47.4
.075	53.5
.075	69.0
.080	77.3
.090	101.1

ALLOY - TD NICR
STRESS (MPA) - 80.7
TEMP. (KELVIN) - 1144
THICKNESS (CM) - .051
TEST DIRECTION - TRANS.
SOURCE - NAS-3-15558

STRAIN (PCT.)	TIME (HOURS)
.015	.1
.015	.2
.020	.3
.035	1.1
.085	5.8
.111	16.5
.140	25.1
.155	40.4
.170	49.3
.180	64.3
.185	69.6
.225	88.9
.250	114.7

ALLOY - TD NICR
STRESS (MPA) - 82.7
TEMP. (KELVIN) - 1144
THICKNESS (CM) - .051
TEST DIRECTION - TRANS.
SOURCE - NAS-3-15558

STRAIN (PCT.)	TIME (HOURS)
.025	.1
.045	.2
.045	.3
.060	.4
.065	.9
.330	18.5
.380	25.0
.510	42.5
.560	45.9
.760	74.4
.875	90.6
.900	96.8
.985	115.0

ALLOY - TD NICR
STRESS (MPA) - 82.7
TEMP. (KELVIN) - 1144
THICKNESS (CM) - .051
TEST DIRECTION - TRANS.
SOURCE - NAS-3-15558

STRAIN (PCT.)	TIME (HOURS)
.010	.2
.015	.3
.025	.4
.025	.5
.040	1.0
.080	4.4
.075	5.6
.100	11.2
.130	20.6
.155	29.8
.205	49.2
.185	53.9
.205	70.1
.215	77.5
.235	94.0
.250	98.7
.245	117.5

ALLOY - TD NICR
STRESS (MPA) - 82.7
TEMP. (KELVIN) - 1144
THICKNESS (CM) - .051
TEST DIRECTION - TRANS.
SOURCE - NAS-3-15558

STRAIN (PCT.)	TIME (HOURS)
.015	.2
.020	.3
.035	.7
.055	1.2
.085	7.2
.125	18.8
.160	25.2
.170	43.6
.195	49.2
.200	64.8
.220	73.3
.235	91.4
.255	125.0
.260	136.9

ALLOY - TD NICR
STRESS (MPA) - 86.2
TEMP. (KELVIN) - 1144
THICKNESS (CM) - .025
TEST DIRECTION - LONG.
SOURCE - NAS-3-15558

STRAIN (PCT.)	TIME (HOURS)
.035	.1
.050	.3
.050	.4
.065	1.2
.095	5.4
.105	9.8
.130	23.2
.135	29.2
.155	53.3
.150	69.0
.170	77.3
.170	92.1
.170	98.4
.170	119.7

ALLOY - TD NICR
STRESS (MPA) - 89.6
TEMP. (KELVIN) - 1144
THICKNESS (CM) - .025
TEST DIRECTION - LONG.
SOURCE - NAS-3-15558

STRAIN (PCT.)	TIME (HOURS)
.020	.1
.020	.2
.020	.3
.040	.4
.035	1.1
.045	2.7
.045	3.3
.085	9.0
.080	20.1
.080	27.6
.090	45.4
.090	51.4
.105	68.2
.110	75.5
.110	91.2
.135	99.9

ALLOY - TD NICR
STRESS (MPA) - 89.5
TEMP. (KELVIN) - 1144
THICKNESS (CM) - .051
TEST DIRECTION - TRANS.
SOURCE - NAS-3-15558

STRAIN (PCT.)	TIME (HOURS)
.025	.1
.045	.2
.065	.4
.065	.5
.100	2.2
.170	6.2
.240	11.3
.300	22.0
.325	30.1
.410	48.2
.425	54.3
.485	70.9
.500	77.9
.550	94.7
.555	98.5
.610	122.5

ALLOY - TD NICR
STRESS (MPA) - 91.7
TEMP. (KELVIN) - 1144
THICKNESS (CM) - .025
TEST DIRECTION - TRANS.
SOURCE - NAS-3-15558

STRAIN (PCT.)	TIME (HOURS)
.020	.1
.025	.2
.045	.3
.045	.5
.105	1.2
.215	2.9
.295	4.2
.300	5.3
.425	10.6
.555	20.6
.625	29.2
.705	45.4
.745	53.2
.785	63.4
.815	77.2
.860	94.9
.820	100.9

ALLOY - TD NICR
STRESS (MPA) - 93.1
TEMP. (KELVIN) - 1144
THICKNESS (CM) - .025
TEST DIRECTION - LONG.
SOURCE - NAS-3-15558

STRAIN (PCT.)	TIME (HOURS)
.025	.1
.025	.2
.025	.5
.040	1.4
.060	3.8
.085	10.7
.085	20.2
.100	27.9
.100	32.5
.120	43.2
.125	51.8
.135	67.1
.135	86.3
.135	91.1
.155	96.3
.190	115.6

ALLOY - TD NICR
STRESS (MPA) - 94.5
TEMP. (KELVIN) - 1144
THICKNESS (CM) - .025
TEST DIRECTION - LONG.
SOURCE - NAS-3-15558

STRAIN (PCT.)	TIME (HOURS)
.035	.1
.040	.2
.070	.4
.190	3.1
.222	4.5
.235	10.1
.375	20.8
.420	28.1
.475	44.1
.500	52.0
.540	68.5
.545	75.9
.580	90.6
.600	97.0
.630	114.8

ALLOY - TD NICR
STRESS (MPA) - 110.3
TEMP. (KELVIN) - 1144
THICKNESS (CM) - .025
TEST DIRECTION - LONG.
SOURCE - NAS-3-15558

STRAIN (PCT.)	TIME (HOURS)
.010	.3
.020	.4
.030	.5
.050	2.2
.065	6.4
.070	11.6
.085	21.2
.095	30.4
.095	36.6
.110	48.0
.115	54.3
.120	72.7
.130	78.2
.140	93.9
.140	101.1

ALLOY - TD NICR
STRESS (MPA) - 110.3
TEMP. (KELVIN) - 1144
THICKNESS (CM) - .051
TEST DIRECTION - LONG.
SOURCE - NAS-3-15558

STRAIN (PCT.)	TIME (HOURS)
.010	.1
.020	.4
.020	.5
.030	1.0
.035	1.5
.045	5.6
.070	17.6
.075	25.3
.075	41.7
.085	49.2
.095	67.0
.095	73.2
.100	97.1
.100	112.0

ALLOY - TD NICR
STRESS (MPA) - 113.8
TEMP. (KELVIN) - 1144
THICKNESS (CM) - .051
TEST DIRECTION - LONG.
SOURCE - NAS-3-15558

STRAIN (PCT.)	TIME (HOURS)
.010	.1
.020	.2
.020	.4
.025	1.3
.015	3.1
.040	5.3
.035	9.8
.060	19.7
.060	29.7
.065	46.1
.065	71.0
.065	77.5
.065	93.6
.070	101.2

ALLOY - TD NICR
STRESS (MPA) - 124.1
TEMP. (KELVIN) - 1144
THICKNESS (CM) - .025
TEST DIRECTION - LONG.
SOURCE - NAS-3-15558

STRAIN (PCT.)	TIME (HOURS)
.080	.1
.130	.2
.140	.3
.140	.4
.155	.5
.165	1.0
.175	3.7
.205	9.4
.240	19.7
.240	27.7
.240	33.9
.255	43.3
.265	51.8
.290	68.6
.280	75.8
.295	91.6
.295	99.4

ALLOY - TD NICR
STRESS (MPA) - 124.1
TEMP. (KELVIN) - 1144
THICKNESS (CM) - .051
TEST DIRECTION - LONG.
SOURCE - NAS-3-15558

STRAIN (PCT.)	TIME (HOURS)
.035	.1
.040	.4
.045	.5
.045	1.4
.075	2.8
.085	5.4
.100	5.6
.115	10.6
.150	21.4
.155	29.5
.195	49.9
.220	72.9
.245	95.0
.255	101.4

ALLOY - TD NICR
STRESS (MPA) - 131.0
TEMP. (KELVIN) - 1144
THICKNESS (CM) - .051
TEST DIRECTION - LONG.
SOURCE - NAS-3-15558

STRAIN (PCT.)	TIME (HOURS)
.035	.1
.035	.2
.050	.3
.055	.4
.070	1.2
.080	2.4
.130	7.7
.170	18.5
.210	26.6
.255	47.0
.355	70.0
.380	92.1
.410	98.6
.435	113.7

ALLOY - TD NICR
STRESS (MPA) - 137.9
TEMP. (KELVIN) - 1144
THICKNESS (CM) - .063
TEST DIRECTION - LONG.
SOURCE - DAC-62124

STRAIN (PCT.)	TIME (HOURS)
.090	.1
.140	.2
.200	.4
.230	.6
.280	1.0
.340	2.0
.400	4.0
.430	6.0
.480	10.0
.500	10.2

ALLOY - TD NICR
STRESS (MPA) - 137.9
TEMP. (KELVIN) - 1144
THICKNESS (CM) - .063
TEST DIRECTION - LONG.
SOURCE - DAC-62124

STRAIN (PCT.)	TIME (HOURS)
.060	.1
.100	.2
.130	.4
.160	.6
.190	1.0
.240	2.0
.300	4.0
.340	6.0
.400	10.0
.450	15.0
.500	20.0

ALLOY - TD NICR
STRESS (MPA) - 143.4
TEMP. (KELVIN) - 1144
THICKNESS (CM) - .063
TEST DIRECTION - LONG.
SOURCE - DAC-62124

STRAIN (PCT.)	TIME (HOURS)
.240	.1
.350	.2
.460	.4
.490	.5

ALLOY - TD NICR
STRESS (MPA) - 151.7
TEMP. (KELVIN) - 1144
THICKNESS (CM) - .063
TEST DIRECTION - LONG.
SOURCE - DAC-62124

STRAIN (PCT.)	TIME (HOURS)
.110	.1
.210	.2
.320	.4
.380	.6
.400	.7
.460	1.0
.500	1.2

ALLOY - TD NICR
STRESS (MPA) - 60.7
TEMP. (KELVIN) - 1200
THICKNESS (CM) - .102
TEST DIRECTION - TRANS.
SOURCE - GE-PVT-4662

STRAIN (PCT.)	TIME (HOURS)
.100	30.0
.200	140.0
.500	420.0

ALLOY - TD NICR
STRESS (MPA) - 62.1
TEMP. (KELVIN) - 1200
THICKNESS (CM) - .152
TEST DIRECTION - TRANS.
SOURCE - GE-PVT-5132

STRAIN (PCT.)	TIME (HOURS)
.100	.3
.200	2.9
.500	60.0

ALLOY - TD NICR
STRESS (MPA) - 65.5
TEMP. (KELVIN) - 1200
THICKNESS (CM) - .152
TEST DIRECTION - TRANS.
SOURCE - GE-PVT-5132

STRAIN (PCT.)	TIME (HOURS)
.100	15.0
.200	90.0
.500	600.0

ALLOY - TD NICR
STRESS (MPA) - 66.2
TEMP. (KELVIN) - 1200
THICKNESS (CM) - .102
TEST DIRECTION - TRANS.
SOURCE - GE-PVT-4662

STRAIN (PCT.)	TIME (HOURS)
.100	40.0
.200	68.0
.500	175.0

ALLOY - TD NICR
STRESS (MPA) - 72.4
TEMP. (KELVIN) - 1200
THICKNESS (CM) - .063
TEST DIRECTION - LONG.
SOURCE - GE-PVT-5132

STRAIN (PCT.)	TIME (HOURS)
.100	.2
.200	1.0
.500	36.0

ALLOY - TD NICR
STRESS (MPA) - 72.4
TEMP. (KELVIN) - 1200
THICKNESS (CM) - .152
TEST DIRECTION - TRANS.
SOURCE - GE-PVT-4662

STRAIN (PCT.)	TIME (HOURS)
.100	150.0
.200	839.0

ALLOY - TD NICR
STRESS (MPA) - 75.8
TEMP. (KELVIN) - 1200
THICKNESS (CM) - .102
TEST DIRECTION - TRANS.
SOURCE - GE-PVT-4662

STRAIN (PCT.)	TIME (HOURS)
.100	1.3
.200	4.0
.500	15.0

ALLOY - TD NICR
STRESS (MPA) - 79.3
TEMP. (KELVIN) - 1200
THICKNESS (CM) - .063
TEST DIRECTION - TRANS.
SOURCE - GE-PVT-5132

STRAIN (PCT.)	TIME (HOURS)
.200	.1
.500	.6

ALLOY - TD NICR
STRESS (MPA) - 77.2
TEMP. (KELVIN) - 1200
THICKNESS (CM) - .152
TEST DIRECTION - TRANS.
SOURCE - GE-PVT-4662

STRAIN (PCT.)	TIME (HOURS)
.100	25.0
.200	83.0

ALLOY - TD NICR
STRESS (MPA) - 79.3
TEMP. (KELVIN) - 1200
THICKNESS (CM) - .152
TEST DIRECTION - LONG.
SOURCE - GE-PVT-5132

STRAIN (PCT.)	TIME (HOURS)
.100	.1
.200	.5
.500	38.0

ALLOY - TD NICR
STRESS (MPA) - 79.3
TEMP. (KELVIN) - 1200
THICKNESS (CM) - .152
TEST DIRECTION - TRANS.
SOURCE - GE-PVT-5132

STRAIN (PCT.)	TIME (HOURS)
.100	.1
.200	1.0
.500	9.5

ALLOY - TD NICR
STRESS (MPA) - 82.7
TEMP. (KELVIN) - 1200
THICKNESS (CM) - .152
TEST DIRECTION - LONG.
SOURCE - GE-PVT-5132

STRAIN (PCT.)	TIME (HOURS)
.100	.4
.200	3.0
.500	215.0

ALLOY - TD NICR
STRESS (MPA) - 86.2
TEMP. (KELVIN) - 1200
THICKNESS (CM) - .152
TEST DIRECTION - LONG.
SOURCE - GE-PVT-5132

STRAIN (PCT.)	TIME (HOURS)
.100	.1
.200	.4
.500	25.0

ALLOY - TD NICR
STRESS (MPA) - 89.6
TEMP. (KELVIN) - 1200
THICKNESS (CM) - .063
TEST DIRECTION - LONG.
SOURCE - GE-PVT-5132

STRAIN (PCT.)	TIME (HOURS)
.100	.2
.200	1.5
.500	25.0

ALLOY - TD NICR
STRESS (MPA) - 93.1
TEMP. (KELVIN) - 1200
THICKNESS (CM) - .152
TEST DIRECTION - LONG.
SOURCE - GE-PVT-5132

STRAIN (PCT.)	TIME (HOURS)
.100	.1
.200	.2
.500	23.0

ALLOY - TD NICR
STRESS (MPA) - 96.5
TEMP. (KELVIN) - 1200
THICKNESS (CM) - .152
TEST DIRECTION - LONG.
SOURCE - GE-PVT-4662

STRAIN (PCT.)	TIME (HOURS)
.100	100.0
.200	270.0

ALLOY - TD NICR
STRESS (MPA) - 114.5
TEMP. (KELVIN) - 1200
THICKNESS (CM) - .152
TEST DIRECTION - LONG.
SOURCE - GE-PVT-4662

STRAIN (PCT.)	TIME (HOURS)
.100	40.0
.200	480.0

ORIGINAL PAGE IS OF POOR QUALITY

ALLOY - TD NICR
STRESS (MPA) - 41.4
TEMP. (KELVIN) - 1255
THICKNESS (CM) - .038
TEST DIRECTION - TRANS.
SOURCE - NAS-8-27189

STRAIN (PCT.)	TIME (HOURS)
.025	1.0
.035	5.0
.043	10.0
.065	20.0
.085	30.0
.118	44.0
.142	56.0
.170	70.0
.188	79.0
.209	93.0
.225	102.0
.255	117.0
.300	140.0
.385	193.0
.425	215.0
.467	239.0

ALLOY - TD NICR
STRESS (MPA) - 44.8
TEMP. (KELVIN) - 1255
THICKNESS (CM) - .025
TEST DIRECTION - TRANS.
SOURCE - NAS-3-15558

STRAIN (PCT.)	TIME (HOURS)
.005	.1
.005	.2
.005	.4
.025	1.4
.045	3.2
.040	5.6
.045	12.5
.060	21.8
.070	29.6
.070	34.3
.075	45.0
.090	53.5
.110	68.9
.115	77.6
.120	92.8
.130	98.1
.145	117.3

ALLOY - TD NICR
STRESS (MPA) - 44.8
TEMP. (KELVIN) - 1255
THICKNESS (CM) - .038
TEST DIRECTION - TRANS.
SOURCE - NAS-8-27189

STRAIN (PCT.)	TIME (HOURS)
.015	.5
.030	1.5
.040	2.0
.065	5.5
.080	7.7
.145	18.4
.210	31.2
.290	42.5
.355	52.2
.440	68.0
.465	73.5

ALLOY - TD NICR
STRESS (MPA) - 44.8
TEMP. (KELVIN) - 1255
THICKNESS (CM) - .038
TEST DIRECTION - TRANS.
SOURCE - NAS-8-27189

STRAIN (PCT.)	TIME (HOURS)
.025	1.0
.030	2.0
.035	4.4
.045	9.0
.085	22.0
.112	29.0
.165	44.0
.188	52.0
.232	68.0
.260	76.0
.310	94.0
.335	102.0
.378	118.0
.430	139.0
.460	148.4
.500	165.0

ALLOY - TD NICR
STRESS (MPA) - 46.9
TEMP. (KELVIN) - 1255
THICKNESS (CM) - .025
TEST DIRECTION - TRANS.
SOURCE - NAS-3-15558

STRAIN (PCT.)	TIME (HOURS)
.015	.1
.020	.2
.030	.4
.025	1.0
.065	2.4
.075	7.5
.100	17.7
.115	25.8
.155	43.9
.145	53.2
.175	65.9
.205	74.0
.225	89.9
.245	122.8

ALLOY - TD NICR
STRESS (MPA) - 48.3
TEMP. (KELVIN) - 1255
THICKNESS (CM) - .025
TEST DIRECTION - TRANS.
SOURCE - NAS-3-15558

STRAIN (PCT.)	TIME (HOURS)
.015	.1
.015	.2
.025	.3
.035	.4
.040	.5
.105	3.2
.125	5.3
.135	6.3
.165	10.7
.205	20.7
.260	30.0
.295	35.7
.340	45.1
.375	54.2
.405	70.6
.460	78.2
.520	94.6
.520	101.9

ALLOY - TD NICR
STRESS (MPA) - 48.3
TEMP. (KELVIN) - 1255
THICKNESS (CM) - .038
TEST DIRECTION - TRANS.
SOURCE - NAS-8-27189

STRAIN (PCT.)	TIME (HOURS)
.040	1.0
.060	2.5
.075	5.7
.105	11.0
.170	22.0
.245	36.0
.285	44.5
.335	55.0
.425	73.5

ALLOY - TD NICR
STRESS (MPA) - 51.7
TEMP. (KELVIN) - 1255
THICKNESS (CM) - .038
TEST DIRECTION - TRANS.
SOURCE - NAS-8-27189

STRAIN (PCT.)	TIME (HOURS)
.085	8.0
.125	13.0
.190	22.0
.265	32.0
.380	48.5
.430	56.0

ALLOY - TD NICR
STRESS (MPA) - 55.2
TEMP. (KELVIN) - 1255
THICKNESS (CM) - .051
TEST DIRECTION - TRANS.
SOURCE - NAS-3-15558

STRAIN (PCT.)	TIME (HOURS)
.015	.1
.025	.3
.025	.4
.030	.5
.035	1.0
.060	5.3
.075	10.3
.095	20.1
.110	29.3
.110	35.3
.125	46.8
.125	53.2
.140	70.6
.140	77.1
.150	92.7
.150	100.0

ALLOY - TD NICR
STRESS (MPA) - 55.2
TEMP. (KELVIN) - 1255
THICKNESS (CM) - .051
TEST DIRECTION - TRANS.
SOURCE - NAS-3-15558

STRAIN (PCT.)	TIME (HOURS)
.005	.1
.005	.2
.025	.4
.070	2.7
.070	5.5
.070	11.1
.085	21.5
.110	29.5
.110	35.6
.120	45.1
.135	53.5
.145	70.3
.140	77.6
.145	93.3
.155	101.2

ALLOY - TD NICR
STRESS (MPA) - 55.2
TEMP. (KELVIN) - 1255
THICKNESS (CM) - .051
TEST DIRECTION - TRANS.
SOURCE - NAS-3-15558

STRAIN (PCT.)	TIME (HOURS)
.010	.3
.010	.4
.015	.5
.015	1.1
.035	4.8
.045	6.4
.025	13.1
.045	21.2
.055	30.1
.070	45.9
.075	54.0
.090	71.9
.090	78.2
.090	94.8
.100	101.9

ALLOY - TD NICR
STRESS (MPA) - 58.6
TEMP. (KELVIN) - 1255
THICKNESS (CM) - .051
TEST DIRECTION - TRANS.
SOURCE - NAS-3-15558

STRAIN (PCT.)	TIME (HOURS)
.015	.2
.010	.3
.035	.5
.040	1.2
.065	10.9
.080	24.6
.100	41.4
.095	48.9
.125	65.1
.120	72.9
.145	87.5
.170	95.4
.200	116.4

ALLOY - TD NICR
STRESS (MPA) - 68.9
TEMP. (KELVIN) - 1255
THICKNESS (CM) - .025
TEST DIRECTION - LONG.
SOURCE - NAS-3-15558

STRAIN (PCT.)	TIME (HOURS)
.020	.1
.030	.2
.035	.3
.040	.4
.045	.5
.045	1.0
.080	3.3
.100	7.8
.115	27.8
.135	44.1
.150	51.8
.160	75.6
.165	91.7
.170	99.5
.170	113.5

ALLOY - TD NICR
STRESS (MPA) - 68.9
TEMP. (KELVIN) - 1255
THICKNESS (CM) - .038
TEST DIRECTION - TRANS.
SOURCE - NAS-8-27189

STRAIN (PCT.)	TIME (HOURS)
.040	.1
.070	.2
.120	.4
.160	.6
.210	.9
.250	1.2
.295	1.6
.340	2.0
.375	2.4
.415	2.8
.435	3.3
.475	3.8

ALLOY - TD NICR
STRESS (MPA) - 72.4
TEMP. (KELVIN) - 1255
THICKNESS (CM) - .051
TEST DIRECTION - LONG.
SOURCE - NAS-3-15558

STRAIN (PCT.)	TIME (HOURS)
.020	.1
.020	.2
.030	.4
.035	.6
.030	1.2
.035	6.1
.030	19.4
.050	26.0
.045	44.9
.045	50.6
.050	68.8
.060	98.5
.065	113.2

ALLOY - TD NICR
STRESS (MPA) - 79.3
TEMP. (KELVIN) - 1255
THICKNESS (CM) - .051
TEST DIRECTION - LONG.
SOURCE - NAS-3-15558

STRAIN (PCT.)	TIME (HOURS)
.010	.1
.025	.2
.020	.4
.035	1.2
.030	4.0
.040	9.1
.055	23.6
.060	29.6
.060	47.5
.075	53.7
.075	70.2
.080	77.4
.085	95.7
.085	100.6

ALLOY - TD NICR
STRESS (MPA) - 89.6
TEMP. (KELVIN) - 1255
THICKNESS (CM) - .051
TEST DIRECTION - LONG.
SOURCE - NAS-3-15558

STRAIN (PCT.)	TIME (HOURS)
.015	.1
.020	.3
.030	.4
.040	.5
.035	1.1
.050	1.9
.050	3.5
.075	18.9
.095	27.5
.100	45.4
.105	50.5
.120	51.6
.130	68.0
.125	75.7
.130	91.2
.135	99.9
.145	116.6

ALLOY - TD NICR
STRESS (MPA) - 93.1
TEMP. (KELVIN) - 1255
THICKNESS (CM) - .025
TEST DIRECTION - LONG.
SOURCE - NAS-3-15558

STRAIN (PCT.)	TIME (HOURS)
.035	.1
.065	.3
.070	.4
.070	.5
.080	1.1
.115	5.3
.120	10.3
.170	21.1
.180	29.2
.205	47.3
.215	53.4
.235	77.3
.270	93.8
.285	121.6

ALLOY - TD NICR
STRESS (MPA) - 93.1
TEMP. (KELVIN) - 1255
THICKNESS (CM) - .051
TEST DIRECTION - LONG.
SOURCE - NAS-3-15558

STRAIN (PCT.)	TIME (HOURS)
.005	.1
.015	.2
.010	.4
.020	.5
.030	1.0
.025	1.8
.055	3.3
.055	6.3
.075	10.8
.095	22.4
.095	30.3
.125	34.9
.130	45.8
.150	53.5
.180	70.3
.195	77.8
.230	94.1
.240	101.7

ALLOY - TD NICR
STRESS (MPA) - 93.1
TEMP. (KELVIN) - 1255
THICKNESS (CM) - .051
TEST DIRECTION - LONG.
SOURCE - NAS-3-15558

STRAIN (PCT.)	TIME (HOURS)
.025	.1
.030	.2
.040	.3
.035	.4
.055	.8
.090	4.3
.105	5.5
.120	11.3
.140	20.6
.165	29.9
.190	46.1
.210	53.8
.225	70.1
.245	77.6
.265	93.8
.270	98.6
.300	117.5

ALLOY - TD NICR
STRESS (MPA) - 100.0
TEMP. (KELVIN) - 1255
THICKNESS (CM) - .051
TEST DIRECTION - LONG.
SOURCE - NAS-3-15558

STRAIN (PCT.)	TIME (HOURS)
.015	.1
.020	.3
.020	.4
.040	.5
.075	1.0
.080	3.8
.110	9.6
.160	19.8
.190	27.9
.220	34.1
.260	43.5
.290	51.9
.355	68.7
.395	76.0
.460	91.7
.490	99.7

ALLOY - TD NICR
STRESS (MPA) - 37.9
TEMP. (KELVIN) - 1311
THICKNESS (CM) - .102
TEST DIRECTION - TRANS.
SOURCE - GE-PVT-4662

STRAIN (PCT.)	TIME (HOURS)
.100	248.0
.200	357.0

ALLOY - TD NICR
STRESS (MPA) - 17.2
TEMP. (KELVIN) - 1366
THICKNESS (CM) - .038
TEST DIRECTION - TRANS.
SOURCE - NAS-8-27189

STRAIN (PCT.)	TIME (HOURS)
.025	2.0
.034	5.0
.045	10.5
.060	20.0
.110	42.0
.195	67.5
.276	90.0
.365	112.0
.482	139.0

ALLOY - TD NICR
STRESS (MPA) - 20.7
TEMP. (KELVIN) - 1366
THICKNESS (CM) - .038
TEST DIRECTION - TRANS.
SOURCE - NAS-8-27189

STRAIN (PCT.)	TIME (HOURS)
.015	1.0
.022	2.0
.022	5.7
.042	19.8
.075	25.5
.100	30.0
.160	41.5
.235	49.5
.265	54.5
.360	65.5
.425	73.3
.475	78.0

ALLOY - TD NICR
STRESS (MPA) - 58.6
TEMP. (KELVIN) - 1255
THICKNESS (CM) - .051
TEST DIRECTION - TRANS.
SOURCE - NAS-3-15558

STRAIN (PCT.)	TIME (HOURS)
.020	.1
.030	.2
.030	.4
.055	.5
.080	1.5
.130	5.6
.180	11.8
.240	21.3
.280	29.7
.370	46.4
.420	53.7
.530	69.4
.590	77.5
.705	92.7
.745	97.7
.915	118.3

ALLOY - TD NICR
STRESS (MPA) - 58.6
TEMP. (KELVIN) - 1255
THICKNESS (CM) - .051
TEST DIRECTION - TRANS.
SOURCE - NAS-3-15558

STRAIN (PCT.)	TIME (HOURS)
.005	.1
.005	.2
.045	.3
.070	3.0
.105	9.4
.130	20.7
.150	27.2
.180	45.5
.185	51.1
.195	66.7
.205	75.2
.240	93.4
.310	128.9
.335	138.7

ALLOY - TD NICR
STRESS (MPA) - 62.1
TEMP. (KELVIN) - 1255
THICKNESS (CM) - .025
TEST DIRECTION - TRANS.
SOURCE - NAS-3-15558

STRAIN (PCT.)	TIME (HOURS)
.020	.1
.035	.3
.055	.4
.060	.5
.055	1.0
.080	2.5
.075	3.5
.105	9.1
.135	20.0
.145	27.7
.170	43.2
.185	51.5
.255	68.6
.250	72.3
.230	91.7
.240	123.5

ALLOY - TD NICR
STRESS (MPA) - 62.1
TEMP. (KELVIN) - 1255
THICKNESS (CM) - .025
TEST DIRECTION - TRANS.
SOURCE - NAS-3-15558

STRAIN (PCT.)	TIME (HOURS)
.050	.3
.040	.4
.040	.8
.045	1.0
.090	17.6
.105	24.7
.115	43.3
.115	48.6
.115	68.2
.105	72.5
.095	85.7
.100	122.2
.130	136.8

ALLOY - TD NICR
STRESS (MPA) - 65.5
TEMP. (KELVIN) - 1255
THICKNESS (CM) - .025
TEST DIRECTION - TRANS.
SOURCE - NAS-3-15558

STRAIN (PCT.)	TIME (HOURS)
.015	.1
.020	.2
.035	.4
.040	.5
.060	1.2
.095	3.8
.125	9.2
.145	19.8
.160	28.1
.170	48.4
.195	71.4
.200	93.4
.200	99.8

ALLOY - TD NICR
STRESS (MPA) - 65.5
TEMP. (KELVIN) - 1255
THICKNESS (CM) - .051
TEST DIRECTION - TRANS.
SOURCE - NAS-3-15558

STRAIN (PCT.)	TIME (HOURS)
.020	.1
.025	.2
.035	.3
.035	.5
.055	1.3
.105	4.1
.140	8.8
.230	20.3
.275	28.1
.270	32.9
.355	43.8
.390	51.5
.445	68.3
.480	75.8
.520	92.0
.540	99.8

ALLOY - TD NICR
STRESS (MPA) - 20.7
TEMP. (KELVIN) - 1366
THICKNESS (CM) - .038
TEST DIRECTION - TRANS.
SOURCE - NAS-8-27189

STRAIN (PCT.)	TIME (HOURS)
.010	2.0
.019	11.0
.045	22.0
.110	37.5
.159	45.5
.260	65.0
.385	87.5

ALLOY - TD NICR
STRESS (MPA) - 24.1
TEMP. (KELVIN) - 1366
THICKNESS (CM) - .038
TEST DIRECTION - TRANS.
SOURCE - NAS-8-27189

STRAIN (PCT.)	TIME (HOURS)
.018	1.0
.040	2.5
.055	4.5
.070	6.5
.120	11.5
.220	23.0
.292	30.0
.462	46.6

ALLOY - TD NICR
STRESS (MPA) - 24.1
TEMP. (KELVIN) - 1366
THICKNESS (CM) - .038
TEST DIRECTION - TRANS.
SOURCE - NAS-8-27189

STRAIN (PCT.)	TIME (HOURS)
.015	1.0
.035	2.2
.041	4.5
.066	9.8
.105	21.6
.150	29.4
.240	45.2
.285	53.5
.385	68.5
.426	74.0

ALLOY - TD NICR
STRESS (MPA) - 27.6
TEMP. (KELVIN) - 1366
THICKNESS (CM) - .038
TEST DIRECTION - TRANS.
SOURCE - NAS-8-27189

STRAIN (PCT.)	TIME (HOURS)
.025	1.0
.038	2.4
.045	4.5
.067	11.5
.110	22.0
.150	30.0
.222	46.5
.245	54.0
.340	69.0
.390	78.0

ALLOY - TD NICR
STRESS (MPA) - 27.6
TEMP. (KELVIN) - 1366
THICKNESS (CM) - .051
TEST DIRECTION - LONG.
SOURCE - NAS-3-15558

STRAIN (PCT.)	TIME (HOURS)
.010	.1
.005	.4
.015	1.0
.020	19.1
.030	24.8
.055	42.5
.065	49.0
.075	67.7
.085	72.9
.090	90.5
.095	97.0
.100	101.0

ALLOY - TD NICR
STRESS (MPA) - 31.0
TEMP. (KELVIN) - 1366
THICKNESS (CM) - .038
TEST DIRECTION - TRANS.
SOURCE - NAS-8-27189

STRAIN (PCT.)	TIME (HOURS)
.015	.4
.030	.6
.045	1.5
.060	3.5
.090	6.5
.150	13.0
.215	21.5
.235	25.2
.278	30.5
.408	46.0

ALLOY - TD NICR
STRESS (MPA) - 32.4
TEMP. (KELVIN) - 1366
THICKNESS (CM) - .025
TEST DIRECTION - TRANS.
SOURCE - NAS-3-15558

STRAIN (PCT.)	TIME (HOURS)
.010	.1
.025	.3
.030	.4
.045	1.0
.060	5.8
.080	16.5
.090	25.1
.110	40.5
.120	49.4
.150	64.4
.155	69.7
.205	89.1
.270	114.9

ALLOY - TD NICR
STRESS (MPA) - 34.5
TEMP. (KELVIN) - 1366
THICKNESS (CM) - .025
TEST DIRECTION - TRANS.
SOURCE - NAS-3-15558

STRAIN (PCT.)	TIME (HOURS)
.020	.1
.025	.3
.030	.4
.035	.5
.035	1.6
.040	3.4
.065	9.3
.090	18.5
.130	27.9
.135	28.0
.185	44.1
.200	51.7
.295	68.0
.335	75.6
.415	91.8
.475	96.5
.630	115.5

ALLOY - TD NICR
STRESS (MPA) - 34.5
TEMP. (KELVIN) - 1366
THICKNESS (CM) - .025
TEST DIRECTION - TRANS.
SOURCE - NAS-3-15558

STRAIN (PCT.)	TIME (HOURS)
.015	.2
.015	.4
.025	1.2
.100	5.4
.095	10.6
.220	20.9
.235	29.0
.320	46.9
.355	53.4
.445	70.0
.495	77.2
.605	93.1
.635	98.2
.805	125.9

ALLOY - TD NICR
STRESS (MPA) - 34.5
TEMP. (KELVIN) - 1366
THICKNESS (CM) - .051
TEST DIRECTION - TRANS.
SOURCE - NAS-3-15558

STRAIN (PCT.)	TIME (HOURS)
.010	.1
.010	.2
.020	.3
.010	.4
.035	1.4
.040	3.3
.070	7.2
.100	19.6
.090	27.7
.105	45.1
.115	51.9
.140	68.0
.140	75.7
.145	92.2
.150	99.5
.150	113.0

ALLOY - TD NICR
STRESS (MPA) - 35.9
TEMP. (KELVIN) - 1366
THICKNESS (CM) - .051
TEST DIRECTION - TRANS.
SOURCE - NAS-3-15558

STRAIN (PCT.)	TIME (HOURS)
.015	.1
.010	.2
.010	.3
.030	1.0
.045	3.4
.050	5.4
.040	10.3
.075	22.2
.080	30.2
.115	47.7
.120	54.2
.135	69.3
.130	75.4
.150	92.9
.160	120.1

ALLOY - TD NICR
STRESS (MPA) - 36.5
TEMP. (KELVIN) - 1366
THICKNESS (CM) - .051
TEST DIRECTION - TRANS.
SOURCE - NAS-3-15558

STRAIN (PCT.)	TIME (HOURS)
.010	.1
.010	.2
.015	.4
.015	.5
.020	1.0
.050	2.4
.030	3.2
.100	18.6
.105	27.0
.145	43.2
.150	50.5
.190	67.7
.195	75.1
.225	100.0

ALLOY - TD NICR
STRESS (MPA) - 37.9
TEMP. (KELVIN) - 1366
THICKNESS (CM) - .025
TEST DIRECTION - TRANS.
SOURCE - NAS-3-15558

STRAIN (PCT.)	TIME (HOURS)
.010	.1
.020	.2
.025	.3
.030	.5
.030	1.3
.105	17.0
.105	24.7
.150	41.5
.165	49.0
.230	65.2
.245	73.0
.315	87.6
.335	95.5
.420	116.6

ALLOY - TD NICR
STRESS (MPA) - 39.3
TEMP. (KELVIN) - 1366
THICKNESS (CM) - .025
TEST DIRECTION - TRANS.
SOURCE - NAS-3-15558

STRAIN (PCT.)	TIME (HOURS)
.010	.1
.030	.2
.030	.3
.040	.5
.040	1.7
.075	5.8
.125	11.2
.120	22.0
.125	30.3
.135	35.9
.155	46.0
.165	53.9
.185	69.9
.200	77.8
.220	94.3
.225	101.8
.240	116.4

ALLOY - TD NICR
STRESS (MPA) - 39.3
TEMP. (KELVIN) - 1366
THICKNESS (CM) - .051
TEST DIRECTION - TRANS.
SOURCE - NAS-3-15558

STRAIN (PCT.)	TIME (HOURS)
.010	.1
.015	.3
.020	.5
.030	1.7
.035	3.2
.060	7.7
.085	19.6
.095	26.8
.140	43.6
.155	50.2
.190	69.1
.210	74.9
.290	92.5
.315	98.9
.460	119.8

ALLOY - TD NICR
STRESS (MPA) - 41.4
TEMP. (KELVIN) - 1366
THICKNESS (CM) - .025
TEST DIRECTION - TRANS.
SOURCE - NAS-3-15558

STRAIN (PCT.)	TIME (HOURS)
.015	.1
.020	.2
.030	.3
.030	1.3
.070	2.1
.070	3.8
.110	9.3
.190	19.5
.225	27.8
.260	46.2
.255	51.8
.280	68.1
.285	75.6
.295	91.8
.290	96.2
.335	121.0

ALLOY - TD NICR
STRESS (MPA) - 41.4
TEMP. (KELVIN) - 1366
THICKNESS (CM) - .051
TEST DIRECTION - TRANS.
SOURCE - NAS-3-15558

STRAIN (PCT.)	TIME (HOURS)
.010	.2
.005	.4
.005	.5
.030	2.3
.030	3.7
.045	10.1
.070	20.4
.090	27.7
.130	43.1
.130	51.2
.160	69.3
.180	75.6
.220	92.3
.210	99.4

ALLOY - TD NICR
STRESS (MPA) - 41.4
TEMP. (KELVIN) - 1366
THICKNESS (CM) - .051
TEST DIRECTION - TRANS.
SOURCE - NAS-3-15558

STRAIN (PCT.)	TIME (HOURS)
.015	.1
.025	.2
.015	.3
.020	.4
.030	1.0
.025	3.4
.030	5.0
.020	5.7
.025	11.3
.060	22.4
.065	29.9
.090	34.4
.110	47.9
.115	53.8
.165	72.6
.170	78.0
.225	93.6
.260	102.1

ALLOY - TD NICR
STRESS (MPA) - 43.4
TEMP. (KELVIN) - 1366
THICKNESS (CM) - .051
TEST DIRECTION - TRANS.
SOURCE - NAS-3-15558

STRAIN (PCT.)	TIME (HOURS)
.005	.3
.010	2.7
.025	7.7
.055	19.5
.075	26.9
.075	32.5
.090	42.6
.115	53.9
.160	69.2
.180	74.9
.225	91.2
.250	98.7
.330	114.8

ALLOY - TD NICR
STRESS (MPA) - 44.8
TEMP. (KELVIN) - 1366
THICKNESS (CM) - .025
TEST DIRECTION - LONG.
SOURCE - NAS-3-15558

STRAIN (PCT.)	TIME (HOURS)
.015	.1
.025	.3
.035	.7
.045	1.6
.045	7.4
.055	19.2
.065	27.1
.070	42.2
.080	51.1
.085	68.7
.095	74.9
.100	88.4
.110	95.4
.130	112.8

ALLOY - TD NICR
STRESS (MPA) - 48.3
TEMP. (KELVIN) - 1366
THICKNESS (CM) - .025
TEST DIRECTION - LONG.
SOURCE - NAS-3-15558

STRAIN (PCT.)	TIME (HOURS)
.010	.1
.015	.2
.015	.4
.020	1.0
.025	2.5
.045	8.1
.055	18.3
.080	26.2
.120	42.2
.155	58.1
.235	66.5
.255	74.0
.340	88.7
.340	95.1
.400	113.0

ALLOY - TD NICR
STRESS (MPA) - 48.3
TEMP. (KELVIN) - 1366
THICKNESS (CM) - .025
TEST DIRECTION - TRANS.
SOURCE - NAS-3-15558

STRAIN (PCT.)	TIME (HOURS)
.015	.1
.010	.3
.035	.4
.035	.5
.030	1.0
.075	3.2
.095	7.7
.140	17.6
.165	27.6
.195	44.0
.215	51.6
.250	69.0
.255	75.4
.285	91.6
.300	99.3

ALLOY - TD NICR
STRESS (MPA) - 48.3
TEMP. (KELVIN) - 1366
THICKNESS (CM) - .051
TEST DIRECTION - LONG.
SOURCE - NAS-3-15558

STRAIN (PCT.)	TIME (HOURS)
.020	.1
.010	.2
.020	.3
.030	.4
.030	3.8
.030	5.6
.055	10.8
.050	21.9
.070	29.8
.070	47.5
.075	53.6
.100	77.4

ALLOY - TD NICR
STRESS (MPA) - 48.3
TEMP. (KELVIN) - 1366
THICKNESS (CM) - .063
TEST DIRECTION - LONG.
SOURCE - GE-PVT-5132

STRAIN (PCT.)	TIME (HOURS)
.100	.6
.200	2.5
.500	63.0

ERROR 84 OUTPUT FILE LINE LIMIT EXCEEDED.
SENSED BY OUTPTC
CALLED BY CONVRT AT 217 (117)

ALLOY - TD NICR
STRESS (MPA) - 51.7
TEMP. (KELVIN) - 1366
THICKNESS (CM) - .025
TEST DIRECTION - LONG.
SOURCE - NAS-3-15558

STRAIN (PCT.)	TIME (HOURS)
.010	.1
.015	.2
.015	.3
.025	.4
.025	.5
.030	1.5
.035	2.6
.050	5.9
.060	10.3
.080	22.3
.090	29.5
.110	46.3
.125	53.0
.150	71.8
.160	77.6
.195	95.2
.200	101.6

ALLOY - TD NICR
STRESS (MPA) - 51.7
TEMP. (KELVIN) - 1366
THICKNESS (CM) - .025
TEST DIRECTION - LONG.
SOURCE - NAS-3-15558

STRAIN (PCT.)	TIME (HOURS)
.010	.1
.020	.2
.030	.3
.030	.4
.080	1.1
.130	4.8
.145	6.3
.245	13.1
.325	21.1
.370	30.1
.440	54.0
.480	72.1
.495	78.2
.510	94.9
.525	102.0

ALLOY - TD NICR
STRESS (MPA) - 51.7
TEMP. (KELVIN) - 1366
THICKNESS (CM) - .025
TEST DIRECTION - LONG.
SOURCE - NAS-3-15558

STRAIN (PCT.)	TIME (HOURS)
.025	.1
.030	.2
.050	.4
.055	1.0
.075	1.8
.085	3.7
.115	8.3
.165	21.4
.190	27.5
.255	42.9
.285	51.3
.380	69.2
.425	75.2
.590	92.7
.605	96.7
.840	120.7

ALLOY - TD NICR
STRESS (MPA) - 51.7
TEMP. (KELVIN) - 1366
THICKNESS (CM) - .152
TEST DIRECTION - LONG.
SOURCE - GE-PVT-5132

STRAIN (PCT.)	TIME (HOURS)
.100	.2
.200	1.0
.500	16.0

ALLOY - TD NICR
STRESS (MPA) - 55.2
TEMP. (KELVIN) - 1366
THICKNESS (CM) - .025
TEST DIRECTION - LONG.
SOURCE - NAS-3-15558

STRAIN (PCT.)	TIME (HOURS)
.030	.1
.035	.2
.035	.3
.040	.4
.070	.5
.070	1.2
.085	5.4
.120	21.1
.130	29.3
.155	47.3
.150	53.5
.160	70.1
.175	77.3
.190	93.9
.190	97.6
.205	122.0

ALLOY - TD NICR
STRESS (MPA) - 58.6
TEMP. (KELVIN) - 1366
THICKNESS (CM) - .152
TEST DIRECTION - LONG.
SOURCE - GE-PVT-5132

STRAIN (PCT.)	TIME (HOURS)
.100	.1
.200	.2
.500	2.0

ALLOY - TD NICR
STRESS (MPA) - 62.1
TEMP. (KELVIN) - 1366
THICKNESS (CM) - .025
TEST DIRECTION - LONG.
SOURCE - NAS-3-15558

STRAIN (PCT.)	TIME (HOURS)
.015	.1
.025	.3
.035	.4
.040	.5
.045	1.1
.085	5.4
.110	10.6
.150	20.2
.170	29.4
.180	35.7
.210	46.9
.235	53.3
.280	71.7
.305	77.5
.345	92.9
.370	100.1

ALLOY - TD NICR
STRESS (MPA) - 62.1
TEMP. (KELVIN) - 1366
THICKNESS (CM) - .051
TEST DIRECTION - LONG.
SOURCE - NAS-3-15558

STRAIN (PCT.)	TIME (HOURS)
.015	.1
.030	.2
.030	.4
.030	.5
.045	5.6
.030	10.4
.030	20.0
.040	29.3
.045	35.0
.030	44.4
.030	53.8
.045	77.6
.045	93.9
.055	101.3

ALLOY - TD NICR
STRESS (MPA) - 55.5
TEMP. (KELVIN) - 1366
THICKNESS (CM) - .025
TEST DIRECTION - LONG.
SOURCE - NAS-3-15558

STRAIN (PCT.)	TIME (HOURS)
.030	.4
.040	1.0
.035	2.0
.050	3.7
.070	9.1
.110	20.0
.135	28.1
.135	32.7
.170	51.6
.200	67.1
.240	75.4
.325	93.3
.355	100.3

ALLOY - TD NICR
STRESS (MPA) - 68.9
TEMP. (KELVIN) - 1366
THICKNESS (CM) - .051
TEST DIRECTION - LONG.
SOURCE - NAS-3-15558

STRAIN (PCT.)	TIME (HOURS)
.020	.1
.010	.2
.010	.3
.015	.4
.020	.5
.020	6.0
.040	19.2
.050	25.3
.070	49.0
.105	66.9
.120	72.9
.165	90.6
.175	94.6
.290	119.2

ALLOY - TD NICR
STRESS (MPA) - 68.9
TEMP. (KELVIN) - 1366
THICKNESS (CM) - .063
TEST DIRECTION - LONG.
SOURCE - GE-PVT-5132

STRAIN (PCT.)	TIME (HOURS)
.100	.2
.200	.4
.500	1.0

ALLOY - TD NICR
STRESS (MPA) - 72.4
TEMP. (KELVIN) - 1366
THICKNESS (CM) - .081
TEST DIRECTION - LONG.
SOURCE - MDAC-W-INTL

STRAIN (PCT.)	TIME (HOURS)
.100	2.0
.200	5.5

ALLOY - TD NICR
STRESS (MPA) - 79.3
TEMP. (KELVIN) - 1366
THICKNESS (CM) - .081
TEST DIRECTION - LONG.
SOURCE - MDAC-W-INTL

STRAIN (PCT.)	TIME (HOURS)
.100	3.0
.100	43.0

ALLOY - TD NICR
STRESS (MPA) - 89.6
TEMP. (KELVIN) - 1366
THICKNESS (CM) - .081
TEST DIRECTION - LONG.
SOURCE - MDAC-W-INTL

STRAIN (PCT.)	TIME (HOURS)
.100	.4
.100	2.1

ALLOY - TD NICR
STRESS (MPA) - 96.5
TEMP. (KELVIN) - 1366
THICKNESS (CM) - .081
TEST DIRECTION - LONG.
SOURCE - MDAC-W-INTL

STRAIN (PCT.)	TIME (HOURS)
.100	1.6
.200	3.5

ALLOY - TD NICR
STRESS (MPA) - 34.5
TEMP. (KELVIN) - 1422
THICKNESS (CM) - .102
TEST DIRECTION - TRANS.
SOURCE - GE-PVT-4662

STRAIN (PCT.)	TIME (HOURS)
.100	4.6
.200	9.0
.100	3150.0

ALLOY - TD NICR
STRESS (MPA) - 18.6
TEMP. (KELVIN) - 1478
THICKNESS (CM) - .025
TEST DIRECTION - TRANS.
SOURCE - NAS-3-15558

STRAIN (PCT.)	TIME (HOURS)
.010	.3
.005	.5
.010	1.1
.010	3.9
.035	8.5
.075	27.8
.075	44.4
.095	51.8
.13[illegible]	68.2
[illegible]	7[illegible].8
.225	[illegible]

ALLOY - TD NICR
STRESS (MPA) - 103.4
TEMP. (KELVIN) - 1366
THICKNESS (CM) - .081
TEST DIRECTION - LONG.
SOURCE - MDAC-W-INTL

STRAIN (PCT.)	TIME (HOURS)
.100	.3
.200	1.0
.100	1.3
.200	3.0

ALLOY - TD NICR
STRESS (MPA) - 17.2
TEMP. (KELVIN) - 1478
THICKNESS (CM) - .025
TEST DIRECTION - TRANS.
SOURCE - NAS-3-15558

STRAIN (PCT.)	TIME (HOURS)
.030	.1
.020	.3
.025	.4
.045	1.4
.040	3.4
.065	8.8
.105	19.7
.111	27.4
.150	43.4
.165	51.4
.235	71.5
.240	75.4
.310	91.5
.335	99.4

ALLOY - TD NICR
STRESS (MPA) - 27.6
TEMP. (KELVIN) - 1422
THICKNESS (CM) - .102
TEST DIRECTION - TRANS.
SOURCE - GE-PVT-4662

STRAIN (PCT.)	TIME (HOURS)
.100	12.0
.200	57.0
.100	1400.0
.200	4200.0
.500	*500.0

ALLOY - TD NICR
STRESS (MPA) - 17.2
TEMP. (KELVIN) - 1478
THICKNESS (CM) - .063
TEST DIRECTION - TRANS.
SOURCE - GE-PVT-5132

STRAIN (PCT.)	TIME (HOURS)
.100	1.0
.200	27.0
.500	190.0

ALLOY - TD NICR
STRESS (MPA) - 18.6
TEMP. (KELVIN) - 1478
THICKNESS (CM) - .025
TEST DIRECTION - TRANS.
SOURCE - NAS-3-15558

STRAIN (PCT.)	TIME (HOURS)
.010	.2
.010	.3
.005	.4
.015	.5
.015	1.0
.020	2.2
.025	2.7
.040	7.3
.050	20.2
.075	27.0
.105	44.7
.125	68.8
.150	74.9
.185	90.3
.225	95.7
.265	117.3

ORIGINAL PAGE IS OF POOR QUALITY

ALLOY - TD NICR
STRESS (MPA) - 20.7
TEMP. (KELVIN) - 1478
THICKNESS (CM) - .025
TEST DIRECTION - LONG.
SOURCE - NAS-3-15558

STRAIN (PCT.)	TIME (HOURS)
.020	.1
.020	.2
.020	.3
.040	1.0
.030	2.0
.035	3.5
.075	8.0
.115	19.0
.165	27.1
.290	50.5
.305	55.4
.395	67.3
.450	75.3
.555	92.8
.595	100.2

ALLOY - TD NICR
STRESS (MPA) - 20.7
TEMP. (KELVIN) - 1478
THICKNESS (CM) - .025
TEST DIRECTION - TRANS.
SOURCE - NAS-3-15558

STRAIN (PCT.)	TIME (HOURS)
.015	.1
.020	.2
.030	.4
.030	.5
.030	1.0
.035	7.9
.090	18.6
.065	26.3
.065	42.4
.090	50.3
.115	70.5
.145	90.5
.165	98.4
.225	113.0

ALLOY - TD NICR
STRESS (MPA) - 20.7
TEMP. (KELVIN) - 1478
THICKNESS (CM) - .051
TEST DIRECTION - TRANS.
SOURCE - NAS-3-15558

STRAIN (PCT.)	TIME (HOURS)
.010	.1
.010	.2
.015	.3
.025	.4
.030	1.0
.035	19.0
.040	24.7
.050	42.8
.035	48.8
.050	67.2
.060	90.3
.075	96.8
.080	101.1

ALLOY - TD NICR
STRESS (MPA) - 22.1
TEMP. (KELVIN) - 1478
THICKNESS (CM) - .025
TEST DIRECTION - TRANS.
SOURCE - NAS-3-15558

STRAIN (PCT.)	TIME (HOURS)
.025	.2
.020	.3
.015	.5
.025	1.0
.030	6.8
.110	18.6
.125	24.8
.190	42.2
.210	48.5
.300	64.5
.300	72.2
.370	91.4
.380	96.3
.430	113.3

ALLOY - TD NICR
STRESS (MPA) - 22.1
TEMP. (KELVIN) - 1478
THICKNESS (CM) - .051
TEST DIRECTION - TRANS.
SOURCE - NAS-3-15558

STRAIN (PCT.)	TIME (HOURS)
.005	.1
.015	.2
.010	.3
.015	.5
.020	.7
.020	1.3
.025	1.8
.025	7.1
.060	18.7
.050	25.0
.065	41.7
.055	50.2
.070	75.3
.095	91.2
.080	97.1
.100	110.8

ALLOY - TD NICR
STRESS (MPA) - 23.4
TEMP. (KELVIN) - 1478
THICKNESS (CM) - .051
TEST DIRECTION - TRANS.
SOURCE - NAS-3-15558

STRAIN (PCT.)	TIME (HOURS)
.005	.1
.015	.3
.015	.4
.025	.5
.025	1.0
.035	2.0
.040	8.0
.065	19.3
.070	27.1
.110	43.9
.135	51.4
.170	67.9
.165	75.2
.200	91.2
.325	128.0

ALLOY - TD NICR
STRESS (MPA) - 24.1
TEMP. (KELVIN) - 1478
THICKNESS (CM) - .025
TEST DIRECTION - TRANS.
SOURCE - NAS-3-15558

STRAIN (PCT.)	TIME (HOURS)
.005	.1
.005	.3
.005	.4
.015	2.5
.015	8.3
.055	17.1
.070	26.7
.110	42.6
.135	50.6
.210	66.9
.230	74.5
.275	89.4
.295	95.5
.370	118.0
.455	137.1

ALLOY - TD NICR
STRESS (MPA) - 25.5
TEMP. (KELVIN) - 1478
THICKNESS (CM) - .051
TEST DIRECTION - TRANS.
SOURCE - NAS-3-15558

STRAIN (PCT.)	TIME (HOURS)
.015	.2
.010	.4
.010	.5
.015	1.3
.030	2.3
.025	3.5
.020	4.5
.035	5.4
.055	11.0
.065	22.6
.055	30.0
.070	45.4
.085	53.8
.090	69.8
.080	78.1
.110	93.9
.105	98.1
.165	129.3

ALLOY - TD NICR
STRESS (MPA) - 24.1
TEMP. (KELVIN) - 1478
THICKNESS (CM) - .051
TEST DIRECTION - TRANS.
SOURCE - NAS-3-15558

STRAIN (PCT.)	TIME (HOURS)
.010	.1
.005	.2
.020	.4
.035	1.2
.035	3.1
.050	5.8
.065	11.8
.075	22.0
.075	30.2
.090	44.8
.105	54.5
.100	70.5
.120	78.2
.140	93.9
.145	101.2

ALLOY - TD NICR
STRESS (MPA) - 27.6
TEMP. (KELVIN) - 1478
THICKNESS (CM) - .025
TEST DIRECTION - LONG.
SOURCE - NAS-3-15558

STRAIN (PCT.)	TIME (HOURS)
.010	.1
.025	.2
.025	.3
.025	.4
.020	.5
.035	7.9
.060	8.7
.060	21.5
.170	42.7
.175	42.8
.195	64.1
.255	74.7
.350	94.3
.460	113.0

ALLOY - TD NICR
STRESS (MPA) - 24.1
TEMP. (KELVIN) - 1478
THICKNESS (CM) - .152
TEST DIRECTION - TRANS.
SOURCE - GE-PVT-5132

STRAIN (PCT.)	TIME (HOURS)
.200	.1
.500	.6

ALLOY - TD NICR
STRESS (MPA) - 24.1
TEMP. (KELVIN) - 1478
THICKNESS (CM) - .152
TEST DIRECTION - TRANS.
SOURCE - GE-PVT-5132

STRAIN (PCT.)	TIME (HOURS)
.100	.3
.200	.7
.500	3.0

ALLOY - TD NICR
STRESS (MPA) - 27.6
TEMP. (KELVIN) - 1478
THICKNESS (CM) - .038
TEST DIRECTION - TRANS.
SOURCE - NAS-8-27189

STRAIN (PCT.)	TIME (HOURS)
.045	1.0
.065	1.8
.100	3.4
.215	7.5
.290	10.4

C-5

ALLOY - TD NICR
STRESS (MPA) - 27.6
TEMP. (KELVIN) - 1478
THICKNESS (CM) - .051
TEST DIRECTION - TRANS.
SOURCE - NAS-3-15558

STRAIN (PCT.)	TIME (HOURS)
.005	.1
.005	.4
.005	1.0
.010	3.5
.035	19.9
.055	27.6
.120	44.9
.140	51.4
.195	69.0
.200	75.5
.350	91.7
.490	96.8
.610	118.5

ALLOY - TD NICR
STRESS (MPA) - 27.6
TEMP. (KELVIN) - 1478
THICKNESS (CM) - .063
TEST DIRECTION - TRANS.
SOURCE - GE-PVT-5132

STRAIN (PCT.)	TIME (HOURS)
.200	.1
.500	.4

ALLOY - TD NICR
STRESS (MPA) - 31.7
TEMP. (KELVIN) - 1478
THICKNESS (CM) - .025
TEST DIRECTION - LONG.
SOURCE - NAS-3-15558

STRAIN (PCT.)	TIME (HOURS)
.020	.3
.010	.5
.020	1.2
.030	2.4
.030	4.2
.055	10.0
.115	28.8
.170	44.2
.215	52.7
.315	68.7
.360	76.9
.425	92.7
.425	97.5
.457	128.1

ALLOY - TD NICR
STRESS (MPA) - 27.6
TEMP. (KELVIN) - 1478
THICKNESS (CM) - .152
TEST DIRECTION - LONG.
SOURCE - GE-PVT-5132

STRAIN (PCT.)	TIME (HOURS)
.100	.5
.200	1.5
.500	5.5

ALLOY - TD NICR
STRESS (MPA) - 33.1
TEMP. (KELVIN) - 1478
THICKNESS (CM) - .025
TEST DIRECTION - LONG.
SOURCE - NAS-3-15558

STRAIN (PCT.)	TIME (HOURS)
.010	.1
.015	.2
.020	.4
.025	.5
.020	1.1
.040	7.0
.060	18.8
.090	24.9
.135	42.3
.160	48.7
.225	64.7
.270	72.3
.390	91.6
.425	96.5
.525	113.5

ALLOY - TD NICR
STRESS (MPA) - 34.5
TEMP. (KELVIN) - 1478
THICKNESS (CM) - .038
TEST DIRECTION - TRANS.
SOURCE - NAS-3-27189

STRAIN (PCT.)	TIME (HOURS)
.170	.6
.286	1.2

ALLOY - TD NICR
STRESS (MPA) - 37.9
TEMP. (KELVIN) - 1478
THICKNESS (CM) - .152
TEST DIRECTION - LONG.
SOURCE - GE-PVT-5132

STRAIN (PCT.)	TIME (HOURS)
.100	.2
.200	.5
.500	3.0

ALLOY - TD NICR
STRESS (MPA) - 39.3
TEMP. (KELVIN) - 1478
THICKNESS (CM) - .051
TEST DIRECTION - LONG.
SOURCE - NAS-3-15558

STRAIN (PCT.)	TIME (HOURS)
.005	.1
.010	.3
.020	.5
.020	1.0
.050	8.0
.050	19.2
.080	27.1
.090	43.8
.100	51.4
.110	67.8
.110	75.2
.120	91.1
.160	127.9

ALLOY - TD NICR
STRESS (MPA) - 41.4
TEMP. (KELVIN) - 1478
THICKNESS (CM) - .063
TEST DIRECTION - LONG.
SOURCE - GE-PVT-5132

STRAIN (PCT.)	TIME (HOURS)
.200	.1
.500	.3

ALLOY - TD NICR
STRESS (MPA) - 41.4
TEMP. (KELVIN) - 1478
THICKNESS (CM) - .152
TEST DIRECTION - LONG.
SOURCE - GE-PVT-5132

STRAIN (PCT.)	TIME (HOURS)
.200	.1
.500	.2

ALLOY - TD NICR
STRESS (MPA) - 41.4
TEMP. (KELVIN) - 1478
THICKNESS (CM) - .152
TEST DIRECTION - LONG.
SOURCE - GE-PVT-5132

STRAIN (PCT.)	TIME (HOURS)
.100	.1
.200	.2
.500	1.0

ALLOY - TD NICR
STRESS (MPA) - 42.7
TEMP. (KELVIN) - 1478
THICKNESS (CM) - .051
TEST DIRECTION - LONG.
SOURCE - NAS-3-15558

STRAIN (PCT.)	TIME (HOURS)
.020	.2
.020	.3
.015	.4
.035	1.0
.040	2.0
.035	3.2
.070	9.5
.080	18.8
.085	33.3
.095	51.8
.190	67.7
.225	75.5
.365	92.0
.455	99.7

ORIGINAL PAGE IS OF POOR QUALITY

APPENDIX F-2

TDNiCr SUPPLEMENTAL STEADY-STATE CREEP TESTS (RAW DATA)

This portion of Appendix F presents the results of the supplemental steady-state creep tests. All strains shown are total plastic strains. For informational purposes the elastic strains are presented below for the individual tests in order of their appearance in this section. Elastic strain "A" was measured at the start of the test while elastic strain "B" was measured at the conclusion of the test.

SPECIMEN #	ELASTIC STRAIN, %	
	A	B
TD02L	.055	.089
TD03L	.045	.065
TD11T	.071	*
TD12T	.054	.042
TD13T	.064	.092
TD21L	.117	.121
TD23L	.104	.121
TD24L	.102	.095
TD25L	.039	.027
TD26L	.118	.058
TD27L	.056	.030
TD28L	.032	.028
TD29L	.052	*
TD30L	.032	.034
TD32L	.062	.065

*Specimen failed

ALLOY - TD-NI-CR
STRESS (MPA) - 110.3
TEMP. (KELVIN) - 1089
THICKNESS (CM) - .025
SPECIMEN NO. - T D21L

STRAIN (PCT.)	TIME (HOURS)
.031	.1
.050	.2
.069	.3
.096	.5
.059	.8
.048	1.0
.051	1.5
.063	2.0
.071	3.0
.073	4.0
.078	5.0
.090	13.0
.092	15.0
.100	20.0
.103	25.0
.106	29.0
.104	37.0
.109	40.0
.107	45.0
.108	50.0
.110	53.0
.107	61.0
.112	65.0
.112	65.0
.115	76.0
.110	85.0
.116	90.0
.125	95.0
.117	100.0
.124	157.0
.132	160.0

ALLOY - TD-NI-CR
STRESS (MPA) - 34.5
TEMP. (KELVIN) - 1200
THICKNESS (CM) - .025
SPECIMEN NO. - T D25L

STRAIN (PCT.)	TIME (HOURS)
.003	.1
.001	.2
.001	.3
.008	.5
.005	.8
.003	1.0
.008	1.5
.012	2.0
.015	3.0
.008	4.0
.008	5.0
.008	10.0
.006	66.0
.002	71.0
.002	76.0
-.002	76.0
.005	81.0
.005	90.0
.015	98.0
.007	103.0
.012	106.0
.012	114.0
.007	119.0
.013	124.0
.013	129.0
-.001	138.0
.011	144.0
.013	149.0
.020	154.0
.011	169.0
.013	173.0
.008	177.0
.008	234.0
.009	258.0

ALLOY - TD-NI-CR
STRESS (MPA) - 62.1
TEMP. (KELVIN) - 1200
THICKNESS (CM) - .025
SPECIMEN NO. - T D24L

STRAIN (PCT.)	TIME (HOURS)
.003	.1
.008	.2
.009	.3
.010	.5
.011	.8
.012	1.0
.013	1.5
.017	2.0
.016	3.0
.024	4.0
.029	5.0
.025	10.0
.023	18.0
.026	20.0
.029	25.0
.029	30.0
.037	35.0
.030	42.0
.024	45.0
.020	50.0
.020	55.0
.012	59.0
.012	66.0
.035	71.0
.030	76.0
.028	81.0
.037	90.0
.026	98.0
.031	102.0
.030	106.0
.030	185.0
.022	195.0
.029	205.0

ALLOY - TD-NI-CR
STRESS (MPA) - 62.1
TEMP. (KELVIN) - 1200
THICKNESS (CM) - .025
SPECIMEN NO. - T 012T

STRAIN (PCT.)	TIME (HOURS)
.001	.1
.004	.2
.002	.3
.002	.5
.002	.8
.002	1.0
.004	1.5
.019	2.0
.023	3.0
.023	4.0
.022	5.0
.021	13.0
.021	16.0
.008	21.0
.006	26.0
.029	29.5
.039	37.0
.026	42.0
.018	47.0
.016	52.0
.025	61.0
.021	67.0
.032	72.0
.035	77.0
.031	133.0
.034	141.0
.034	146.0
.041	150.0
.039	158.0
.031	166.0
.035	173.0
.035	182.0
.041	190.0
.041	191.0

ALLOY - TD-NI-CR
STRESS (MPA) - 62.1
TEMP. (KELVIN) - 1200
THICKNESS (CM) - .063
SPECIMEN NO. - MDAC-E-TD2L

STRAIN (PCT.)	TIME (HOURS)
.009	.083
.016	.170
.026	.250
.026	.500
.022	.750
.028	1.000
.031	1.500
.034	2.000
.042	3.000
.037	4.000
.039	5.000
.044	7.500
.037	15.000
.037	20.000
.049	25.000
.053	30.000
.047	39.000
.036	45.000
.052	50.000
.065	55.000
.059	70.000
.068	74.000
.067	78.000
.071	135.000
.076	159.000
.080	183.000
.084	207.000

ALLOY - TD-NI-CR
STRESS (MPA) - 110.3
TEMP. (KELVIN) - 1200
THICKNESS (CM) - .025
SPECIMEN NO. - T 023L

STRAIN (PCT.)	TIME (HOURS)
.006	.1
.030	.2
.040	.3
.052	.5
.072	.8
.083	1.0
.104	1.5
.125	2.0
.135	3.0
.157	4.0
.179	5.0
.263	15.0
.290	20.0
.294	25.0
.312	30.0
.350	40.0
.357	45.0
.375	50.0
.384	55.0
.400	63.0
.403	65.0
.416	70.0
.422	75.0
.442	79.0
.452	87.0
.461	90.0
.467	95.0
.473	100.0

ALLOY - TD-NI-CR
STRESS (MPA) - 110.3
TEMP. (KELVIN) - 1200
THICKNESS (CM) - .025
SPECIMEN NO. - T D11T

STRAIN (PCT.)	TIME (HOURS)
.053	.1
.077	.2
.094	.3
.117	.5
.145	.8
.159	1.0
.175	1.5
.191	2.0
.207	3.0
.233	4.0
.236	5.0
.333	13.0
.346	16.5
.397	21.5

ALLOY - TD-NI-CR
STRESS (MPA) - 110.3
TEMP. (KELVIN) - 1202
THICKNESS (CM) - .063
SPECIMEN NO. - MDAC-E-TD1L

STRAIN (PCT.)	TIME (HOURS)
.080	.083
.138	.170
.238	.250

ALLOY - TD-NI-CR
STRESS (MPA) - 17.2
TEMP. (KELVIN) - 1339
THICKNESS (CM) - .025
SPECIMEN NO. - T D28L

STRAIN (PCT.)	TIME (HOURS)
.007	.1
.013	.2
.015	.3
.016	.5
.018	.8
.019	1.0
.020	1.5
.018	2.0
.018	3.0
.020	4.0
.020	5.0
.018	19.0
.017	25.0
.018	43.0
.019	45.0
.019	50.0
.021	55.0
.022	60.0
.026	116.0
.026	120.0
.028	125.0
.028	130.0
.028	132.0
.024	140.0
.024	145.0
.030	150.0
.030	155.0
.024	165.0
.016	170.0
.030	175.0
.030	180.0
.020	190.0
.027	195.0
.027	200.0

ALLOY - TD-NI-CR
STRESS (MPA) - 34.5
TEMP. (KELVIN) - 1339
THICKNESS (CM) - .025
SPECIMEN NO. - T D27L

STRAIN (PCT.)	TIME (HOURS)
.005	.1
.001	.2
.009	.8
.010	1.0
.012	1.5
.012	2.0
.009	3.0
.007	4.0
.012	5.0
.035	13.0
.043	20.0
.057	25.0
.065	29.0
.091	37.0
.094	40.0
.090	45.0
.099	50.0
.108	61.0
.107	85.0
.112	90.0
.140	95.0
.153	100.0
.122	157.0
.130	160.0
.135	165.0
.139	170.0
.136	173.0
.134	181.0
.145	185.0
.141	190.0
.136	195.0
.141	197.0
.135	205.0

ALLOY - TD-NI-CR
STRESS (MPA) - 62.1
TEMP. (KELVIN) - 1339
THICKNESS (CM) - .025
SPECIMEN NO. - T D26L

STRAIN (PCT.)	TIME (HOURS)
.002	.1
.003	.2
.004	.3
.005	.5
.007	.8
.009	1.0
.017	1.5
.020	2.0
.022	3.0
.024	4.0
.028	5.0
.037	10.0
.066	15.0
.097	71.0
.098	75.0
.093	80.0
.102	85.0
.119	93.0
.123	95.0
.131	100.0

ALLOY - TD-NI-CR
STRESS (MPA) - 62.1
TEMP. (KELVIN) - 1339
THICKNESS (CM) - .025
SPECIMEN NO. - T 013T

STRAIN (PCT.)	TIME (HOURS)
.013	.1
.017	.2
.025	.3
.047	.5
.055	.8
.066	1.0
.073	1.5
.077	2.0
.098	3.0
.111	4.0
.117	5.0
.186	10.0
.245	15.0
.342	24.0
.396	30.0
.451	35.0
.476	40.0
.946	96.0

ALLOY - TD-NI-CR
STRESS (MPA) - 62.1
TEMP. (KELVIN) - 1339
THICKNESS (CM) - .063
SPECIMEN NO. - MDAC-E-TD3L

STRAIN (PCT.)	TIME (HOURS)
.013	.063
.028	.170
.039	.250
.048	.500
.055	.750
.065	1.000
.071	1.500
.078	2.000
.100	3.000
.120	4.000
.130	5.000
.148	10.000
.225	15.000
.482	24.000
.850	29.000

ALLOY - TD-NI-CR
STRESS (MPA) - 17.2
TEMP. (KELVIN) - 1478
THICKNESS (CM) - .025
SPECIMEN NO. - T 030L

STRAIN (PCT.)	TIME (HOURS)
.002	.1
.004	.2
.006	.3
.007	.5
.008	.8
.010	1.0
.015	1.5
.016	2.0
.017	3.0
.018	4.0
.016	5.0
.012	10.0
.002	14.0
.019	21.0
.013	25.0
.020	30.0
.017	35.0
.017	38.0
.015	45.0
.020	53.0
.013	94.0

ALLOY - TD-NI-CR
STRESS (MPA) - 27.6
TEMP. (KELVIN) - 1478
THICKNESS (CM) - .025
SPECIMEN NO. - T 032L

STRAIN (PCT.)	TIME (HOURS)
.003	.1
.005	.2
.006	.3
.012	.5
.014	.8
.015	1.0
.018	1.5
.019	2.0
.023	3.0
.029	4.0
.031	5.0
.033	10.0
.040	14.0
.043	21.0
.046	26.0
.047	31.0
.041	36.0
.043	45.0
.033	50.0
.038	55.0

ALLOY - TD-NI-CR
STRESS (MPA) - 34.5
TEMP. (KELVIN) - 1478
THICKNESS (CM) - .025
SPECIMEN NO. - T 029L

STRAIN (PCT.)	TIME (HOURS)
.008	.1
.011	.2
.011	.3
.012	.5
.011	.8
.012	1.0
.022	1.5
.027	2.0
.025	3.0
.028	4.0
.030	5.0
.033	10.0
.036	15.0
.042	27.5
.042	35.5
.055	43.0
.054	45.0
.066	50.0
.068	55.0
.069	60.0
.090	67.0
.092	70.0
.110	75.0

APPENDIX F-3

TD-Ni-Cr CYCLIC CREEP TESTS

(RAW DATA)

This section presents the results of the 12 cyclic creep tests that were performed on TD-Ni-Cr tensile specimens.

TDNiCr
Cyclic Creep Data

Cyclic Test Number	1				
Alloy Designation	TDNiCr				
Heat Number	TC3875				
Supplier	NASA-Lewis*				
Test Temperature (°K)	1089				
Test Direction	Longitudinal				
Sheet Thickness (cm)	0.024 cm ±0.004				
Specimen Number	TD95L	TD96L	TD97L	TD98L	TD93L
Specimen Thickness (cm)	.0241	.0239	.0239	.0241	.0249
Specimen Width (cm)	1.2682	1.2684	1.2684	1.2684	1.2684
Applied Load (Kg)	(See Table - Page F-3-4)				
Test Stress (MPa)	(See Table - Page F-3-4)				
Pressure (Pa)	Constant (< 1.333)				

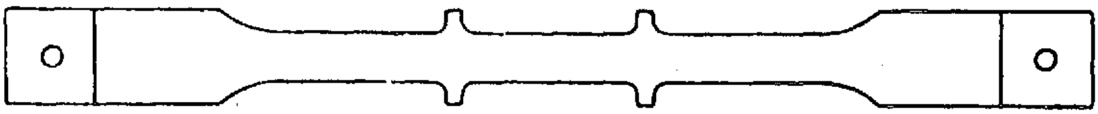

Cycle Number		% Creep TD95L	TD96L	TD97L
1	Side A	.02	.01	.19
	Side B	.03	.02	.01
	Ave.	.025	.015	.10
5	Side A	.03	.01	(Specimen broke at start
	Side B	.05	.02	of Cycle 2 and was
	Ave.	.04	.015	replaced by TD98L)
15	Side A	.05	.02	
	Side B	.05	.02	
	Ave.	.05	.02	
25	Side A	.06	.03	
	Side B	.06	.02	
	Ave.	.06	.025	
50	Side A	.05	.02	
	Side B	.06	.03	
	Ave.	.055	.025	
75	Side A	.06	.03	
	Side B	.07	.03	
	Ave.	.065	.03	
100	Side A	.06	.03	
	Side B	.08	.03	
	Ave.	.07	.03	

* Produced by Fansteel Inc. for NASA Lewis Research Center under Contract NAS3-13490.

Cycle Number		% Creep TD98L
4	Side A	.06
	Side B	.05
	Ave.	.055
14	Side A	.09
	Side B	.09
	Ave.	.09
24	Side A	.10
	Side B	.10
	Ave.	.10
49	Side A	.11
	Side B	.10
	Ave.	.105
74	Side A	.13
	Side B	.11
	Ave.	.12

(Specimen broke at cycle 87 and was replaced by TD93L)

Cycle Number		% Creep TD93L
12	Side A	.07
	Side B	.10
	Ave.	.085

TDNiCr TEST NO. 1

SPECIMEN	LOAD ∿ Kg
TD95L	32.3
TD96L	26.5
TD97L	38.2
TD98L	38.8
TD93L	—

SPECIMEN	STRESS ∿ MPa
TD95L	103.3 (1)
TD96L	85.7 (1)
TD97L	123.6 (2)
TD98L	124.2 (3)
TD93L	— (4)

NOTE:

(1) Stress level average for cycles 1 through 88. Cycle 89-100 not recorded.

(2) Specimen broke at start of cycle 2. Material flaw noted in test zone. Replaced by specimen TD98L.

(3) Specimen broke at cycle 88.

(4) This specimen replaced TD98L in whiffle tree for cycle 89-100. Stress not recorded - assumed to be same as for TD98L

TDNiCr
Cyclic Creep Data

Cyclic Test Number	2			
Alloy Designation	TDNiCr			
Heat Number	T3875			
Supplier	NASA-Lewis*			
Test Temperature (°K)	1200			
Test Direction	Longitudinal			
Sheet Thickness (cm)	0.024 cm ±0.004			
Specimen Number	TD45L	TD47L	TD52L	TD75L
Test Stress (MPa) (Approx. Values)	85.5	62.1	108.6	108.6
Pressure (Pa)	Constant (< 1.333)			

Side A

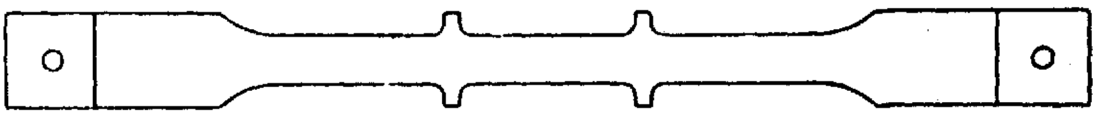

Side B

Cycle Number		% Creep TD45L	TD47L	TD52L	
1	Side A	.07	.01	Specimen broke on 1st cycle and was replaced by Specimen TD75L which broke on 1st cycle)	
	Side B	.05	.02		
	Ave.	.06	.015		
					Broke

NOTE: This test was replaced by Test 3.

* Produced by Fansteel Inc. for NASA Lewis Research Center under Contract NAS3-13490.

TDNiCr
Cyclic Creep Data

Cyclic Test Number	3		
Alloy Designation	TDNiCr		
Heat Number	TC3875		
Supplier	NASA-Lewis*		
Test Temperature (°K)	1200		
Test Direction	Longitudinal		
Sheet Thickness (cm)	0.024 cm $\pm$0.004		
Specimen Number	TD44L	TD80L	TD81L
Specimen Thickness (cm)	.0246	.0246	.0246
Specimen Width (cm)	1.2667	1.2682	1.2680
Applied Load (Kg)	23.5	18.3	28.0
Test Stress (MPa)	73.8	57.2	87.7
Pressure (Pa)	Constant (< 1.333)		

Side A

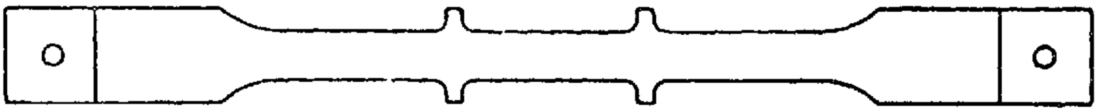

Side B

Cycle Number		% Creep TD44L	TD80L	TD81L
1	Side A	.02	.01	.02
	Side B	.01	.01	.03
	Ave.	.015	.01	.025
5	Side A	.05	.02	.04
	Side B	.02	.02	.05
	Ave.	.035	.02	.045
15	Side A	.06	.03	.06
	Side B	.05	.04	.08
	Ave.	.055	.035	.07
25	Side A	.07	.03	.05
	Side B	.03	.03	.07
	Ave.	.05	.03	.06
50	Side A	.07	.03	.07
	Side B	.05	.03	.09
	Ave.	.06	.03	.08
75	Side A	.09	.04	.09
	Side B	.05	.03	.10
	Ave.	.07	.035	.095
100	Side A	.10	.03	.09
	Side B	.06	.04	.11
	Ave.	.08	.035	.10

* Produced by Fanstell Inc. for NASA Lewis Research Center under Contract NAS3-13490.

TDNiCr
Cyclic Creep Data

Cyclic Test Number	4			
Alloy Designation	TDNiCr			
Heat Number	TC3875			
Supplier	NASA-Lewis *			
Test Temperature (°K)	1339			
Test Direction	Longitudinal			
Sheet Thickness (cm)	0.024 cm ±0.004			
Specimen Number	TD55L	TD57L	TD59L	TD67L
Specimen Thickness (cm)	.0259	.0259	.0259	.0262
Specimen Width (cm)	1.2682	1.2682	1.2682	1.2680
Applied Load (Kg)	(See Table - Page F-3-9)			
Test Stress (MPa)	(See Table - Page F-3-9)			
Pressure (Pa)	Constant (< 1.333)			

Side A

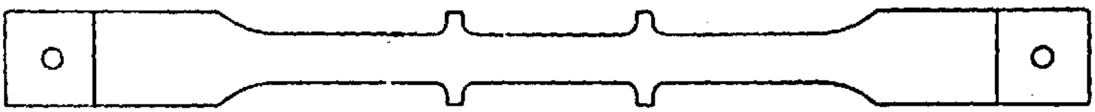

Side B

Cycle Number		% Creep TD55L	TD57L	TD59L
1	Side A	.02	.02	.05
	Side B	.02	.01	.03
	Ave.	.02	.015	.04
5	Side A	.03	.02	.07
	Side B	.03	.02	.05
	Ave.	.03	.02	.06
15	Side A	.03	.02	.09
	Side B	.04	.02	.06
	Ave.	.035	.02	.075
25	Side A	.04	.03	.13
	Side B	.05	.02	.07
	Ave.	.045	.025	.10
50	Side A	.04	.04	(Broke on Cycle 46
	Side B	.05	.04	Replaced by Specimen
	Ave.	.045	.04	TD67L)
75	Side A	.05	.03	
	Side B	.05	.03	
	Ave.	.05	.03	
100	Side A	.05	.03	
	Side B	.05	.03	
	Ave.	.05	.03	

* Produced by Fansteel Inc. for NASA Lewis Research Center under Contract NAS3-13490.

Cycle Number		% Creep TD67L
4	Side A	.03
	Side B	.03
	Ave.	.03
29	Side A	.03
	Side B	.09
	Ave.	.06
54	Side A	.05
	Side B	.10
	Ave.	.075

TDNiCr TEST NO. 4

SPECIMEN	LOAD ∿ Kg
TD55L	16.0
TD57L	10.3
TD59L	20.2 (1)
TD67L	20.1

SPECIMEN	STRESS ∿ MPa
TD55L	47.6
TD57L	30.6
TD59L	60.3
TD67L	59.2

NOTE: (1) Specimen TD59L broke on Cycle 46. Replaced by Specimen TD67L.

TD NiCr Cyclic Creep Data

Cyclic Test Number	5		
Alloy Designation	TD NiCr		
Heat Number	TC 3875		
Supplier	NASA-Lewis*		
Test Temperature (°K)	1478		
Test Direction	Longitudinal		
Sheet Thickness (cm)	0.024 cm ±0.004		
Specimen Number	TD35L	TD62L	TD63L
Specimen Thickness (cm)	.0277	.0274	.0277
Specimen Width (cm)	1.2672	1.2685	1.2685
Applied Load (Kg)	12.1	10.4	5.8
Test Stress (MPa)	33.7	29.3	16.1
Pressure (Pa)	Constant (< 1.333)		

Side A

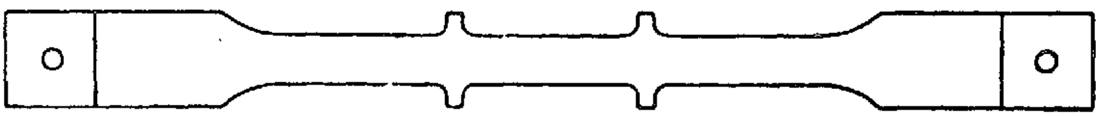

Side B

Cycle Number		% Creep TD35L	TD62L	TD63L
1	Side A	.03	.01	.02
	Side B	.02	.00	.02
	Ave.	.025	.005	.02
5	Side A	.03	.01	.03
	Side B	.03	.00	.02
	Ave.	.03	.005	.025
15	Side A	.03	.02	.04
	Side B	.02	.01	.04
	Ave.	.025	.015	.04
25	Side A	.06	.01	.04
	Side B	.06	.01	.04
	Ave.	.06	.01	.04
50	Side A	.10	.02	.05
	Side B	.08	.02	.06
	Ave.	.09	.02	.055
75	Side A	.10	.02	.05
	Side B	.11	.02	.06
	Ave.	.105	.02	.055
100	Side A	.13	.03	.07
	Side B	.13	.02	.07
	Ave.	.13	.025	.07

*Produced by Fansteel, Inc. for NASA Lewis Research Center under Contract NAS3-13490.

TD NiCr Cyclic Creep Data

Cyclic Test Number	6						
Alloy Designation	TD NiCr						
Heat Number	TC 3875						
Supplier	NASA-Lewis*						
Test Temperature (°K)	1478						
Test Direction	Longitudinal						
Sheet Thickness (cm)	0.024 cm ±0.004						
Specimen Number	TD72L	TD77L	TD85L	TD102L	TD40L	TD36L	TD43L
Specimen Thickness (cm)	.0257	.0254	.0257	.0257	.0257	.0257	
Specimen Width (cm)	1.2685	1.2687	1.2680	1.2682	1.2667	1.2667	
Applied Load (Kg)	(See Table - Page F-3-13)						
Test Stress (MPa)	(See Table - Page F-3-13)						
Pressure (Pa)	Constant (< 1.333)						

Side A

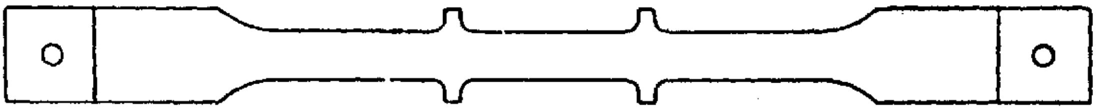

Side B

Cycle Number		% Creep TD77L	% Creep TD85L
1	Side A	.05	.05
	Side B	.05	.05
	Ave.	.05	.05
5	Side A	.03	.06
	Side B	.03	.07
	Ave.	.03	.065
15	Side A	.03	.09
	Side B	.03	.09
	Ave.	.03	.09
25	Side A	.04	.09
	Side B	.06	.11
	Ave.	.05	.10
50	Side A	.05	.11
	Side B	.06	.16
	Ave.	.055	.135
75	Side A	.05	.15
	Side B	.08	.18
	Ave.	.065	.165
100	Side A	.05	.17
	Side B	.07	.22
	Ave.	.06	.195

*Produced by Fansteel, Inc. for NASA Lewis Research Center under Contract NAS3-13490.

Cycle Number		% Creep
		TD72L
1		(Broke)

Cycle Number		% Creep
		TD102L
4	Side A	.07
	Side B	.09
	Ave.	.08
14	Side A	.08
	Side B	.13
	Ave.	.105
24	Side A	.11
	Side B	.15
	Ave.	.13
49	Side A	.22
	Side B	.22
	Ave.	.22
		(Broke on Cycle 56)

Cycle Number		% Creep
		TD40L
18	Side A	.08
	Side B	.14
	Ave.	.11
		(Broke on Cycle 78)

Cycle Number		% Creep
		TD36L
13	Side A	.11
	Side B	.09
	Ave.	.10

TDNiCr TEST NO. 6

SPECIMEN	LOAD ~ Kg
TD72L	14.6 (1)
TD77L	7.2
TD85L	12.4
TD102L	14.7 (2)
TD40L	14.5 (3)
TD43L	14.4 (4)
TD36L	14.5

SPECIMEN	STRESS ~ MPa
TD72L	44.0
TD77L	21.8
TD85L	37.5
TD102L	44.2
TD40L	43.8
TD43L	43.4
TD36L	43.6

NOTE:
(1) Specimen failed on Cycle 1. Replaced by Specimen TD102L.
(2) Specimen failed on Cycle 57. Replaced by Specimen TD40L.
(3) Specimen failed on Cycle 78. Replaced by Specimen TD43L.
(4) Specimen failed on Cycle 88. Replaced by Specimen TD36L.

TD NiCr Cyclic Creep Data

Cyclic Test Number	7		
Alloy Designation	TD NiCr		
Heat Number	TC 3875		
Supplier	NASA-Lewis*		
Test Temperature (°K)	1478		
Test Direction	Longitudinal		
Sheet Thickness (cm)	0.024 cm ±0.004		
Specimen Number	TD60L	TD61L	TD65L
Specimen Thickness (cm)	.0259	.0259	.0259
Specimen Width (cm)	1.2680	1.2682	1.2685
Applied Load (Kg)	(See Table - Page F-3-15)		
Test Stress (MPa)	(See Table - Page F-3-15)		
Pressure (Pa)	Constant (< 1.333)		

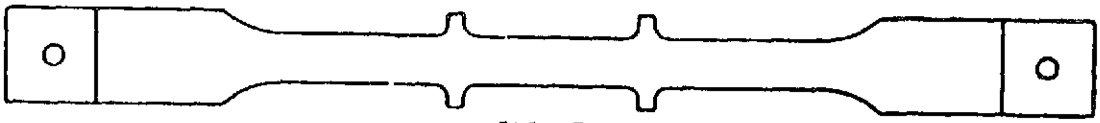

Cycle Number		% Creep TD60L	TD61L	TD65L
1	Side A	.02	.02	.02
	Side B	.03	.01	.03
	Ave.	.025	.015	.025
5	Side A	.05	.02	.04
	Side B	.05	.01	.03
	Ave.	.05	.015	.035
15	Side A	.05	.02	.05
	Side B	.06	.03	.05
	Ave.	.055	.025	.05
25	Side A	.10	.03	.07
	Side B	.06	.02	.07
	Ave.	.08	.025	.07
50	Side A	.12	.05	.07
	Side B	.09	.03	.07
	Ave.	.105	.04	.07
75	Side A	.13	.05	.07
	Side B	.10	.03	.10
	Ave.	.115	.04	.085
100	Side A	.21	.05	.09
	Side B	.10	.03	.13
	Ave.	.155	.04	.105

*Produced by Fansteel, Inc. for NASA Lewis Research Center under Contract NAS3-13490.

TDNiCr TEST NO. 7

	LOAD ~ Kg	
SPECIMEN	1st Step (10 Minutes)	2nd Step (10 Minutes)
TD60L	10.1	12.8
TD61L	4.8	6.1
TD65L	38.6	11.2

	STRESS ~ MPa	
SPECIMEN	1st Step (10 Minutes)	2nd Step (10 Minutes)
TD60L	30.0	38.3
TD61L	14.2	18.3
TD65L	25.8	33.4

TD NiCr Cyclic Creep Data

Cyclic Test Number	8		
Alloy Designation	TD NiCr		
Heat Number	TC 3875		
Supplier	NASA-Lewis*		
Test Temperature (°K)	1478		
Test Direction	Longitudinal		
Sheet Thickness (cm)	0.024 cm ±0.004		
Specimen Number	TD87L	TD88L	TD100L
Specimen Thickness (cm)	.0257	.0254	.0251
Specimen Width (cm)	1.2685	1.2682	1.2687
Applied Load (Kg)	(See Table - Page F-3-17)		
Test Stress (MPa)	(See Table - Page F-3-17)		
Pressure (Pa)	Constant (< 1.333)		

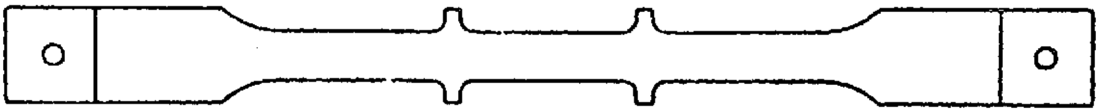

Cycle Number		% Creep TD87L	TD88L	TD100L
1	Side A	.05	.01	.03
	Side B	.04	.02	.05
	Ave.	.045	.015	.04
5	Side A	.07	.02	.05
	Side B	.05	.03	.05
	Ave.	.06	.025	.05
15	Side A	.10	.02	.05
	Side B	.06	.03	.07
	Ave.	.08	.025	.06
25	Side A	.11	.03	.06
	Side B	.06	.03	.07
	Ave.	.085	.03	.065
50	Side A	.14	.03	.07
	Side B	.08	.05	.09
	Ave.	.11	.04	.08
75	Side A	.18	.05	.10
	Side B	.09	.05	.10
	Ave.	.135	.05	.10
100	Side A	.20	.05	.11
	Side B	.10	.05	.11
	Ave.	.15	.05	.11

*Produced by Fansteel, Inc. for NASA Lewis Research Center under Contract NAS3-13490.

TDNiCr TEST NO. 8

SPECIMEN	LOAD ~ Kg 1st Step (10 Minutes)	2nd Step (10 Minutes)	3rd Step (5 Minutes)	4th Step (10 Minutes)
TD87L	3.5	7.23	12.6	15.5
TD88L	2.8	6.1	10.8	14.5
TD100L	1.6	3.4	6.2	7.9

SPECIMEN	STRESS ~ MPa 1st Step (10 Minutes)	2nd Step (10 Minutes)	3rd Step (5 Minutes)	4th Step (10 Minutes)
TD87L	10.5	21.7	38.0	46.8
TD88L	8.6	18.6	33.0	44.2
TD100L	5.0	10.4	19.1	24.2

TD NiCr Cyclic Creep Data

Cyclic Test Number	9		
Alloy Designation	TD NiCr		
Heat Number	TC 3875		
Supplier	NASA-Lewis*		
Test Temperature (°K)	(See Table - Page F-3-19)		
Test Direction	Longitudinal		
Sheet Thickness (cm)	0.024 cm ±0.004		
Specimen Number	TD49L	TD76L	TD83L
Specimen Thickness (cm)	.0249	.0249	.0251
Specimen Width (cm)	1.2670	1.2680	1.2677
Applied Load (Kg)	(See Table - Page F-3-19)		
Test Stress (MPa)	(See Table - Page F-3-19)		
Pressure (Pa)	(See Table - Page F-3-19)		

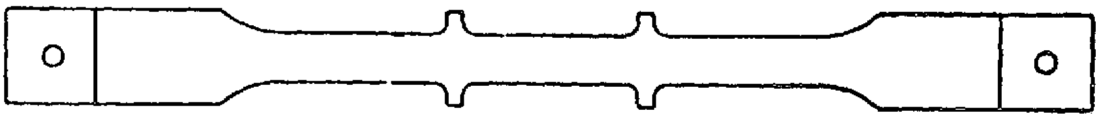

Cycle Number		% Creep TD49L	TD76L	TD83L
1	Side A	.03	.02	.02
	Side B	.03	.02	.03
	Ave.	.03	.02	.025
5	Side A	.05	.03	.03
	Side B	.04	.03	.03
	Ave.	.045	.03	.03
15	Side A	.05	.03	.03
	Side B	.05	.02	.04
	Ave.	.05	.025	.035
25	Side A	.06	.04	.04
	Side B	.06	.03	.05
	Ave.	.06	.035	.045
50	Side A	.06	.04	.04
	Side B	.06	.04	.05
	Ave.	.06	.04	.045
75	Side A	.07	.03	.04
	Side B	.06	.05	.05
	Ave.	.065	.04	.045
100	Side A	.09	.03	.05
	Side B	.09	.05	.06
	Ave.	.09	.04	.055
150	Side A	.10	.04	.06
	Side B	.09	.05	.06
	Ave.	.095	.045	.06
200	Side A	.11	.04	.07
	Side B	.11	.05	.06
	Ave.	.11	.045	.065

*Produced by Fansteel, Inc. for NASA Lewis Research Center under Contract NAS3-13490.

TDNiCr TEST NO. 9

CYCLE TIME (SEC.)	TEMP. (°K)	PRESSURE (Pa)	STRESS ∿ MPa		
			TD49L	TD76L	TD83L
300	955	1.5	4.2	1.7	3.8
400	1200	2.4	9.9	4.4	8.6
500	1339	4.0	13.7	6.2	11.6
600	1439	5.2	16.0	7.4	13.3
700	1479	6.4	17.9	8.3	14.6
800	1482	7.2	18.8	8.8	15.3
900	1466	8.3	19.2	8.9	15.6
1000	1450	9.3	20.4	9.4	16.8
1100	1444	10.4	22.1	10.2	18.4
1200	1428	10.7	25.2	11.7	21.2
1300	1405	12.5	27.8	13.0	23.7
1400	1389	18.7	31.8	15.1	27.6
1500	1361	33.3	37.0	18.1	32.8
1600	1337	56.0	42.7	20.8	37.2
1700	1228	77.3	45.4	22.7	40.5
1800	1111	100.0	48.2	24.4	43.8
1900	1010	126.6	48.2	24.4	44.5
2000	944	319.9	46.0	23.1	42.9
2100	872	693.2	41.7	20.6	39.1
2200	813	1333.0	35.7	17.6	33.8
2300	750	41323.0	28.2	13.2	26.7
2400	694	101308	19.7	8.6	18.8
2500	649	101308	11.7	4.5	11.0

TD NiCr Cyclic Creep Data

Cyclic Test Number	10		
Alloy Designation	TD NiCr		
Heat Number	TC 3875		
Supplier	NASA-Lewis*		
Test Temperature (°K)	1478		
Test Direction	Longitudinal		
Sheet Thickness (cm)	0.024 cm ±0.004		
Specimen Number	TD53L	TD54L	TD73L
Specimen Thickness (cm)	.0249	.0251	.0251
Specimen Width (cm)	1.2680	1.2680	1.2677
Applied Load (Kg)	(See Table - Page F-3-21)		
Test Stress (MPa)	(See Table - Page F-3-21)		
Pressure (Pa)	(See Table - Page F-3-21)		

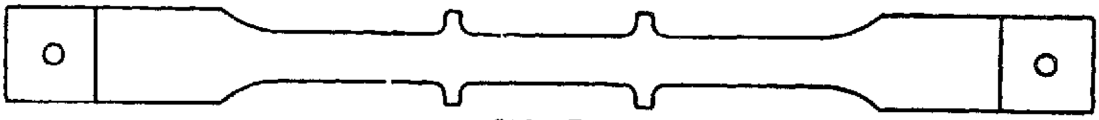

Cycle Number		% Creep TD53L	TD54L	TD73L
1	Side A	.05	.03	.02
	Side B	.03	.02	.03
	Ave.	.04	.025	.025
5	Side A	.06	.02	.04
	Side B	.06	.03	.05
	Ave.	.06	.025	.045
15	Side A	.08	.02	.06
	Side B	.07	.03	.07
	Ave.	.075	.025	.065
25	Side A	.09	.03	.06
	Side B	.09	.05	.07
	Ave.	.09	.04	.065
50	Side A	.12	.03	.06
	Side B	.10	.05	.09
	Ave.	.11	.04	.075
75	Side A	.15	.05	.08
	Side B	.13	.05	.09
	Ave.	.14	.05	.085
100	Side A	.18	.05	.10
	Side B	.16	.06	.12
	Ave.	.17	.055	.11

*Produced by Fansteel, Inc. for NASA Lewis Research Center under Contract NAS3-13490.

TDNiCr TEST NO. 10

SPECIMEN	LOAD ~ Kg 1st Step (10 Minutes)	2nd Step (10 Minutes)	3rd Step (5 Minutes)	4th Step (10 Minutes)
TD53L	3.4	7.0	12.2	14.9
TD54L	1.6	3.4	6.3	7.9
TD73L	2.6	5.7	10.3	13.3

SPECIMEN	STRESS ~ MPa 1st Step (10 Minutes)	2nd Step (10 Minutes)	3rd Step (5 Minutes)	4th Step (10 Minutes)
TD53L	10.4	21.6	38.0	46.4
TD54L	5.1	10.6	19.3	24.4
TD73L	8.0	17.5	31.5	41.0

TD NiCr Cyclic Creep Data

Cyclic Test Number	11		
Alloy Designation	TD NiCr		
Heat Number	TC 3875		
Supplier	NASA-Lewis*		
Test Temperature (°K)	1478		
Test Direction	Longitudinal		
Sheet Thickness (cm)	0.024 cm ±0.004		
Specimen Number	TD69L	TD86L	TD103L
Specimen Thickness (cm)	.0262	.0259	.0259
Specimen Width (cm)	1.2682	1.2680	1.2682
Applied Load (Kg)	13.0	6.4	11.0
Test Stress (MPa)	38.5	19.2	32.7
Pressure (Pa)	Constant (< 1.333)		

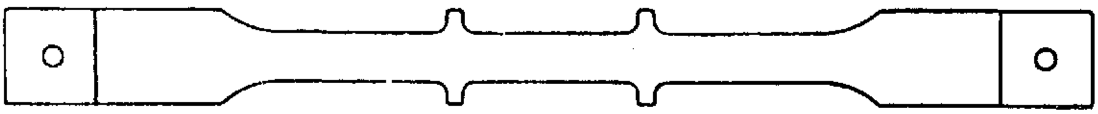

Cycle Number		% Creep TD69L	TD86L	TD103L
1	Side A	.05	.01	.02
	Side B	.03	.02	.02
	Ave.	.04	.015	.02
5	Side A	.06	.01	.03
	Side B	.05	.02	.04
	Ave.	.055	.015	.035
15	Side A	.09	.02	.04
	Side B	.06	.03	.06
	Ave.	.075	.025	.05
25	Side A	.11	.02	.05
	Side B	.07	.05	.07
	Ave.	.09	.035	.06
50	Side A	.14	.03	.06
	Side B	.10	.05	.07
	Ave.	.12	.04	.065
75	Side A	.17	.03	.06
	Side B	.11	.05	.09
	Ave.	.14	.04	.075
100	Side A	.18	.03	.06
	Side B	.13	.05	.09
	Ave.	.155	.04	.075

*Produced by Fansteel, Inc. for NASA Lewis Research Center under Contract NAS3-13490.

TD NiCr Cyclic Creep Data

Cyclic Test Number	12		
Alloy Designation	TD NiCr		
Heat Number	TC 3875		
Supplier	NASA-Lewis*		
Test Temperature (°K)	1478		
Test Direction	Longitudinal		
Sheet Thickness (cm)	0.024 cm ±0.004		
Specimen Number	TD63L	TD77L	TD85L
Specimen Thickness (cm)	.0277	.0254	.0257
Specimen Width (cm)	1.2685	1.2687	1.2680
Applied Load (Kg)	10.9	6.7	12.5
Test Stress (MPa)	30.3	20.4	37.7
Pressure (Pa)	Constant (< 1.333)		

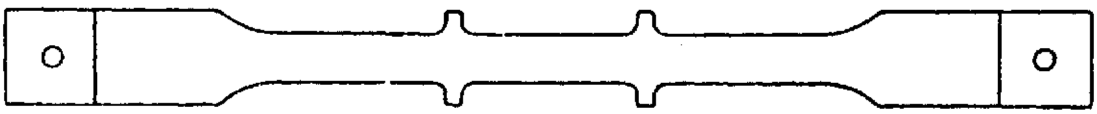

Cycle Number		% Creep TD63L	TD77L	TD85L
1	Side A	.02	.01	.01
	Side B	.02	.01	.01
	Ave.	.02	.01	.01
5	Side A	.02	.01	.01
	Side B	.01	.01	.01
	Ave.	.015	.01	.01
15	Side A	.02	.02	.02
	Side B	.01	.01	.02
	Ave.	.015	.015	.02
25	Side A	.02	.02	.02
	Side B	.03	.02	.03
	Ave.	.025	.02	.025
50	Side A	.03	.02	.05
	Side B	.03	.02	.04
	Ave.	.03	.02	.045

*Produced by Fansteel, Inc. for NASA Lewis Research Center under Contract NAS3-13490.

Appendix G

ALTERNATE APPROACHES TO THE DEVELOPMENT OF EQUATIONS

During the course of this study limited investigations were performed on various data sets in an attempt to develop equations that had lower standard errors of estimates (better data fit).

The first of these investigations, as described in Appendix G-1, was the attempt to take the literature survey data base for Ti-6Al-4V and orthogonalize it. The reason for the orthogonalization was that during the development of the literature survey creep equation it was felt that the independent variables in the regression analysis were interrelated (i.e. time, stress, and temperature) which produced problems with multi-colinearity. Orthogonization was a way of reducing this problem. Our approach to using orthogonalization is presented in Appendix G-1. (For further information on this subject see Ref. 27, pages 150-158.) This approach was successful, however it required the use of a large number of terms in the equation which made it more difficult to work with than the existing equation and as a result this technique was not pursued further.

A second approach examined was for the Rene '41 literature survey data and involved the use of a finite difference equation. In the development of a literature survey equation for Rene '41 it was found that the equation was essentially a "best fit" type and did not always describe the shape (time function) of the individual creep curves. Therefore, using the concept that in any given creep test the next data point will be a function of the previous data point a finite difference approach was examined. The results of this study are presented in Appendix G-2. The equation developed using this approach described the shape of the creep curve but could not conform to the boundary condition of $\varepsilon = 0$, at $\sigma = 0$ and $t = 0$ and as a result this approach was not pursued.

The last approach was a nonliner least squares analysis of L605 and Ti-6Al-4V data. During the program it appeared that there was a correlation between cyclic and steady-state creep data for equal total time at load and temperature. The correlation could not be found using the linear least squares analysis approach so a nonlinear analysis was performed. Through the use of this approach we were able to correlate the function of stress with strain for combined steady-state and cyclic data, however, we could not correlate the function of temperature or time. While this approach offers potential, program schedule and budget would not permit further exploration in this area. Appendix G-3 describes our efforts in nonlinear least squares analysis.

APPENDIX G-1

AN APPROACH TO ORTHOGONALIZING THE INDEPENDENT VARIABLES IN A REGRESSION EQUATION

I. Definitions (initial):

$Y = \{y_i\}_{T\times1}$ is a column vector of T observations on the dependent variable.

$X = \{x_{ij}\}_{T\times n}$ is a matrix of T observations on n independent variables.

X_i refers to independent variable i.

$\bar{X}_i$ refers to the mean of independent variable i.

$\hat{Y} = \{\hat{y}_i\}_{T\times1}$ is a vector of T estimates of the dependent variable. ($\hat{y}_i$ is an estimate of y_i).

$E = \{e_i\}_{T\times1} = \{y_i\} - \{\hat{y}_i\}$ is a vector of T residuals (errors).

$S_{1\times1} = \{e_i\}^T_{1\times T} \times \{e_i\}_{T\times1}$ is the sum of squares of the error terms.

$\succ$ means precedes in order.

II. Desired Results:

A. Derive a column vector of coefficients

$B = \{b_i\}_{n\times1}$

such that

$\hat{Y}_{T\times1} = X_{T\times n} B_{n\times1}$ and S is minimum and <u>all</u> b_i are significant.

B. In the event that there is any collinearity among the columns of X (i.e., for some column i, for some columns j_k (k = 1...) and for some coefficients a_ℓ

$$(\ell = 1 \ldots r), \quad \sum_{m=1}^{T} (x_{mi} - \bar{X}_i) \left(\sum_{l=1}^{r} a_l (x_{m\ell} - \bar{X}_\ell) \right) > 0,$$

there may be difficulty in estimating the vector of coefficients in such a way that S is minimum.

C. If there is an exact collinearity (i.e., one independent variable is an exact linear function of the other independent variables), there is no unique solution to deriving the vector $\underline{B}$.

D. If the collinearity is not quite exact, and if the whole set of independent variables is 'forced,' there is a potential problem in that the standard errors of the coefficients may cast some doubt on the significance of the coefficients. Thus one may end up with the embarrassing situation of having a significant equation (as measured by the multiple R, or the overall F) and few, if any, significant coefficients.

E. To circumvent these problems, the method of stepwise regression was devised. It operates in such a manner that one variable at a time is brought into the equation. The criteria for entry quite simply are (a) significance of the variable in explaining variance and (b) independence of the entering variable relative to the independent variable already in the equation.

F. This method circumvents the multicollinearity problem but at a cost. First, there is the cost in form (or meaning); then there is the cost in precision. In form, this cost manifests itself in restricting itself to the earliest entering variables in a collinear set. Thus higher order terms may lock out lower order terms. The loss of precision may come about when the dependence of the candidate variable, relative to the independent variables already in the equation, is too great to allow the candidate's entry, but where the candidate can account for a significant portion of the residual variation of the dependent variable.

G. A technique has been devised to correct this condition by transforming the original independent variables into a new orthogonal set. The original variables are linear combinations of the new variables and vice versa. The new set is orthogonal in the sense the intercorrelations among them is low. In a perfect orthogonalization technique, the intercorrelation between the new variables would be exactly zero. In our more practical approach, the new variables are generated in such a way that their intercorrelations are low enough to alleviate the problem of form and precision.

H. The technique of orthogonization is not new, having been employed in polynomial regression in the method of orthogonal polynomials and in factor analysis in the regression on principle components.

III. Technique of Regression on Near Orthogonal Variables:

First order the independent variables according to two criteria and relable them Z_1 = some X_1, Z_2 = some X_j ordered higher than X_i such that

$$Z_1 \succ Z_2 \succ Z_3 \ldots \succ Z_n \text{ in the ordering.}$$

Then derive regression equations relating each Z_i (except Z_1) to those Z's which precede it in the ordering. Preceding Z's are entered into the equation until the standard error of estimate begins to increase (until F to enter is less than 1.0). The residual from each equation $\left[\text{residual} = Z_i^* = Z_i - f(Z_1, Z_2 \ldots Z_{i-1})\right]$ form a variable in our new set. Let $Z_1^* = Z_1$. By the method of least squares, each residual has zero correlation with those variables entering the equation and thus may be expressed as "variable Z_i adjusted for $Z_1, Z_2 \ldots Z_{i-1}$." If all the preceding variables entered in each of the above regression equations, the new variables (residuals) would be perfectly orthogonal, since for any residual Z_i^*, all the preceding residuals $(Z_1^*, \ldots Z_{i-1}^*)$ are functions of the preceding variables $(Z_1, Z_2 \ldots Z_3)$.

Since the residuals are independent of the preceding variables, they are independent of each other. In the case where only some of the preceding variables enter into the equations, they correlations between the residuals may be greater than zero, but in any event, they should suffice as an approximation to the process.

The new set of variables (consisting of $Z_1 = Z_1^*$ and $Z_2^* \ldots Z_n^*$) is then run against the dependent variable to derive a column vector of coefficients

$$C = \left\{c_i\right\}$$

such that

$$\hat{Y} = \left\{z_{it}^*\right\} \left\{c_i\right\}$$

or

$$Y = \left\{z_{it}^*\right\} \left\{c_i\right\} + \left\{e_i\right\}$$

Let the set of coefficients relating Z_i^*'s with Z's be represented by the matrix $G = \left\{g_{ik}\right\}$ such that

$$\left\{z_{it}^*\right\} = \left\{z_{it}\right\} - \left\{z_{it}\right\} \left\{g_{ik}\right\}$$

or

$$\left\{z_{it}^*\right\} = \left\{z_{it}\right\} (I - G)$$

where I is the identity matrix. Then substitute $\left\{z_{it}\right\} (I - G)$ for $\left\{z_{it}^*\right\}$ to yield $Y = \left\{z_{it}\right\} (I - G) \left\{c_i\right\} + E$.

The product $(I - G) \left\{c_i\right\}$ gives a column vector $D = \left\{d_{ij}\right\}$ such that $Y = \left\{z_{it}\right\} D + E$.

By rearranging the columns of $\left\{z_{it}\right\}$ and the rows of D, we can express this equation in original form $Y = XB + E$ or $\hat{Y} = XB$.

Utilizing orthogonalizing procedures the following equation was derived for the Reactive Metals portion of the Ti-6Al-4V data:

$$\ln\varepsilon = \underset{}{-1.60105} + \underset{(.08247)}{.76778Z_2^{**}} + \underset{(.03822)}{1.39468Z_4^{**}} + \underset{(.01625)}{.24348Z_6^{**}} - \underset{(.05316)}{1.18079Z_7^{**}}$$

$$+\underset{(.09507)}{3.60467Z_8^{**}} - \underset{(.02030)}{.10396Z_{11}^{**}} - \underset{(.10484)}{1.09665Z_{12}^{**}} - \underset{(.10459)}{.50740Z_{13}^{**}}$$

$$+\underset{(.02846)}{.11015Z_{14}^{**}} + \underset{(.12843)}{.72766Z_{16}^{**}} + \underset{(.10602)}{.62602Z_{17}^{**}} + \underset{(.02807)}{.85095Z_{20}^{**}}$$

$$+\underset{(.04119)}{.65313Z_{21}^{**}} + \underset{(.05184)}{.30998Z_{24}^{**}}$$

R = .9729
SE = .1754

The standard error of the coefficients are the figures in parentheses; * = significant at the 95% level, ** = significant at the 99% level.

where:

$$Z_2 = (X_2 - 229.6774 + 264.768X_3) \times 10^{-2}$$

$$Z_4 = (X_4 - 2708.787 + 8.76202X_2 + 2994.652X_3) \times 10^{-3}$$

$$Z_6 = (X_6 - 50.56067 - .04075X_2 + 35.54213X_3 + .00027X_4 + 16.64302X_7) \times 1$$

$$Z_7 = (X_7 - 2.91615 + 2.08822X_3) \times 10^{1}$$

$$Z_8 = (X_8 - 38.59265 + .13689X_2 + 42.84755X_3 - .00396X_4 + .15648X_6) \times 10^{-1}$$

$$Z_{11} = (X_{11} - 94.6895 - .73939X_2 + 79.713X_3 - .09289X_4 - 1.65322X_6 - .80516X_8 + 2.09007X_9 + 17.46747X_{10} + .00006X_{19} + .00284X_{20}) \times 10^{-1}$$

$$Z_{12} = (X_{12} - 27.75812 - 5.19467X_6 + 17.22734X_7 + .12260X_{11} - 2.55488X_{14} + 25.86461X_{18} - .00039X_{20} + .00729X_{21} + .29827X_{22} - .00013X_{23}) \times 10^{-1}$$

$$Z_{13} = (X_{13} + 3.11399 - .00957X_2 - 1.07833X_3 - 1.24902X_6 - .01214X_8 + .02755X_9 - 1.45858X_{10} + .00184X_{11}) \times 10^{1}$$

$$Z_{14} = (X_{14} + 24.13931 - 20.9303X_3 + .00081X_4 - 1.23404X_8 - 4.13036X_{10} - .02142X_{11} + .00034X_{20} - .04262X_{22} - .00002X_{23}) \times 1$$

$$Z_{16} = (X_{16} + 15542.488 + .15819X_4 + 9.94253X_9 - 4866.97X_{10} + 2.21308X_{11} - 130.1504X_{13} - 5.9535X_{14} - 12374.320X_{18} - .05248X_{20} - .27890X_{21}) \times 10^{-2}$$

$$Z_{17} = (X_{17} + 5183.19922 - 13443.8X_3 + 3.77204X_4 + 1547.665X_8 - 131.697X_{11} - 855.631X_{12} + 5969.641X_{13} - 7.40512X_{16} + 3.5764X_{20} - 801.125X_{22} - .09379X_{23}) \times 10^{-4}$$

$$Z_{20} = (X_{20} - 7808.86328 - 100.71542X_2 + 8273.63672X_3 - .24669X_4 + 984.1379X_6 + 174.171X_8) \times 10^{-3}$$

$$Z_{21} = (X_{21} - 463.50928 - .7699X_4 + 22.00688X_6 + 5.16804X_8 + 84.767X_{10} + 408.36768X_{18} + .00009X_{19}) \times 10^{-2}$$

$$Z_{24} = (X_{24} - 665.85156 - 1.80408X_4 + 347.87134X_6 + 343.60107X_8 - 20.18231X_{11} - 130.64374X_{12} + .07985X_{17} + .00047X_{19} + .06608X_{20} - 24.84586X_{22} - .5659X_{23}) \times 10^{-3}$$

Where:

$X_2 = \sigma$	$X_{12} = (\ln\sigma)(\ln t)$	$X_{22} = T\sigma$
$X_3 = T\ (°K)$	$X_{13} = (\ln\sigma)[T(°K)]^{-1}$	$X_{23} = t\sigma$
$X_4 = t$	$X_{14} = (\ln t)[T(°K)]^{-1}$	$X_{24} = t\sigma T$
$X_6 = \ln\sigma$	$X_{16} = \ln\sigma e^{4.(T°K)^{-1}}$	
$X_7 = [T(°K)]^{-1}$	$X_{17} = \ln(t)\ln\sigma e^{4.(T°K)^{-1}}$	
$X_8 = \ln t$	$X_{18} = T°K^2$	
$X_9 = (\ln\sigma)^2$	$X_{19} = t^2$	
$X_{10} = [T(°K)]^{-2}$	$X_{20} = \sigma^2$	
$X_{11} = (\ln t)^2$	$X_{21} = Tt$	

NOTE: ($X_{15} = T^{-1}\sigma t$) does not enter as independent variables

APPENDIX G-2

AN APPROACH TOWARD DEVELOPING A FINITE DIFFERENCE EQUATION FOR RENE' 41

The predictive equations developed to describe the data are essentially "best fit" equations and may or may not describe the shape of the individual creep curve. In an attempt to better describe individual creep curves the finite difference approach was applied to develop an equation for the same Rene' 41 steady-state data base used in development of Equation (3-19). The additional variable strain at time t was included as a function of strain at time t-Δt, using a Δt of 20 hours for the data set. This allowed creep strain to be expressed as a function of the previous time history at any given stress and temperature.

The following finite difference equation was computed, using the BMD02R computer program.

$$\varepsilon_{t+1} = 1.057 + .053 \ln\sigma - 1.289/T + .878\, \varepsilon_t + .195\, \varepsilon_t^2 \qquad (1)$$

where σ = stress, MPa

T = temperature, °K/1000

ε_{t+1} = Creep strain at time $t + \Delta t$ where Δt = 20 hours

ε_t = Creep strain at time t

In order to determine the form of the equation for strain as a function of time, a solution was developed for an approximate differential equation form of Equation (1).

A brief development of the solution is presented below. Suggestions by Mr. Lars Sjodahl, General Electric Company, Evendale, were extremely helpful in the analysis.

Subtracting ε_t from each side of Equation (1) and substituting the expression

$$A = 1.057 + .053 \ln\sigma - 1.289/T,$$ the equation can be rewritten as:

$$\Delta\varepsilon = \varepsilon_{t+1} - \varepsilon_t = A - .122\ \varepsilon_t + .195\ \varepsilon_t^{\ 2} \qquad (2)$$

The expression A may be considered a constant for any particular steady state creep test. Dividing both sides of Equation (2) by the time increment, Δt, we obtain

$$\frac{\Delta\varepsilon}{\Delta t} = \frac{1}{\Delta t}\left[A - .122\ \varepsilon_t + .195\ \varepsilon_t^{\ 2}\right] \qquad (3)$$

For small Δt, $\frac{\Delta\varepsilon}{\Delta t} \sim \frac{d\varepsilon}{\Delta t}$, and separation of variables yields:

$$\int_o^t dt = \int_o^t \frac{d\varepsilon}{1/20\ \left[A - .122\varepsilon_t + .195\ \varepsilon_t^{\ 2}\right]} \qquad (4)$$

Integrating, the expression and solving for strain, the equation becomes

$$\varepsilon = 51.282\ \sqrt{q}\ \tan\ (\gamma t + \beta) + .312 \qquad (5)$$

where:

$$q = .00195\ A - .0000372$$

$$\gamma = \sqrt{q}/2$$

$$\beta = \arctan\ \left(- \frac{.0061}{\sqrt{q}}\right)$$

The finite difference prediction equation developed (Equation (5)) was found to provide excellent predictions in the stress and temperature range of the data. However, a study of the equation showed that extrapolation outside the data base range could result in erroneous predicted values of strain. This can be noted from the equation since $\varepsilon \neq 0$ at $t = 0$.

Since it will, in general, be difficult to solve resulting finite difference equations and may be impossible to control resulting boundary conditions of $\varepsilon = 0$ at $\sigma = 0$ and $t = 0$, which must be met for application of the equation to TPS creep deflection analysis, the approach was not pursued further during this program.

APPENDIX G-3

NONLINEAR LEAST SQUARES FIT TO L605 AND Ti-6Al-4V DATA

Based on plots of L605 and Ti-6Al-4V cycles and steady-state creep data it appears that one equation may be used to describe each data set (L605 and Ti-6Al-4V). In an attempt to develop a common equation, a nonlinear least squares analysis was attempted using the titanium and L605 data. Temperatures and stresses are in °F and ksi respectively.

The first form attempted was

$$\varepsilon = \sinh\left[(\beta\sigma)^n\right] \tag{1}$$

where ε=strain, σ=stress, and β and n are unknown coefficients. Temperature and time were constant for each set of data used to obtain β and n. Steady-state and cyclic data were combined for each constant temperature and time. Table 1 shows the results of the fits obtained. The error in these fits was considered unacceptably high.

The second form attempted was

$$\varepsilon = c_0 e^{-bt} + c_1 t + c_2 \tag{2}$$

where ε=strain, t=time, and c_0, c_1, c_2, and b are unknown coefficients. Stress and temperature were held constant and coefficients (c_0, c_1, c_2, and b) were generated for each combination of stress and temperature. Attempts to use this form were unsuccessful. Intermediate results printed showed that c_o and b both grew simultaneously and did not appear to be approaching any limit. It was decided to modify this form to eliminate this problem and at the same time ensure that the new form had the properties:

(a) $\varepsilon(t)$ was linear for large t;

(b) $\varepsilon'(t)$ was "large" for small t, but decayed rapidly to some value appropriate for large t; (derivative of ε with respect to t)

(c) $\varepsilon(0) = 0$.

The third form attempted was

$$\varepsilon = c_0 \ (1 - e^{-bt}) + c_1 t \tag{3}$$

where t and ε are the same parameters as in Equation 2. This form has the properties described in the next paragraph. The results obtained were very good for all data sets used. Table 2 shows the coefficients obtained for various combinations of strain and temperature.

Since each coefficient c_0, c_1, and b (in Equation 3) is a function of temperature and stress, the next step attempted was to perform a linear regression analysis on each of these coefficients including such terms as T, σ, σ^2, Tσ, and Tσ^2. The residual for this equation was .9705. The resulting fits were not sufficiently close to the previously calculated c_0, c_1, and b values. (See Tables 3, 4, and 5.) At this point, the values for the coefficients (c_0, c_1, and b) were separated into two groups corresponding to steady state and cyclic data. Again a linear regression analysis was performed. The results were somewhat better but still unacceptable.

After plotting the "steady-state" c_0 and c_1 as a function of σ, it became clear that one possible form for these variables would be

$$c = \sinh \ [\beta\sigma] \tag{4}$$

where c = c_0 or c_1. The results were encouraging, although the calculated value was usually too large for small σ. As an attempt to improve the fit, the form

$$c = \sinh \ [(\beta\sigma)^2] \tag{5}$$

was also tried on the "steady-state" c_0 and c_1 values. The fit was in many cases better. As a final attempt to improve these fits, the form

$$c_j = \sinh \ [(\beta_j\sigma)^{n_j}] \tag{6}$$

was used. The results were very good. The values for n and β are shown in Tables 6 and 7. Unfortunately, the values for n and β shown there do not suggest a simple

functional relationship with the temperature. However, the intermediate results suggest that any point in a fairly large region in the β, n plane can produce an "acceptable" fit. Thus it may be possible to obtain an acceptable fit for all temperature, T, by using a relatively simple form such as

$$\beta_j = \beta_{j_0} + \beta_{j_1} T$$

and (7)

$$n_j = n_{j_0} + n_{j_1} T$$

This possibility was not explored because of time limitations. The calculations described in this paragraph also have not been attempted with the "cyclic" coefficients because of time limitations.

The relationship between b (in Equation 3) and σ and T has not been explored to any great extent. However, preliminary results suggest that any point in a fairly wide range can serve as an acceptable value for b. That is, Equation 3 is not particularly sensitive to the value of b. Thus it should be possible to use a fairly simple relation in fitting b as a function of σ and T.

The resulting form would then look like

$$\varepsilon = \sinh\left[(\beta_0\sigma)^{n_0}\right]\{1-e^{-b(T,\sigma)t}\} + \sinh\left[(\beta_1\sigma)^{n_1}\right]t \qquad (8)$$

where β_0, β_1, n_0, n_1 are some functions of T (e.g., equation 7) and b (T, σ) is the function described in Equation 3.

Table 1 . . . . $\varepsilon = \sinh [(\beta\ )^n]$

Input			Calculated		
Temperature °F	stress(σ) ksi	strain(ε) %	strain %	β	n
1300	7.40	.050	.05220	.011131	1.182886
	8.00	.070	.05725		
	11.70	.090	.08982		
	16.00	.115	.13026		
	16.00	.120	.13026		
	18.70	.174	.15685		
1435	4.00	.062	.02169	.059777	2.677391
	7.57	.155	.11996		
	8.00	.175	.13920		
	12.10	.440	.43256		
	16.00	.950	1.00880		
	18.50	1.740	1.71669		
1600	2.00	.043	.00157	.101148	4.041910
	4.00	.081	.02580		
	4.30	.141	.03457		
	6.85	.330	.22890		
	8.00	.424	.43786		
	8.00	.318	.43786		
	8.00	.457	.43786		
	10.66	1.820	1.81129		
1800	1.92	.060	.00485	.193888	5.391857
	2.00	.069	.00605		
	2.00	.070	.00605		
	2.98	.155	.05196		
	4.00	.189	.25672		
	4.90	.845	.83349		
900	7.00	.225	.26308	.051557	1.321247
	7.30	.250	.27844		
	12.00	.620	.55545		
	19.00	1.120	1.13413		
825	7.00	.045	.04127	.015592	1.439139
	17.00	.140	.14849		
	28.00	.310	.30806		
	45.00	.680	.63728		
	46.00	.620	.66028		
725	24.00	.040	.04275	.008279	1.950928
	30.00	.070	.06610		
	43.00	.130	.13372		
	46.00	.155	.15266		

Table 2 . . . . $\varepsilon = c_0(1-e^{-bt}) + c_1 t$

Temperature °F	Stress ksi	b	c_0	c_1
650	46.00	1.2452	.02675	.00082
	69.00	1.0663	.04726	.00215
725	24.00	.6279	.02469	.00078
	30.02	1.1332	.05212	.00074
	43.40	1.2218	.09592	.00109
	46.00	.5677	.07138	.00281
	57.86	.9363	.14805	.00321
	69.00	.4075	.21548	.01279
825	7.00	.4178	.02053	.00081
	16.63	.8501	.06182	.00252
	24.00	.3427	.07640	.00326
	27.85	.6778	.11338	.00656
	44.57	.3757	.24689	.01490
	46.00	.5815	.17893	.01149
950	7.00	.4056	.07126	.00514
	7.31	.4425	.07305	.00588
	12.12	.4689	.23018	.01294
	18.81	.2891	.35600	.02550
	24.00	.8148	.19001	.05505
1050	2.85	*	.04100	.01123
	4.43	*	.07362	.02508
	6.85	*	.10645	.05269

* Computed value considered to be unreliable.

Table 3 . . . . Linear Regression for b

$$b = BS2T*\sigma^2*T + BST*\sigma*T + BT*T + BCON + BS*\sigma$$

Input			Calculated
Temperature (T) °F	Stress (σ) ksi	b	b
650	46.00	1.245	1.256
	69.00	1.066	1.050
725	24.00	.628	.815
	30.02	1.133	.902
	43.40	1.222	.948
	46.00	.568	.933
	57.86	.936	.769
	69.00	.408	.469
825	7.00	.418	.387
	16.63	.850	.590
	24.00	.343	.668
	27.85	.678	.683
	44.57	.376	.533
	46.00	.582	.504
950	7.00	.406	.437
	7.31	.443	.441
	12.12	.469	.492
	18.81	.289	.511
	24.00	.815	.485

Values for b at temperature=1050 were considered unreliable and were not used in the regression.

The term b is from the equation (3) $\varepsilon = c_o\,(1-e^{-bt}) + c_1 t$ where σ, T are stress and temperature respectively, while BCON, BS, BT, B 55T, and B 52T are constants from a linear regression analysis.

Table 4 . . . . Linear Regression for c_0

$$c_0 = COS2*\sigma^2 + COST*\sigma*T + COT*T + COS*\sigma + COCON$$

Input			Calculated
Temperature (T) °F	Stress (σ) ksi	c_0	c_0
650	46.00	.0268	-.0043
	69.00	.0473	.0042
725	24.00	.0247	.0279
	30.02	.0521	.0479
	43.40	.0959	.0947
	46.00	.0714	.1042
	57.86	.1481	.1487
	69.00	.2155	.1928
825	7.00	.0205	.0225
	16.63	.0618	.0759
	24.00	.0764	.1179
	27.85	.1134	.1402
	44.57	.2469	.2400
	46.00	.1789	.2487
950	7.00	.0713	.0822
	7.31	.0731	.0849
	12.12	.2302	.1263
	18.81	.3560	.1846
	24.00	.1900	.2303
1050	2.85	.0410	.0843
	4.43	.0736	.1017
	6.85	.1065	.1283

The term b is from the equation (3) $\varepsilon = c_o\ (1-e^{-bt}) + c_1 t$ where σ, T are stress and temperature respectively, while BCON, BS, BT, B 55T, and B 52T are constants from a linear regression analysis.

Table 5 . . . . Linear Regression for c_1

$$c_1 = C1S2T*\sigma^2*T + C1ST*\sigma*T + C1T*T + C1CON + C1S2*\sigma^2$$

Input			Calculated
Temperature (T) °F	Stress (σ) ksi	c_1	c_1
650	46.00	.00082	-.00241
	69.00	.00215	.00480
725	24.00	.00078	-.00766
	30.02	.00074	-.00223
	43.40	.00109	.00547
	46.00	.00281	.00627
	57.86	.00321	.00701
	69.00	.01279	.00340
825	7.00	.00081	-.01072
	16.63	.00252	.00291
	24.00	.00326	.01430
	27.85	.00656	.01335
	44.57	.01490	.01805
	46.00	.01149	.01785
950	7.00	.00514	.01286
	7.31	.00588	.01339
	12.12	.01294	.02084
	18.81	.02550	.02879
	24.00	.05505	.03303
1050	2.85	.01123	.02368
	4.43	.02508	.02689
	6.85	.05269	.03145

The term c_1 is from equation (3) $\varepsilon = c_0 (1-e^{-bt}) + c_1 t$

where σ, T are stress and temperature respectively, while CICON, CIT, CIST, C1S2, and C1S2T are constants from a linear regression analysis.

Table 6 . . . . $c_0 = \sinh\left[(\beta_0\sigma)^{n_0}\right]$

Input			Calculated		
Temperature °F	Stress (σ) ksi	c_0	c_0	β_0	n_0
650	46.00	.02675	.02651	.00172*	1.43263*
	69.00	.04726	.04740		
725	24.00	.02469	.01472	.00786	2.52945
	46.00	.07138	.07638		
	69.00	.21548	.21440		
825	7.00	.02053	.01683	.00545	1.25070
	24.00	.07640	.07868		
	46.00	.17893	.17828		
950	7.00	.07126	.07110	.00511	.79387
	24.00	.19001	.19007		

* Value of coefficient is unreliable but is reported because a reasonable fit was obtained.

Table 7 . . . . $c_1 = \sinh [(\beta_1 \sigma)^{n_1}]$

Input			Calculated		
Temperature °F	Stress (σ) ksi	c_1	c_1	β_1	n_1
650	46.00	.00082	.00028	.00424*	5.00050*
	69.00	.00215	.00215		
725	24.00	.00078	.00025	.00451	3.73737
	46.00	.00281	.00281		
	69.00	.01279	.01279		
825	7.00	.00081	.00030	.00217	1.93637
	24.00	.00326	.00326		
	46.00	.01149	.01149		
950	7.00	.00514	.00511	.00927	1.92939
	24.00	.05505	.05505		

* Value of coefficient is unreliable but is reported because a reasonable fit was obtained.

APPENDIX H

ERROR ANALYSIS FOR CYCLE CREEP FURNACE STRESS MEASUREMENTS

I. Introduction

The stress and temperature data are recorded with a miniature 50 channel digital data system after the required signal conditioning has been performed. The data errors, which are the subject of this discussion, are the static errors of the system. Dynamic errors are not involved in the analysis since the sampling rate and software tend to eliminate dynamic effects by 1) using a record rate of one sample every 50 seconds and 2) deleting the first and last samples of a cycle in an effort to stay off the slope of the stress curve. It is assumed that system noise results in load fluctuations which are random in nature and that the mean value of data over a cycle has a mean deviation that is negligible. This does not imply that the standard deviation will be negligible. Noise levels may cause significant load variations which, if recorded, may result in a substantial standard deviation.

II. Basis for Analysis

A. Statistics

1. Mean Value

$$X_m = \frac{1}{n} \sum_{i=1}^{n} X_i \qquad (1)$$

2. Mean Deviation

$$\bar{S} = \frac{1}{n} \sum_{i=1}^{n} (X_m - X_i) \qquad (2)$$

3. Standard Deviation

$$\sigma = \left(\frac{1}{n-1} \sum_{i=1}^{n} |X_m - X_i|^2 \right)^{1/2} \qquad (3)$$

III. System Analysis

A. Transducer-Stress

The data system is used to record the millivolt output of a strain gage bridge force transducer. Several factors affect the uncertainty which should be assigned to the magnitude of load measured with this transducer. These factors are discussed and their effects are evaluated in the following paragraphs. The equation for transducer output may be written as follows:

$$e_o = F K_c \left[1 + f_t \left(t_r - t \right) \right] \tag{4}$$

where = transducer output in mV

F = applied force-pounds

K_c = calibration factor in mV/pound/Volt Excit.

f_t = fractional temperature sensitivity

t = operating temperature

(temperature must be expressed in consistent units, i.e., ^oF or ^oC)

1. Transducer Calibration

The calibration is performed at discrete points covering the specified range, the load being applied in both the ascending and descending directions. The result of the calibration should be incremental e_o, (Equation 4) versus incremental load. The calibration statement may include a tolerance for linearity and hysteresis, repeatability and for the standards used to perform the calibration. The temperature at which the calibration was performed must be specified. If the transducer temperature

coefficient is unknown, tests at two or three temperatures are needed.

a) Nonlinearity and hysteresis are determined by a best straight line through zero. This imposes some unnecessary restraints and results in a tolerance generally larger than simple best straight line fit which is recommended.

b) Repeatability is a measure of the ability of the transducer to produce the same output each time a given load is applied, approaching the load level from the same direction each time. This is the figure specified on the certificate. The figure used in the analysis should include long-term stability as this historical data is obtained for a given transducer.

c) The statement of tolerance for the standards used is a measure of the accuracy with which a given e_o versus load was determined.

d) Analysis of Data

(1) use the statement of accuracy for the standards, converted to fractional form.

(2) use the figure for repeatability, again converted to fractional form.

(3) calculate the average mV/pound/volt by obtaining the mV/pound/volt value for each increment (e_{si}) and then average. Include data for both directions of load.

$$e_s = \frac{1}{n} \sum_{i=1}^{n} e_{si} \qquad (5)$$

where e_{si} = the mV/pound/Volt sensitivity for the ith increment

e_s = transducer sensitivity in mV/pound load/Volt

The figure e_s is the slope of the straight line which fits in the data. The need for close tolerance has not (so far) justified the more rigorous least squares fit).

(4) Combine non-linearity and hysteresis into a single tolerance based upon the fractional maximum deviation from the straight line f_n:

where $$f_n = \frac{|(e_s - e_{si})|}{e_s} \tag{6}$$

and e_{si} is that increment having the greatest deviation from e_s.

(5) The tolerance to be used for nonrepeatability is that specified by the calibration certificate, usually in percent, converted to fractional form. Designate f_n.

(6) The uncertainty in calibration is f_s = the fractional error equivalent to the tolerance specified for the standards.

(7) Convert the data which defines f_t to f_t as follows:

a. Calculate e_s for each temperature

$$f_t = \frac{e_{st_r} - e_{st_z}}{\delta t} \tag{7}$$

where t_r is the reference temperature

t_z is a temperature higher than t_r

$\delta t = t_z - t_r$

* t_r and t_z should be close to and bracket the expected operating temperature.

(8) Expressing again the transducer equation

$$e_o = FK_c\left[1 + f_t\,(t_r - t)\right] \tag{8}$$

$$= F e_s [1 + f_t (t_r - t)] \cdot V_v \qquad (9)$$

where V_v is the bridge excitation.

(9) The uncertainty in the calibration may be evaluated as follows:

$$f_c = f_h + f_n + f_s \qquad (10)$$

This expression assumes the error in f_t is negligibly small. (Typical ϵ_t = .015% for MAC made transducers. If t is measured to $\pm$ 1°F the temperature error f_t, in fractional form, is .00015.

(10) The Rcal specifies equivalent load. This factor is derived from a best straight line through zero analysis. Unless the equivalent mV level is given, this value cannot be converted directly to equivalent pounds for straight line not thru zero.

The equivalent can be found by applying the Rcal to to the bridge and get $mV/_{V_v\ (cal)}$

than $\text{Equiv} = mV/_{V_c\ (cal)} \cdot e_s \qquad (11)$

[See 2-a-(5)]

B. Transducer Signal Conditioning

1. Repeating equation (9) $e_o = F\, e_s [1 + f_t (t_r - t)] \cdot V_v$

the factors directly affected by the signal conditioning are:

a) Ve - the bridge excitation voltage

- the stability of the power supply is not perfect.
- the resistors used to adjust the excitation to the required

level vary with time and temperature.

Variations in bridge voltage have a direct effect on e_o. Since the recorded calibration level on the data system constitutes the reference level until a new calibration level is recorded, it is necessary that Ve be stable, within the limits required for measurement accuracy from one calibration to the next.

The instability of V_v is ϵ_v the fractional equivalent is

$$f_v = \frac{\epsilon_v}{V_v} \tag{12}$$

measurements indicate this may be ± 0.001.

b) f_t - the error due to a change in transducer sensitivity versus temperature. The contribution to this factor by calibration was stated to be negligible. This is not necessarily true for use. The error in temperature measurement is somewhat larger and will determine the magnitude of this contribution. The fractional error is f_t. $f_t = \epsilon_t(100)$.

c) If bridge balance is used a balancing current is caused to flow through the bridge. The stability of this current, relative to bridge current, is determined by the stability of the components in the balance circuit. The variation observed is 0.2 to 0.3%, depending upon the relative size of adjustable and fixed resistors in the balance network and the change in all these resistors due to temperature. The fractional error, directly contributing to a change in e_o:

$$f_d = \frac{\Delta e_o / V_v}{e_s} \tag{13}$$

Balance networks are not normally used in the creep test except for the control transducers.

d) If the procedure suggested in d(10) are followed in establishing the Rcal equivalent, the error resulting from the procedure is due to the relative accuracy of the measurements of voltage made at the time of the determination and those made in the calibration process. If proper procedures, such as zeroing the measuring instruments, sufficient resolution, careful calibration, etc. have been observed; these measurements can be made with a combined uncertainty of .03%. The error, otherwise, results from the difference between the specified Rcal and the one actually used. A ±.01% resistor is specified by the calibration laboratory. Available laboratory instruments permit measurements to be made so that the specified value of resistance can be matched within 0.1%.

The fractional uncertainty due to this factor is f_e.

e) Other Effects - The sketch below is used for reference:

SIMPLIFIED SIGNAL CONDITIONER SCHEMATIC

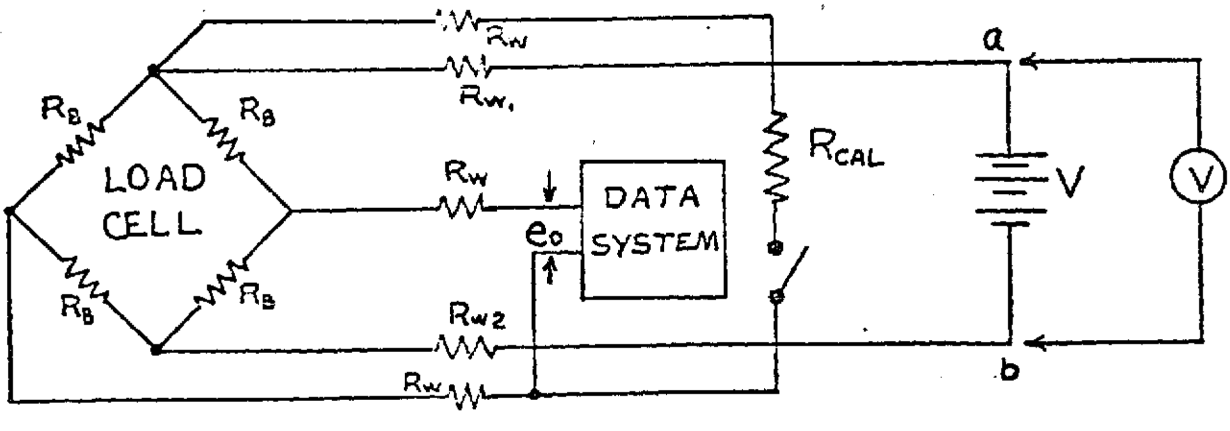

FIGURE (1)

- The leads which connect the load cell to the data system have a resistance of approximately 0.5 ohm per single line or conductor. The voltage applied to the bridge is then

  (1 - 1/350) = .997 of the voltage measured by

V at ab. Calculations of load based upon measurements of V and e_o at the data system terminals are in error by ~0.3%. However, the Rcal is applied to the bridge with the same excitation so the recorded equivalent is correct.

* An error will result in determining the Rcal equivalent as specified in step 1-d(10) if this factor is not accounted for in V_v. The value of resistance R_{W_1} and R_{W_2} Figure (1) must be measured.

o The addition of lead resistance to the Rcal resistor does not contribute significant error - approximately 1 in 10^4 or less depending upon the size of the Rcal and the actual value of 2 Rw. For 22 AWG wire, RW is about 0.016 ohms per foot of 19 strand conductor.

C. Data System Contribution to Total Error ϵ_d

1. The data system consists of the elements shown below which bear directly upon the accuracy of measurements made.

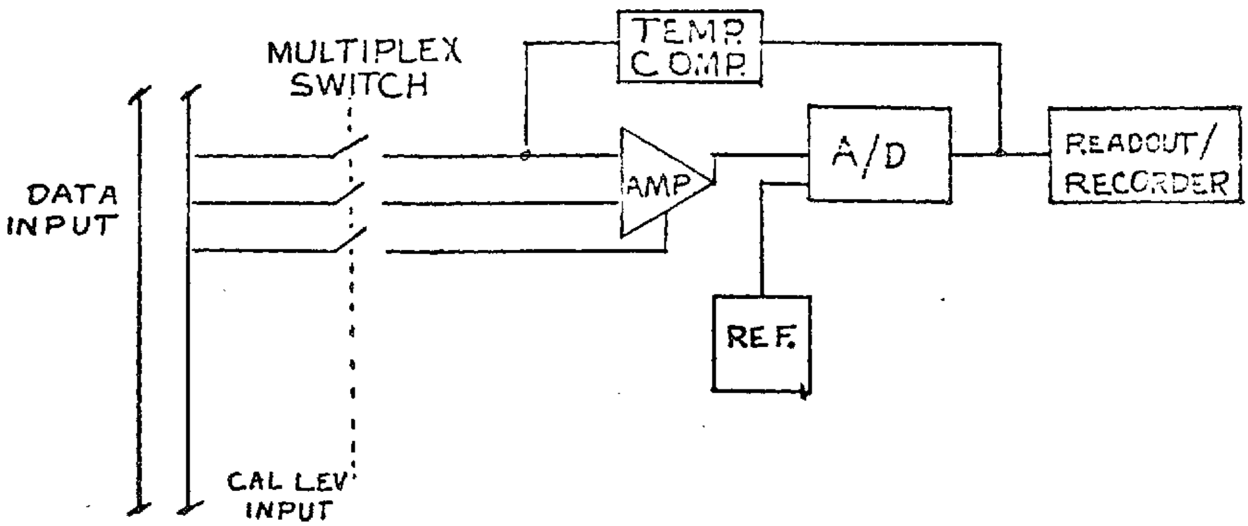

FIGURE (2)

2. The use of an Rcal equivalent for transducer inputs calibrates the system-from transducer through data system-each time a Zcal/Rcal record is made. The data processing software uses this recorded calibration signal for scaling. If the amplifier gain or zero changes or an A/D conversion error due to a resistor change would occur, the software will correct for that. However, if the internal calibration reference level changes, a correction may be applied which will be erroneous. The stability of the reference supply is, therefore, a key parameter. e_r is the variation in the reference voltage (V_r). The fractional error f_r

$$f_r = \frac{e_r}{V_r} \tag{14}$$

A more useful form is f_r (counts equivalent to V_r). Measurements indicate f_r is less than .001.

3. If the amplifier is non-linear, this will result in an error related to level of signal. This effect has been evaluated by measurements. This error is designated f_ℓ. The magnitude of this factor is .0005.

4. The data system direct measurement accuracy must be assigned to data from thermocouples since no calibration level is used. This factor is part of the evaluation, designated ϵ_d.

Interims of Counts

$\epsilon_d/100$ (counts full scale) = (f_r + f_ℓ) (counts full scale)

5. This analysis of the data system makes some assumptions.
   a) That the thermal units of the input circuits are negligible.
   b) That the digitizing error is constant.
   c) That for typical applications and installations the effect

of temperature is negligible.

Bench tests indicate the effect of these factors to be negligible.

6. The following is a summary of the data obtained using the digital system to measure reference inputs over a period of three months.

   a) The stability of the reference - deviation is less that 0.1% of full scale or f_r (counts) = 2; fractional = .001.

   b) Non-linearity - 0.05% or 1 count. So f_ℓ (counts) = 1
   fractional = .0005

D. Analysis Applied to Direct Voltage Inputs

1. The system can be analyzed as a voltmeter since the only consideration is the direct measurement accuracy of the digital data system which has been expressed in fractional form (fraction of full scale) as:

$$f_D = f_r + f_\ell \text{ (in counts)} = 3$$
$$\text{fractional} = .0015$$

2. For thermocouples the error can be expressed in equivalent temperature as

$$\frac{f_D \text{ (mV f.S. - data system)}}{(\text{mV}/^\circ\text{F})_{T/C}} = \epsilon_T$$

$$\epsilon_T = \frac{15 \times 10^{-6} v}{22 \times 10^{-6} v/^\circ F} = .68 \simeq 0.7^\circ F$$

IV. Summary of the Analysis

A. Transducer Uncertainty

1. Equation - re-writing equation (9)

$$F = \frac{e_o}{e_s \left[1 + f_t(t_r - t)\right] V_v} \tag{15}$$

the error in e_s may be expressed as

$$e_s = e_s' \; (1 \pm f_c) \tag{16}$$
$$= e_s' \; (1 \pm f_h \pm f_n \pm f_s)$$

therefore

$$F = \frac{e_o}{e'_s\left[(1 + f_c) \quad 1 + f_t(t_r - t)\right] V_v} \tag{17}$$

The uncertainty can be expressed simply as $f_c = f_h + f_n + f_s$ - the maximum fractional error in the calibration. If a dead wt. calibration is performed typical figures are $f_h = .0015$, $f_n = .0005$, $f_s = .0005$ and $f_c = .0015$. Each calibration must be evaluated.

B. Contributions of Signal Conditioning:

Signal conditioning errors explained in detail in the text can be expressed as the sum of fractional errors.

$$f_a = f_v + f_t + f_d + f_e \tag{18}$$

for the creep test system

f_d does not apply

f_e: error can be as small as .03% so $f_e = .0003$

f_t: the error in temperature measurement is about 1°F (0.7°F for data system + 0.4 for T/C Calibration)

If transducer temperature sensitivity ϵ_t is ±.02%/°F, $f_t = .0002$

f_v: a stability of 0.1% or better indicates $f_v = .001$

So $f_a = .0003 + .0002 + .001$

$f_a = .0015$

C. Contribution of Data System

$f_D = f_r + f_\ell \quad .001 + .0005$

counts = 3 = .0015 (2000)

fractional = .0015

D. If the inaccuracy of the measurement (f_m) is assumed to be the sum

$$f_m = f_c + f_a + f_D \tag{19}$$

f_c will vary with transducer range.

If the example given for f_c is used:

$$f_m = f_c + f_a + f_D$$

$$= .0015 + .0015 + .0015 = .0045$$

$$= 0.45\%$$

MCDONNELL DOUGLAS ASTRONAUTICS COMPANY - EAST

Saint Louis, Missouri 63166 (314) 232-0232

MCDONNELL DOUGLAS

CORPORATION